



Latvia University of Agriculture
Faculty of Rural Engineering

CIVIL ENGINEERING'13

4th International Scientific Conference

Part I

PROCEEDINGS

Volume 4

Jelgava 2013

International Scientific Conference and Proceedings “Civil Engineering 13” – dedicated to the 150th anniversary of the higher agriculture education in Latvia and the Latvia University of Agriculture, and the 275th anniversary of the Jelgava Palace

The 4th International Scientific Conference „Civil Engineering 13” is organized on a regular basis and this year it was held on May 16-17, 2013. More than 80 reports were presented at six conference sections. Reports were presented by scientists and civil engineering professionals from the Latvia University of Agriculture, Riga Technical University as well as scientists from universities of Lithuania, Estonia, Russia, Poland, Netherlands and other countries. The main research directions represented at the conference were: construction and materials, landscape architecture, land management and geodesy, building and renovation, structural engineering, environment and environmental effects, industrial energy efficiency and others. One of the nowadays research priorities – effective usage and saving of energy resources, received a lot of attention - 10 scientific reports were presented at the “Industrial Energy Efficiency” section.

The conference „Civil Engineering 13” international scientific committee is represented by civil engineering experts and academic staff from Latvia, Lithuania, Estonia, Poland, Finland, Sweden, Czech Republic, Netherlands.

The 4th International Scientific Conference „Civil Engineering 13” Proceedings are developed in a notable anniversary year for all of us – the conference and proceedings are dedicated to the 150 anniversary of the higher agriculture education in Latvia and the Latvia University of Agriculture. The home of the Latvia University of Agriculture is the Jelgava Palace - the largest architectural monument in the Baltic States. The Jelgava Palace this year is celebrating its 275 anniversary years. We are proud that this monument is fundamental and outstanding and it definitely influences also modern building tendencies in Latvia and abroad.

It is important to note that scientific papers from previous International Scientific Conference „Civil Engineering 11” Proceedings were included in the AGRIS, CAB ABSTRACTS, EBSCO Central & Eastern European Academic Source and SCOPUS databases.

Scientific Conference "Civil Engeneering" has become very traditional and I hope that in future it will expand and will provide a collection of excellent researches.

Sincerely,
Dr. sc. ing., prof. Juris Skujans
Rector of Latvia University of Agriculture

Organizing Committee

Chairpersons:

Dr.sc.ing. Janis Kreilis, Latvia University of Agriculture
Dr.arch. Una Ile, Latvia University of Agriculture

Co-chairperson:

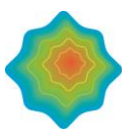
Mg.sc.ing. Silvija Strausa, Latvia University of Agriculture

Members:

Dr.sc.ing. Guntis Andersons, Latvia University of Agriculture
Dr.habil.sc.ing. Janis Brauns, Latvia University of Agriculture
Mg.sc.ing. Raitis Brencis, Latvia University of Agriculture
Mg.sc.ing. Arturs Gaurilka, Latvia University of Agriculture
Dr.oec. Sandra Gusta, Latvia University of Agriculture
Mg.sc.ing. Linda Grinberga, Latvia University of Agriculture

Mg.arch. Lilita Lazdane, Latvia University of Agriculture
Dr.sc.ing. Andris Steinerts, Latvia University of Agriculture
Dr.arch. Daiga Zigmunde, Latvia University of Agriculture
Mg.arch. Kristine Vugule, Latvia University of Agriculture
Dr.sc.ing. Reinis Ziemelnieks, Latvia University of Agriculture
Dr.arch. Aija Ziemelniece, Latvia University of Agriculture

ISSN 2255-7776



cluster
of industrial
energy efficiency



VIDES AIZSARDZĪBAS UN
REĢIONĀLĀS ATTĪSTĪBAS MINISTRĪJA

**LATVIA UNIVERSITY OF AGRICULTURE
FACULTY OF RURAL ENGINEERING**

Department of Architecture and Building

Department of Structural Engineering

**CIVIL ENGINEERING '13
4th International Scientific Conference
PROCEEDINGS**

Volume 4

Part I

Jelgava 2013

Civil Engineering` 13

4th International Scientific Conference Proceedings, Vol. 4

Jelgava, Latvia University of Agriculture, 2013, 371 pages

ISSN 2255-7776

SCIENTIFIC COMMITTEE

Chairperson

Dr.sc.ing. Juris Skujans, Latvia University of Agriculture, Latvia

Co-chairpersons

Dr.sc.ing. Andris Steinerts, Latvia University of Agriculture, Latvia
Dr.arch. Daiga Zigmunde, Latvia University of Agriculture, Latvia

Members

Ainars Paeglitis, Dr.sc.ing., Riga Technical University, Latvia
Juris Skujans, Dr.sc.ing., Latvia University of Agriculture, Latvia
Arturs Lesinskis, Dr.sc.ing., Latvia University of Agriculture, Latvia
Eriks Tilgalis, Dr.sc.ing., Latvia University of Agriculture, Latvia
Gintaras Stauskis, Dr., Vilnius Gediminas Technical University, Lithuania
Jaan Miljan, Dr.sc.ing., Estonian University of Life Science, Estonia
Janis Brauns, Dr.habil.sc.ing., Latvia University of Agriculture, Latvia
Janis Kreilis, Dr.sc.ing., Latvia University of Agriculture, Latvia
Lilita Ozola, Dr.sc.ing., Latvia University of Agriculture, Latvia
Simon Bell, Dr., Estonian University of Life Science, Estonia
Daiga Zigmunde, Dr.arch., Latvia University of Agriculture, Latvia
Ralejs Tepfers, Dr.sc.ing., Chalmers University of Technology, Sweden
Raimondas Sadzevicius, Dr.sc.ing., Aleksandras Stulginskis University, Lithuania
Ugis Bratuskins, Dr.arch., Riga Technical University, Latvia
Uldis Iljins, Dr.habil.sc.ing., Latvia University of Agriculture, Latvia
Velta Parsova, Dr.oec., Latvia University of Agriculture, Latvia
Anatolijs Borodinecs, Dr.sc.ing., Riga Technical University, Latvia
Nico Scholten, PhD, Expert Centre Regulations in Building, Netherland
Aija Ziemelniece, Dr.arch., Latvia University of Agriculture, Latvia
Reinis Ziemelnieks, Dr.sc.ing., Latvia University of Agriculture, Latvia

Reviewers

J. Skujans, A. Paeglitis, A. Lesinskis, E. Tilgalis, G. Stauskis, J. Miljan, J. Brauns, J. Kreilis, L. Ozola, S. Bell,
D. Zigmunde, R. Tepfers, U. Bratuskins, U. Iljins, S. Strausa, G. Andersons, S. Gusta, A. Ziemelniece, A. Borodinecs,
R. Sadzevicius, R. Ziemelnieks, K. Zaleckis, U. Ile, R. Misius, I. Niedzwiecka-Filipiak, E. Navickiene, N. Liba,
J. Kaminskis, I. Bimane, A. Jankava, U. Skadins, V. Parsova, M. Pelse

ABSTRACTED AND INDEXED: AGRIS, CAB ABSTRACTS, EBSCO Central & Eastern European Academic Source, SCOPUS. Note: the data bases select the articles from the proceedings for including them in their data bases after individual qualitative examination.

EDITORS

Editor of language

Diana Svika, Mg.paed., Larisa Malinovska, Dr.paed.

Technical editor

Madara Markova, Mg.arch.

© Latvia University of Agriculture

Printed in SIA Puse Plus

The collection of articles provides important ideas for further scientific activities and is dedicated to the 150 anniversary of the Latvia University of Agriculture.

PROCEEDINGS ARE SUPPORTED BY



Projekts tiek atbalstīts ar LIAA Latvijas Investīciju un attīstības aģentūra

CONTENT

Structural Engineering	8
Vadims Goremkins, Karlis Rocens, Dmitrijs Serduks, Raimonds Ozolins BEHAVIOUR OF CABLE TRUSS WEB ELEMENTS OF PRESTRESSED SUSPENSION BRIDGE	8
Liga Gaile, Normunds Tirans, Jans Velicko EVALUATION OF HIGHRISE BUILDING MODEL USING FUNDAMENTAL FREQUENCY MEASUREMENTS	15
Guntis Andersons, Lilita Ozola EFFICIENCY OF THERMAL DESIGN OF SHALLOW FOUNDATIONS	21
Renno Reitsnik, Harri Lille, Alexander Ryabchikov, Kauni Kiviste DETERMINATION OF SHRINKAGE STRESSES IN CONCRETE FLOOR COATINGS	31
Rytis Skominas, Vincas Gurskis, Algimantas Patasius RESEARCH OF MATERIALS SUITABILITY FOR CRACK REPAIR IN REINFORCED CONCRETE STRUCTURES	36
Eduards Skukis, Kaspars Kalnins, Olgerts Ozolins ASSESMENT OF THE EFFECT OF BOUNDARY CONDITIONS ON CYLINDRICAL SHELL MODAL RESPONSES	41
Liene Sable, Kaspars Kalnins EVALUATION OF GLASS IN DESIGN OF LOAD BEARING STRUCTURES	49
Mihails Lisicins, Viktors Mironovs, Irina Boiko BUILDING CONSTRUCTIONS MADE OF PERFORATED METALLIC MATERIALS	53
Liga Gaile, Ivars Radinsh FOOTFALL INDUCED FORCES ON STAIRS	60
Edgars Labans, Kaspars Kalnins INVESTIGATON OF WOOD BASED PANELS WITH PLYWOOD AND GFRP COMPOSITE COMPONENTS	69
Janis Sliseris, Girts Frolovs, Karlis Rocens OPTIMAL DESIGN OF VARIABLE STIFFNESS PLYWOOD- PLASTIC PLATE	75
Galina Harjkova, Pavels Akishins, Olga Kononova FINITE ELEMENT ANALYSIS OF WEFT KNITTED COMPOSITES	82

Andrejs Kovalovs, Georgij Portnov, Vladimir Kulakov, Alexander Arnautov, Ellen Lackey ANALYSIS OF INTERFACIAL STRESS BETWEEN COMPOSITE REBAR AND CONCRETE	86
Ulvis Skadins, Janis Brauns INFLUENCE OF FIBRE AMOUNT ON SFRC PRE- AND POST-CRACK BEHAVIOUR.....	91
Angelina Galushchak, Olga Kononova MICROMECHANICS OF ELASTO-PLASTIC FIBER PULL OUT OF ELASTIC MATRIX	99
Arturs Macanovskis, Vitalijs Lusis, Andrejs Krasnikovs POLYMER FIBER PULL OUT EXPERIMENTAL INVESTIGATION	104
Vitalijs Lusis TECHNOLOGY FOR CONCRETE SHELLS FABRICATION REINFORCED BY GLASS FIBERS	112
Vitalijs Lusis, Andrejs Krasnikovs BENDING STRENGTH OF LAYERED FIBERCONCRETE PRISM	117
Construction and Materials.....	122
Genady Shakhmenko, Diana Bajare, Inna Juhnevica, Nikolajs Toropovs, Janis Justs, Aljona Gabrene PROPERTIES AND COMPOSITION OF CONCRETE CONTAINING DIVERSE POZZOLANIC ADMIXTURES	122
Nikolajs Toropovs, Diana Bajare, Genadijs Shakhmenko, Aleksandrs Korjakins, Janis Justs EFFECT OF THERMAL TREATMENT ON PROPERTIES OF HIGH STRENGTH CONCRETE	129
Olga Finozenok, Ramune Zurauskiene, Rimvydas Zurauskas, Linas Mikulenas, Aleksandrs Korjakins, Genadijs Shakhmenko INFLUENCE OF POLYMERIC ADDITIVES ON THE PROPERTIES OF CONCRETE MANUFACTURED ON THE BASIS OF AGGREGATES PRODUCED FROM CRUSHED CONCRETE WASTE.....	134
Girts Bumanis, Diana Bajare, Aleksandrs Korjakins THE ECONOMIC AND ENVIRONMENTAL BENEFITS FROM INCORPORATION OF COAL BOTTOM ASH IN CONCRETE	142
Raitis Brencis, Juris Skujans, Uldis Iljins ACOUSTIC AND MECHANICAL PROPERTIES OF FOAM GYPSUM DECORATIVE CEILING PANELS	153

Janis Kazjonovs, Diana Bajare, Aleksandrs Korjakins, Ansis Ozolins, Andris Jakovics ANALYSIS OF SIMULATION MODELS OF PCM IN BUILDINGS UNDER LATVIA'S CLIMATE CONDITIONS.....	160
Aleksandrs Korjakins, Liga Upeniece, Diana Bajare HEAT INSULATION MATERIALS OF POROUS CERAMICS, USING PLANT FILLER.....	169
Martti-Jann Miljan, Matis Miljan, Jaan Miljan THERMAL CONDUCTIVITY OF WALLS INSULATED WITH NATURAL MATERIALS	175
Marija Masonkina, Kaspars Kalnins APPLICATION OF ULTRASONIC IMAGING TECHNIQUE AS STRUCTURAL HEALTH MONITORING TOOL FOR ASSESSMENT OF DEFECTS IN GLASS FIBER COMPOSITE STRUCTURES	180
Viktors Haritonovs, Martins Zaumanis, Guntis Brencis, Juris Smirnovs COMPARISON OF ASPHALT CONCRETE PERFORMANCE USING CONVENTIONAL AND UNCONVENTIONAL AGGREGATE	185
Atis Zarins, Viktors Haritonovs, Juris Smirnovs INTERPRETATION OF ASPHALT MATERIAL DESIGN PARAMETERS	192
Viktors Haritonovs, Martins Zaumanis, Janis Tihonovs, Juris Smirnovs DEVELOPMENT OF HIGH PERFORMANCE ASPHALT CONCRETE USING LOW QUALITY AGGREGATES.....	197
Peteris Skels, Kaspars Bondars, Aleksandrs Korjakins UNCONFINED COMPRESSIVE STRENGTH PROPERTIES OF CEMENT STABILIZED PEAT	202
Bruno Kirulis, Janis Kreilis, Linda Krage, Inta Barbane, Inese Sidraba MECHANICAL PROPERTIES OF LOW TEMPERATURE HYDROLYC BINDERS ...	207
Building and Renovation	212
Arturs Brahmanis, Arturs Lesinskis INDIRECT EVAPORATIVE PRE-COOLED COMPRESSOR COOLING SYSTEM PERFORMANCE UNDER VARIOUS OUTDOOR AIR HUMIDITY CONDITIONS ..	212
Sandra Gusta, Gints Skenders CONSTRUCTION WASTE MANAGEMENT PROCESS IN LATVIA: PROBLEMS AND POSSIBLE SOLUTIONS	217
Peter H.E. van de Leur, Nico P.M. Scholten DESIGN OF FLOW AND HOLDING CAPACITY OF ESCAPE ROUTES IN BUILDINGS.....	225

Arturs Macanovskis, Vitalijs Zaharevskis, Andrejs Krasnikovs NON-DESTRUCTIVE EVALUATION OF FIBER ORIENTATION IN FIBERCONCRETE PRISM.....	233
Gatis Plavenieks, Arturs Lesinskis CASE STUDY OF HEAT RECOVERY IN AIR HANDLING UNITS WITH HEAT EXCHANGERS FOR RESIDENTIAL APPLICATION IN LATVIA	240
Nico P.M. Scholten, Harry A.L. van Ewijk ENVIRONMENTAL PERFORMANCE REGULATIONS IN THE NETHERLANDS ..	245
 Landscape Architecture	 250
Una Ile, Silvija Rubene INTERACTION AREAS OF THE CULTURAL AND HISTORICAL TERRITORIES AND THE SOVIET PERIOD RESIDENTIAL AREAS	250
Natalija Nitavska, Daiga Zigmunde THE IMPACT OF LEGISLATIVE RULES AND ECONOMIC DEVELOPMENT ON THE COASTAL LANDSCAPE IN LATVIA	259
Lilita Lazdane, Madara Markova, Aija Ziemelniece REGIONAL STRUCTURE OF CULTURALLY-HISTORICAL LANDSCAPE OBJECTS AVAILABILITY IN LATGALE UPLAND AREA	272
Lukasz Pardela FLOODING AS A MEANS OF MILITARY DEFENCE: LANDSCAPE OF THE 20TH CENTURY FORTRESS WROCŁAW	283
Aija Ziemelniece THE ROOF LANDSCAPES, THE HISTORIC CITY CENTRES AND CONTEXTUAL SEARCHES OF THE GREEN STRUCTURE	288
 Land Management and Geodesy	 299
Vivita Baumane, Armands Celms EVALUATION OF INDICATORS OF CADASTRAL ASSESSMENT	299
Diana Haritonova, Janis Balodis, Inese Janpaule, Madara Normand DISPLACEMENTS AT THE GNSS STATIONS	305
Armands Celms, Maigonis Kronbergs, Vita Cintina, Vivita Baumane PRECISION OF LATVIA LEVELING NETWORK NODAL POINT HEIGHT	310

Environment and Environmental Effects.....	318
Dace Arina, Ausma Orupe COMPARISON OF MUNICIPAL SOLID WASTE CHARACTERISTICS AFTER SEPARATION BY STAR AND DRUM SCREEN SYSTEMS	318
Otilija Miseckaite, Liudas Kinciu FORECAST FOR DRAINAGE RUNOFF AT DIFFERENT THICKNESS OF HUMUS SOIL LAYER	323
Eriks Tilgalis, Reinis Ziemelnieks, Marcis Sipols CALCULATION OF RAINWATER SEWAGE SYSTEMS	328
Dainius Ramukevicius, Petras Milius GROUND TEMPERATURE REGIME IN THE COWSHED ENVIRONMENT.....	332
Raimondas Sadzevicius, Tatjana Sankauskiene, Feliksas Mikuckis LIMIT DEFORMATIONS OF RETAINING WALLS IN LITHUANIAN HYDROSCHMES	336
 Industrial Energy Efficiency.....	 341
Anda Kursisa, Laura Gleizde DEVELOPMENT OF INDUSTRIAL ENERGY EFFICIENCY IN LATVIA, LEGISLATION AND STATISTICS	341
Karlis Grinbergs, Sandra Gusta ENERGY AUDIT METHOD FOR INDUSTRIAL PLANTS	350
Karlis Grinbergs ENERGY EFFICIENT ELECTRICITY USAGE AND LIGHTING SOLUTIONS FOR INDUSTRIAL PLANTS	356
Anda Kursisa, Laura Gleizde ENERGY CONSUMPTION AND ITS REDUCTION POTENTIAL IN LATVIAN INDUSTRY SECTORS	363

STRUCTURAL ENGINEERING

BEHAVIOUR OF CABLE TRUSS WEB ELEMENTS OF PRESTRESSED SUSPENSION BRIDGE

Vadims Goremkins*, Karlis Rocens**, Dmitrijs Serdjuks***, Raimonds Ozolins****

Riga Technical University, Institute of Structural Engineering and Reconstruction

E-mail: *goremkins@gmail.com, ** rocensk@latnet.lv, *** dmitrijs@bf.rtu.lv,

**** raimonds.ozolinsh@apollo.lv

ABSTRACT

A suspension bridge is more appropriate type of structure for extremely long-span bridges due to the rational use of structural materials. Increased deformability, which is conditioned by the appearance of the elastic and kinematic displacements, is the major disadvantage of suspension bridges.

Prestressing can solve the problem of increased kinematic displacements under the action of non-symmetrical load. A prestressed suspension bridge with the spans of 50, 200 and 350 m was considered as the object of investigation. The cable truss with the cross web was considered as the main load carrying structure of the prestressed suspension bridge.

Optimization of the cable truss web by 9 variables was realized using genetic algorithm. It was obtained, that the displacements of the prestressed suspension bridge with the proposed cable truss are smaller by 26–30% than the displacements of the structure with the single main cable for the span interval from 50 to 350 m in the case of the worst situated load.

Key words: Suspension bridges, topology optimization, genetic algorithm

INTRODUCTION

Suspension bridges are structures where the deck is continuously supported by the stretched catenary cable (Chen and Lui, 2005). Suspension bridges are the most important and attractive structures possessing a number of technical, economical and aesthetic advantages (Grigorjeva et al., 2010a).

A suspension bridge is the most suitable type of structure for very long-span bridges at the present moment. Suspension bridges represent 20 or more of all the longest span bridges in the world. The bridge with the longest centre span of 1991m is the Akashi Kaikyo Bridge (Chen and Duan, 2000). So, long spans can be achieved because the main load carrying cables are subjected to tension and the distribution of normal stresses in the cable cross-section is close to uniform (Juozapaitis et al., 2010). Increased deformability is one of the basic disadvantages of suspension bridges (Walther et al., 1999). Increased deformability is conditioned by appearance of elastic and kinematic displacements. The elastic displacements are caused by the large tensile internal forces. The elastic displacements are maximal at the centre of the span in the case of symmetrical load application. The kinematic displacements are caused by the initial parabolic shape change, resulting from non-symmetrical or local loads (Fig. 1) (Juozapaitis and Norkus, 2004; Grigorjeva et al., 2010b). These displacements are not connected with the cable elastic characteristics.

Serviceability limit state is dominating for suspension cable structures.

The elastic displacements can be reduced by applying of low strength steel structural profiles, elastic modulus increase, reinforced concrete application and cable camber increase (Кирсанов, 1973).

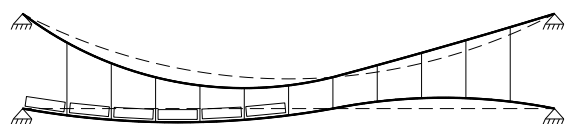


Figure 1. Initial shape change under the action of non-symmetrical load

The problem of increased kinematic displacements can be solved by increasing of the ratio of dead weight and imposed load values, which is achieved by adding of cantledge (Fig. 2). However, this method causes the increase of material consumption. Stiffness of suspended structures can be increased also by increasing of girder stiffness (Fig. 3), increasing of main cable camber, connecting of main cable and girder at the centre of the span (Fig. 4), application of diagonal suspenders (Fig. 5) or inclined additional cables (Fig. 6), application of two chain systems (Fig. 7), stiff chains (Fig. 8) and stress ribbons (Fig. 9) (Кирсанов, 1973; Strasky, 2005; Бахтин et al., 1999; Качурин et al., 1999). Nevertheless, these systems are characterized also with the increased

material consumption, and system stiffness is not sufficient in many cases.

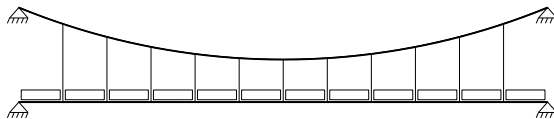


Figure 2. Suspension bridge stabilization by adding of cantledge

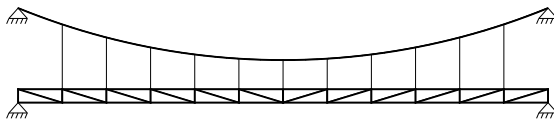


Figure 3. Suspension bridge stabilization by increasing of girder stiffness



Figure 4. Suspension bridge stabilization by connecting of main cable and girder at the centre of the span

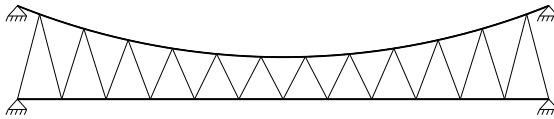


Figure 5. Suspension bridge stabilization by application of diagonal suspenders

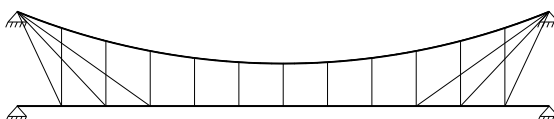


Figure 6. Suspension bridge stabilization by application of inclined additional cables

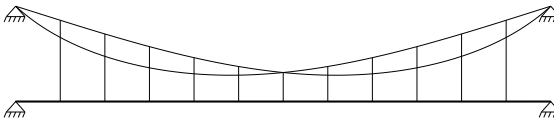


Figure 7. Suspension bridge stabilization by application of two-chain system

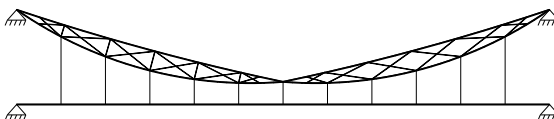


Figure 8. Suspension bridge stabilization by application of stiff chains



Figure 9. Suspension bridge stabilization by application of stress ribbons

Use of prestressed cable truss is another method to solve the problem of increased kinematic displacements under the action of unsymmetrical load (Serdjuks and Rocens, 2004; Goremikins et al., 2011a). Different types of cable trusses are known, such as convex cable trusses, convex-concave cable trusses, cable trusses with centre compression strut or parallel cable truss (Schierle, 2012). But one of the most efficient and convenient for application for bridges is the concave cable truss (Fig. 10) (Goremikins et al., 2011). Cable truss usage allows developing bridges with reduced requirements for girder stiffness, where overall bridge rigidity will be ensured by prestressing of the stabilization cable (Кирсанов, 1973). The deck can be made of light composite materials (Goremikins et al., 2010a; Goremikins et al., 2010b).

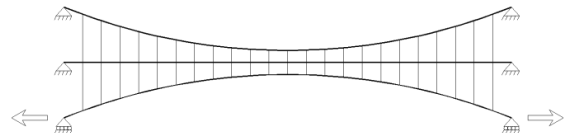


Figure 10. Suspension bridge stabilization by prestressing

The kinematic displacements of a prestressed suspension bridge can be decreased by replacing of the main single cable with the cable truss with a cross web (Fig. 11) (Goremikins et al., 2012a; Goremikins et al., 2012b; Goremikins et al., 2012c; Serdjuks et al., 2005).

Cables can be cambered in horizontal plane to increase the structure stiffness in the same plane (Fig. 12) (Кирсанов, 1973).

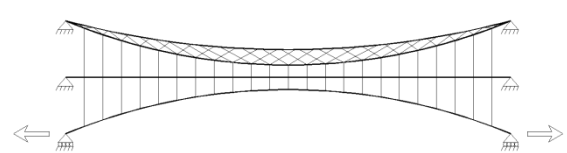


Figure 11. Suspension bridge stabilization by using of prestressed stabilization cable and cable truss

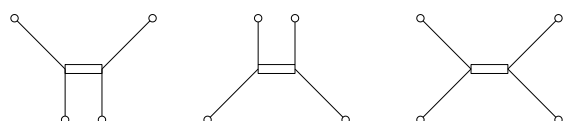


Figure 12. Suspension bridge stabilization in horizontal plane by cambering of main or stabilization cables. Cross-sectional view

Decrease of displacements can be achieved by rational positioning of the cable truss elements and rational material distribution between them. Topology optimization of the cable truss web is presented in this paper.

MATERIALS AND METHODS

Description of Investigation Object

A prestressed suspension bridge with a cable truss with cross web was chosen as the object of the investigation (Fig. 13) (Goremkins et al., 2012a).

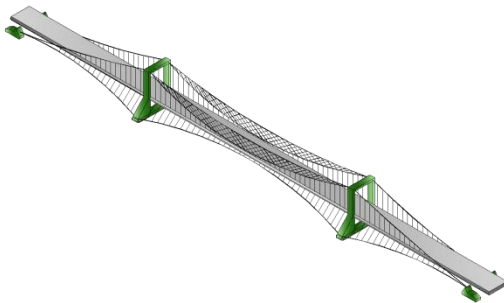


Figure 13. Prestressed suspension bridge with cable truss load carrying structure

Three different spans were considered for the bridge. The main span l of the considered bridge is equal to 50, 200 and 350 m. The bridge has two lines in each direction, two pedestrian lines and their total width is equal to 18.2 m (Fig. 14). The chamber of the bottom chord of the cable truss f_b is equal to 1/10 from the span. The bridge is prestressed in horizontal and vertical planes by the stabilization cables. The camber of the stabilization cable is equal to 1/200 from the span. The deck is connected with the main load-carrying cables by the suspensions with a step a equal to 5 m (Fig. 15). The cable string is placed between suspensions to minimize the horizontal prestressing force effects acting in the deck. Prestressed horizontal cables are placed along the deck to minimize the effects of horizontal transport braking force (Fig. 16). The deck of the bridge is made of pultrusion composite trussed beams, pultrusion composite beams with the step 1 m and pultrusion composite plank with the height 40 mm that is covered with asphalt layer (Fig. 14) (Goremkins et al., 2010a; Goremkins et al., 2010b; Fiberline Composites A/S, 2002). It is assumed that cables are covered with high-density polyethylene and are heated with electricity to reduce the influence of temperature effects (Xiang et al., 2009). Possible prestressing loosing is reduced by active tendons (Achkire and Preumont, 1996). It is possible to reduce the requirements for girder stiffness by bridge prestressing. This allows using the composite pultrusion materials in the deck

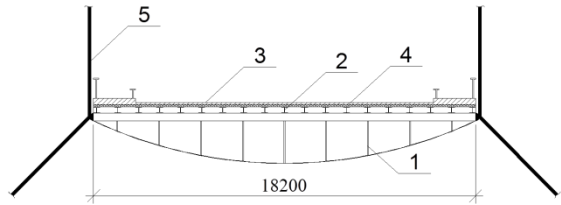


Figure 14. The bridge deck structure.

1 – composite trussed beam, 2 – composite I type beams, 3 – composite plank, 4 – cover of the bridge, 5 – suspensions

structure and makes it possible to develop constructions of bridges with a large span and reduced dead weight in comparison with steel or concrete bridges (Бахтин et al., 1999).

The design scheme of the investigation object is shown in Fig. 15 and Fig. 16. The structural material is a prestressed steel rope (Eurocode 3, 2003; Feyrer, 2007). The dead load g that is applied to the structure is equal to 51.1 kN/m. The bridge is loaded by the imposed load q , which is equal to 82.2 kN/m (Eurocode 1, 2009). Imposed load can be applied to any place of the span. Distributed load is transformed to the point load and is applied to the connections of the deck and suspensions. There are 39 possible points of load application (Fig. 15).

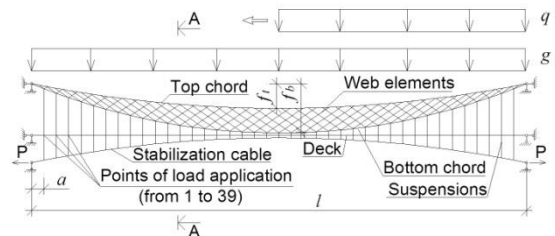


Figure 15. Design scheme of suspension bridge.
 q – imposed load, g – dead load, P – prestressing, f_b – bottom chord camber, f_t – top chord camber, l – main span, b – width, a – suspension step

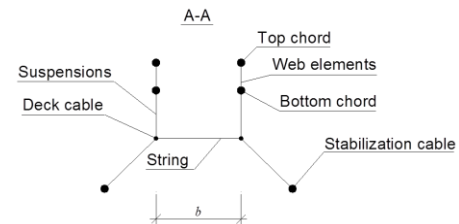


Figure 16. Cross section of prestressed suspension bridge

Position of each web element of the cable truss is defined by the distance from the pylon to the connection of the web element with the top chord, depending on the distance from the pylon to the connection of the same element with the bottom

chord (Fig. 17). The web elements are divided into two groups – the elements inclined to the centre of the cable truss and the elements inclined to the edges of the cable truss. Each element of the web may have its own angle on inclination. The second order polynomial equation is assumed to express the position of each web element and to minimize the amount of variable factors.

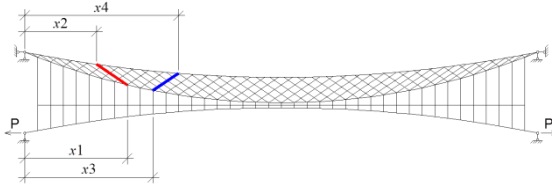


Figure 17. Position of web elements

The position of the web elements, which are inclined to the edges of the cable truss, is expressed by Eq. (1), the position of the web elements, inclined to the edges of the cable truss, is expressed by Eq. (2) (Goremikins et al., 2012a; Goremikins et al., 2012b).

$$x_2 = x_1 - (\text{root1} \cdot x_1^2 + \text{root2} \cdot x_1 + \text{root3}), \quad (1)$$

$$x_4 = x_3 + (\text{root4} \cdot x_3^2 + \text{root5} \cdot x_3 + \text{root6}), \quad (2)$$

where x_2 and x_4 – distances from the pylon to the connection of the web element and top cord;
 x_1 and x_3 – distances from the pylon to the connection of the web element and bottom cord;
 $\text{root1} \dots \text{root6}$ – roots of the system of Eqs. (3) and Eqs. (4).

The roots of the polynomial equation for the web elements were found by solving the system of Eqs. (3) and Eqs. (4).

$$\begin{cases} s_1 = \text{root1} \cdot a_1^2 + \text{root2} \cdot a_1 + \text{root3} \\ s_2 = \text{root1} \cdot a_2^2 + \text{root2} \cdot a_2 + \text{root3}, \\ s_3 = \text{root1} \cdot a_3^2 + \text{root2} \cdot a_3 + \text{root3} \end{cases} \quad (3)$$

$$\begin{cases} s_4 = \text{root4} \cdot a_1^2 + \text{root5} \cdot a_1 + \text{root6} \\ s_5 = \text{root4} \cdot a_2^2 + \text{root5} \cdot a_2 + \text{root6}, \\ s_6 = \text{root4} \cdot a_3^2 + \text{root5} \cdot a_3 + \text{root6} \end{cases} \quad (4)$$

where s_1 – distance x_2 for $x_1 = a_1$;
 s_2 – distance x_2 for $x_1 = a_2$;
 s_3 – distance x_2 for $x_1 = a_3$;
 s_4 – distance x_4 for $x_3 = a_1$;
 s_5 – distance x_4 for $x_3 = a_2$;
 s_6 – distance x_4 for $x_3 = a_3$;
 a_1 – distance from the pylon to the connection of the first web element with bottom chord;

a_2 – distance from the pylon to the connection of the middle web element with bottom chord;
 a_3 – distance from the pylon to the connection of the last web element with bottom chord, counting for the middle of the span.

Distribution of the material among the cable truss elements can be expressed by Eq. (5):

$$\begin{aligned} g &= g_b + g_t + g_w, \\ g_t &= g - g_b - g_w, \end{aligned} \quad (5)$$

where g – material consumption of cable truss;

g_b – material consumption of bottom chord;

g_t – material consumption of top chord;

g_w – material consumption of all web elements;

Definition of Optimization Problem

The aim of optimization is to evaluate rational, from the point of view of total vertical displacements minimization, characteristics of the cable truss for the prestressed suspension bridge.

The bottom chord camber f_b , material consumption of the cable truss g , material consumption of the stabilization cable, level of prestressing, bridge geometrical parameters: pylon height, main span and suspension step are considered as constants in objective function.

Relation of the top and bottom chord cambers f_t/f_b , the distances $s_1, s_2, s_3, s_4, s_5, s_6$, the ratios g_b/g and g_w/g are variables of the optimization, 9 factors in all.

The optimization problem is to minimize the objective function:

$$w_{tot} \left(s_1, s_2, s_3, s_4, s_5, s_6, \frac{g_b}{g}, \frac{g_w}{g}, \frac{f_t}{f_b} \right), \quad (6)$$

subject to:

$$[K(U)] \cdot \{U\} = [F(U)], \quad (7)$$

and Eqs. (1) – (5),

where $[K(U)]$ is the stiffness matrix, $\{U\}$ is the displacement vector and $[F(U)]$ is the force vector.

Total displacements w_{tot} are found by summing the displacements upwards w^+ and downwards w^- (Fig. 18). Maximum vertical displacements for suspended cable structures appear under the action of load applied to different parts of the span, therefore 39 different loading cases were analysed. The problem has been solved for elastic material behaviour stage taking into account geometrical non-linearity.

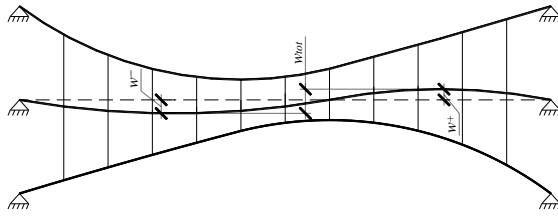


Figure 18. Deformed shape of prestressed suspension bridge in non-symmetrical loading case

Optimization Method for Calculation of Rational Characteristics of Cable Truss

The optimization of the cable truss by 9 variable factors for three different spans was done by the genetic algorithm (Goremkins et al., 2012a; Lute et al., 2009; Šešok and Belevičius, 2008).

The genetic algorithm is a method for solving both constrained and unconstrained optimization problems that are based on natural selection, the process that reproduces a biological evolution. The genetic algorithm repeatedly modifies population of individual solutions. At each step, the genetic algorithm selects individuals at random from the current population to be parents and uses them to produce the children for the next generation. Over successive generations, the population “evolves” towards an optimal solution. Genetic algorithms are used to solve a variety of optimization problems that are not well suited for standard optimization algorithms, including problems in which the objective function is discontinuous, non-differentiable, stochastic, or highly nonlinear (MathWorks, 2011).

The genetic algorithm uses three main types of rules at each step to create the next generation from the current population:

-Selection rules select the individuals, called parents, which contribute to the population at the next generation.

-Crossover rules combine two parents to form children for the next generation.

-Mutation rules apply random changes to individual parents to form children (MathWorks, 2011).

GA Toolbox of mathematical software MatLAB was used in the optimization. A special program was written in MatLAB programming environment to calculate the fitness using FEM. FEM program ANSYS was used to calculate displacements of the suspension bridge. A specially written MatLAB function calls ANSYS and ANSYS returns vertical displacements. The cable truss is modelled by two-node link type compression less finite elements (LINK10 in ANSYS). The analysis type is geometrically nonlinear static including large-deflection effects, because suspension cable structures are characterized with large deflections before stabilization (Sliseris and Rocens, 2011; Ozoliniš et al., 1979).

RESULTS AND DISCUSSION

Topology optimization by the genetic algorithm was realized, using 10 generations, population size was equal to 50, elite child number was equal to 5. The rational characteristics of the cable truss were evaluated and are generalized in the Table 1.

Table 1

Characteristics of Rational Cable Truss

Characteristic	Symbol	Value		
		Span 50 m	Span 200 m	Span 350 m
Ratio of top and bottom chord cambers	f_t/f_b	0.4293	0.5089	0.5358
Ratio of material consumption of bottom chord and whole truss	g_b/g	0.5870	0.4512	0.4684
Ratio of material consumption of web elements and whole truss	g_w/g	0.0842	0.0673	0.0673
Distances, which define position of web elements	s_1, m	0.7785	4.8147	1.5595
	s_2, m	7.1937	16.3004	24.6802
	s_3, m	9.6487	16.3190	28.5679
	s_4, m	0.7150	0.9800	0.5029
	s_5, m	7.9753	12.6897	24.2618
	s_6, m	2.4367	16.2324	22.7034

The displacements of the prestressed suspension bridge with the rational cable truss were compared with the displacements of the prestressed suspension bridge with a single main cable for three selected spans. The material consumption of the cable truss was the same as the material consumption of the single cable. The analysis were carried out by the FEM software ANSYS.

The maximum total displacements are reduced from 26 to 30% depending on the span by using of the cable truss instead of the single cable in the case of the worst situated load. The dependence between the differences of displacements of structures with a single cable and cable truss and span of structures in the case of the worst situated load is shown in Fig. 19.

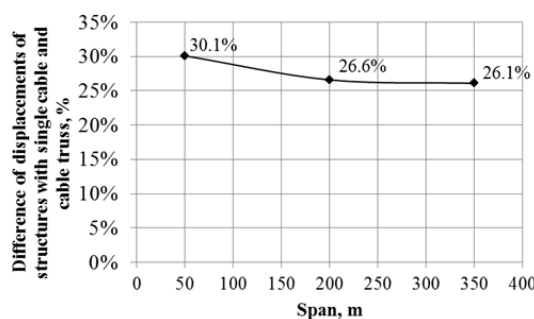


Figure 19. Dependence between differences of displacements of structures with single cable and cable truss and span of structures in the case of worst situated load

CONCLUSIONS

The application of the cable truss with concave chords, optimized chord shape and cross web topology considerably decreases displacements of the prestressed suspension structure.

The displacements of the prestressed suspension bridge with the proposed cable truss are smaller by

REFERENCES

- Achkire Y., Preumont A. (1996) Active tendon control of cable-stayed bridges. *Earthquake Engineering and Structural Dynamics*, 25(6), pp. 585–597. Chen W. F., Lui E. M. (2005) *Handbook of structural engineering*. New York: CRC Press, 625 p.
- Chen W. F., Duan L. (2000) *Bridge Engineering Handbook*. New York: CRC Press LLC, 452 p.
- European Committee for Standardization (2004) *Eurocode 1: Actions on structures - Part 2: Traffic loads on bridges*, Brussels.
- European Committee for Standardization (2003) *Eurocode 3: Design of steel structures – Part 1.11: Design of structures with tensile components*, Brussels.
- Feyrer K. (2007) *Wire Ropes*. Berlin: Springer-Verlag Berlin Heidelberg.
- Fiberline Composites A/S. (2002) *Design Manual*, Middelfart: Fiberline Composites A/S, 326 p.
- Goremkins V., Rocens K., Serduks D. (2012a) Decreasing Displacements of Prestressed Suspension Bridge. *Journal of Civil Engineering and Management*, 18(6), pp. 858-866.
- Goremkins V., Rocens K., Serduks D. (2012b) Decreasing of Displacements of Prestressed Cable Truss. *World Academy of Science, Engineering and Technology*, 63, pp. 554-562.
- Goremkins V., Rocens K., Serduks D. (2012c) Cable Truss Analyses for Suspension Bridge. In *Proc. of 10th International Scientific Conference “Engineering for Rural Development”*, Jelgava, Latvia, Vol. 11, pp. 228-233.
- Goremkins V., Rocens K., Serduks D. (2011) Rational Structure of Cable Truss. *World Academy of Science, Engineering and Technology*, 76, pp. 571-578.
- Goremkins V., Rocens K., Serduks D. (2010a) Rational Large Span Structure of Composite Pultrusion Trussed Beam. *Scientific Journal of RTU. Construction Science*, Vol. 11, pp. 26-31.
- Goremkins V., Rocens K., Serduks D. (2010b) Rational Structure of Composite Trussed Beam. In *Proc. of the 16th International Conference “Mechanics of Composite Materials”*, Riga, Latvia, p. 75.
- Grigorjeva T., Juozapaitis A., Kamaitis Z. (2010a) Static analyses and simplified design of suspension bridges having various rigidity of cables. *Journal of Civil Engineering and Management*, 16(3), pp. 363-371.

26–30% than the displacements of the structure with the single main cable for the span interval from 50 to 350 m.

Rational characteristics of the cable truss with spans 50, 200 and 350 m and bottom chord camber 1/10 of the span from the point of view of structural stiffness are the following: the ratio between the top and bottom chord chambers is 0.429, 0.510 and 0.536, the ratio between the bottom chord material consumption and material consumption of the whole truss is 0.587, 0.451 and 0.468, the relation between material consumption of the web elements and the whole truss is 0.084, 0.067 and 0.067, respectively. The position of the web elements was evaluated in the form of the second order polynomial.

ACKNOWLEDGMENTS

This work has been supported by the European Social Fund within the project “Support for the implementation of doctoral studies at Riga Technical University”.

- Grigorjeva T., Juozapaitis A., Kamaitis Z., Paeglitis A. (2010b) Finite element modeling for static behavior analysis of suspension bridges with varying rigidity of main cables. *The Baltic Journal of Road and Bridge Engineering*, 3(3), pp. 121-128.
- Juozapaitis A., Idnurm S., Kaklauskas G., Idnurm J., Gribniak V. (2010) Non-linear analysis of suspension bridges with flexible and rigid cables. *Journal of Civil Engineering and Management*, 16(1), pp. 149-154.
- Juozapaitis A., Norkus A. (2004) Displacement analysis of asymmetrically loaded cable. *Journal of Civil Engineering and Management*, 10(4), pp. 277-284.
- Lute V., Upadhyay A., Singh K. (2009) Computationally efficient analysis of cable-stayed bridge for GA-based optimization. *Engineering Applications of Artificial Intelligence*, 22, pp. 750–758.
- MathWorks (2011) *MATLAB User's manual. What Is the Genetic algorithm*. MathWorks.
- Schierle G. G. (2012) *Structure and Design*. San Diego: Cognella, 624 p.
- Serdjuks D., Rocens K., Ozolons R. (2005) Influence of the Diagonal Cables Strengthening by the Trusses on the Saddle-Shaped Roof Rigidity. *Scientific Journal of RTU. Architecture and Construction Science*, Vol. 6, pp. 210-218.
- Serdjuks D., Rocens K. (2004) Decrease the Displacements of a Composite Saddle-Shaped Cable Roof. *Mechanics of Composite Materials*, 40(5), pp. 675-684.
- Šešok D., Belevičius R. (2008) Global optimization of trusses with a modified Genetic Algorithm. *Journal of Civil Engineering and Management*, 14(3), pp. 147-154.
- Sliseris J., Rocens K. (2011) Rational structure of panel with curved plywood ribs. *World Academy of Science, Engineering and Technology*, 76, pp. 317-323.
- Strasky J. (2005) *Stress Ribbon and Cable Supported Pedestrian Bridge*. London: Thomas Telford Publishing, 213 p.
- Walther R., Houriet B., Isler W., Moia P., Klein J. F. (1999) *Cable Stayed Bridges. Second Edition*. London: Thomas Telford, 236 p.
- Xiang R., Ping-ming H., Kui-hua M., Zhi-hua P. (2009) Influence of Temperature on Main Cable Sagging of Suspension Bridge. *Journal of Zhengzhou University Engineering Science*, 30(4), pp. 22-25.
- Бахтин С., Овчинников И., Инамов Р. (1999) *Висячие и вантовые мосты [Suspension and Cable Bridges]*. Саратов: Сарат. гос. техн. ун-т, 124 с.
- Качурин В., Брагин А., Ерунов Б. (1971) *Проектирование висячих и вантовых мостов*. Москва: Издательство «Транспорт», 280 с.
- Кирсанов Н. М. (1973) *Висячие системы повышенной жесткости [Suspension Structures with Increased Stiffness]*. Москва: Стройиздат., 116 с.
- Озолиньш Р.Р., Завицкий Я.А., Сальцевич В.Я. (1979) Универсальный способ расчета сложных пространственных комбинированных стержневых систем, не следующих принципу независимости действия сил. *Проектирование и оптимизация конструкций инженерных сооружений*, с. 97-103.

EVALUATION OF HIGHRISE BUILDING MODEL USING FUNDAMENTAL FREQUENCY MEASUREMENTS

Liga Gaile*, Normunds Tirans **, Jans Velicko **

*Riga Technical University, Department of Structural Analysis

E-mail: liga.gaile_1@rtu.lv

**Engineers group Kurbads (SIA „IG Kurbads”)

E-mail: kurbads@ig-kurbads.lv

ABSTRACT

This paper proposes a potential method to evaluate the degree of assumption precision made during the finite element model construction. It is very important to precisely model the stiffness properties of the whole building in order to choose the correct dimensions of the load bearing elements of the building. The finite element models of two 35 story high-rise buildings were verified with the real high-rise building structure using the experimental data. The two high-rise building fundamental frequencies data were experimentally obtained during the different stages of the construction process. The data were compared with the numerically calculated to evaluate the precision of the assumptions made during the FEM model creation process.

Key words: finite element method, high-rise building, oscillations, reinforced concrete, vibration

INTRODUCTION

Nowadays, the finite element method (FEM) is the dominating technique for load bearing structure computer analysis. The structural engineer must accept many simplifications of the real structure geometry, loads, stiffness and other parameters during creation of FEM calculation model; otherwise it would take an extensive amount of time and expenditures. Therefore, it is important to control calculations by taking on-site measurements, to ensure the accepted simplifications do not disturb the structure adequate analysis.

Since the year 2007 in Riga, Latvia the multifunctional complex “Z-towers” that consists of four underground levels and two cylindrical towers above them has been built.



Figure 1. Multifunctional complex “Z-towers” construction process

The complex main load bearing structures are made of in-situ reinforced concrete (RC). The foundation is the drilled RC piles based on the dolomite rock layer. Both tower structures consist of the central core and perimeter columns. The “O” tower has the outer diameter of 37,2 m, 12 perimeter columns and the cylindrical core with the outer diameter of 17,8 m. And the smaller “H” tower has the outer diameter of 30,9 m, 14 perimeter columns and the cylindrical core with the outer diameter of 13,8 m. The “O” tower RC structure height above the ground without the roof steel structure is planned to be 124,600 m and 117,870 m for the ‘H’ tower.

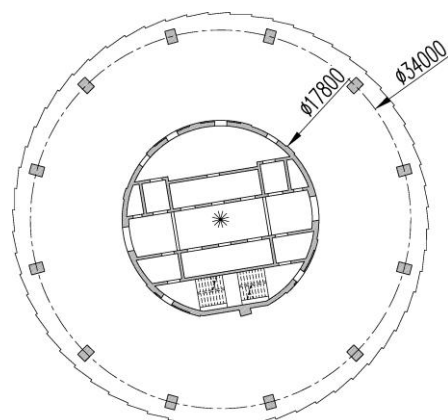


Figure 2. Typical floor plan of the ‘O’ tower

Both towers at the 5th level above the ground will have the outrigger structure – in-situ reinforced concrete walls of 600 mm and 500 mm (for ‘H’ tower) thickness between the central core and perimeter columns. These walls will provide translation of the internal forces between the columns and the core, hence it promotes combined

work to increase the global stiffness of the building, reduces wind induced dynamic effects, reduces loads on the piles under the central core and provides greater security level against progressive collapse.

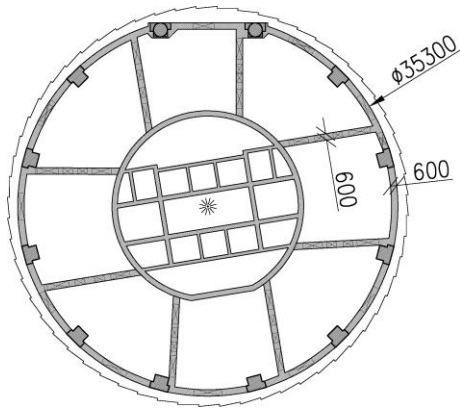


Figure 3. Plan of the ‘O’ tower outrigger level walls

The dynamic characteristic precise estimation of such a high structure is vitally important. This directly affects the structural solutions of the building.

The structural dynamic behavior denotes modal parameters of the structure (natural frequencies, damping ratios and mode shapes). The field of the research the so called “modal analysis” is dealing with identification of these parameters. Basically, there are two ways of extracting them:

1. Theoretical modal analysis where the stiffness matrix, mass matrix and damping matrix are known, and by solving the eigenvalue problem the required dynamic parameters of the structure can be obtained (used in FEM analysis software);
2. Experimental modal analysis that starts with the measurement of the input forces and output responses of the structure of interest (Heylen, et.al., 2007)

In case of tall buildings it is almost impossible to measure the input forces, therefore the output or operational modal analysis should be used that aims to determine the dynamic characteristics of the structure under operational conditions. Usually, the operational analysis drawback is that the method assumes the input signal to be a white noise sequence but the peaks in an input spectrum will yield in responses that might not be the structural mode.

This drawback might be utilized in a positive way. The usual assumption in response calculations of tall structures like high-rise buildings is that it will mainly respond in fundamental modes (Zhou, 1999) due to wind loading. This assumption might be confirmed by many case studies, for example (Li, Wu, et. al 2007), (Li, Fu, et. al 2006), (Zhao, 2011),

(Gu, 2009). Therefore, to identify only the fundamental frequency of the structure extracted from measurements in time domain (e.g., accelerations) does not require expensive dynamic testing methods but still it provides a valuable tool for checking assumptions made during the numerical model construction.

The wind induced displacement of a structure mainly consists of a mean component and dynamic fluctuating component.

To measure the output response of the structure accelerometers that generally are capable to measure the resonant components can be utilized (Li, Wu, 2007).

In this way, the measurements of the tower response during the construction process using simple accelerometers might give the confidence of the finite element model reliability.

TOWER NATURAL OSCILLATION FREQUENCIES ESTIMATION

FEM analysis

High-rise FEM analysis was made using Lira 9.4 computer program. The calculation model consists of linear (beams, columns and piles) and shell (walls and slabs) finite elements. The structure dimensions were assumed according to nominal project dimensions. In-situ reinforced concrete structure dead weight was assumed regarding the density 2.5 t/m^3 .

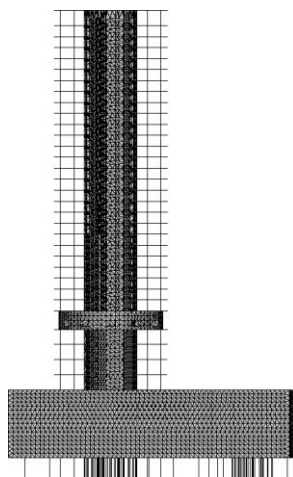


Figure 4. FEM calculation model of the “O” tower for full height

The tower overall calculations were carried out in the linear elastic phase. The modulus of elasticity for mainly compressed vertical elements (columns and walls) was assumed based on the concrete elasticity properties and reinforcement amount. The modulus of elasticity E of homogeneous cross-sections for mainly bended horizontal elements (slabs, plates and beams) was determined by calculations to take into account cracking of the

elements under the characteristic self-weight load. In the FEM model of the structure the supports are located at the bottom ends of the piles. The pile modulus of elasticity was reduced to provide equal load-deformation relationship as it was obtained in the full scale static pile tests.

A number of simplifications were made during the FEM analysis:

1. Taking into account the amount of levels and complex configuration some geometry features were ignored, such as one slab elevation local changes, small openings in walls and slabs, etc. The calculation models were made maximally close to the design project, but some simplifications were made to decrease the amount of the finite elements to get the model of the whole building in order to calculate the natural frequencies.

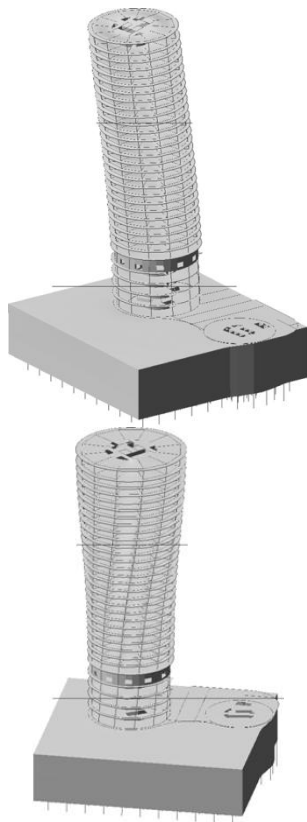


Figure 5. The FEM calculation model of the “O” tower; natural oscillations in the 1st (bending) and 3rd (torsion) modes. Displacement scale is increased

2. Stiffness values should be specified for RC elements during the FEM modeling. They are different for cracked and non-cracked sections. The cracked section stiffness reduction varies depending on the current loads and loading history, used materials, section geometry, used RC analysis model, etc. This complicates a precise estimation of the stiffness parameters. Also the RC stiffness can vary depending on

the specific concrete compound, compacting quality, climatic conditions during concrete works and hardening process, etc. All of these factors are difficult to predict and can be evaluated only in a simplified way.

3. The towers are supported by a 12m deep underground structure that is loaded with the ground water pressure from the bottom. The RC piles are drilled to the dolomite layer and work in compression or tension depending on the load from the supported structure. Geotechnical data and deformation characteristics of the piles can vary in a very wide range and the stiffness of the supports is difficult to predict precisely.

All these factors influence the theoretical calculations; therefore behavior of the real building can be different. That is why the FEM analysis should be checked with on-site measurements. The estimation of the structure natural frequency can be obtained theoretically and experimentally. These dynamic parameters can be used to validate the FEM model.

To compare the natural frequencies obtained from the FEM model with on-site measurements at the particular construction stage the finite elements of the model that were not built yet at the relevant stage were deleted.

On-site measurements

The on-site oscillations measurements were periodically conducted during the tower construction. It allows controlling the dynamic characteristics of the towers and observes changes depending on the tower height and construction work progress.

The measurements were conducted in windy weather, when the wind gusts provoked significant horizontal deformations of the towers due to natural oscillations.

One of the aims of on – site experiments was to identify weather without the expensive dynamic testing methods and instruments it is possible to identify the fundamental mode frequency of the structure. Therefore, simple 3-axis light-weight (55g) USB accelerometers (Model X6-1A) were used to record the accelerations. The measurement sample rate was 160 Hz.

The placement of the accelerometers was chosen after examination of the existing FEM model. The maximum and minimum vertical stiffness planes of each of the two towers were found. Accelerometers were tightly attached to the upper floor outer perimeter columns that were built at the particular construction stage and crossed these planes. One of the accelerometers was attached to the main lateral stiffness element - central core of the tower, which gives a possibility to identify the torsional modes later. Already from the raw accelerometer readings

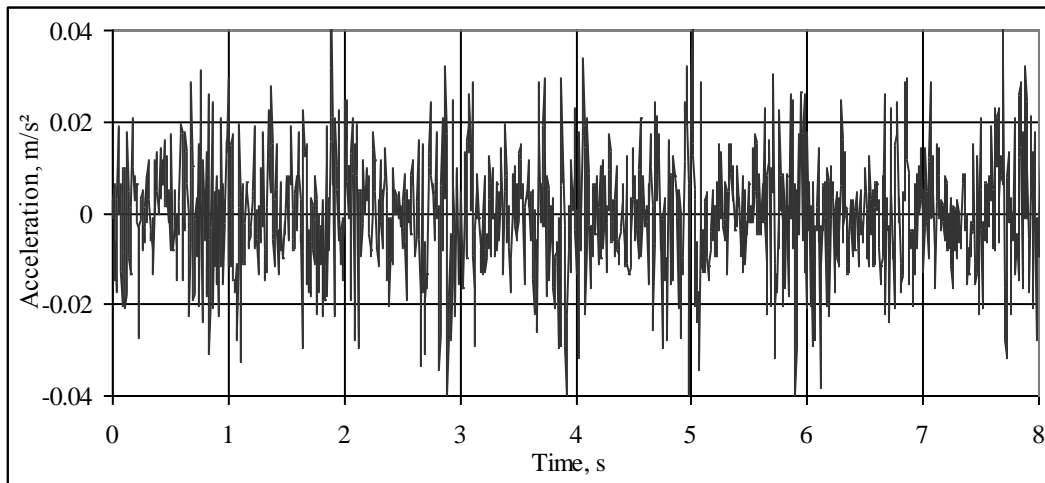


Figure 6. An example of the recorded measurements by accelerometer (conducted at level 65.720m of the “H” tower)

it is possible to identify the presence of harmonic oscillations (Fig. 6). The autocorrelation function (1) shows how the mean power in a signal is distributed over frequency. It is also a very handy tool to detect harmonic signals buried in the noise (Heylen, et.al., 2007).

$$G_{AA}(f) = A(f) \cdot A^*(f), \quad (1)$$

where $A(f)$ is the Fourier transform of the time trace $a(t)$ and “*” indicates the complex conjugate.

To reduce the leakage effects due to the non-periodicity of the time signal records the “Hanning window” was applied to each sampling window before the FFT (Fast Fourier Transform) was applied. In the next step Auto Spectrum was “normalized” by the frequency resolution of the Auto Spectrum and thereby the power spectral density was obtained (PSD). The PSD is very useful even if data do not contain any pure oscillatory signals and it is the easiest way to identify the peaks. In the experiments 3-axis accelerometers that simultaneously measured accelerations in three directions were used, and then the obtained frequency response function amplitudes were summed to improve the identifying process of the physical and meaningful poles. As a check the stabilization diagram that subsequently assumes an increasing number of poles was used. Physical poles (excited frequencies) always appear as “stable poles”, consequently unrealistic poles are filtered out.

Fig. 7 presents the example of the obtained acceleration response spectra for the largest lateral stiffness direction.

To compare the numerically obtained frequencies with the experimentally ones the FEM model was loaded only with permanent load – RC self-weight

because during the experiment generally only this load was represented.

RESULTS

Generally, the FEM analysis results show a good correspondence with on-site measurements for the first oscillation mode. According to the FEM analysis the first two oscillation modes of both towers are bending in two perpendicular directions. The performed measurements do not allow to receive precise oscillation mode shapes but generally there is no doubt that oscillations could happen in a different manner as it was estimated by the FEM calculations.

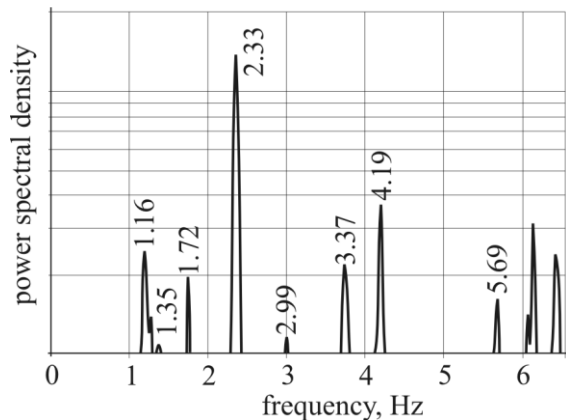


Figure 7. Power spectral density of acceleration along stiffer axis of the structure (“H” tower level 65.720 m)

Similar measurements were also conducted earlier when the heights of the towers were smaller. When the structure with a smaller height and fundamental frequencies close to 2.0Hz was measured using the same devices, there were no clear results obtained and extraction of the building fundamental

frequency was problematic. The first reliable results were obtained when the first 11 levels above the ground were built.

The experimentally obtained fundamental frequency of the “O” tower was ~0.9 Hz, on the other hand the FEM calculation result was 0.77 Hz which makes the difference of 15%. The experimentally obtained fundamental frequency of the “H” tower was ~1.0 Hz and the FEM calculation result was 1.10 Hz which makes the difference of 10%.

The dynamic behavior of both towers is similar. It appears in the similar acceleration levels and dominating natural frequencies.

The “O” tower real behavior is better than estimated by the FEM analysis (oscillation frequency is greater). The “H” tower real behavior is slightly worse as it was estimated by the FEM analysis (oscillation frequency is smaller) but by a small non-critical value that does not affect the safety or serviceability parameters. Generally, there was good correspondence between the on-site measurements and the FEM analysis showing that the adopted simplifications of the numerical

calculation model are adequate. The information extracted from the experimental measurements of the “O” tower reveals that foundation restrain of the real structure is better than modeled in the FEM model. There is no reason to assume that the “H” tower does not have the same degree of foundation restraint. The fact, that the “H” tower has lower values of the numerically calculated fundamental frequencies than the experimentally obtained ones could be explained with the assumption that the slabs real stiffness is smaller than modeled. Following, the “H” tower stiffness of the slabs and column involvement in overall stiffness have a bigger role than in the “O” tower case.

The obtained results can be used as the basis for the existing FEM model update that allows getting more precise calculation results. In case if significant difference between the FEM calculations and the experimentally obtained results would be found, the assumptions made during the FEM model construction should be analyzed and the model revised.

Table 1
The fundamental frequencies of the “O” tower

Construction stage	Oscillation mode	Oscillation frequency according to FEM analysis, Hz	Oscillation frequency according to on-site measurements, Hz
“O” tower 58.400m above the ground (16.07.2012; 14 levels without outrigger walls)	1 st	1.04	1.11
	2 nd	1.11	1.18
“O” tower 79.750m above the ground (28.12.2012; 20 levels with partly constructed outrigger walls)	1 st	0.768	0.9
	2 nd	0.833	1.15
“O” tower 124.600m above the ground (full height of RC structure)	1 st	0.419	Under construction
	2 nd	0.444	

Table 2
The fundamental frequencies of the “H” tower

Construction stage	Oscillation mode	Oscillation frequency according to FEM analysis, Hz	Oscillation frequency according to on-site measurements, Hz
“H” tower 46.050m above the ground (16.07.2012; 11 levels without outrigger walls)	1 st	1.57	1.3
	2 nd	1.59	1.4
“H” tower 65.720m above the ground (28.12.2012; 17 levels with partly constructed outrigger walls)	1 st	1.10	1
	2 nd	1.13	1.16
“H” tower 117.87m above the ground (full height of RC structure)	1 st	0.454	Under construction
	2 nd	0.481	

DISCUSSION

The accuracy of the developed calculation model of the structure with relatively small natural frequencies can be evaluated by conducting the on-site frequency measurements.

Usually the dynamic testing is performed for the finished building when nonstructural parts (e.g., partition walls or facades) add additional stiffness to the whole building. A simplified dynamic testing (when there is an aim to determine only the fundamental frequencies of the building) during the different stages of the load bearing structure construction process creates the possibility to verify the correspondence of the existing calculation model with the real structure behavior by comparing the stiffness parameters. In this case if there a necessity arises, the FEM model could be corrected in relatively early stage. And strengthening of the real structure can be performed before the building is finished so avoiding the extensive additional expenses.

This method has its restrictions – the structures must have uncoupled natural frequencies that are well separated. Therefore, the method of calculation model verification cannot be used for the buildings with a low-rise structure and non-consistent structural element arrangement. Still, a large amount of the engineering judgment and experience is necessary to extract proper dynamic parameters from the accelerometer measurements.

Such simplified calculation model evaluation is specifically applicable for high-rise buildings, tall towers and other similar line – like vertical structures.

As the tower construction process has not ended yet, the measurements will continue to be carried on, additional data will be collected and used for further analysis.

CONCLUSION

During construction stage of two high-rise concrete towers a simplified dynamic testing was performed and a good correlation between finite element method and on-site measurement were obtained. Consequently, no significant imperfections were applied in analytical calculations. Several assumptions were assumed during the design stage, such as linear elastic behavior of the structure, homogeneous cross-sections of the main concrete members, geometrical simplifications in order to reduce the FEM model size and complexity and approximate modulus of elasticity. These assumptions are acceptable, therefore can be used in engineering practice of high-rise concrete buildings. Nevertheless, it is recommended to control stiffness parameters of high-rise buildings during the construction stage by determining the fundamental frequencies of bare load bearing structure to ensure the assumptions and simplifications made during the design stage are valid.

REFERENCES

- Grafe H. (1998) *Model Updating of Large Structural Dynamics Models Using Measured Response Functions*, A thesis submitted to the University of London for the degree of Doctor of Philosophy. Imperial College of Science, Technology and Medicine, University of London.
- Gu Ming (2009) Study of Wind Loads and Responses of Tall Buildings and Structures. *The Seventh Asia-Pacific Conference on Wind Engineering*, Taipei, Taiwan.
- Heylen W., Lammens S., Sas P. (2007) *Modal analysis theory and testing*. Leuven: Katholieke Universiteit Leuven. 295p.
- Li Q.S., Fu J.Y., Xiao Y.Q., Li Z.N., Ni Z.H., Xie Z.N., Gu M. (2006) Wind tunnel and full-scale study of wind effects on China's tallest building. *Engineering structures*, Vol. 28, Issue 12, p. 1745–1758.
- Li Q.S., Wu J.R. (2007) Time-frequency analysis of typhoon effects on a 79-storey tall building. *Journal of Wind Engineering and Industrial Aerodynamics*, Vol. 95, Issue 12, p. 1648–1666.
- Zhao X., Ding M.J., Sun H.H. (2011) Structural Design of Shanghai Tower for Wind Loads. *Procedia Engineering*, Vol. 14, p. 1759-1767.
- Zhou Y., Gu M., Xiang H. (1999) Alongwind Static Equivalent Wind Loads and Responses of Tall Buildings. Part I: Unfavorable Distributions of Static Equivalent Wind Loads. *Journal of Wind Engineering and Industrial Aerodynamics*, Vol. 79, Issue 1, p. 135-150.

EFFICIENCY OF THERMAL DESIGN OF SHALLOW FOUNDATIONS

Guntis Andersons*, Lilita Ozola**

Latvia University of Agriculture, Department of Structural Engineering

E-mail: *Guntis.Andersons@llu.lv, **Lilita.Ozola@llu.lv

ABSTRACT

The article contains results of a preliminary study of specific local prerequisites for the application of a frost protected shallow foundation design method presented in the European standard LVS EN ISO 13793 with the purpose to make a reasonable decision for implementation in the design practice for buildings in frost susceptible soils in the areas of Latvia. The design base is the Latvian building code: LBN 207-01 and valid climatic data for some localities in Daugavpils. The article contains the results of external air temperature data processing and consequently analysis of a freezing index value variation depending on the reference period of frost seasons. The specific design results were obtained for eccentrically loaded columnar spread foundations of an unheated building and insulated to reduce heat loss from the soil below the foundations keeping the subgrade soil unfrozen. As a result of the research the conclusion about the benefits has been presented, based on the comparison of material and labour-consumption. It has been concluded that the cost effectiveness of heated foundations correlates closely to the type of frost-heaving soil. Use of frost protected shallow foundations in clayey gravel soils leads to an increase of ground volume to be excavated and filled back, and concrete consumption for foundations decreases. In silty sand soils, if the required foundation depth is less than 0.8 m, both reductions are achieved by earth-moving and in concrete consumption.

Key words: Foundations, Thermal Insulation, Codes and Standards

INTRODUCTION

In the majority of locations within Latvia's territory the soils are susceptible to frost heaving, and building foundations must normally be built below the frost depth for this reason. During the last decades the frost protected shallow foundation method has been used in many cold regions (Nordic countries, USA, Canada and others) as a practical alternative to deeper, more expensive foundations (Farouki, 1992; Revised Builder's Guide..., 2004). The frost-protected shallow foundation technique is an advanced building technology to achieve both lower initial costs and increased energy savings. The risk of frost heave to foundations may be avoided in various ways, such as:

- to have foundations deep enough so they are below the frost penetration depth,
- to replace the frost-susceptible soil with a non frost-susceptible material before constructing the foundations,
- to set up the insulation so as to avoid frost penetrating below the foundations,
- a worthwhile utilization
- of heat loss from the building to keep the soil below the foundations unfrozen.

Furthermore the solution adopted can be a combination of methods listed above.

The simplified procedures for the design of building foundations to avoid damage resulting from frost heave are given in standard LVS EN ISO 13793. Yet these methods are new for construction practices in Latvia because they should be carefully

approved of first taking into account the local geological and climatic conditions.

The geotechnical specifications for areas inspected testifies that the water table rests less than 2 m below the depth at which fully frozen soil lies. For such conditions the Latvian code LBN 207-01 specifies that a foundation depth should be not less than 1.4 m for undisturbed clayed soils and not less than 1.7 m for undisturbed sandy-soils. Correspondingly to insulation layer constructed the foundation depth may be reduced up to 0.4 m.

The current study contains the comparison of effectiveness of foundation insulation methods presented in standard LVS EN ISO 13793 with the design results obtained using the Latvian building code LBN 207-01 for columnar spread foundations of an unheated building sized by 18×36 m in plan and insulated to reduce heat loss from the soil below the foundations keeping the soil unfrozen.

AIM AND SCOPE

The aim of this study is to provide some insight on the problem regarding conditions of Latvia's regions and to draw up a methodological background for frost protected shallow foundation design, including analysis of input data range and effectiveness, and practical usefulness of the implementation of a new method regarding local climatic conditions and subgrade soil properties. The study provides background information for decision making when an innovative construction method has been advanced.

BACKGROUND

Recent investigations in geotechnical engineering clarifies the frost heave phenomena in more detail (Noon, 1996; Manz, 2011). Frost heave i.d., the nonuniform change of a volume of a subgrade matrix occurs not only due to the expansion of freezing water in the soil, since, frequently, the heave effect is much greater than the freezing water in the soil is capable of producing. The process is exceedingly complex and still not fully understood. Frost heave is caused by the formation of ice lenses in the soil below the foundation (Fig. 1). Water expands roughly nine percent by volume when frozen. When freezing temperatures penetrate a subgrade soil, water moves from the unfrozen area towards the frozen zone. If the soil is susceptible to capillary action, the water migrates to previously formed ice crystals and freezes. The size of the ice lens depends on the quantity of free water available within the soil, from the water table, and time.

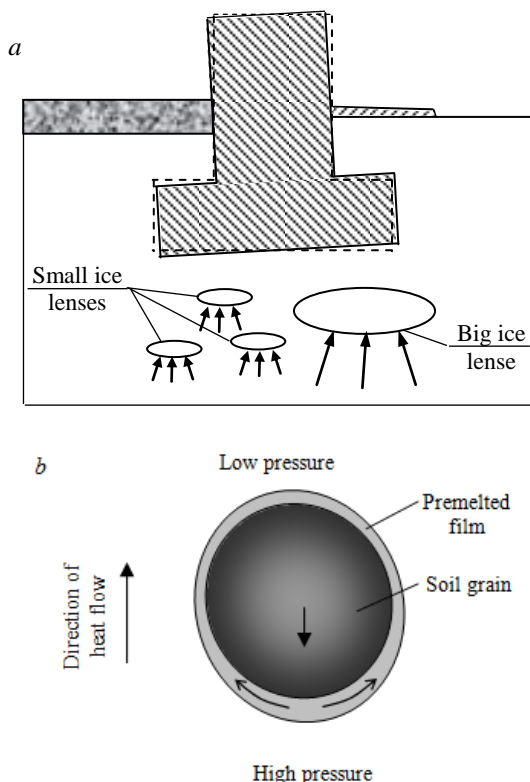


Figure 1. Simplified illustration for frost heave effect in subgrade soil: *a*- growing of ice lenses due to the feed of groundwater from warmer deeper zones, *b*- formation of pressure gradient around soil grain due to grains and ice molecular interactions

In an up-close or secondary frost heave zone of ice lens, a structure of matrix is composed of a multitude of thin crystals growing due to capillary water supply and oriented parallel to the direction of heat flow.

The frost susceptible soil must be sufficiently porous to allow capillary action, yet not so porous as to break capillary continuity.

Water movement in freezing soils is also supported by suction forces (due to pressure differences) that are induced by microscopic interactions between soil grains, nanometer-thick premelted film (formed by liquid water below-freezing temperature), ice, and water within a partially frozen region below the ice lens.

The result of the frost heave force complex is an upward pressure attached to foundations embedded in frost susceptible soil, ranging from 1200 kPa in clay soils, and up to 3000 kPa in silty sand recognized in field tests by researchers during the last decades. Moreover an upward drag of the foundation has been caused by adfreeze stress generated at the side interfaces of foundations ranging from 45 to 1600 kPa for concrete regarding soil type (Domaschuk, 1982).

The incidence of frost heave occur when all of the following three conditions are present:

- 1) The soil is frost susceptible due to a large silt fraction
- 2) Soil is above approximately 80 percent water saturation due to the supply in the surrounding area
- 3) From below, above and/or laterally into the freezing zone subfreezing temperatures penetrate the soil.

Removing one of these factors prevents the possibility of frost damage. Insulation helps with the third one, shielding the foundation from the freezing underlying soil. Soil can hold a great deal of thermal energy, particularly if damp, but it is not a good insulator. For example, 25 mm of polystyrene insulation has an equivalent U-value with 100 mm of soil on average. Depending on the soil type, a layer of 200 - 300 mm depth would be required to provide the same insulation as 50 mm of foam or 80 mm of fiberglass insulation.

Now, a few insulation materials are able to maintain a dry U-value in a moist, below the ground environment over any great length of time. The stress limits declared for insulation material must provide a factor of safety required, according to LVS EN 1990, and a means to limit long-term compressive creep in the insulation layer as well. The high strength extruded polystyrene rigid insulation boards must be appropriate for use under concrete floors and foundations meeting the requirements stated by LVS EN 13164.

Basing on results of the investigations in the related field and due to production of durable insulation materials developed, background has been established for the implementation of insulated foundations.

For unheated buildings the frost protected foundation design methodology is based on conception about the prevention of heat loss from

the subgrade soil stored in the ground during the summer.

SOURCE DATA AND METHODS

Design data for building foundations analysed

A numerical analysis has been performed based on real climatic data for an insulated foundation of a single storey building. The main load bearing structure of the building is a planar steel frame (span 18 m, space 6 m) formed by restrained steel columns and simply supported lightly loaded roof trusses (Fig.2a). The enclosure system is composed of sandwich panels including a 100 mm thick insulation layer. The cladding panels are supported on purlins which transmit the loads to trusses. Lightweight Z-profiles perform the function of secondary bearing members - purlins. Fourteen column foundations are placed correspondingly in rectangular form (Fig. 2). To corner foundations, placed on axes 1-1 and 7-7, the distinctive portion of external load will be transferred, and the ground insulation layer may be of different sizes. Taking into account these differences, the internal foundations have been chosen for analysis in this study. Generally the height of the foundation depends on the depth. The sizes of the rectangular pad of the foundation depend on the subgrade soil's resistance but no less than the required size at the section of column restraint- 600x600 mm.

The vertical force transferred to bearing system is calculated taking into account a permanent load representing the selfweight of cladding and bearing structures ($g_k= 0.6 \text{ kN/m}^2$) and variable snow load. For Latvia's territory the characteristic value of snow load (s_k) declared by Latvian building code LBN 003-01 ranges from 1.10 to 2.80 kN/m^2 . In this study the value $s_k= 1.60 \text{ kN/m}^2$ has been accepted as defined more often (approximately 80% of territory of Latvia). Eccentrically loaded foundation has been designed for four fundamental combinations of actions according LVS EN 1990:

- 1) permanent load (selfweight) + snow load;
- 2) selfweight+ full snow load+decreased wind pressure;
- 3) selfweight+decreased snow load+ full wind pressure;
- 4) selfweight+ wind pressure.

Depth of foundation

The depth of the frozen ground depends on climatic conditions of an area and the properties of the soil (porosity, moisture content, particle sizes). For locations within Latvia the characteristic frost depth values range from 1.20 up to 1.35 m for clayed soils as it is defined by Latvian building code LBN 003-01. The codified values are based on the analysis of

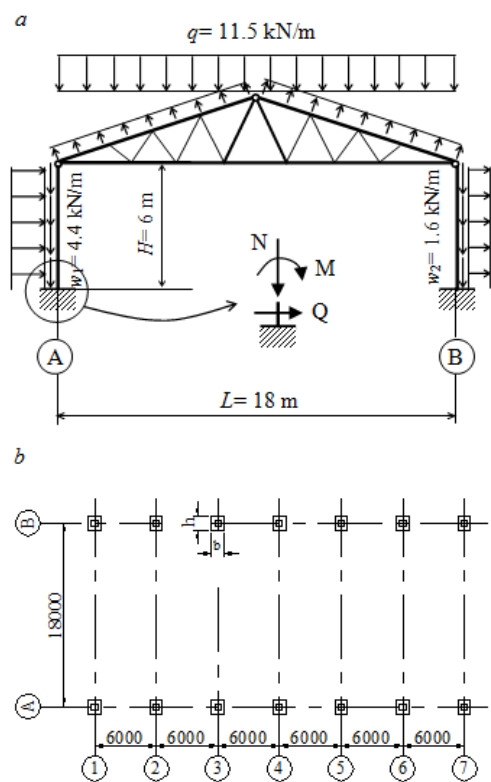


Figure 2. Design model of test building: *a*- design model of planar bearing frame, *b*- plan of column foundations

a valid data set (years 1923-1998), and defined as frost depth values which are expected to exceed one time during 100 years. A real depth of the foundation has been determined depending on the heat regime in the building. In this study the method for an unheated building has been applied, consequently the depth of foundation (d_f) for clayey soils is defined $d_f= 1.3 \times 1.1 \approx 1.4 \text{ m}$, but for silty sand $d_f= 1.3 \times 1.1 \times 1.2 = 1.7 \text{ m}$, and provided that the water table is nearer 2 m from the level of the frost depth. Usually the snow cover insulates the ground and retards heat loss from the earth decreasing the frost depth except in the cases of weathered ground surfaces or cleaned up from the snow. The unfavourable situation should be taken into account in construction, and thereby there is no consideration about snow cover influence on foundation depth in this study.

Design bearing capacity of soil

Some types of soils typical for locations of Latvia including Daugavpils region, such as clays, clay sands, sandy clays and silt sand were chosen for the analysis regarding effectiveness of subgrade insulation.

The existing Latvia building codes (LBN 207-01, article 58) recommend the equation for calculation of design bearing capacity value is not essentially different from that proposed by Terzaghi many

decades before (Terzaghi, 1961) and developed for general failure case assuming that resistance expected to be inherent for subgrade soil depends on shear stresses in the frictional-cohesive material (soil) at edges of three zones under the footing and of overburden pressure.

Consequently a bearing capacity may be explained by three factors every one being a function of internal friction angle and related to: 1) cohesion of the soil, 2) depth of the footing and overburden pressure, 3) width of the footing and the length of shear zone in the limit state. The soil capacity to vertical load increases linearly with depth as illustrated by graphs for some characteristic soil types in Figure 3. The following values of soil properties have been introduced for analysis: coefficient of porosity $e = 0.65$, unit weight $\gamma = 17.5 \text{ kN/m}^3$, plasticity index $I_L > 0.5$. An angle of internal friction φ and effective cohesion c values are as follows correspondingly: $\varphi = 30^\circ$, $c = 4 \text{ kPa}$ for silt sand; $\varphi = 24^\circ$, $c = 13 \text{ kPa}$ for clay sand; $\varphi = 19^\circ$, $c = 25 \text{ kPa}$ for sandy clay; $\varphi = 15^\circ$, $c = 45 \text{ kPa}$ for clay. Note that soil classification corresponds to that specified in LBN 207-01.

The width of footing (b) has been found as optimal for transmitting of forces from restrained columns. The capacity values in Fig. 3 correspond to width value $b = 1.2 \text{ m}$.

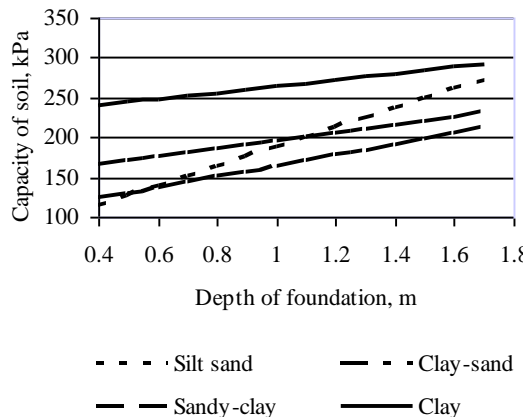


Figure 3. Resistance of soil versus depth of foundation

Analysis of frost season's data

The frost protected shallow foundation design method described in LVS EN ISO 13793 has been recommended for columnar and strip foundations, for slabs on ground and also in regions where the average annual temperature of external air remains above 0°C as the averages range from $+4.5^\circ\text{C}$ to $+6.7^\circ\text{C}$ referring to observations over a 30-year period (LBN 003-01).

Another more labour-consuming procedure deals with winter temperature data processing in order to

make an assessment of duration for each year's freezing season. The frost characteristic is defined as the difference between the freezing point ($\theta_f = 0^\circ\text{C}$) and the daily mean external air temperature. The freezing season starts at the point from which the accumulation of aforementioned differences remain positive throughout the winter. If there is initially some freezing followed by complete thawing, the corresponding days are not included. The accumulation, therefore, starts after this. The freezing season ends at the point which results in the largest total accumulation for the winter. If a short thawing period is followed by a longer freezing period both are included; if a thawing period is followed by a shorter freezing period neither is included.

In this study the external air temperature data (averages of daily data set from October 20 until April 10) were collected for 62 seasons from 1950 until 2012 from records at Daugavpils station available in Web page of State Ltd "Latvian Environment, Geology and Meteorology Centre". There are great variations in both duration of the frost season and temperature range from year to year, as it is typical for a coastal region, see Figure 4 for illustration. Similar graphs were drawn for every winter. The frost season duration was estimated manually following the standard conditions described in the previous paragraph. The illustration is presented in Figure 5. Freezing depth of the soil is more affected by temperatures characterised by the sum of differences between freezing point and the daily mean during the frost season (Fig. 6). It is clear from both column graphs presented that uncertainty of the frost season data is explicitly large, particularly as regard temperatures. The extreme value theory was used for estimation of confident parameters for design as the upper tails of distributions are of great significance.

From different probabilistic models developed for statistical characterisation of extremal values in engineering, the Gumbel model is the most widely applied (Kotz and Nadarajah, 2000). Also the design characteristics presented in LVS EN ISO 13793 have been derived using the Gumbel model. For this reason data samples of frost duration and temperature cumulates were verified using cumulative distribution function of the Gumbel model defined as follows:

$$G(z) = \exp(-e^{-z}), \quad (1)$$

where $G(z)$ – the cumulative distribution function, z – normalized variable useful for simplified calculation. For data processing of freezing temperature cumulates variable z is taken as:

$$z = (\theta_{y,i} - \text{Mod}(\theta)) / \beta, \quad (2)$$

where $\theta_{y,i} = \sum_k (0^\circ - \theta_{\text{daily},i})$
 $\text{Mod}(\theta)$ – mode of data sample,

β – positive real number.

The variables of frost duration were normalized in a similar manner for the Gumbel test. Evidently the Gumbel distribution shapes produce sufficiently

good compatibility with observed data (Fig.7,8), and consequently we can use the probabilistic parameters recommended by standard LVS EN ISO 13793 with good reason.

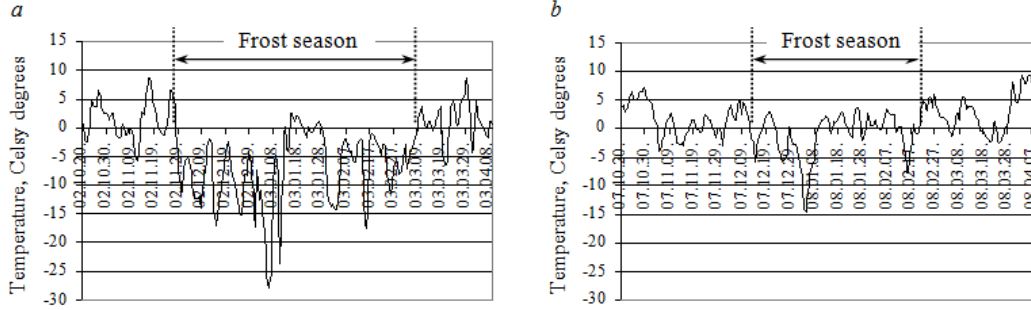


Figure 4. Examples of external air temperature fluctuations in Daugavpils area during time period from October 20 until April 10: a- season 2002/2003, b- season 2007/2008

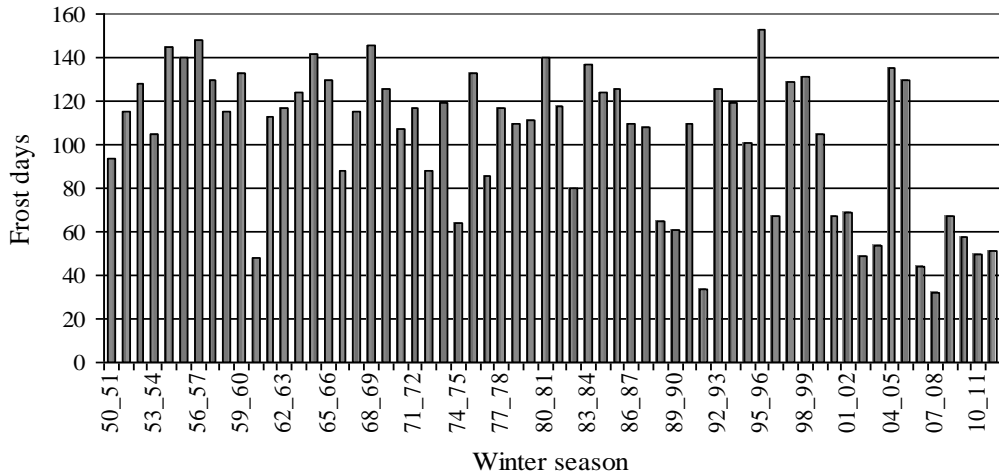


Figure 5. Durations of frost seasons during winters in Daugavpils, years 1950-2012

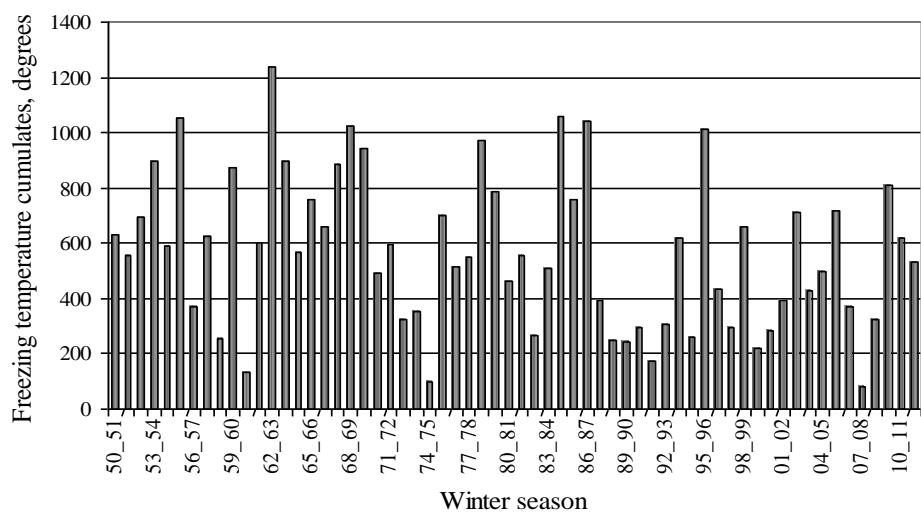


Figure 6. Data range of temperature cumulates during frost seasons in Daugavpils (1950-2012)

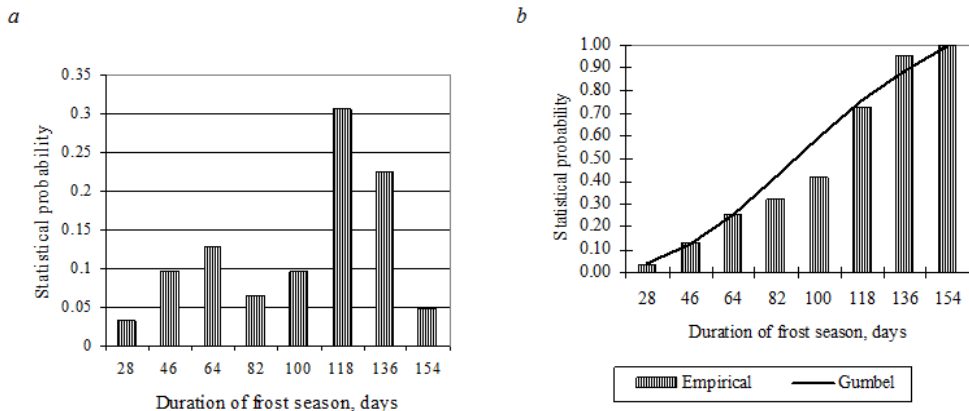


Figure 7. Distributions of frost season duration probabilities : a- empirical; b- empirical and theoretical cumulates (Daugavpils, years 1950-2012)

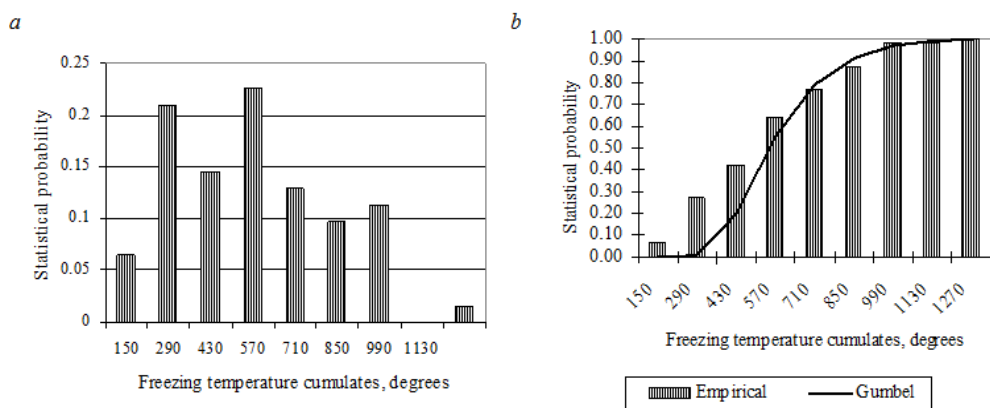


Figure 8. Distributions of freezing temperature cumulates during frost season: a- empirical; b- empirical and theoretical cumulates of probabilities (Daugavpils, years 1950-2012)

Evaluation of design freezing index

The insulation required for frost protection depends on the severity of the design winter, expressed in terms of the freezing index together with the annual average external air temperature. The design freezing index (F_n) is the value which statistically is exceeded once in n years for the locality concerned, based on recorded meteorological data and calculated according to Annex A of LVS EN ISO 13793. F_n has a 1 in n probability of being exceeded in a given winter. For permanent buildings n is normally chosen as 50 or 100 years; for the test building in this study $n = 50$.

In this study the design freezing index F_d has been calculated from meteorological records of daily mean external air temperatures for the Daugavpils region. The freezing index F_i (in °K·h) for one frost season were calculated as 24 times the sum of the difference between freezing point ($\theta_f = 0^\circ\text{C}$) and the daily mean external air temperature:

$$F_i = 24 \sum_{j=1}^k (\theta_f - \theta_{d,j}), \quad (3)$$

where $\theta_{d,j}$ – the daily mean external air temperature the average of several readings for day j , in °C; k - all days in the freezing season. Both positive and negative differences, within the freezing season, are included in the accumulation. A negative difference implies some thawing of the ground reducing the frost penetration in the ground. The design freezing index for a given location is obtained from a set of freezing indexes F_i , calculated of m winters at the location ($m \geq 20$, in this case $m = 62$). The Gumbel distribution has been recognized as a suitable statistical distribution that realistically reflects extreme events and recommended for determination of design freezing index (F_n). According to Gumbel the design freezing index is given by:

$$F_n = \bar{F} + \frac{s_F}{s_y} (y_n - \bar{y}), \quad (4)$$

where \bar{F} - average of freezing indexes;

$$\bar{F} = \frac{\sum_{i=1}^m F_i}{m} = \frac{844450.9}{62} = 13620 \text{ } ^\circ\text{h},$$

s_F - standard deviation for index data sample;

$$s_F = \sqrt{\sum_{i=1}^m (F_i - \bar{F})^2 / (m-1)} = \\ = \sqrt{2674563867 / (62-1)} = 6621.6 \text{ } ^\circ\text{h},$$

y , s_y – reduction factors for variables in Gumbel distribution regarding the reference period of data processed; in this study $\bar{y} = 0.55$, $s_y = 1.17$ correspondingly to data sample of 62 years (LVS EN ISO 13793, Table A.1).

y_n – statistical parameter with regard to the level of safety of the building, dependent on the expected lifetime, $y_n = 3.9$ correspondingly 50 years lifetime of permanent building. The values estimated were put into formulae (4) resulting to the freezing index for Daugavpils locality according to temperature data sample of 62 winter seasons: $F_{50} = 32579 \text{ } ^\circ\text{K}\cdot\text{h}$ which may be exceeded once in 50 years, and $F_{100} = 36541 \text{ } ^\circ\text{K}\cdot\text{h}$ once in 100 years basing on the Gumbel prognosis.

The prognosticated value of the freezing index for Daugavpils region is quite dependent on the chosen time period upon which the temperature data are processed. The variation of freezing index values determined according to different reference data periods is illustrated by column graphs in Figure 9. It is useful to note that the maximal value of freezing index was obtained upon data of the winter seasons for the years of 1960-1980 (not displayed in Fig.9): $F_{50} = 43548 \text{ } ^\circ\text{K}\cdot\text{h}$ and $F_{100} = 49317 \text{ } ^\circ\text{K}\cdot\text{h}$ for building of life time 100 years.

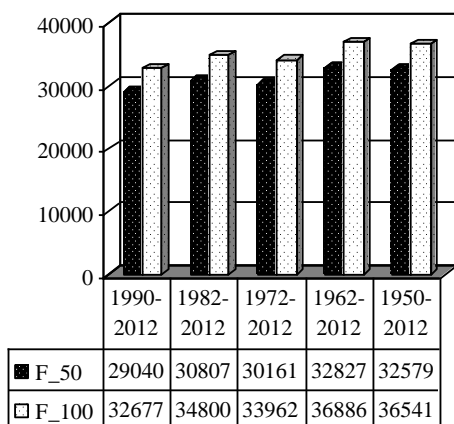


Figure 9. Freezing index (in $^\circ\text{K}\cdot\text{h}$) versus reference period

Characterisation of average year temperatures

The protection of cold structures relies on the heat consumption available in soil that has been stored in the ground during summer. Therefore the average

temperature in a region is one more important factor for design. Figure 10 represents the graph of average temperature values calculated from data of Daugavpils station.

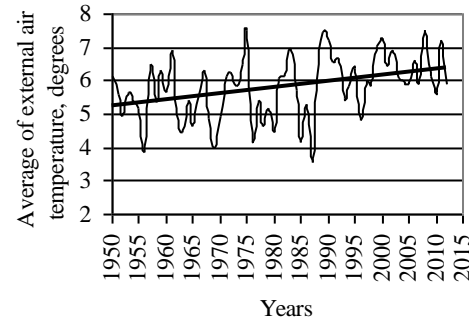


Figure 10. Variation of average temperatures

Frost protected foundation design for unheated building

The main purpose of the thermal design of foundations is to avoid frost heave. The design methodology used in this study has been provided by LVS EN ISO 13793 where it is proposed that no fully frozen soil occurs below the foundation during the design winter. The design procedure presented in the standard has been developed according to the investigations and practical experience for many decades. The parameters included in this study and relevant to frost protection are:

- freezing index and annual average temperature;
- frost susceptibility of the soil;
- thermal properties of the ground, both frozen and unfrozen;
- insulation of the floor;
- internal temperature in the building;
- the geometry, and especially the overall dimensions of the building and the type of foundation used.

The width of ground insulation for an unheated building is determined based upon the data shown in Table 10 presented in standard LVS EN ISO 13793 corresponding to the design freezing index $F_d = F_n$. The required width of the insulation layer, i.d., widening around footing is $b_g = 1.7 \text{ m}$ (Fig. 11). Such width of the ground insulation for an unheated building may be applied for foundation depth from 0.4 to 1.0 m. Insulation is placed on a drainage layer. The drainage layer consists of coarse material that is not frost susceptible.

The minimum thermal resistance of the ground insulation, R_g , is determined according to the tabulated values in standard LVS EN ISO 13793 for foundations at least 0.4 m up to 1.0 m deep (see Table 1). Expanded or extruded polystyrene with a density of at least 30 kg/m^3 can normally be used in the construction of insulation layer under loaded foundation. Extruded polystyrene (XPS) has the largest compressive strength and can be used in

various applications for insulating of building foundations. As compressive loads in value up to the ground bearing capacity may be applied and transferred to the insulation layer, the insulation material selected must be verified for stress limits providing a factor of safety and a means to limit long-term compressive creep in the insulation layer, and the allowable stress limits are defined based on a percentage of minimum insulation compressive resistance.

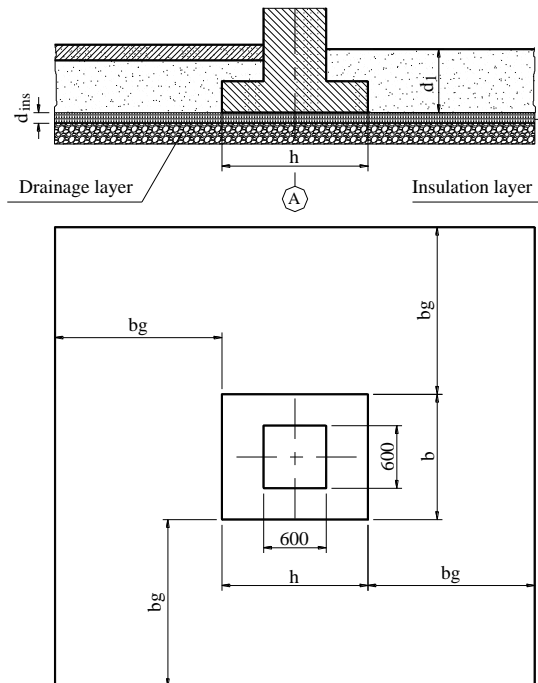


Figure 11. Frost protected shallow foundation

Table 1
Characteristics of ground insulation

d_1 , m	R_D , $\text{m}^2 \cdot \text{K}/\text{W}$	U , $\text{W}/\text{m}^2 \cdot \text{K}$	λ_D , $\text{W}/\text{m} \cdot \text{K}$	d_{ins} , m
0.4	1.90	0.53	0.035	70
0.5	1.68	0.60	0.034	60
0.6	1.47	0.68	0.033	50
0.7	1.25	0.80	0.032	40
0.8	1.03	0.97	0.032	40
0.9	0.82	1.22	0.032	40
1.0	0.60	1.67	0.032	40

Symbols: d_1 – depth of foundation; R – minimal unit thermal resistance of ground insulation required; λ , U – thermal transmission coefficients, d_{ins} - thickness of insulation layer.

For this study extruded polystyrene Styrodur 4000CS (density 30 kg/m³) has been selected as the material used in related practice of European countries, Canada and the United States in recent decades. The verified acceptable long-term (50 years) compressive stress for this material is declared 180 kPa, and creep deformation less than

2% and compression strength at 10% deformation – 180 kPa (Technical Data... BASF).

RESULTS AND DISCUSSION

Numerical results for case study

The foundation under an unheated buiding has been designed to support the loads (Fig. 2) according to serviceability limit state criteria (LBN 207-01) stated as follows: maximal pressure (σ_{max}) around side line of footing must be less or equal to bearing capacity (R) multiplied by 1.2, and the calculated value of average compression stresses (σ_{mean}) must be less or equal to capacity ($\sigma_{mean} \leq R$). See Table 2. Cost-effectiveness of building depends considerably on the bulk of ground excavation needed for the foundation. With regard to economical estimations in this case study (Fig. 12), the comparison of soil volumes to be moved during construction for insulated foundations as ratio to deep ones depending on the depth of foundation has been illustrated in graphs in Fig. 13. It is clear that frost protected shallow foundations are effective at a depth less than approximately 0.8 m.

Also the concrete consumption for insulated foundations has been estimated in comparison with ones to be built in freezing depth (see Fig. 14), and savings may be achieved of up to 50 per cent.

Table 2
Design characteristics

d_1 , m	Sizes of footing, m	σ_{max} , kPa	σ_{mean} , kPa	R , kPa	$\sigma_{max}/1.2R$
Silty Sand					
0.4	1.5 × 1.2	133	78.6	114	0.98
0.6	1.4 × 1.2	159	87.5	138	0.96
1.0	1.3 × 1.2	167	91.6	163	0.86
1.7	1.2 × 1.1	294	130	273	0.90
Claysand					
0.4	1.5 × 1.2	133	78.6	123	0.90
0.6	1.4 × 1.2	159	87.5	137	0.97
1.0	1.4 × 1.2	167	91.6	151	0.93
1.4	1.3 × 1.2	220	109	191	0.96
Sandy Clay					
0.4	1.3 × 1.2	174	89.2	165	0.87
0.6	1.3 × 1.2	183	93.3	175	0.87
1.0	1.3 × 1.2	192	97.3	186	0.86
1.4	1.2 × 1.2	257	116	216	0.99
Clay					
0.4	1.1 × 1.0	290	122	239	1
0.6	1.1 × 1.1	278	116	247	0.93
1.0	1.1 × 1.1	291	120	255	0.95
1.4	1.1 × 1.1	332	133	280	0.99

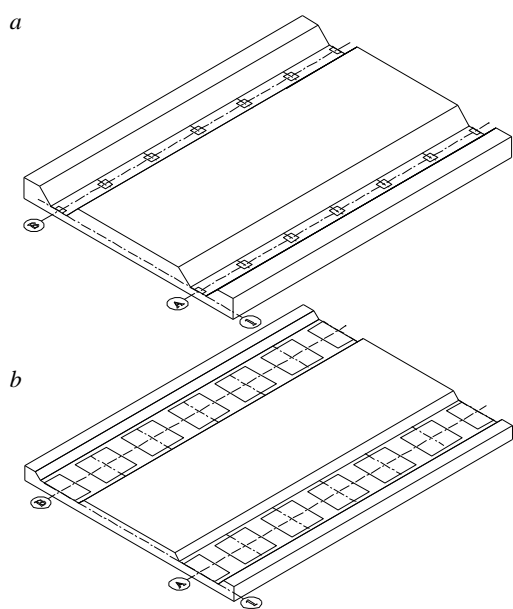


Figure 12. Soil excavation schemes: a- for traditional deep foundations, b- frost protected shallow foundations

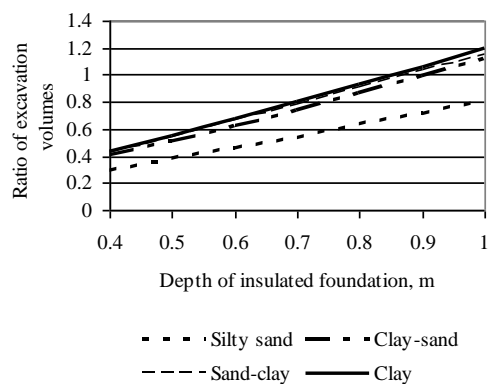


Figure 13. Variation of relative ground excavation volumes versus depth

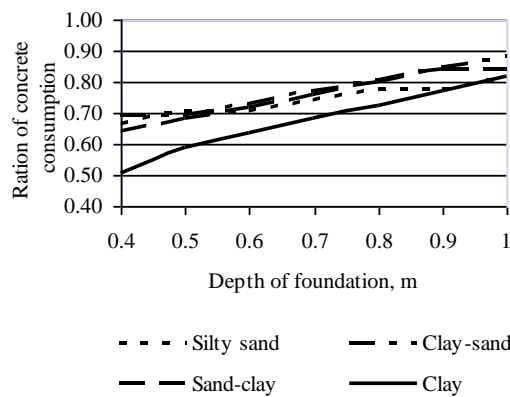


Figure 14. Illustration of relative concrete consumption for insulated foundations

Discussion on uncertainty of freezing index

It is clear that the implementation of frost protected shallow foundation design in the construction practice of Latvia may be accepted when there is no doubt of the fulfillment of the basic requirements for safety and durability of structure performing procedures stated by the standards and code. The main objective in this relation is the value of the freezing index.

Results of temperature data processing for 62 winter seasons according to temperature records in Daugavpils station testify that quite distinctive reliability levels may be defined for shallow foundation design depending on the number of frost seasons (m) sampled remaining under condition ($m \geq 20$) stated by LVS EN ISO 13793. As it is shown in Figure 9, the range of variation of freezing index exceeds 15000 that involves the range of uncertainty for insulation size selected of about 25-30 cm. Normally, the freezing index value derived from a longer reference data period should be of higher confidence level. At the same time the graph of annual average temperatures (Fig. 10) displays some trend of increase as it is found from the trendline equation an increment is $\Delta T = 0.019^\circ$ per year according to the recent 62 year external air temperature data in Daugavpils. Note that this tendency may be characterised as inherent of high statistical uncertainty. Also the development of frozen depth in time under small negative degrees correlates with the thermal conductivity of the soil, and consequently with soil saturation, water table and soil type.

Discussion on future trends

The thermal design method of shallow foundations offers several advantages over the traditional practice when a new building has to be designed in a densely property development area, and moreover the deeper soil layers inherent of lower capacity characteristics and/or the water table is so high that groundwater lowering techniques are needed during construction that may induce an additional nonuniformly settlement of subgrade under the buildings nearby.

Also the use of insulated foundations may be an effective and acceptable method when the required depth of foundations for a new building exceeds the one of an existing building nearby, for example, the design of unheated building close to residence.

Some benefit may be achieved in areas of high water table while construction of shallow foundations enable builders to avoid additional expenses for groundwater lowering, and to reduce the duration of construction.

Lightly loaded frost protected foundations may be a more effective solution in special cases when there is a good chance to remain with footing in the upper sufficiently thick layer of soil inherent of higher

capacity not disturbing the deeper layer of lower capacity.

CONCLUSIONS

Some conclusions made as a result of this research could be useful for the evaluation of insulated foundation(s) method and making decisions on their implementation in the construction practice of Latvia:

- Cost effectiveness of insulated foundations according to LVS EN ISO 13793 correlates closely with the type of frost-heaven soil. For example, the use of heated foundations in clayey soils, including silty sand leads to increase of soil volume to be excavated and filled back but concrete consumption for foundations decreases. In dusty sand soils, if the required foundation depth is less than 0.8 m, both

reductions are achieved in earth-moving and concrete consumption

- The decreased side area of foundations obtained applying the insulation leads to a decrease of heave forces and consequently to more safety in construction regarding human errors in construction (if the backfill is non-quality or the material is off-grade, i.e., contains a clay fraction)

- There is a lack of tabulated data and/or maps for Latvia regions regarding the design freezing index needed for design, and it is labour consuming procedure to be undertaken.

- The thermal design may be recommended when the groundwater level is high, since using this method there is no need to lower the water table during the construction.

REFERENCES

- Design Guide for Frost protected shallow Foundations. NAHB Research Center, Springfield, Virginia, 1994. 30 pages + Appendixes A1-A4.
- Domaschuk L. (1982). Frost Heave Forces on embedded structural Units. Proceedings of 4th Canadian Permafrost Conference, p. 487-496
- Farouki, O. (1992). European foundation designs for seasonally frozen ground. Monograph 92-1, U.S. Army Corps of Engrs., Cold Regions Res. & Engrg. Lab., Hanover, N.H. 113 p.
- State Ltd "Latvian Environment, Geology and Meteorology Centre: <http://www.meteo.lv>
- Kotz S. and Nadarajah S. (2000), Extreme Value Distributions. Theory and Applications, Imperial College Press, London, 185 p.
- Latvijas būvnormatīvs LBN 003-01. Būvklimatoloģija.
- Latvijas būvnormatīvs LBN 207-01. Geotehnika. Būvju pamati un pamatnes.
- LVS EN 13164:2009. Siltumizolācijas izstrādājumi ēkām. Rūpnieciski ražotie ekstrudēta putu polistirola (XPS) izstrādājumi. Specifikācija/ EN 13164. Thermal Insulation Products for Buildings - Factory made Products of extruded Polystyrene Foam (XPS) – Specification
- LVS EN 1990:2006 /A1:2008 L. Eirokodekss. Konstrukciju projektēšanas pamatprincipi/ EN 1990: Eurocode - Basis of structural design
- LVS EN ISO 13793:2003 L. Ēku siltumtehniskās īpašības - Pamatu termiskā projektēšana, lai izvairītos no grunts izcilāšanās salā/ EN ISO 13793. Thermal Performance of Buildings - Thermal Design of Foundations to avoid Frost Heave
- Manz Lorraine (2011). Frost Heave. Geo News, July, p. 18-24.
- Merkel H. (2004) Determination of Long-Term Mechanical Properties for Thermal Insulation under Foundations. Proceedings of Performance of the Exterior Envelopes of Whole Buildings IX International. Conference, ASHRAE, December, p.1-7
- Noon, C. (1996). Secondary Frost Heave in Freezing Soils. A thesis for the degree of Doctor of Philosophy at the University of Oxford, Oxford, 189 p.
- Revised Builder's Guide (2004) to Frost Protected Shallow Foundations/ National Association of Home Builders (NAHB), Upper Marlboro, Washington DC, 34 p.
- Technical Data. Recommended Applications. BASF, The Chemical Company Web page <http://www.styrodur.de>
- Терцаги К. (1961). Теория механики грунтов. Госстройиздат, 507 с.

DETERMINATION OF SHRINKAGE STRESSES IN CONCRETE FLOOR COATINGS

Rенно Reitsnik, Харри Лиле, Александр Рыбчиков, Кауни Кивисте

Estonian University of Life Sciences, Institute of Forestry and Rural Engineering

Address: Fr. R. Kreutzwaldi 5, 51014, Tartu, Estonia

Phone: +372 731 3181

E-mail: renno.reitsnik@emu.ee

ABSTRACT

Durability of concrete floors is a major problem in many industrial facilities nowadays. Particular attention is paid to the wear resistance of floors and different surface hardeners are used to improve this property. There are situations where floor surface separates from the subbase and delamination takes place. Surface hardeners and subbases have different shrinkages, which should be taken into consideration as one of the reasons that can weaken floor structure.

The aim of this study was to explore the shrinkage of different surface hardeners, to calculate shrinkage stresses and to compare them with the shrinkage of concrete. Determination of shrinkage was carried out by two methods: length change measurement and semi-destructive hole-drilling according to the standards ASTM C490 and ASTM E837-08, respectively. Shrinkage stresses depend on the modulus of elasticity and Poisson's ratio of hardeners which affect shrinkage stresses in the system subbase-coating.

Test results showed that surface hardeners had higher shrinkage than plain concrete. The difference in shrinkage stresses becomes more significant when a surface hardener is poured onto the hardened subbase.

Key words: shrinkage stresses, surface hardeners, concrete floors, length change measurements, hole-drilling method

INTRODUCTION

High quality surface hardeners are applied on the concrete floor base to prolong the floor's service life. Solid waste management has the highest requirements for floors because continuous friction with heavy machinery and contact with different chemical compounds take place. These processes accelerate deterioration of the quality of most common concrete floors. Frequent repair and maintenance are expensive, not to mention the holdups of business activity (Kurtz, 1998).

During solidification of mixtures tensile shrinkage stresses are induced, which can cause crack formation and surface layer delamination.

A dry-shake hardener is applied to freshly poured concrete and rubbed into complete monolithic surface. Since a dry-shake hardener consists of quartz sand and cement, it can be assumed that its shrinkage takes place similarly to that of concrete.

Shrinkage of concrete can be divided into two different stages: early and late age shrinkage. Early stage shrinkage of concrete is defined as the first 24 hours when fresh concrete is cast. Later age, or long term shrinkage, refers to volume changes of concrete after 24 hours (Holt, 2001).

Early stage shrinkage can be divided into two types: plastic and autogeneous. Plastic shrinkage takes place in the first hours of curing when the evaporation speed of water is higher than the speed of the migration of water from the inside to surface.

Bleed water rises to concrete surface and is exposed to the environment and evaporation. Long term shrinkage can be divided into three types: autogeneous, drying, and carbonation. Autogeneous shrinkage is defined as volume change of concrete without moisture transfer to the surrounding environment. Drying shrinkage is decrease of concrete volume caused by water loss. Early stage drying shrinkage can be reduced by proper curing conditions and surface handling, ensuring stronger finish and uniform hardening. Carbonation occurs when cement paste in hardened concrete reacts with moisture and carbon dioxide in the air.

Three series of specimens were prepared using different dry-shake hardeners and a mixture was made by adding water to powder. The dry-shake hardeners used in the experiments were Qualitop Master (QT) and Qualidur Premix (QD) by Rocland (Qualitop, 2010; Qualidur, 2010) and Monoshake TF (MS) manufactured by DCP Baltics (Monoshake TF, 2006). One series of specimens were prepared from industrial concrete class C25/30 (PC). Shrinkage strain was investigated for different materials (mixtures). The moduli of elasticity and Poisson's ratios for hardeners and for concrete and the calibration coefficients of the hole-drilling method rosette were determined for calculation of shrinkage stresses.

EXPERIMENTAL PROCEDURE AND METHOD

Specimens were prepared according to the standard (ASTM C490, 2008). Measurements of the specimens were $(75 \times 75 \times 285)$ mm³. A special mould has been designed and manufactured from plastic and was used to cast these specimens. Gauge studs were fixed to each end of a specimen for measurement of length change. Each mould was equipped by the end plate to hold the studs properly in place during the curing period. The gauge length between the bottom ends of the studs was 250 mm. The measuring equipment (Fig. 1) was designed and manufactured for determining the length change of the specimens.



Figure 1. Equipment for measuring the length change of the specimens

Length change was measured by the digital dial gauge *Mitutoyo ID-C112B* to 0.001 mm. Four series of experiments were carried out, each consisting of 12 specimens. One series of specimens were prepared from industrial concrete class C25/30. The water/cement ratio was 0.5. Mix details of concrete are presented in Table 1.

Table 1
Mix details of PC

Material	Quantity
Cement CEM II A-T 42.5 R	344.5 kg/m ³
Sand	1124.0 kg/m ³
Gravel, 4-12 mm	482.7 kg/m ³
Gravel, 8-16 mm	394.0 kg/m ³
Water	172.1 dm ³

For calculation, the needed moduli of elasticity and the Poisson's ratios of the investigated hardeners and concrete were determined. Wire strain gauges with a length of base 20 mm, resistance 200 Ω and gauge factor 2.0 were glued in the longitudinal (LSG) and transverse (TSG) directions onto the two opposite sides of the specimen (see Fig. 2 a). The specimen was loaded up to 49 kN by the compressive testing machine *H-20*. (Fig. 2 b).

The hole-drilling method was used to check the results obtained by measuring length change. This is one of the most widely used semi-destructive methods for determining residual and shrinkage

stresses (ASTM E837-08, 2009). Relieved strains were measured with a strain gauge rosette (SGR) (*Vishay Micro-Measurements EA 06-125RE-120*) which was glued onto the specimen with the two-component adhesive *M-Bond 200* and a hole was drilled through the geometric centre of the rosette (Fig 3a). The rosette was wired and connected to the *Vishay Strain Indicator and Recorder Model P3*. The specimen was placed in a rig which had been specially designed and manufactured for this study (Fig. 3b).

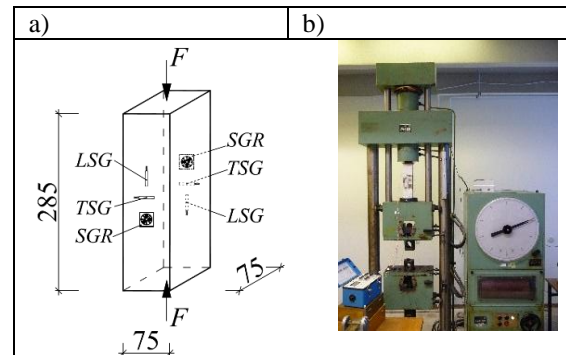


Figure 2. Scheme (a) and photo (b) of the compressive test

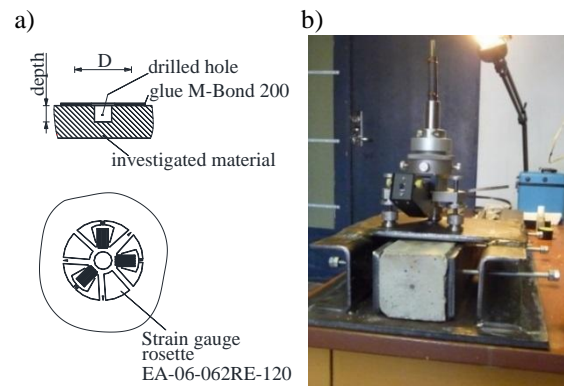


Figure 3. The hole-drilling technique (a) and rig for fixing a specimen (b)

Calibration constants \bar{a} and \bar{b} for the SGR *EA 06-125RE-120* were calculated according to the standard (ASTM E837-08, 2009) from the measured strains obtained from the compressive test. The maximum load was 49 kN (stress 8.71 N/mm²). Loading was done before and after drilling a hole into SGR. Hole drilling was conducted using a 1.53 mm increment and the hole was drilled to a depth of 4.59 mm, i.e. corresponding to three increments. After each increment the readings were allowed to stabilize for 120 seconds before recording. The obtained values of calibration constants are presented in Table 2. Constants are necessary for calculation of residual

stresses, because they are dependent on material properties.

RESULTS AND DISCUSSION

The major part of this study was carried out within a Master's course. The duration of shrinkage was 60 days. In this period of time the shrinkage of concrete is 80% (Holt, 2001). During measurements the humidity and temperature in the storage room remained uniform for 60 days. Thereafter, central heating was turned off for the spring season and the conditions of the storage room affected the results of measurements.

In the case of short term measurements, experimental data can be approximated by the following analytical equation (1) (Kivisté, 2011)

$$s(t) = c_1 \cdot \ln(1.0 + t^{c_2}), \quad (1)$$

where t – time, days;

c_1, c_2 – dimensionless parameters.

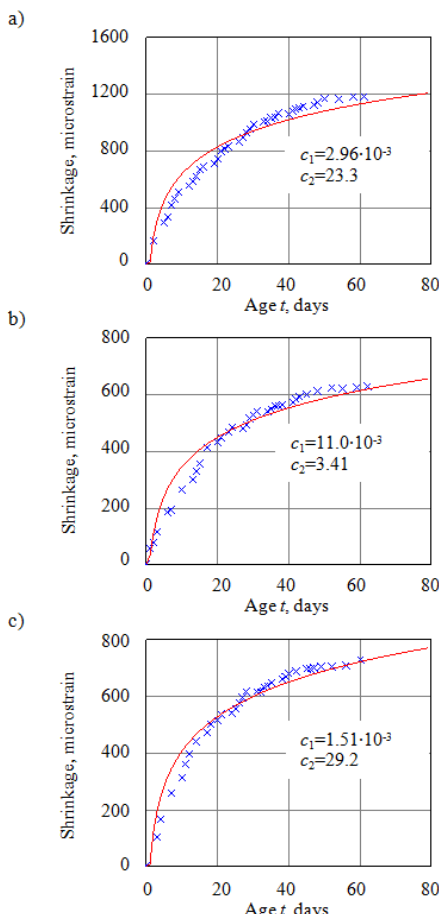


Figure 4. Experimental data and the curve of approximation for the specimens cast from a) MS; b) QT; c) QD

The purpose was to find unknown constants so that the measured displacements $s(t)$ could be approximated in the best way. This problem was

solved by using the regression function *genfit(vx, vy, vg, F)* of the mathematical program *Mathcad 15.0* (Makarov, 2008).

The results of the measurements and the approximation curves are presented in Figs. 4 and 5. The specimens of QT and QD did not practically reveal changes in shrinkage, but the shrinkage of MS was about two times as high at the same age. The shrinkage of PC was the smallest compared to the shrinkage of surface hardeners. It can be seen that the values of the currently studied shrinkage strain of the hardeners QT and QD and the values of the previously investigated shrinkage strain of concrete containing 0.51% of crimped steel fibres are practically similar, see paper (Kivisté, 2011).

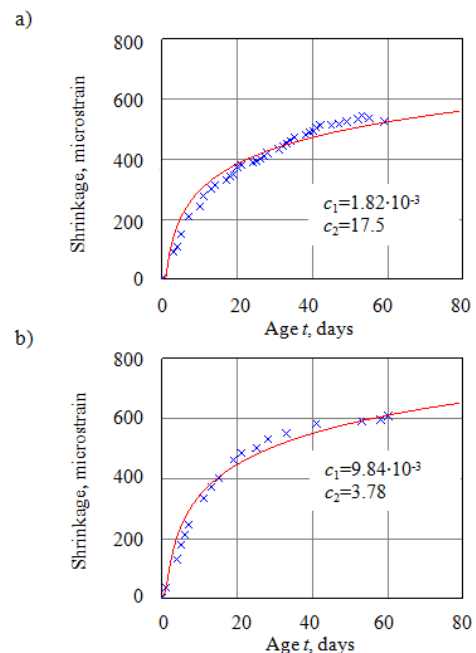


Figure 5. Experimental data and the curve of approximation for the specimens cast from a) PC; b) PC containing crimped fibres 0.51%

Consequently, this kind of hardener on fibre reinforced concrete floor has small shrinkage stresses.

Note that the determined numerical values of hardeners can be used for determining shrinkage stresses on concrete floors covered with surface hardeners.

It is evident that the determined moduli of elasticity and Poisson's ratios are quite similar, whereas the calibration coefficients differ to some degree.

We assume that in the case of free shrinkage the stresses of specimens are absent (i.e. equal to zero). However, as we measured 1.59 N/mm^2 in the surface layer of MS, 0.48 N/mm^2 in the surface layer of QT, -0.25 N/mm^2 in the surface layer of QD and 0.48 N/mm^2 in the surface layer of PC, using hole drilling. The results are measured in the surface layer because the hole depth is relatively small compared to specimen dimensions. The

results remained within experimental uncertainty except one MS, they can be taken equal to zero in the following example of applications.

Table 2
Determined modulus of elasticity,
Poisson's ratio and calibration coefficients
 \bar{a} and \bar{b} for the type of rosette used

Material	Modulus of elasticity E , GPa	Poisson's ratio μ	Depth/D =	
			0.45	\bar{a}
MS	21.9	0.14	0.259	0.569
QT	26.9	0.19	0.222	0.625
QD	26.9	0.19	0.381	0.822
PC	27.1	0.19	0.346	0.717

EXAMPLE OF APPLICATIONS

For example, shrinkage stresses in the system subbase (concrete floor) – coating (hardener) can be calculated after a certain number of days have passed from pouring, assuming that shrinkage stresses are distributed uniformly through the coating and subbase (Fig. 6).

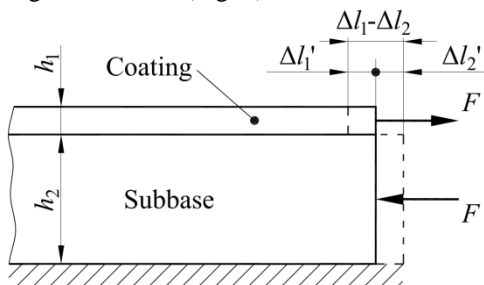


Figure 6. A fragment of the edge region of hardened concrete floor and formation of F generated by shrinkage

Shrinkage strain of the system subbase-coating

$$\Delta\varepsilon = \frac{\Delta l_1 - \Delta l_2}{l}, \quad (2)$$

where Δl_1 – shrinkage of coating;
 Δl_2 – shrinkage of subbase.

Such differential shrinkage rate usually produces tensile stresses which are relieved by cracking of the coating.

Compatibility equation (3) in the case of equilibrium of the initial forces assuming that Poisson's ratio $\mu_1 = \mu_2 = \mu$ (valid condition $\Delta l_1 - \Delta l_2 = \Delta l'_1 + \Delta l'_2$) yields

$$\Delta\varepsilon = F \left(\frac{1-\mu}{E_2 h_2} + \frac{1-\mu}{E_1 h_1} \right), \quad (3)$$

where F can be calculated and the shrinkage stresses per unit width of the hardener and the floor are expressed as equation (4)

$$\sigma_1 = \frac{F}{h_1}, \quad \sigma_2 = -\frac{F}{h_2}, \quad (4)$$

where σ_1 – shrinkage stress in coating, N/mm²;
 σ_2 – shrinkage stress in subbase, N/mm².

Stress gradients are induced between the surface hardener and the substrate, however, arising stresses have unequal values due to the different cross-sections of the hardener and the substrate. Stress gradients diminish when a surface hardener is applied onto freshly poured concrete. Again, the smaller is the difference between the shrinkage of coating and subbase, the lower shrinkage stresses arise. The purpose is to minimise differential shrinkage stresses.

When the hardener QD was set on a fresh plain concrete floor the obtained shrinkage stresses were after 60 days of pouring: $\sigma_1 = 5.7$ N/mm² (tensile), $\sigma_2 = 1.1$ N/mm² (compressive).

The preceding results were obtained, when $h_1 = 15$ mm, $h_2 = 80$ mm, $\Delta l_1 = 0.182$ mm, $\Delta l_2 = 0.131$ mm, $\mu = 0.19$, $E_1 = 26.9 \cdot 10^3$ N/mm², $E_2 = 27.1 \cdot 10^3$ N/mm².

Calculated (tensile) stresses are quite close to the coating's flexural strength (8 N/mm²) (Qualidur, 2010). This is one of the main reasons why cracks are induced.

CONCLUSIONS

The following conclusions were made on the basis of the experiments:

- The shrinkage of concrete was the least compared to the shrinkage of surface hardeners. This is the reason why tensile shrinkage stresses arise in concrete floors coated with surface hardeners.
- Formation of shrinkage stresses can be postponed by reducing plastic shrinkage, which emerges during the first hours when concrete is in the liquid state. Faster evaporation of water causes larger shrinkage and hence higher shrinkage stresses.
- The modulus of elasticity, the Poisson's ratio, calibration coefficients \bar{a} and \bar{b} for the type of rosette used were determined.
- An example of applications is presented where presumable stresses are calculated in QD and PC.
- This analysis was limited to the data obtained from the above described experiments.

ACKNOWLEDGEMENT

This study was partially supported by the Estonian Ministry of Education and Science (SF0140091s08) and by the Estonian Science Foundation (grant ETF8459).

REFERENCES

- ASTM C490/C490M-08. (2008) *Standard Practice for Use of Apparatus for the Determination of Length Change of Hardened Cement Paste, Mortar, and Concrete*. ASTM International. 5 p.
- ASTM E837-08. (2009). *Standard Test Method for Determining Residual Stresses by the Hole-Drilling Strain-Gauge Method*. ASTM International. 17 p.
- Holt, E.E. (2001) *Early-age autogeneous shrinkage of concrete*. Espoo: Technical Research Centre of Finland, VTT Publications 446. 197 p.
- Kiviste, K., Ryabchikov, A., Lille, H. (2011) Determination of Shrinkage of Fibre Reinforced Concrete. *Civil Engineering '11. 3rd International Scientific Conference Proceedings*, Vol. 3, p. 113-116.
- Kurtz, F.S. (ed.). (1998) *Practitioner's guide to slabs on ground*. USA: American Concrete Institute. 567 p.
- Makarov, E.G. (2008) *Mathcad 2014. Manual for Self-tuition*. Electronic book, Novyj disk, CD-ROM (in Russian).
- Monoshake TF data sheet (2006) [online] [accessed on 27.01.2013].
Available: <http://www.dcpbaltics.com//failid/File/MONOSHAKE2006.pdf>
- Qualidur data sheet (2010) [online] [accessed on 27.01.2013]
Available: http://www.rocland.eu/en/component/docman/doc_download/107-data-sheet.html
- Qualitop Master data sheet (2010) [online] [accessed on 27.01.2013]
Available: http://www.rocland.eu/en/component/docman/doc_download/101-data-sheet.html

RESEARCH OF MATERIALS SUITABILITY FOR CRACK REPAIR IN REINFORCED CONCRETE STRUCTURES

Rytis Skominas*, Vincas Gurskis**, Algimantas Patasius***

Aleksandras Stulginskis University, Institute of Hydraulic Constructional Engineering

E-mail: *rytis.skominas@asu.lt, **vincas.gurskis@asu.lt, ***algimantas.patasius@asu.lt

ABSTRACT

Cracks are one of the serious problems appearing in reinforced concrete. The reasons that cause the cracking of structures could be different: load impact, corrosion of reinforcement, unsteady settlement of framework, environmental effect etc. The cracks cause a decrease of the structure's durability and longevity. Therefore it is important to repair damaged structures.

To estimate the materials' suitability for crack repair a slant shear strength test and a water penetration test were used. The results show that polymer injection materials A and B can restore the strength of concrete. The repair carried out with modified cementitious material (for modification used expansive additive and polymer additive) has the same effect. Water penetration test shows, that all polymer injection materials are quite water resistant.

Keywords: reinforced concrete, crack, repair, cementitious material, injection material.

INTRODUCTION

Reinforced concrete structures are one of the most popular in the world. They are often used in civil and hydraulic engineering. During their service time, reinforced concrete structures tend to deteriorate. Cracks are one of the biggest problems appearing in reinforced concrete. The reasons that cause cracking of structures could be different: load impact, corrosion of reinforcement, unsteady settlement of framework, environmental effects, etc. The cracks cause the decrease of the structure's durability and longevity (Poursaei et al., 2008; Vidal et al., 2004; Zhao et al., 2011). Therefore, it is important to repair these damaged structures. Different repair techniques have been successfully developed to strengthen a given structure or part of it to restore its serviceability and strength. It is also prudent to consider the durability aspect when repair or strengthening is carried out. The final selection of a suitable and most effective method generally depends on simplicity, speed of application, structural performance and total cost (Thanoon et al., 2005). The proper repair of cracks depends on knowing the causes and selecting the repair procedures that take these causes into account; otherwise, the repair may only be temporary. Successful long-term repair procedures must attack the causes of the cracks as well as the cracks themselves (Issa et al., 2007).

Nowadays all manufacturers of repair materials try to improve their products in order to give more universal and technologically simpler repair materials for the market.

There are a number of studies carried out on crack repair. In scientific articles it is possible to find about crack repair using cementitious materials with shrinkable polymers (Ahmad et al., 2012; Jefferson et al., 2010), epoxy repair systems (Issa et al., 2007; Shin et al., 2011), synthesizing super-absorbent

resins (Song et al., 2009). Kim Van Tittelboom, Nele De Belie, Willem De Muynck, Willy Verstraete and Jianyun Wang (2010; 2012) recommends to use a bacteria to repair cracks in concrete. Ureolytic bacteria such as *Bacillus sphaericus* are able to precipitate CaCO_3 in their micro-environment by conversion of urea into ammonium and carbonate. The bacterial degradation of urea locally increases the pH and promotes the microbial deposition of carbonate as calcium carbonate in a calcium rich environment. These precipitated crystals can thus fill the cracks. It is of considerable interest to compare commercially available injection materials with cementitious materials and to estimate the suitability of them for the cracks repair in different conditions.

MATERIALS

In the research 3 cementitious mortars (1st without additives, 2nd modified with expansive additive and 3rd modified with polymer additive) and 4 different polymer injection materials were used.

Cementitious mortars were prepared using the Portland cement CEM II/A-L-42,5N, natural sand (fraction 0...1 mm) and water. Sand and water meet the requirements described in European standards EN 13139:2002 and EN 1008:2002. For modification of cementitious mortars the expansive additive (5 % amount from mass of cement) and acryl based polymer additive (10 % amount from mass of cement) were used.

Injection material A is a low viscosity polyurethane-based elastomer resin for use in flexible sealing and filling of cracks, joints and voids in building construction, underground and civil engineering under dry, water-bearing and high-pressure water-bearing conditions.

Injection material *B* is a low viscosity duromer resin based on epoxy for use in rigid filling of cracks, joints and voids in building construction, civil and underground engineering under dry and slightly damp conditions.

Injection material *C* is a polyurethane-based adhesive for use in tamping of cracks and open voids for force fit and non-force fit injection in construction and civil engineering under dry conditions.

Injection material *D* is a low viscosity polymer-modified, acrylic-based hydro-structural resin for use in sealing injection of joints, cracks and cavities in masonry and concrete without reinforcement.

As a base, for the slant shear strength test fine-grained concrete specimens (160×40×40 mm) were prepared using the Portland cement CEM II/A-L-42.5 N, natural sand (fraction 0...4 mm) and water. Sand and water meet the requirements described in European standards EN 13139:2002 and EN 1008:2002.

In order to evaluate the watertightness of the repaired cracks, concrete specimens ($d=150$ mm, $D=180$ mm, $h=150$ mm) were prepared using Portland cement CEM II/A-L-42.5 N, natural gravel (fraction 4...16 mm), natural sand (fraction 0...4 mm) and water. Gravel, sand and water meet the requirements described in European standards EN 12620:2002+A1:2008 and EN 1008:2002. The strength class of concrete specimens C30/37.

TEST METHODS

In order to evaluate the compression and flexural strength of mortars, the specimens (40×40×160 mm) were prepared and tested after 28 days by standard test methods (EN 196-1:2007).

The slant shear strength of the repaired specimens was estimated according to the European standard EN 12615:1999. The principal scheme of specimen used in test is presented in figure 1. Performing a test the specimens were split into the two parts according to the requirements presented in standard.

Subsequently the specimen's parts were pasted with repair materials and tested for compression.

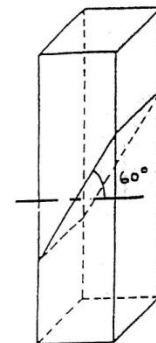


Figure 1. Principal scheme of specimen

The watertightness of repaired cracks was estimated according to the European standard EN 12390-8:2009. Before the test specimens were split into the two parts and pasted with repair materials. The test lasted 72 hours pressing the specimens with 5 atm. water pressure and keeping the close watch on leakage.

TEST RESULTS AND DISCUSSION

In order to estimate the influence of expansive and polymer additives on mortar, the specimens (40×40×160 mm) with and without additives were made, and they were tested after 28 days of solidification (1 day in the form and 27 days in the water). The test results of flexure and compression strength are presented in Table 1.

The test results show that modification of mortar has a positive effect on the mechanical properties of mortar. The compression strength of mortar increased by 12 % using an expansive additive and by 39 % using a polymer additive. The flexure strength of mortar increased by 21 % using an expansive additive and by 6 % using a polymer additive

Table 1

Test results of fresh mortar which are used for crack repair

Cementitious mortar	Flexure strength, N/mm ²	Compression strength, N/mm ²
Non modified cementitious mortar	4.40	20.94
Cementitious mortar modified with expansive additive	5.33	23.50
Cementitious mortar modified with polymer additive	4.68	29.10

During the slant shear test, two different failure types of specimens occurred (Table 2). The failure type of specimens repaired with polymer injection materials *A*, *B* and *D* was cohesive through mortar substrate (A). The failure type of specimens

repaired with all cementitious mortars and polymer injection material *C* was dual (A/B) – partly cohesive through mortar substrate and partly adhesive between mortar substrate and repair material. According to the dual failure results (Table 2) the dominant average (76.7 – 91.2 %) of

failure is cohesive. Summarizing the results it is possible to state that all repair materials carry sufficient adhesive features, because of worst case only 23.3 % of specimen failure was adhesive (between mortar substrate and repair material).

Evaluating the strength of the repaired concrete a slant shear test was used and determined that all the

repair materials had various influences (Figure 2). Comparing the strength of repaired specimens the results can be grouped into three types: a) the strength decreased by more than 5 %; b) the strength decreased under 5 %; c) the strength increased.

Table 2
The specimens failure types

Repaired crack with	Failure, %		
	Type A (cohesive through mortar substrate)	Type B (adhesive between mortar substrate and repair material)	Type A/B (partly cohesive through mortar substrate and partly adhesive between mortar substrate and repair material)
Cementitious mortar	-	-	(82.5/17.5)
Cementitious mortar modified with expansive additive	-	-	(76.7/23.3)
Cementitious mortar modified with polymer additive	-	-	(78.0/22.0)
Polymer injection material A	100	-	-
Polymer injection material B	100	-	-
Polymer injection material C	-	-	(91.2/8.8)
Polymer injection material D	100	-	-

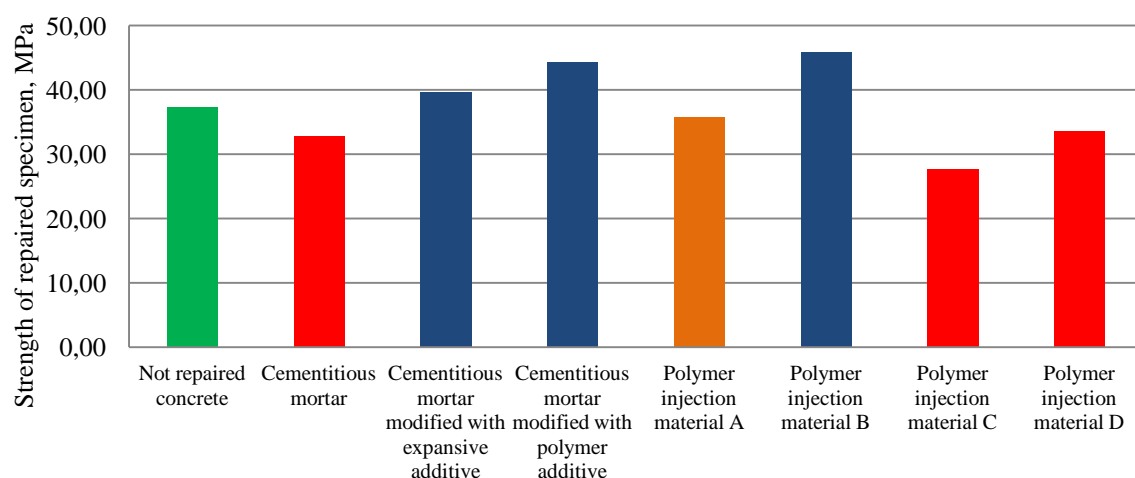


Figure 2. Repair materials influence on specimen strength

In the first group (red color in Figure 2) there are non-modified cementitious mortar (strength decreased by 12.2 %) and injection materials C and D (strength decreased by 25.8 % and 9.9 % respectively). All these materials are not suitable for constructional repair and can be used only for non-

constructional repair. It is noticeable, that according to the manufacturer's technical data of injection materials C and D that they are not useful for constructional repair. These two materials are suitable for moving crack repair, where elastic materials are needed. So the research confirms the

information published in the technical list of materials.

In the second group (orange color in Figure 2), there are injection material A (strength decreased by 4.3 %). As we see the strength loss did not reach 5 %, therefore it can be used for constructional repair.

In the third group (blue color in Figure 2) are cementitious mortars modified with expansive and polymer additives (strength increased by 6.1 % and 15.8 % respectively) and injection material B (strength increased by 18.3 %). The modification of cementitious mortar with an expansive additive decreased the shrinkage deformations, therefore the mortars have better adhesive properties. The

polymer additive increased the sticky properties of the mortar, which partly penetrated into the concrete surface and formed a solid monolith. In all three cases the strength of specimens increased due to the achieved monolithic performance between repair materials and parent concrete.

The results of water tightness test show (Table 3), that all tested injection materials are suitable for the crack's repair when the purpose of repair is hermetisation. The injection materials did not let in water through the repaired specimen over the test time (72 hours). Therefore, these materials are suitable for repair in environmental exposure classes XO, XC, XD, XS and XF.

Table 3
Water tightness of repaired cracks

Repaired concrete with	Water penetration through the specimen time
Cementitious mortar	17 min
Cementitious mortar modified with expansive additive	33 min
Cementitious mortar modified with polymer additive	19 min
Polymer injection material A	> 72 h
Polymer injection material B	> 72 h
Polymer injection material C	> 72 h
Polymer injection material D	> 72 h

The cementitious materials show different results comparing them with injection materials. The water penetrated through the repaired cracks with all cementitious materials in a short time (17 – 33 min). Such fluctuation is connected with shrinkage deformations, which occur during the solidification of mortars. The shrinkage of the solidified concrete is lower during its drying as compared to mortar during its solidification. Using the expansive additive, the comparative shrinkage deformation decreased as compared to the mortar prepared without expansive additive, but not enough. With the weaker shrinkage, acting intermolecular forces become weaker as well, due to which mortar particles lose the bond. This influenced the microcracking in the mortar. In such case, the cementing materials used in research are suitable for repair in the environmental exposure class XO.

CONCLUSIONS

- According to the failure types of the slant shear test the dominant failure is cohesive. Therefore, it is possible to state, that all repair materials used in the research carry sufficient adhesive features.
- The cementitious mortar modified with expansive and polymer additives and injection materials A and B are suitable for constructional repair. Other repair materials (non-modified cementitious mortar and injection materials C and D) used in the research proved to be suitable only for non-constructional repair.
- Having carried out research of water tightness it was determined that all injection materials used in the research are suitable for repair in environmental exposure classes XO, XC, XD, XS and XF. The cementitious mortars used in the research are suitable only for repair in environmental exposure classes XO.

REFERENCES

- Ahmad S., Elahi A., Barbhuiya S. A., Farid Y. (2012) Use of polymer modified mortar in controlling cracks in reinforced concrete beams. *Construction and Building Materials* Vol. 27, p. 91-96.
- EN 196-1:2005 Methods of testing cement - Part 1: Determination of strength.
- EN 1008:2002 Mixing water for concrete - Specification for sampling, testing and assessing the suitability of water, including water recovered from processes in the concrete industry, as mixing water for concrete.
- EN 12390-8:2009 Testing hardened concrete - Part 8: Depth of penetration of water under pressure.

- EN 12615:1999 Products and systems for the protection and repair of concrete structures - Test methods - Determination of slant shear strength.
- EN 12620:2002 Aggregates for concrete.
- EN 13139:2002 Aggregates for mortar.
- Issa C. A., Debs P. (2007) Experimental study of epoxy repairing of cracks in concrete. *Construction and Building Materials* Vol. 21, p. 157-163.
- Jefferson A., Joseph C., Lark R., Isaacs B., Dunn S., Weager B. (2010) A new system for crack closure of cementitious materials using shrinkable polymers. *Cement and Concrete Research* Vol. 40, p. 795-801.
- Poursaei. A., Hansson. C.M. (2008) The influence of longitudinal cracks on the corrosion protection afforded reinforcing steel in high performance concrete. *Cement and Concrete Research* Vol. 38, p. 1098-1105.
- Shin. H.C., Miyauchi. H., Tanaka. K. (2011) An experimental study of fatigue resistance in epoxy injection for cracked mortar and concrete considering the temperature effect. *Construction and Building Materials* Vol. 25, p. 1316-1324.
- Song. X.F., Wei. J.F., He.T.SH. (2009) A method to repair concrete leakage through cracks by synthesizing super-absorbent resin in situ. *Construction and Building Materials* Vol. 23, p. 386-391.
- Thanoon. W.A., Jaafar. M.S., Razali. A., Kardin. A., Noorzaei. J. (2005) Repair and structural performance of initially cracked reinforced concrete slabs. *Construction and Building Materials* Vol. 19, p. 595-603.
- Tittelboom. K.V., De Belie. N., Muynck. W.D., Verstraete. W. (2010) Use of bacteria to repair cracks in concrete. *Cement and Concrete Research* Vol. 40, p. 157-166.
- Wang J., Tittelboom K. V., De Belie N., Verstraete W. (2012) Use of silica gel or polyurethane immobilized bacteria for self-healing concrete. *Construction and Building Materials* Vol. 26, p. 532-540.
- Vidal. T., Castel. A., Francois. R. (2004) Analyzing crack width to predict corrosion in reinforced concrete. *Cement and Concrete Research* Vol. 34, p. 165-174.
- Zhao Y., Yu J., Jin W. (2011) Damage analysis and cracking model of reinforced concrete structures with rebar corrosion. *Corrosion Science* Vol. 53, p. 3388-3397.

ASSESSMENT OF THE EFFECT OF BOUNDARY CONDITIONS ON CYLINDRICAL SHELL MODAL RESPONSES

Eduards Skukis, Kaspars Kalnins, Olgerts Ozolinsh

Riga Technical University

Institute of Materials and Structures

E-mail: eduards.skukis@rtu.lv

ABSTRACT

The modal analysis of circular cylindrical shells with general boundary conditions is rarely studied in the literature probably because of a lack of viable experimental verification. Moreover, the utilization of existing solution procedures, which are often only customized for a specific set of different boundary conditions, can easily be inundated by the variety of possible boundary conditions encountered in the real life practice. Present research focusing on an assessment of boundary condition effects in modal response estimation. For this study a circular cylindrical shells with outer diameter of OD300 employing arbitrary boundary conditions has been fabricated and physically tested. A set of four cylinders with fixed thickness of 0.5 mm has been rolled from the stainless steel AISI 304 grade and joined by plasma welding. The self-frequency measurements have been performed by means of laser scanning vibrometer (Polytech PSV400). Several boundary conditions have been studied during the experimental setup: free/free, simply supported/free and simply supported/simply supported in order to assess the robustness of modal responses. A numerical verification with FE code ANSYS has been performed in parallel in order to demonstrate the accuracy and convergence of the current solutions. The modal characteristics and vibration responses of elastically supported shells are summarized and the effect of various boundary conditions over stiffness configurations has been discussed.

Key words: Circular cylindrical shells; Modal response; Numerical techniques; Boundary conditions.

INTRODUCTION

One of challenges in assessment of self-frequencies of cylindrical shells, the lowest natural frequencies do not necessarily correspond to the lowest number of waves in corresponding modes. In fact, the natural frequencies do not fall in ascending order of the wave index either. Moreover the mode shapes associated to each natural frequency are combination of radial (flexural); longitudinal (axial); and circumferential (torsional) modes. Even though an analytical eigenvalue analysis could be employed as reference for identification of corresponding mode shapes the extraction of similar mode shapes from physical tests may still cause troubles.

In present paper, the modal testing employing fixed response approach was performed to obtain self-frequency modal characteristics of the cylindrical shell in spectrum between 0 and 800 Hz. Identification of the natural frequencies of a structure is normally done through experimental modal analysis (EMA). EMA is primary intended to obtain the structural modal characteristics i.e., natural frequencies, damping coefficient and mode shapes (Bucalem and Bathe, 2011). An influence of the different boundary conditions on structure stiffness parameters was recently studied (by Dai et al. 2012) for development of analytical method the vibration analysis of circular cylindrical shells with arbitrary boundary conditions. Nevertheless such a

method could not be utilised for identification of material properties as it has been shown by (Čate et al. 2001; Alzahabi and Natarajan 2003). In those studies applying the finite element method allowed to determine and to optimise the dynamic response of the cylindrical structures. For this particular study two different types of boundary conditions were primary selected: free-free boundary conditions and a single edge axially supported (UZ) identified as pinned/free boundary conditions as described in Fig. 1. Four different cylinders having two different manufacturing approaches (one or two longitudinal welds) have been studied. Experimental modal response data was compared with the finite element modal analyses. Laser vibrometer equipment has been utilised for modal excitation and self-frequency mode capture.

ANALYSIS APPROACH

Geometry of the Cylindrical Shell

The specimens have been produced by rolling of thin stainless steel sheet ($t = 0.5$ mm) in line with longitudinal plasma joint welds has been utilised to form a cylindrical shell structure. Two shells per each manufacturing type were realized: single and double longitudinal weld specimens. No further weld treatment was made, thus a slight deformation of welding line was noted. Nevertheless these geometrical imperfections haven't been further

implemented in finite element simulations. Moreover a 2 mm drill holes has been processed in order to hang the specimen in rubber slings and to form a free from any restrictions a boundary conditions.

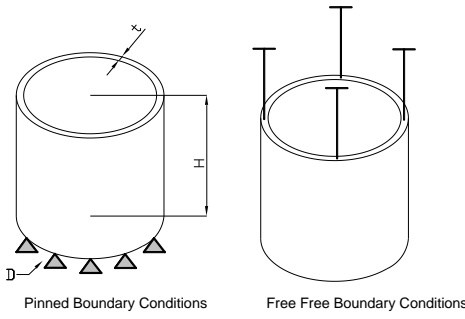


Figure 1. The dimension parameters of the cylindrical shell

The geometry of manufactured cylindrical shells were met following dimensions: outer diameter: $D=300\text{mm}$ and the free length $L=400\text{mm}$. The material properties defined for finite element analysis have been extracted from material datasheets for AISI type 304 stainless steel are listed in Table 1.

Table 1
The material properties of the AISI 304.

Material Properties	Value
Young's modulus (E)	193-200 [GPa]
Shear's modulus (G)	86 [GPa]
Density (ρ)	7850 [kg/m^3]

Finite Element Mesh Convergence Study

All numerical calculation has been performed employing FEM commercial code ANSYS. The 8-node element Shell 281 has been selected for study as this element is most suitable for analysing thin to moderately-thick shell isotropic/anisotropic structures including material properties as plasticity etc. A geometrically perfect cylinder model has been considered neglecting the weld seams and weld/handling related deformations.

Furthermore one of most essential features dealing with finite element method (FEM) is correct selection of mesh density. Therefore a particular attention has been denoted to mesh correlation analysis in order to establish optimal ratio between mesh density and computational time and eigenfrequency sensitivity. Obtained convergence results are summarised in Table 2.

Experimental Modal Analysis

For physical measurement of self-frequencies and vibration modes a non-contact measurement, visualization and analysis vibrometer PSV-400 has

been employed. A test set up scheme is presented in the Fig. 2. Due excitation a vibrometer has a potential to determine the natural frequency modes and nodal accelerations from entire testing surface

Table 2
Verification of Eigenfrequencies and Eigenmodes (BC: UZ).

Nr.	Eigenmodes	D/a		
		24	12	6
(1&2)		14.82	14.82	14.83
(3&4)		41.93	41.94	42.02
(5&6)		80.39	80.43	80.92
(7&8)		130.0	130.20	132.00

in planar view. The measurement process can be scanned and probed automatically using flexible and interactive measurement grids. Measurements can be made over a wide frequency bandwidth in current test set-up up to 300Hz. Depending on structure stiffness, excitation of the structure could be made by the software controllable piezoelectric sensor, excitation hammer or loudspeaker. It should be noted that for set-up with 122 scan point grid a full measurement scan cycle is up to 70 minutes and if the grid is extended to 448 points a single test may lead up to 270 minutes.

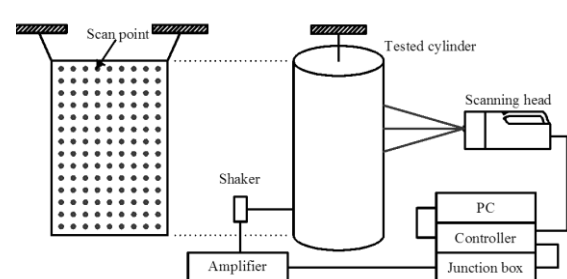


Figure 2. Experimental Measurement Set-up for Cylindrical Shell

SELF FREQUENCY VERIFICATION WITH EIGENFREQUENCY RESULTS

Captured frequency response has been measured in form of amplitude M versus frequency f range such graphs are plotted in Fig. 3. and Fig. 4. For initial test set up a cylinder has been positioned on testing table, therefore boundary condition has been assumed single edge axially supported in Fig. 3 and free/free boundary conditions for Fig. 4. For given boundary conditions, one may observe that all initial six self-frequencies are within range of up to 300Hz. Moreover among all four specimens amplitude peaks are close to each other, thus confirming robustness of manufacturing process. One may observe that for larger diameter cylinders frequency range of up to 300Hz contains more than ten initial frequencies. Furthermore it should be noted that higher frequencies develop a scatter among tested specimens which could be explained with insufficient structural stiffness.

It should be noted that for free/free boundary conditions the first vibration mode and self-frequency could not be determined from dynamic tests as large scatter has been overlapped. Moreover cylinders with double side welds had comparatively lower self-frequencies and some shift for lower frequencies and frequencies above 200 Hz. Moreover it could be observed that often for each frequency corresponding two vibration modes which has 90° inclinations among each other.

Similar results have been observed earlier by (Čate et al. 2001).

Verification study overlaying the FEM eigenfrequency results over experimental results of cylinders has been performed and given in Table 5. It has been noted that by increment of cylinder diameter the eigenmodes becomes finer and easier to identify and to compare with FEM. Nevertheless it is not easy to identify both vibration modes corresponding to each eigenmode as in case of finite element calculations. A statistical estimate of divergence among numerical and dynamical test results is outlined in Table 6. It should be noted that OD300 specimens with two side welds have lower discrepancy among the analysis and test results showing an average (AVE) error below 2%. Nevertheless the highest divergence from numerical and physical model is systematically observed in initial frequencies which indicate insufficient stiffness in boundary conditions. At the same time it could be generalised that specimens with only one side weld are more robust and showing lower than 4% error margin where additional weld actually increase the average error up to 6%.

Moreover from physical tests one may recognise that measurements up to 50Hz range show low fidelity and high noise level. This is due free boundary conditions on one our both sides however these values has to be neglected in numerical verification study.

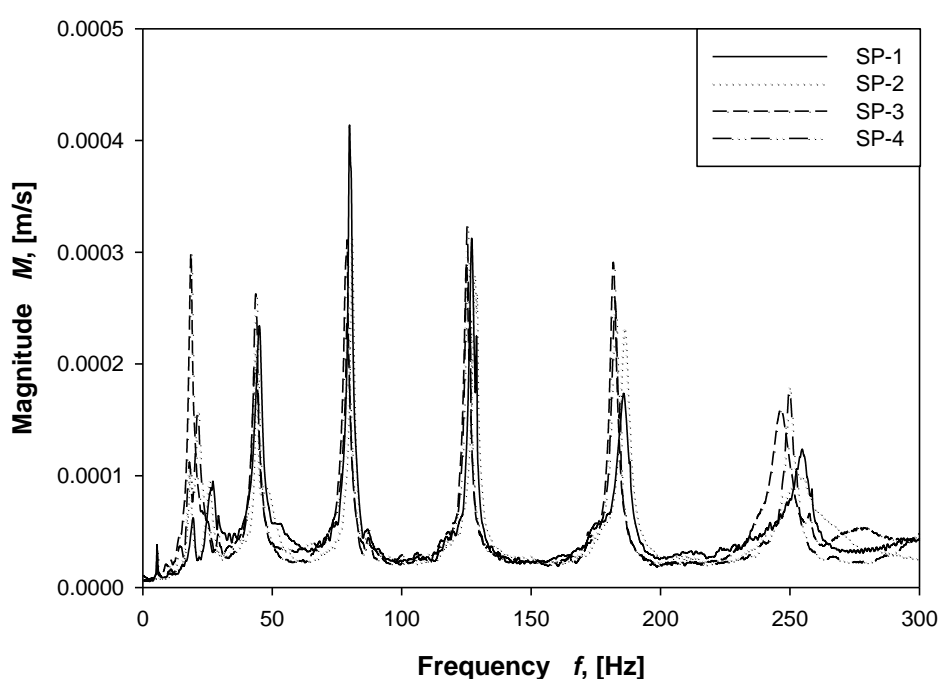


Figure 3. Self-frequency response for specimen OD300 (BC: Single edge pinned)

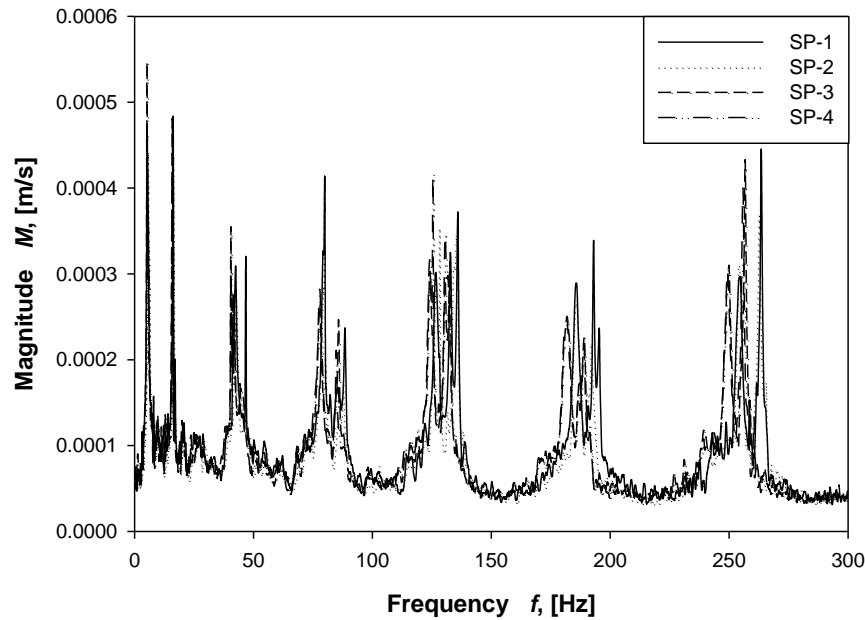


Figure 4. Self-frequency response for specimen OD300 (BC: Free/Free)

Verification among self -frequency mode and eigenfrequency modes are demonstrated in Table 5, where one may observe that in both numerical and experimental study each frequency is associated with similar pair of vibration modes. Furthermore an annotation of number of symmetrical half waves propagated through the structure has been identified and noted as Nr*, where 0 means symmetrical straight mode, and 1 stands for symmetrical one half wave mode. More than one half waves could be observed in much higher frequencies like 13&14, thus is not shown in current example.

For verification of experimental results as a reference has been set the FEM eigenfrequency

values and then extracted the divergence in form of percentage error summarised in Table 6. It should be noted that for initial self-frequency values a significant (above 10% for free/free boundary conditions and above 20% for single side pinned boundary conditions) systematical scatter of results could be observed. This suggests and confirms that for cylinders boundary conditions significantly influence physical response of the structure. Having this in mind one may conclude that non-destructive determination of cylindrical structure by vibration tests would not be efficient and reliable means for determining of mechanical properties as long the structure is not placed in final assembly state.

Table 5
Verification of Self-frequencies and Vibration modes (BC: Free / Free).

FEM							
EXPERIMENT							
	126.5	128	133.3	135.5	185.7	191.7	199.4
Nr *.	0	0	1	1	0	1	1
	253.8						

Table 6

Validation of numerical versus experimental frequency responses (BC: UZ and Free / Free).

	BC: FREE/FREE					BC: Single side pinned				
	FEM	AVE (SP-1, SP-2)	Δ, %	AVE (SP-3, SP-4)	Δ, %	FEM	AVE (SP-1, SP-2)	Δ, %	AVE (SP-3, SP-4)	Δ, %
(1&2)	14.8	Too high experimental noise			14.8	18.7	21.1	18.3	19.1	
(3&4)	18.0	16.2	10.0	15.8	12.1	41.9	44.4	5.6	43.8	4.3
		17	5.3							
(5&6)	42.0	41.3	1.6	40.5	3.5	80.4	80.5	0.1	78.9	-1.9
		42.5	-1.3	41.7	0.7					
(7&8)	46.6	46.8	-0.3	44.3	5.1	130.0	127.5	-2.0	125.2	-3.8
							128.9	-0.9	126.5	-2.8
(9&10)	80.5	79.4	1.3	77.9	3.2	191.0	185.8	-3.0	182.2	-4.8
		80	0.6						184.5	-3.5
		AVG	2.5	AVE	4.92		AVE	6.0	AVE	5.7

CONCLUSIONS

It has been physically and experimentally demonstrated that for determination of self-frequencies of thin walled cylinder structures the boundary conditions are essential to obtain reliable results. It has been confirmed that for cylinder structure without edge restraints a couple of initial self-frequency modes may be lost in numerical noise. By adding at least one side restraints all modes could be determined physically, however again initial self-frequency mode one has unreliable discrepancy compared to numerical results. This is due fact that thin-walled cylinder is so tolerant to geometrical imperfections and only proper boundary conditions may assure the nominal geometry of the structure. Results obtained during experimental investigations confirmed, that further

investigations should be carried out for the specimens with clamped or simply supported boundary conditions, which improves structure stiffness and let to extend the research towards buckling versus frequency response for loaded specimens.

Experimental investigations reviled that all of the specimens are thoroughly manufactured employing the same quality manufacturing practice, without influence in structural performance. In order to improve the agreement with FE analyses, a further mechanical properties of the material used should be studied by the small coupon testing.

REFERENCES

- Alzahabi, B., Natarajan, L. K. (2003) Frequency Response Optimization of Cylindrical Shells using MSC.NASTRAN. In: *The 1st International Conference on Finite Element Process*, Luxembourg City, LUXFEM, Luxembourg
- “ANSYS” (2007), Inc., Theory Reference for ANSYS and ANSYS Workbench Release 11.0, Canonsburg, PA. [online] [accessed on 01.04.2013].
- Available: <http://progdata.umflint.edu/MAZUMDER/ANSYS/Theory%20of%20ANSYS.pdf>
- Bucalem, M. L. and Bathe, K. J. (2011) *The Mechanics of Solid and Structures: Hierarchical Modeling and the Finite Element Solution*, Springer Verlag.
- Čate A., Rikards R., Ozoliņš O. (2001) Analysis for Buckling and Vibrations of Composite Stiffened Shells and Plates. *Composite Structures*. Vol. 51, p. 361-370.
- Dai, L.a, Yang, T.a, Li, W.L.b, Du, J.a, Jin, G.a (2012) Dynamic analysis of circular cylindrical shells with general boundary conditions using modified fourier series method. *Journal of Vibration and Acoustics*, Vol. 134, No. 4.
- Shah, A.G., Mahmood, T., Naeem, M.N. (2009) Vibrations of FGM thin cylindrical shells with exponential volume fraction law. *Applied Mathematics and Mechanics*. Vol. 30, No. 5, p. 607-615

EVALUATION OF GLASS IN DESIGN OF LOAD BEARING STRUCTURES

Liene Sable*, Kaspars Kalnins**

Riga Technical University

Institute of Materials and Structures

E-mail: *lienesable@gmail.com, **kaspars.kalnins@sigmanet.lv

ABSTRACT

Transparent glass staircase landings platforms are one of the load bearing structural components which do not have established design practice by national or international codes. Experimental tests are practically only option to assess the behavior of glass and to certificate it. Glass may be assumed as isotropic material; mechanical properties do not depend on direction for orientation thus easy for modeling. The main issue once designing staircase landings assumptions of critical stress in particular as tensile and in certain extend bending strength of glass is not a constant value. This stress level depending on glass type, location of the load and glass laminate panel compilation. This paper presents the assessment of the existing design practice in contrary to physical experiments of single glass stair landing plate. In order to perform an optimization task, different kinds of glass samples have been tested in 4-point bending using testing equipment INSTRON 8802. Bending test settings are correspond to LVS EN 1288-3 standard requirements and based on similar research performed earlier at DTU Netherlands. The results demonstrated that the glass mechanical and physical properties such as Young's modulus, the Poisson ratio and the density, of the annealed and tempered glass are practically the same nevertheless the bending stress is dependent on glass type.

Key words: glass, 4-point bending, tempered glass, annealed glass, finite element analysis

INTRODUCTION

In 21st century the glass is not anymore considered just as a material for producing household goods, but becoming a material widely utilised in load bearing structures. This is due fact that production quality has improved dramatically and building industry has progressed like never before.

Initially glass as material is obtained liquid cooled to the rigid state without crystallizing. Raw materials for glass production are 75% silica (SiO_2), sodium oxide Na_2O from soda ash, lime CaO , and several minor additives. (Button, 1993) In the production process all ingredients were heated at a temperature much higher than 1200°C . (Button, 1993) The main advantage of the application of glass is its high mechanical and physical properties. At the same time glass is well known for its fragile and brittle/ instantaneous collapse behaviour which does not encourage designers to sufficiently exploit glass material.

This is due fact that at higher levels of stress most materials deform plastically, that is the atoms or molecules in the structure become rearranged or crystals slide past each other. These materials can often accommodate large strains without failure, although they may be permanently deformed. (Button, 1993) The structure of glass cannot accommodate this plastic deformation, so the stress-strain curves for glass show perfect linearity. (Button, 1993) Such behaviour is easy to simulate in modern analysis codes, however requires robust and reliable knowledge of glass failure stress levels.

General ceramic including glass material properties are described by U.S. researchers Marshall W. and Rudnicki A. (Marshall et al.) which are basis of defining character of the glass. Mathematical calculations for determination of mechanical properties from 3 and 4 point bending tests, assuming that samples have a square cross-section have been developed by Davies G.S. (1972) (Davies, 1973). Moreover, this approach has been extended for circular cross-section by Kittl.P (1978), Medrano R.E and Grills P.P (1978) (Kittl, 1980). There are several alternative bending methods, for example, one of the most specific test method is "Brazil" disk test method, described by Handros G. (1974) and Oh. K.P. and co-authors (1973) (Migliore et al., 1996).

Glass brittle failure is the reason why it is necessary to clarify the failure strength of glass in bending. Delft University of Technology had developed a whole series of glass bending tests. F.A. Veer (Veer, 2007) main research related to the bending strength for different types of glass samples in 4 point bending, setting the average failure stress values, which depend on the sample size. Bending tests values can be employed for load-bearing structural calculation, which display actual situation for glass's behaviour.

For tailor made glass designs, one may require curved glass which do change the mechanical performance of the glass. J.Belis, et. al. have set an experimental study investigating curved glass to design for design "cold bending" processing (Belis et al., 2007).

Recent research by Maria Froling (Froling, 2011) has demonstrated the advanced strength design approach for laminated glass, applying numerical solid-shell element of the commercial finite element software ABAQUS and established the maximum principal stresses for laminated glass samples with holes for bolt binding.

MATERIALS AND METHODS

FEM solution

For the highest design reliability, particularly when applying a material which is not commonly utilized by civil engineers, one of strategies is to employ a detailed design finite element engineering simulation software. This creates an alternative to physical test as set up of a numerical model has to be prepared as close to the actual physical model as possible. The finite element method (*FEM*) software ANSYS 11.0 was utilized for simulation as it has sole potential for design of various complexity structural components. In ANSYS code the model is divided into finite elements for analyzing thin to moderately thick shell structures (Figure 1), in the current research the 4-node SHELL 181 elements.

The main goal was verify the numerical results against the experimental test data.

A single glass sheet has been tested initially and then manufactured glass laminate decks composed from two to three glass sheets. Mechanical properties which has been assumed in numerical simulation were density $\rho=2500\text{kg/m}^3$ (prEN 13474-3, 2008), Young Modulus $E=70\text{kN/mm}^2$ (prEN 13474-3, 2008) and Poisson's ratio $\nu=0.23$ (prEN 13474-3, 2008).

Experimental investigation

All glass panels have been tested in 4-point bending set up according to LVS EN 1288-3:2001 (LVS EN 1288-3, 2001) at the Riga Technical University, Institute of Materials and Structures (IMS). For bending tests was utilised INSTRON 8802 testing machine (Figure 2), which can perform tests in tension, compression, bending and fatigue. It can be set up to do static and dynamic loads up to a maximum load of 250 kN.

Glass panel samples of size $L_p=1100\text{ mm}\pm5\text{mm}$ long and $b_p=360\text{mm}\pm5\text{mm}$ wide were cut from a single glass plate with a thickness of 10 mm (h_p). These were industrially cut on cutting machines and finished by grinding and polishing as required for the best quality glass product. The distance between supports was assumed to be constant of 1000 mm and the distance between the loading points set 200 mm.

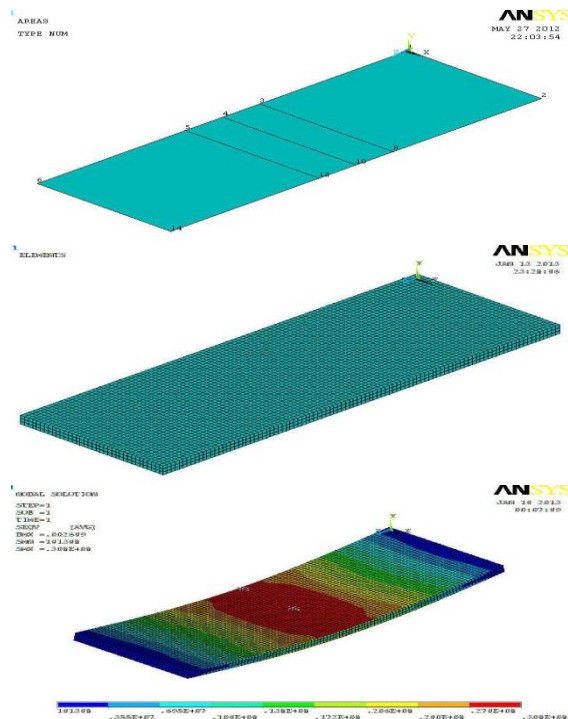


Figure 1. a) model geometry; b) FE meshed structure; c) deformed state

All specimens were divided in three groups for tests (Figure 2a): annealed float glass without polishing edges (AN); annealed glass with polishing edges (AP); tempered glass (T).

After estimation of the mechanical behaviour of each type of glass samples, these sheets were laminated in given combinations (Table 1). A glass laminate test set up is given in (Figure 2b).

Table 1
Laminated glass samples

	T	A^+	A^+	T	A^-
	A^+	T	A^+	A^+	A^-
	T	A^+	T		A^-
Number of samples	1	1	1	1	2

where T-tempered glass;
A-annealed glass;
+-with polishing edges;
--without polishing edges.

The main emphasis for testing of glass laminates in four point bending set up, was establishing the strength relationship among tempered and annealed glasses. Estimated mechanical behavior confirmed that stiffness properties are similar among these two glass types.

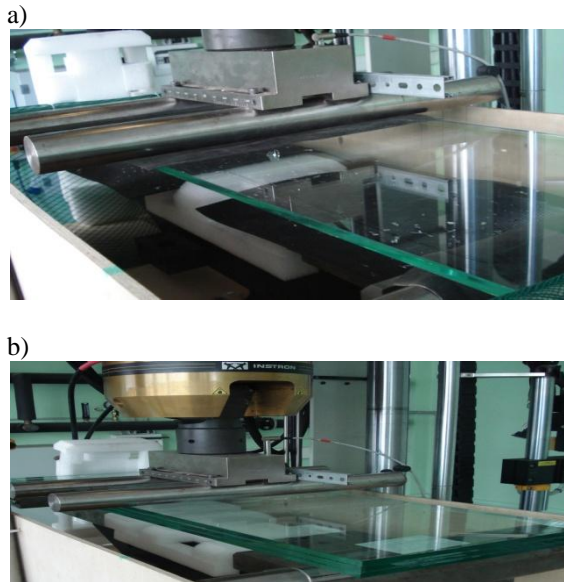


Figure 2. a) single glass sheet sample b) laminated glass sample in bending test set up (INSTRON 8802)

RESULTS AND DISCUSSION

Single glass sheet samples

Indeed it is evidently that glass is brittle and once reaching the ultimate load fails instantly. It would be of advantage if one may determinate the cause of the failure for glass only from size and shape of broken glass samples as it is for concrete samples. One of the factors influencing load carrying capacity of glass is micro cracks (Button, 1993). Conventional glass cutting is done by "scoring" and breaking which produces micro-cracks (Mangeron, 2010) an alternative is stress concentration during the transportation and handling. Even if they are up to 100 micro meters, it may be sufficient reason for the reduction in bending strength of the glass, especially vital in load-bearing structures.

During the physical experiments, before sample has been placed in bench, it has been visually examined whether annealed glass edges hasn't been damaged during the transportation. After examining, it was concluded that no visual damage had been observed, so it can be assumed that the samples could be accepted for testing of mechanical properties.

Once brittle fracture was observed the annealed float glass samples without polished edges (Figure 3.a) crumbled into tiny, incisive, elongated fragments, forming a triangle or rectangular-shaped area at the site where the load has been applied. The sample of span length of about 30 cm in width remained solid. It suggests that this type of glass breaks in areas where stress concentrations have accrued.

Table 2
Test results for annealed glass samples without polishing edges

Number of test	Failure load F_{max} [N]	Deflection u [mm]	Young's Modulus E [GPa]	Bending strength F_m [MPa]
1AN	692	6.1	94.6	23.1
2AN	1 467	12.9	92.0	48.9
3AN	1 549	13.6	89.5	51.6
4AN	948	8.3	93.6	31.6
5AN	1 021	9.1	90.7	34.0
6AN	990	8.7	93.8	33.0

In the next step annealed glass samples were tested (Figure 3.b). It should be noted that specimen had polished edges which basically eliminates any possibility of micro cracks. Bending strength of this type of glass samples resulted in load-bearing capacity increment of 1.5 times higher than initial sample (Table 3).

This finding may suggest that the glass is one of those materials, whose behaviour of the load response depends on the quality of the glass. For samples with polished edges one may observe a small inconsistency of the results, thus one recommendation may be concluded that special attention should be given to sample preparation. Furthermore, annealed glass samples with polished edges once failed, form a set of small, elongated and sharp pieces, under load, but unlike the previous panels, these samples are of collapse were larger with size range from a few mm to 20 cm.

Table 3
Test results for annealed glass samples with polishing edges

Number of test	Failure load F_{max} [N]	Deflection u [mm]	Young's Modulus E [GPa]	Bending strength F_m [MPa]
1AP	1 664	13.4	92.1	55.5
2AP	1 497	13.3	89.2	50.0
3AP	1 709	15.0	92.1	57.0
4AP	2 031	17.9	91.8	67.7
5AP	1 242	11.0	104.5	41.4
6AP	1 609	14.1	117.0	53.6

Finally one may observe that tempered glass (Figure 3.c) bending strength is almost twice higher than annealed glass (Table 3). Meanwhile, one may see that once reaching the maximum bending stress the sample broke into enormous small around 2-5 mm to 2 cm "crystals", Such result was observed in five samples out of six in each set (Table 4). The modulus of elasticity of glass is typically assumed to be 70 GPa, only about a third of that of steel but five times greater than hardwood. (Wurm, 2007) It should be noted that after thermal enhancement of glass the Young's modulus doesn't change (Table2) or the difference is insignificant. For tempered and annealed glass modulus of elasticity it may be assumed exactly the same. In present research the

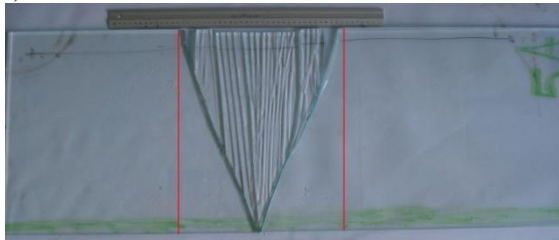
tests average value for modulus of elasticity is 88 ± 6 GPa.

Table 4

Test results for tempered glass

Number of test	Failure load F_{max} [N]	Deflection u [mm]	Young's Modulus E [GPa]	Bending strength Fm [MPa]
1T	3 764	30.3	79.0	125.5
2T	4 243	38.2	74.7	141.4
3T	3 458	30.6	72.8	115.3
4T	3 974	35.5	75.1	132.5
5T	4 390	39.0	72.9	146.3
6T	3 896	34.4	75.2	129.9

a)



b)



c)



Figure 3. Samples after testing a) annealed glass without polishing edges, b) annealed glass with polishing glass, c) tempered glass

Laminated glass samples

The current Latvian legislation has not developed rules which provide a combination for glass (tempered and annealed) for load bearing structural applications. In European for design of staircase landings the choice is made to apply the annealed glass only because, the strength of the laminate is sufficient and these types of glasses do not contain nickel sulphide (Barry) in contrary to tempered glass.

Table 5

Test results for laminated glass

Number of test	Thickness h_l [mm]	Failure load F_{max} [N]	Deflection u_f [mm]	Bending strength Fm_l [MPa]
TAT	32.58	20 002	21.1	157.0
ATA	32.85	9 006	7.0	69.5
AAT	32.63	7 398	22.5	57.9
TA	21.30	2 825	6.4	51.9
AAA	33.29	8 513	6.8	64.0
AAA	33.28	8 557	6.8	64.4

a)



b)



c)



d)



e)

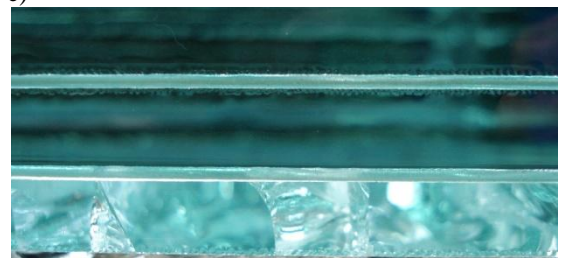


Figure 4. Laminated samples after testing a) TAT, b) ATA, c) AAT, d) TA, e) AAA

Laminated glasses typically consist of three glass plates bonded by a polyvinyl butyral (PVB) interlayer (Table1). This kind of combination is the

basis for glass stair step, so it was important to conduct an experiment and find the corresponding behaviour in bending.

One may observe that the best combinations are that in which in tension zone tempered glass sheet was placed (Table 5). Such a solution provides tension zone stability (Figure 4a, 4c).

Once inserting an annealed glass between two tempered glasses (Figure 4a) as middle layer is unable to hold high bending strength which was generated in the top and bottom tempered glass sheets. All laminate samples has crashed in a they characteristic manner as described in previously test (Figure 4b, 4d).

Figure 5,6,7 summarise verification among the physical test and numerical model showing that the calculation is identically corresponding to single sheet glass (Figure 5) panel only. A laminate consisting of two (Figure 6) or three (Figure 7) sheets, should be modelled involving a thin polymer thin film as there is no sufficient stiffness if adhesive film layer. It should be noted that those plies haven't been considerate in the FE simulation. Thus differences in response can be observed in the bending stiffness. For further studies both adhesive film properties and failure criteria should be implemented in this preliminary study.

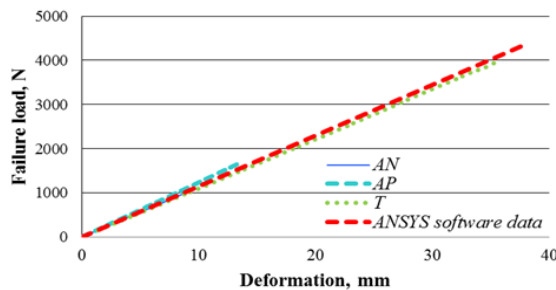


Figure 5. Experimental data compared with ANSYS results for single sheet glass samples

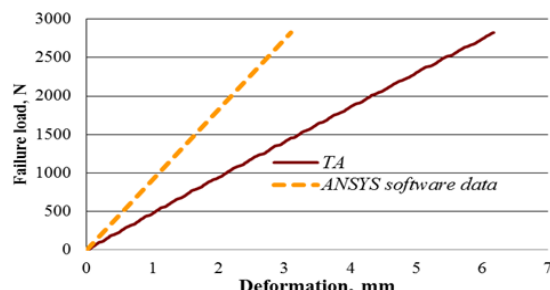


Figure 6. Experimental data compared with ANSYS results for two layers samples

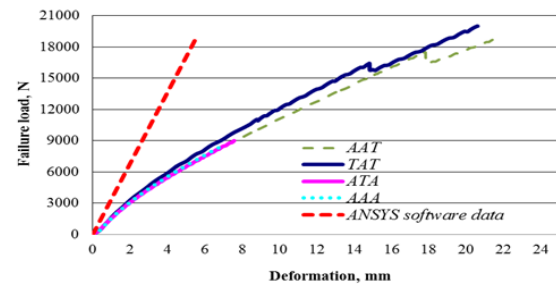


Figure 7. Experimental data compared with ANSYS results for three layers samples

Metamodelling approach

Metamodelling is a set of tools, based on design of experiments and approximation of mathematical model of the system. Approximation model should be unsophisticated enough to guarantee short calculation times at the same time keeping sufficient prediction accuracy – for example determined applying cross-validation error estimation. The main steps in design optimization process employing metamodels are: a) defining the design space of the experiments, b) selecting factors (independent variables) and responses (dependent variables), c) setting levels of each factor according prescribed plan of experiments, d) conducting of experiments and recording the system behaviour, e) approximation of system responses, f) minimizing or maximizing responses using approximation model, g) development of recommendations for further product modification.

For creating of efficient design guidelines, three cross-section parameters of the plate have been defined in Table 6.

Table 6

Domain of interest			
Parameters	Units	Lower bound	Upper bound
Length L	m	0.6	2.4
Width B	m	0.22	0.4
Thickness T_1, T_2	m	0.003	0.019

Design of experiments was made employing Latin Hypercube design with Mean Square Error (MSE) space filling criteria in order to uniformly redistribute the points inside domain of interests.

In order to obtain statistically reliable mathematical approximation functions it is necessary to carry out a definite number of numerical experiments. *EdaOpt* (Auzins, 2007) optimisation software was used to create experimental design with 120 and 140 experiments and 3 variables. For approximation purposes freeware software *VariReg* was utilised with ability to approximate experimental data by full or partial polynomials and Kriging. Analysing error estimates was concluded that the smallest

error was conducted by partial polynomial function based on Adaptive Basis Function Construction (ABFC).

This approach allows generating polynomials of arbitrary complexity and degree without the requirement to predefined any functions or to set the maximal degree of the polynomial- all the required basis functions are constructed adaptively specifically for the data at hand. (Jekabsons, 2010)

Verification of the optimisation results

For design of glass material stair landings, the main load need to be considered is load equivalent to human weight. Thus the development of an optimal design practice a load level was assumed at 125 kg and panel is simply supported at both ends of the panel. Summarising the experimental results, one may draw a conclusion that the single glass can take a significant load, but for increased level of safety the stair should be laminated from at least two sheets of glass which bonded together by a polyvinyl butyral (PVB) interlayer. The PVB-material is a rubber like elastomer that keeps the shards of broken glass plates in the frame of the glass unit after the failure. (Hills, 2006)

The graphs show (Figure 8, 9, 10) the optimal step thickness dependence versus span length at a limiting relative deformation level. The step width is assumed constant 0.35 m and 1 kN load is applied. If the glass panel span is longer, than glass thickness is thicker. The optimal configurations found for a single sheet panel of maximum span is set at 2.0 m and glass thickness 19 mm (Figure 8). For two (Figure 9) and three (Figure 10) sheet glass laminate the thickness is smaller but span may be extended.

In order to create a staircase glass landing optimal design guidelines, two most important parameters were assessed. The landing span and width parameters have been evaluated and obtained graphs indicate (Figure 11, 12, 13), that thickness decreases if the glass width increases.

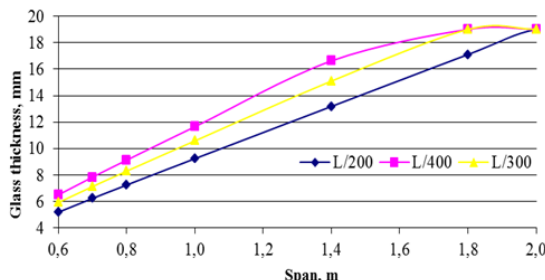


Figure 8. Glass thickness depending on the span of step: for one layer glass

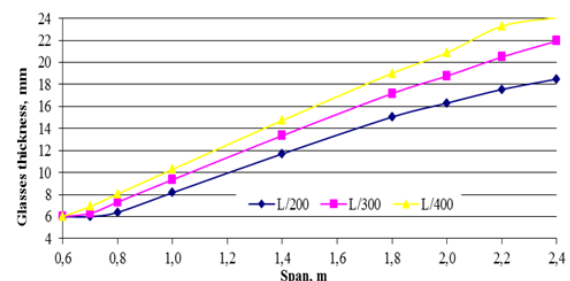


Figure 9. Glass thickness depending on the span of step: for two layers glass

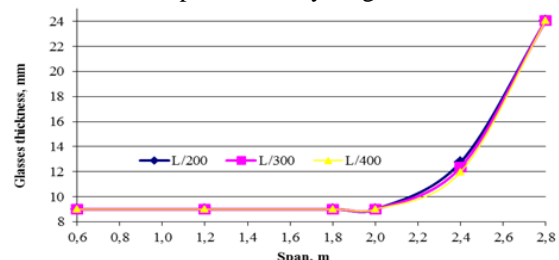


Figure 10. Glass thickness depending on the span of step: for three layers glass

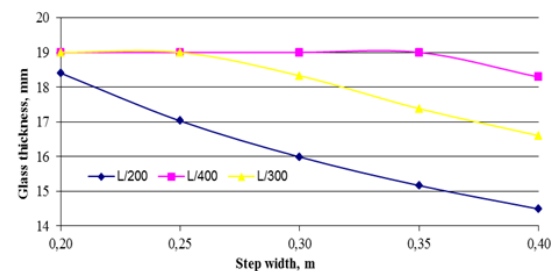


Figure 11. Glass thickness depending on the step width: for one layer glass

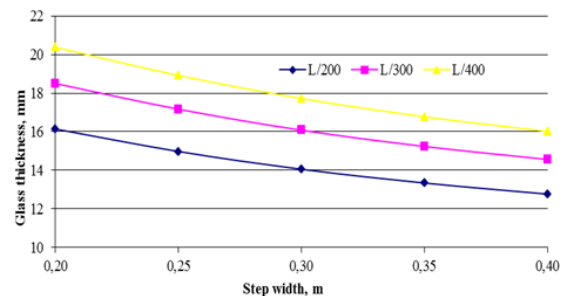


Figure 12. Glass thickness depending on the step width: for two layer glass

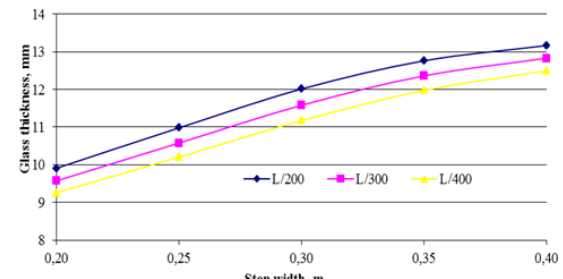


Figure 13. Glass thickness depending on the step width: for three layer glass

CONCLUSIONS

It may be concluded and confirmed that for structural designing one may assume Young's modulus for glass 70 GPa however actual, experimental results confirm a much higher modulus of elasticity reaching 88 ± 5 GPa value. Moreover it was confirmed that for tempered and annealed glass, the modulus of elasticity may be assumed equivalent or the difference is insignificant. In order to achieve a high load carrying capacity, annealed glass edges should be polished, then load carrying capacity will increase up to 1.5 times compared to annealed glass without polished edges. Tempered glass is useful for load-bearing constructions because its bending strength, deflection and relative deflection are at least three times higher than for annealed glass.

After experimental data and calculation of the relative deformation of the glass sheet, it can be assumed that annealed glass relative deflection range of annealed glass is from L/300 to L/250, for tempered glass the same configurations, but the design margins may be increased by at least 70%. For design of laminated stair glass step the highest load - bearing characteristics may be achieved if the tempered glass is placed in the tension zone. Such a design will increase the load carrying capacity, compared with the all annealed glass combination at least 3 times. Optimizing the glass landing dimensions, it should be noted, that increasing the span length proportionally increases the glass thickness or step's width. Drawing up the triplex design, the lower sheet of the pack should be thicker glass than the other parts, moreover, it should be tempered as well.

REFERENCES

- Belis J., Inghelbrecht B., Impe R.V., Callewaert D., *Cold bending of laminate glass panels*. HERON Vol.52, 2007, p. 123- 146.
- Davies, G.S. In Proc. N 22- British Ceramic Society. 1973. Edited by D. J. Godfrey. British Ceramic Society, Stoke-on-Trent. Proceeding of the Meeting in Cambridge, July 1972. P 429.
- European Standard DRAFT prEN 13474-3*, Berlin, June 2008
- Froling M., *Strength design methods for laminated glass*. Lund University, 2011.
- Haldimann M., *Fracture strength of structural glass elements- analytical and numerical modelling, testing and design*. THESE N°3671, Switzerland, 2006, p.202.
- Hills, D.A., "Analysis, modelling, and optimization of laminated glasses as plane beam." International Journal of Solids abvnd Structures 43, Bulgaria, 2006, pp.6887-6907.
- Kittl, P. Res. Mechanica, 1980, 1,161.
- LVS EN 1288-3:2001 "Glass in building-Determination of the bending strength of glass- Part3: Test with specimen supported at two points (four point bending)", Brussels, 2001.
- Mangeron D., *Glasses as engineering materials: A review*. Gh. Asachi Technical University of Iasi, Romania, 2010.
- Marschall, W.&Rudnick A. *In Fracture mechanics of ceramics*. Vol.1. Plenum Press, New York. P.69.
- Migliore A.R. Jnr & Zanotto E.D., *Fracture strength of glass analysed by different testing procedures*. Glass Technology Vol37, No3, Brazil, 1996, p. 95- 98.
- Veer F.A., Boss F.P., Zuidema J., Romein T. *Description of the experiment: Strength and fracture behaviour of annealed and tempered float glass*. Delft University of Technology, 2005.
- Veer F.A., *The strength of glass, a nontransparent value*. HERON Vol.52, 2007, p. 88- 104.
- Button D., at el. *Glass in buildings: a guide to modern architectural glass performance*.- England, 1993,p. 372.
- Jekabsons G. *A software tool for regression modelling using various modelling methods*. RTU, 2010
- Auziņš J., Januševskis A. (2007) *Eksperimentu plānošana un analīze*. Riga, RTU publishing. p. 208. (in Latvian lang.)
- Wurm J. *Glass structures: design and construction of self-supporting skins*. Springer, 2007.p. 255.
- Barry J. Toughened glass: A wonderful material, but with an "Achilles heel" [online][accessed on 15.01.2013.]

BUILDING CONSTRUCTIONS MADE OF PERFORATED METALLIC MATERIALS

Mihails Lisičins*, Viktors Mironovs**

Riga Technical University, Faculty of Civil Engineering, Institute of Building Production

E-mail: *mihails.lisicins@gmail.com, **viktors.mironovs@gmail.com

Irina Boiko

Riga Technical University, Institute of Mechanical Engineering

E-mail: irinaboyko@inbox.lv

ABSTRACT

The formation of cellular building constructions made of perforated steel band is presented in the paper. The information about the main mechanical properties of perforated tapes and plates is provided. Basic technological methods for obtaining cellular structures from perforated metallic tape achieved from waste material by stamping are suggested. The main attention is focused on the analysis of the compressive strength of key elements of cellular structures. Examples of the use of cellular structures made of perforated metallic materials in building construction are given. Special attention is paid to the manufacturing of sandwich panels based on a honeycomb structure made of perforated metal tape.

Key words: metallic sheets and profiles, perforation, welding, sandwich panels

INTRODUCTION

Perforated metallic materials have a big potential to be used in construction. Stiffness, strength and elastic/plastic properties of perforated metallic materials open up good opportunities for their wide range of use in the building industry.

For example they could be used as spacers for wall and floor constructions, reinforcement materials, fixtures and connectors for nodes of wooden constructions, etc. (Ozola, 2011; Kalva, 2011) Because of high strength, light weight, good painting abilities and easy installation, perforated materials are becoming widely used in the design of building facades.

The main aim of the investigation is to propose different cellular building structures and constructions made from perforated plates or tapes.

MATERIALS AND METHODS

The properties of perforated metallic materials as end products directly depend on the mechanical and technological properties, intended perforation types, shapes, sizes, steps and other characteristics of used material. The technology of perforation also affects mechanical properties of the perforated end product. In order to select the required perforation technology and related equipment we should know the mechanical properties of the used material - density, tensile strength, hardness, etc.

The main materials for producing perforated construction elements are the steel, aluminium and copper. Sheet materials from aluminium and copper could be used in construction due to their high

corrosion resistance and architectural impression, but steel – due to its relatively high strength. Besides, aluminium alloys are lightweight and have sufficiently high strength they have good machinability during perforating and durability. Copper is widely used for roof covering. The oxide layer provides high corrosion resistance and, consequently, durability. Copper sheets have good machinability during perforating as well as good weldability. Nevertheless, steel perforated materials have better perspectives for use as a material for cellular building structures and constructions due to their lower cost and higher strength.

The weight of perforated aluminium products will be lower, but at the same time, the final products from perforated aluminium will have worse tensile strength properties compared to other materials, referred to in Table 1. Harder workable materials due to their mechanical properties are steel and different copper alloys. However, the strength of constructions is much better.

Mechanical properties of different types of metallic materials (tapes, plates) change during punching (Fig. 1, Fig. 2). The relationships shown, characterise the yield strength ratio and effective elastic properties depending on the percentage of perforation (O'Donell & Associates, Inc. 1993). The above mentioned relationships achieved for a perforated plate with round holes in a standard staggered 60° pattern are shown in Fig. 3. It is evident that the perforation reduces the yield strength ratio and effective elastic properties. The modulus of elasticity and Poisson's ratio of metallic material shows ultra-rapid changes.

Table 1
Mechanical properties of metallic materials used in the production of perforated tapes and plates

Materials	$\rho, \frac{kg}{m^3}$	σ_t, MPa	HB (MPa)	Marks of material
Steel	7700 – 7900	320 – 930	1310 – 2550	C50E, C22E, C8E, S235JRG2
Aluminium alloys	2700	60 – 310	520 – 847	AMg2H2, AD31T1
Copper alloys	8920 – 8980	220 – 640	1186 – 2430	M1-M3

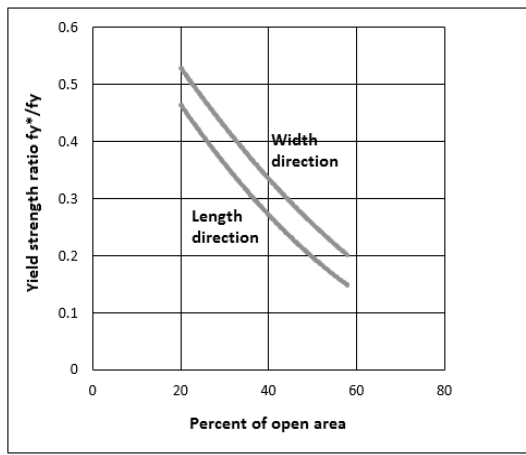


Figure 1. Yield strength ratio depending on percent of perforation,
where f_y^* - yield strength of perforated plate; f_y - yield strength of unperforated plate

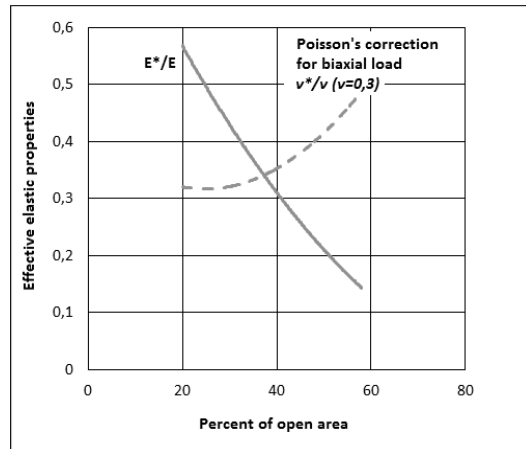


Figure 2. Effective elastic properties depending on the percentage of perforation,
where E^* - elastic modulus of perforated plate; E - elastic modulus of unperforated plate; v^* - Poisson's ratio of perforated plate; v – Poisson's ratio of unperforated plate

Main methods for manufacturing of different types of cellular building constructions from perforated metallic materials are stretching, corrugation, plate shearing, cut-sheet and stretching, perforated tape twisting, method of interlacement, profiling and welding (Wadley et al., 2003; Mironovs et al., 2012,

Bogojavenskij et al., 1978). The right choice of method is directly affected by the properties of raw and perforated materials. For example, the method of stretching requires a slightly high strength of glued locations of connected plates

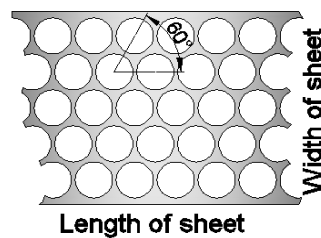


Figure 3. Perforated plate with round holes arranged in 60° angle

(enough to allow the stretching of the structure) which in the case of a thin cell wall is usually provided with modern adhesive polymers. The value of force necessary for stretching the cells steadily approaches the strength of adhesion between the plates, when the ratio of the cell wall's thickness against the cell size increases. In this case, for the production of a honeycomb structure with a higher relative density, another method of manufacturing (corrugation) or method of joining the elements (welding, soldering) is necessary. The usage of perforated metallic materials opens up new possibilities for the production of fundamentally new cellular materials and constructions. There are a variety of cellular structures with different types of structure and mechanical properties that can be produced using different profiling and bonding methods. The usage of such structures in sandwich panel core raises particular interest.

EXPERIMENTAL STUDIES

Formation of cellular building constructions

In the experimental investigation we used samples from perforated steel tapes, obtained from waste in the production of driving chain (Lisicins et al., 2011; Mironovs et al., 2006; Products 2013). This structure was made from bands of LPM-1 – trade mark of JSC “Ditton Driving Chain Factory”, Latvia (Table 2).

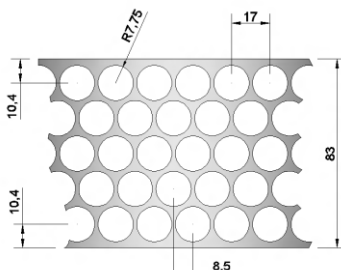
Samples of cellular structures were made from perforated steel tape using profiling and welding. Profiling was made in crosswise direction (Fig. 4) and in longitudinal direction (Fig. 5). Previously profiled tapes were joined. As a result, cavities were generated between the tapes (Fig. 6, a and Fig. 6, b). Subsequently cavities may be filled, for example, by insulating filler.

It was experimentally determined that profiling of tape of C50E steel is hard to implement and possible only with high curvature. For example, there was cracking observed with a bend radius of less than 30 mm for several types of tape.

The profiling by bending in the case of C8E steel was much easier. This material is soft and ductile.

Table 2

Mechanical and geometrical characteristics of perforated steel band produced by punching

Type of band & geometrical characteristics	Designation	Material	Permeable area, %	Thickness, mm	Tensile strength, N/mm ²
	LPM - 1	Steel S235JRG2	66.97	1.50	320.70

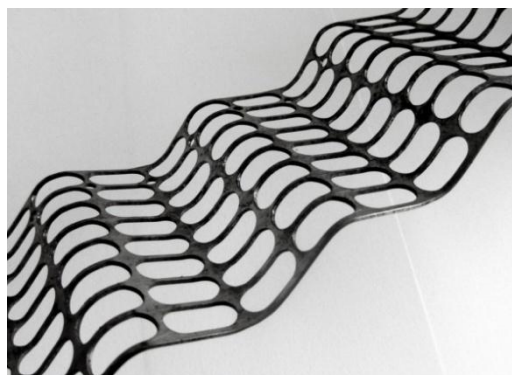


Figure 4. The crosswise profiling

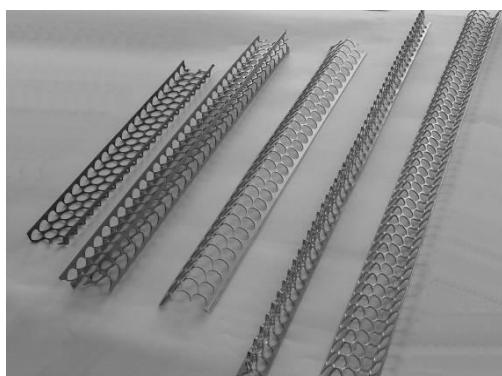


Figure 5. The longitudinal profiling

There were different profiles experimentally obtained by bending in the profiling machine – with a radial curvature of 90° and a greater angle

curvature. LPM – 1 sample of tape can be bent even slightly less than 180° due to its thin dimension.

Previously profiled tapes were joined by resistance spot welding (RSW) using experimental AC RSW equipment „Impulse KM” earlier elaborated in Riga Technical University. The outer diameter of the spot weld is in the range of 4...5 mm (Mironovs et al., 2012). RSW welding parameters are given in Table 3.

Table 3
RSW welding parameters for steel S235JRG2 welding

Welding parameters	Welding current range, kA	Electrode force, kN	Weld time, sec (50 Hz cycles)
Conditions	8...9	3.5...4.0	0.18...0.20

Assessment of deformation of cellular structures

One of the aims of modeling cellular structures with complex shapes and structures of the material is the determination of their deformation properties. Computer modeling using FEM (Finite Element Method) was done using CAE module of design software SolidWorks – COSMOSWorks. Experimental tests performed on the compression setting Zwick Z100.

Evaluation of mechanical properties was carried out using an elaborated model of the basic element (Fig. 7.) of the structure shown in Fig. 8. The

collapse of cellular structure element occurred as a result of local carrying capacity loss (Fig. 9.).

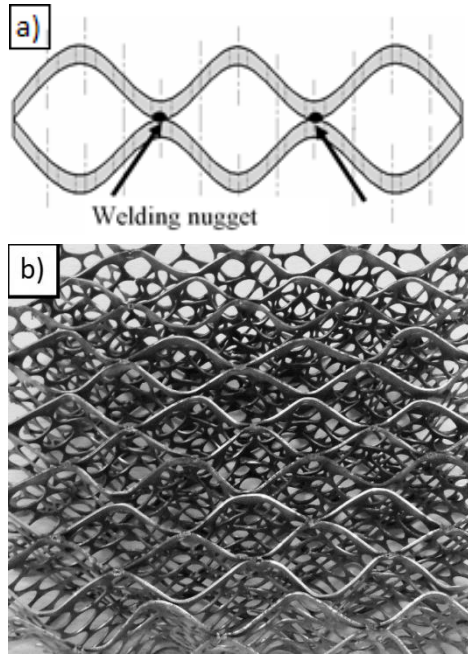


Figure 6. Scheme of assembly (a) and cellular structures from S235JRG2 perforated tapes (width 100 mm, thickness 1.2 mm) produced by RSW (b). The scheme of the welded cellular structure is given in Fig. 6 a, but the view of the cellular structure is shown in Fig. 6, b. Preliminary experiments were

revealed that resistance welding is an appropriate technology for the generation of cellular structures.

Results of tests are shown in Fig. 9 and Fig. 10. Compression force ranged from 2644 N to 2815 N. The maximum deformation by the y-axis is 1.0...1.4 mm. The average load capacity (2744 N) results in average deformation 1.17 mm.

The maximum deformation was 1.15 mm, which is at 1.17% lower than experimental results. The difference between results obtained by computer simulation and experimental work is in the range of 5%. Thus, computer simulation is a feasible way to predict the deformation of geometrically complex cellular structures, using perforated bands.

The compressive strength test results for the metallic core elements of the cell structure are shown in Table 4, where:

H – height of cellular structure

$A_{s,eff}$ – effective cross-sectional area

$F_{c,max}$ – maximal load carrying capacity

$\Delta l_{c,Fmax}$ – maximal deformation

ε_{Fmax} – maximal strain

σ_c – compressive stress

It is also worth noting that all the welds passed the above-mentioned load, and hence the strength of the pins provided no less strength than that of the construction. The local loss of load carrying capacity was observed in the walls between perforation.



Figure 7. The model of basic the element of the cellular structure for FEM calculation

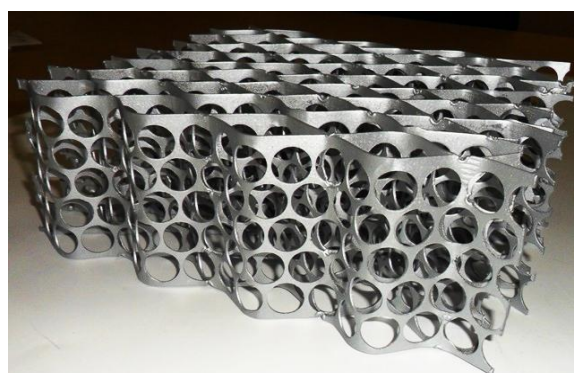


Figure 8. Cellular structure made of perforated bands

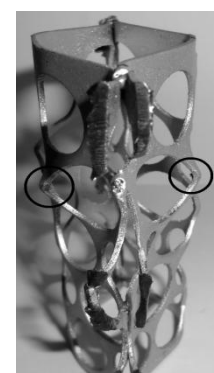


Figure 9. The tested element of cellular structure

Compressive strength test results for the metallic core elements of the cell structure

No.	H , mm	$A_{s,eff}$	$F_{c,max}$, N	$\Delta l_{c,Fmax}$, mm	ε_{Fmax} %	σ_c , N/mm ²
1.	83	14.40	2773.20	1.0	1.20	192.58
2.	83	14.40	2643.93	1.5	1.81	183.61
3.	83	14.40	2814.98	1.0	1.20	195.48
Average results:		14.40	2744.04	1.17	1.40	190.56

Table 4

CELLULAR METALLIC STRUCTURES IN BUILDING CONSTRUCTION

One of the usage possibilities of perforated metallic materials in building construction is sandwich panels.

Sandwich panel is a composite structure in which two stiff outer skins are bonded to a relatively thick but lightweight core. The panels are preferred in applications requiring a structure that is both highly resistant to bending and extremely lightweight. The facing skins of a sandwich panel can be compared to the flanges of an I-beam, as they carry the bending stresses to which the beam is subjected.

One facing skin is in compression, the other - in tension. The core resists the shear loads, increases the stiffness of the structure by holding the facing skins apart, and improving on the I-beam, it gives continuous support to the flanges or facing skins to produce a uniformly stiffened panel. The core-to-skin adhesive rigidly joins the sandwich components and allows them to act as one unit with a high torsional and bending rigidity. The separation of the skins by the core increases the moment of inertia of the panel with little increase in weight – in such a way an efficient construction with good bending and buckling strength is obtained.

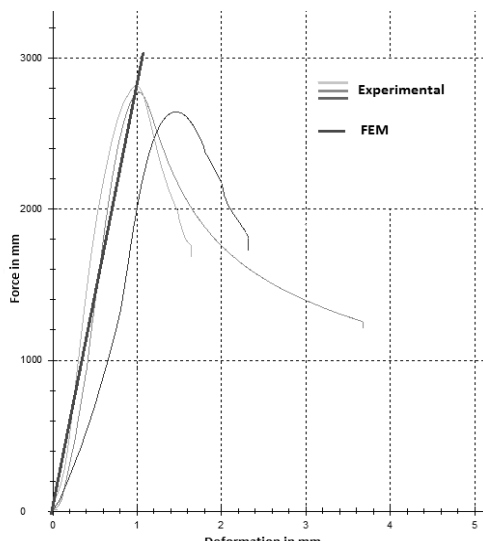


Figure 10. The curves of the deformation of the load

By splitting a solid laminate down the middle and separating the two halves with a core material, the result is a sandwich panel. The new panel weighs a little more than the laminate, but its flexural stiffness and strength are much greater (Table 5). By doubling the thickness of the core material, the difference is even more striking (Petras et al., 1998).

By use of perforated metallic tapes or plates the weight of the sandwich panel can be reduced even more. In that case, the load carrying capacity of the panels will be reduced. However, in most cases it is enough to provide functioning of the construction under load (especially in the case of facade panels). The use of perforated sheets also provides additional opportunities for the installation of fastenings of the panels depending on the constructive solution. There are the opportunities to join the elements of the core of the sandwich panel by wire, sleeves, nuts, etc. Using perforated steel waste materials, the compressive strength of the cell structure is sufficient (Table 4) to ensure safe work

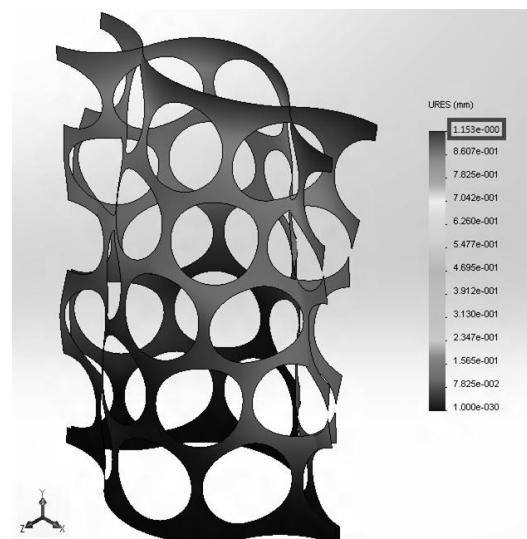


Figure 11. View of deformation

of panels even in floor constructions, but lower costs significantly increase the economic efficiency. Sandwich panels shown in Fig. 11 and Fig. 12 are diverse in terms of the types of profile and their distribution. Profiles can be based on the perforated tape with different widths and thicknesses. The percentage of open area (perforation) also may vary. The profiling of tape may vary depending on the engineering solution of the construction and expected load. Profiles of the core can be arranged upright (Fig. 11) or flatwise (Fig. 12) relative to the cladding. All these parameters are chosen according to the mechanical properties of the profiles (and their material) and expected service circumstances of the end product (panel). For example, profiles arranged upright have a greater load carrying capacity, but those placed flatwise – better connection options with cladding sheets, as well as mechanical energy absorption capability. Core sheets are commonly completed with profiling in the transversal direction. The method of stretching, corrugation or slotting (especially in the case of the

perforated metallic waste materials) can be efficiently used for production of the core.

Cavities between the plates of the panel may be empty or filled by thermal or acoustic insulating materials. The upper cladding sheet of the panel can consist of only one layer, for example, in the case of interior facing panels, or multilayer, where the lower layer smoothly splits the load, but the upper layer is decorative and connected to the upper layer with a layer of glue or a damping layer is applied on top – in the case of floor panels.

Artificial or natural stone materials – granite, marble, limestone, sandstone, etc, may create the upper decorative layer.

Panels based on a metallic cell structure can be used as load carrying or non-load carrying constructions. They can be used for wall, floor, stairs and door constructions, scaffolding and gantry constructions, pre-manufactured and pre-fabricated garages, car shelters, bus stops, shower and toilet modules.

The main benefits of perforated metallic materials usage in sandwich panel's constructions:

- weight reduction (compared with non-perforated metallic materials);
- fire resistance;
- noise reduction or acoustic effects;
- ventilation possibilities;
- durability and vandal proof.

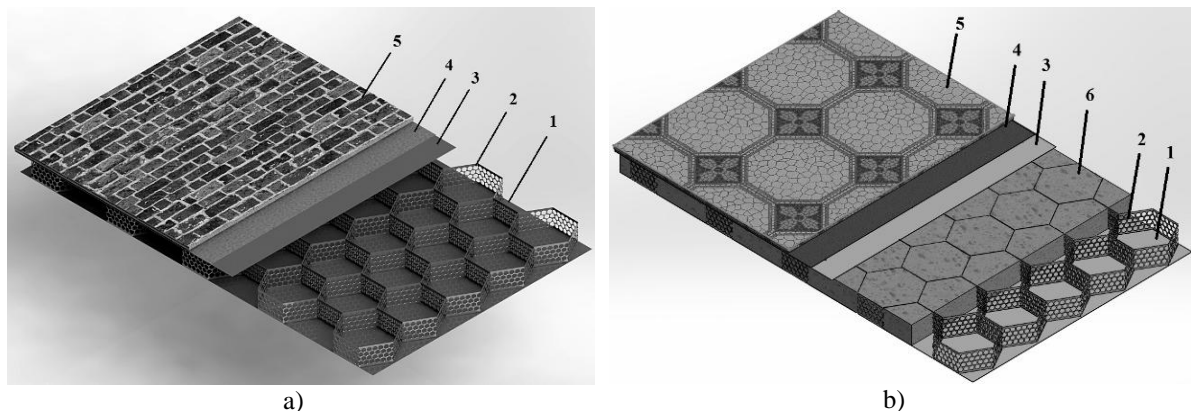


Figure 11. Example of sandwich panel based on perforated and profiled metal tape placed upright without an insulation layer (a) and with an insulation layer (b):

1 – lower metallic sheet; 2 – perforated and profiled metal tape; 3 – upper metallic sheet; 4 – layer of glue, 5 – facing (finishing) material; 6 – insulation material

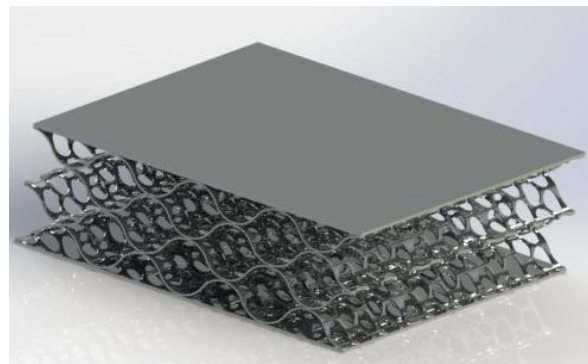


Figure 12. Example of a multilayer sandwich panel for absorption of mechanical energy based on perforated and profiled metal tape placed flatwise

CONCLUSION AND FOLLOW-UP STUDIES

Perforated metallic materials (tapes, plates, strips) have a big potential to be used in construction. It was shown that by profiling and welding - it is possible to produce different cellular structures, matching with filler material and decoration.

The computer simulation is a feasible way to predict the deformation of geometrically complex cellular structures, using perforated bands as well as

for form optimization in regard to the effective use of the material. The difference between results obtained by computer simulation and experimental work is in the range of 5%. Experiments (computer and mechanical testing) prove, that a cellular structure from perforated steel S235JRG2 strip have a high compressive strength, when the average carrying capacity is 2744 N.

One of the possible applications of perforated metallic materials in building construction, is

sandwich panels. Such sandwich panels after a detailed studies have good opportunities to be used as supporting or decorative structures. According to the core material and core location in the panel, the sandwich panels could be with high stiffness as well as with good absorption ability of mechanical energy. Filling of the cellular structure with insulating filler allows heat-insulating and sound-insulating properties of the sandwich panels to be improved.

Further studies will be linked to the development of effective methods for interconnection of metallic elements.

The obtained panel prototypes will be tested in 4 – point bending. The multilayer numerical model of sandwich panel will be created with aim to draw correlations, validate calculated results with experimental strain and deflection measurements, and optimise the design of sandwich panel.

REFERENCES

- Ozola L. (2011) Savienojumi ar perforētām zobotām metāla plāksnēm. In: *Koka būvkonstrukciju aplēse un konstruešana II: 1. Un 5. Eirokodeksa pielietošana būvprojektēšanā*. Latvia, Jelgava: Latvia University of Agriculture, p. 89–91.
- Kaļva L. (2011) *Metallic perforated materials in concrete works*. Latvia, Riga: Riga Technical University. 87 p.
- O’ Donell & Associates, Inc. (1993). Strength of Perforated Metal. In: *Designers, Specifiers And Buyers Handbook For Perforated Metals*. A publication of the Industrial Perforators Association, p. 12–15.
- Wadley H. N. G, Fleck N. A., Evans A. G. (2003) Fabrication and structural performance of periodic cellular metal sandwich structures. *Composites Science and Technology*, No. 63, p. 2331–2343.
- Mironovs V., Lisicins M., Boiko I., Zemchenkovs V. (2012) Manufacturing of Cellular Structures of the Perforated Steel Tape. *Proceedings of the 8th International Conference of DAAAM Baltic Industrial Engineering*. Otto T. (ed.). Estonia, Tallinn: Tallinn University of Technology, p. 688–693.
- Lisicins M., Mironovs V., Kaļva L. (2011) *Proceedings of 3rd International Scientific Conference “Civil Engineering’11”, vol. 3*. Latvia, Jelgava: Latvia University of Agriculture, p. 95–102.
- Calva C. M., Eagar T. W. (1990) Enhancement on the Weldability in Resistance Spot Welding. In *AWS Detroit Section Sheet Metal Welding Conference IV*, USA, Southfield, p. 1–33.
- Mironovs V., Boyko I., Serduks D. (2006) Recycling and application of perforated steel band and profiles. In *Proceeding of the 5th Int. DAAAM Conference*, Estonia, Tallinn: Tallinn University of Technology, p. 285–288.
- Petras A., Sutcliffe M. P. F. (1998) *Design of sandwich structures*. United Kingdom: Cambridge University Engineering Department, 99 p.
- Bogojavenskij K., Neubauer A., Ris V. (1978) *Technologie der Fertigung von Liechtauprofilen*. Leipzig: VEB DeutscherVerlag fur Grundstoffindustrie, 565 p.
- Daugavpils Driving Chain plant: Products (2013) [online] [accessed on 10.01.2013]. Available: <http://www.dpr.lv/index.php?lang=en&id=produkt>
- Aluminium honeycomb panel (2013) [online] [accessed on 10.01.2013] Available: <http://www.aluminum-honeycomb-panel.com/aluminum-honeycomb-core-manufacturing.html>
- Online product catalog of Perfo Linea (2013) [online] [accessed on 10.01.2013] Available: <http://www.perfolinea.ru>

FOOTFALL INDUCED FORCES ON STAIRS

Liga Gaile*, Ivars Radinsh**
Riga Technical University, Department of Structural Analysis
E-mail: *liga.gaile_1@rtu.lv, **ivarsr@bf.rtu.lv

ABSTRACT

To get a reliable dynamic performance of the modern flexible light-weight structures such as pedestrian bridges, flexible stairs, long span floors and tall public observation towers it is important to check the structure vibrations induced by human movement dynamic loads.

The paper gives some background information about recent advances determining the human induced dynamic forces. The paper presents a convenient method in order to obtain the equivalent continuous walking force histories and therefore essential parameters (dynamic load factors and corresponding phase shifts) that can be used in the structural design. The imperfection of individual footfall forcing functions and differences between continuous walking force histories among individuals is taken into account. There are analyzed the experimental data obtained by using the inverse dynamic method (accelerometer technology) for walking load amplitude dependence on various pacing frequencies during the stair ascending or descending action.

Key words: dynamic load factor, footfall, human induced loading, stairs

INTRODUCTION

There are structures like slender stairs, footbridges, slender floors, grandstands or even light-weight observation towers where the most common source of the vibration is human activity (Kasperski et.al., 2011; Caetano, et. al., 2009; Feldmann et. al. 2009; Gaile, Radinsh, 2011; Gaile, Radinsh, 2012a; Straupe, Paeglis, 2012). Increasing vibration issues for light-weight structures show that to perform design only based on the static loads is not enough anymore. Several recent extensive literature reviews and new guidelines highlight researchers interest in experimental identification and modeling human walking forces (Racic et. al., 2009; Zivanovic et. al., 2005; Venuti et. al., 2009; Butz et. al., 2008). The problem is the major part of these researches is done for human walking forces on flat surfaces. Still there is a little work done for studying the walking forces on stairs. The most relevant and recent on this subject is done by S.C. Kerr, N.W.M. Bishop and M. Kasperski (Kerr et. al., 2001; Kasperski et. al., 2011a). But researchers who applied the existing load models for the stair ascending or descending cases reported a very noticeable differences between the predicted and measured accelerations due to climbing (Davis et. al., 2009; Zhou et. al., 2011). In those works as a dynamic load for predictions seems to be applied only the vertical force component. However, for examples during the stair ascend the longitudinal force component amplitude is approximately 30% of the person's weight (Gaile, Radinsh, 2012b) and should be taken into account (Fig. 4). This indicates that loading models are still not complete and tuned properly. This correlates with the conclusion in the recent literature review done by V. Racic that

disregarding the activity investigated, only the vertical ground reaction forces (GRF) on rigid surfaces for a single person are tested with modern non direct measurement technologies.

Riener (Riener et.al. 2001) in his experimental investigation found that ground reaction forces (GRF) were not significantly affected by the staircase inclination (tests were performed on the following stair inclinations: 24°, 30°, 42°).

This paper presents a new and relatively easy method for obtaining the equivalent continuous walking force histories where the imperfection of the individual footfall forcing functions are taken into account. It is done by utilizing the modern accele-rometry technology. There is presented the force amplitude dependence on the pacing rate during the stair ascending and descending case for all three components: vertical, lateral and longitudinal direction based on the experimental results. There are analyzed the walking harmonics that are mostly relevant in the structural design and parameters of the critical ones presented.

BACKGROUND

There are many different types of human activities such as walking, running, jumping and intentional swaying (vandal loading), that induce dynamic forces on structures. Except the vandal loading that is a provision of the accidental limit state according to so-called the limit state design code format (Eurocode 0, 1990), other activities mostly are associated with the comfort of the users of light-weight structures and therefore fall under the serviceability limit state. If the stairs are under consideration, the most frequent and therefore important dynamic loading is the stair ascending

and descending action at human natural pacing rate. And there is a clear necessity to improve the existing load model of pedestrian induced forces to obtain better agreement between numerically calculated and experimentally measured structure response to human activities.

Experimental background

A lot of research is done on human ground reaction forces in the field of biomechanics (Ayyappa, 1997). The interest mostly is GRF values for distinct points and their chronological occurrence on the single foot step force time history (Gordon et. al., 2004). In the field of civil engineering dynamics there is an interest to simulate the continuous walking force histories that can be applied to the structure during the design process. The common way to obtain the GRF is using the force platforms (Fig. 1).



Figure 1. Example of the force platform for GRF measurements

It is an instrumented plate installed flush with the ground to register GRF (Gordon et. al., 2004). Also the main results in the field of civil engineering dynamics regarding the GRF on stairs are obtained using this technology (Kerr et. al., 2001; Kasperski et. al., 2011b), where one of the steps being replaced with the force plate. Comparing to the single force plate, the treadmill technology allows analysis of many consecutive cycles over a longer period of time (Racic et. al., 2009) but it is suitable only for obtaining forces on flat or inclined surfaces. One of the most recent works to obtain experimental values of the walking force lateral component with the treadmill technology is done by Ingolfsson (Ingolfsson et. al., 2011). Both methods have a serious drawback because the measurement devices have a strong influence on human ability to move naturally.

Relatively a new concept to measure the GRF is using accelerometers that are capable of monitoring, storing, and downloading data of relatively small time intervals over a long period of time. Accelerometers are sensors that produce electrical signals proportional to the acceleration in particular frequency band and might be based on different working principles (Cunha et. al., 2008). The benefits of using accelerometers compared to more traditional gait analysis instruments include low cost, testing is not restricted to laboratory environment, accelerometers are small in size, therefore walking is relatively unrestricted and with an option of direct measurement of 3D accelerations

(Kavanagh et. al., 2008). Another way with a great potential to obtain GRF is during the analysis to combine the visual motion tracking data recorded using cameras or sensors (Cappozzo, et. al., 2005) with known body mass distribution (Gordon, et. al., 2004). Both of these methods are so called the inverse dynamic methods and could be valuable in civil engineering applications to estimate the continuous human induced forces applied to the structure under a wide range of conditions.

Theoretical background

Theoretically the continuous walking force histories can be obtained by using kinematics of the motion of the human centre of gravity (COG) (Winiarski, et. al. 2009; Whittlesey, et. al., 2004) because dynamics of different parts of the body translate the center of gravity from one point to another in the most energy efficient way (Amin, 2012). The vertical walking force function can be obtained from a simple dynamic equilibrium based on the Newton's Second law (1).

$$F(t) = Mg + Ma(t), \quad (1)$$

where M is a body mass of the person, g – gravitational constant, a – acceleration of the COG. COG or also known as a body center of mass (BCOM) represents the mean position of the total mass of human body as a multi-segment system (Racic et. al., 2009). The segmental masses and their centers can be found from different authors (Wu et. al., 2005; Vaughan et. al., 1999; Dumas et. al., 2006). This approach usually is used in the field of the inverse dynamics (Fig. 2).

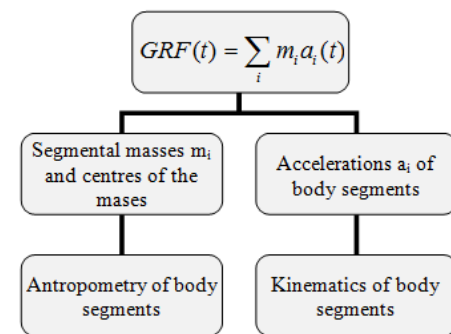


Figure 2. Flow chart of indirect measurement interpretation of human – induced loading

The drawbacks of the method are an incorrect assumption that body segments are rigid and placing markers or sensors accurately on the relevant segment of the body is problematic. As well the huge amounts of data due to the number of body segments under consideration are subject to errors. Therefore, for the civil engineering

applications more convenient would be the placement of the sensor close to the actual COG of the whole body and not to the separate segments. It should be done tightly attaching the sensor on the body through the part that reduces the effect of the “soft tissue artifact (Leardini, 2005)”. In the field of biomechanics it is known that approximate location of COG for women is 55% of height from the floor and 57% for men (Bartlett, 1997).

Although the probabilistic force models would be more suitable when simulating the walking forces as it is a stochastic narrow band process and depends on many parameters (Racic et. al., 2012) more convenient from the designing point of view would be a deterministic force model that takes into account non-periodicity of the force.

The most common way based on the Fourier decomposition for perfectly repeatable footfalls is to represent the walking force in the time domain as a sum of Fourier harmonic components, where the Fourier coefficient of the i^{th} harmonic often referred as the dynamic loading factor (DLF_i) is the base of this model. The example in Fig. 3 shows very significant scatter of the obtained DLF_i values of vertical force second harmonic (according to different authors). But the experimental measurements reveal that the character of the walking time history of different persons appears to be similar (Gaile, Radinsh, 2012b). Therefore, the authors suggest performing the averaging of individuals’ continuous walking time histories instead of separate DLF_i values as it is usually done.

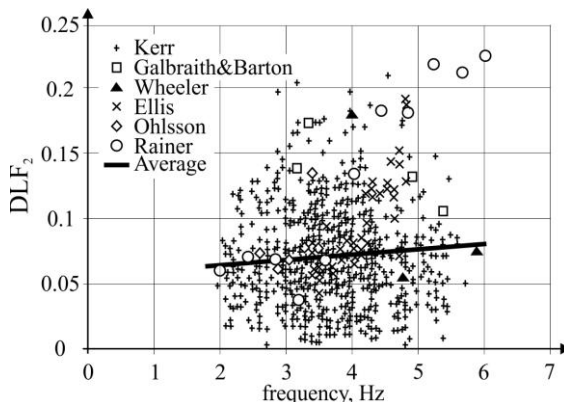


Figure 3. DLF values of second harmonic of walking force vertical component (Zivanovic, 2005)

EXPERIMENTAL INVESTIGATION

During the experiment to verify the proposed methodology for obtaining analytical expressions of human walking forces that took place in the Riga Technical University where accelerations of 22 persons’ (mixed group of men and women) COG were measured and recorded as they ascended and

descended the stair. Each participant of the experiment had several attempts with freely-chosen different pacing rates.

Two 3-axis light-weight (55g) USB accelerometers (Model X6-1A) were used to record the accelerations. The accelerometers were attached to the foam plastic light-weight boards tightly strapped to the COG horizontal axis of the subject in the front and back of the body (Fig. 4). The equipment is very light and does not vibrate independently from the individual’s body. The measurement sample rate was 160 Hz.

Two flights of the stair (12 steps in each flight) were used to perform the test but only the second flight data, when the test subjects obviously were moving more naturally, was taken for the processing.

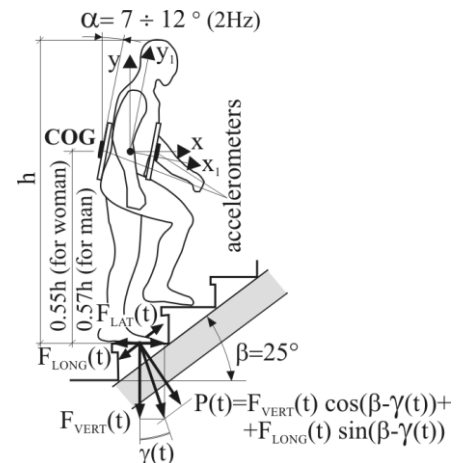


Figure 4. Illustration of the experimental setup

The experiment once again confirmed the sensitivity of the data when the test subject is under experimental conditions. The second flight measurements were always noticeably more stable and with smaller amplitudes. Additionally, some attempts during the experiment were completed with a laser streamer mounted on the front of the board lasing the staircase wall while a video camera recorded the change of the angle α from Fig. 4.

RESULTS OF THE RESEARCH

The presented method of obtaining the equivalent continuous walking histories that takes into account the imperfection of the repeated footfall of the individual as well as differences between the individual walking force histories by averaging them is presented in Table 1. Consequently, it is possible to obtain the mean values of the DLF_i and the corresponding phase shifts. This is convenient to use in analytical or numerical calculations of the structure response under various human induced dynamic loading conditions.

To check the new method there were compared the S.C. Kerr's obtained results of the vertical force component DLF_i values with the new mean DLF_i values (for ascending (2Hz) and descending (2.15Hz) cases) and found to be in a very good agreement for the first harmonics. The results of the second harmonics slightly differ that correlate with the proposition of Davis (Davis et. al., 2009) to take a higher value for the second harmonic. The mean value obtained by the presented methodology is plotted on the S.C. Kerr's obtained results (Fig. 5).

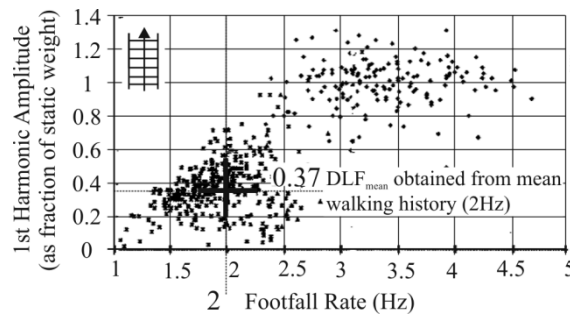


Figure 5. First harmonic amplitude of vertical force for ascending the stair

There are still no results to compare the longitudinal and lateral force component directions in the case of stair ascending/descending.

During the double averaging process the experimentally measured peaks smoothen and widen accordingly due to the lack of perfect periodicity between footsteps and individuals, therefore this effect on the response of the structure is investigated by numerical calculations. It is found that the error is less than 1% and therefore negligible (Fig. 6).

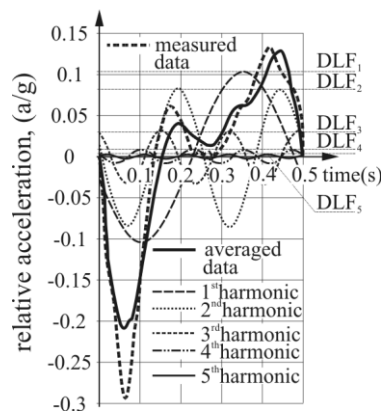


Figure 6. Walking force history averaging

The data in Fig. 7 and Fig. 8 that are obtained from the mean walking force history reveal differences between the stair ascending and descending process. The weight of the person was taken 740N. From the presented figures it follows that in contradiction to

the vertical forces, the lateral and longitudinal components of the force reached the highest magnitudes during the ascending process that seems to be logical. A closer look at the middle part (small loops) of the figures reveals that during the ascending process a person tries to balance oneself in the lateral direction but during descending more in the longitudinal direction due to the inertia. The lack of the symmetry confirms that the presented method has taken into account the "leading leg" effect that especially becomes apparent for the stair ascending process.

To obtain the relationship between the walking force amplitudes and pacing frequencies it is suggested not to look at the separate DLF_i values corresponding to the relevant frequency but to take the mean value of the individual's experimental walking force history of n periods expressed as a range from maximum to minimum amplitude (2):

$$A = \frac{1}{n} \sum_{i=1}^n A_i^{poz} + |A_i^{neg}|. \quad (2)$$

These relationships are obtained from the experimental data of the recoded walking histories of individuals and presented in Fig. 9 - 14.

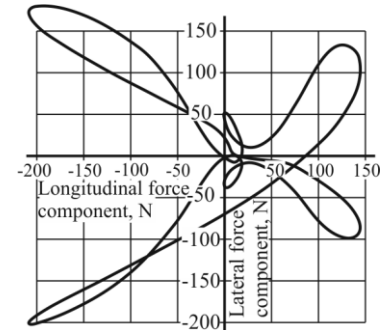


Figure 7. Path of the mean pedestrian force vector end point (ascending case at rate 2Hz)

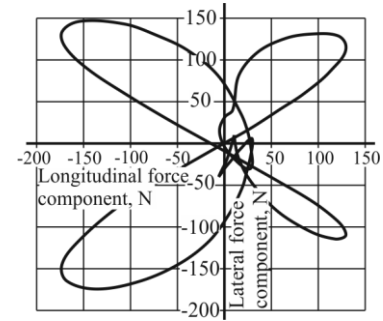


Figure 8. Path of the mean pedestrian force vector end point (descending case at rate 2,15Hz)

Table 1

Description of the new method for obtaining the equivalent continuous walking histories (analytical expressions)

Step Nr.	Action		Illustration
1.	Measure individual walking acceleration histories (WAH_i) and transform the recorded measurements from the local axis of the sensors into global directions taking into account the angle α in Fig. 4, then divide into periods p_n		
2.	Perform period averaging to obtain the equivalent period and further WAH of the person:	(3)	
3.	Perform transformation from the time domain to the frequency domain via FFT (Fast Fourier Transform):	(4)	
4.	Find the DLF value and relevant phase shift for each individual in order to obtain separate harmonics and further the analytical expression of individuals' walking force history (WFH_i)(5):	(5)	
	where i – order number of the harmonic, n – total number of contributing harmonics, λ^i – Fourier coefficient of the i^{th} harmonic often referred as the dynamic loading factor (DLF), f_i - i^{th} harmonic frequency (Hz), φ^i – phase shift of the i^{th} harmonics. If necessary, use the correction coefficient for magnitude to maintain the same area under the function as the experimental data have:		
	$\sum_n A_{ave} = \sum_n A_{exp}$	(6)	
5.	Perform averaging between the functions of WFH_i to obtain the equivalent (mean) continuous walking time history:	(7)	
6.	Transformation from the time domain to the frequency domain via FFT:	(8)	
7.	Find the DLF value (λ_{eq}^i) and relevant phase shift of mean walking history in order to obtain separate harmonics and further the analytical expression of the mean walking force history in vertical (9) and lateral or longitudinal directions (10):	(9) (10)	
	$F_y(t) = G + \sum_{i=1}^n G \lambda_{eq,y}^i \sin(2\pi f_i t + \varphi_y^i),$ $F(t) = \sum_{i=1}^n G \lambda_{eq}^i \sin(2\pi f_i t + \varphi^i),$ where G is a static weight of the subject's body (N)		

Each of the experimental points on the chart is the mean value of 12 periods (number of steps in the

stair flight). The vertical dynamic walking forces are sensitive to the pacing frequency until the point of noticeable scatter in the values of each test subject and therefore the mean value might be taken as constant. The shape of the mean value function is similar to other researchers' works. The longitudinal and lateral force component is sensitive to changes of the pacing frequency with a tendency to increase by adding the walking speed in the case of the stair ascending. For the descending case these components seem to be very slightly dependent on the persons' pacing frequency and therefore could be regarded as constant.

If assumed that changes in the force amplitude due to different pacing frequencies divide proportionally between the harmonics and therefore DLF values, it is possible to find relationship that describes each of the relevant DLF value dependence from the person's pacing frequency (Table 2). As an example, there were calculated DLF values for the pacing frequency 1.6Hz and compared to the Kerr data.

Most of the data correlate very well except the second harmonic for the descending case. By analyzing the mean values obtained by Kerr (in Figure 18 (Kerr et. al., 2001)), it follows that the second harmonic does not depend on the pacing frequency for the stair descending case and

therefore the shape of the walking force history should differ dramatically even if there is a slight change in the walking speed. Apparently, it is due to the rapid change of the first harmonic values. However, this does not appear in the experimental data for fundamental pacing frequency range of $1\text{Hz} \leq f \leq 2.3\text{Hz}$. On the other hand, Kerr in his paper states that "...the weight is transferred quickly from one leg to the other, which creates a deeper hollow between the humps. The greater the distance between the hollow and the humps, the greater the second harmonic". Therefore, the second harmonic amplitude should change if the pacing frequency changes for the stair descending or ascending case. This example demonstrates the advantage of the new method based on the averaging of the continuous walking histories and not the separate DLF values obtained from one or few steps. Also to get a correct analytical function of human induced forces, the phase shift of each harmonic is an important parameter. By averaging only DLF values this information is lost. Another aspect is that the averaging of particular Fourier coefficient between the different Fourier series will not necessarily give the average forcing function due to the connection between the coefficients in each of the function.

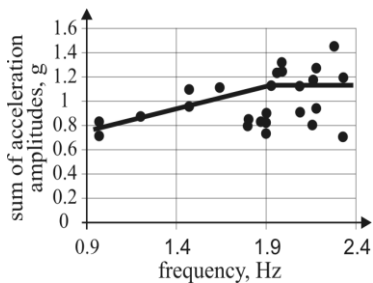


Figure 9. Relationship of amplitude and pacing frequency (vertical direction, ascend)

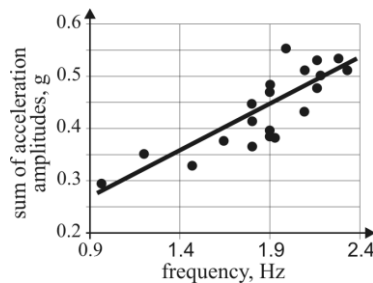


Figure 10. Relationship of amplitude and pacing frequency (longitudinal, ascend)

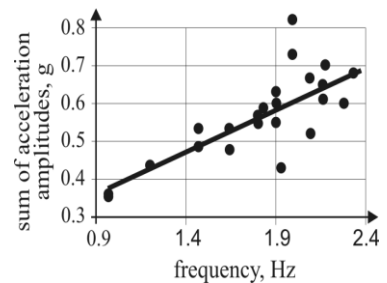


Figure 11. Relationship of amplitude and pacing frequency (lateral, ascend)

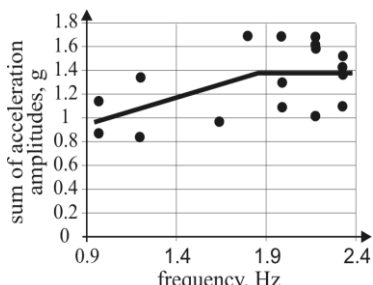


Figure 12. Relationship of amplitude and pacing frequency (vertical direction, descend)

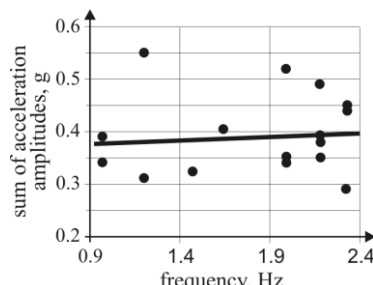


Figure 13. Relationship of amplitude and pacing frequency (longitudinal, descend)

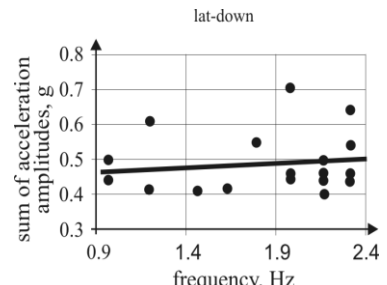


Figure 14. Relationship of amplitude and pacing frequency (lateral, descend)

Table 2
DLF values of stair ascending and descending dominant harmonics

Action	Proposed $DLF_n(f)$	Calculated DLF_i at 1.6Hz	Average DLF by Kerr at 1.6Hz (Kerr et. al., 2001)
Ascending, vertical	$DLF_n(2\text{Hz}) \cdot (0.94f - 0.88); 1 \leq f < 1.95$	0.23(DLF_1)	0.27(DLF_1)
	$DLF_n(2\text{Hz}); 1.95 \leq f \leq 2.3$	0.13(DLF_2)	0.12(DLF_2)
Descending, vertical	$DLF_n(2\text{Hz}) \cdot (0.99f - 1.13); 1 \leq f < 1.85$	0.27(DLF_1)	0.24(DLF_1)
	$DLF_n(2.15\text{Hz}); 1.85 \leq f \leq 2.3$	0.06(DLF_2)	0.22(DLF_2)
Ascending, longitudinal	$DLF_n(2\text{Hz}) \cdot (1.49f - 1.98); 1 \leq f \leq 2.3$	0.049(DLF_1) 0.044(DLF_2)	- -
	$DLF_n(2.15\text{Hz}); 1 \leq f \leq 2.3$	0.07(DLF_1) 0.1(DLF_2)	- -
Descending, lateral	$DLF_n(2\text{Hz}) \cdot (2.2f - 3.4); 1 \leq f \leq 2.3$	0.012(DLF_1) 0.013(DLF_3)	- -
	$DLF_n(2.15\text{Hz}); 1 \leq f \leq 2.3$	0.08(DLF_1) 0.11(DLF_3) 0.07(DLF_5)	- - -

where f – pacing frequency, Hz;

n – number of the harmonic;

$DLF_n(f)$ - dynamic load factor at pacing frequency f for the harmonic n ;

$DLF_n(2\text{Hz})$ - dynamic load factor at pacing frequency 2Hz and corresponding phase shifts for the harmonic n found from Table II – IV (Gaile, Radinsh, 2012b).

CONCLUSIONS

The presented new method of obtaining analytical functions of continuous walking histories is based on experimentally obtained continuous walking histories of individuals that are found by the inverse dynamic method and uses kinematics of the human center of gravity. Instead of the traditional approach when relationship between the walking pace and force amplitudes is based on the average harmonic (DLF) amplitude, this method proposes averaging between continuous walking histories priorly proceeded in order to take into account the imperfections of repeated footfall. In this way there is preserved information about the phase shifts – necessary parameter to obtain analytical function based on the Fourier series. The main advantages of using the presented method are as follows:

- 1) Possibility to estimate continuous human-induced forces of different actions applied to the structure under a wide range of the conditions due to the non-laboratory restrictions;

- 2) The measurement devices do not have a strong influence on human ability to move naturally;
- 3) Requirement of a low cost instruments: few accelerometers capable of storing and downloading data with relatively small time intervals;
- 4) Allows to obtain not only dynamic load factors but also the phase shift values associated with the mean walking history;
- 5) The obtained analytical mean function contains information about imperfections of the person's footfalls and differences between the continuous walking histories but still it is a deterministic force model. Unlike the probabilistic force models it is more convenient to handle when performing analytical or numerical calculations of the structure under consideration.

To test the method there were obtained equivalent DLFs and their dependence on the walking pace for all three force directions (the stair ascending and descending case): vertical, longitudinal and lateral. Vertical results are compared with the measurements of the vertical component done by

Kerr using the force plate technology. The overall results correlate very well except the second harmonic were the Kerr's data have a very significant scatter and the mean value does not depend on the walking pace (stair descending case) that seems not to be quite realistic.

Descending the stair produces higher vertical force amplitudes than ascending that is logical and in agreement with other researchers' works. The lateral and longitudinal direction force amplitudes strongly depend on the walking pace only in the case of the stair ascending. In the case of the stair descending these might be considered as constant but with smaller amplitudes. The authors are not aware of any information that could be compared

with the obtained results for these two directions. Recent concerns about some of the light-weight public observation towers excessive vibrations and dissatisfaction of the visitors' comfort criteria call for greater attention to longitudinal and lateral force components during a long stair ascending or descending process.

ACKNOWLEDGMENT

This work has been supported by the European Social Fund within the project "Support for the implementation of doctoral studies at Riga Technical University".

REFERENCES

- Amin. T., Hatzinakos D. (2012) Determinants in human gait recognition, *Proceedings from 25th IEEE Canadian Conference on Electrical and Computer Engineering: Vision for a Greener Future, CCECE 2012*, Montreal: pp.1-4.
- Arizona State University, Department of Kinesiology [online] [accessed on 27.12.2012.]
- Ayyappa E. (1997) Normal human locomotion, part 1: basic concepts and terminology, *Journal of Prosthetics and Orthotics*, Vol. 9, p. 1-10.
- Bartlett R., (1977). *Introduction to Sports Biomechanics*. Great Britain: Alden Press. 289 p.
- Butz C., Feldmann M., Heinemeyer C, et. al. (2008) *Advanced load models for synchronous pedestrian excitation and optimized design guidelines for steel footbridges*. Luxembourg: Office for Official Publications of the European Communities. 168p.
- Gordon D., Robertson D.G.E., Whittlesey G. E. et.al. (2004). *Research Methods in Biomechanics*. USA, IL: Champaign. 311 p.
- Cappozzo A., Leardini A., et. al. (2005) Human movement analysis using stereophotogrammetry. Part 1: theoretical background, *Gait & Posture*, Vol. 21, pp. 186-196.
- Caetano E., Cunha A, et. al. (2009) *Footbridge Vibration Design*. Netherlands: CRC Press/Balkema. 192 p.
- Leardini A., Chiari. et. al. (2005) Human movement analysis using stereophotogrammetry. Part 3. Soft tissue artifact assessment and compensation, *Gait Posture*, Vol. 21(2), pp. 212-25.
- Cunha A., Caetano E., et. al. (2008) The role of dynamic testing in design, construction and long – term monitoring of lively footbridges. *Proceedings of 3rd International Footbridge Conference*, Portugal, Porto: p.
- Davis B., Murray T. M. (2009) Slender Monumental Stair Vibration Serviceability, *Journal of Architectural Engineering*, Dec., pp. 111–121.
- Dumas R., Cheze L., Verriest J. P. (2006) Adjustments to McConville et. al. and Young et. al. body segment inertial parameters, *Journal of Biomechanics*, Vol. 40, pp. 543-553.
- Eurocode 0. (1990) Eurocode - Basis of Structural Design. EN 1990.
- Feldmann M., Heinemeyer C, et. al. (2009) *Design of Floor Structures for Human Induced Vibrations*. Luxembourg: Office for Official Publications of the European Communities. 67p.
- Gaile L., Radinsh I. (2011) Time depending service load influence on steel tower vibrations. *Proceedings of Civil Engineering '11 - 3rd International Scientific Conference*, Jelgava: Vol. 3, pp. 144-149.
- Gaile L., Radinsh I. (2012a) Eccentric Lattice Tower Response to Human Induced Dynamic Loads. *Proceedings of 19th International Congress on Sound and Vibration (ICSV19)*, Vilnius: pp. 560-567
- Gaile L., Radinsh I. (2012b) Human Induced Dynamic Loading on Stairs, *Proceedings of International Conference on Civil and Construction (ICSC 2012)*, Stockholm: Issue 67, pp. 626-632.

- Ingolfsson E. T., Georgakis C. T. (2011) Experimental identification of pedestrian – induced lateral forces on footbridges, *Journal of Sound and Vibration*, Vol. 330, 1265-1284.
- Kasperski M., Czwikla B. (2011a) A Refined Model for Human Induced Loads on Stairs, *Conference proceedings of the Society for Experimental Mechanics Series, Topics on the Dynamics of Civil Structures*, Proulx: Tomson Edition, pp.27-39.
- Kasperski M., Czwikla B. (2011) Men – induced loads on stairs, *Proc. 8th International Conf. on Structural Dynamics, EURODYN 2011*, Leuven, Belgium: pp. 949–956.
- Kavanagh J. J., Menz H., B. (2008) Accelerometry: A technique for quantifying movement, *Gait & Posture*, Vol. 28, pp. 1-15.
- Kerr S. C., Bishop N. W. M. (2001) Human induced loading on flexible staircases, *Engineering Structures*, Vol. 23, pp. 37–45.
- Racic V., Brownjohn, J. M. W. (2012) Mathematical modeling of random narrow band lateral excitation of footbridges due to pedestrians walking, *Computers and Structures*, Vols. 90-91, p. 116-130.
- Racic V., Pavic A, Brownjohn, J. M. W. (2009) Experimental identification and analytical modeling of human walking forces: Literature review. *Journal of Sound and Vibration*, Vol. 326, p. 1–49.
- Riener R., Rabuffetti M., Frigo C. (2002) Stair ascent and descent at different inclinations, *Gait & Posture*, Vol. 15, p. 32-44.
- Straupe, V., Paeglitis, A. (2012) Analysis of interaction between the elements in cable-stayed bridge, Baltic Journal of Road and Bridge Engineering, Vol. 7 (2), pp. 84-9.
- Vaughan C. L., Davis B. L. O'Connor J. C. (1999) *Dynamics of Human Gait*, Cape Town: Kiboho Publishers.
- Venuti F., Bruno L., (2009) Crowd – structure interaction in lively footbridges under synchronous lateral excitation: A Literature review, *Physics of Life Reviews*, Vol. 6, p. 176-206.
- Winiarski S, Rutkowska – Kucharska A. (2009) Estimated ground reaction force in normal and pathological gait, *Acta of Bioengineering and Biomechanics*, Vol. 11, no. 1, pp. 54–60.
- Wu G., van der Helm F. C. T., et, al (2005) ISB recommendation on definitions of joint coordinate systems of various joints for the reporting of human joint motion – part II: shoulder, elbow, wrist and hand, *Journal of Biomechanics*, Vol. 38, pp. 981-982.
- Zhou B., Ren X., Lu X. (2011) Vibration Analysis and Evaluation of the Indoor Spiral Steel Stair, *Advanced Materials Research*, Vols. 163-167, pp. 36–43.
- Zivanovic S., Pavic A., Reynolds P. (2004) Vibration Serviceability of Footbridges under Human – Induced Excitation: A Literature Review, *Journal of Sound and Vibration*, Vol. 279 (1-2), p. 1–74.

INVESTIGATION OF WOOD BASED PANELS WITH PLYWOOD AND GFRP COMPOSITE COMPONENTS

Edgars Labans^{*}, Kaspars Kalnins^{}**

Riga Technical University

Institute of Materials and Structures

E-mail: *edgars.labans@rtu.lv, **kaspars.kalnins@sigmanet.lv

ABSTRACT

The current research aims to extend the existing knowledge about weight reduction of wood based panels with plywood faces and glass fibre reinforced plastic (GFRP) stiffeners, where experimental prototypes have been analysed and optimized utilizing ANSYS finite element code and design of computer experiments. The initial study demonstrated that replacing homogeneous core of plywood boards with corrugated glass fibre composite hollow core it is possible to reach up to 65 % weight reduction at the same time keeping stiffness unchanged.

Key words: finite element analysis, glass fibre composites, plywood, metamodelling, optimization

INTRODUCTION

It is generally well known that oriented fibre composite materials have advantages over traditional isotropic materials when concerning lightweighting of the load bearing structures in transport or civil engineering. Densities of laminate materials are usually lower than those of traditional materials like steel and plastics, besides orientation of fibres could be tailored according to the main load directions. In some cases a more efficient result could be achieved combining several types of fibre reinforced laminates to gain cost advantage (Zhang, 2012) or improve the resistance under specific load cases (Akhbari, 2008). Mostly glass and carbon fibres are compounded together to improve the product stiffness without major cost increasing while other combinations of fibre composites are not widely studied. However, taking into account that mechanical properties of a wood layer (veneer) integrated in the plywood structure are closer to glass fibre fabric laminate than a clear wood specimen, it makes reasonable to combine these two materials for overall benefit in lightweight structure design. Typical modulus of elasticity for glass laminate made of plain woven fabric and epoxy resin is about 18-24 GPa. The same property for veneer subjected to hot pressing and adhesive impregnation is only little lower 14-17 GPa.

In such a way disadvantages of one material component could be compensated by advantages of the other material. Thin glass fibre reinforced plastic (GFRP) layers could be applied for parts requiring complicated geometrical shapes and large bending angles; in opposite plywood sheets could successfully substitute GFRP for straight surfaces requiring increased thickness to prevent local damage. This concept could be further developed

replacing thermo reactive laminates made from epoxy resin with glass fibre/ polypropylene woven fabric capable of one shot manufacturing process by hot pressing and demonstrating great potential as future material for transport structures (Zike, 2011). The current research deals with investigation of 3D structural sandwich panels made of plywood skins and corrugated glass fibre laminate core.

One of the possible applications for similar structures is offered by Hudson (Hudson, 2010) where rail vehicle floor arrangement consisting of the main structural panel with a corrugated core covered with thinner sandwich-type plates has been optimized to find the best trade-off between the floor mass and price per unit. Optimisation employing mechanical responses acquired by numerical models is one of the most efficient ways of advance necessary structure qualities, because large numbers of cross-section parameters are not allowing making sufficient quantity of experimental prototypes or makes such an approach too expensive.

Previous scientific research in optimisation of corrugated sandwich structures mainly covers isotropic materials where the governing mechanics of corrugated structures has been described and methods compared like in research of \Luo et al., (1992).

Meanwhile several papers deal with corrugated structures from wood origin materials. Hunt (2004) performed experimental tests and FEM analysis for 3D wood fibreboards, confirming the potential of a corrugated structure as an easy producible component for lightweight panels. FEM analysis of conventional corrugated paper structures, used in packaging applications, (Rahman, 2004) demonstrated significant buckling load dependency on adhesive mechanical properties. Sandwich plywood panels with a rib-stiffened and corrugated

core have been investigated by Zudrags et al. (2009) with the aim to increase plywood specific stiffness. Optimisation procedures using the stiffness and weight ratio for plywood sandwich panels with rib-stiffened core were described in the previous study (Kalinins et al., 2009). Also the mechanical behaviour of sandwich panels with a corrugated plywood core has been investigated (Labans, 2011). It has been noted that corrugated structure has a potential for replacing traditional plywood boards, however, birch veneer is not suited for corrugated structure forming with a small section height (<50 mm). Also thin corrugated plywood core could be applied for large span panels ($L > 5$ m) for civil engineering purposes where stability of the core is provided by foam matrix (Sliseris, 2011). The aim of this research is to study feasibility of manufacturing GFRP/plywood sandwich panels, their mechanical properties in comparison with traditional plywood boards. Applying validated numerical model bending stiffness of panels has been optimized employing the metamodelling technique to find ways of reducing the structure's mass.

MATERIALS AND METHODS

FEM solution

Mechanical bending responses of the sandwich panel have been acquired by a numerical model made in ANSYS finite element code (2009). In order to accelerate the finite element analysis geometry of the structure has been modelled with SHELL 181 elements. Reaching short calculation times it is especially important to bear in mind that same model will be further employed for parametrical optimisation with several hundreds of trial runs. Loading and boundary conditions have been modelled in accordance to the EN789 (2004) standard with two linear loads near the centre of the panel assigned to coupled sets of nodes. The mesh step for the final model has been assigned to 10 mm

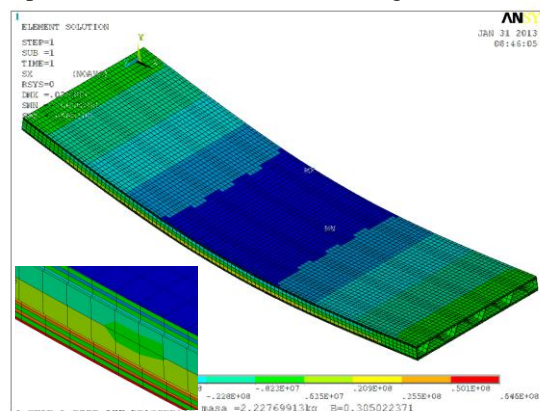


Figure 1. Distribution of stresses along longitudinal axis of the panel

(Figure 2). The model is considered of multilayered nature of plywood where single veneer properties (shown in Table 1) have been assigned to odd number of plies. The thicknesses of the upper plies has been reduced by 20 % according to manufacturing tolerances at plywood industry. The corrugated core has been modelled with only one 0.8 mm thick woven textile layer with the properties summarised in Table 1.

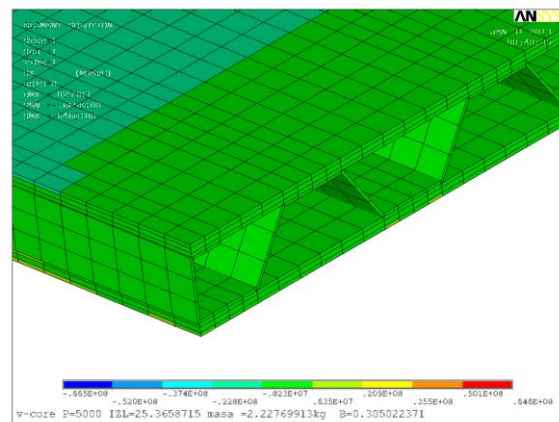


Figure 2. Mesh of the corrugated core

Table 1

Properties of panel materials

Name of the elastic property	Symbol	Mechanical properties	
		Veneer	GFRP
Modulus of elasticity in fibre direction	E_x	17 GPa	18 GPa
Modulus of elasticity perpendicular to fibre direction	E_y	0.5 GPa	18 GPa
Poisson's ratio in fibre direction	P_{xy}	0.35	0.35
Poisson's ratio perpendicular to fibre direction	P_{yx}	0.03	0.35
Shear modulus	G	0.7 GPa	3.2 GPa
Density	R_o	680 kg/m ³	1400 kg/m ³

Experimental investigation

Experimental prototypes for bending tests have been manufactured in a two step process at first creating the corrugated core from 5 layers of plain woven glass fibre fabric and epoxy resin. In the result of vacuum pressing a laminate structure with average thickness of 0.8 mm has been acquired. At the second step plywood surfaces have been

attached to the corrugated core with the same epoxy resin. Three panels with the same geometrical parameters have been manufactured and tested in 4-point bending set up according to the EN 789 standard using INSTRON 8802 servo-hydraulic testing rig (Figure 3.)



Figure 3. Bending set-up on INSTRON 8802

Deflections under the symmetrical loading conditions have been recorded with LVDT extensometer at the midspan of the panel. The geometrical properties of the prototype panels are shown in Table 2 marked as reference.

Metamodelling procedure

Regarding the ability to improve the efficiency of simulations and optimization of the designs requiring computationally expensive algorithms metamodelling techniques have been widely employed in engineering applications. Metamodels also called surrogate models can be constructed to replace the original response with the approximation functions, therefore significantly

increasing the optimisation/design time (Kalnins et al, 2009).

The design optimization process employing metamodels usually consists of three major steps: 1) design of computer experiments 2) construction of approximation functions that describe the behaviour of the problem more appropriate 3) employing the developed metamodels for the optimization or the derivation of the design guidelines.

In the present research a sequential space filling design based on Latin Hypercube with Means Square error criterion has been evaluated in-house EdaOpt software (Auzins, 2007). For common engineering tasks low order global polynomial approximations (for example, 2nd order polynomial) have been widely accepted as they do not require a large number of sample points and are computationally effective.

However, they fail to approximate most of non-linear model behaviours. In such a case a higher order polynomial could be utilised, but if no special control algorithms are assigned, they tend to overfit the data and produce even larger approximation errors. An alternative approach for polynomial model building which does not assume a predefined set of the basis functions has been proposed by (Jekabsons, 2010). The Adaptive Basis Function Construction (ABFC) approach allows generating polynomials of arbitrary complexity without the requirement to predefine any base functions or to set the maximal order of the polynomial (or any other hyper parameters) – all the required basis functions are constructed adaptively.

Table 2
Cross section design variables

Parameter	Label	Reference	Lower limit	Upper limit	Increment step	Units
Number of cover plate plies	P1	5	3	7	2	-
Total section height	P2	28.4	30	50	-	mm
Core wall thickness	P3	0.8	1	2.5	-	mm
Corrugated ply angle	P4	45	30	60	-	Deg
Glue line width	P5	20	10	40	-	mm

The cross section of the corrugated panel has been characterised with five design variables (Figure 4) corresponding to the thicknesses of skins **P1**, core layer **P3**, overall thickness **P2** and glue line **P5** width. A separate parameter is assigned for the corrugated core angle **P4** as displayed in Figure 4. The design space and parametrical increment for the variables are given in Table 2. The core wall thickness has been restricted to 1 millimetre in order to avoid local buckling. The acquired response parameters resulting from the numeric

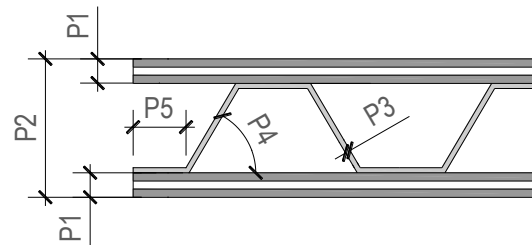


Figure 4. Variable cross section parameters

calculations are the maximum deflection at the midspan U and mass of the panel M calculated by means of densities of plywood and GFRP. The span length of the four point loading model was kept constant; however, the width of the panel has been linked with the corrugated ply angle parameter **P4** and corrugate attachment zone width **P5**. This constraint assures that the acquired results for different topology models would be comparable, as the width parameter and deflection magnitudes have linear dependency in the elastic region. This means that the acquired response values (numerical output) were multiplied with the coefficient k_r characterizing the relation of the actual panel width against the standard width of the panel of 300 mm.

RESULTS AND DISCUSSION

Validation of numerical model

The test load/deflection curves have been compared with the numerical results from ANSYS as shown in Figure 5 in order to validate the numerical model accuracy. The numerical and experimental curves have been compared to the experimental ones in the region of elastic mechanical behaviour of the panel until the load magnitude up to 5000 N. Large scatter of the experimental results could be observed between the panel 1.1 and 1.1, 1.3. A possible cause of such a large scatter could be the non-uniform quality of the bond line between the skins and the core. Moreover, the numerical results using ANSYS code are within domain of the experimental load/deflection curves closer to the panels 1.1 and

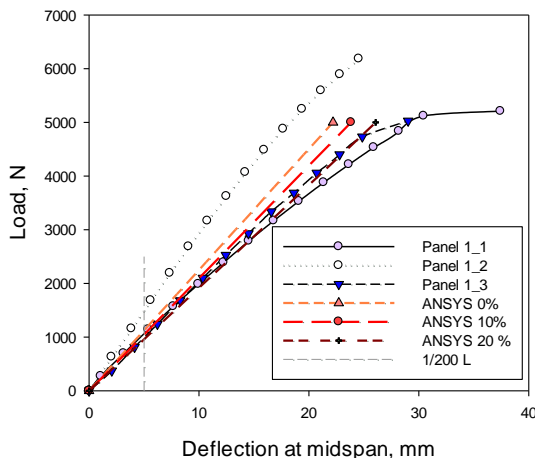


Figure 5. Load/deflection curves of sandwich panels

1.3. Depending on the upper ply thickness reduction additional ANSYS plots have been added indicating the models with 0, 10 and 20% upper ply thickness reduction. It has been set to default, that a model with 10 % thickness reduction is further most appropriate in optimisation tasks.

The vertical line is added to the graph in order to identify the deflection limit state (0.5% of span length) prescribed by the structural design codes as (Eurocode 5 , 1994). It could be concluded from the verification study that the parametrical model elaborated in ANSYS code matches the mechanical behaviour of the sandwich panel observed in the experimental tests.

Optimisation of initial design

Improving of the cross-section design for the prototype was considered as the initial step of the optimisation. The aim of optimization was to minimize the mass of the panel. Combinations of cross section topology parameters have been selected to guarantee deflection not over exceeding those original values obtained from the initial designs. The parameters of optimal and initial designs are displayed in Table 3. One could notice that the lower mass in the optimised structure is achieved by slightly increasing the overall thickness by 1.5 mm and a larger corrugated core angle equal to 60 %. The mass of the optimised panel is decreased by 10 % comparing with the initial prototype.

Table 3
Initial and optimised design of the panels

Panel characteristics	Initial design	Optimal Design
Cross-section parameter values	P1=3; P2=0.0284; P3=0.0009; P4=52; P5=0.011	P1=3; P2=0.03; P3=0.001; P4=60; P5=0.02
Load, N	5000	5000
Deflection, mm	29.84	26.43
Mass, kg	2.29	2.08
Absolute mass, %	100.0	90.3

Sandwich panels compared to traditional plywood

One of the best ways how to evaluate the efficiency of sandwich panels is to compare them with traditional wood based plate materials as plywood. Employing the same optimisation approach but constituting deflection restraints to those of full plywood boards, sandwich configurations with stiffness equivalent to traditional plywood could be found. Deflection values of plywood boards have been acquired by a layered numerical model with the assigned material properties from Table 1. Detailed summary of a sandwich panel design versus full plywood cross-section is listed in Table 3. It could be seen that self weight of the sandwich panels in general terms is at least two times lower

comparing to a plywood board with corresponding stiffness. Sandwich panels are most efficient comparing with plywood boards the thicknesses of which exceeds 30 mm. In order to keep the sandwich design rational at conventionally large plywood board thicknesses (>40 mm) the overall

sandwich panel cross-section height should be raised above the bounds of this variable stated in Table 2. However, in that case special attention to buckling stability should be paid.

Equivalent stiffness boards

Table 3

Nominal plywood thickness	Mass, kg		Differ. %	Deflection at 5kN, mm	Parameters of sandwich panel				
	Sandwich panel	Conventional plywood			P1	P2	P3	P4	P5
24	2.03	4.68	56.62	33.50	3	30.26	1.00	30.00	20.00
30	2.05	5.58	63.26	17.26	3	41.60	1.00	30.00	15.94
35	2.41	6.83	64.71	10.38	3	50.00	1.79	30.00	5.00
40	3.12	7.76	59.79	7.80	5	50.00	1.00	42.62	11.06
45	3.27	8.77	60.89	6.01	5	50.00	1.30	65.00	15.00

Optimal designs based on Pareto optimality

In order to assess the most effective combinations of design variables of the sandwich panel cross section in line with plywood boards with similar total thickness, the Pareto optimality problem has been formulated where maximization of the relative stiffness ΔK is performed simultaneously minimizing the relative mass ΔM of the panel. Relative stiffness is acquired by dividing the numerically calculated conventional plywood board deflection value by the results of the sandwich panel at the same length and thickness configurations assuming that both numerical models have the same loading configurations. Moreover, the relative mass is acquired by dividing the sandwich panel mass by full plywood panel mass. Once the relative stiffness ΔK is close to 1, this indicates that the sandwich panel stiffness is similar to the stiffness of the plywood board. At the same time the parameter ΔM close to 1 means that the sandwich panel mass is reaching the mass of the full-cross section panel. The results of Pareto optimality are outlined graphically in Figure 6. The points on Pareto front line are marked with darker colour.

One may observe that average difference between the relative mass and stiffness is 30 %. For example, the sandwich panel which total volume bay is as low as 50 % of full plywood board maintaining 80 % of conventional plywood stiffness. Increasing the GFRP core wall thickness is possible to reach configurations where the sandwich panel stiffness is equivalent to the plywood board stiffness at the same time with 25 % reduced self weight. The acquired results serve as a tool for effective assessment of the bearing capacity of sandwich panels with a GFRP corrugated core.

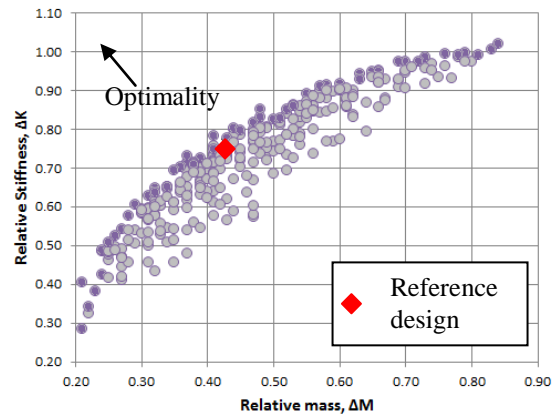


Figure 6. Pareto optimality between relative stiffness and mass

CONCLUSIONS

Several wood based sandwich panels with plywood skins and a corrugated GFRP core were prototyped and the stiffness properties evaluated in 4-point bending. The acquired mechanical responses served as means of validation of the numerical model. It has been confirmed that the numerical model has an ability to predict the mechanical behaviour of the panels in the region of linear elasticity where the calculated results are within scatter of the experimental load/deflection curves. Moreover, it has been recognised that deviation of the plywood upper plies thicknesses, as a result of surface grinding, has significant influence on the sandwich panel overall stiffness. Therefore it should be considered designing sandwich structures with plywood components.

The optimisation results demonstrated that the initial design of the corrugated core could be slightly improved, reducing the structural weight at the same time keeping the initial stiffness by increasing the angle of the corrugated layer. However, such a design makes manufacturing more complex. Once comparing the sandwich panel

design with conventional plywood board it may be concluded that the sandwich structure could be up to 65 % weight effective in bending load case up to the serviceability limit state. Pareto plot between the relative stiffness and mass indicates the region of the most efficient combinations where utilising the GFRP corrugated core is the most reasonable in order to match the conventional plywood board stiffness.

A similar design methodology could be further extended for optimisation of one shot thermoplastic composites with glass fibre reinforcement.

Additional experimental work is required to reduce the scatter of the experimental results in such a way improving the accuracy of the numerical model.

Acknowledgements

This study has received the support from the European Commission through the large-scale integrating collaborative project MAPPIC 3D - number 263159-1 and entitled: One-shot Manufacturing on large scale of 3D up graded panels and stiffeners for lightweight thermoplastic textile composite structures.

REFERENCES

- Akhbari, M., Shokrieh, M.M. & Nosratty, H. (2008) A study on buckling behavior of composite sheets reinforced by hybrid woven fabrics, *Transactions of the Canadian Society for Mechanical Engineering*, vol. 32, no. 1, pp. 81-90.
- Auziņš J., Januševskis A. (2007) *Eksperimentu plānošana un analīze*. Riga, RTU publishing. p. 208. (in Latvian lang.)
- ANSYS Version 11. (2009) *User Manual*, Papenburg, USA
- EN 789:2004. Timber structures. Test methods. Determination of mechanical properties of wood based panels. European Committee for Standardization (CEN), Brussels, Belgium
- Hudson C. W., Carruthers J.J., Robinson A.M. (2010) Multiple objective optimisation of composite sandwich structures for rail vehicle floor panels. *Composite Structures* 92, p. 2077–2082.
- Hunt J.F. (2004) 3D Engineered Fiberboard: Finite Element Analysis of a New Building Product. 2004 International ANSYS Conference. Pittsburg, PA, May, p. 24-26.
- Jekabsons G. (2010) VariReg: A software tool for regression modelling using various modelling methods, available at <http://www.cs.rtu.lv/jekabsons/> [online] [accessed on 04.04.2013.]
- Kalnins K., Jekabsons G., Zudrags K., Beitlers R. (2009) Metamodels in optimisation of plywood sandwich panels. *Shell Structures: Theory and Applications*, Vol. 2. Pietraszkiewicz W. and Kreja I. (eds.), CRC press /Taylor & Francis Group, London, UK, p. 291-294.
- Labans, E. & Kalniņš, K. (2011), Numerical versus experimental investigation of plywood sandwich panels with corrugated core, *Civil Engineering '11 - 3rd International Scientific Conference, Proceedings*, pp. 159.
- Luo S., Suhling J. C., Considine J. M., Laufenberg T. L. (1992) The bending stiffness of corrugated board. AMD-Vol. 145/MD-Vol. 36, *Mechanics of Cellulosic Materials*, ASME, p. 15-26.
- Rahman, A.A., Abubakr, S. (2004) A finite element investigation of the role of adhesive in the buckling failure of corrugated fiberboard, *Wood and Fiber Science*, vol. 36, no. 2, pp. 260-268.
- Šlisseris, J., Rocens, K. (2011) Rational structure of panel with curved plywood ribs, *World Academy of Science, Engineering and Technology*, Vol. 76, pp. 317-323.
- Zike, S., Kalnins, K., Ozolins, O. & Knite, M. (2011) An experimental and numerical study of low velocity impact of unsaturated polyester/glass fibre composite, *Medziagotyra*, Vol. 17, no. 4, pp. 384-390.
- Zudrags K., Kalnins K., Jekabsons G., Ozolins O. (2009) Bending properties of plywood I-core sandwich panel. *Proceedings of the 5th Nordic-Baltic Network in Wood Material Science and Engineering*. Meeting, Copenhagen, p. 169-175.
- Zhang, J., Chaisombat, K., He, S. & Wang, C.H. (2012) Hybrid composite laminates reinforced with glass/carbon woven fabrics for lightweight load bearing structures, *Materials and Design*, vol. 36, pp. 75-80.
- Eurocode-5 (1994). Design of timber structures, common rules and rules for buildings. *European Standard*, Bruxelles

OPTIMAL DESIGN OF VARIABLE STIFFNESS PLYWOOD- PLASTIC PLATE

Janis Sliseris*, Girts Frolovs**, Karlis Rocens***

Riga Technical University, Department of Structural Engineering

E-mail: *janis.sliseris@gmail.com, **girts.frolovs@gmail.com, ***rocensk@latnet.lv

ABSTRACT

A new optimization method of outer layer fibre directions and fiber relative concentrations of plywood plate with glass fibre-epoxy outer layers is proposed. The method minimizes structural compliance. It consists of two phases. The fibre directions are optimized in the first phase and concentrations in the second phase. The increase of stiffness is about 31% of the plate with optimized fibre direction and concentration comparing to a similar non-optimized plate.

Key words: plywood, glass fibre, fibre orientation, fibre concentration, minimal compliance

INTRODUCTION

Laminated plates and shells with variable stiffness have been intensively investigated during the past two decades.

These kinds of structures are becoming more popular due to the ability to achieve increased strength-to-mass and stiffness-to-mass ratios by tailoring the material properties. The fibre steering machines are becoming more popular in manufacturing variable stiffness glass or carbon fibre plates.

An optimal variable stiffness plate could be obtained by optimization of the fibre orientation angle (Keller, 2010; Pelletier, Vel, 2006; Gurdal, Olmedo, 1993) or thickness optimization (Almeida, Awruch, 2009; Muc, Muc-Wierzgon, 2012). A lamina with variable stiffness and curved fibres provides great flexibility to achieve the needed natural frequencies, mode shapes (Akhavan, Ribeiro, 2011), vibration amplitudes (Akhavan, Ribeiro, 2012) and buckling load (Setoodeh et.al., 2009). It is necessary to design constant thickness plates in many cases. Optimal properties of a constant thickness plate or shell are obtained by using the Genetic Algorithm (Sliseris, Rocens, 2011; Sliseris, Rocens, 2012) or Ant Colony algorithm (Sebaey et. al., 2011; Wang et.al., 2010; Hudson et. al., 2010) in cases of complicated objective function or many design variables. It is necessary to take into account the inter-laminar stress of variable stiffness lamina (Diaz et. al., 2012) in some cases.

The problem of optimal fibre orientation angle of multilayer lamina is successfully solved by using of the topology optimization approach (Diaz, Bendsoe, 1992; Bendsoe, 1989), discrete material optimization method (Lund, 2009; Niu et.al., 2010; Stegmann, Lund, 2005), Ant colony algorithm (Kaveh et.al., 2008) or Genetic algorithm (Hansel et.al., 2002). Optimizations of structural elements are done by taking into account uncertainty and

nonlinear effects (Jung, Cho, 2004; Asadpoure et.al., 2011).

Flexural plates, like glass fibre reinforced polymer(GFRP)-plywood, with variable stiffness have not been investigated enough by now. The optimization method for this type of structure should be specially created. Therefore, this publication is proposing a new optimization method for GFRP-plywood lamina fibre direction and concentration optimization and providing some typical results.

OPTIMIZATION METHOD

The lamination parameters that define stacking sequence of lamina by 12 parameters are usually used in optimization because relationship between stiffness and lamination parameters is convex. The lamination parameters are related to each other, therefore the problem with feasible region always appears in the optimization procedure. As well as an extra procedure for stacking sequence rendering from lamination parameters is necessary. To simplify this optimization technique and make it more applicable to flexural plates with symmetrical layup the authors of this publication are proposing a new method.

This method is based on structural compliance minimization:

$$\min_{\phi, k} U^T(\phi, k) K(\phi, k) U(\phi, k), \quad (1)$$

where

$U(\phi, k)$ – displacement vector;

$K(\phi, k)$ – global stiffness matrix;

$\phi = \{\phi_1, \phi_2, \dots, \phi_{Ne}\}$ - fibre orientation angles;

$k = \{k_1, k_2, \dots, k_{Ne}\}$ - fibre concentrations, that is volume fractional part of fiber in GFRP layer.

This method directly optimizes the fibre orientation angle and concentration of only outer layers of

symmetrical lamina. The outer layers play the most significant role in stiffness of flexural plate.

The material flexural stiffness matrix D_i of i -th finite element is modified by using the coordinate transformation matrix N and the fibre concentration coefficients k :

$$D_i = k_i N^T(\phi_i) D_i^0 N(\phi_i). \quad (2)$$

The proposed method is based on the algorithm that is shown in Fig.1. The algorithm consists of three loops. The first loop runs until the convergence criteria are satisfied. The second loop goes through all finite elements from 1 to N_e (number of finite elements). The third loop goes through all discrete values of the fibre orientation angles from 1 to N .

The fibre orientation angles are changed by special procedure $R(x)=x_j$. This procedure changes the orientation angle to x_j in the region with the centre in i -th finite element and influence radius R_{inf} .

The finite element analysis is done inside all loops. The value of the compliance function $C(i,j)$ (index i indicates i -th discrete angle and index j indicates j -th finite element) is calculated by using the results of the finite element analysis.

There is a special procedure that updates values of fibre orientation angles x inside the first loop. The updated value of x is obtained in each finite element according to minimal compliance.

The fibre concentrations are updated by using the following algorithm:

$$k_i = \max \left\{ \min \left\{ \frac{k_{min}}{\left(k_i * \frac{C(i)}{L} \right)^{0.5}}, \frac{k_{max}}{\left(k_i * \frac{C(i)}{L} \right)^{0.5}} \right\} \right\}, \quad (3)$$

where k_{min}, k_{max} –minimal/maximal value of possible concentration;

L –parameter that is used to limit the sum of concentrations in all finite elements.

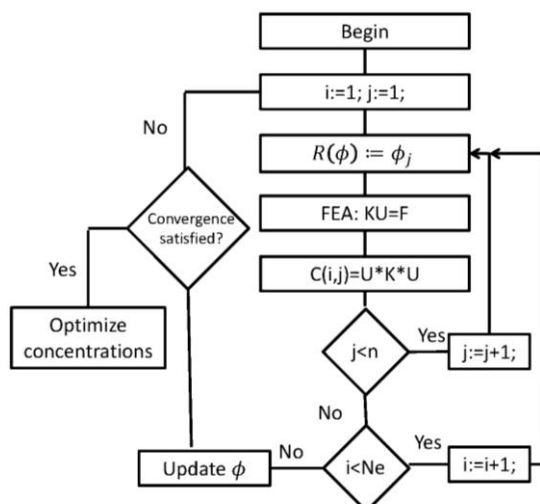


Figure 1. Fibre direction ϕ optimization algorithm

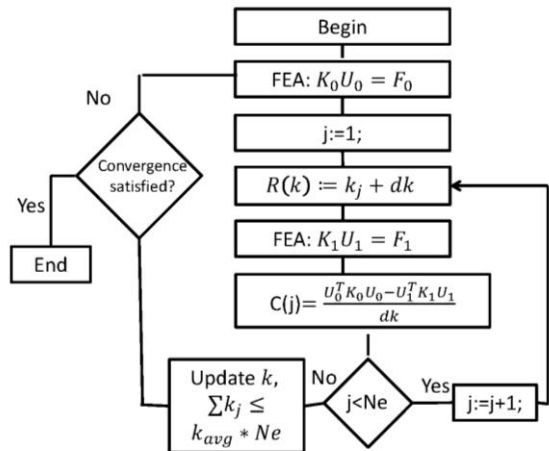


Figure 2. Fibre concentration k optimization algorithm

RESULTS AND DISCUSSION

The optimal fibre orientation angles and concentration ratio were obtained for a 19 layer symmetrical birch plywood sheet. The plywood sheet has the following lay-up $[\phi_1, 0, 90, \dots, 90, 0, \phi_1]$. The total thickness of the sheet is 26 mm. The outer layer of the sheet was made of glass fibre- epoxy. The birch plywood was used with the following elastic properties (Sliseris, Rocens, 2012): $E_1 = 16400 \text{ MPa}$, $E_2 = 500 \text{ MPa}$, $G_{12} = 890 \text{ MPa}$, $v_{12} = 0.3$. The glass fibre of grade E was analyzed using the following elastic properties: $E_1 = E_2 = 85000 \text{ MPa}$, $G_{12} = 35420 \text{ MPa}$, $v_{12} = v_{21} = 0.2$ (Bank 2006). The epoxy glue was assumed to have the following elastic properties: $E_1 = E_2 = 3400 \text{ MPa}$, $v_{12} = v_{21} = 0.3$, $G_{12} = 1308 \text{ MPa}$ (Clarke, 2005). Four discrete values of the fibre orientation angle were used: 0/45/90/135.

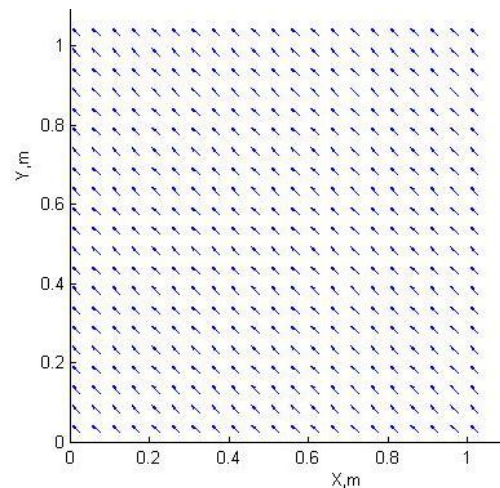


Figure 3. Fibre direction plot of a single span rectangular plate with dimensions 2.1 m x 2.1 m (due to symmetry shown one quarter of the plate)

The angle is between the x-axis (horizontal axis) and the fibre longitudinal axis. In all cases the influence radius (radius of domain where is changed fibre orientation angles) was constant $R_{inf}=0.15(m)$. The plates are loaded by 1 KPa uniformly distributed transversal load when searching for minimal compliance.

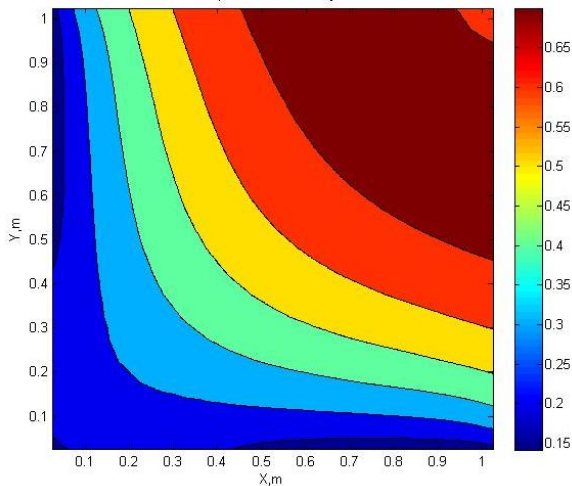


Figure 4. Fiber relative concentration plot of a single span rectangular plate with dimensions 2.1 m x 2.1 m (due to symmetry shown one quarter of the plate)

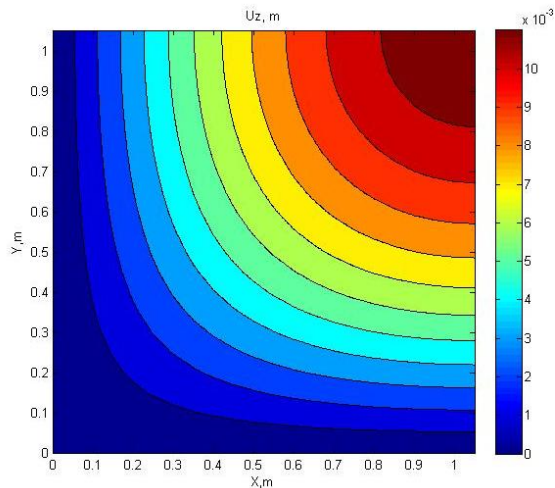


Figure 5. Deflection plot of a single span rectangular non-optimized plate with dimensions 2.1 m x 2.1 m (due to symmetry shown one quarter of the plate)

The optimal fibre concentration plot is shown in Fig. 4. It can be seen that the maximal amount of fibres should be put in the central part of the plate. The maximal deflection of a non-optimized plate is 0.0117 m. The maximal deflection of a plate with optimized fibre directions and constant concentration is 0.0101 m. The maximal deflection of the plate with optimal fibre directions and concentrations is 0.008 m. The difference between

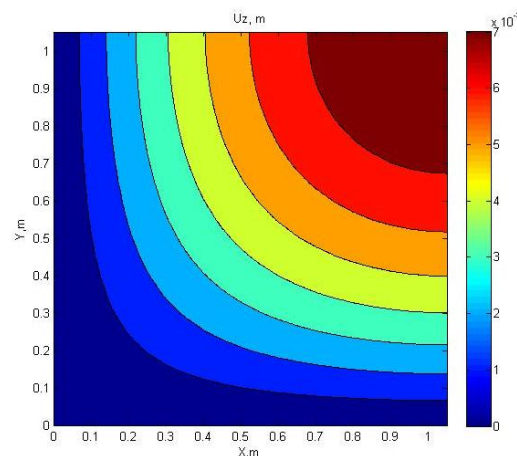


Figure 6. Deflection plot of a single span rectangular optimized plate with dimensions 2.1 m x 2.1 m (due to symmetry shown one quarter of the plate)

rotation angles of non-optimized and optimized plates is the same as for maximal deflection. The increase of stiffness of the optimized plate is not significant when a single span plate has one dimension significantly bigger than other. The optimization was done also for three span plates. The plots of optimal fibre directions and concentration of plate 0.7 m equal spans in both directions as it is shown in Fig. 7 and Fig. 8. The fibre direction is orthogonal with support lines. Maximal fibre concentrations are necessary on support lines. The fibre relative concentrations in the middle of spans are about 25% less than on support lines.

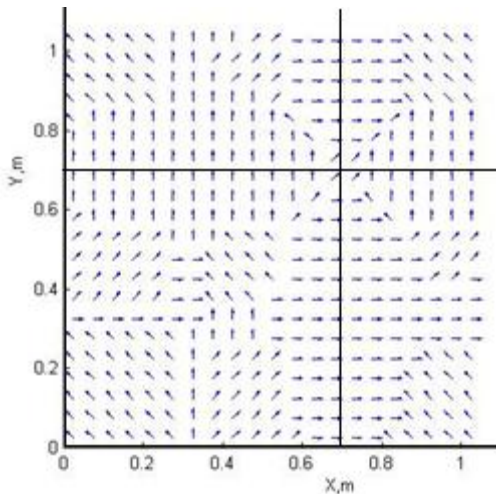


Figure 7. Fiber direction plot of a three span rectangular plate with spans 0.7 m x 0.7 m x 0.7 m in both directions (due to symmetry shown one quarter of the plate)

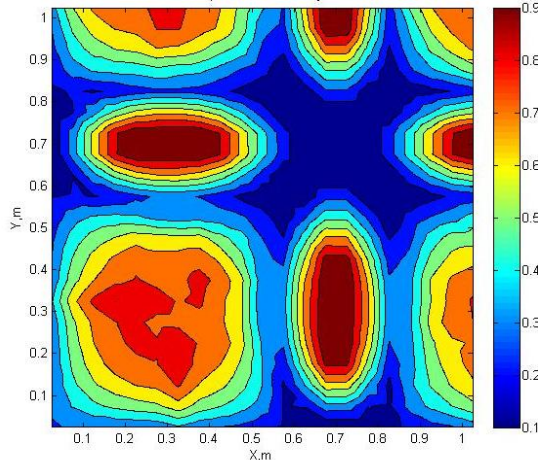


Figure 8. Fiber relative concentration plot of a three span rectangular plate with spans 0.7 m x 0.7 m x 0.7 m in both directions (due to symmetry shown one quarter of the plate)

The obtained optimal fibre orientation results show that a single simply supported plate could be effectively manufactured by making four different regions of the plate (see Fig. 3.). However, the concentration that is close to the necessary one could be achieved when additional four discrete regions are made (see Fig. 4.).

The three span plates could be divided in rectangular discrete domains to obtain fibre orientation and concentrations that are close to the necessary ones (see Fig. 7 and Fig. 8).

THE BEHAVIOR OF A PLATE WITH DISCRETE VARIABLE STIFFNESS

The manufacturing of continuously varying fibre placement may cause difficulties in manufacturing of GFRP-plywood composite. Therefore, the authors of this publication are proposing to make composite with discrete variable stiffness. It means that in discrete areas of the plate there are different fibre orientation and concentrations. Only discrete fibre orientation angles (0/45/90/135 degrees) and relative concentrations I (0.16/0.50/0.64/0.85); (0.18/0.50/0.67/0.85); (0.16/0.50/0.65/0.85) are used.

For each area the direction of glass fibres (0/45/90/135 degrees) and fibre relative concentration I are chosen. For each division three types of plates were analyzed – non-optimized directions (0 degrees) and non-optimized relative concentration (0.5); optimized directions (0/45/90/135 degrees) and non-optimized relative concentration (0.5); optimized directions (0/45/90/135 degrees) and optimized relative concentrations I .

Reduced modulus of elasticity (for relative concentration 0.5) for glass fibre layer is calculated

(Bank 2006) $E_1=58000$ MPa; $E_2=E_3=16400$ MPa; $G_{12}=G_{13}=6000$ MPa; $G_{23}=15000$ MPa; $v_{12}=v_{23}=0.233$; $v_{13}=0.056$

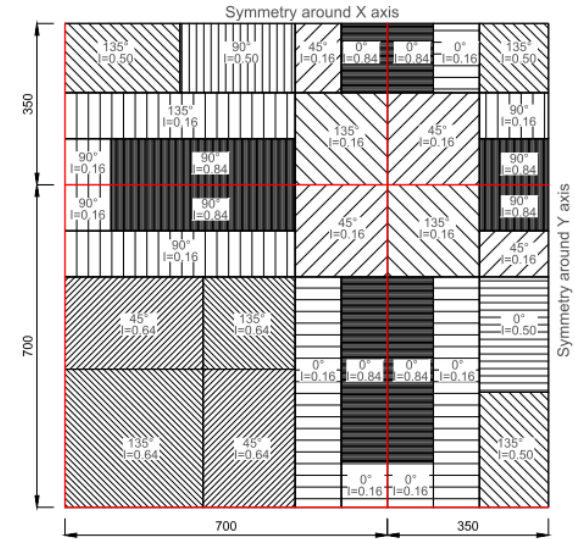


Figure 9. The plot of simply rectangular discrete domains including fibre orientations and concentrations of a three span rectangular plate (1 variant) with spans 0.7 m x 0.7 m x 0.7 m in both directions (due to symmetry shown one quarter of the plate)

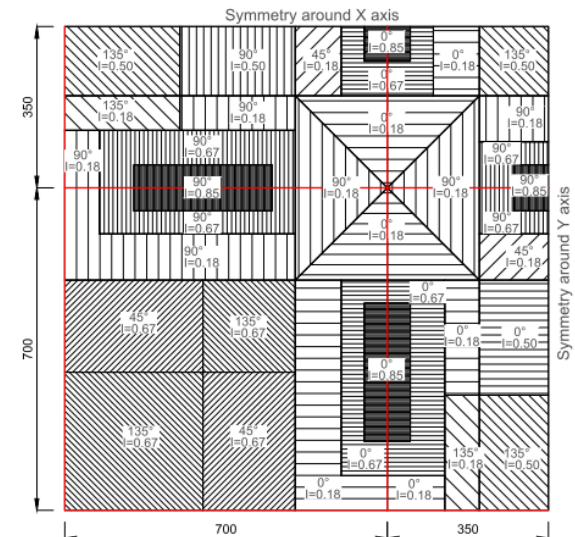


Figure 10. The plot of normal discrete domains including fibre orientations and concentrations of a three span rectangular plate (2 variant) with spans 0.7 m x 0.7 m x 0.7 m in both directions (due to symmetry shown one quarter of the plate)

The chosen discrete domains for 3 different complexities (1, 2, 3 variants) of discrete areas with intensities are shown in Fig. 9 - Fig. 11.

The plates are loaded by 1 kPa uniformly distributed transversal load the same as for one span plate example. Due to symmetry, one quarter of the plate was analyzed.

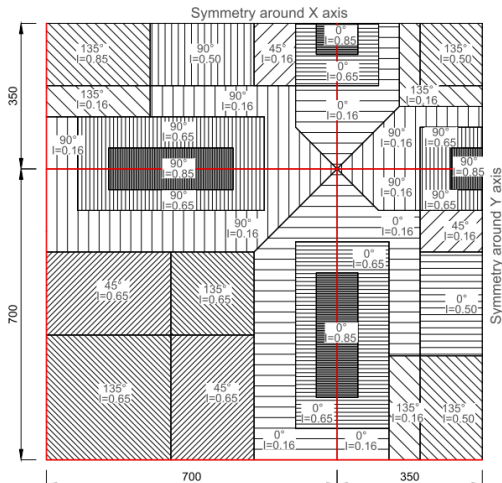


Figure 11. The plot of complex discrete domains including fibre orientations and concentrations of a three span rectangular plate (3 variant) with spans 0.7 m x 0.7 m x 0.7 m in both directions (due to symmetry shown one quarter of the plate)

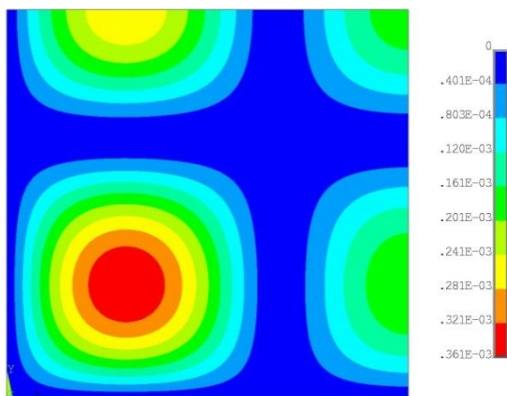


Figure 12. Deflection plot of a three span rectangular plate with spans 0.7 m x 0.7 m x 0.7 m in both directions for non-optimized plate (due to symmetry shown one quarter of the plate)

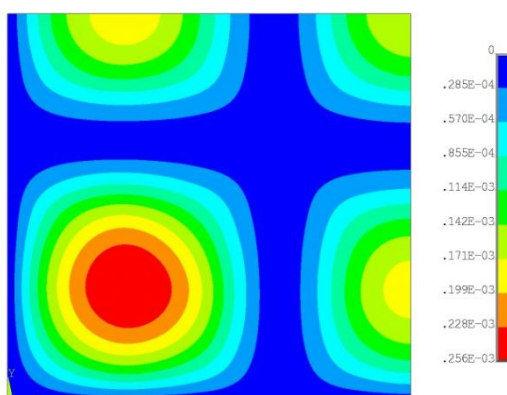


Figure 13. Deflection plot of a three span rectangular plate with spans 0.7 m x 0.7 m x 0.7 m in both directions for plate (1 variant) with optimized fibre directions and concentrations for simply rectangular division (due to symmetry shown one quarter of the plate)

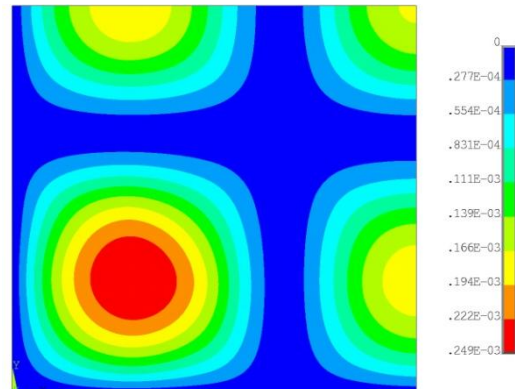


Figure 14. Deflection plot of a three span rectangular plate with spans 0.7 m x 0.7 m x 0.7 m in both directions for plate (2 variant) with optimized fibre directions and concentrations for normal division (due to symmetry shown one quarter of the plate)

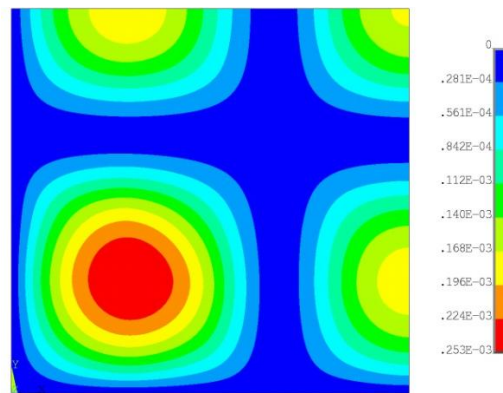


Figure 15. Deflection plot of a three span rectangular plate with spans 0.7 m x 0.7 m x 0.7 m in both directions for plate (3 variant) with optimized fibre directions and concentrations for complex division (due to symmetry shown one quarter of the plate)

The thickness of the GFRP layer is 1.75 mm, but the thickness of the plywood layers is 1.21 mm. The maximal deflection of a non-optimized plate is 0.000361 m (see Fig. 12). For the plate with optimized fibre directions and concentrations the maximal deflection is 0.000256 m (see Fig. 13) for simply division; 0.000249 m (see Fig. 14) for normal division and deflection of the plate with optimal fibre directions and concentrations it is 0.000253 m (see Fig. 15). The difference between the rotation angles of non-optimized and optimized plates is the same as for maximal deflection.

The comparison between analyzed structures of plate is shown in Table 1.

It is found that differences of displacements between all three cases (type of division) are similar (decrease of displacements is 18% when only the fibre direction is optimized and 31 % when fibre directions and concentrations are optimized) that

shows that even simpler division may lead to decrease of displacements).

The maximum displacements were in the middle of the first and last span of the plate for the three span plate.

Stresses in the direction of glass fibres increase for about 12% (from 9 MPa to 10 MPa, see Table 2). It means that stress in plywood reduces (see Table 3).

The values of stresses reduce for 8% with optimization of fibre directions and 35% with optimization of fibre directions and concentrations for tension. But for compression stresses reduce for 6% with optimization of fibre directions and 16% by optimization of fibre directions and concentrations. All values for three types of divisions are shown in Table 3.

Table 1
Comparison of maximal deflection (m) for different variants

	var. 1	var. 2		var. 3	
Not optimized:	0.000361	0%	0.000361	0%	0.000361
Optimized directions:	0.000295	-18%	0.000299	-17%	0.000299
Optimized directions and Intensities:	0.000256	-29%	0.000249	-31%	0.000253

Table 2
Comparison of maximal stress (MPa) in direction of glass fibre for different variants

	var. 1	var. 2		var. 3	
Not optimized:	8.960	0%	8.960	0%	8.960
Optimized directions:	8.405	-6%	8.380	-6%	8.389
Optimized directions and Intensities:	9.970	11%	10.036	12%	10.002

Table 3
Comparison of maximal stress in direction of wood fibre for different variants

	var. 1	var. 2		var. 3	
σ_{\max} not optimized:	2.170	0%	2.170	0%	2.170
σ_{\max} optimized directions:	1.989	-8%	1.984	-9%	1.986
σ_{\max} opt. directions and concentrations:	1.434	-34%	1.416	-35%	1.413
σ_{\min} not optimized:	-1.387	0%	-1.387	0%	-1.387
σ_{\min} optimized directions:	-1.291	-7%	-1.310	-6%	-1.311
σ_{\min} opt. directions and concentrations:	-1.179	-15%	-1.148	-17%	-1.169

CONCLUSIONS

New fibre direction and concentration optimization methods, which minimize the structural compliance, are proposed.

The GFRP-plywood composite plates provide a good possibility to increase the stiffness for more than 30%.

The maximal stress in the direction of glass fibre increases for 12%, but the maximal tensile stress in the direction of wood fibres decreases for 35 % for the optimized cases.

In future there should be a method created that calculates the optimal dimensions of discrete domains of the plate. Experimental investigations of GFRP-plywood plates should be made in future.

REFERENCES

- Akhavan H., Ribeiro P. (2011) Natural modes of vibration of variable stiffness composite laminates with curvilinear fibers. *Composite Structures*, Vol. 93, No. 11, p. 3040-3047.
- Akhavan H., Ribeiro P. (2012) Non-linear vibrations of variable stiffness composite laminated plates. *Composite Structures*, Vol. 94, No. 8, p. 2424-2432.
- Almeida F.S., Awruch A.M. (2009) Design optimization of composite laminated structures using genetic algorithms and finite element analysis. *Composite Structures*, Vol. 88, No. 3, p. 443-454.

- Asadpoure A., Tootkaboni M., Guest J. K. (2011) Robust topology optimization of structures with uncertainties in stiffness – Application to truss structures. *Computers and Structures*, Vol. 89, No. 11-12, p. 1131-1141.
- Bank L.C. (2006) *Composites for Construction Structural Design with FRP Materials*. Jon Willey & Sons. 567 p.
- Bendsoe M. (1989) Optimal shape design as a material distribution problem. *Structural and Multidisciplinary Optimization*, Vol.1, No. 4, p. 193-202.
- Clarke J.L. (2005) *Structural design of polymer composites*. London: E&FN SPON. 660 p.
- Diaz A., Bendsoe M. (1992) Shape optimization of structures for multiple loading conditions using a homogenization method. *Structural and Multidisciplinary Optimization*, Vol. 4, No. 1, p. 17-22.
- Diaz J., Fagiano C., Abdalla M.M., Gurdal Z., Hernandez S. (2012) A study of interlaminar stresses in variable stiffness plates. *Composite Structures*, Vol. 94, No. 3, p. 1192-1199.
- Gurdal Z., Olmedo R. (1993) In-Plane Response of Laminates with Spatially Varying Fiber Orientations: Variable Stiffness Concept. *AIAA Journal*, Vol. 31, No. 4, p. 751-758.
- Hansel W., Treptow A., Becker W., Freisleben B. (2002) A heuristic and a genetic topology optimization algorithm for weight-minimal laminate structures. *Composite Structures*, Vol. 58, No. 2, p. 287-294.
- Hudson C. W., Carruthers J. J., Robinson A. M. (2010) Multiple objective optimization of composite sandwich structures for rail vehicle floor panels. *Composite Structures*, Vol. 92, No. 9, p. 2077-2082.
- Jung HS., Cho S. (2004) Reliability-based topology optimization of geometrically nonlinear structures with loading and material uncertainties. *Finite Element Analysis and Design*, Vol. 41, No. 3, p. 311-331.
- Kaveh A., Hassani B., Shojaee S., Tavakkoli S.M. (2008) Structural topology optimization using ant colony methodology. *Engineering Structures*, Vol. 30, No. 9, p. 2559-2565.
- Keller D. (2010) Optimization of ply angles in laminated composite structures by a hybrid, asynchronous, parallel evolutionary algorithm. *Composite Structures*, Vol. 92, No. 11, p. 2781-2790.
- Lund E. (2009) Buckling topology optimization of laminated multi-material composite shell structures, *Composite Structures*, Vol. 91, No. 2, p. 158-167.
- Muc A., Muc-Wierzgon M. (2012) An evolution strategy in structural optimization problems for plates and shells. *Composite Structures*, Vol. 94, No. 4, p. 1461-1470.
- Niu B., Olhoff N., Lund E., Cheng G. (2010) Discrete material optimization of vibrating laminated composite plates for minimum sound radiation. *International Journal of Solids and Structures*, Vol. 47, No. 16, p. 2097-2114.
- Pelletier J. L., Vel S.S. (2006) Multi-objective optimization of fibre reinforced composite laminates for strength, stiffness and minimal mass. *Computers and Structures*, Vol. 84, No. 29-30, p. 2065-2080.
- Sebaey T.A., Lopes C.S., Blanco N., Costa J. (2011) Ant Colony Optimization for dispersed laminated composite panels under biaxial loading. *Composite Structures*, Vol. 94, No. 1, p. 31-36.
- Setoodeh S., Abdalla M. M., IJsselmuiden S. T., Gurdal Z. (2009) Design of variable-stiffness composite panels for maximum buckling load. *Composite Structures*, Vol. 87, No. 1, p. 109-117.
- Sliseris, J.; Rocens, K. 2013. Optimal design of composite plates with discrete variable stiffness, *Composite Structures* 98 (April): 15-23
- Sliseris, J., Rocens K. (2012) Optimization of multispan ribbed plywood plate macro-structure for multiple load cases, *Journal of Civil Engineering and Management* (accepted to publish).
- Sliseris J., Rocens K. (2011) Rational structure of panel with curved plywood ribs. *in proceedings of ICBSE 2011 : "International Conference on Building Science and Engineering"*, April, p. 317-323.
- Stegmann J., Lund E. (2005) Discrete material optimization of general composite shell structures. *International Journal for Numerical Methods in Engineering*, Vol. 62, No. 14, p. 2009-2027.
- Wang W., Guo S., Chang N., Yang W. (2010) Optimum buckling design of composite stiffened panels using ant colony algorithm. *Composite Structures*, Vol. 92, No. 3, p. 712-719.

FINITE ELEMENT ANALYSIS OF WEFT KNITTED COMPOSITES

Galina Harjkova

Riga Technical University, Institute of Mechanics

E-mail: Galina.Harjkova@rtu.lv

Pavels Akishins

Riga Technical University, Institute of Materials and Constructions

E-mail: Pavels.Akisins@rtu.lv

Olga Kononova

Riga Technical University, Institute of Mechanics

E-mail: Olga.Kononova@rtu.lv

ABSTRACT

In the present paper mechanical properties of knitted fiber reinforced polymer laminates are investigated experimentally and numerically, using unspecialized FEA. For this purpose the material unit cell was observed and its stress-strain statement was simulated using ANSYS commercial software depending on applied external loads. As example tensile properties (namely elastic modulus) in two principal directions of epoxy matrix E-glass knitted fabric laminated composites were obtained. The numerically predicted composite material mechanical parameters were compared with the experimental results and with the data obtained from previously performed analysis based on FEA software Solid Works. The numerically obtained longitudinal and transverse modulus comparison with the performed experiments has shown the ability to predict the material properties with reasonable accuracy.

Key words: textile composites, knitted fabric reinforcement, modeling, mechanical properties

INTRODUCTION

Knitted fabric reinforced composites show attractive properties - good impact resistance and high energy absorption, simultaneously high reinforcement deformability makes them possible to fit various complex preform shapes without forming folds (Miravete 1999). At the same time, mechanical properties prediction for such composite materials still needs additional investigations. It is worth mentioning that direct experimental determination of stiffness and strength for textile composites may be expensive and time consuming (Ernst 2010), however the results may be disappointing. Therefore, it is important to attempt to predict the composite materials properties and behavior and to optimize their internal structure and components features.

In the present paper the material (namely glass weft-knitted fabric/epoxy laminate) structure unit cell was recognized and its numerical model, based on ANSYS software, was elaborated and numerically exploited. Tensile testing in two principal directions of material was simulated. The obtained results (elastic modulus in two principal directions) were compared with the experimental data and the similar case study previously made by numerical simulation analysis executing SolidWorks (Kononova 2012, Krasnikovs 2012) software.

MATERIALS AND METHODS

Materials

The subject of investigation was weft-knitted glass fabric/epoxy laminated composite. E-glass fiber yarns, produced by JSC "Valmieras stikla šķiedra" (Latvia), were used. Density of the glass fibers was $\rho=2540 \text{ kg/m}^3$, diameter of the yarn $d=0.37 \times 10^{-3} \text{ m}$. Linear density of the glass yarn was calculated and it was equal to 275.6 tex. The value of elastic modulus for glass yarn was adjusted by the manufacturer and it was equal to 73.4 GPa.

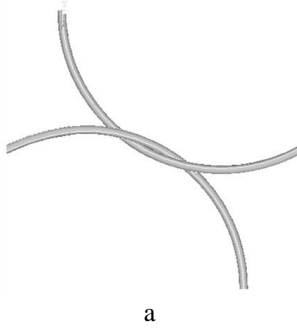


Figure 1. Structure of weft knitted fabric laminate
(created in WeftKnit software (KU Leuven))

Glass knitted fabric with stitch density $W=1.053 \text{ loops/cm}$, $C=2 \text{ loops/cm}$ was prepared by the authors on a flat-bed type knitting machine Neva-5. The fabrics were stacked and impregnated by polymer thermoset resin at room temperature. Epoxy resin was used. The laminate lay-up was $[0]_4$ (Fig. 1). Two plates were produced with thicknesses 0.176 and 0.202 cm.

Modeling

The material structural repeating element (unit cell) is shown in Figure 2. The material internal structure model was based on Leaf and Glaskin (Ramakrishna 1997, Ramakrishna 2000) geometrical formulas and was created using properties of real knitted textiles. The basic assumptions were: a) each yarn has a circular cross-section and it remains constant along the length of the yarn; b) the projection of the central axis of the yarn on the plane of the fabric is composed of circular arcs. Yarn is modeled as a solid element,



a

although in reality the structure of each yarn consists of fibers. The fabric in composite is in a relaxed state without pre-stretching.

Yarn 3D model was obtained, inputting x, y and z coordinates for both yarns after they were approximated by spline functions. Each yarn was simulated as a curved homogeneous elastic rod that creates a base by moving a profile (circle with certain diameter) along a particular spline curve. The model was meshed by eight-node Solid 45 elements.

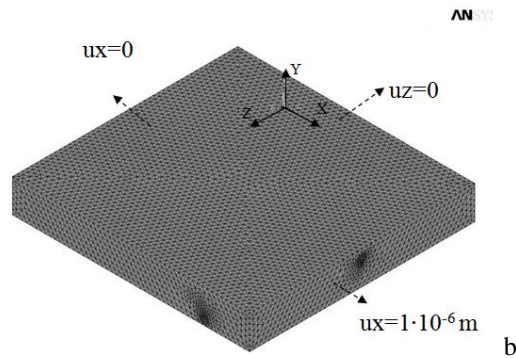


Figure 2. Material unit cell komponents: a – yarns in knitted fabric (top view), b – meshed unit cell (isometric view)

And at last, the assembly between the yarns and matrix was created. In the framework of this study it was accepted that between the yarns and matrix there is perfect bonding.

Performing tensile loading simulation, displacements were applied to the boundaries of the unit cell. The boundary condition for the studied laminate unit cell (with the goal to obtain longitudinal elastic modulus) is displacement along axis x direction equal to zero ($ux = 0$). On the opposite boundary $ux=1\cdot10^{-6}$ m. On other sides symmetry boundary condition was applied, boundaries of the unit cell remain flat during the deformation process. The coordinate axis and boundary conditions for longitudinal elastic modulus evaluation are shown in Fig. 2b. The scheme of the deformation process is shown in Fig. 3.

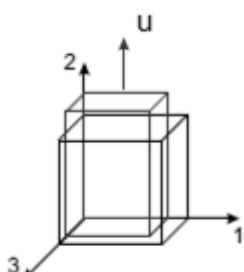


Figure 3. Deformed shape of the material unit cell

When deformed volume condition was achieved, the average value of longitudinal stress component on the stretched sample edge was obtained and the

elastic modulus in the stretching direction was calculated. Figure 4 shows the yarn-matrix meshed contact zone.

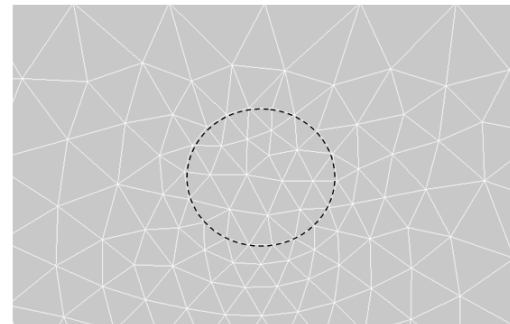


Figure 4. Yarn-matrix meshed contact zone on one of the boundaries

RESULTS AND DISCUSSION

In this paper FE model is used for predicting the elastic modulus of knitted glass fiber fabric reinforced epoxy composites. This methodology allows predicting the preliminary elastic properties of weft knitted fabric-reinforced composites.

The principal elastic modulus (longitudinal and transverse) obtained from the finite element analysis and from the tensile testing according ASTM D 5083-02 (Kononova 2012) in the wale and course directions with respect to the knitted fabric are summarized in Table 1. FE model shows

higher modulus especially in the course direction (Fig. 5 and 6).

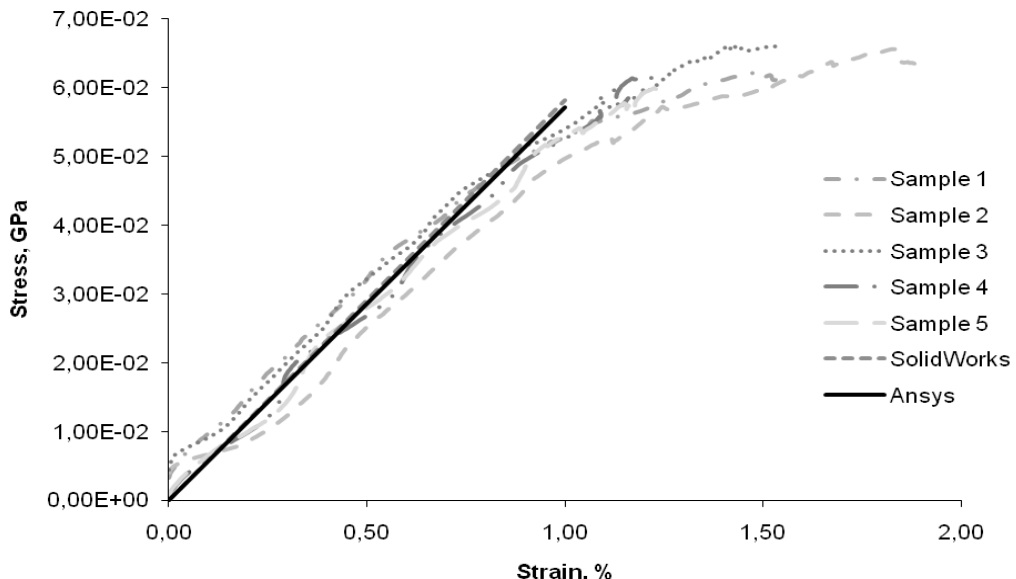


Figure 5. Stress-strain graphs for experimental, SolidWorks and Ansys FEM results for tensile testing in the wale direction

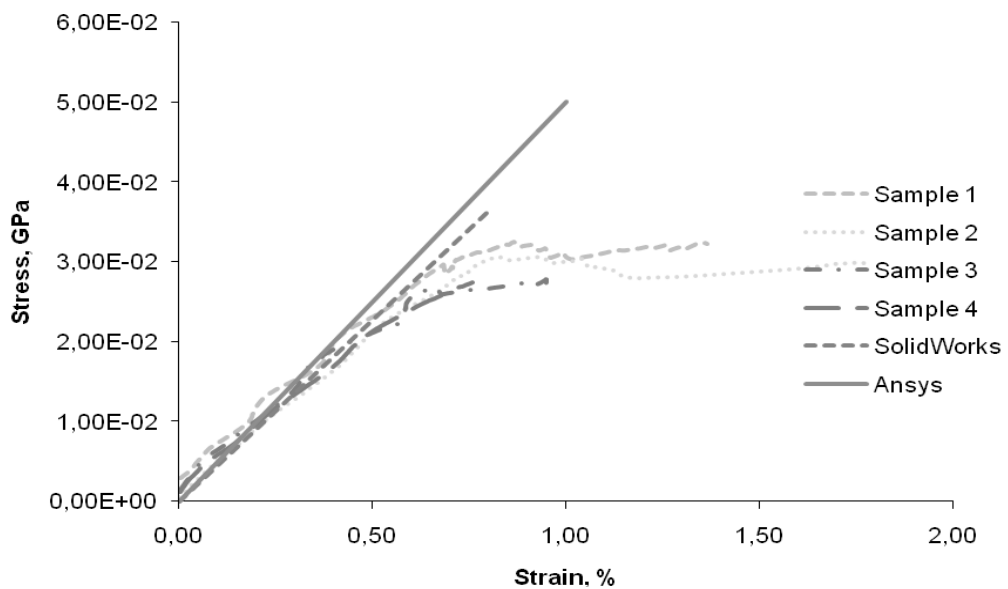


Figure 6. Stress-strain graphs for experimental, SolidWorks and Ansys FEM results for tensile testing in the course direction

Table 1
Comparison of the obtained elastic modulus of plain knitted glass fiber fabric/epoxy composite

Method	Longitudinal modulus E_x , [GPa]	transverse modulus E_z , [GPa]
Experiments	5.46	3.95
Ansys	5.71	5.00
SolidWorks (previous studies)	5.82	4.55

The differences between the experimental and simulation results may be attributed to inhomogeneous microstructure of the real material and the uncertainty on the fabric parameters as the fiber content, orientation and distribution in yarns, contact between composite components and yarns diameter variability, especially in yarn intersection zones.

Both the FE model yarn and matrix materials are considered isotropic, that can be a true assumption for epoxy resin, but unlikely for glass fibers and yarns. Also, there is a difference of load between the FEM simulation and experimental. Deviation between the results from different software can be explained with different mesh size and different solvers.

Efforts are being made to improve the described model and obtain realistic and reliable FEM modeling of this material model. Using the described unit cell FEA predicting the strength properties can be possible. Anisotropic material models can also be analyzed in future work.

CONCLUSIONS

The effective elastic constants (longitudinal and transverse modulus) of plain weft knitted glass fiber fabric reinforced epoxy 4-ply laminate were calculated. The unit cell approach was used; the spatial geometry of yarns were obtained using Leaf-Glaskin model. According used geometrical model yarns central axis projections are assumed composed of circular yarns and cross-sections are circular and constant. In the framework of this study yarns and matrix are perfectly bonded. Unit cell were simulated in FEM software (namely Ansys). Tensile properties in two principal directions were obtained and compared with the previously obtained experimental results. The predicted values show acceptable results comparing with the experimental results and previously obtained results in another FE program. This study shows that mechanical behavior of knitted textiles and its composites can be modeled using universal FEA software packages

REFERENCES

- Ernst G., Vogler M., Hühne C., Rolfs R. (2010) Multiscale progressive failure analysis of textile composites. Composites Science and Technology, Vol. 70, Iss. 1, p. 61–72
- Huang Z.M., Zhang Y., and Ramakrishna S. (2001) Modeling of the progressive failure behavior of multilayer knitted fabric-reinforced composite laminates. Composites Science Technology, 61(14): p. 2033-2046;
- Kononova O., Krasnikovs A., Harjkova G., Zaleskis J., Macanovskis E. (2012) Mechanical Properties Characterization by Inverse Technique for Composite Reinforced by Knitted Fabric. Part 1: Material Modeling and Direct Experimental Mechanical Properties Evaluation. Journal of Vibroengineering, Vol.14, Iss.2, p. 681-690.
- Krasnikovs A., Kononova O., Harjkova G., Zaharevskis V., Galuscaka A. (2012) Mechanical Properties Characterization by Inverse Technique for Composite Reinforced by Knitted Fabric. Proceedings of the 15th European Conference on Composite Materials (ECCM15), Italy, Venice, 24. June-28. July, 2012. – p. 42-45.
- Miravete A., (1999) 3-D textile reinforcements in composite materials. Cambridge, England, Woodhead Publishing Ltd, p. 180.
- Ramakrishna S., Hamada H., Cheng K. B., (1997) Analytical procedure for the prediction of elastic properties of plain knitted fabric-reinforced composites. Composites Part A, 28A: p. 25-37.
- Ramakrishna S., Huang Z. M., Teoh S. H., Tay A. A. O. and Chew C. L. (2000) Application of the model of Leaf and Glaskin to estimating the 3D elastic properties of knitted-fabric-reinforced composites. Journal of the Textile Institute, 91(1): p. 132 - 150.

ANALYSIS OF INTERFACIAL STRESSES BETWEEN COMPOSITE REBAR AND CONCRETE

Andrejs Kovalovs*, Georgij Portnov, Vladimir Kulakov, Alexander Arnautov **, Ellen Lackey ***

*Riga Technical University

Institute of Materials and Structures

E-mail: andrejs.kovalovs@rtu.lv

** University of Latvia

Institute of Polymer Mechanics

***University of Mississippi

Department of Mechanical Engineering

ABSTRACT

The objective of this study is to investigate and compare the interfacial stresses between glass-fiber reinforced polymer (GFRP) composite rebar and concrete under axial loading. Rebars of three different cross-sections are considered: circular one and circular with two and four longitudinal ribs. The design analyses of the rebar configurations embedded in concrete are investigated by the 3D finite element method (FEM) using ANSYS software. FEM results convergence was examined with different FE mesh sizes comparing the calculated stresses. The influence of rib geometry on the operating stresses was also studied. The results of the interfacial stresses calculated are applied as a basis for estimation of the effectiveness of composite rebar configurations in concrete structures, which can provide good bond characteristics.

Key words: composite rebars, design analysis, concrete structure, parametric study

INTRODUCTION

Fibre reinforced polymer (FRP) bars have become commercially available as reinforcement for concrete over the last decades. Durability, lightweight, long fatigue life and good corrosion resistance in aggressive environments are the main reasons of implementation into the civil engineering structures (Barboni et al., 1997, Emmons et al., 1998, Midwater et al., 1997, Nanni et al., 1995, Bakis et al., 1998).

Composite rebars made of glass, carbon and aramid fiber reinforced composites can be readily formed into complex shapes through the pultrusion manufacturing process. (Wallenberger et al., 2001, Walsh, 2001).

The most common manufacturing process is the pultrusion process, when the longitudinal fibers are drawn through a resin bath and then passed through a die, which gives the rebar of a final shape.

Recent studies have shown that, generally, the bond between the concrete and smooth FRP rods is affected by the non-isotropic mechanical properties of the FRP. The mechanical properties in the longitudinal direction are controlled by the fibres, but the stiffness and strength in the transversal direction depend on the resin matrix, low elastic modulus which can reduce the bond strength (Al-Zahrani et al., 1995). Moreover, the relative smoothness of FRP rods in the longitudinal direction compared to steel reinforcing bars can also reduce friction and thus the bond strength with concrete.

Additional techniques are required to improve the bond between the rebar and the surrounding concrete. Several techniques can be used, including surface deformations, sand coating, over-moulding a new surface on the bar or a combination of the techniques. Many researchers have brought up various formulae to estimate the bond strength of deformed composite reinforcement and studied experimentally and numerically the use of composite rebars as reinforcement in concrete structures.

Tighiouart et al. (1998) presented experimental investigations of concrete beams reinforced with two types of FRP rebars. The results of the tests indicated that the applied tensile load approached the tensile strength of rebars as the embedment length increased and the GFRP rebars showed lower bond strength values compared to steel rebars. The average maximum bond strength of the FRP rebars depends on the diameter and the embedment length. The GFRP rebars showed lower bond strength values compared to steel rebars. Nanni et al. (1994) presented experimental and analytical results for beams reinforced with hybrid rebars for the evaluation of the flexural behavior of the composite system. The tensile and interface bond strengths of composite rebars are the most important characteristics for establishing design procedures for reinforced composite concrete structures. Mirmiran and Shahawy (1996) considered that an effective use of fiber-reinforced plastic (FRP) rebar shapes in infrastructure is in the form of composite construction with reinforced concrete.

The finite element research of composite rebars with different shape has been proposed by (Kadioglu, 2005). Specifically four different composite rebar configurations under axial, bending and torsional loadings are investigated using the 3D finite element analysis. The composite rebar configurations investigated include square rebar, circular rebar with ribs, and ribs oriented at an offset angle along the length of the rebar. The results of interface stresses obtained are presented and compared among various rebar configurations under axial, bending and torsional loadings. The idea of using ribs is to improve the bond characteristics with the surrounding concrete. The results presented in this research illustrate that various design features added to the circular composite rebar may provide good bonding characteristics and can be used in reinforced concrete structures.

The objective of this study is to investigate and compare the interfacial stresses between glass-fiber reinforced polymers (GFRP) composite rebar and concrete under axial loading using finite element software. The influence of rib geometry on the operating stresses is presented to illustrate the effectiveness of composite rebar configurations in beam type reinforced concrete structures. The bond stress of a usual smooth composite rod was used as reference.

COMPOSITE REBAR

Materials and configuration

Three different types of concrete composite rebar configurations for improving the bond properties under axial loading are considered in this research. The first rebar R1 (Fig. 1a) has a standard circular

cross-section that is commonly used in construction industry (Fig. 1). The second R2 and third R3 rebars have circular cross-sections with two and four longitudinal ribs respectively (Fig. 1b, c).

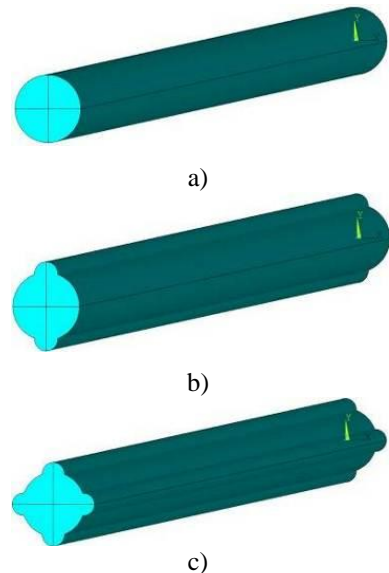


Figure 1. Shape of rebars (R1), (R2) and (R3)

Other possible configurations of this rebar type are not considered in this study. All rebars are made of fiber-reinforced polymer composite, which can be easily manufactured through the pultrusion process. Composite rebar embedded in a cylindrical concrete block: $D = 39$ mm (diameter) and $L = 20$ mm (length). The height of rib (h) is 2 mm, width of rib (w) is 4.5 mm, diameter of rod (d) is 13 mm and length of composite rebar (l) is 250 mm (Fig. 2).

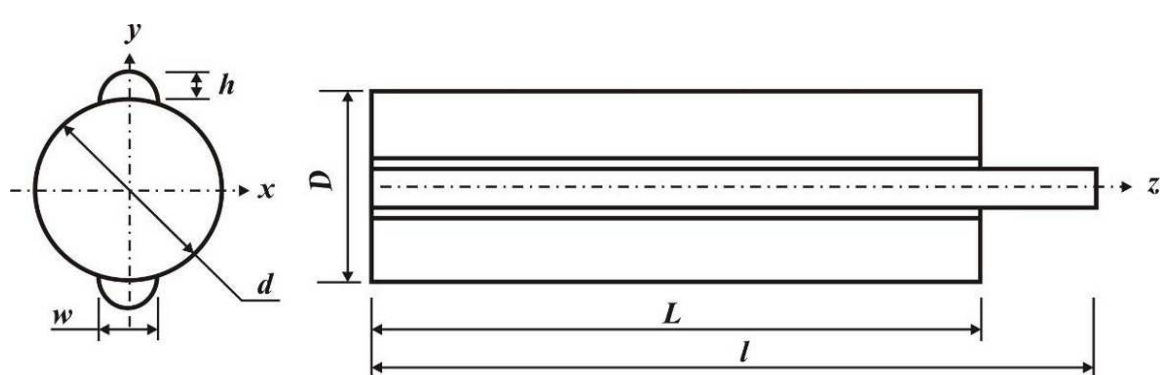


Figure 2. Cross-sectional geometry of a composite rebar R2

The following properties are used in the finite element analysis for the concrete ($E = 30$ GPa and $\nu = 0.15$) and composite rebars UD GFRP/epoxy ($E_1 = 54$ GPa; $E_2 = E_3 = 18$ GPa; $G_{12} = G_{13} = 4.9$ GPa, $\nu_{12} = \nu_{13} = 0.25$).

Uniaxial loading was carried by axial displacement of 2 mm applied to one side of the composite rod with rebars.

Finite element models

The 3D finite element models of the composite rebars and the surrounding concrete were simulated

by software ANSYS. The composite rebar and concrete are modelled using 3D brick elements SOLID185. The SOLID185 element type is defined by eight nodes and has three degrees of freedom (translations in x , y , z directions) at each node. The concrete rebar having circular and circular with ribs configurations enclosed in a concrete block are considered. Due to the geometrical symmetry of the configurations considered, one quarter of their volume was modelled.

At the beginning, it is necessary to conduct the convergence tests for the finite element model developed and validate the correctness of FEM discretization for the next calculation work. Convergence of the FEM results was examined for

several models with different mesh sizes and by comparing the resulting stresses. Based on these results, the appropriate mesh with brick finite elements was chosen as primary for FEM model. Fragments of FEM models are shown in Fig. 3 for rebars with different cross-sections.

All calculations were made with the finite element method by creation of a friction interface between the composite rod and concrete. 3D contact FEM problems for the research system were considered and the compressive strength is analyzed.

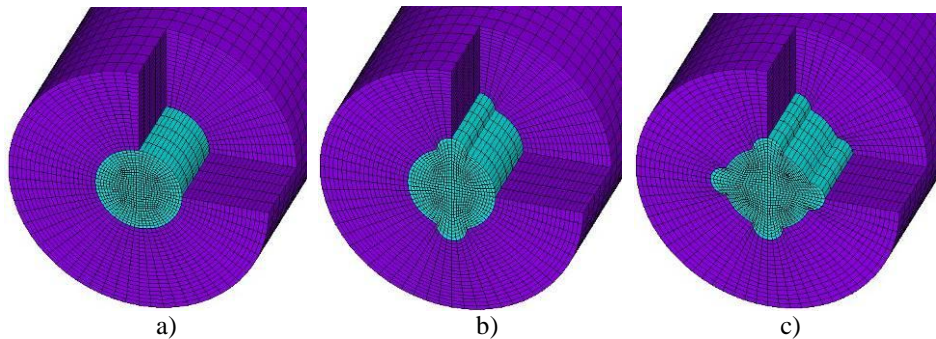


Figure 3. Finite element models for composite rebars R1 (a), R2 (b) and R3 (c)

RESULTS AND DISCUSSION

Interfacial stresses distributions

The distribution of interfacial shear stresses τ_{yz} at the interface of the rebars R1, R2 and R3 under axial loading is shown in Fig. 4.

It is seen that the rebar with 2 ribs is subject to shear stress of about 25 % higher than the rebar with 4 ribs ($|\tau_{yz}^{\max}| = 51.3$ and 38.3 MPa, respectively). Moreover, location of maximum shear stress depends also on the rebar configuration (Fig. 5).

Rib height effect

An important geometrical parameter of the rebars is the height of the ribs. The results presented in Fig. 6 illustrate the influence of the rib height on the maximum interfacial shear stresses for rebars with 2 ribs and 4 ribs under axial loading. The width of the ribs was 4.5 mm in all rebars studied.

It is seen that the maximum interfacial shear stresses for the rebar with 2 ribs is much higher than with 4 ribs. Depending on the rib height, this difference changes from 25% ($h = 2$ mm) to 45% ($h = 4$ mm).

Rib height and width effect

The following step of FEM calculations was concerned with estimation of interfacial shear stresses in the case of simultaneous variation of the

rib height and width. The maximum interfacial shear stresses calculated for rebars with 2 and 4 ribs under axial loading are shown in Figure 9.

The data of Figures 10 and 11 show the distribution of interfacial shear stresses along the length of the rebars with 2 and 4 ribs depending on the rib height and width.

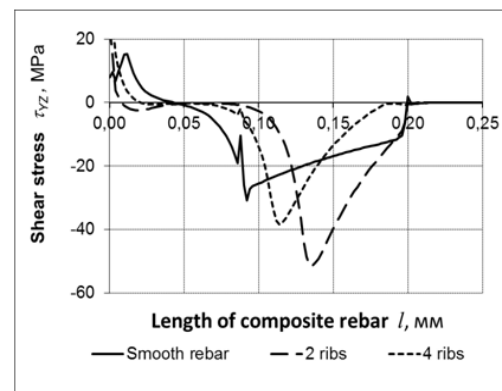


Figure 4. Distribution of interfacial shear stresses at the interface of the rebars R1, R2, R3

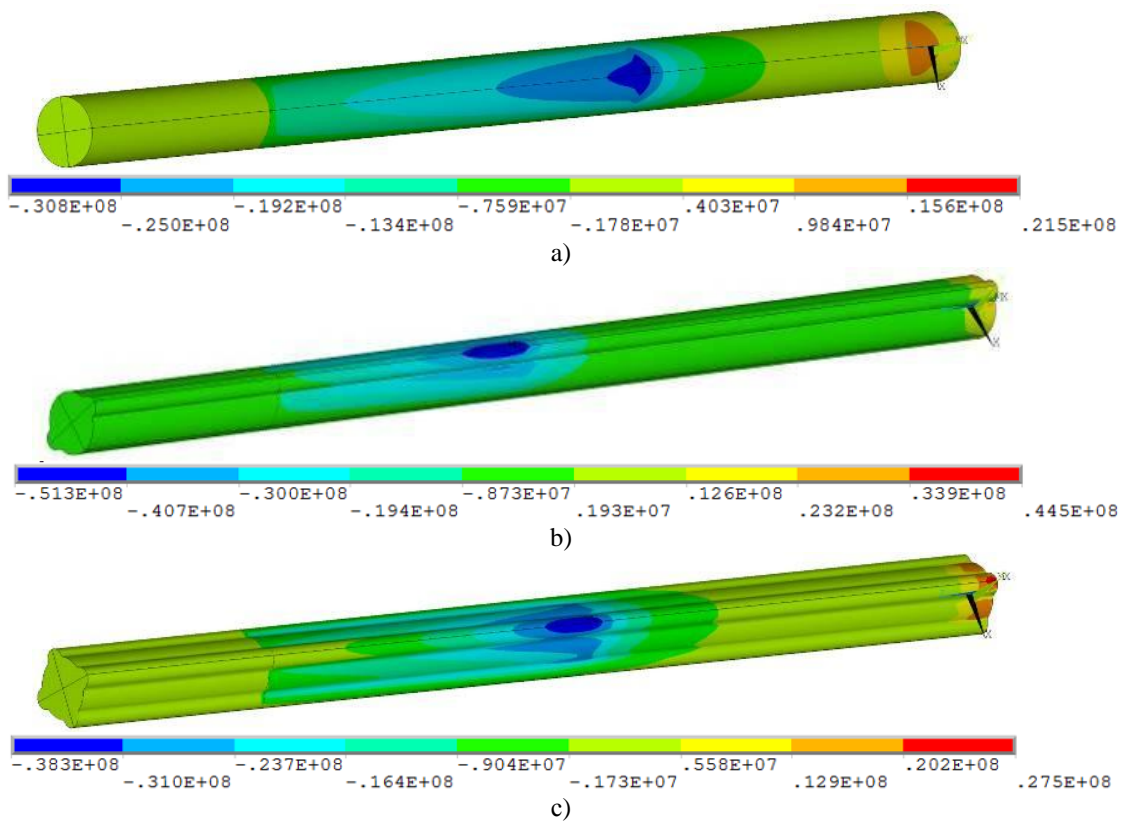


Figure 5. Distribution of shear stresses in rebars R1 (a), R2 (b) and R3 (c)

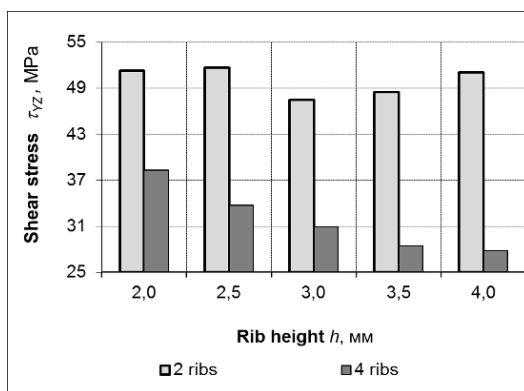


Figure 6. Maximum interface shear stresses for rebars R2 and R3 via rib height

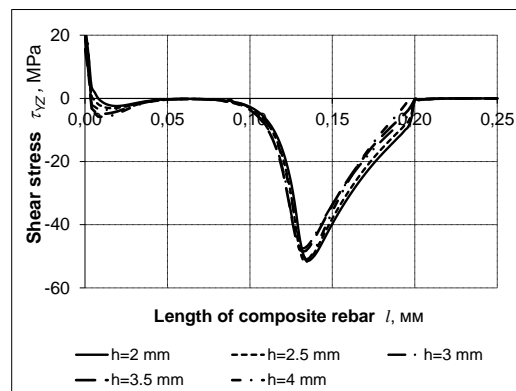


Figure 7. Shear stress distributions in rebar R2

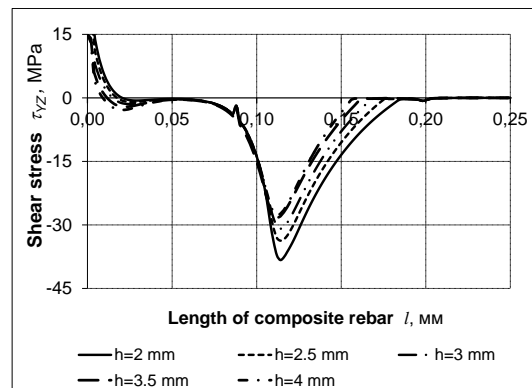


Figure 8. Shear stress distributions in rebar R3

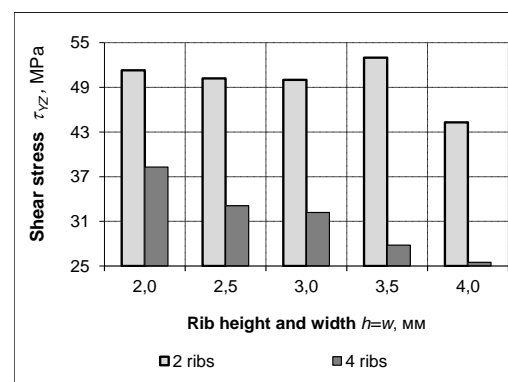


Figure 9. Maximum interface shear stresses for rebars R2 and R3 via rib height and width

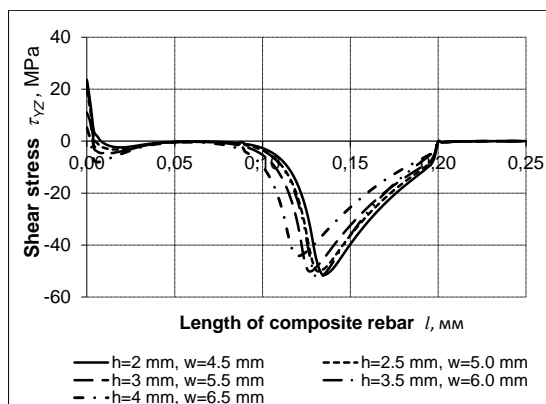


Figure 10. Shear stress distributions in rebar R2

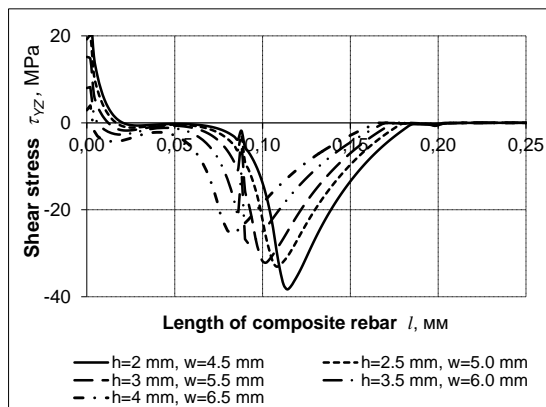


Figure 11. Shear stress distributions in rebar R3

CONCLUSION

The numerical stress analyses for the composite rebars embedded in concrete are investigated by the 3D finite element method (FEM) using ANSYS software. The rebars of circular cross-section with two and four longitudinal ribs, as well without ribs were studied. Based on the results of the preliminary parametric analysis of interfacial shear stresses under uniaxial tension of the composite rebars, the following conclusions can be made.

- Number of the longitudinal ribs influences significantly on the mechanical bond between composite rebars and concrete.
- In the case of rebars with four longitudinal ribs, maximum shear stresses τ_{yz}^{\max} are 25% less than that for rebars with two ribs.
- It was shown that height and width of the ribs were also strongly effect of the magnitude of interfacial stresses τ_{yz}^{\max} .

Thus, solution of the optimization problem with searching the optimal set of the parameters of composite rebars enhancing their mechanical bond with concrete will be the further step of the investigation.

ACKNOWLEDGEMENT

This work has been supported by ERAF project Nr/2010/0296/2dp/2.1.1.1.0/10/APIA/VIAA/049

REFERENCES

- Al-Zahrani M.M. and Al-Dulaijan S.H. (1995) Annotated bibliography of bond behavior in FRP/concrete systems. Report CMTG-9501. Composite Manufacturing Technology Centre. p.72.
- Bakis C.E., Uppuluri V.S., Nanni A, and Boothby T.E. (1998) Analysis of bonding mechanisms of smooth and lugged FRP rods embedded in concrete. *Composite Science and Technology*. Vol. 58, p. 1307–19.
- Barboni M., Benedetti A., and Nanni A. (1997) Carbon FRP strengthening of doubly curved precast PC shell. *Journal of Composite Construction*, Vol. 1, p 168–74.
- Emmons P.H., Vaysburt A.M., and Thomas J. (1998) Strengthening concrete structures, part II. *Concrete International*, Vol. 20, No. 3, p. 56-60.
- Fethi Kadioglu, Ramana M., and Pidaparti (2005) Composite rebars shape effect in reinforced structures. *Composite Structures*, Vol. 67, No. 1, p. 19–26.
- Midwater KR. (1997) Plate bonding carbon fiber and steel plates. *Construction Repair*, Vol. 11. p. 5–8.
- Mirmiran A. and Shahawy M. (1996) A new concrete-filled hollow FRP composite column. *Composites Part B*, Vol. 27, No. 3–4, p. 263–8.
- Nanni A., Henneke M.J., and Okamoto T. (1994) Behaviour of concrete beams with hybrid reinforcement. *Construction and Building Materials*, Vol.8, No. 2, p. 89–95.
- Nanni A. (1995) Concrete repair with externally bonded FRP reinforcement: examples from Japan. *Concrete International*, Vol. 17, p. 22–6.
- Tighiouart B., Benmokrane B., and Gao D. (1998) Investigation of bond in concrete member with fibre reinforced polymer (FRP) bars. *Construction and Building Materials*, Vol.12, No. 10, p. 453–462.
- Wallenberger F.T., Watson J.C. and Hong L. (2001) Glass Fibers. *ASM Handbook-Composites*. Vol. 21, p. 27-34.
- Walsh P. J. (2001) Carbon Fibres, *ASM Handbook-Composites*. Vol. 21, p. 35-40.

INFLUENCE OF FIBRE AMOUNT ON SFRC PRE- AND POST-CRACK BEHAVIOUR

Ulvis Skadins, Janis Brauns

Latvia University of Agriculture
Department of Structural Engineering
E-mail: ulvis.skadins@llu.lv

ABSTRACT

Researchers agree that the number and orientation of the fibres largely influence the properties of steel fibre reinforced concrete (SFRC) member before and after cracking. There are proposed models in the literature, which can be used to predict the fibre number per cross-section assuming homogeneous fibre distribution. Thus, the expected number of fibres in every section can be calculated from the total fibre amount per volume. Nevertheless, other researches based on experimental data have shown that there is a difference between the theoretical and actual number of fibres, and it varies for different fibre volume fractions. In this paper experimental investigation of fibre distribution and orientation is represented. The location of cracks with respect to the fibre distribution in flexural elements is studied. It is shown by this research, that the theoretical prognosis of the fibre number per cross-section may largely overestimate the actual number of fibres in the fracture plane.

Key words: steel fibres, fibre density, fibre distribution, fibre orientation, cracks

INTRODUCTION

One of the most important factors, influencing behaviour of a structural element, is the distribution of reinforcement in the material. If SFRC is compared with conventionally reinforced concrete, the main difference is the uncertainty and unpredictability of the location and orientation of reinforcement in SFRC. Indeed, fibres are randomly distributed throughout the concrete and their spatial position can be influenced by numerous factors.

Experimental studies have shown that strong connection exists between the fibre distribution, workability and the mechanical properties of fibre reinforced concrete (Ferrara and Meda, 2006). It was observed for a large number of test series that the measured equivalent flexural tensile strength is proportional to the number of effective fibres crossing the crack (Dupont, 2003).

Deformation and strength properties of uncracked and cracked SFRC elements are affected by fibre distribution in terms of the three main aspects: 1) fibre amount bridging a fracture plane; 2) uniformity of the distribution of fibres all through the cross-section; 3) orientation of fibres corresponding to the longitudinal axis of the element. Although there are analytical methods for predicting the fibre number per cross-section of a structural element, most of them are based on assumptions of homogeneous fibre distribution, where no segregation of fibres is considered. Thus, the number of fibres in a particular section is proportional to the total number of fibres per unit of volume. Actually, many authors have studied the relationship between the content of fibres V_f and the number of fibres n_f counted on the fracture surface

of the tested specimens. As it was expected, n_f increased with V_f , but the $V_f - n_f$ relationship has large scatter since the fibre distribution depends on many factors such as the fibre geometric characteristics, concrete composition and cross section dimensions of the element (Barros et al., 2005; Barragán et al., 2003). Due to uneven fibre distribution the number of effective fibres along the length of a structure is also different.

Besides the fibre amount, the distribution of fibres throughout the particular cross-section is significant. The efficiency of fibres reduces, if they are not distributed evenly or they are concentrated in regions, where no tensile stress needs to be transferred. On the other hand, Stahli et al. (2008) observed that fibre segregation led to a much higher bending strength than expected due to fibre alignment only, at least as long as the segregated fibres are located along the tensile stressed part of the beam.

The effectiveness of fibres in the fracture plane is largely influenced by the orientation of the fibres. There is a correlation between the bending strength and fibre alignment: better fibre-alignment leads to a higher bending strength (Stahli et al., 2008). The analysis of the bond properties between the fibres and concrete shows that the maximum pull-out force has to be applied to the fibres with the inclination angle of 0 ... 20 (Robins et al., 2002). Furthermore, the fibres oriented almost parallel to the crack plane, have no direct contribution in stress bridging. The average orientation of fibres is commonly characterized through the so-called orientation number which varies from 0.0 to 1.0 referring to fibres parallel and orthogonal to the

analysed cross-section, respectively. Large orientation numbers not only provide improved properties, but also induce smaller scattering on the performance, which may be an aspect of superior importance for design purposes (Laranjeira et al., 2011).

The aim of this study is to investigate the influence of fibre distribution and orientation on the crack initiation in SFRC flexural elements and to evaluate the applicability of analytical methods for predicting number of fibres in fracture plane. Concrete beams with normal dosage of fibres, beforehand tested in four-point bending till failure, were sawn in multiple sections in three main directions, and fibres were manually counted on all surfaces. The obtained data are compared with the results calculated by an analytical method available in literature.

EXPERIMENTAL STUDY

Manufacturing of the specimens

The experimental investigations on fibre distribution and orientation were performed on SFRC beams with dimensions of $100 \times 100 \times 500$ mm. Samples with different types and amount of fibres were manufactured, tested under four-point bending till failure and then sawn for counting the number of fibres on every "new" surface of prismatic specimens.

Fibres of three different shapes were used: 1) crimped, 2) hooked with round cross-section, and 3) crimped with flat cross-section. The samples with crimped round fibres were marked as group S1, samples with hooked fibres – as group S2, and samples with crimped flat fibres – as group S3.

There were three specimens in every group, thus altogether 9 specimens were observed. The nominal fibre amount for groups S1 and S3 was 1% by volume (or approx. 80 kg/m^3) and 0.75% by volume (approx. 60 kg/m^3) for group S2. The length of the fibres of all types was 50 mm. Crimped-round and hooked fibres were of equal diameter of 0.75 mm, while crimped flat fibres were with a larger cross-sectional area thus less in number per kg.

Counting of fibres

Hardened samples, after testing under four-point bending, were sawn with a diamond circular saw and every specimen was marked according to its position in the specimen. For determining the fibre distribution the manual fibre counting method was used, which is applicable for specimens with normal fibre dosages up to 80 kg/m^3 (Gettu, 2005). The number of cut fibres was registered for three main directions. The fibres crossing X-planes were considered as ones oriented in the longitudinal direction. The fibres counted on Y- and Z-planes are considered as ones aligned transversally to the main axis of the beams in vertical and horizontal directions respectively. The direction of concrete casting and compacting is considered as the vertical direction, which is represented by Y-planes. The cutting planes are shown in Figure 1.

Longitudinal planes were located in the middle and at a distance of 10 mm from each side of the beams. Transversal cuts were made with a distance of 40 mm starting at a distance of 10 mm from each end of the specimen. Thus, from each specimen 48 sample cubes with the length of the edge of 40 mm and area of a side of 16 cm^2 were obtained.

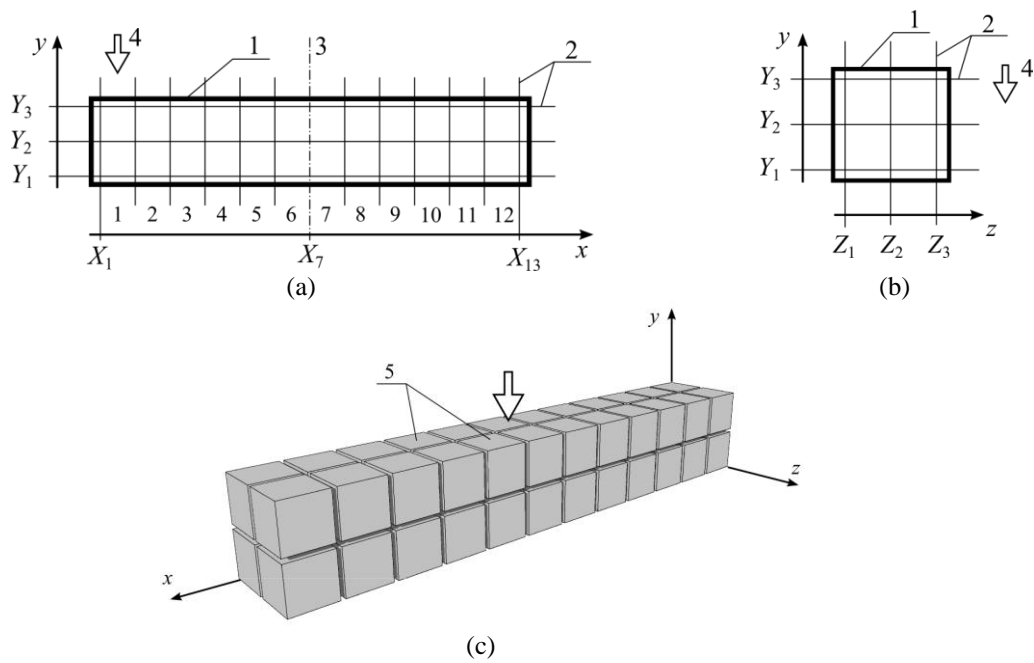


Figure 1. Position of planes used for fibre distribution analysis,

Where: (a) longitudinal side view, (b) cross-section, (c) 3D view; 1 – sample beams, 2 – cutting planes, 3 – plane of symmetry, 4 – casting direction, 5 – cube specimens

For every beam there were 52 planes with the dimensions of 40×40 mm normal to the longitudinal axis. The planes parallel to the longitudinal axis were 72 in each direction. The total number of the observed planes was 196. The fibres in each plane were counted and the average was noted.

Results and analysis

It was observed that the distribution and orientation of the fibres in the manufactured specimens were influenced by two main factors, which are mentioned by other researchers as well. First, the fibre orientation is much influenced in the regions near the walls of the moulds, which is called the wall-effect. In the observed specimens the number

of the cut fibres is notably smaller in the outer planes compared with the number in the middle planes. Second, the distribution and orientation of the fibres is affected by the technique used for concrete placing and compacting.

If fibre distribution along the length of the beam specimen is assessed, the difference between the average values of the fibre count in the longitudinal and transversal planes is insignificant. However, there are differences in the "shape" of the distributions. The comparison of the fibre density (number of fibres per 1 cm^2) for different directions along the length of the beams of group S1 is illustrated in Figure 2.

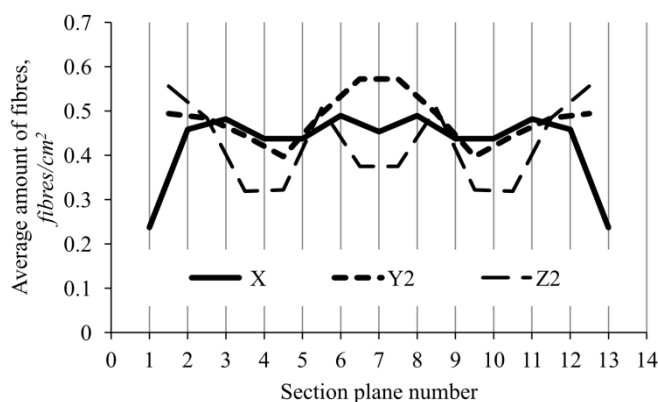


Figure 2. Variation of fibre density along the length of the beam (sample group S1)

Distribution and orientation of fibres

The study of the distribution and orientation of fibres was done in three ranges with respect to the longitudinal direction of the beams. The ranges are: 1) along the whole length of the beam or all X-planes and the regions between them, which allows to evaluate the wall-effect; 2) part of the beam between the planes X_2 and X_{12} to exclude the wall-effect when statistical quantities are calculated; 3) interval between the applied concentrated loads (in four-point bending test), i.e., between the planes X_5 and X_9 . This is the region of the maximum bending moment, where cracks are expected to occur. This range is used to study the influence of fibre distribution on initiation of cracks in SFRC beams, discussed later.

The total number of fibres per beam specimen, counted on the surfaces of the cut planes, was from 1006...1156 fibres for group S1, 682...725 fibres for group S2, and 535...625 fibres for group S3.

The specimens from groups S1 and S3 had the same nominal fibre amount per volume (80 kg/m^3), while the relationship between the number of fibres in group S3 and S1 is 53%, which is due to different cross-sectional areas of the fibres.

Analysing the obtained data, some characteristics and tendencies of fibre distribution and orientation can be pointed out. First, as it can be expected, there is a tendency for fibres to be oriented more in horizontal position, though a minimal compacting was applied. Considering the horizontal planes, more fibres were in the transversal (crossing Z-planes) than longitudinal (crossing X-planes) direction.

Data dispersion of the fibre density is higher for the specimens with a larger number of fibres (Fig. 3). That leads to comparatively small difference between the properties of the weakest sections, though the average fibre amount is different. Thus, the properties of the weakest section of a SFRC beam, which determines the behaviour of the element under flexure, may not be proportional to the total or average number of fibres per sample. No significant correlation between the number of fibres and the dispersion of fibre orientation was observed.

Variation of fibre orientation within a specimen is rather large. If the ratio of the fibres aligned with the longitudinal direction to the fibres of the transversal direction is considered, the variation coefficient is 0.25...0.42. In this case neither the

number of fibres nor the amount of fibres by volume correlate with the variation coefficients of both the fibre density and orientation. The variation coefficient of the fibre density is similar for all specimen groups: 0.2...0.33 for S1, 0.2...0.33 for S2, and 0.23...0.32 for group S3.

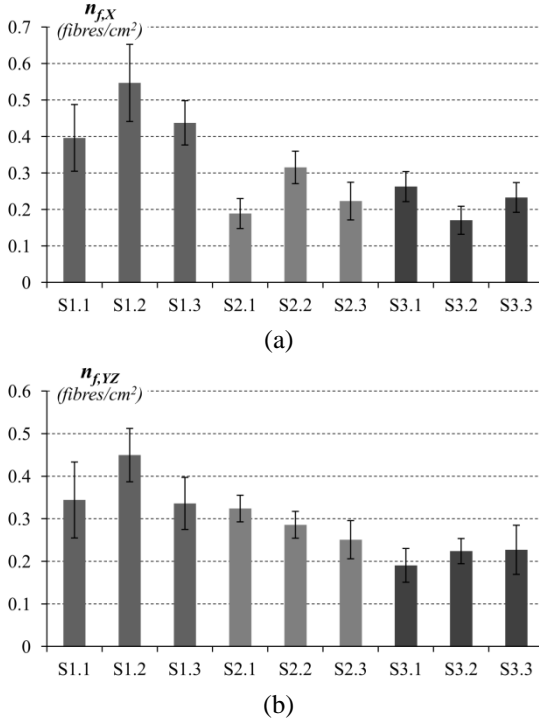


Figure 3. Mean values of fibre densities in longitudinal (a) and transversal (b) directions and confidential interval for probability of 95%

The results show, that fibres may also align in all directions equally making a particular SFRC element more or less an isotropic material, however, mostly it is not the case. Within a specimen every section may have distinct shapes of the orientation patterns, thus possessing different orientation coefficients.

The variation of the mean values of fibre orientation for the specimens of the same mix is significant for the specimens of groups S2 and S3 with a smaller fibre per volume amount, where the variation coefficients are 0.3 and 0.27 respectively. In the group S1, where the number of fibres per volume is greater, the variation coefficient is as small as 0.08. Relation between mean values of the fibre density in the longitudinal $n_{f,X}$ and transversal $n_{f,YZ}$ directions together with the confidential interval for probability of 95% are shown in Fig. 4.

INFLUENCE OF FIBRE DISTRIBUTION ON CRACK FORMATION

In this section the number of fibres with respect to the fracture plane of the tested beams is analysed. Mean fibre densities per cross-section of the test beams are given in Table 1. The underlined values

show the fibre amount in the cracked section. As it can be seen from the data, all cracks formed in the region between the section planes X_5 and X_9 , which conforms to the region between the applied forces.

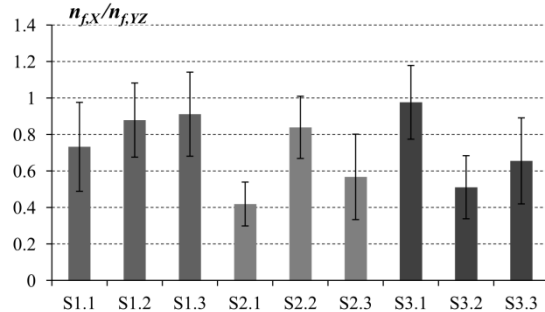


Figure 4. Relation between mean values of fibre density in longitudinal $n_{f,X}$ and transversal $n_{f,YZ}$ directions and confidential interval for probability of 95%

It is assumed that tensile stresses on the most tensioned side are uniform between the applied forces, thus, regarding the stresses, the crack can be expected to appear in any section of this region with equal probability.

On the other hand, the tensile strength of SFRC cannot be considered uniform along the beam, because it is affected by fibre reinforcement, which is randomly distributed with uneven denseness. If the ratio of stresses to strength σ_t/f_i is variable, it is obvious to expect for a crack to initiate in the section where stresses reach the tensile strength first. Besides fibre distribution and orientation, the strength is influenced also by the heterogeneous properties and imperfections of concrete itself.

The fibre density in the crack plane is compared to the densities in other X-planes of the same beam specimen. To evaluate whether fracture plane develops in the section with the smallest number of fibres all section planes located in the range of the maximum bending moment were sorted by the values of fibre density. The sorted planes of each beam with the values of the densities are given in Fig. 4. The bold underlined values indicate the position of the fracture planes.

Fig. 4 shows that there is a strong tendency for cracks to occur in the sections having smaller fibre density. Cracks were never observed in the sections, where the number of fibres was above the mean value. In the case of beams S1.1...S1.3 cracks always developed in the regions with the smallest fibre density. However, for half of the specimens of groups S2 and S3 the weakest sections do not correspond to the planes with the least number of fibres. It is suggested by the authors that the difference is connected with the number of fibres per volume or unit area. As it was observed for the tested beam specimens, the higher mean value of

the fibre density, the more explicit the effect of fibres, even if the nominal fibre amount fraction by volume V_f is the same.

Table 1
Fibre densities in X -planes

Section number	S1.1	S1.2	S1.3	S2.1	S2.2	S2.3	S3.1	S3.2	S3.3
1	0.25	0.38	0.31	0.17	0.14	0.22	0.17	0.23	0.14
2	0.45	0.58	0.59	0.19	0.25	0.23	0.28	0.23	0.23
3	0.39	0.72	0.41	0.16	0.36	0.22	0.27	0.16	0.25
4	0.42	0.61	0.5	0.13	0.44	0.33	0.39	0.16	0.31
5	0.42	0.73	<u>0.23</u>	0.16	0.36	0.31	<u>0.22</u>	0.09	0.25
6	0.61	0.56	0.41	<u>0.20</u>	<u>0.27</u>	0.25	0.28	<u>0.14</u>	0.2
7	0.64	<u>0.28</u>	0.44	0.33	0.28	0.25	0.3	0.16	<u>0.11</u>
8	0.3	0.61	0.45	0.16	0.34	<u>0.16</u>	0.27	0.28	0.22
9	<u>0.28</u>	0.53	0.42	0.25	0.34	0.28	0.2	0.09	0.19
10	0.3	0.38	0.42	0.2	0.27	0.16	0.3	0.19	0.23
11	0.27	0.67	0.44	0.19	0.34	0.19	0.22	0.19	0.33
12	0.28	0.34	0.5	0.13	0.22	0.08	0.17	0.19	0.23
13	0.16	0.17	0.16	0.28	0.17	0.2	0.06	0.13	0.22

	S1.1	S1.2	S1.3	S2.1	S2.2	S2.3	S3.1	S3.2	S3.3
Max. value	0.64	0.73	0.45	0.33	0.36	0.31	0.30	0.28	0.25
	0.61	0.61	0.44	0.25	0.34	0.28	0.28	0.16	0.22
	0.42	0.56	0.42	0.20	0.34	0.25	0.27	0.14	0.20
	0.30	0.53	0.41	0.16	0.28	0.25	0.22	0.09	0.19
Min. value	0.28	0.28	0.23	0.16	0.27	0.16	0.20	0.09	0.11

Figure 4. Fibre densities in planes $X_5 - X_9$ of every beam sorted by values of densities, where bold underlined values represent fibre density in fracture plane

Although it is attested that cracking is influenced by fibres, the results show that there are also other factors, which can determine the strength of the section besides the number of fibres per unit area. The orientation, anchorage length, distribution of fibres and imperfections of concrete micro-structure in the particular section of the element can be some of them.

Relationship between the fibre orientation and crack formation was studied as well. The fibres aligned with the longitudinal axis of the beams are considered to have more influence on crack formation than the ones aligned transversally. Therefore, the ratios of fibre density, $n_{f,X}$, registered on X -planes to the average fibre density, $n_{f,YZ}$, registered on both Y - and Z -planes were determined. The fibre densities in transversal directions were calculated as the average of fibre densities in two adjacent regions, which are on both sides of the

corresponding X -plane. The obtained values are given in Table 2.

To evaluate the influence of fibre orientation on the location of the developed crack, a similar procedure as for evaluating the influence of the fibre density was used. In this case all middle sections ($X_5 - X_9$) were sorted by the values of the ratio of longitudinal to transversal fibres, $n_{f,X} / n_{f,YZ}$. The sorted planes of each beam with the values of the ratio are given in Fig. 5. The bold underlined values indicate the position of the fracture planes.

There is observed a tendency for cracks to develop in sections, where the ratio of longitudinal to transversal fibres is smaller, though the influence is not as strong as of fibre density. However, no crack has occurred in the section planes with the highest value of the ratio $n_{f,X} / n_{f,YZ}$. For two beams the crack occurred in the sections, where the ratio was slightly higher than the mean value. For half of the specimens the fracture planes correspond to the

planes, where $n_{f,X}/n_{f,YZ}$ has the minimum value in the considered range. The tendency of a crack to initiate in the sections, where the fibres are less orientated in the longitudinal than in transversal direction, is a bit more pronounced in specimens with higher fibre densities. To analyse the

correlation between the influence of orientation of fibres on the crack position and the number of fibres, more investigations of specimens with a wider range of fibre volume fraction V_f are necessary.

Table 2

Section number	Ratio of fibre density in longitudinal to transversal directions								
	S1.1	S1.2	S1.3	S2.1	S2.2	S2.3	S3.1	S3.2	S3.3
2	1.16	1.01	1.21	0.57	0.70	0.79	0.88	0.79	0.75
3	1.43	1.48	1.13	0.50	1.05	0.93	1.06	0.53	0.84
4	1.35	1.30	1.94	0.33	1.51	1.20	1.56	0.64	0.95
5	1.13	1.16	<u>0.77</u>	0.36	1.31	1.08	<u>1.27</u>	0.38	0.73
6	1.32	0.88	1.18	<u>0.49</u>	<u>0.79</u>	0.94	1.24	<u>0.55</u>	0.49
7	1.02	<u>0.57</u>	1.43	0.87	0.74	0.62	0.91	0.65	<u>0.36</u>
8	0.58	1.15	1.04	0.43	0.94	<u>0.40</u>	1.13	1.24	1.47
9	<u>1.03</u>	1.11	0.82	0.73	1.10	1.33	1.37	0.48	1.09
10	0.78	1.20	0.87	0.67	0.95	0.67	1.73	1.00	1.25
11	0.49	1.41	0.95	0.63	1.10	0.65	1.00	0.71	1.20
12	0.45	0.63	1.23	0.36	0.93	0.22	0.81	0.57	0.67

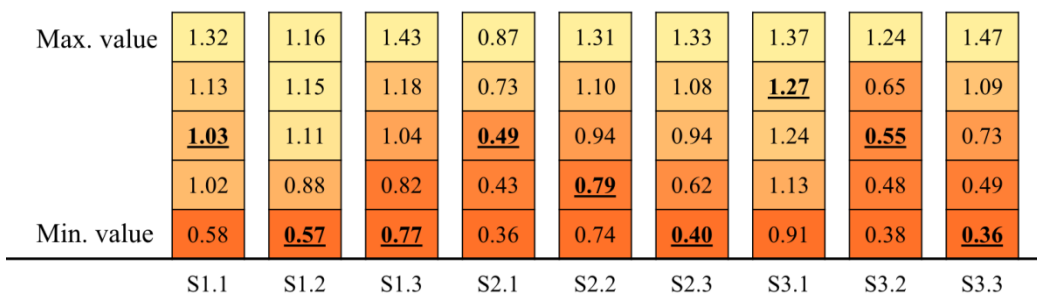


Figure 5. Fibre density ratio of longitudinal to transversal directions ($n_{f,X}/n_{f,YZ}$) in the range between planes X5 – X9 sorted by the values of the ratio, where bold underlined values represent fibre density ratio in fracture plane

NUMERICAL ANALYSIS AND DISCUSSION

From a mechanical point of view, there is an obvious interest in knowing the number of fibres crossing a given cracked section of a structural element. If we assume that the concentration of fibres can be considered as homogeneous, this number is proportional to the total number of fibres per unit of volume multiplied by the parameter α called the orientation factor (Krenchel, 1975; Martinie and Roussel, 2011):

$$n_f = \alpha \frac{V_f}{A_f} \quad (1)$$

where n_f – fibre density;
 V_f – fibre volume fraction;
 A_f – cross-sectional area of fibres.

The value for α is 0, if no fibre crosses the considered section; α equals 1.0 if all fibres cross the studied section. For isotropic materials α is 0.5. From a simple geometrical point of view, fibres cannot be equally oriented throughout the cross section. If the distance between the wall of a mould and the centre of gravity of a particular fibre is smaller than the half of the fibre length, this particular fibre cannot be orientated perpendicular to that wall. Therefore, the studied cross-section should be divided into at least three zones (bulk, at mould side, and in a corner of the mould) having distinct fibre orientation coefficients.

Dupont and Vandewalle (2005) offer a simple method for calculating the coefficients α for each area of the cross-section, denoting them as α_1 , α_2 , α_3 for bulk, mould side, and corner of the mould respectively. The overall orientation factor can be

calculated as follows by taking the geometrical average over the section:

$$\alpha = \frac{\alpha_1(b-l_f) + \alpha_2[(b-l_f)l_f + (h-l_f)l_f] + \alpha_3l_f^2}{bh} \quad (2)$$

where b – width of cross-section;

h – depth of cross-section;

l_f – fibre length.

According to Dupont and Vandewalle the values of the calculated orientation factors are $\alpha_1 = 0.50$, $\alpha_2 = 0.60$, and $\alpha_3 = 0.84$. Applying these values to the prismatic specimens studied in this work, the theoretical orientation factor is obtained, $\alpha = 0.635$. Based on the cross-sectional area of the fibres and the nominal fibre volume fraction, the theoretical fibre density, $n_{f,\text{theor}}$, can be predicted. The comparison between the predicted and experimentally obtained fibre densities is given in Table 3. In the table $n_{f,X,\text{mean}}$ is the mean value of densities and $n_{f,X,\text{crc}}$ is the fibre density in the fracture plane of the tested beams.

Table 3
Theoretically predicted and experimentally obtained fibre densities

Sample	$n_{f,\text{theor}}$	$n_{f,X,\text{mean}}$	$n_{f,X,\text{crc}}$	$n_{f,\text{theor}} / n_{f,X,\text{crc}}$
S1.1	1.44	0.40	0.28	5.14
S1.2	1.44	0.55	0.28	5.14
S1.3	1.44	0.44	0.23	6.26
S2.1	1.08	0.19	0.20	5.40
S2.2	1.08	0.32	0.27	4.00
S2.3	1.08	0.22	0.16	6.75
S3.1	0.74	0.26	0.22	3.36

REFERENCES

- Barragán B.E., Gettu R., Martín M.A., Zerbino R.L. (2003) Uniaxial Tension Test for Steel Fibre Reinforced Concrete – a Parametric Study. *Cement and Concrete Composites*, Vol. 25, No. 7, pp. 767–777.
- Barros J., Cunha V., Ribeiro A., Antunes J. (2005) Post-Cracking Behaviour of Steel Fibre Reinforced Concrete. *Materials and Structures*, Vol. 38, pp. 47–56.
- Dupont D. (2003) Modelling and Experimental Validation of the Constitutive Law ($\sigma-\varepsilon$) and Cracking Behaviour of Steel Fibre Reinforced Concrete. Ph.D. thesis. Katholieke Universiteit Leuven, Belgium, 198 p.
- Dupont D., Vandewalle L. (2005) Distribution of Steel Fibres in Rectangular Sections. *Cement and Concrete Composites*, Vol. 27, No. 3, pp. 391–398.
- Ferrara L., Meda A. (2006) Relationships between Fibre Distribution, Workability and the Mechanical Properties of SFRC applied to Precast Roof Elements. *Materials and Structures*, Vol. 39, pp. 411–420.
- Gettu R., Gardner D.R., Saldivar H., Barragán B. (2005) Study of the Distribution and Orientation of Fibers in SFRC Specimens. *Materials and Structures*, Vol. 38, pp. 31–37.
- Krenchel H. (1975) Fibre Spacing and Specific Fibre Surface. In: *Fibre Reinforced Cement and Concrete*. Edited by A. Neville. New-York: Construction Press, pp. 69–79.
- Laranjeira F., Grunewald S., Walraven J., Blom C., Molins C., Aguado A. (2011) Characterization of the Orientation Profile of Steel Fiber Reinforced Concrete. *Materials and Structures*, Vol. 44, pp. 1093–1111.

S3.2	0.74	0.17	0.14	5.29
S3.3	0.74	0.23	0.11	6.73

Table 3 shows, that the fibre amount predicted by the method, where homogeneous concentration of fibres is assumed, is significantly overestimated in the case of the studied prismatic specimens. Comparing analytically the calculated fibre densities with the average fibre amount in the test specimens, the overestimation is 2.6 to 5.7 times. Furthermore, comparison between the theoretical fibre densities and the densities in the crack planes gives even greater overestimation of 3.3 to 6.7 times (the last column in Table 3).

CONCLUSIONS

The influence of the fibre distribution and orientation on the deformation and strength characteristics of SFRC elements is determined by the fibre counting method on the tested flexural samples sawn into prismatic specimens. It is confirmed that cracks tend to propagate in the regions with a smaller number of fibres and large orientation angles of fibres with respect to the direction normal to the crack plane.

The fibre amount per cross-section, calculated according to the methods assuming that the concentration of fibres is homogeneous, may differ significantly from the actual fibre amount in the section where the crack is located. The method proposed by Krenchel using orientation factors derived by Dupont and Vandewalle gives overestimation of the fibre amount up to 6.7 times in the studied prismatic specimens.

Martinie L., Roussel N. (2011) Simple tools for Fiber Orientation Prediction in Industrial Practice. *Cement and Concrete Research*, Vol. 41, No. 10, pp. 993–1000.

Robins P., Austin S., Jones P. (2002) Pull-out Behaviour of Hooked Steel Fibres. *Materials and Structures*, Vol. 35, pp. 434–442.

Stahli P., Custer R., van Mier J.G.M. (2008) On Flow Properties, Fibre Distribution, Fibre Orientation and Flexural Behaviour of FRC. *Materials and Structures*, Vol. 41, pp. 189–196.

MICROMECHANICS OF ELASTO-PLASTIC FIBER PULL OUT OF ELASTIC MATRIX

Angelina Galushchak*, Olga Kononova**

Riga Technical University

Institute of Mechanics and Concrete mechanics laboratory

E-mail: *Galushchak.a@gmail.com, **Olga.Kononova@rtu.lv

ABSTRACT

It has been proven by many researchers that the overall behavior of concrete can be improved by the addition of fibers. In the present investigation numerical (FEM) modeling of elastically plastic single straight fiber pull out of elastic matrix volume was realized. Comparison was done with steel fiber is pulling out of concrete matrix. Fiber pulling out micromechanics is governing the macro-crack opening process - fiberconcrete post cracking load bearing capacity is dependent on each single fiber pull out force. Numerical modeling was performed using 3D approach, which takes into account the non-linearity is presenting in physical model in combination with a finite element method (FEM). Straight shape fiber pulling out of concrete block in fiber direction was investigated earlier (Li et al., 1998; Mobasher et at., 1995). In our investigation numerical modeling was performed for straight shape fiber was embedded into elastic matrix under variable angle to applied pulling force and at variable depth.

Key words: pullout, fiber, concrete, micromechanics

INTRODUCTION

Pull out process is the process of pulling a single fiber from concrete matrix. Knowing the force that must be applied for a single fiber to pull it out, we can predict the strength of the structure that is made of fiber reinforced concrete. In fiber concrete fibers which are bridging each particular crack are arranged irregularly and have different angles to the crack plane and depth of each fiber ends embedment into concrete is also variable.

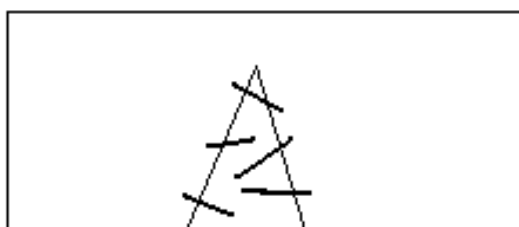


Figure 1. Fibers are bridging the particular crack in fiber concrete. Their location and orientation

In presenting work experiments were made as well as were used earlier obtained results (Krasnikovs A et.al., 2009, 2010), with the goal to clarify what is happening with a single fiber, which is located in the concrete matrix having variable angle and different embedment length in the concrete and is pulling out by external load. Simultaneously the pullout process was modeled, using computer technology. The aim was in comparison of experimental and theoretical data to clarify

micromechanical picture of single fiber pull out process and particular this process components – friction, fiber plastic deformation.

MATERIALS

Fibers

Maximum efficiency of fiber-reinforced concrete (reinforced by steel fibers), is possible to achieve with proper component selection and combination of their micromechanical properties. In the case of fiberconcrete ingredients having affordable relative cost, suitable kind of fibers are steel fibers, and their elasticity modulus is 5-6 times higher than the elasticity modulus of concrete. With a certain amount of fibers in the concrete, there is possible to achieve the best strength of the fiber-reinforced concrete, and that will make the greatest contribution to the fiber and concrete mutual withstand to external loads, before and after the formation of cracks in the concrete.

Steel fiber importance in concrete

Differently oriented fibers in concrete can prevent spread of micro-cracks in it. The effect of the fibers depends on their amount and size. Micro-cracking begins at the hydration process stage in cement, so the deformation can be reduced by forming the solid skeleton of the filler particles. Fibers bridging micro-cracks can reduce and delay their growth, despite before cracking fibers are not loaded in concrete. Important is the ratio of the length and

diameter of fiber. Fiber is starting to work when the crack is starting to growth in length and width. Steel fibers are obtained at the market can be divided into two groups: a) fibers that are pulling out of concrete without rupture; b) fibers that are not possible to pull out of concrete without their rupture. First type of fibers- straight, undulated, with different form hooks on the ends etc., second type – fibers with cones or balls on the ends, etc. Straight fibers belong to first group of above mentioned fibers. Commercial fibers are designed in such way that each fiber start to slide in the concrete before it will reach the limit of elasticity. If the fiber is broken, in the concrete, it cannot continue to carry the tensile load. If the fiber in concrete remains intact, it works together with a concrete and is able to constrain even wide cracks.

Fiber load bearing properties are highly dependent on the fiber's steel strength, shape, surface geometry, strength of concrete, as well as adhesion to concrete (specially for coated fibers).

Pull out experiments

Fibers pullout micro mechanism is governing structural elements mechanical behavior under applied external loads. With the goal to more closely examine this phenomenon, experiments with single fiber pull out of the concrete matrix were executed.

Pull out specimen elaboration

Moulds of wooden plywood, consisting out of two separated similar parts, were manufactured. Each formwork internal sides were covered by plastic tape, to prevent the matured sample from sticking to the mould. Between the form's parts was placed a plastic film (separator). Single fiber was embedded into both sample parts going through the separator at its middle part. This film is separating concrete parts of the sample from each other and is simulating the crack. This ensures that only fiber is bearing the external stretching load in the process of tearing the sample. The fiber is placing at a certain angle to direction of the stretching force and at a certain depth by pulling out end. Embedment was: 5, 10, 15, 20 and 25mm, and the fiber inclination angle to the stretching force direction: 0 °, 10 °, 20°, 30°, 45°, 60°. Samples were matured at least 28 days. Then with the Zwick / Roell Z150 computer governing mechanical loading machine with additional 1kN dynamometer, experiments on the fiber pulling-out were conducted. Concrete sample both parts mutual displacement was fixed by video extensometer "Messphysik". As results of the Pull out experiment F- δ (force-displacement) curves for fibers with different inclinations and different embedment in concrete were obtained. Concrete compressive strength was 70Mpa. Steel fibers had strength equal to 1050Mpa.

Simultaneously, numerical simulation of the elasto-plastic fiber pull out process was executed using finite element method (FEM).

MODELING AND RESULTS

Creating a pull out model using FEM is necessary to consider parameters that determine the outcome of modeling. In our investigation friction between concrete matrix and steel fiber surfaces is taking into account using finite contact elements. If we are observing two rigid bodies are sliding one corresponding to other and between them is appearing dry, called Coulomb, friction force (see Fig.2) the coefficient of friction between them is 0.45 if one body material is steel and other is concrete. If dry friction is realizing between two bodies, the value of friction force is dependent on friction coefficient and force is compressing bodies. In the case when steel fiber is in a concrete, as compressing force is acting concrete matrix shrinkage.

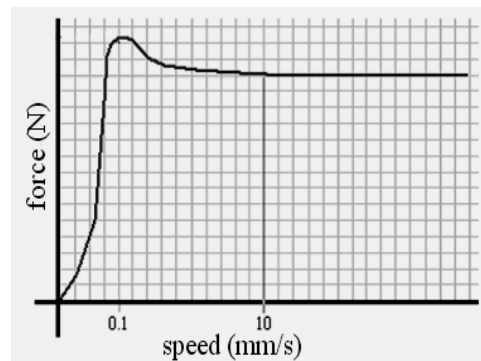


Figure 2.Coulomb friction curve

The reason of concrete shrinkage is removal of excess water when it dries. In order to obtain the value of shrinkage, an experimental investigation was conducted. Plain concrete specimen with dimensions 300x55x55mm and an extensometer mounted on one of the sample end was exposed 28 days under room external conditions (see Fig.3). During this time the concrete dried and shranked, and after 28 days was found that the concrete shrinkage is 0,073%.

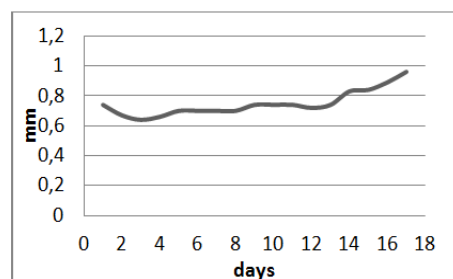


Figure 3.Shrinkage experimental curve

Modeling volume consists of a straight steel fiber with a length 50 mm and a diameter is equal to 0.75 mm that is placed in the concrete matrix (see Fig.4). Volume with a straight fiber is radially symmetric, because that for stress fields calculation only a quarter of the volume was taken for numerical modeling. The fiber was placed into the matrix for different lengths: 5, 10, 15, 20 and 25 mm. Displacement of dead end of the concrete matrix in fiber direction is equal to zero (see Fig.4), on all planar side surfaces symmetry boundary conditions were applied. Fibers outer end was pulled out with constant velocity and between fiber and concrete matrix were placed contact elements with dry Coulomb friction in a form shown at figure 2 between them.

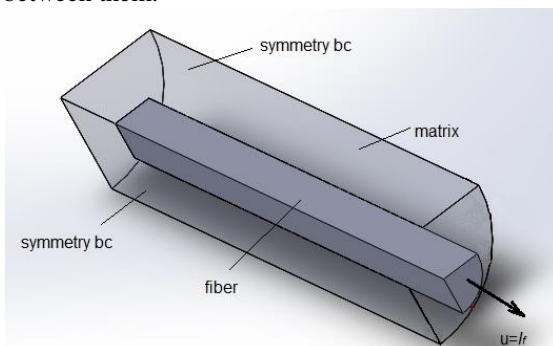


Figure 4.FEM modeling volume geometry and boundary conditions

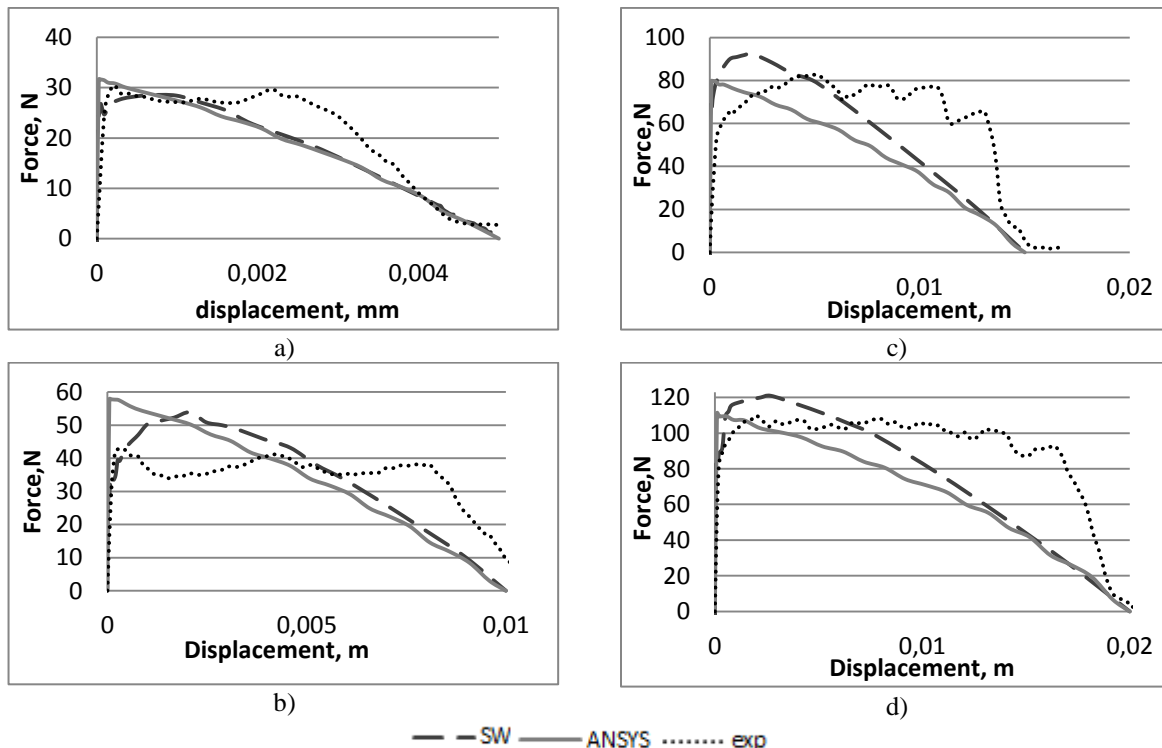


Figure 5a-d. Pull out experimental curvecomparison with numerical modeling data(were obtained using SolidWorks and ANSYS FEM software) for steel fibers were embedded in concrete at different depth: a) 5mm; b) 10mm; c) 15mm; d) 20mm

Young modulus of concrete matrix was: $E = 30000$ Mpa; Poisson's ratio of concrete matrix $\nu = 0.2$; Young modulus of steel fiber: $E = 200$ GPa, Poisson's ratio of steel fiber: $\nu = 0.32$. Concrete matrix was elastic, fiber was elasto plastic. In result of numerical simulation, curves "force-displacement" for the straight fibers that were placed in the concrete for 5, 10, 15 and 20 mm

were obtained and were compared with experimentally obtained (see Fig.5). Simulations comparison with experimental data was shown inability to approximate experimental curves at fiber pull stage. Is possible to conclude- fiber movement in the channel in concrete matrix is not happen as movement under dry friction movement conditions with constant friction coefficient.

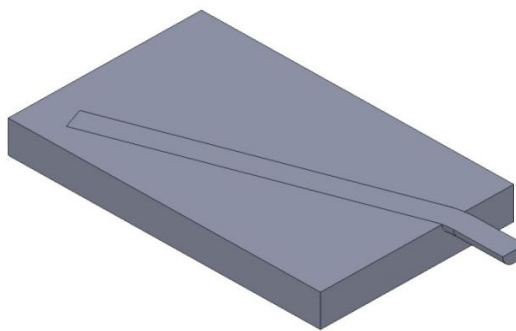


Figure 6. Pull out model for fiber is embedded under the angle to pulling out force direction

Only if friction coefficient is non-linearly changing during motion successful approximation can be done. Was supposed, that during fiber sliding small concrete matrix particles (small grains of sand or cement stone) are separated from concrete matrix channel internal surface and rolling between

concrete and steel surfaces are making plugs. Such plug existence leads to increase of applied force till the plug is demolish and sliding is continuing till future plug formation (peaks on experimental curves in figure 5).

Similar model was created in a case when fiber had different declination angle to pulling out force direction and different embedment depth (see Fig.6). In this case two micromechanical mechanisms – friction and plasticity of the fiber are working simultaneously. Curves "force-displacement" numerically obtained in the simulations by finite element method were compared with the curves obtained experimentally and are shown in Fig.7.a-d for fibers inclined under different angles to load direction and in Fig.8.a-d for fibers embedded at different depth.

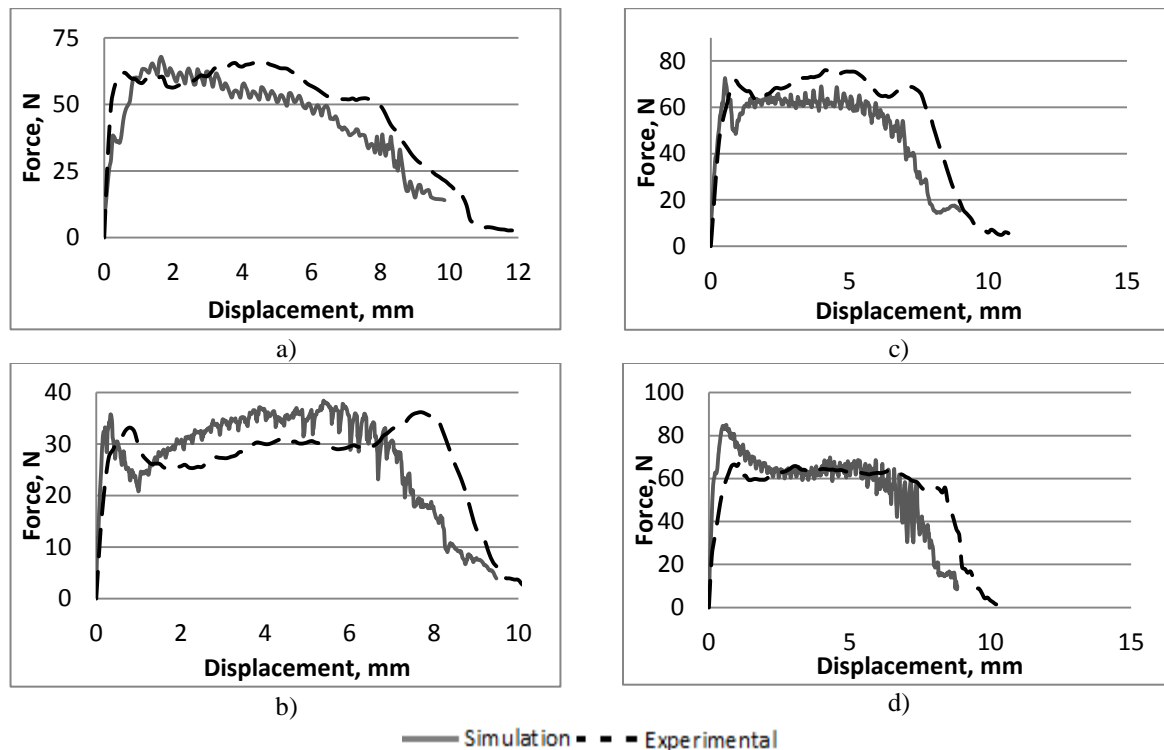


Figure 7. Experimental and modeling curves for fibers were embedded into the matrix on a depth 10mm: a) fiber is oriented under the angle 20° to the applied force direction; b) fiber is oriented under the angle 30° to applied force direction; c) fiber is oriented under the angle 45° to applied force direction; d) fiber is oriented under the angle 60° to applied force direction

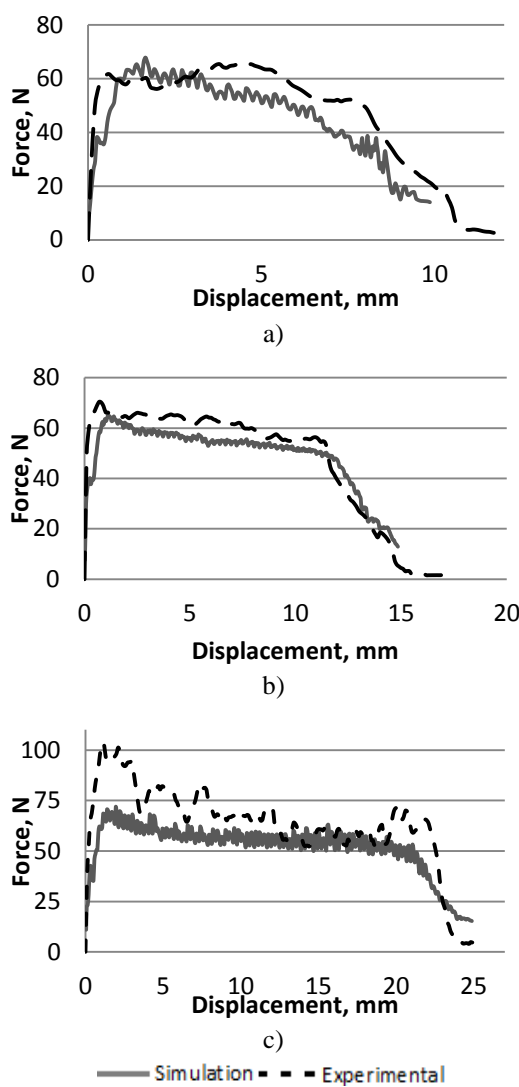


Figure 8. Experimental and modeling curves for fibers were oriented under the angle 20° to applied force direction: a) fiber is embedded into the matrix on a depth 10 mm; b) Fiber is embedded into the matrix on a depth 15 mm; c) Fiber is embedded into the matrix on a depth 25 mm

REFERENCES

- Li C., Mobasher B. (1998) Finite element simulations of fiber pull out toughening in fiber reinforced cement based composites. *Journal of Advanced Cem. Based Materials*, 7, No 3–4, pp 123–132;
- Mobasher B, Li C. (1995) Modelling of stiffness degradation of the interfacial zone during fiber debonding. *Journal of Compos. Eng.*, 5, No 10–11, pp 1349–1365;
- Krasnikovs A., Khabaz A. and Kononova O. (2009) Numerical 2D Investigation of Non-metallic (glass and carbon) Fiber Micro-mechanical Behaviour in Concrete Matrix. *Sc. Proceedings of Riga Technical University, Architecture and Construction Science*, 2. V.10, pp 67-78;
- Krasnikovs A., Khabaz A., Telnova I., Machanovsky A. and Klavinsh J. (2010) Numerical 3D investigation of non-metallic (glass, carbon) fiber pullout micromechanics (in concrete matrix). *Sc. Proceedings of Riga Technical University, Transport and engineering*, 6, vol.33, pp103-108;

CONCLUSIONS

Detailed 3D numerical (FEM) investigation for elasto-plastic single fiber pull-out of concrete matrix was realized. Comparing pull out theoretical data for fibers which were embedded orthogonally to concrete block with experimental results, was shown, that model based on assumptions about dry friction between fiber and matrix and elastic fiber and matrix deformations fail to predict experimentally obtained curves. Micro-mechanical mechanism of small concrete particles separation out of internal fiber channel surface in concrete cause fiber friction and plugs formation around the fiber can be mentioned as possible this situation explanation. Plug in the channel between fiber and matrix is triggering fiber motion increasing resistance to motion. After that plug is failing, allowing fiber to move simultaneously decreasing applied pulling load. Small particles in the channel between fiber and matrix are rolling after some time forming next plug. Experimental and numerical data coincidence increase for fibers which are pulling out under an angle. Plastical fiber behavior incorporation into solution compensates uncertainty in nonlinear friction simulation.

POLYMER FIBER PULL OUT EXPERIMENTAL INVESTIGATION

Arturs Macanovskis **, Vitalijs Lusis *, Andrejs Krasnikovs *,**

**Riga Technical University

Institute of Mechanics

E-mail: artursmacanovskis@inbox.lv

* Riga Technical University

Concrete mechanics laboratory

E-mail: Vitalijs.Lusis@rtu.lv

*,** Riga Technical University

Institute of Mechanics and Concrete mechanics laboratory

E-mail: Krasnikovs.Andrejs@gmail.com

ABSTRACT

Advanced polymer fibers are used in structural applications as micro reinforcement in composite materials with a concrete matrix. Comparing to other fibers such as steel, glass, carbon etc., polymer fibers behave visco-elastically or visco-elasto-plastically. Such fibers having moderate starting elastic modulus are characterized by relatively large elastic deformations and pronounced Poisson's effect during stretching. Concrete prisms with dimensions 10x10x40 cm were fabricated, having different amounts of 3 cm long and 0,75 mm in diameter polymer fibers. All prisms were tested under four point bending conditions and loading velocity $v = 150 \text{ N/s}$. An elaborated numerical fiberconcrete cracking model was exploited for prism load – deflection mechanical behavior prediction under four point bending conditions. Numerical results were compared with experimental data.

Key words: polymer fibers, concrete prisms, pull-out, four point bending

INTRODUCTION

The need to use high-quality concrete increases every day. An important role among such materials belongs to fiberconcretes - concrete with the addition of different fibers - metal, glass, carbon, polymer and some others. Adding fibers into the concrete matrix causes a situation when the load bearing capacity of the material after cracking of the concrete matrix (appearances of magistral cracks) decreases within acceptable limits or does not decrease at all. In this work, single polymer synthetic fiber pull -out from a concrete matrix is under investigation. A short synthetic polymer fiber is immersed by one end into the concrete matrix at a certain depth and at a certain angle to the direction of the pulling out force. Thereby - the fiber is oriented (has its angle to the direction of the pulling force from the concrete matrix) and has the embedded length in the concrete matrix. Experimental and theoretical data were obtained for the single fiber pull-out phenomena, as well as for the fiberconcrete prisms four point bending.

CONCRETE COMPRESSIVE STRENGTH EXPERIMENTAL EVALUATION

With the goal to control the class of a concrete used in experiments, 10 samples, having dimensions of 10x10x10 cm of a concrete without fibers, were prepared and tested under compression loading conditions. Samples were elaborated and were

matured for 28 days and afterwards were tested using the testing machine Controls AUTOMAX System V1.04. Average samples compressive strength was equal to 72 MPa.



Figure 1. The sample is centered in the testing machine for compression test

SINGLE POLYMER FIBER PULL-OUT EXPERIMENTAL INVESTIGATION

A single polymer synthetic fiber (Fig. 2.) was placed in a concrete matrix (Fig. 3) and was oriented at an angle to the future stretching direction. Each fiber was embedded at a specific depth (less or equal to fibers half-length)

corresponding to the accepted experimental program (Fig. 4). Specimens were prepared in the following sequence: Step 1: Were prepared a concrete mix. In the concrete mix, used in experiments a relatively small amount of water was added.

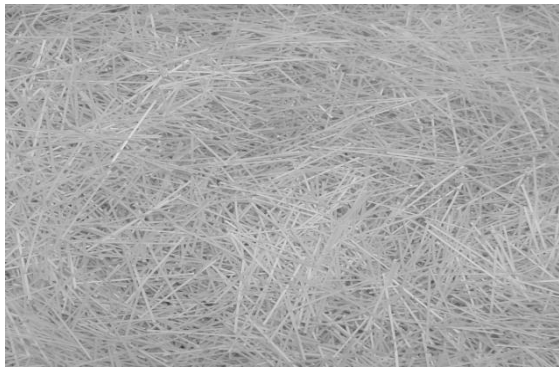


Figure 2. Polymer synthetic fibers with the length equal to 3 cm and with the diameter equal to 0.75 mm



Figure 3. Samples view for pull-out tests. Is shown how were oriented single fibers in the concrete matrix corresponding to future stretching direction

Step 2: Polymer synthetic fiber is placed into the concrete matrix. Specimen mould was poured in four steps (layers) (Fig. 5).

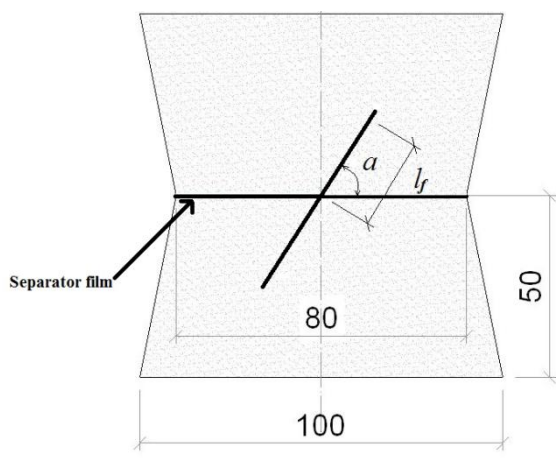


Figure 4. A) Configuration of a pull-out test specimen: l_f - embedded length, α – inclination angle

The first and second layers were poured into the mould and were well compacted. Layers were rammed carefully with the goal to avoid air bubbles and voids in the concrete. The first and second layers were poured in the form filling exactly half of the depth of a form, in order to facilitate future

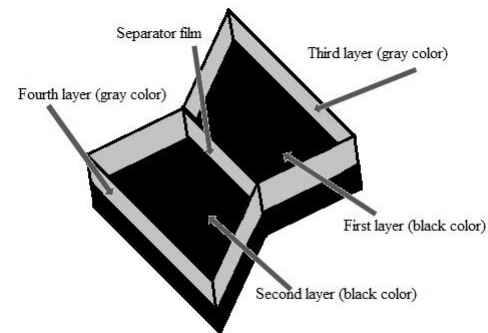


Figure 5. Mould filling sequence in the pull-out experiment

fiber emplacement (and orientation) in the mould. Both geometrically similar parts of the sample were separated by a plastic film. Then, after placing the oriented polymer fiber a third layer was poured into one half of the sample mould. The third layer was placed in such way: the concrete mix was taken and superimposed on the fiber, thereby fixing its position and orientation and then the concrete in the form was compacted. Ramming is important otherwise after aging due to macro and micro cavities between fiber and concrete matrix, the polymer fiber without resistance will be pulled out of the concrete. Then the 4th layer was poured. Step 3: Aged specimens experimentally were tested using the tensile testing machine Zwick Roell Z150



Figure 6. Sample with fiber oriented under the angle (particular sample shown in the picture has an angle 60°) to the tension direction

with an additional 1kN load sensor (Fig. 6). Each specimen was placed into the grips and was carefully centered. Two stickers (each with a black horizontal line) were glued on the specimen's both parts, in order to determine their mutual displacement increase, using the noncontact extensometer (camera) MESSPHYSIK (extensometer allows to fix displacement in a thousandth part of a millimeter).

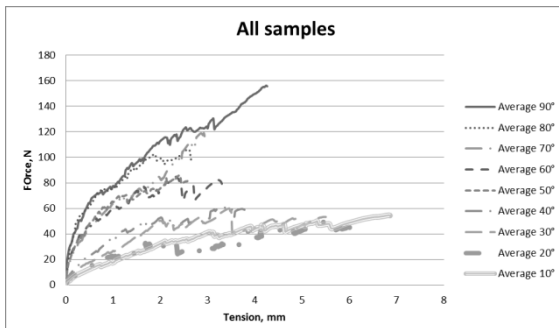


Figure 7. Pull-out curves for a polymer synthetic fiber embedded into a concrete under different angles

Fig. 7 shows the applied pulling force- pulled out displacement curves for the polymer macro synthetic fiber which is embedded into the concrete at different angles to the direction of the pulling out force. Each curve was obtained averaging results over eight to ten tested samples.

Pull-out process observation shown two different scenario of fiber pull-out, depended on the angle between the fiber and the stretching direction:

a) if an angle is small (10° - 20°) fiber release in crack zone is happening by concrete matrix spalling and fiber's middle part rotation according to embedment points in both crack flanks. Such oriented fibers can easily break down the concrete matrix and the release of the fiber due to the spalling of the concrete matrix adds to the length which is pulled out of the concrete. Fiber pull-out process starts when distance between crack flanks is reaching few millimeters; b) for fibers oriented under angles from 30° to 90° fiber that is pulled out of the concrete breaks at a certain depth and the detached end is pulled out by friction which is possible to see in figure 8. For fibers that were oriented under an angle 90° it was about 4.5 mm (averaged value over tested fibers were oriented at such angle) and was longer than for fibers oriented under the angles from 80° to 40° , that was probably caused by the fact that the fibers oriented at angles of 40° - 80° during pulling out are subjected to cutting shear stresses (spalling of the concrete in the output of the fiber out of concrete only shifts crossection in which the fiber is subjected to shear).

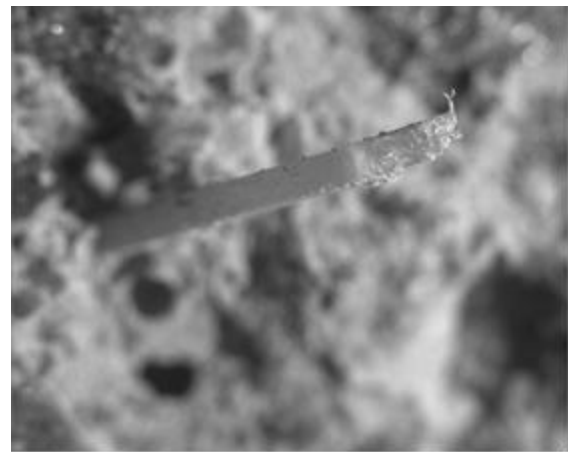


Figure 8. Macro synthetic fiber torn out from the concrete (under a microscope)

ELABORATION OF FIBERCONCRETE SAMPLES WITH HOMOGENEOUS POLYMER MICRO AND MACRO SYNTHETIC FIBERS SPATIAL DISTRIBUTION

Experimentally samples were elaborated (prisms having dimensions $100 \times 100 \times 400$ mm) with different fiber concentrations in the concrete matrix. Polymers macro synthetic fibers (Fig. 2) and micro synthetic fibers (Fig. 9) were homogeneously distributed in the material volume.



Figure 9. Polymeric micro synthetic fibers (fiber length $\approx 5\text{-}6$ mm , diameter $\approx 1\text{mkm}$)

Samples were possible to subdivide into following groups (Fig. 10):

- a) fiberconcrete samples with micro synthetic fibers;
- b) fiberconcrete samples with macro synthetic fibers;



Figure 10. Samples tested for four point bending

c) fiberconcrete samples with micro and macro synthetic fibers.

Fiberconcrete with micro synthetic fibers was created in follow way:

- 1) all concrete ingredients, without micro synthetic fibers were mixed;
- 2) micro synthetic fibers were added to the concrete. Specimens were prepared with fiber concentrations: $1\text{kg}/1\text{m}^3$, $2\text{kg}/1\text{m}^3$ and $3\text{kg}/1\text{m}^3$.

Fiberconcrete with macro synthetic fibers was created in the following way:

- 1) all concrete ingredients, without macro synthetic fibers were mixed;
- 2) macro synthetic fibers were added to concrete. Specimens were created with concentrations of fibers: $1\text{kg}/1\text{m}^3$, $2\text{kg}/1\text{m}^3$, $3\text{kg}/1\text{m}^3$, $5\text{kg}/1\text{m}^3$, $6\text{kg}/1\text{m}^3$ and $8\text{kg}/1\text{m}^3$.

Fiberconcrete with micro and macro synthetic fibers was created in following way:

- 1) all concrete ingredients, without micro and macro synthetic fibers were mixed;
- 2) in the second step, gradually micro synthetic fibers were added into the mix and then the macro synthetic fibers added. Specimens were created with fibers concentrations of: $1\text{kg}/1\text{m}^3$ micro and $1\text{kg}/1\text{m}^3$ macro; $2\text{kg}/1\text{m}^3$ micro and $5\text{kg}/1\text{m}^3$ macro; $2\text{kg}/1\text{m}^3$ micro and $5\text{kg}/1\text{m}^3$ macro; $4\text{kg}/1\text{m}^3$ micro and $4\text{kg}/1\text{m}^3$ macro; $5\text{kg}/1\text{m}^3$ micro and $4\text{kg}/1\text{m}^3$ macro; $8\text{kg}/1\text{m}^3$ micro and $3\text{kg}/1\text{m}^3$ macro synthetic fibers.

All the samples obtained after complete solidification (28 days) were subjected to experimental testing by four points bending using the tensile testing machine AUTOMAX Controls System V1.04 (Fig. 11).

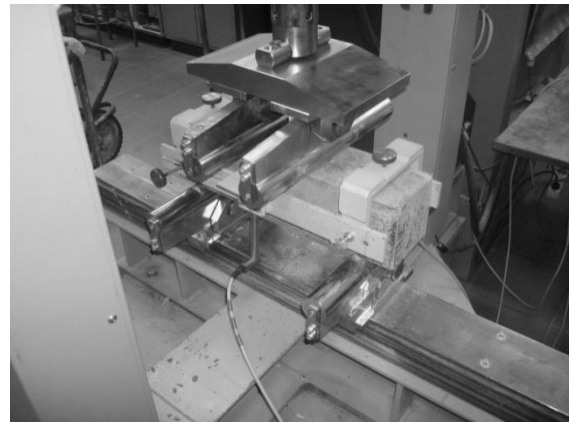


Figure 11. Fiberconcrete prism with macro synthetic polymer fibers (concentration – $8\text{ kg}/1\text{ m}^3$) test by four point bending

EXPERIMENTALLY OBTAINED POLYMER MACRO SYNTHETIC FIBERS DISTRIBUTIONS (ACCORDING TO PULL-OUT LENGTH AND ANGLE TO CRACK'S PLANE)

Experimentally distribution of macro synthetic fibers on the crack surface was studied according to location. During the bending test each sample was separated into two pieces. Each sample's both cracked halves surfaces were covered by graphic mesh (mesh cell size $1\text{cm} \times 1\text{cm}$). On both surfaces of the crack location, all of the pulled out macro synthetic fibers were recognized (Fig. 13 and Fig. 14). In table 1 and 2 show every particular fiber crossing of the crack pulled out length and angle to the crack surface plane.

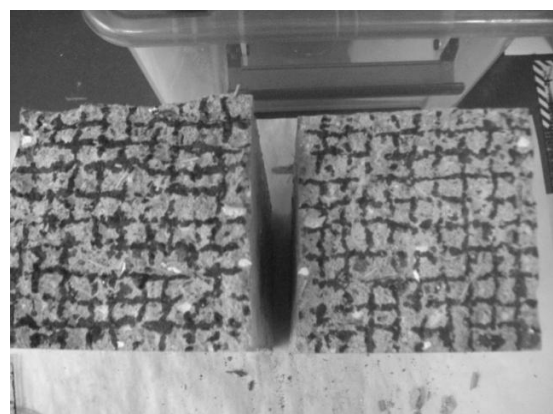


Figure 12. View of the grid on one broken sample both parts (concentration of macro synthetic fibers - $6\text{ kg}/1\text{ m}^3$)

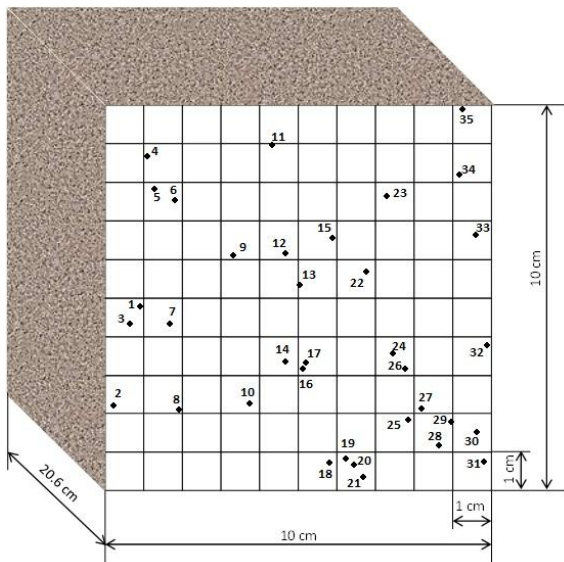


Figure 13. Experimental macro synthetic fibers distributions (according to the pulled out length and fiber angle to crack surface) counted on first (left side) crack's side in sample N3. The concentration of fibers in the concrete matrix is 6kg/1m³

30	47	5
31	87	13
32	79	14
33	58	8
34	45	3
35	65	9

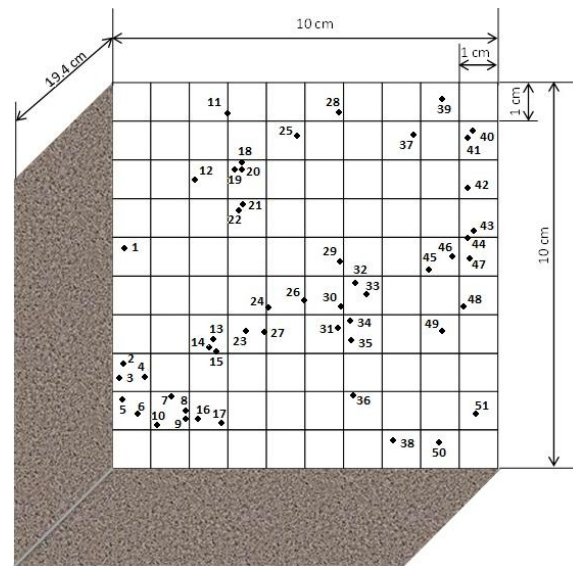


Figure 14. Experimental macro synthetic fibers distributions (according to the pulled out length and fiber angle to crack surface) counted on the second (right side) crack's side in sample N3. The concentration of fibers in the concrete matrix is 6kg/1m³

Table 1
Experimental macro synthetic fibers distributions (according to the pulled out length and fiber angle to the crack surface) counted on the first (left side) of the crack's side in sample N3

Sample	N3	
Number	Angle, °	Length, mm
1	70	4
2	70	10
3	18	13
4	60	9
5	42	5
6	78	4
7	82	5
8	40	8
9	36	4
10	42	5
11	63	7
12	36	12
13	46	6
14	26	9
15	25	7
16	57	2
17	90	4
18	54	3
19	76	8
20	53	7
21	47	5
22	45	9
23	25	10
24	42	5
25	73	5
26	57	7
27	78	5
28	65	8
29	70	4

Table 2
Experimental macro synthetic fibers distributions (according to the pulled out length and fiber angle to crack surface) counted on the second (right side) of the crack's side in sample N3

Sample	N3	
Number	Angle, °	Length, mm
1	82	8
2	90	4
3	85	17
4	50	6
5	80	9
6	78	6
7	50	7
8	64	10
9	69	7
10	62	4
11	66	4
12	90	2
13	61	10
14	53	9
15	19	15
16	66	4
17	40	10
18	78	6
19	62	4
20	17	7
21	54	5

22	52	3
23	37	4
24	81	4
25	90	7
26	55	3
27	90	2
28	65	2
29	54	2
30	90	7
31	58	6
32	42	6
33	51	3
34	45	6
35	60	5
36	17	16
37	50	6
38	70	2
39	62	5
40	63	7
41	73	4
42	72	4
43	54	8
44	52	10
45	90	2
46	74	3
47	45	3
48	64	2
49	70	6
50	50	6
51	19	4

Following graphics were made:

- a) The distribution of macro synthetic fibers (crossing the macro-crack) according to angles between the fiber and crack plane (Fig. 15);
- b) The distribution of macro synthetic fibers on crack surface according to the pulled out ends' lengths (Fig. 16).

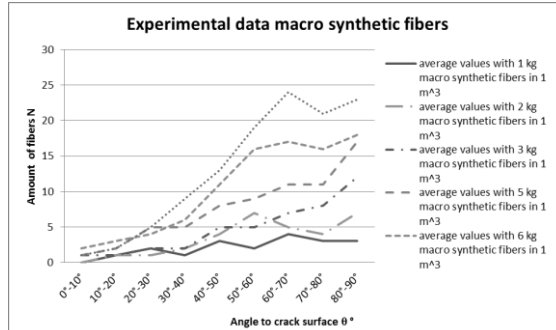


Figure 15. Angles to crack surface distribution for pulled out macro synthetic fibers' ends

Looking at figure 15. It is possible to see that those fibers' orientation which are crossing the macro-crack to the crack's plane is non-uniform in all spatial directions. The main reasons for such phenomena may be two: a) fibers are located under an angle to the pulling out force are obtaining a "quazi" plastic deformation during pulling out;

b) fibers obtained orientation along each prism longitudinal direction when the mould is filled with fresh fiberconcrete. Figure 16 shows that among the pulled out fibers ends, the dominate length is less than 5 mm.

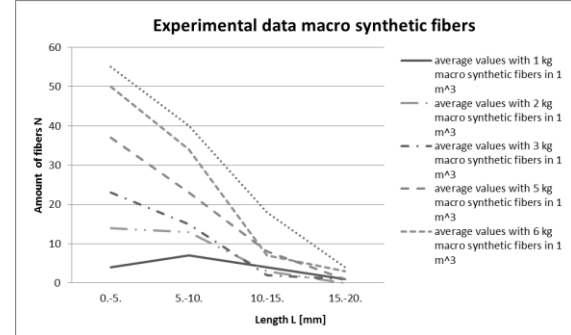


Figure 16. Macro synthetic fibers ends distribution according to pulled out lengths

FIBERCONCRETE SAMPLES LOAD BEARING CAPACITY

Applied force-deflection graphs of the middle of the prism (for material containing micro synthetic fibers), loaded under four point bending conditions, are shown in figure 17. In the figure it is possible to see how the applied force and deflection are increasing, depending on the increasing amount of micro synthetic fibers per 1 m³. Samples contained micro synthetic fibers in a range from 1 kg to 3 kg per 1 m³. The highest bearing load and maximal deflection (≈ 0.052 mm) was obtained for the highest amount of fibers. Reaching the highest deflection, each prism broke the "quazi" brittle way, separating in two

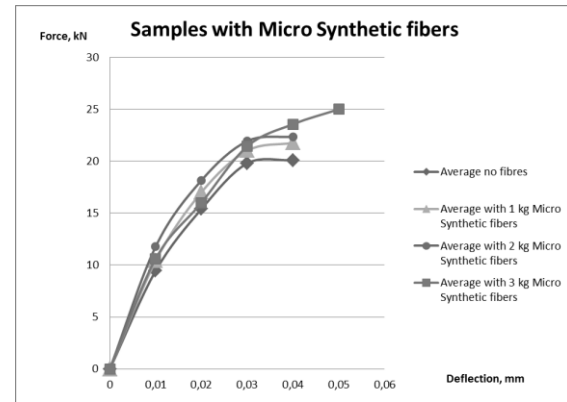


Figure 17. Averaged force curves - the vertical deflection of the middle fiberconcrete prisms with micro synthetic fibers when testing on four point bending

parts. Since the micro synthetic fiber is relatively short and small in diameter, the number of such fibers in the material is much higher compared with the concrete containing the same concentration of

macro synthetic fibers. At the same time, the length of pulled out fibers ends of micro synthetic fibers is much shorter than for macro synthetic fibers. Visual view (using a microscope) of the crack's surface is shown in figure 18.



Figure 18. Micro synthetic fibers on a macro-crack surface

In figure 19, experimental data obtained in the four point bending tests of fiberconcrete samples are plotted - where macro synthetic fibers are contained. Graphs have two stages at the part corresponding to macro-crack opening (graph's part at which the entire load is carried by stretching and pulling out fibers). Stage 1 – macro- crack cuts a major part of the sample prism crossection, the prism shows a sharp decrease of bearing capacity, this is explained by the fact that the macro synthetic fiber has a low modulus of elasticity and only fibers are carrying the load. Stage 2 – Repeated increase of the load carrying capacity is explained by the fact that the macro synthetic fibers are stretched and after that break in the concrete, the elasto-plastic deformation of the fibers themselves, maintain the highest load.

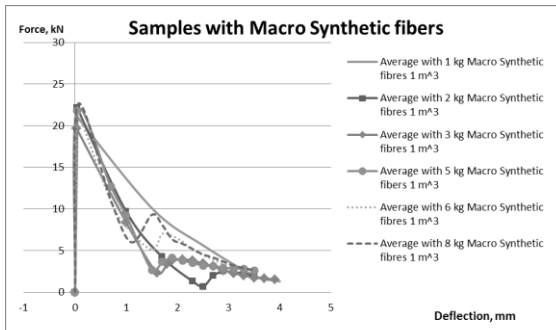


Figure 19. The average values of fiberconcrete with macro synthetic fibers after testing on four point bending

In fig. 20 - graphs of the experimental data for fiberconcrete with micro and macro synthetic fibers

that were tested under four point bending conditions are displayed. Adding micro and macro synthetic fibers in concrete, leads to an increase in carrying capacity of fiberconcrete, increase of strength, at the same time, two stages of destruction still remain, as was previously discussed for the graphs in fig.19.

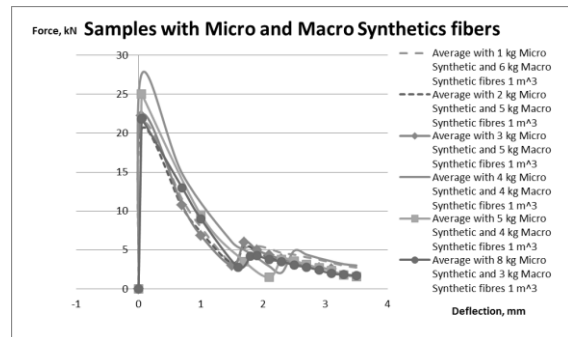


Figure 20. The average values fiberconcrete with micro and macro synthetic fibers after testing on four point bending

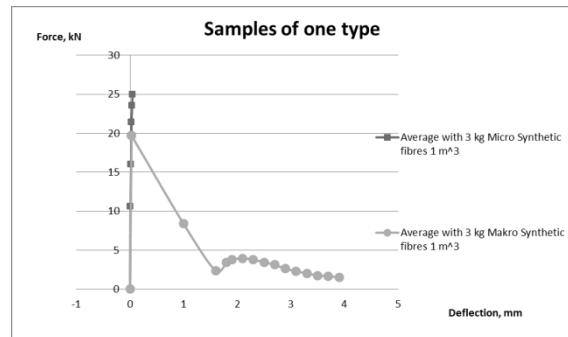


Figure 21. The average values of the same type fiberconcrete after testing on four point bending

Figure 21 shows the results of testing for one prism with micro synthetic fibers and one prism with macro- synthetic fibers. It is easy to see that the micro - synthetic fibers are working in fiber cocktails only at the starting stage of rupture. At the same time increase of the material's integrity leads to a higher load bearing capacity of fiberconcrete with a fiber cocktail comparing with material having the same amount of macro- synthetic fibers only.

THE THEORETICAL MODEL FOR POLYMER FIBER CONCRETE CRACKING N 4 POINT BENDING TESTS

Experimentally obtained pull-out observations were used as the main input data for the numerical model with the goal to predict the linear and non-linear behavior of fiberconcrete beams under bending loads. Because the fibers during being pulled out of the concrete matrix the ability of the FRC beam to carry applied load in the post-cracking state purely depends on the capacity of fibers in broken crossection to carry pull-out loads. In the model the

behavior of fiberconcrete beam was simulated by calculating internally existing load bearing value of each fiber crossing the crack (using this fiber experimentally measured pull-out curve), depending on crack opening value b_i at the location of this particular fiber. The iteration procedure of beam behavior modeling in bending was performed according to step sequence. Further, number of fibers on one crack's surface unit was used as was obtained in experiment. Relation of externally applied load P as a function of crack opening displacement b_i is thus obtained at each step. The force P represents total force applied to the beam that is divided in two symmetrical forces. To run the algorithms of the model, computer software was elaborated. In figure 22: δ_i - is the current crack opening at the bottom side of the beam (is called crack mouth opening displacement CMOD). In the same figure $b(y)$ - is the local opening of the crack at distance y in crack depth direction from the bottom beam surface.

Since the local opening of crack $b(y)$ is not constant and varies along the height of the crack the bridging force must be dependent on the local crack opening. In our model, we know all fibers coordinates on the macro-crack surface and every particular fiber orientation angle to crack surface and each fiber shortest end embedded length, as well as how far it is pulled out if CMOD is equal δ .

ACKNOWLEDGMENT



This work has been supported by the European Social Fund within the project «Support for the implementation of doctoral studies at Riga Technical University».

REFERENCES

1. ShaoY., Li Z. and Shan S. (1993) *Journ. Adv. Cem. Based Materials*, 1,p. 55-66.
2. Li V.C. and Chan Y. W. (1994) *ASCE J. Eng. Mech.*, 120, p.707-719.
3. Krasnikovs A., Khabaz A., Telnova I., Machanovsky A. and Klavinsh I. (2010) Numerical 3D investigation of non-metallic (glass, carbon) fiber pull-out micromechanics (in concrete matrix), *Sc. Proceedings of Riga Technical University, Transport and engineering*, 6, vol.33, p.103-108
4. Lapsa V., Krasnikovs A., Eiduks M., Pupurs A. "Method for production the oriented fiberconcrete structures". LV 13929 B. 20.07.2010.

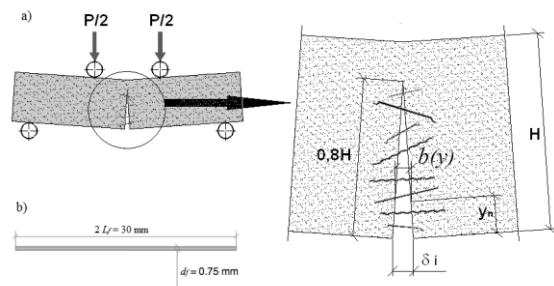


Figure 22. a) Schematic representation of beam loads bearing mechanisms during macro-crack opening. Maximal crack opening δ = CMOD and local opening of crack $b(y)$ (at depth y). b) Polymer macro synthetic fibers under investigation – straight form

CONCLUSIONS

Detailed experimental and numerical fiberconcrete strength and post cracking behavior investigation was performed for material with macro and micro synthetic polymer fibers. Broad experimental program for macro- synthetic fibers pull out of concrete was realized. Peculiarities of fracture for such materials were investigated. Beams with uniformly distributed macro- synthetic fibers, micro- synthetic fibers and simultaneously with macro and micro- synthetic fibers were tested and their mechanical behavior under bending loading conditions was numerically simulated. Numerical modeling results were compared with experiments and recommendations were done.

TECHNOLOGY FOR CONCRETE SHELLS FABRICATION REINFORCED BY GLASS FIBERS

Vitalijs Lusis*

*Riga Technical University

Concrete mechanics laboratory

E-mail: Vitalijs.Lusis@rtu.lv

ABSTRACT

The use of fiberconcrete, leads to a variety of innovative designs as a result of its many desirable properties. Not only can it be cast in diverse shapes; but in thin –wall structural elements also, possessing high compressive strength and stiffness. The promise of thinner and stronger elements, reduced weight and controlled cracking by simply adding fibers is an attractive feature of fiber-reinforced concrete.

Key words: concrete shells, glass fibers, fiberconcrete, FEM modeling

INTRODUCTION

New form architecture has a thin concrete shell created in the form of cylinders, circles, paraboloids and hyperboloids. In order to achieve the required geometrically complicated forms and surfaces of textured concrete a flexible and adjustable formwork system is necessary (Krasnikovs A.et al., 2012, Lusis V. 2011, LapsaV.et.al. 2010).

Pneumatic formwork with changeable lifting form adjustment and adjustment abilities allow the use of them effectively as complete flexible and adjustable formwork systems, in order to create geometrically complicated architecture forms, at the same time not losing the strength indexes of constructed surfaces. The new offered technology is foreseen for plain wall structures, that allows one to create and have different shells, including domelike structures, in one direction curved shell, in two directions curved shell etc., for example, for building roof covering structures (Figure 2). Its field of usage is in manufacturing and building of concrete and fibro concrete precast and monolith shells.

Pneumatic mould use is an approach with a set of advantages among thin wall structural element fabrication technologies. In the reported work, a flat surface of a non- inflated pneumatic mould was imposed and smoothed down (forming a thin layer of a glass fiberconcrete mix). Before concrete binding, the mould was inflated by air forming a moderate curvature shell. Till the moment when the concrete was hardened, air pressure in pneumatic mould was kept at a constant value. Then the air in the pneumatic mould was blown out and the shell was demoulded.

Two variants were observed:

a) the shell is reinforced by uniformly distributed short glass fibers (concretes with three different fiber concentrations were investigated);

b) the shell is reinforced by weft knitted glass fiber textiles (were fabricated in the laboratory). Simultaneously flat material samples were fabricated and experimentally tested. Composite materials elastic moduli as well as tensile strength were obtained.



Figure 1. Short glass fiber concrete is evenly placed on the surface of a rubber membrane (pneumatic mould)

With the goal to predict the mechanical behavior of produced thin fiberconcrete shells a detailed micromechanical investigation for single fiber and few fibers bundle pull-out micro-mechanics was performed numerically (using FEM modeling) and experimentally. The macro-crack opening structural model, based on data sets with information about single fiber and few fibers bundle pull-out micro-



Figure 2. Concrete shell fabrication reinforced by three layers of knitted glass fiber fabric

mechanics, (that was elaborated earlier) was exploited predicting shell load bearing facility depending on the opening of a crack in the loaded shell.

Concrete is a brittle material, if we want to fabricate thin wall (few centimeters) construction elements (thin wall shells) made out of concrete we are forced to use a small diameter densely placed reinforcement. One solution can be - short AR glass fibers homogeneously distributed in the concrete, another – a few layers of knitted AR glass fiber fabrics (filled with concrete) and placed at an even distance one to another through the thickness of the structure.

MATERIALS AND METHODS

A pneumatic formwork with a changeable lifting was elaborated. Use of a pneumatic formwork advantages can be mentioned as follows:

1. Flexible shapes (being curved created surfaces are of architecturally and technologically complicated shapes);
2. Smooth concrete surface quality;
3. Transporting: formwork weight and volume of tissue is very small compared to wooden or steel formwork.

In the first case the flat surface of a non-inflated pneumatic mould was spread out and smoothed down with a short glass fiberconcrete mix (Figure 1). In the second case the flat surface of a non-inflated pneumatic mould was covered by three layers of glass fiber knitted fabrics penetrated by fine aggregate concrete (Figure2).

Knitted fabric reinforced concrete matrix composites have grew rapidly during recent years. Such materials are exhibiting attractive mechanical properties including high energy absorption and impact resistance.

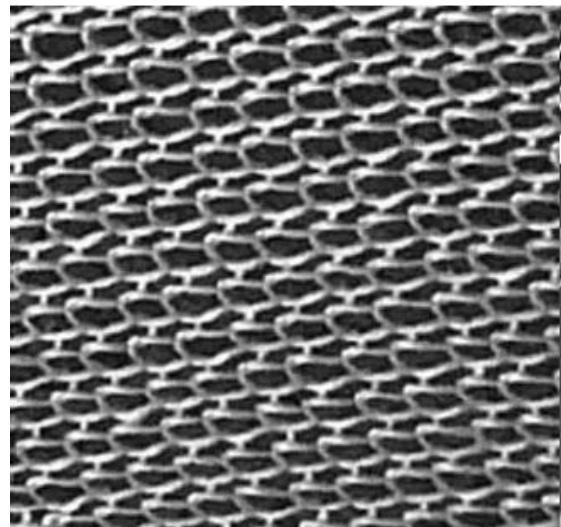


Figure 3. Knitted fabric for concrete shell reinforcement

Yarns loops are arranged in structures. In woven fabric, threads traditionally run horizontally and vertically. Contrary, in the case of knitted fabric, strands form loops see Figure 3. A knitted fabric is highly deformable in all directions. Depending on the fibers used, some of them are more deformable than others. The reason is – yarns do not make straight lines anywhere in the knitted fabric. It is easy to recognize the possible motions in the fabric – threads sliding, loops twisting, bending and stretching leading to a technological advantage – excellent deformability, shape forming ability and flexibility, which allows it to be used in any complex shape mould without folds. Glass fiber weft knitted fabrics were investigated. Type E glass fiber yarns, produced by JSC “Valmieras stikla šķiedra” (Latvia), were used. The density of the glass was $\rho = 2540 \text{ kg/m}^3$, diameter of the yarn d was determined and was equal to $0.37 \times 10^{-3} \text{ m}$. Linear density of the glass yarn was calculated and was equal to 275.6 tex. Value of the elastic modulus for glass yarn was obtained from the manufacturer and was 73.4 GPa (Krasnikovs A. et al., 2012). Before concrete binding, the mould is inflated with air till its final shell shape size is obtained (moderate curvature shells were elaborated (shell surface maximal deviation from the plane was 110mm, see Figure 4)). During concrete hardening the air pressure in the pneumatic mould sustains a constant value. After the concrete becomes hard, air in the pneumatic mould blows out and the shell is demoulded. Experimentally fabricated and investigated shells were curved quadratic plates



Figure 4. Short glass fiber concrete shell

with a thickness of 15mm. The horizontal plane created shells dimensions were 940x940 mm. Matured short glass fiber concrete shell is shown in Figure 4.

Stress –deflection fields numerical modeling in the shell under applied distributed surface load

Elaborated, reinforced by glass fibers, concrete shells were numerically simulated and loaded with external load distributed on shell's surface. Areas of maximal tensile and compressive loads were numerically recognized. The reinforced concrete shell geometry was numerically modeled.

SHELL GEOMETRY MODELING

The shell geometry that was used for numerical calculations, was created using parts of a geometrical arcs. Such shell's form approximates an actual shell's geometry, that was obtained experimentally, that is because a more detailed description of the geometry creation procedure must be completed. At the beginning a plane was created. The additional plane (Plane 2) parallel to the top plane was created at a distance of 110 mm and an additional point was created on plane 2 over the origin point. A 2D chart of the square form with the dimensions of 940×940 mm was created on the top plane. The origin coincides with the centre of the square. The additional planes (Plane 4 and Plane 5) were created on the diagonals of the 2D chart. See Figure 5. The 2D charts of the arc part, were obtained on planes: Plane 4, Plane 5, Front Plane, and Right Plane as shown in Figure 4. The 2D chart of the arc part was created by two points: the first point belongs to the square chart and the second point is located on Plane 2 and is the top point of shell.

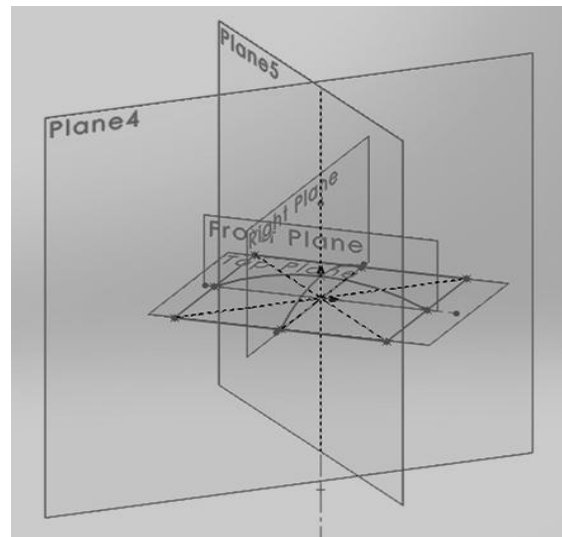


Figure 5. 2D charts of arc part were obtained on planes: Plane 4, Plane 5, Front Plane and Right Plane

The arc part is coincident with the first point and is tangential to second point.

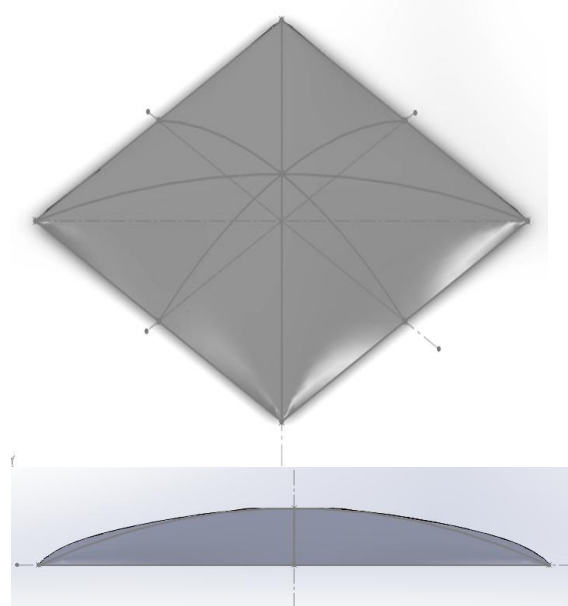


Figure 6. Created shell geometry

The surface-fill operation was used as a patch boundary and a square sketch, as constrain curves, were used with four arc parts. Shell modeling results were shown in Figure 6. The 2D chart of the square with the dimensions of 970×970 mm was created on the top plane. The origin coincides with the centre of the square.

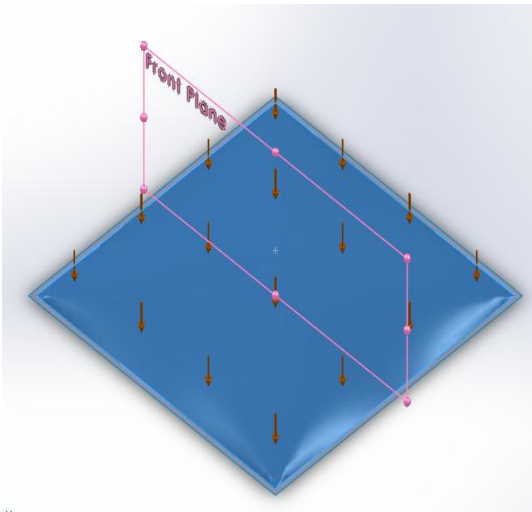


Figure 7. Applied distributed force

A surface-loft operation was used for modeling the technological edge of the shell, as profiles were used from the square chart with the dimensions of 940×940 mm and the square chart with the dimensions of 970×970 mm. On the upper surface of the shell distributed force equal to 1MPa was applied. The force applied direction was strictly vertical (see Figure 7).

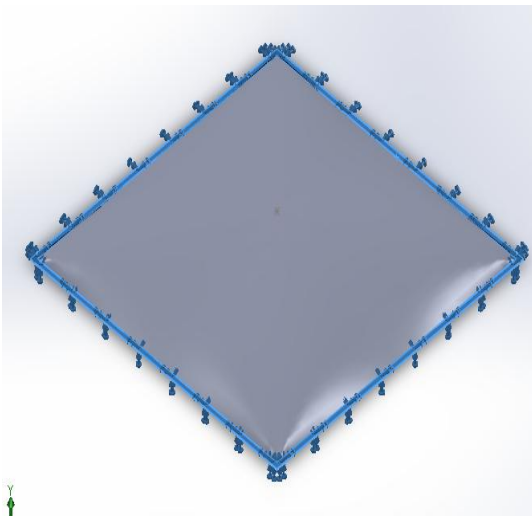


Figure 8. Shell boundary conditions

The shell was freely supported along its entire free edge see Figure 8. The shell was meshed see Figure 9. Looking at Figure 9 it is easy to recognize the shell's geometric deviations, experimentally obtained by inflating fiberconcrete

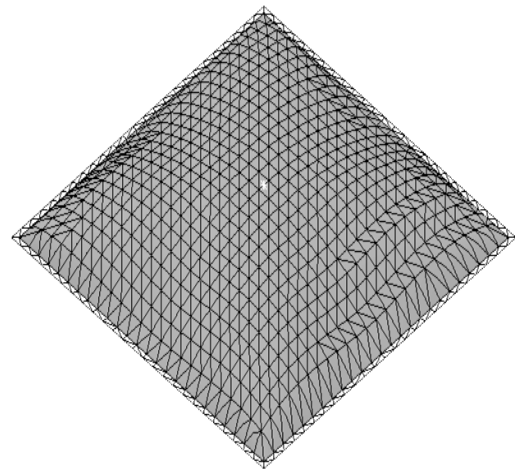


Figure 9. Meshed Shell

shell by air – small depressions between every two corners. Calculated shell's top point vertical deflection for short fibers concrete shell was 2.72 mm and for concrete shell reinforced by three knitted glass fiber fabrics was 2.718 mm.

Vertical displacement view is shown in figure 10. Membrane stresses (stresses according to Mises)

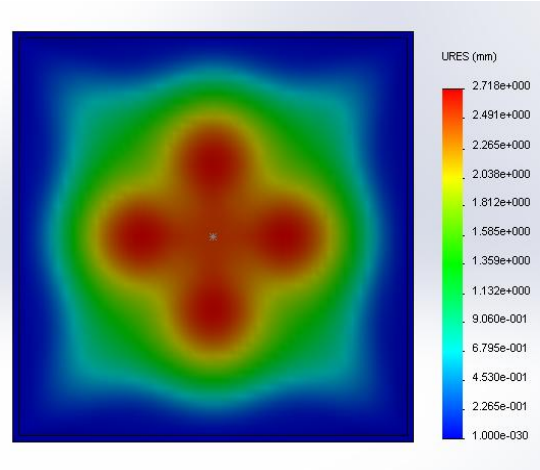


Figure 10. Vertical displacement in loaded shell.
Top view

in loaded shell are shown in Figure 11. Missed stresses were described only as equivalent stress form (because the shell's material is not metal). Stretched zones at the middle of each side of the shell can be observed as potential places of macro-crack formations.

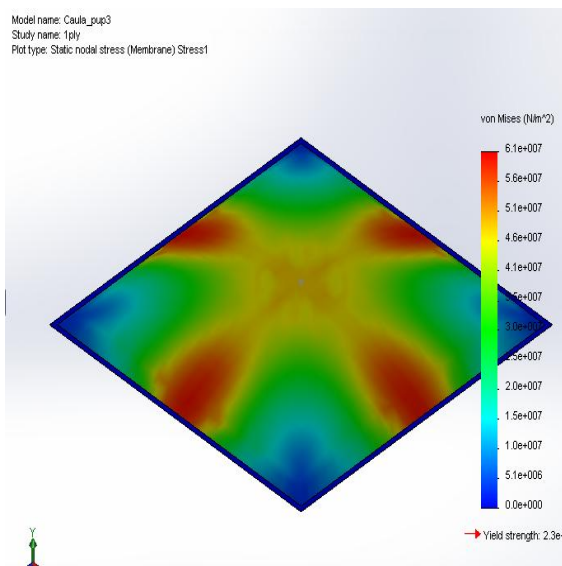


Figure 11. Membrane stresses (equivalent stresses according to Mises) in loaded shell isometric view

CONCLUSIONS

Existing views about techniques and technology of constructions built from monolithic concrete mostly are based on plane construction building experience. Pneumatic formworks with changeable lifting provide an ideal concrete solution for formwork adjustment without any restricting factors connected to complicated geometry. Shells reinforced by chopped glass fibre bundles as well as by knitted glass fibre fabric were fabricated. The shells load bearing capacity was numerically investigated, applying distributed force on the upper surface of the shell. Theoretical results were compared with the data obtained in the experiments.

ACKNOWLEDGMENT

This work has been supported by the European Social Fund within the project “Support for the implementation of doctoral studies at Riga Technical University”.



REFERENCES

- Lapsa V., Krasnikovs A. Technological process for concrete shell formation”, Latvian patent Nr. P-10-162, 2010, November 30.
- Lusis V. Production Technology for Concrete Shells Using Pneumatic Formwork with Variable Elevation// Sc. Proceeding of Riga Technical University 2, Construction science, 12. (2011), P. 35-39.
- Krasnikovs A., Lusis V., Lapsa V., Zaleskis J., Zaharevskis V. and Machanovskis E., Concrete shells reinforced by glass fibers Sc. Proceedings of Riga Technical University, Transport and engineering, 6, 2012, 6.p. (submitted 2012)

BENDING STRENGTH OF LAYERED FIBERCONCRETE PRISMS

Vitalijs Lusis*

*Riga Technical University

Concrete mechanics laboratory

E-mail: Vitalijs.Lusis@rtu.lv

Andrejs Krasnikovs**

**Riga Technical University

Institute of Mechanics and Concrete mechanics laboratory

E-mail: Krasnikovs.Andrejs@gmail.com

ABSTRACT

Fiber reinforced concrete is an important material for structural applications. Traditionally fibers are homogeneously dispersed in concrete volume. At the same time in many situations material with homogeneously dispersed fibers is not optimal (the majority of added fibers are not participating in the load bearing process). In the present research fiber reinforced concrete prisms with layers contained different fibers concentrations inside them were elaborated. Prisms were tested under four point bending conditions, experimental results were discussed.

Key words: fiber concrete, layered structure, numerical modelling

INTRODUCTION

While in most of the currently available design recommendations fiber reinforced concrete strength properties are observed using the inverse approach (approximating the experimentally obtained curve), it should be noted that the direct modelling approach allows one to perform an economically optimal design of fiber reinforced concrete structure and to obtain the characterization of fibers distribution and their spatial orientations in structural element volume (Krasnikovs A. et all., 2008; Krasnikovs A. et all., 2009; Krasnikovs A. et all., 2012; Li V. C., 2003). In the present research three different types of layered prisms with the same amount of fibers in them were experimentally produced, three samples with the dimensions of 100×100×400 mm were created for each type and four prisms with homogeneously dispersed fibers were produced for reference as well. Prisms were tested under four point bending conditions until crack openings in each prism reached 6 mm. Simultaneously, prism cracking was simulated numerically using an elaborated numerical model for neutral axes location in the prism during crack growth and cracked beam load bearing capacity during crack growth and opening. The numerical modelling results were compared with the experimentally obtained ones. Finally, conclusions about fracture process features were made.

EXPERIMENTAL INVESTIGATION

In the framework of this research prisms of non-homogeneous fiber reinforced concrete with the dimensions 100×100×400 mm were designed. The technology of specimen preparation is described in the patent (Lapsa V. et all., 2011). Three identical

prisms of each type of non-homogeneous fiber reinforced concrete were prepared. Prisms were tested under four point bending conditions using the „CONTROLS” Automax 5 loading machine.

Specimens preparation

Groups of specimens are presented in the Table 1. Group 1 consists of fiber reinforced concrete with fibers homogeneously dispersed in the sample volume. These prisms were used as reference. As seen in Table 1, while the total amount of fibers is identical for all four groups of specimens, the difference is in their distribution. For specimens of Groups 2, 3 and 4, fibers are distributed in different layers with various concentration and orientation. These specimens can be defined as layered prisms with oriented distribution of fibers.

Steel end-hooked fibers Dramix RC 80/30 BP with the following parameters were used: length - 30 mm, fiber aspect ratio 80, and tensile strength 1020Mpa.

Fibers were added to the mix during the concrete mixing process and moulds were filled by such fiberconcrete for specimens representing Group 1 see in figure 1. For the specimens from Groups 2, 3, and 4, moulds were gradually filled with the concrete mix according to the description of each group. Then fibers were uniformly scattered on the concrete surface in the mould and were pressed into concrete (figure 2, 3 and 4).

Table 1
Distribution and concentration of fibers in specimens

Group Nr.	Distribution and concentration of fibers
Group Nr.1.	Fibers mixed in concrete mixer and homogeneously dispersed in the specimen (classical method)
Group Nr.2.	1. 25mm of concrete – 1/2 of the total amount of fibers (60 kg/m^3) were pressed into concrete 2. 25mm of concrete – 1/2 of the total amount of fibers (60 kg/m^3) were pressed into concrete 3. 50mm of concrete without fibers
Group Nr.3.	1. 25 mm of concrete – 2/3 of the total amount of fibers (60 kg/m^3) were pressed into concrete 2. 50 mm of concrete – 1/3 of the total amount of fibers (60 kg/m^3) were pressed into concrete 3. 25mm of concrete without fibers
Group Nr.4.	1. 25 mm of concrete – 2/3 of the total amount of fibers (60 kg/m^3) were pressed into concrete 2. 75mm of concrete – 1/3 of the total amount of fibers (60 kg/m^3) were pressed into concrete

Figure 1

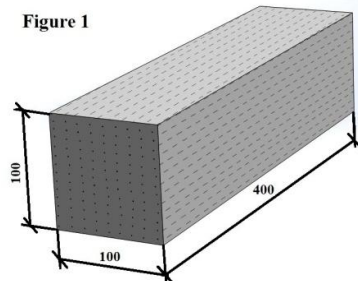


Figure 2

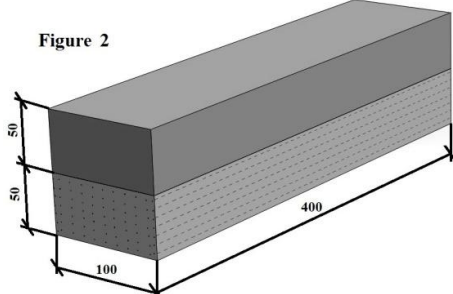


Figure 3

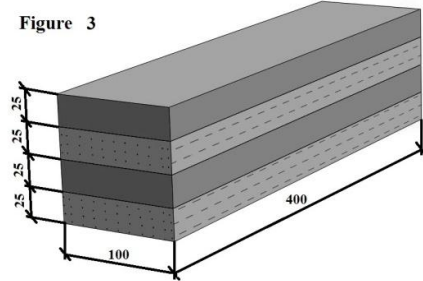


Figure 4

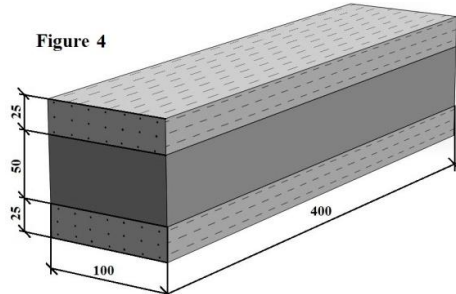


Figure 1; 2; 3; 4. Fibers distribution and concentration in samples



Figure 5. Testing device with fiber reinforced concrete prism

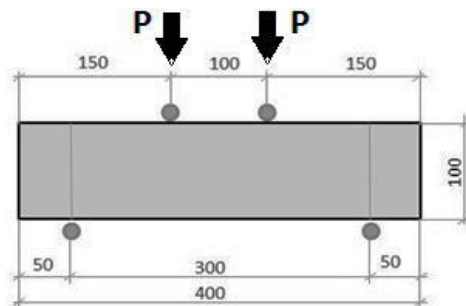


Figure 6. Picture of loads application to a fiber reinforced concrete beam

Table 2
Concentrations of fibers in the layers of specimen

Group Nr.	Fiber dispersion in the height of prisms and concentration of fibers in specimens kg/m^3
Group Nr.1.	1. 100mm - 60 kg/m^3 . Fibers are homogeneously and chaotically dispersed in the volume of prism.
Group Nr.2.	1. 50mm – 120 kg/m^3 . Fibers are homogeneously and chaotically dispersed in the layer with thickness 50mm. 2. 50mm – concrete without fibers.
Group Nr.3.	1. 25mm – 160 kg/m^3 . Fibers are homogeneously and chaotically dispersed in the layer with thickness 25mm. 2. 25mm – concrete without fibers. 3. 25mm – 80 kg/m^3 . Fibers are homogeneously and chaotically dispersed in the layer with thickness 25mm. 4. 25mm – concrete without fibers.
Group Nr.4.	1. 25mm – 160 kg/m^3 . Fibers are homogeneously and chaotically dispersed in the layer with thickness 25mm. 2. 50mm – concrete without fibers. 3. 25mm – 80 kg/m^3 . Fibers are homogeneously and chaotically dispersed in the layer with thickness 25mm.

During testing, the vertical deflection at the centre of a prism and crack opening were fixed by the linear displacements transducers in real time. Sensors were connected through a data acquisition unit to the computer where the obtained data were recorded and were available after experiments.

NUMERICAL MODELING

The computer modeling of fiber reinforced concrete cracking was performed using the previously developed numerical model (Krasnikovs A.et all., 2008; Krasnikovs A.et all., 2009; Krasnikovs A.et all., 2012). Assumptions regarding the fiber distribution in samples are shown in the Table 2.

RESULTS AND DISCUSSION

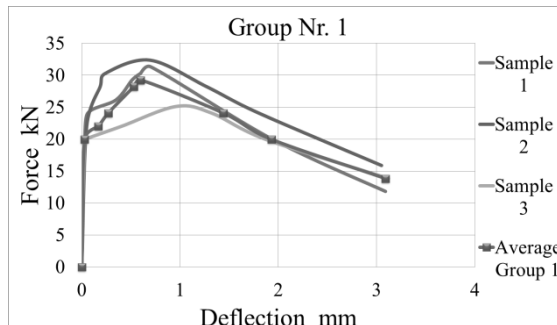


Figure 7. Load – sample centre vertical deflection graphs for specimens are representing group Nr.1

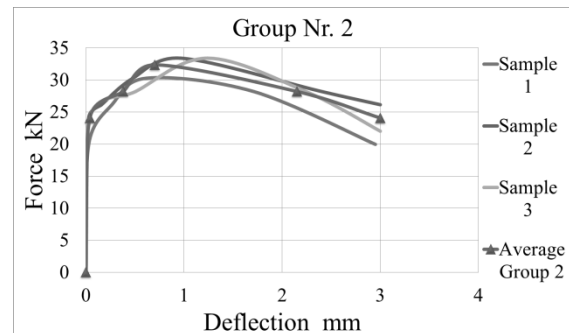


Figure 8. Load - sample centre vertical deflection graphs for specimens are representing group Nr.2

Specimens were tested under four point bending conditions. Load bearing - vertical deflection at the centre of each prism graphs for the specimens of Group 1 are given in figure 7.

The diagram shows the experimental curve of each specimen as well as the average value curve. Three stages are seen in each curve; first of them is linear elastic deflection (corresponds to deflection under 0,01mm). In this stage the fiber reinforced concrete prisms become deformed without visible crack openings.

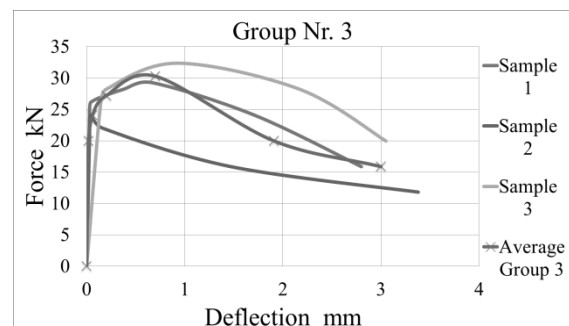


Figure 9. Load - sample centre vertical deflection graphs for specimens are representing group Nr.3

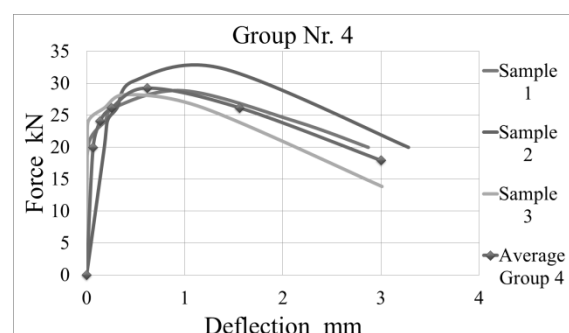


Figure 10. Load - sample centre vertical deflection graphs for specimens are representing group Nr.4

Fibers in the concrete do not bear significant load. The next stage begins with deviation of curves from the straight line and terminates reaching the maximum value on curve (with deflection of prisms 0,75mm – 1mm).

In this stage concrete micro cracks accumulate and grow forming a macro crack network. The macro cracks are formed perpendicularly to the longitudinal axis of prism. The density of the macro crack network depends on the specimen's geometry, size of fibers and their amount. Fibers traversing the macro cracks begin to bear load, while the cracks are still invisible on the outer surface of specimen.

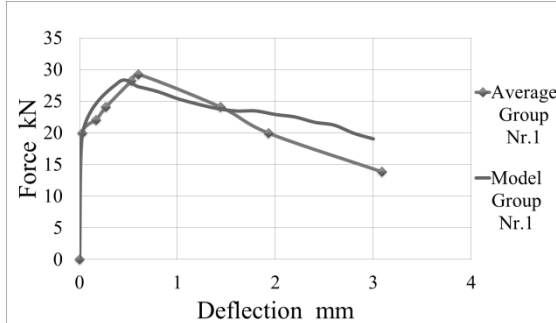


Figure 11. Load - sample centre vertical deflection graphs for specimens in Group Nr.1. The average result and modeling curve

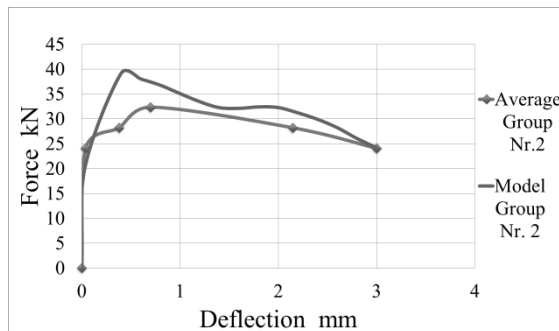


Figure 12. Load - sample centre vertical deflection graphs for specimens in Group Nr.2. The average result and modeling curve

The crack with the lowest resistance to opening (the one with the lower amount of fibers traversing it or fibers located and oriented in a less optimal way) starts to open. It proceeds the following way: fibers which are bearing load are delaminated from the concrete and start to pull out by one or both ends. The individual load carrying capacity of fiber depends on its orientation towards the crack plane and how far it is extracted.

Experimental observation of fiber pull-out micromechanics (Krasnikovs A.et all., 2009) showed that the maximum load carrying capacity of fiber depends on the orientation of fiber towards the direction of extraction force and how much the fiber has been extracted. The third stage is characterized by the decline of the total load carrying capacity of fiber. The capacity decreases proportionally to the size of the crack opening. Applied load - vertical deflection at the center of the prism for the specimens of Groups 2, 3 and 4 are given in figures 8, 9 and 10. Diagrams in figures 11, 12, 13 and 14 show the average experimental curves (from three

specimens) compared to the results of the numerical modeling. The modeling results approximate the data obtained experimentally in the first and second stage of curves. In the third stage the modeling results show a higher load carrying capacity for the specimens of Groups 1, 2 and 4 compared to the ones obtained experimentally.

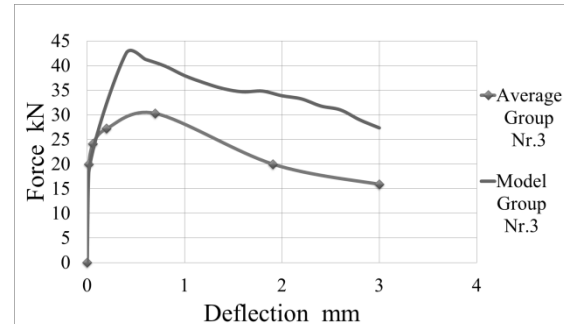


Figure 13. Load - sample centre vertical deflection graphs for specimens in Group Nr.3. The average result and modeling curve

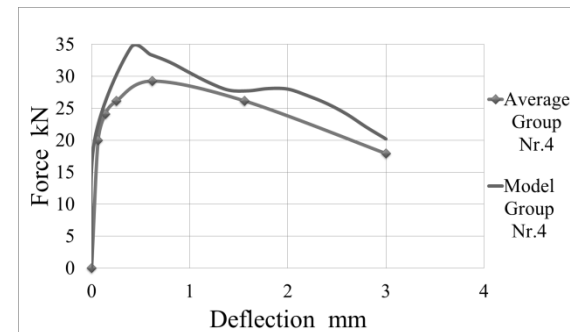


Figure 14. Load - sample centre vertical deflection graphs for specimens in Group Nr.4. The average result and modeling curve

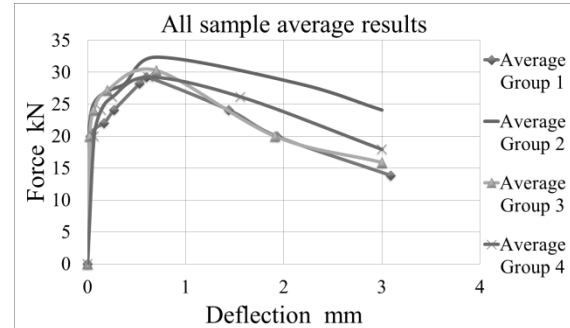


Figure 15. Load - sample centre vertical deflection graphs for specimens in comparison of average of all sample groups

The difference grows proportionally to the size of the crack opening. It can be explained by the homogenous distribution of fibers used in the model versus the non-homogenous in reality, for the specimens of Group 1, in the entire prism and for the specimens of Groups 2 and 4, in layers. Experimental (average) curves for all four groups are given in figure 15. It can be observed, that

Group 2 reaches the highest load carrying capacity during the crack opening stage due to the highest concentration of fibers compared to other groups in the lower part of the prism which bears the maximum tensile load. It can be observed, Group 1 (reference specimens) reaches lower average load carrying capacity in the third stage (macro cracks) compared to the specimens with the non-homogeneous distribution of fibers. Certain similar tendencies can be observed among the diagrams of the average results of the specimens – the maximal load carrying capacity is reached with deflection of prisms 0,75 mm – 1 mm, which correlates with the crack opening size.

CONCLUSIONS

According to the testing results, specimens of Group 2 reached the highest load carrying capacity during the crack opening stage as they had the highest concentration of fibers in the part of prisms experiencing maximum tensile load. Specimens of Group 1 showed a lower average load carrying capacity during the crack forming stage compared to the specimens with the non-homogeneous distribution of fibers. The load carrying capacity of

the fiber reinforced concrete was compared with the numerical modelling. The modelling results approximate the data obtained experimentally in the first and second stage of curves. In the third stage (macro crack opening) the modelling results showed a higher load carrying capacity for the specimens of Groups 1, 2 and 4 compared to the ones obtained experimentally. The difference increases proportionally to the size of the crack opening. It can be explained by the assumption about homogenous distribution of fibers that were used in the model versus the non-homogenous in reality.

ACKNOWLEDGMENT

This work has been supported by the European Social Fund within the project “Support for the implementation of doctoral studies at Riga Technical University”.



REFERENCES

- Krasnikovs A., Kononova O. and Khabaz A. (2009) Fracture and Post-cracking Behavior Prediction for Glass and Carbon Fiber Reinforced Concrete Construction Members, Proceedings of 5th International Conference Fiber Concrete2009 Technology, Design, Application, Prague p.161-166.
- Krasnikovs A., Kononova O. and Pupurs A. (2008) Steel Fiber Reinforced Concrete Strength. Sc. Proceedings of Riga Technical University. Transport and Engineering, 6. 28, p. 142-150.
- Krasnikovs A., Kononova O., Khabaz A., Machanovsky E. and Machanovsky A. (2012) Post-Cracking Behavior of High Strength (Nano Level Designed) Fiber Concrete Prediction and Validation. CD-Proceedings of 4th International Symposium on Nanotechnology in Construction, 20-22 May 2012, Crete, Greece, 6 p.
- Krasnikovs A., Kononova O. strength prediction for concrete reinforced by different length and shape short steel fibers// Sc. Proceedings of Riga Technical University. Transport and Engineering, 6, vol.31, p.89-93, 2009.
- Li V. C. (2003) On Engineered Cementitious Composites a Revue of the Material and it's Applications. Journal of Advanced Concrete Technology, Vol.1, No3, p. 215-230.
- Lapsa V., Krasnikovs A., Strauts K., (2011.20.04) „Fiberconcrete Non- Homogeneous Structure Element Building Technology Process and Equipment”, Latvian patent LV14257.

CONSTRUCTION AND MATERIALS

PROPERTIES AND COMPOSITION OF CONCRETE CONTAINING DIVERSE POZZOLANIC ADMIXTURES

Genady Shakhmenko^{*} Asist Prof. Dr.sc.ing., **Diana Bajare**^{*}, Assoc Prof. Dr.sc.ing., **Inna Juhnevica**^{**},
Leading researcher. Dr.sc.ing., **Nikolajs Toropovs**^{*}, PhD student, **Janis Justs**^{*}, PhD student, **Aljona Gabrene**^{**}, PhD student

^{*} Riga Technical University, Faculty of Civil Engineering, Institute of Materials and Structures
^{**} Riga Technical University, Faculty of Material Science and Applied Chemistry, Institute of Silicate Materials

Address: Kalku Street 1, Postal index LV-1658, Riga, Latvia
Phone: 371+29160832, e-mail: genadijs.sahmenko@rtu.lv

ABSTRACT

Micro-sized particles are used in modern concrete technology as a part of multi-component cementitious systems. Adding of micro-filler admixtures improves the properties of both fresh and hardened concrete. Local and commercially available micro-fillers were used in this research: dolomite powder, microsilica, calcined local (illite) clay and calcined kaolinite clay. Firstly, the basic micro-filler properties were studied, such as particle size distribution, particle morphology, specific surface and content of reactive components. The second experimental part covered production of fine-grained mixes, sample curing and testing. Compressive strength and water absorption were tested. Mineral formation processes were investigated using X-Ray analysis and IR spectroscopy.

As a result, it is concluded that the main factors, which determine the effectiveness of admixture, are pozzolanic reactivity, particle grading and morphology. The most effective fillers in this research were silica fume and calcinated kaolinite clay. Results for dolomite fillers were the same as for the inert fillers. Addition of local calcined illite clay improved tested concrete properties; consequently other locally available clay materials should be investigated more specifically as potential pozzolanic materials in future.

Keywords: Calcined clay, pozzolanic admixture, High performance concrete.

INTRODUCTION

The task of modern concrete industry is producing durable and sustainable concrete. It means: a highly workable concrete mix, stable and predictable properties of hardened concrete, high durability and other high performance characteristics. Traditional concrete consists of cement and macroscopic aggregates - sand and coarse aggregate. Modern concrete is a multi-component composite material, its structure can be regarded in 3 levels: macro (sand and coarse aggregate), micro (cement, micro-fillers) and nano-sized modifiers. Micro and nano elements compose cementitious system or cement paste. The current trend in concrete production worldwide is to use multi-component cementitious systems, which allows obtaining of high performance concrete with high durability (Presuel-Moreno, 2012). At the same time it contributes to the following ecological and economic benefits:

- to reduce clinker content (clinker is the most energy consuming component which is responsible for the majority of carbon dioxide emissions);
- to utilise industrial waste and by-products as mineral admixture;

- to minimize concrete price and transport charge. Most often multi-component cementitious systems are obtained by combining cement with supplementary fine-graded materials (powders) having pozzolanic activity (Cook, 1980). The most popular pozzolanic admixtures are silica fume and fly ash. Pozzolanic reaction is a simple acid-based reaction between calcium hydroxide $\text{Ca}(\text{OH})_2$ or CH and silicium acid H_4SiO_4 (Cook, 1986). As a result the calcium silicate hydrate (CSH) gel is formed that fills in pores and strengthens the cement matrix.

Authors (Sabir et al, 2001) emphasize that nowadays the term pozzolans has been extended to cover all siliceous/aluminous materials which react with calcium hydroxide (CH). Clay is among the natural hydrous siliceous/aluminous raw materials. Pozzolanic admixture can be obtained from clay with thermal treatment at 600-900°C. Metakaoline is an aluminium silicate mineral ($\text{Al}_2\text{O}_3\text{xSiO}_2$, or AS_2), it is considered as the most effective pozzolanic admixture obtained from clay after thermal treatment. Pozzolanic reaction between clay aluminium silicate AS_2 and CH forms additional aluminium containing CSH gel (Sabir et al, 2001). Some industrial wastes, for example, fluid cracking

catalyst (FCC), may also be used as siliceous/aluminous pozzolanic admixture (Žvironaitė et al, 2011).

Kaoline clay is not among the natural resources available in the Baltic States. However, according to the experience of other countries, other types of local clay can be used as pozzolanic admixture of concrete after thermal treatment as well. It has been proved that carefully calcined marl (calcareous clay) can be transformed to a very effective pozzolan that can replace cement in mortar (Ostnot et al, 2011).

It must be noted that mainly one-component cement is used nowadays in the Baltic States for concrete production. The main reasons for this situation are lack of experience and absence of available local high quality pozzolans. The price of imported pozzolans, such as fly ash, is much higher than the price of cement.

This paper discusses the possibilities of using diverse locally available pozzolanic admixtures, including the ones obtained from local clay.

The basic properties of micro filler are its pozzolanic activity, grading and morphology of particles. Particles with high pozzolanic activity are more effective as they react with cement, but inactive micro fillers can improve particle packing and rheological properties of concrete mix (for example, dolomite powder; micro-filler obtained from crushed concrete waste (Finoženok, 2011)). Micro fillers can be divided in three groups: based on natural materials, derived from industrial by-products and commercial products. The suggested scheme of classification is shown in Figure 1.

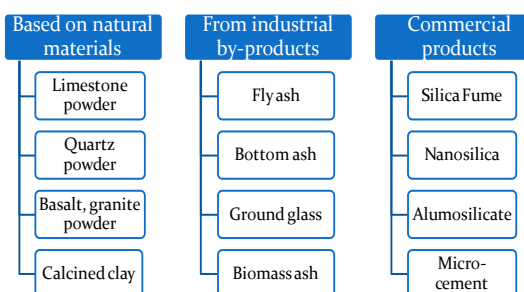


Figure 1. Classification of micro/pozzolanic admixtures

In this research the use of diverse pozzolanic admixtures, such as silica fume, dolomite powder (local material), calcined kaoline clay and local (illite) clay as part of two-component cementitious system, has been discussed.

METHODS

Investigation methods of micro admixtures

When preparing micro-filler admixtures it is important to examine them in detail as it allows one to assess the effectiveness of micro fillers and to

eliminate possible consequences if micro fillers contain substances having a negative impact on the cement hydration process.

The basic properties and their assessment methods in this research are the following:

Grading (particle size distribution) was determined by Dynamic Light Scattering (DLS) method;

Specific surface was determined by BET method using nitrogen absorption;

Pozzolanic reactivity was estimated taking into account the content of active $\text{SiO}_2/\text{R}_2\text{O}_3$. The principle of this method is determination of content of amorphous oxide reacting with calcium hydroxide (product of cement hydration);

SEM (Scanning Electron Microscope) microscopy (MiraLMU "Tescan") was used to determine real size and morphology of micro-particles.

Concrete preparation and testing methods

The effect of admixtures was estimated by testing specially prepared fine-graded concrete samples based on cement and quartz sand. The sample producing procedure included mix preparation, sample moulding and curing.

Raw materials were dosed by mass and mixed in the laboratory high shear mixer at a speed of 150 rotations per minute, total mixing time 4 minutes.

Standard samples (prisms) with the dimensions of 40x40x160 mm were produced from the concrete mix. After 2 days the samples were demoulded, then measured and weighted. Samples were cured in normal hardening conditions, ensuring the temperature at +20°C and relative humidity not falling below 95%.

The testing program of hardened concrete samples included mechanical testing, water absorption testing and the physical study of hydrated products. Mechanical properties were determined according to LVS EN 12390-3 Testing hardened concrete - Part 3: **Compressive strength** of test samples. Density was determined according to LVS EN 12390-7 Testing hardened concrete - Part 7: Density of hardened concrete.

Water absorption was calculated taking into account: the mass of water saturated samples and the mass of oven-dried samples (105°C during 48 hours).

Mineralogical composition of hardened specimens was investigated using X-Ray analyse equipment with Rigaku Optima Plus diffractometer and CuK α .

Hardening processes of cement paste was investigated using Fourier Transmission Infrared Spectroscopy (FTIS). The method is based on activating the molecules by means of infrared ray energy and recording the intensity curve after energy transmission through material. The character of absorbed energy curve depends on the nature of chemical bonds in the material. The method allows one to control the forming of functional groups and new chemical bonds. Average infrared wave range

2.5 – 25 µm (4000 – 400 cm⁻¹) was applied in this research.

MATERIALS USED

In the frame of this work the following micro powdered materials were applied as concrete admixture: dolomite powder (Saulkalne, commercially available), Silica fume (Elkem microsilica 971U, commercially available), Illite type local Latvian clay (deposit Liepa) and kaoline clay (commercially available). Chemical compositions of raw materials are summarised in Table 1. Clay materials were specially prepared (dried, calcined and ground) prior to use as a concrete admixture. The basic properties of used fillers were determined.

The target of clay thermal treatment is dehydration and decarbonation of clay minerals and the transformation of SiO₂ and R₂O₃ into amorphous oxides. In the process of thermal treatment, water of crystallization is released from the structure of clay and chemical bonds disappear. As a result, the material becomes chemically active and capable of reacting with free calcium hydroxide. By analysing the literature sources it can be concluded that the optimum calcination temperatures for clay - ranges from 600-800 °C (Ambroise, 1986). Chemically bonded water from the kaoline clay is mainly released at a temperature of 600°C, but for montmorillonite clay, the temperature range is higher, namely, 600-780°C (Bain, 1974). Kurss (1972) has performed research on mineralogical changes of the Latvian clay during the thermal treatment process and has concluded that the mineral structure remains without significant changes up to 400 – 500°C. At a higher temperature the release of water can be observed. For the kaolinite it is most intense at the temperature between 450 and 650°C. By fast thermal treatment hydroxyl groups are released at high temperature. Vertical shaft kiln and rotary kiln are usually used for calcination of clay materials.

Table 1
Chemical composition of raw materials
(mass percentage)

	SiO ₂	Al ₂ O ₃	Fe ₂ O ₃	CaO	MgO	Na ₂ O+K ₂ O	SO ₃	LOI	Other
C	25.0	2.1	3.0	66.0	0.7	0.2	2.3		0.7
K	52.1	41.0	4.32	0.07	0.19	0.89		0.6	0.8
M	54.83	19.05	6.0	9.39	1.77	3.65	2.9	1.48	0.9
SF	92.0	0.7	1.2	0.2	0.2	2.0		3.0	0.7

C- Cement; K- Kaoline clay; M- Illite clay; SF-Silica fume

Clay preparing procedure in laboratory was the following:

Clay was broken into smaller pieces and dried at a temperature of 100°C to remove free water. Then the clay was additionally ground before calcination to obtain a particle size of <5 mm.

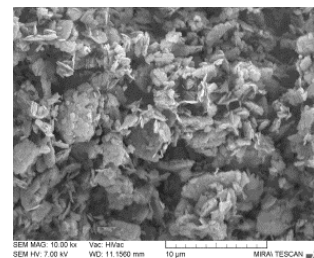
Clay calcination (burning) was done in a laboratory rotary kiln (diameter 70 mm, rotation speed 30 rpm) for about 15 minutes with designed temperature 700 °C.

After burning the material, it was ground in the laboratory planetary ball mill Retsch PM 400 for 15 minutes, providing a rotation speed of 300 rpms.

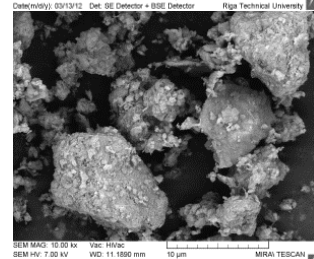
Estimating the environmental impact of using thermally treated clay, calcining energy consumption must be taken into account. It must be stressed that clay calcining requires much less energy (68 kJ/kg) than cement production (372 kJ/kg) (Cook, 1980). Additionally, this process is associated with significantly lower level of carbon dioxide emissions compared to cement production.

Grading and morphology

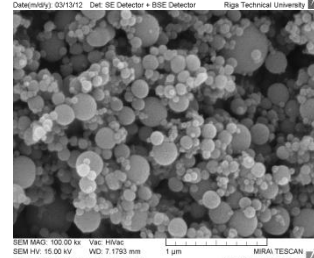
Particle size distribution and shape of particles are the basic parameters which determine rheological properties of mix and density of microstructural packing (Ulm and Acker, 2008). The shape of particles is an important parameter affecting the total specific surface and chemical reactivity.



Calcined Kaoline (metakaoline)
Shape of particles:
irregular, flake-shaped, disperse packing



Calcined Illite clay
Shape of particles:
irregular, flake-shaped, particle agglomerates (up to 10 µm)



Silica fume
Very fine material,
shape of particles
ideally rounded, wide
range of sizes
(20...450 nm)

Figure 2. SEM images and description of micro admixtures

Particle shape characteristics of used pozzolanic admixtures were investigated by means of a Scanning Electron Microscope, typical SEM pictures and particle characteristics are described in Figure 2. Basic characteristics of micro powdered admixtures and used cement are summarised in Table 2.

Particle size distribution (grading curves) of calcined clay and silica fume are summarised in Figure 3. It must be noted that the calcined clay materials (both matalaoline and illite) are characterised by an extremely high specific surface (more than 15 m²/g), 2-3 times exceeding the specific surface value of silica fume. Particle size distribution curves (Figure 3) are characterized by narrow range of sizes (low polydispersity) and very small particle size (<1 µm), placing clay between silica fume and cement. However, the dimensions of metakaolin particle sizes mentioned in different literature sources range from 1 to 10 µm. Possible reasons for these differences might be the following:

1. DLS analysing system outputs particle sizes, which are reduced to spheres of similar volume. If the particles are thin and flake-shaped, their real dimensions (length) could be considerably bigger.
2. Coarse particles can be observed in the SEM images, which can be agglomerated fine particles. Performing DLS test agglomerates dissolved in water, but rough particle sedimentation can take place in an environment of water suspension. However, in this case small dimensions of calcined clay particles from the DLS test confirm the high value of the specific surface from the BET analysis (Tab.2).

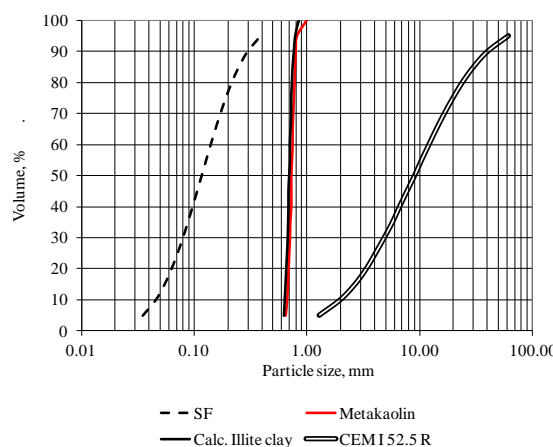


Figure 3. Particle size distribution

Table 2
Basic characteristics of used admixtures and cement

Powdered material	Effective particle size, µm	Specific surface (BET), m ² /g	Active SiO ₂ and R ₂ O ₃ , %
Cement CEM I 52,5 R	40	0.45	
Dolomite powder	<...50	0.8	
Calcined illite clay	0.71	21.9	0.89 / 7.92
Calcined kaoline clay	0.74	16.5	1.10 / 32.76
Silica fume	0.3	7.92	>90/0

MIX DESIGN AND SAMPLE PREPARATION

White high-strength alite based cement CEM I 52.5R was used as a binding agent and pure quartz sand 0/1 mm was used as a filling agent. The experimental phase involved producing mix compositions replacing cement by different micro admixtures in the amount of 20% from the total amount of cement. The compositions of raw materials are summarised in Table 3.

All the mixes are characterised by homogenous and flowable consistence. Water content was provided constant for all mixes.

Table 3
Concrete mix composition

	K15	M15	D	SF	C
Cement CEM I 52,5 R	1	1	1	1	1.2
Sand 0/1 mm	2.64	2.64	2.64	2.64	2.64
Calcined kaoline clay	0.2				
Calcined illite clay		0.2			
Dolomite powder			0.2		
Silica fume				0.2	
Superplasticizer	0.01	0.01	0.01	0.01	0.01
Water	0.43	0.43	0.43	0.43	0.43

RESULTS AND DISCUSSION

Compressive strength and density

Concrete specimens were tested at the age of 7, 28 and 49 days of normal curing. The compressive strength results are summarised in Figure 4. Values of density of hardened specimens varied in range: 2140 – 2200 kg/m³ for all mixes. Therefore it can be concluded that the deviation of density is insignificant and admixtures do not have a significant impact on density.

Summarizing compressive strength results: it may be said that the long-term hardening effect is related to composition based on calcined clay and silica fume. In addition, metakaoline (K15) composition results after 7 days of curing are similar to those of silica fume (SF) and cement without admixtures (CEM) composition, but at the age of 28 and 49 days, the compressive strength results of

composition K15 are the highest, exceeding even the composition with silica fume. The lowest compressive strength results after 7 days are for composition D with dolomite powder, it increases and stabilises at the age of 28 and 49 days. Composition with calcined local metakaoline clay (M15) shows lower compressive strength results as composition CEM, but it increases after 28 days and continues to increase afterwards, becoming similar to the results of CEM, while 17% of the cement was replaced.

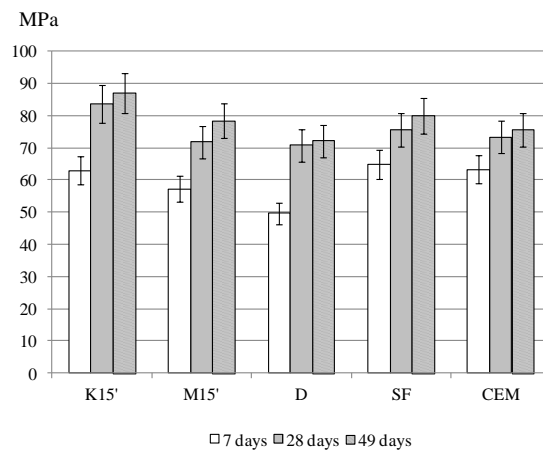


Figure 4. Compressive strength results: K15' - with metakaoline ground for 15 min., M15' - with calcined illite clay ground for 15 min, D - with dolomite powder, SF – with silica fume, CEM - cement without admixtures

Water absorption

Water absorption test provides information about open porosity of the material. Comparing water absorption results of different samples, the biggest water uptake values are indicated for mixes D (5.7%) and CEM (5.4%), which do not contain pozzolanic admixtures. The results are almost two times lower for the mixes containing silica fume and metakaoline (about 2%). Composition containing calcined illite clay also has quite a high value of absorption (4.9%), but the results are lower compared to compositions D and CEM. It indicates that the local clay have slight pozzolanic effect and microstructural packing capability of concrete. Water absorption data correlates with compressive strength results; the strongest compositions SF and K15 have the lowest values of water absorption.

X-ray diffraction analysis

X-Ray diffraction analysis was performed for concrete specimens after 28 days of curing. The results show the presence of mineral portlandite (Calcium hydroxide) in all samples. The biggest concentration of this mineral is indicated in samples

CEM and D. Low content of portlandite is found in samples SF and K15 as well, this effect can be interpreted by the pozzolanic reactions (because silica fume and metakaoline are the most active pozzolans). Cement mineral hatrurite (alite) was found in samples CEM, D, K15, M15 and SF. The most typical X-ray diagrams (for mixes SF and D) are shown in Figures 6.

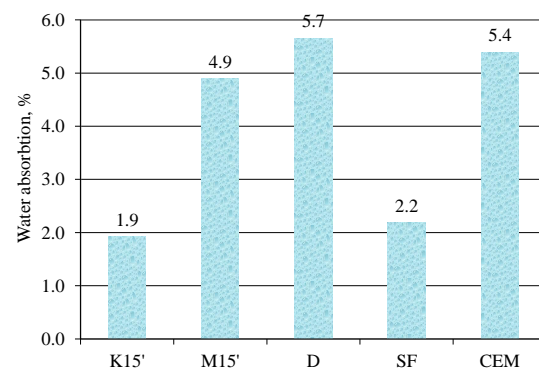


Figure 5. Water absorption results: : K15' - with metakaoline ground for 15 min., M15' - with calcined illite clay ground for 15 min, D - with dolomite powder, SF – with silica fume, CEM - cement without admixtures

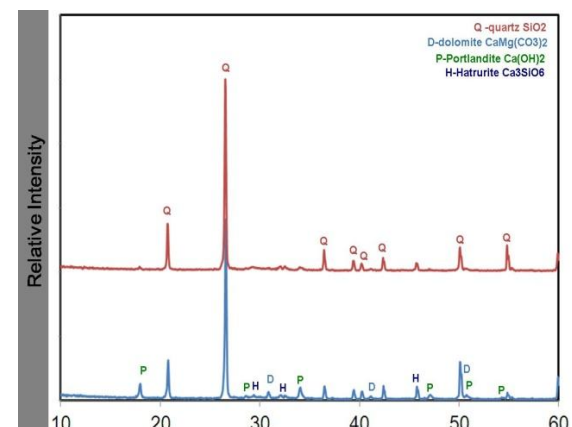


Figure 6. X-Ray diffraction results: mix D (below) with dolomite powder and mix SF (above) with silica fume

FTIR analysis

According to the results of the Fourier Transmission Infrared Spectroscopy (Fig. 7, 8) the following can be concluded:

- For samples with calcined clay (M15 un K15) infrared wave absorption is 671 cm^{-1} due to functional groups O-Al-O, which indicates the presence of aluminium containing CSH gel.
- Hydrated samples with dolomite (D) are characterised with infrared wave absorption in the range of 871 cm^{-1} and 1620 cm^{-1} , which corresponds

to fluctuations of C-O. It indicates a significant presence of CO_3^{2-} groups in sample

- Absorption in range 455 ... 520 cm^{-1} corresponds to valence fluctuations of Si-O in the hydrated sample of cement paste (C-S-H gel).

- Intensity increase of the infrared wave absorption in the range of 3400...3500 cm^{-1} , responsible for the valence fluctuations of O-H group, and absorption of 1620 cm^{-1} (deformation fluctuations of H-O-H) in infrared spectrum of silica fume (SF) and dolomite (D) can be explained by a high level of absorbed water in the admixtures compared to the spectrum of M15 and K15.

- Si-O fluctuations in the structure of C-S-H can be observed at 779 cm^{-1} . Fluctuations at 671 cm^{-1} correspond to the Si-O fluctuations in tetrahedron $[\text{SiO}_4]^{4-}$, which might indicate the presence of quartz.

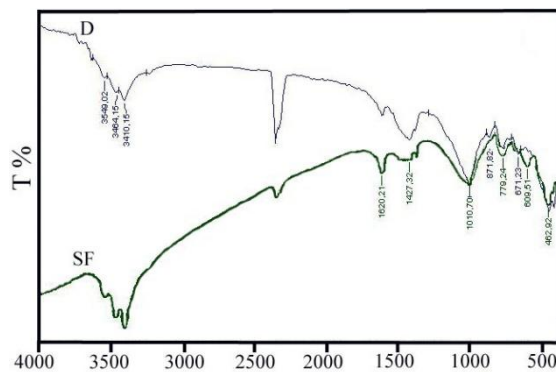


Figure 7. FTIS results: mix D with dolomite powder and SF with silica fume

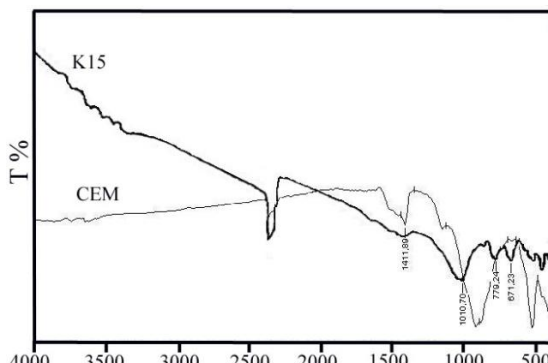


Figure 8. FTIS results: mix CEM - cement without admixtures and K15 with calcined illite clay ground for 15 min

- Absorption range 1010 cm^{-1} corresponds to asymmetric fluctuations of Si-O-Si, which indicates the presence of amorphous silica compounds (characteristic to all silicates), which are formed during the cement hydration process and which are impossible to detect with the X-ray test. Wide range of infrared wave absorption 879...918 cm^{-1} for the specimen CEM compared to the narrow range of infrared wave absorption 1100 cm^{-1} for the

specimens D, SF, K15 indicates a higher level of amorphisation.

It must be emphasised, that the method of the Fourier Transmission Infrared Spectroscopy can be used additionally to X-Ray diffraction analysis to understand the mechanism of pozzolanic reactions.

CONCLUSIONS

Basic factors such as pozzolanic reactivity, particle grading and morphology determine the effectiveness of cement admixtures. Particle size distribution is the parameter, which may have an insufficient objectivity characterising a particular material, because the particles could be thin and flake-shaped. For this reason it is recommended to perform a BET analysis and particle morphology investigation as well.

Four admixtures have been compared in this research. It was tested and verified that the admixtures do not have a significant impact on the density of hardened concrete.

Mixes based of cement and cement combination with dolomite powder are non-effective binders, having a high water absorption rate and low compressive strength.

The most effective fillers in this case are calcined kaoline clay (metakaoline) and silica fume characterised by a high level of pozzolanic activity and specific surface. These mixes showed the highest mechanical strength results and low water absorption.

Calcined local illite clay demonstrated an insignificant effect comparing to metakaoline and silica fume, but some improvement in properties and long term curing effect took place. Red colour of calcined illite clay may be used for creating an aesthetic concrete surface. Local Latvian clays are an unlimited natural resource, which successfully may be used as cement admixtures having some pozzolanic activity. Research in the future may be carried out, varying the clay type and conditions of production (temperature and grinding time).

The use of calcined locally available clay as a cement replacing admixture is an environmentally friendly way, because the calcining process requires 5 times less energy than cement production and is not associated with high level carbon dioxide emissions. Possibilities for the use of local calcined clay to improve concrete durability properties, must be investigated in the future.

ACKNOWLEDGEMENT

The financial support of the ERAF project Nr. 2010/0286/ 2DP/2.1.1.0/10/APIA/VIAA/033 „High efficiency nano concretes” is acknowledged.

REFERENCES

- Ambroise J., Murat M., Pera J. (1986) Investigation of synthetic binders obtained by middle-temperature thermal dissociation of clay minerals. *Silicates industrie*, Vol. 7(8):99-107.
- Bai J., Wild S., Sabir BB., Kinuthia JM. (1999) Workability of concrete incorporating PFA and metakaolin. *Mag. Concrete Res.*, Vol. 51(5):207-16
- Bain, J.A. (1974) Mineralogical assessment of raw material for burnt clay pozzolanas. Spence, R. ed., Lime & Alternative Cements, *Proc. of a One-day Seminar on Small-Scale Manufacturing of Cementitious Materials*, Intermediate Technology Development Group, London, England, p. 60-69
- Cook, D.J., (1980) Using rice-husk for making cement-like materials. *Appropriate Technology*, Vol. 6, p. 9-11
- Cook D.J. (1986) Natural pozzolans. In: Swamy R.N., Editor (1986) Cement Replacement Materials, Surrey University Press, p. 200
- Costa U., Massazza F. (1977) Influence of the thermal treatment on the reactivity of some natural pozzolanas with lime. *II Cemento*, V3, p. 105-122
- Finoženok O., Zurauskene R., Rūrauskas R. (2011) Influence of various size crushed concrete waste aggregate on characteristics of hardened concrete. *Proceeding of '11: International Scientific Conference Civil Engineering*, Latvia, Jelgava, 12.-13. May, p. 7-13
- Kuršs V., A. Stinkule (1972) *Māli Latvijas zemes dzīlēs un rūpniecībā*, Rīga: LU
- Lea F.M. (1974) *The Chemistry of Cement and Concrete*. 3rd ed., London: Edward Arnold.
- LVS EN 12390-3. *Testing hardened concrete - Part 3: Compressive strength of test samples*
- LVS EN 12390-7. *Testing hardened concrete - Part 7: Density of hardened concrete*
- Ostnor T., Justnes H., Martius-Hammer T.A. and Danner T. (2011) Calcined marl as alternative pozzolan. *Proceedings of the 7th Central European congress on concrete engineering*, Balatonfured, Hungary, p. 151-154
- Presuel-Moreno F., Paredes M. (2012) 16 years' exposure of fly ash and silica fume concretes on salt induced reinforcing steel corrosion: corrosion potential, resistivity and diffusivity. *Proceeding of International congress on durability of concrete*, Trondheim, Norway, p.83
- Sabir B.B., Wild S., Bai J. (2001) Metakaolin and calcined clays as pozzolans for concrete: a review original research article. *Cement and Concrete Composites*, Vol. 23, Issue 6, p. 441–454
- Ulm F. J., Acker P. (2008) Nanoengineering UHPC materials and structures. *Proceedings of the 2nd international symposium of Ultra High Performance Concrete*, Kassel, Germany, March 05-07, p. 3-9
- Žvironaitė, Jadvyga; Pundienė, Ina; Antonovič, Valentin; Balkevičius, Valdas (2011) Investigation of peculiarities in the hardening process of portland cements with active additives out of waste. *Materials science, Medžiagotyra*. ISSN 1392-1320. Vol. 17, no. 1, p. 73-79

EFFECT OF THERMAL TREATMENT ON PROPERTIES OF HIGH STRENGTH CONCRETE

Nikolajs Toropovs, Diana Bajare, Genadijs Shakhmenko, Aleksandrs Korjakins, Janis Justs

Riga Technical University, Faculty of Civil Engineering, Institute of Materials and Structures

Address: Azenes Street 16, Postal index LV-1658, Riga, Latvia

Phone: +371 67089248, e-mail: diana.bajare@rtu.lv

ABSTRACT

High Performance Concrete (HPC) and Ultra-High Performance Concrete (UHPC) are modern building materials with advanced mechanical properties and durability compared with traditional concrete. Increasing of their mechanical properties allows reducing cross section of construction element. As a result, less raw materials are consumed.

Obtaining of concrete with high mechanical strength is related to a low W/C ratio, superplastificators and use of specific mixing and hardening technologies. One of the factors that influence properties of concrete is thermal treatment during hardening process. For traditional concrete steam treatment is used, but in the case of specific modern materials like HPC and UHPC increasing of mechanical properties can be achieved with the thermal treatment at temperature over 100°C.

The effect of thermal treatment on concrete compressive strength was investigated on cube-shaped specimens of 5cm. The heat treatment temperature varied from 50°C to 200°C with a 50°C increment. The specimens were heated under the same conditions for each temperature level; speed of increasing the temperature was 2°C per minute, thermal treatment at maximal temperature lasted 4 hours. Thermal treatment and compressive strength tests were carried out on the 3rd and 28th days. Tests were performed with specimens cooled down slowly to room temperature after heating.

Additional tests were made for water absorption and permeability, including SEM analysis comparing concrete specimens with and without specific thermal treatment applied.

The results showed that, despite the possible dehydration, compressive strength of thermally treated HPC specimens has improved. Maximal compressive strength was achieved for specimens thermally treated at 200°C. Compressive strength of non-heated specimens was about 80 MPa (on 3rd day) and 130 MPa (on 28th day), and thermally treated specimens showed a strength about 155 MPa (on 3rd and 28th day).

Results for SEM, water absorption and permeability, compressive strength of specimens at different thermal treatment conditions are summarized in this paper.

Key words: High strength concrete, HPC, thermal treatment, permeability of HPC

INTRODUCTION

Construction sector is one of the biggest industries having an enormous impact on the economic development. 4.6 trillion USD were spent in the world in this sector, in 2011 (Crosthwaite, 2012). Concrete is the most widely used construction material in the world with an annual use of cement estimated to constitute 3.86 billion tons in 2012 (For Construction Pros.com, 2011). The cement production industry generates up to 5% of the total amount of CO₂ emissions (Flower et al, 2007).

Considering the huge amount of concrete used in the world, qualitative changes in the material and its production process could have a significant impact on global economic development and the total amount of CO₂ emissions. Improvement of mechanical properties of concrete would allow the size of constructions to be reduced and less concrete would be necessary decreasing the amount of raw materials used.

Introduction of high strength concrete (with a compressive strength more than 100 MPa) in

particular construction elements of civil engineering would give an economic benefit. Dimensions of columns often used in high-rise buildings could be decreased therefore increasing the total useful floor area. Without changing dimensions of columns it is possible to reduce the amount of necessary reinforcement in columns. Here is the economic benefit – while high strength concrete might be more expensive than an equal amount of traditional concrete, the total costs can be lower due to improved concrete properties. Increased modulus of elasticity of high strength concrete increases stiffness of high-rise buildings and reduces deformations due to wind load. Design of parking facilities improves as well if the supporting columns are smaller.

According to the results of the recent research, it is possible to reduce by 50% the amount of gases causing the greenhouse effect in the production of building materials by using high strength concrete (Habert et al, 2012). Consequently, not only the economic benefit can be observed, but sustainable development is encouraged as well.

Obtaining of concrete with high mechanical strength is related to a low W/C ratio, superplastifiers and use of specific mixing and hardening technologies. One of the factors that influence properties of concrete is thermal treatment during the hardening process. For traditional concrete, steam treatment is used, but in the case of specific modern materials like HPC and UHPC increasing of mechanical properties can be achieved with thermal treatment at a temperature of over 100°C.

Concrete is non-flammable and is considered to be a fire-proof material, thus it is used in constructions with increased requirements for fire safety, for example, firewalls and fire-proof sections in buildings (Mehta et al, 2006). Thermal treatment is used in the process of concrete curing as well in order to obtain a higher early age strength. For example, this method is widely used for the production cycle optimisation in the production of precast concrete elements. Several researches regarding the impact of thermal treatment on concrete properties and its application time and application period have been performed since 1950. Research results have been included in various design norms and guidelines. However, the research object usually has been traditional concrete with a compressive strength of 15-30 MPa. As the use of high strength concrete and the research on its properties has expanded during the last years, there are well-founded suspicions that the performance of high strength concrete under thermal treatment is not characterised precisely in design norms.

Thermal treatment of concrete is used separately or as a steam-heat treatment with possible high-pressure steam. Treatment at an elevated temperature accelerates cement hydration or reactions of other cementitious materials, therefore resulting in higher early age strength compared to the normal conditions. It is observed that after a 28 day curing period, at a temperature regime +5°C – +46°C the difference between concrete which has been thermally treated or cured under normal conditions becomes less evident as the similar hydration stage is reached after 28 days. It should be noted that according to practical observations the higher thermal treatment temperature results in a lower final strength of concrete, for example, after 180 days (Mehta et al, 2006).

In modern concrete more and more attention is paid to fine mineral additives, for example, microsilica. However, the results of researches on thermal treatment of concrete containing amorphous silica and conclusions regarding the impact of the fine mineral additives are contradictory. For example, M.S.Morsy and others concluded that microsilica additives have a positive impact on the concrete after 28 days of curing at a temperature of up to 400°C (thermally treated for 2 hours), because the compressive strength of treated specimens increased

in comparison with the non-treated specimens (Morsy et al, 2010). Ali Behnood and Hasan Ziari in turn argue that the presence of microsilica in concrete do not have a positive contribution to its mechanical properties apart from the higher compressive strength in comparison with concrete without microsilica (Behnood et al, 2008). The compressive strength of concrete increases only slightly compared with the thermal treatment of 100°C and 200°C. Concrete mixes with amorphous silica which were thermally treated at a temperature exceeding 200°C showed more significant strength reduction in comparison with concrete without this additive. It should be noted that the initial strength of concrete in the research of M.S.Morsy and others was up to 50MPa, while in the research of Ali Behnood and Hasan Ziari it ranged from 60-85MPa. The initial strength of concrete is one of the factors having an impact on concrete properties at a high temperature.

MATERIALS AND METHODS

In this research the impact of high temperature regime on high strength concrete was examined. Concrete with the approximate compressive strength of 100 MPa and chemical composition shown in Table 1 was used.

Table 1
Chemical composition of concrete used in research

Components	Amount, kg/m3
Cement CEM I 42,5 N	800
Sand 0,3- 2,5 mm	510
Sand 0-1,0 mm	480
Sand 0-0,3 mm	100
Ground quartz sand	100
Microsilica	100
Nanosilica	20
Superplasticizer	20
Water	200

Thermal treatment of specimens was performed on 3rd and 28th days, while physical and mechanical properties were tested on 4th and 29th days of curing respectively. Compressive strength was also tested on the 58th and 86th days to assess the dynamics of curing without thermal treatment. Thermal treatment was performed applying temperatures of 50, 100, 150 and 200°C, compressive strength, water absorption and water permeability of the specimens were tested as well. Thermal treatment of specimens at temperatures of 250°C and 300°C was performed on the 3rd day as well in order to test the impact of temperature on the concrete at a high temperature, which is close to the temperature of possible concrete destruction under the impact of increased steam pressure.

Technology of the concrete mix preparation consisted of several stages. First all the dry

components were mixed in a mixer for approximately 1.5 minutes in order to obtain a homogenous mix. Then nanosilica was added in the form of a water suspension with a ratio of 1:2 (water:nanosilica) according to the mass. Next 2/3 of the necessary water was added followed by 1/3 of water mixed with superplasticizer. The mixing process was continued until a homogenous fluid mix was obtained. The total mixing time was about 6 minutes.

The prepared concrete mix was moulded in respective moulds (steel moulds including 5x5x5 cm cubes for mechanical tests, 4x4x16 cm prisms for water absorption tests and 10x10x10 cm cubes for water permeability tests). Specimens were vibrated on a vibrating table for about 10 seconds. Moulds were covered with a polyethylene film to limit the vaporising of water and left for curing at the room temperature. On the 3rd day of curing specimens were demoulded. Part of the specimens was placed in the water to continue curing process, while the rest of them were thermally treated. Temperatures of 50, 100, 150, 200, 250, 300°C were used in this research. The thermal treatment cycle consisted of heating phase when increasing of the temperature was 2°C per minute, thermal treatment at maximal temperature phase, which lasted for 4 hours and cooling down phase when the specimens were left to cool down to the room temperature (Fig. 1).

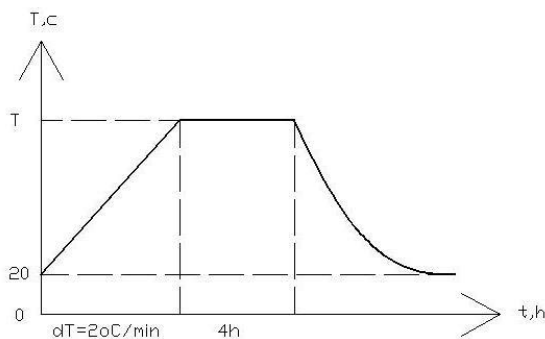


Figure 1. Furnace operating mode,
Where T – temperature, °C;
t – time, hours

Compressive strength of the specimens after the application of various temperatures was tested in this research depending on the time of thermal treatment and testing time. Labelling of specimens:

- Thermal treatment was applied on the 3rd day, compressive strength tested on the 4th day of curing. Labelling 3/4 (thermal treatment day/testing day);
- Thermal treatment was applied on the 3rd day, compressive strength tested on the 29th day of curing. Labelling: 3/29;
- Thermal treatment was applied on the 28th day, compressive strength tested on the 29th day of curing. Labelling: 28/29.

Specimens without thermal treatment, which were cured in water, were used for reference. Specimens 28/29 were taken out of the water 7 days prior to the thermal treatment and left to dry at room temperature. Specimens 3/29 were immersed in water again after thermal treatment and treated similarly to the 28/29 specimens until the testing of compressive strength.

Dynamics of the reference specimens' compressive strength was tested on the 4th, 29th, 58th and 86th days. Specimens were cured in water at room temperature and taken out of the water 7 days prior to mechanical tests. 5x5x5 cm cubes were used for compressive strength tests.

4x4x16 cm prisms were used for water absorption tests. Water absorption of 3/29 and 28/29 specimens were tested by treating them at temperatures of 50-200°C with 50°C increments.

Water permeability tests were performed with reference specimens and the specimens which were thermally treated at 200°C on the 3rd day and then immersed in water until the 29th day. Specimens were tested on the 31st day according to the standard LVS EN 12390-8:2009 Testing hardened concrete - Part 8: Depth of penetration of water under pressure.

The concrete microstructure was investigated using a scanning electron microscope (SEM) as well as by X-ray analysis of reference specimens without thermal treatment and specimens treated at 200°C for 4 hours.

RESULTS AND DISCUSSION

The obtained compressive strength results are shown in Fig. 2. Growth of compressive strength can be observed with a temperature increase. However, regardless of the maximal compressive strength at the maximal temperature of (153.1 MPa for 28/29 specimens at 200°C) and the following thermal treatment, even this treatment effect decreases with the increase of curing time and temperature.

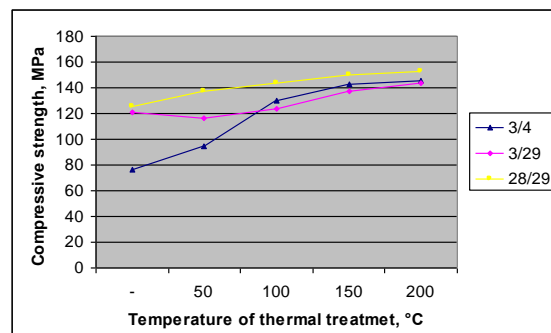


Figure 2. Compressive strength of the specimens

Compressive strength development dynamics of the specimens without thermal treatment was tested, which reached 123 MPa and 139.8 MPa on the 29th

and 58th days respectively. It corresponds to 160% and 170% strength activity index compared to the compressive strength on the 4th day (76.8 MPa). Up to 29 days compressive strength increased rapidly, then it slowed down, but did not stop completely, which is typical for concrete mixes with such pozzolanic additives as microsilica and nanosilica. Compressive strength of concrete specimens was 137.9 MPa on 86th day which corresponds to 180% strength activity index.

Treating ¾ specimens at temperature 300°C for 4 hours the critical value of the steam pressure for the chosen composition was reached and the specimens exploded during the thermal treatment which could be expected.

Compressive strength of 3/4 specimens after treatment at temperature 250°C was 177.7 MPa, which corresponds to 231% of specimens without thermal treatment 3/4 (76.8 MPa). Water absorption results are given in Table 2.

Table 2

Water absorption results of specimens

		day of treatment	
		3	28
temperature of treatment	50	2.8%	3.0%
	100	2.9%	3.0%
	150	2.9%	3.0%
	200	2.9%	3.0%

The overall trend is that specimens thermally treated on the 3rd day have lower water absorption. However, taking into account the dispersion of results and close mean values, it is not possible to draw apparent conclusions about the impact of thermal treatment on water absorption.

Depth of penetration of water under pressure was not observed for the specimens without thermal treatment by splitting the specimens. For the specimens treated at 200°C it was 3 mm. It indicates the presence of cracks in the upper layers of concrete which have appeared as a result of thermal treatment and encouraged water penetration in contradistinction to the dense structure of specimens without thermal treatment. The map of cracking of specimens is shown in Fig. 3.

High density of concrete is regarded as a factor encouraging the spalling in the top layer of concrete because it limits moisture migration and heat transfer processes in the concrete significantly.

Observing the microstructure of specimens under the SEM, formations shown in Fig. 4 were found. They were present in the specimens treated at 200°C and are similar to aluminium silicate hydrate. These formations were not present in the specimens without thermal treatment. Taking into account the shape of formations, they possibly might weaken concrete structure and encourage the complete or

partial destruction of concrete under the impact of increased steam pressure or spalling in the top layer of concrete.

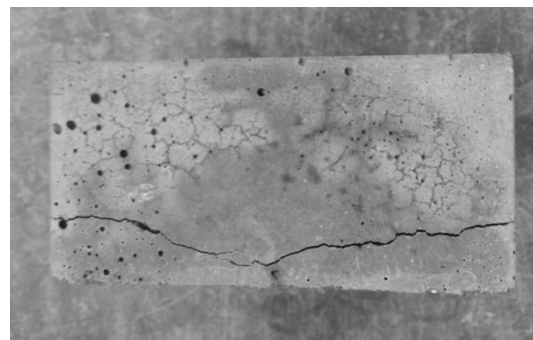


Figure 3. Map of cracking of concrete specimens after thermal treatment at 200°C

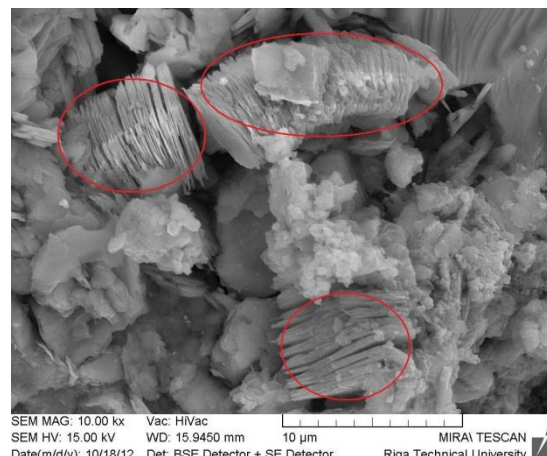


Figure 4. SEM image of the concrete specimen thermally treated at 200°C

By comparing the results obtained with the RDX method of specimens without thermal treatment (Fig. 5) and specimens treated at 200°C (Fig. 6), in addition to quartz (Q), larnite (L) and plagioclase (P), calcite (C) can be observed which is not present in specimens without thermal treatment.

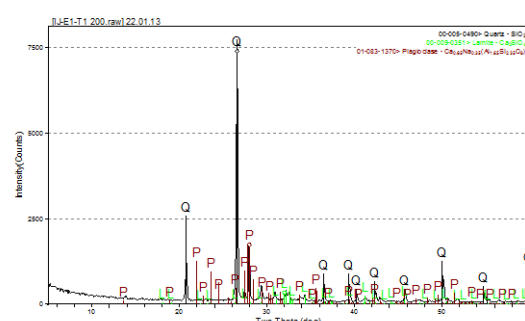


Figure 5. Results of X-ray analysis of specimens without thermal treatment

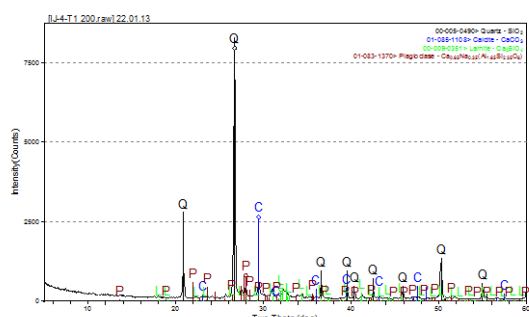


Figure 6. Results of X-ray analysis of specimens treated at 200°C

CONCLUSIONS

Thermal treatment at the temperature up to 250°C increases the compressive strength of concrete, especially in the early curing stage of the high strength concrete (compressive strength of 3/4 specimens without thermal treatment is 76.8 MPa, but it reaches 177.7 MPa or 231% of the compressive strength without thermal treatment after 4 hours of thermal treatment at 250°C); The treatment temperature exceeding 200°C creates irreversible changes in the structure of high strength concrete and has an impact on its properties, for example, water permeability (water permeability for the specimens after thermal treatment at 200°C

REFERENCES

- Behnood A., Ziari H. (2008) Effect of silica fume addition and water cement ratio on properties of high-strength concrete after exposure to high temperatures. *Cement & concrete composites*, Vol. 30, Issue 2, p. 106-112.
- Crosthwaite D. (2012) World Construction 2012 [online] [accessed on 08.01.2013.]. <http://www.davilangdon.com/EME/Research/ResearchFinder/OtherResearchPublications/World-Construction-2012/>
- Flower D., Sanjayan J. (2007) Green house gas emissions due to concrete manufacture. *The international Journal of life cycle assessment*, Vol. 12, Issue 5, p. 282-288.
- For Construction Pros.com (2011) Global Cement Consumption Expected to Reach New Highs [online] [accessed on 08.01.2013.] http://www.forconstructionpros.com/press_release/10366676/global-cement-consumption-expected-to-reach-new-highs
- Habert G., Arribe D., Debove T., Espinasse L., Le Roy R. (2012) Reducing environmental impact by increasing the strength of concrete: quantification of the improvement to concrete bridges. *Journal of Cleaner Production*, Vol. 35, p. 250-262.
- Mehta P.K., Monteiro P.J. (2006) *Concrete Microstructure, Properties, and Materials*, 3rd Edition. New York: The McGraw-Hill Companies. 669 p.
- Morsy M.S., Alsayed S.H., Aqel M. (2010) Effect of elevated temperature on mechanical properties and microstructure of silica flour concrete. *International journal of civil & environmental engineering*, Vol. 10, Issue 01, p. 1-6.

grows to 3 mm compared to 0 mm for the specimens without thermal treatment), while the compressive strength may not indicate it (the overall trend is increase of compressive strength according to the Fig. 2);

Using high strength concrete in the production of concrete elements thermal treatment at temperature up to 100°C might be a balanced solution taking into account the shorter period which is necessary to create constructions as well as minimise the negative impact on the concrete properties. Applying this temperature, it is possible to reach the same concrete compressive strength as after 58 days of curing;

Creating constructions from ,high strength concrete, it is necessary to pay attention to the fact that temperatures exceeding 250°C, for example, in the case of fire, increase the risk of spalling in the top layer of concrete.

ACKNOWLEDGMENT

The financial support of the Ministry of Education and Science of the Republic of Latvia and the ERAF project Nr. 2010/0286/2DP/2.1.1.0/10/APIA/VIAA/033 „High efficiency nanoconcretes” is acknowledged.

INFLUENCE OF POLYMERIC ADDITIVES ON THE PROPERTIES OF CONCRETE MANUFACTURED ON THE BASIS OF AGGREGATES PRODUCED FROM CRUSHED CONCRETE WASTE

Olga Finozenok*, Ramune Zurauskienė**, Rimvydas Zurauskas***, Linas Mikulenas***, Aleksandrs Korjakins* ***, Genadijs Shakhmenko** *

*,**,*** Vilnius Gediminas Technical University, Department of Building Materials

E-mail: *olga.finozenok@yahoo.com; **ramune.zurauskienė@vgtu.lt; ***linasmikulenas@gmail.com;

***Vilnius Gediminas Technical University, Department of Water Management

E-mail: ***rzuster@gmail.com

**** Riga Technical University, Faculty of Civil Engineering, Institute of Materials and Structures

E-mail: ****; ***gs@apollo.lv;

ABSTRACT

The research is devoted to the analysis of the influence of various polymeric additives on the properties of hardened concrete with aggregate made from concrete waste. The following materials were used during the research: coarse aggregate - crushed concrete waste, fine aggregate - natural sand with 0.1/0.5 mm fraction and crushed concrete waste with particles' size of 0.125–4 mm, composite Portland limestone cement, water and 4 polymeric additives. 9 compositions of concrete mixtures were produced: the reference mixture and 4 concrete mixtures prepared by adding 1 % and 2 % (of the cement mass) from each of the polymeric additives. During the calculation of concrete composition, the selected slumping class of the concrete mixture was S1, and compressive strength class of the hardened concrete – C25/30. The following parameters of concrete samples were determined during the research: density, compressive strength, bending strength, water absorption, structural properties. Forecasted performance frost resistance was calculated and frost resistance was determined, as well as the alkali corrosion of concrete samples was analysed.

Key words: concrete waste, recycled aggregate, vinyl acetate copolymer, frost resistance, alkali-reactivity

INTRODUCTION

Concrete is one of the oldest and widely employed materials, prepared from natural components, such as sand, breakstone, cement and water. Nearly all of these materials belong to the group of non-renewable natural resources. Therefore, in order to save natural resources, scientists look for the best methods to replace these resources with waste materials. Buildings' demolition waste can be utilized for the production of the concrete with low and average strength. Nowadays more and more old buildings are being rebuilt, repaired or demolished. Moreover, there are a lot of unfinished constructions throughout the world and frameworks of these constructions have to be demolished in the course of time. In many countries, demolition waste is transported to the landfills that occupy a lot of space. This type of waste does not decompose in landfills, does not emit gas, and is not used in the production cycle of energy resources. Therefore, scientists look for methods to decrease the amount of this waste and utilise it in the new products.

Nowadays, reinforced concrete constructions and concrete products are crushed at a building demolition site or in some special area, where the metal (used for reinforcement of reinforced concrete constructions) is separated and concrete is stored in separate stacks. In Lithuania, such concrete is used as a road pavement base, however it is not used for the manufacturing of any new

products. Currently, in various areas of the country, large amounts of crushed concrete are stored, and the demand for this concrete in road construction is lower than the amount of crushed concrete produced. The crushed concrete is stored at demolitions sites, some of which are located within the city boundaries (Figure 1). At some sites concrete is stored until the moment when higher growth of demand for this material is achieved. The storage period may even exceed one year.



Figure 1. Storage of crushed demolition waste in Vilnius city (where the building of the Lithuanian film production studio was earlier located)

Many researchers have analysed the influence of concrete waste on the properties of hardened cement concrete and came to the conclusion that the strength of such concrete decreases by approximately 30 % (Finoženok et al., 2011;

Richardson et al., 2010) while water absorption increases (Finoženok et al. 2010). During the previous analysis it was determined that in order to maintain concrete strength within the specified range, it is necessary to separate fine aggregate fractions, which size is smaller than 0.125 mm, from the crushed concrete and to add in addition 40 % fine sand with the particle size up to 1 mm (Finoženok et al., 2012).

Analysis developed by the scientists (Shehata et al., 2010) shows that reduction of the amount of fine aggregate, produced from concrete waste, should also result in the decrease of the expansion of concrete during vitriolic corrosion. The provided analysis shows that application of the finer fraction of the aggregate produced from concrete waste in concrete mixtures, results in larger expansions during the sample vitriolic corrosion.

There are practically no investigations of alkali corrosion of concretes made with the aggregate obtained from concrete waste. Therefore, this research is focused on investigation of the behavior of concrete produced by using concrete waste, in alkaline environment.

It is obvious that properly selected chemical additives can increase concrete strength, its frost resistance and improve rheological properties of concrete mixture. There are no special additives developed for the mixtures from crushed concrete waste. Each chemical additive in the cement system fulfills one or another task: modifies mixture viscosity, increases mixture diffusiveness and fluidity, prevents mixture lamination segregation, increases adhesion to the base material, etc. There are chemical element products that increase the adhesion of cement systems to the base material - polymeric additives in the base material: vinyl acetate copolymers. In accordance with the manufacturer's recommendations, these additives increase the adhesion of repaired concrete and reinforced concrete products to the repaired cement mixture, decrease humidity with saline CO₂ penetration through the hardened layers, as well as increase frost resistance. Therefore, vinyl acetate copolymers have been chosen for concrete mixtures with filler made from crushed concrete waste. It was assumed the additives should increase the adhesion of concrete pieces with cement paste and, possibly, change rheological properties of concrete mixtures.

This research was carried out with the aim to investigate the possibility of improving the properties of hardened concrete by using the selected polymeric additives when the concrete is produced by using crushed concrete waste.

MATERIALS AND METHODS

Research materials

Cement, coarse aggregate - crushed concrete waste, fine aggregate - sand and crushed concrete waste, and polymeric additives were used for the tests.

Cement: composite Portland limestone cement CEM II/A-L 42.5 N, satisfying the requirements of standard LST EN 197-1 "Cement. Part 1. Composition, technical requirements and conformity criteria of regular cements". Other properties of this cement are described in the article (Finoženok et al., 2011).

Coarse aggregate: 4/16 mm crushed concrete waste. Crushed concrete waste is obtained from crushing the internal partitions of multistorey large-panel buildings built in 1977-1990s. Coarse fractions were used as the coarse aggregate, and fine fractions were refined and used for the production of fine aggregate. Concrete compressive strength before crushing - 25 MPa. Water absorption of coarse aggregate produced from concrete waste reached 10.5 % after 3 minutes of soaking in water, and - 13 % after 48 hours of soaking. These properties were considered during selection of the composition of concrete mixture.

Fine aggregate: 0.1/0.5 mm natural sand and crushed concrete waste with 0.125/4 mm fractions. The crushed concrete waste was obtained by sieving the remaining particles after the coarse fractions were sorted out. The finest particles smaller than 0.125 mm were not used, because, these considerably decrease concrete strength (Finoženok et al., 2011). 60 % of sand (of the weight of fine aggregate) was added. This amount was selected proceeding from the earlier conducted research, which proved that such amount of sand with 1 mm particles makes it possible to prepare concrete with the intended properties from crushed concrete waste.

The main characteristics of coarse and fine aggregates are presented in Table 1.

Table 1
Characteristics of coarse and fine aggregates

Aggregate	Title and value of the parameter		
	Bulk density, g/cm ³	Particles density, g/cm ³	Hollow ness, %
4/16 mm crushed concrete waste	1.09	2.04	47
0.125/4 mm crushed concrete waste	1.21	2.56	53
0.1/0.5 mm sand	1.4	2.38	41

The granulometric composition of coarse aggregate, produced from crushed concrete waste, is shown in Figure 2, and the granulometric composition of fine aggregate from concrete waste used in the research - in Figure 3

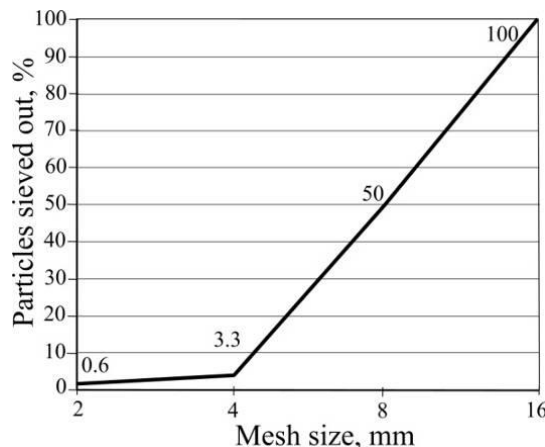


Figure 2. Granulometric composition curve of coarse aggregate from crushed concrete waste

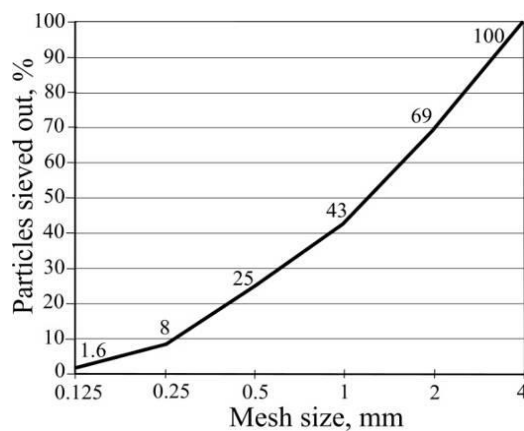


Figure 3. Granulometric composition curve of fine aggregate from crushed concrete waste

Additives: the following selection of polymeric additives were used: vinyl acetate copolymer (E), copolymer from vinyl acetate and ethylene with mineral additives and protective colloid (V5), copolymer from vinyl acetate and ethylene with higher vinylesters with mineral additives and protective colloid (V7), synthetic copolymer with a large molecular mass (R). All additives were in powder form, except for the last one, which was in a liquid state. The characteristics of the additives are presented in Table 2.

Table 2
Characteristics of polymeric additives

Marking of the additive	Title and value of the parameter		
	Bulk density, g/cm ³	Density, g/cm ³	pH
E	0.35–0.55	–	4–6
V5	0.38–0.48	–	7
V7	0.40–0.55	–	8
R	–	1.0	5–8

Liquid additive is used to modify the viscosity of concrete mixtures according to the manufacturer's recommendations. The mixture becomes less sensitive to water amount variations, and the recommended amount is 0.1–1.5 % with relation to the amount of fine particles (<0.125 mm) in the mixture.

Composition of the mixtures analysed

9 compositions of concrete mixtures were prepared: reference mixture K (containing no additives), and concrete mixtures prepared by adding 1 % and 2 % (by weight of cement mass) of one of the above listed additives. In mixture E (E1 and E2), 1 % and 2 % (by weight of cement mass) vinyl acetate copolymer was used; V5 (V51 and V52) – copolymer from vinyl acetate and ethylene with mineral additives and protective colloid; V7 (V71 and V72) – copolymer from vinyl acetate and ethylene with higher vinylesters with mineral additives and protective colloid; R (R1 and R2) – synthetic copolymer with a large molecular mass. For calculation of concrete composition, the selected slumping class of the concrete mixture was S1 according to LST EN 206-1 „Concrete - Part 1: Specification, performance, production and conformity“, and the compressive strength class of the hardened concrete – C25/30. The concrete composition was selected depending on the characteristics of raw materials, by implementing computational - experimental methodology and by using tables, diagrams and nomograms. The composition of concrete mixture is presented in Table 3.

Initially, the dry concrete components, such as cement, fine aggregates and coarse aggregate as well as powder additives, were mixed in dry conditions. After the mixing of dry components, water was poured and the concrete mixture was remixed until an even consistency was obtained. After mixing, the concrete mixture was left for 5 minutes, and remixed afterwards. This procedure was completed in compliance with the recommendations of the manufacturers of polymeric additives. The liquid polymeric additive initially was mixed in water, and later water was added to the dry components.

After the preparation of the mixture the slumping factor of the concrete mixture was verified according to LST EN 12350-2 "Testing of fresh concrete. Part 2. Slump test". Concrete was classified as belonging to slumping class S1. Although the used additives change the amount of water required for preparation of the cement paste of normal consistency, these additives did not change the concrete mixture consistency in concrete mixtures. Most likely, high water absorption of the aggregates used has the greatest influence during the initial stage.

The prepared concrete mixture of the required consistency was poured into the moulds. Samples were vibrated on a laboratory vibrating platform for approximately 1 min. Samples were cured in

accordance with LST EN 12390-2 "Testing of hardened concrete. Part 2. Making and curing specimens for strength tests".

Table 3
Compositions of concrete mixtures

Concrete marking	Cement, kg/m ³	Coarse aggregate, kg/m ³	Fine aggregate, kg/m ³		Additive, kg/m ³	Water, l/m ³	W/C
		Crushed concrete waste, 4/16mm	Fine sand, 0.1/0.5 mm	Crushed concrete waste, 0.125/4mm			
K	450	560	631	421	—	328	0.73
E1, V51, V71, R1	450	560	631	421	4.5	328	0.73
E2, V52, V72, R2	450	560	631	421	9	328	0.73

After 7 and 28 days of hardening, mechanical properties were determined. Other concrete samples after 28 days of hardening were dried out in a laboratory dryer, after that the physical as well as mechanical properties of the samples were determined.

Research methodology

The following parameters of concrete samples were determined during the research: density, compressive strength, bending strength, water absorption, structural properties. Predicted performance frost resistance was calculated and frost resistance as well as resistance against vitriolic corrosion were determined.

Density of the concrete samples was determined according to LST EN 12390-7 "Testing of hardened concrete. Part 7. Density of hardened concrete". Absorption of the concrete samples was established by soaking for 24, 48 and 72 hours in 20±1°C temperature water.

Bending strength of concrete samples was estimated after 7 and 28 days of hardening by testing the produced 40x40x160 mm prism-shaped samples. Compressive strength of the concrete was determined in accordance with LST EN 12390-3 "Testing of hardened concrete. Part 3. Compressive strength of test specimens" after 7 and 28 days of hardening. Samples were compressed by using the press "AUTOMAX 3000" in compliance with the requirements of LST EN 12390-4 "Testing of hardened concrete. Part 4".

The structural properties of concrete samples, such as effective porosity of concrete body, total open porosity, reserve of porous volume, qualified thickness of the wall of capillaries, the capillary rate of mass flow in a vacuum in the direction of freezing, the capillary rate of mass flow in a vacuum in a perpendicular direction of freezing, degree of structural inhomogeneity, capillary rate of mass flow, set under normal conditions, were determined

in accordance with the special methodology described in literature (Kičaitė et al., 2010; Mačiulaitis et al., 2007). These parameters were considered when the predicted performance frost resistance was calculated by the equations proposed in (Mačiulaitis et al., 2010).

Frost resistance of the samples was estimated in accordance with LST CEN/TS 12390-9:2006/P:2007 "Testing of hardened concrete - Part 9: Freeze-thaw resistance. Scaling". Testing was carried out in accordance with alternative CF/CDF test method considered in (Ceprūtis et al., 2012) where the authors studied the testing methodology and temperature variation curves.

Alkali-reactivity of the hardened formation masses was determined according to RILEM TC 219-ACS (Alkali-Aggregate Reactions in Concrete Structures) as AAR-2. 40x40x160 mm prism-shaped samples were prepared from the concrete mixture and hardened for 28 days according to LST EN 12390-2. After 28 days of hardening each element was measured and the main reference point for the prism length estimation was inserted. Prism-shaped samples were stored in 80 °C±2 °C temperature water for 24 hours. Afterwards, their initial (zero) reference length was measured. After the measurements the prism-shaped samples were soaked into 1M NaOH solution with 80 °C±2 °C temperature. In these conditions the prism-shaped samples were stored for 14 days. Length of the specimens was measured periodically.

RESULTS AND DISCUSSION

Resulting density values of the samples are provided in Figure 4. Density of all the batches of concrete mixtures is similar, results vary from 1.89 g/cm³ to 1.95 g/cm³.

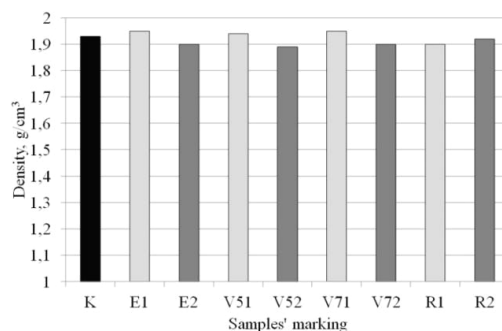


Figure 4. Density results of the samples

Compressive and bending strength of the concrete samples were determined after 7 and 28 days of hardening. The obtained results of compressive strength are shown in Figure 5, and the resulting values for bending strength - in Figure 6. It can be seen that highest results for compressive and bending strength are reached in the reference samples. When the analysed chemical additives are added to the concrete mixtures, compressive and bending strengths do not reach these values.

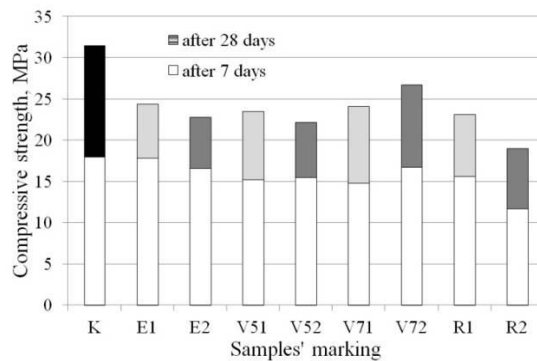


Figure 5. Results of estimation of sample compressive strength

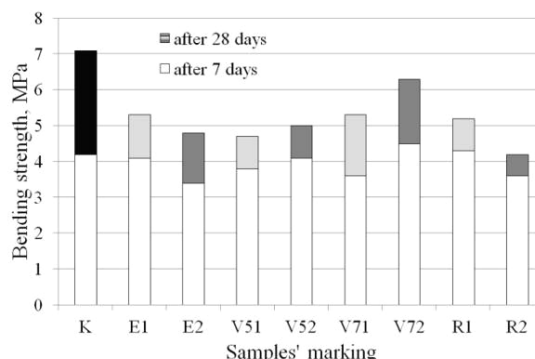


Figure 6. Results of estimation of sample bending strength

Results of the research show that after 7 days concrete with polymeric additives reached similar

strength values as the reference concrete. However, after 7 days of hardening, the strength growth rate in the samples with the additives decelerated, which produced a large effect on the final results of compressive and bending strengths. No samples with the additives had as large an increase of the strength value after 8-28 days of hardening as it was observed in the reference samples. It can be assumed that polymeric additives slow down the strength increase processes at a later stage.

Water absorption was determined after 24, 48 and 72 hours of soaking in water. The results for water absorption are shown in Figure 7. It can be noticed that when 1 % (by weight of the cement) of additives of vinyl acetate copolymer is added to the formation mass, the absorption rate in the samples (E1, V51, V71) decreases. By adding 2 % (by weight of the cement) of these additives, absorption of the samples (E2, V52) becomes higher than that of the reference samples (K). After three days of soaking in water absorption of all samples, except for V72 samples, changed insignificantly. A larger amount of V72 additive determines the period of water absorption in the samples. It is possible that, if the samples are soaked further, absorption of these samples would increase, and absorption of other samples would remain unchanged because they reach the absorption saturation limit in normal conditions. It is worth noting that values for the absorption of R1 and R2 samples after 72 hours of soaking, are very similar to that of the reference sample. Therefore, synthetic copolymer with a large molecular mass added to the formation mass does not change absorption of the samples.

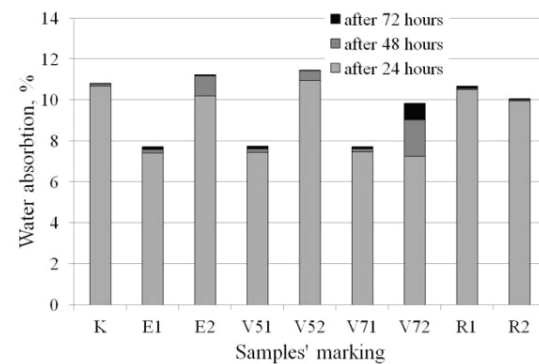


Figure 7. Results of estimation of sample absorption

The determined structural characteristics of the samples are shown in Table 4. Predicted performance frost resistance of the samples was calculated according to the structural characteristics presented in the table. According to the performed calculations E2 samples would have the highest frost resistance, R1, V72 and K samples - the lowest.

Table 4
Structural characteristics of the samples

Sample marking	W_e	W_r	R	D	N	g_1	G_1	G_2	FRE
K	20.8	22.0	6.50	4.30	3.55	0.25	0.35	0.82	13
E1	16.0	16.8	4.60	4.96	1.40	0.18	0.55	0.51	24
E2	21.2	23.2	8.35	3.32	3.40	0.40	0.44	1.08	32
V51	15.5	16.1	4.20	5.20	1.40	0.14	0.51	0.54	25
V52	22.0	24.3	9.45	3.11	6.50	0.38	0.42	0.96	19
V71	14.7	15.3	3.80	5.53	1.00	0.14	0.49	0.48	21
V72	18.1	19.8	8.90	4.04	2.70	0.18	0.34	0.81	14
R1	20.5	22.7	9.90	3.40	0.18	0.23	0.15	0.13	12
R2	19.4	21.5	10.0	3.65	0.18	0.27	0.18	0.27	20

Notes: W_e – effective porosity of concrete body, %; W_r – total open porosity, %; R – the reserve of porous volume, %; D – the qualified thickness of the wall of capillaries, units; G_1 – the capillary rate of mass flow in a vacuum in the direction of freezing, g/cm^2 ; G_2 – the capillary rate of mass flow in a vacuum in a perpendicular direction of freezing, g/cm^2 ; N – degree of structural inhomogeneity, units; g_1 – the capillary rate of mass flow, set under normal conditions, $\text{g}/\text{cm}^2 \cdot 0.5\text{h}$; FRE – forecasted exploitational frost resistance of the samples, in cycles.

Estimated results of frost resistance of the concrete are presented in Figure 8. In this figure the extent of mass losses during the testing of samples in accordance with the freeze-thaw cycle methodology can be seen. According to the alternative CF/CDF test method of testing methodology LST CEN/TS 12390-9:2006/P: 2007, the largest mass loss in one sample can reach 15 g. The results presented in Figure 8 show that mass loss did not exceed the acceptable limits in any of the samples. During the inspection of the samples after 28 testing cycles, the decision was made to continue tests because only small cracks were noticed in some samples. After 56 testing cycles full fragmentation of one sample (E1) was observed. Cracks developed in the following samples: in the two samples - E1 and V51, as well as in one sample V52. Other samples examined after 56 testing cycles had small cracks. The V71 and R1 samples showed the best results - the lowest mass loss and the smallest cracks.

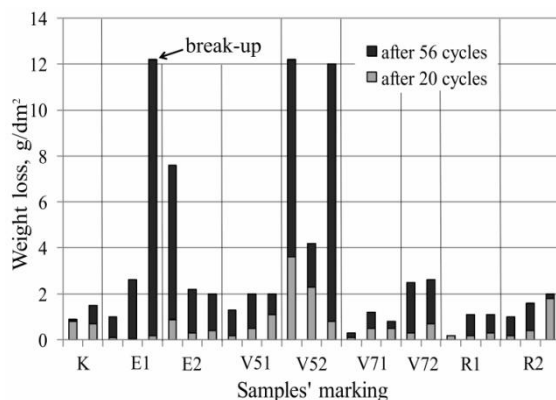


Figure 8. Results of the estimation of samples' frost resistance

Cracks and fractures after 56 testing cycles are clearly seen in Figure 9.



Figure 9. View of the samples V51 after 56 testing cycles

Given the results obtained during the frost resistance testing, V71 and R1 samples can be singled out as the most resistant to freeze-thaw cycles in aggressive conditions. In addition, R2 samples, as well as the reference samples K, can be marked as formation masses, which could be employed in the conditions of moderate aggressiveness.

Upon comparing the results in Table 4, showing predicted performance frost resistance of the samples and the results in Figure 8, it can be concluded that the forecast methodology cannot be used to clearly predict frost resistance results when samples are tested in accordance with the described experimental method. The authors (Nagrockienė et al., 2004) suppose that this prediction methodology is most suitable for the evaluation of frost resistance when samples are tested by applying the one side freeze-thaw method. However, as we can see from the results, this methodology cannot be used to predict frost resistance when CF/CDF testing methodology is applied.

Moreover, during the alkali corrosion the expansion of the samples prepared from the analysed mixtures

was determined. Expansion values of the samples after 28 days of investigation in an aggressive alkaline environment are shown in Figure 10. As seen in this figure, during testing V52, V71, V72, R2 samples did not reach the expansion limit. Expansion of R2 samples was minimal and reached only 0.02 %.

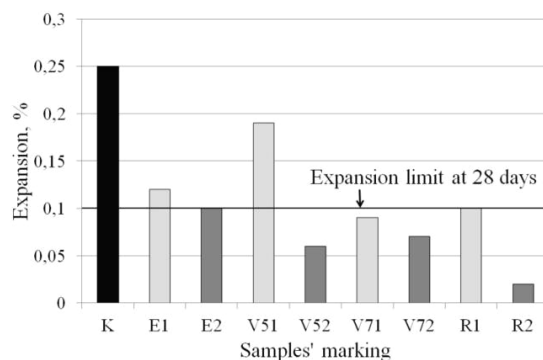


Figure 10. Expansion of the samples after 28 days

Expansion of the reference samples (K) and V7 series is presented in Figure 11.

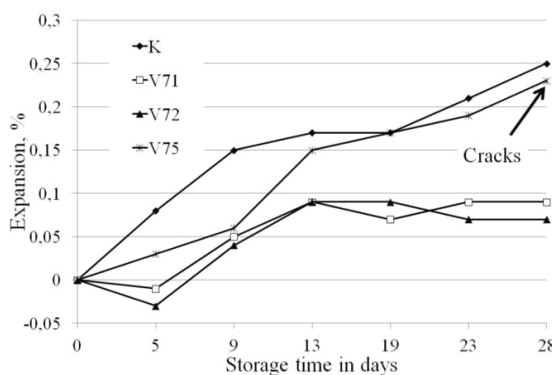


Figure 11. Results of the estimation of sample expansion

It can be observed that upon adding the copolymer additive from vinyl acetate and ethylene with higher vinylesters and mineral additives to the concrete mixture, sample expansion in aggressive alkaline environment does not exceed the defined limits. For comparison, the samples with 5 % (in relation to the cement mass) of this polymeric additive (V75) were prepared. It can be observed from the V75 curve in

Figure 11 that the larger amount of the additive influences the behaviour of the concrete in the aggressive environment, and expansion of the samples is similar to the one of the reference samples. Moreover, after 28 days of testing in the alkaline environment, not only expansion was observed in the above mentioned sample (V75), but also cracks appeared.

CONCLUSIONS

1. To conclude, it can be stated that the studied polymeric additives reduce the compressive and bending strength. However, sample density remains similar to the reference samples (prepared without additives).
2. The effect produced by additives on the water absorption parameter was also examined. The extent of influence depends on the amount of polymeric additive. By adding 1% (by cement mass) polymeric additives water absorption decreases to 25%. By adding 2% (by cement mass) polymeric additives water absorption increases and exceeds the absorption value of the reference mixture for vinyl acetate copolymer (E) and copolymer from vinyl acetate and ethylene with mineral additives and protective colloid (V5) by ~6%, at the same time, causing a decrease of water absorption by 5% as a result of using synthetic copolymer with large molecular mass (R).
3. CF/CDF testing methodology was employed to determine the frost resistance of concrete samples. The best results were observed in the samples, which had the following chemical additives (1 % of each): V7 – copolymer from vinyl acetate and ethylene with higher vinylesters with mineral additives and protective colloid R – synthetic copolymer with large molecular mass.
4. The examined polymeric additives influence the processes occurring in concrete samples during the alkali corrosion. Concrete expansion during alkali corrosion can be reduced when additives in question are added to the mixture. The lowest expansion of concrete samples during the study of alkali-reaction was achieved when the synthetic copolymer with a large molecular mass was added to the concrete mixture. However, this additive considerably reduced the strength properties of the prepared concrete.

REFERENCES

- Cepuritis R., Shakhmenko G. (2012) Frost durability of reinforced concrete research on effect of steel fibres. *International congress on durability of concrete. Selected Papers*.
- Finoženok O., Žurauskienė R., Žurauskas, R. (2010) Analysis of the physical-mechanical concrete properties when concrete waste additives are used in the mixtures. *The 10th International Conference Modern Building Materials, Structures and Techniques: selected papers*, Vol. 1, p. 64–70.

- Finoženok O., Žurauskienė R., Žurauskas, R. (2011) Influence of various size crushed concrete waste aggregate on characteristics of hardened concrete. *Civil Engineering'11: 3rd international scientific conference proceedings*, Vol. 3, p. 7-13.
- Finoženok O., Žurauskienė R., Žurauskas, R. (2012) Reprocessing of buildings' demolition waste and utilization for the manufacturing of new products. *Journal of Civil Engineering and architecture*, Vol. 6, p. 1230-1239.
- Kičaitė A., Malaiškienė J., Mačiulaitis R., Kudabienė G. (2010) The analysis of structural and deformational parameters of building ceramics from Dysna clay. *The 10th International Conference Modern Building Materials, Structures and Techniques: selected papers*, Vol. 1, p. 143–148.
- Mačiulaitis R., Malaiškienė J. (2010) Frost Resistant Porous Ceramics. *Materials Science*, Vol. 16, No. 4, p. 359-364.
- Mačiulaitis R., Žurauskienė R. (2007) *Low Porosity Building Ceramics Produced from Local Technogenic Raw Materials*. Vilnius, Technical. 220 p.
- Nagrockienė D., Kičaitė A., Mačiulaitis R. (2004) Possibilities to Forecast the Frost Resistance of Constructional Concrete. *The 8th International Conference “Modern Building Materials, Structures and Techniques”. Selected Papers*, p. 120 – 123.
- Richardson A., Allain P., Veuille M. (2010) Concrete with crushed, graded and washed recycled construction demolition waste as a coarse aggregate replacement. *Structural Survey*, Vol. 28 No. p. 142-148.
- Shehata M. H., Christidis Ch., Mikhaiela W., Rogers Ch., Lachemia M. (2010) Reactivity of reclaimed concrete aggregate produced from concrete affected by alkali–silica reaction. *Cement and Concrete Research*, Vol. 40, Issue 4, p. 575–582.

THE ECONOMIC AND ENVIRONMENTAL BENEFITS FROM INCORPORATION OF COAL BOTTOM ASH IN CONCRETE

Girts Bumanis*, Diana Bajare**, Aleksandrs Korjakins***

Riga Technical University, Institute of Materials and Structures,

Professors Group of Building Materials and Products

E-mail: *Girts.Bumanis@rtu.lv, **Diana.Bajare@rtu.lv, ***Alex@latnet.lv

ABSTRACT

Coal is a fossil fuel and an important natural resource. Combustion of coal provides high energy production. Total coal production in 2011 was 7678 Mt and lignite production was 1041 Mt. Coal provides 30.3% of the total world primary energy demand and 42% of the world's electricity is produced from the combustion of coal. Coal production will continue to increase and in the 2030's 44% of the world's electricity will be produced from coal (from Data courtesy). Coal combustion is provided in thermal power plants. A significant amount of coal ash is produced burning coal and utilization of ash is an important issue in the world. The sustainable utilization of coal ash could improve production efficiency, reduce production costs and diminish waste product disposal problems.

In this research coal combustion product – coal bottom ash - was investigated regarding its application as a micro filler in conventional concrete production. Coal bottom ash was taken from a local boiler house in Latvia and preliminary processing of coal bottom ash was done. Coal bottom ash was ground for 15, 30 and 45 minutes respectively. The grading analysis of obtained microfiller was done with standard sieves and grading curves were obtained. Scanning electron micrographs were obtained and energy-dispersive X-ray spectroscopy was performed.

In the current study, conventional concrete mixture with the cement amount of 350kg/m³ and W/C 0.61 was chosen to integrate it with coal bottom ash as a microfiller. The integration ratio of microfiller was chosen 10, 20, 30 and 40% by the mass of cement for each type of prepared coal bottom ashes. Reference concrete mixture consisted of 0% coal bottom ash. The concrete workability was kept constant for all mixtures and the chosen cone slump class was S4 (160-210mm). Fresh and hardened concrete properties were obtained. Compressive strength was determined at the age of 7, 14 and 28 days.

Processed coal bottom ash could be used as a microfiller for conventional concrete production. Higher concrete strength class with the same amount of cement could bring economic benefit up to 3.6%. By incorporation of coal bottom ash in concrete environmental benefits could be achieved due to reduced cement consumption and effective disposal of coal bottom ash. The integration level of coal bottom ash could not exceed 30% by the mass of cement. At low rates of incorporation (<20%) coal bottom ash provides the same W/C for concrete and fresh concrete density increases. Mechanical and physical properties of concrete can be improved by choosing appropriate amount of coal bottom ash microfiller.

Key words: concrete, coal bottom ash, microfiller, environmental and economic benefit.

INTRODUCTION

Burning of coal generates a significant amount of coal combustion products (CCPs), especially in the countries where large quantities of low quality coal is used in thermal power plants; therefore coal ash recycling is an important environmental issue in the EU. Total production of CCPs is estimated to be more than 100 million tonnes annually in the EU 27 (ECCPA, 2011). CCPs endanger the environment if they are deposited without taking measures to reduce environment pollution. However, the overall situation is quite positive, because at least half of the coal ash is recycled in many developed countries. The CCPs are mainly utilised in the building material industry, in civil engineering, in road construction, for construction work in underground coal mining as well as for recultivation and restoration purposes in open cast mines (ECCPA, 2011). As coal is not among the natural resources available in Latvia and it has to be

imported from the neighbouring countries for energy production purposes, it constitutes only 2.2 % from the total amount of primary energy resources compared to the overall indicators in the world (Ministry of Economics, 2011). However, coal burning in Latvia generates a significant amount of waste in the form of coal ash, which could cause serious environment pollution problems on a local scale.

Industry development in the local, national regional and the EU level is determined not only by the interests of companies operating in the respective industry, but also by the planning documents at multiple levels. The EU energy policy aims to ensure environmentally friendly energy production and use, and also to reduce energy delivery risks.

One of the problems is collecting, storage and recycling of waste generated in power and heating plants. In order to coordinate the reduction of industrial pollution among the EU member states

more effectively, Council Directive 96/61/EC of 24 September 1996 concerning integrated pollution prevention and control was adopted aiming to achieve an integrated prevention and control of pollution arising from the activities listed in the directive. It lays down measures designed to prevent or, where it is not practical, to reduce emissions in the air, water and land (Council directive, 1996).

Integrated approach regarding environment pollution prevention and control is an important step towards legislation improvement. The above mentioned directive also concerns energy generation installations. According to the Council Directive 96/61/EC the national Law on Pollution was developed which came into force as of 1 July 2001 identifying the order of a gradual transition to the integrated environment pollution prevention and control.

As generation of waste is an integral part of the production process, it is necessary to coordinate proper waste management. Waste management in Latvia at the moment concerns building up the legal basis according to the basic principles of waste management in the EU, creation of an infrastructure for both municipal and industrial waste as well as implementation of legal provisions.

By burning solid fuel in furnaces at around 1700 – 1900 on the Kelvin scale, thermal power plants generate tons of solid mineral waste in the form of bottom ash and fly ash. Modern thermal power plants use pulverized coal. Bottom ash is formed from the completely melted and partially melted ash particles inside the furnace and fall through open grates to an ash hopper at the bottom of the furnace. Bottom ash particle size is 1 to 50 mm. Two types of ashes are formed in the process of pulverized coal burning: bottom ash that fall through open grates to the bottom of the furnace and fly ash that rise with the flue gas and can be collected by flue gas purification. The chemical composition of ash may vary significantly. It may contain SiO_2 47.5-57.32 %, Al_2O_3 19.00-30.22 %, CaO 2.53-28.75 %, Na_2O 0.9-1.22 %. The chemical composition depends on the coal mining area, their quality as well as the combustion process (We Energies, 2003). According to X-ray structural analysis the majority of ashes consist of quartz, anhydrite, calcium oxide together with iron and aluminium oxides (dicalcium silicate, tetracalcium aluminoferrite, calcium aluminates, calcium ferrites). These compounds are followed by glass phase, hematites and admixtures as well as CaO and MgO (Zakharova, 2008).

Several applications are found for coal combustion products. However, huge quantities of the coal combustion products are still deposited in waste sites. Recycling of the coal combustion residuals could bring an economic benefit to some of the production industries and contribute to

environmental quality improvement. Use of coal ash leads to the economizing of natural resources as well as diminishing of costs associated with the storage and depositing of coal combustion waste. By using 30 million tons of coal combustion products, 620 million US dollars as well as an area of 1.416 km² necessary for the depositing of coal combustion products can be spared. Finding a useful application for the above mentioned amount of coal combustion products can bring a profit of 150 million US dollars, raising the total benefit to 770 million US dollars. (Data courtesy, 2001).

The angular form of coal ash particles allows using it as an anti-slip substance on driveways covered with snow and ice. As the coal combustion ashes do not have distinct pozzolanic properties and spheric form as do the electrofilter ashes (fly ashes), they latter are more often used as a partial replacement of cement in concrete mixes. However, coal ashes often are used to replace the traditional fillers in concrete mixes, asphalt concrete and the production of concrete blocks. Often they are used in cement production as flux and for clinker production, also as mineral additives in several commercial products and replacement for sand with wide possible application (Data courtesy, 2001).

There are several researches performed on the use of coal ash as a filler in traditional concrete. As it comprises large amount of carbon from partially burned coal, coal ashes are rinsed in separate cases. It allows to obtain ashes with a lower carbon level, but their production costs raise significantly (Mohd Sani et al., 2010). By using rinsed coal ash to replace 30% of sand in concrete, improved mechanical properties were obtained. Other researches show (Data courtesy, 2001), that washing or rinsing of coal ashes can have a negative impact on the mechanical properties of concrete, because in the rinsing process small particles rinse out thus weakening the bond between hydrated cement paste and filler. The rinsing process lowers effectiveness of coal ash as a pozzolanic additive, because usually the particles are small and can be rinsed out. In addition, researchers explain it with the properties of pozzolanic materials – pozzolanic materials react with calcium hydroxide in the presence of water and form calcium silicate hydrates. After reacting with rinsing water the activity of coal ash may decrease significantly. In addition, water may impact the transformation of chemical elements to the heavy metals thus having an important impact on the physical properties of concrete. For this reason it is essential to determine whether processing of coal ashes by rinsing is necessary, because it decreases their effectiveness. Coal ashes have been used as a replacement for cement concluding that concrete containing coal ashes show higher mechanical properties in the later stages of curing. Possibly, it can be observed due to the pozzolanic reactions provoked by coal ashes

(Cherif et al., 1999; Garboczi, Bentz, 1991). After long-term curing (90 days) compressive strength of the specimens containing coal ashes exceeds the compressive strength of the reference mix.

Consulting with scientific literature sources, it has been decided not to include rinsing of coal ashes in this research to avoid the weakening of coal ash pozzolanic properties. In the framework of scientific research coal bottom ash was used as a micro and pozzolanic additive in order to improve the physical and mechanical properties of the concrete. Coal bottom ash was ground in a planetary ball mill for 15, 30 and 45 minutes before use. The prepared ashes were integrated into the concrete replacing 0; 10; 20; 30 and 40% of cement mass.

MATERIALS AND METHODS

Coal bottom ash

Coal bottom ash was obtained from burning coal in a thermal power plant. The obtained coal bottom ash was homogenised by grinding it in the planetary ball mill for 15, 30 and 45 minutes before use in the concrete preparation. Density of the homogenised coal bottom ash is 2.47 g/cm^3 , which corresponds to the reference data taken from the literature ranging from $1.86\text{-}2.7 \text{ g/cm}^3$ (Federal Highway Administration, 2011; Shah et al. 2005).

From the results of particle size distribution analysis the impact of the grinding period on the particle size distribution of coal bottom ash is clearly visible. Coal bottom ash with a grinding period 15 minutes is coarser than others with longer grinding periods. Amount of particles with the size smaller than 0.125 mm constitute only 47.4%, by extending the grinding period up to 30 minutes the amount of smaller particles increases to 51.5% and up to 45 minutes – to > 74.9 %. Coal bottom ash with a grinding period of 15 minutes is coarser making their particle size distribution similar to particle size distribution of traditional fine sand. By extending the grinding period, the amount of smaller particles increases, which can raise the activity of coal bottom ash during the concrete curing process, because the specific surface area increases and the surface interaction with the hydrated cement paste intensifies. In the particle size distribution of coal bottom ash ground for a shorter period (15 minutes) particles that exceed size of 0.25 mm are observed and they constitute 36.4%. It may have a positive impact on the particle size distribution in concrete by ensuring optimal particle packing. Particle size distribution for coal bottom ash and traditional fillers is given in Figure 1.

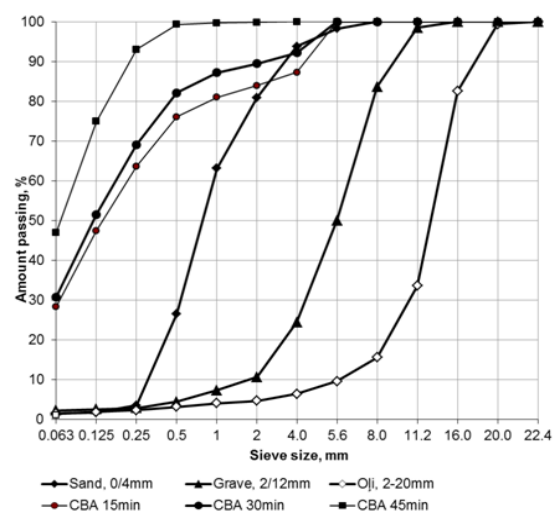


Figure 1. Particle size distribution of ground coal bottom ash and fillers used in concrete production

SEM scanning of coal bottom ash ground for 15, 30 and 45 minutes

The obtained coal bottom ashes from a grinding period of 15, 30 and 45 minutes were scanned by a SEM in order to determine structure of particles and their size. In the SEM it is possible to observe the ash surface as well as the evenness of particle distribution for ash with a different grinding period and to determine the particle size. Particles of coal bottom ash from a grinding period of 15 minutes are presented in Figure 2, particles from a grinding period 30 minutes magnified 10000 times – in Figure 3. Size of the bigger particles is $73.92 \mu\text{m}$ with a grinding period of 15 minutes and it decreases to $1\text{-}3 \mu\text{m}$ after a grinding period of 30 minutes. In addition, regardless of the grinding period, some of the particles are significantly larger compared to the overall particle size. These particles are harder and are not reduced to smaller pieces during the grinding process.

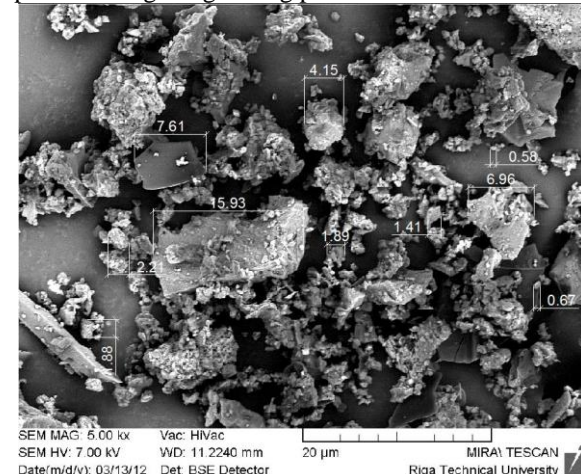


Figure 2. SEM image of coal bottom ash ground for 15 minutes

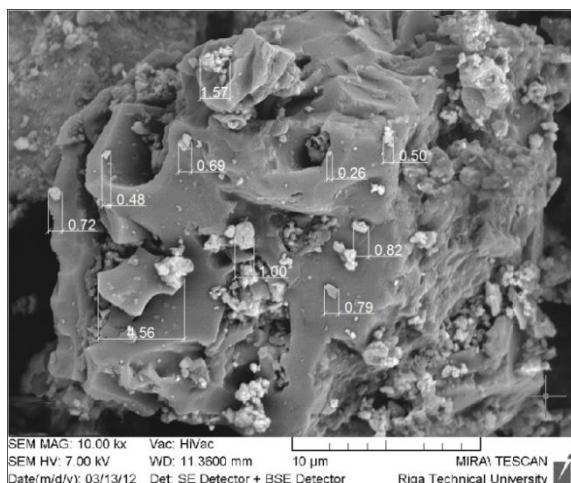


Figure 3. SEM image of coal bottom ash ground for 30 minutes

The ash particles mainly have an angular form. A lot of finer particles can be observed on the surface of larger particles, which have the appearance of metallic lustre and could be the metals present in the coal bottom ash. Larger particles could be partially burned pieces of coal according to literature sources (Pollocka et al., 2000; Karayigita et al., 2000). Additional EDX analysis is necessary in order to determine the elements present in the particles more precisely.

EDX analysis

EDX analysis was performed in order to determine the elements present in the coal bottom ash. It may consist of 88.78% carbon (C) and 10.44% oxygen (O), indicating presence of coal pieces which are not burned or burned partially. Presence of metallic elements were detected in separate locations. In most cases it is aluminium – 3.23 - 10.77%; silica with 3.41 - 11.49 % and calcium with 7.42 % are detected as well. Results are given in Table 1.

Table 1
Distribution of elements in typical locations of coal bottom ash

Elements, atomic weigh,%	EDX analysis location		
	Spectrum 1	Spectrum 2	Spectrum 3
C	88.78	23.63	34.36
O	10.44	54.1	49.82
Mg	0.22	-	1.26
Al	0.13	10.77	3.26
Si	-	11.49	3.41
S	0.26	-	0.18
Ca	0.17	-	7.42
Fe	-	-	0.3

Preparation of concrete mixtures

Concrete mix composition of traditional pumpable concrete was chosen with the mechanical properties meeting the demands of concrete technologists and civil engineers. Reference mix consists of a cement amount of 350 kg/m³, gravel fraction 2/12 mm and 5/20 mm – 500 kg/m³ of each fraction, sand 0/4 mm – 750 kg/m³. The reference W/C ratio was 0.61. Coal bottom ash (with a grinding period of 15, 30 and 45 minutes) was added to the concrete mix replacing 10, 20, 30 and 40 % of the cement mass. Concrete mix compositions with various amounts of coal bottom ash and W/C ratio are given in Table 2. Water to the concrete mix compositions consisting of coal bottom ash was added according to the cone slump class of S4, which range from 160 – 210 mm. The added coal bottom ash may improve the concrete flow and reduce W/C ratio or increase W/C ratio depending on the amount of coal bottom ash added and their particle size distribution. As it can be seen in Table 2, adding 10% of coal bottom ash with a grinding period of 15 minutes does not increase the necessary W/C ratio in order to ensure the initial cone slump class, but increasing the amount of added coal bottom ash to 40% increases the W/C ratio up to 0.69. 10% of coal bottom ash with a grinding period of 30 minutes reduces the necessary amount of water and therefore the W/C ratio to 0.60, while adding 40% of the same coal bottom ash increases it slightly to 0.62. 10% of coal bottom ash with a grinding period of 45 minutes reduces the W/C ratio significantly to 0.58, but the larger amount of the coal bottom ash increases it to 0.63.

A gravity type concrete mixer was used for the concrete mixes. Initially the dry components were measured and put into the mixer. The dry components were mixed for 1.5 minutes in order to obtain a homogenous dry concrete mix. Water was added in two steps. At first 70% of the water was added to the mix and it was mixed for 1.5 minutes. Then the rest of the water was added and the concrete was mixed for an additional 1.5 minutes. If the concrete consistency (workability) still did not correspond to the initial demands, an extra amount of water was added, and the concrete was mixed for an additional 1 minute and its consistency was checked repeatedly. Fresh concrete was moulded into standard size moulds of 100x100x100 mm. Half of the mould was filled with fresh concrete mix, and then it was put on a vibrating table for 5 seconds in the intensive mode. Finally, the rest of the fresh concrete mix was added into the mould and it was put on the vibrating table for another 10 seconds in the intensive mode.

Testing methods

Testing of concrete workability was performed according to the standard LVS EN 12350-2:2009 Testing fresh concrete - Part 2: Slump-test. For the

purposes of this research traditional concrete with the cone slump class of S4 was prepared. Cone slump (LVS EN 12350-2) and bulk density of fresh concrete was determined.

Compressive strength of concrete was determined according to the standard LVS EN 12390-3:2009 Testing hardened concrete - Part 3: Compressive strength of test specimens. Compressive strength was determined for the specimens sized 100x100x100 mm. Compressive strength of concrete was tested after an initial curing period of 7 and 14 days after a standard curing period of 28 days. Depth of penetration of water was tested according to the standard LVS EN 12390-8:2009 Testing hardened concrete - Part 8: Depth of penetration of water under pressure. Concrete specimens with the dimensions of at least 100x100x100 mm were tested under a pressure of 500 KPa for 72±2 h.

RESULTS AND DISCUSSION

Fresh concrete properties

Fresh concrete properties were tested in the process of concrete preparation. Reference consistency and workability demands were set for each of the concrete mixes. The amount of water added and cone slump varied depending on the amount of coal bottom ash added and their grinding period. Data on the cone slump is given in Table 3. For the concrete without coal bottom ash added cone slump is 180 mm and W/C ratio 0.61. Adding coal bottom ash with a grinding period of 15 minutes, the concrete workability decreases; by replacing 10% of cement with coal bottom ash without increasing W/C ratio, the cone slump decreased to 170 mm. Replacing up to 40% of cement with coal bottom ash it was necessary to increase the W/C ratio up to 0.69 in order to maintain the minimum cone slump. The workability of concrete improved by replacing 10% of the cement with coal bottom ash with a grinding period of 30 minutes – cone slump 165 mm with W/C ratio 0.62 was obtained. By increasing the amount of coal bottom ash up to 20%, W/C ratio remained 0.61; while cone slump decreased to 170 and 165 mm. Replacing 40% of the cement with coal bottom ash cone slump 165 mm with W/C ratio 0.62 was obtained. 10% of coal bottom ash with a grinding period of 45 minutes showed lower W/C ratio – 0.58 – and maintained the previous cone slump of 180 mm. However, further increase of coal bottom ash amount did not improve properties of fresh concrete; replacing 30% of cement W/C ratio 0.63 was necessary to ensure a cone slump of 160 mm. 40% of coal bottom ash resulted in a cone slump of 170 mm with W/C ratio 0.63.

Table 3
Cone slump of concrete mix

Cone slump, mm	CBA in concrete				
	REF	10%	20%	30%	40%
CBA15	180	170	160	160	170
CBA30	180	195	170	165	165
CBA45	180	180	180	160	170

Hardened concrete properties

Compressive strength of hardened concrete was determined. The results are given in Figure 4. Compressive strength of 7 days old concrete specimens reached 33-41 MPa depending on the amount of coal bottom ash added. Reference mix without coal bottom ash showed 38 MPa compressive strength. Coal bottom ash with a grinding period of 15 minutes replacing 10, 30 and 40% of cement decreased the compressive strength after initial curing period to 36, 37 and 33MPa respectively, but replacing 20% of cement slightly increased it to 39 MPa. Coal bottom ash with a grinding period of 30 minutes showed compressive strength 38 MPa that was equal to the reference mix. Coal bottom ash with a grinding period of 45 minutes showed the best results after 7 days of curing; replacing 10, 20 and 30% of the cement compressive strength increased to 41, 38 and 39 MPa, but replacing 40% of cement it decreased to 37 MPa. Compressive strength of 14 days old concrete specimens reached 42-47 MPa. Compressive strength slightly decreased in general. Reference mix showed compressive strength 45 MPa. Coal bottom ash with a grinding period of 15 minutes replacing 10-40% of cement showed slightly lower compressive strength – amount 10 - 30% showed 44 MPa and amount 40 % - 42 MPa. Coal bottom ash with a grinding period of 30 minutes showed equivalent results and 20-40% of coal bottom ash added increased the compressive strength of specimens exceeding the reference mix with 45; 47 and 47 MPa respectively, 10% ensured a compressive strength of 44 MPa. Coal bottom ash with a grinding period of 45 minutes showed a compressive strength of 43-45 MPa after 7 days of curing.

The lowest the compressive strength was observed for concrete specimens with 40% of cement replaced by coal bottom ash. Compressive strength after 28 days of curing is used to determine the concrete strength class. The compressive strength of the reference mix increased very slightly reaching 47 MPa. Mixes with the coal bottom ash with a grinding period of 15 minutes showed equivalent results to those of the reference mix; by increasing the amount of coal bottom ash to 30% the compressive strength reached 48, 50 and 51 MPa respectively, by 40% it remained at 47 MPa. Mixes with the coal bottom ash with a grinding period of 30 minutes showed a higher compressive strength

of 53 - 54 MPa. However, mixes with the coal bottom ash with a grinding period of 45 minutes showed the highest compressive strength of 54 – 57 MPa. It was rising by increasing the amount of coal

bottom ash up to 30%, where it slightly decreased to 55 MPa.

Concrete mixture composition

	kg/m ³				
	REF	10%	20%	30%	40%
Portland cement Kunda CEM I 42.5 N	350	350	350	350	350
Gravel 5/20	500	500	500	500	500
Gravel 2/12	500	500	500	500	500
Sand0/4	750	750	750	750	750
Coal bottom ash	0	35	70	105	140
REF W/C	0.61	-	-	-	-
CBA 15min W/C	-	0.61	0.62	0.65	0.69
CBA 30min W/C	-	0.60	0.61	0.61	0.62
CBA 45min W/C	-	0.58	0.61	0.63	0.63

Taking into account the compressive strength results after 28 days of curing it is possible to conclude that the reference mix with a compressive strength of 47 MPa corresponds to the concrete strength class C30/37 with a guaranteed compressive strength of cube 37 MPa. The next concrete strength class C35/45 demands a compressive strength of cube 45 MPa, which is difficult to ensure with a compressive strength of 47 MPa. Concrete specimens with coal bottom ash with a grinding period of 15 minutes showed a compressive strength of 47-51 MPa, which corresponds to the concrete strength class C30/37 and specimens with 30% of coal bottom ash were closer to the concrete strength class C35/45 with 51 MPa exceeding the necessary 45 MPa. Concrete specimens with the coal bottom ash with a grinding period of 30 minutes reached 49-54 MPa, which is closer to the concrete strength class C35/45. Specimens with 10, 20 and 40% of coal bottom ash and compressive strength 53 - 54 MPa correspond to the strength class C35/45 already having a strength reserve and can be compared to the next strength class of C40/50 with the guaranteed compressive strength of cube 50 MPa.

Water permeability, splitting strength, water absorbtion

Water permeability or depth of water penetration in concrete specimens was tested after 28 days. Water absorbtion and tensile splitting strength was tested as well. Results of water absorbtion, water permeability and splitting strength are given in Table 4. Depth of water penetration for concrete reference mix specimen is 28 mm, other specimens with various amounts of coal bottom ash and

grinding periods were compared to it. Depth of water penetration for concrete mix with 10% of coal bottom ash with a grinding period of 15 minutes showed the maximum depth of water penetration 30 mm. 20% of coal bottom ash decreased it to 14 mm, but 30 and 40% of coal bottom ash increased depth of water penetration to 25 mm un 32 mm respectively. Coal bottom ash with a grinding period of 30 minutes diminished depth of water penetration significantly. The lowest depth of water penetration was observed for 20% of coal bottom ash – 10 mm and for 30% of coal bottom ash – 12 mm.

Table 4
Results of water absorbtion, water permeability and splitting strength

Mixture design	Depth of water penetrat- ion, mm	Splitting tensile strength, MPa	Water absorbtion, %
ET	28	2	6.1
CBA15/10	30	2	5.7
CBA15/20	14	2	5.7
CBA15/30	25	2	5.7
CBA15/40	32	2	6.2
CBA30/10	20	2	6.2
CBA30/20	10	2	6.1
CBA30/30	12	2	5.8
CBA30/40	18	2	6.1
CBA45/10	42	2	5.0
CBA45/20	18	2	4.9
CBA45/30	23	2	4.6
CBA45/40	16	2	4.7

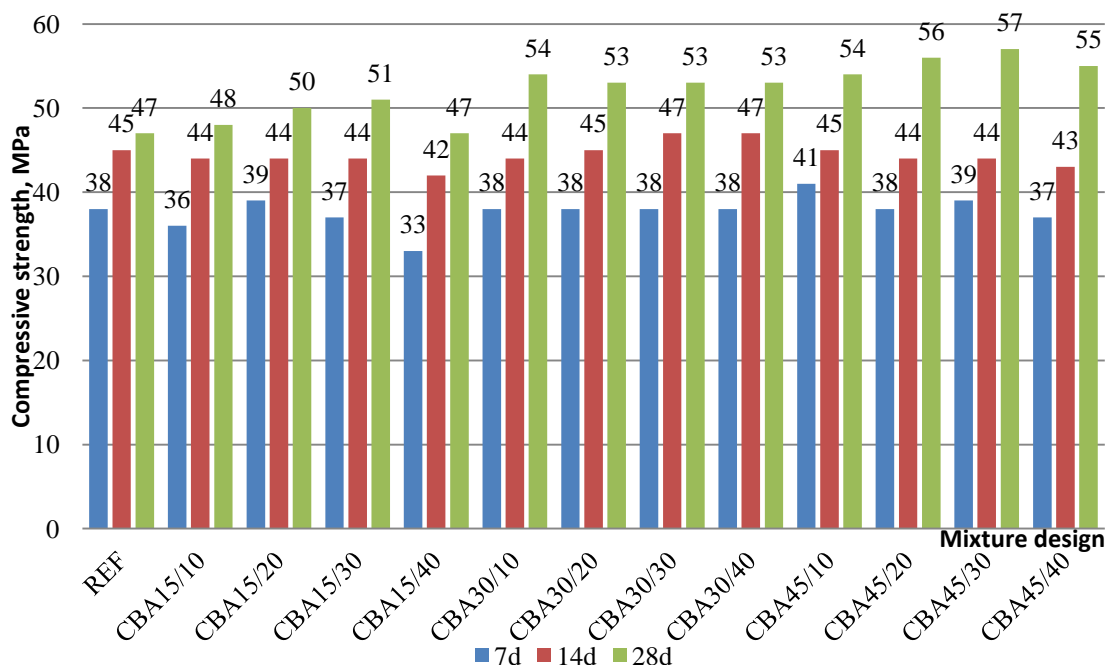


Figure 4. Concrete compressive strength after 7; 14; 28 days

For 10% of coal bottom ash it was 20 mm and for 40% of coal bottom ash – 18 mm. The highest depth of water penetration was observed for coal bottom ash with a grinding period of 45 minutes and replacing 10% of cement with it - 42 mm, replacing 20% of cement it decreased significantly to 18 mm and replacing 30 and 40% of cement it was 23 mm and 16 mm respectively.

In order to test the water absorbtion the concrete specimens were immersed in water for 72 hours. The excess water was wiped off afterwards and specimens were weighted. Finally, the specimens were dried and weighted. The concrete reference mix specimen showed water absorbtion rate of 6.1%. Coal bottom ash with a grinding period of 45 minutes added up to 30% lowered the water absorbtion rate to 5.7%, but 40% raised it to 6.2%. Coal bottom ash with a grinding period of 30 minutes showed water absorbtion rate to 6.2% by replacing 10% of cement with it. By increasing the amount of coal bottom ash up to 30%, the water absorbtion rate was 6.1 and 5.8% respectively, by 40% it slightly increased to 6.1% which corresponds to the water absorbtion rate of reference mix. Coal bottom ash with a grinding period of 45 minutes lowered the water absorbtion rate significantly compared with the results of the reference mix. Even replacing 10% of cement with it the water absorbtion rate was 5.0% and decreased up to 30% showing water absorbtion rate 4.9 % and 4.6 %. Replacing 40% of cement water absorbtion rate slightly increased to 4.7%.

Tensile splitting strength of concrete specimens was tested as well. As it is shown in the Table 4, it is 2

MPa and does not change adding various amounts of coal bottom ash with different grinding period.

Economic and ecological benefits

Economic substantiation of using ground coal bottom ash as a concrete micro additive is necessary for utilization of ash in the concrete industry to be cost effective. The economic benefit should be reasonable as recycling of coal bottom ash in concrete micro additives demands certain investments. Coal bottom ash recycling includes transportation costs from heating plants and costs related to the grinding of coal bottom ash for fixed period of time to obtain the necessary fineness. As transportation costs occur by transporting the natural resources for the concrete production as well, it can be assumed that this price formation factor is equal with the delivery of raw material to the concrete plant. Grinding is one of the most energy-intensive processes related to the ash preparation for use in concrete production. Ash grinding for industrial use is similar to the cement clinker grinding. As the fineness of clinker and ash is similar, energy and costs of ash grinding will be equivalent to the power-intensity and costs of cement grinding. Output data for energy and costs of ash grinding will be assumed equivalent to those of cement clinker grinding.

The grinding process is an important stage both in cement production and ash processing for their use in concrete production. Considerable amount of CO₂ is generated in cement production process. Cement production industry generates 5% of the total amount of CO₂ emissions. Cement production generates 222 kg of CO₂ in average on 1 ton of

cement produced (Jankovic, Valery, 2004). Energy consumed by mills in the cement grinding process generates 50 kg of CO₂ in average on 1 ton of cement produced (50 kg CO₂/t) (Research profile letter, 2011). An equivalent amount of CO₂ would be generated in the process of ash grinding as well. Cement production industry consumes 110 kWh of electricity to produce 1 ton of Portland cement. Around 40% of the energy necessary for 1 ton Portland cement production is consumed for clinker grinding (Jankovic, Valery, 2004). The current standard that allows estimating energy consumption in the grinding process is specified with the empiric formula which is based on cement specific surface area (Blein method) and specific energy consumption for grinding. A relation is discovered experimentally that defines energy consumption according to the specific surface area (cement fineness). It can be observed that cement consists of two components which demand different energy consumption in order to obtain equivalent fineness. Consequently ~47 kWh of energy is necessary for producing 1 ton of cement with specific surface area 450 m²/kg (Research profile letter).

Economic benefit

Ecological and economic benefits were determined for the concrete mix with the highest compressive strength, where 30% of coal bottom ash with grinding period 45 minutes were added, which is 105 kg/m³ of coal bottom ash in the concrete. The highest compressive strength was chosen, because this is one of the most important concrete properties and the choice of concrete is based mainly on the strength class of concrete. Economic benefit can be determined by the strength class and current market price of concrete. Reference mix with 0% of coal bottom ash has the compressive strength class C30/37 with compressive strength of cube 47 MPa. The concrete mix with where 30% of coal bottom ash with a grinding period of 45 minutes were added has compressive strength class C40/50 with

compressive strength of cube 57 MPa. For the purposes of economic comparison it will be assumed that the respective concrete mix has the compressive strength class C35/45 leaving a compressive strength reserve. Economic comparison is given in Table 5. Concrete price is indicated according to information on company Kolle Beton website in April, 2012 (Kollebeton, 2012). The price of traditional concrete is 53.24-55.66 LVL depending on the compressive strength class (C30/37-C40/50). Based on data of the reference mix C30/37 with the price 53.24 LVL/m³, economical calculations were made and costs for m³ of concrete estimated, replacing 30% of the cement mass with coal bottom ash ground for 45 minutes (assuming that for the concrete C30/37 it would be 350 kg/m³). The price of the energy consumed for coal bottom ash grinding is assumed 0.1074 LVL/kWh. As coal bottom ash was ground for 45 minutes and the amount 30% of the cement mass (350 kg/m³) constitute 105 kg/m³, the price of coal bottom ash preparation for 1 m³ is 0.48 LVL. The price of new concrete with higher compressive strength is calculated by adding this price to the price of concrete C30/37. Economic benefit is 0.70 LVL for 1 m³ of concrete assuming that it corresponds to the compressive strength class C35/45 or 2.00 LVL if the compressive strength class is C40/50. Costs of concrete decrease by 1.4 and 3.6% respectively compared to the market price for the particular compressive strength class concrete without coal bottom ash micro additive.

Ecological benefit

In addition to the economic benefit there is an ecological benefit as well. Ecological benefit comes from the economizing of cement and deposition costs of coal bottom ash. Estimation of deposition costs differs in each individual case and therefore it is difficult to assess them, therefore the ecological benefit will be based on the theoretical reduction of CO₂ emission in the cement production.

Economical comparison for concrete with coal bottom ash added

	Compressive strength class of concrete		
	Concrete C30/37	Concrete C35/45	Concrete C40/50
Market price for m ³ of concrete* [17]	53.24	54.45	55.66
Amount of coal bottom ash in concrete, kg/m ³	0	105	105
Price of coal bottom ash grinding, LVL/t**	4.03	4.03	4.03
Price of coal bottom ash for 1m ³ of concrete (140kg), LVL	0	0.42	0.42
Costs of concrete with coal bottom ash (price for concrete 30/37)	53.24	53.66	53.66
Economic benefit LVL/m ³ concrete	0.00	0.79	2.00
Price changes, %	0.00	-1.4	-3.6

*Concrete C40/50 (B40) with the maximal aggregate size 16 mm;

Concrete C30/37 (B30) with the maximal aggregate size 16 mm

** Calculated for the electricity consumption 50 kWh/t, tariff 0.1074 Ls/kWh

Table 6
Calculations of CO₂ emission amount of cement production for 1 m³ of concrete

	Concrete C30/37	Concrete C35/45	Concrete C40/50
Amount of cement for concrete without coal bottom ash, kg/m³	350	370	390
Concrete with coal bottom ash, kg/m³:			
<i>Cement</i>	350	350	350
<i>Ash with grinding period 45 min 40 %</i>	0	105	105
CO₂ emissions for cement without coal bottom ash, kg/m³ concrete	78	82	87
CO₂ emissions for cement with coal bottom ash, kg/m³ concrete:	78	83	83
<i>CO₂ from cement</i>	78	78	78
<i>CO₂ from grinding of ashes</i>	0	5.25	5.25
CO₂ emission changes, kg/m³ concrete:	0	1	-4
CO₂ changes, %	0	1.0	-4.2

By including coal bottom ash in the concrete mix it raises the compressive strength class of concrete (from C30/37 to C35/45 or C40/50). If coal bottom ash would not be included in the concrete mix it can be assumed that the amount of cement necessary for 1 m³ of concrete would be increased in order to raise the compressive strength. By estimating economizing of cement for 1 m³ of concrete it is possible to calculate CO₂ emission reduction for 1 m³ of concrete with ground coal bottom ash. By estimating the necessary amount of cement, it was assumed that compressive strength of cube for specimens correspond to the standards of compressive strength classes. Namely, it is 53 MPa for compressive strength class C35/45 and 58 MPa for compressive strength class C40/50, which is close to the compressive strength of the specimens with coal bottom ash (57 MPa).

In order to produce concrete with a definite compressive strength class without the coal bottom ash micro additive, 370 kg/m³ of cement is necessary for concrete with the compressive strength class C35/45 and 390 kg/m³ of cement is necessary for concrete with the compressive strength class C40/50. Calculations of CO₂ emission amount in production of 1 m³ of concrete including various compressive strength classes and option of replacing 30% of cement with coal bottom ash ground for 45 minutes are given in Table 6. CO₂ emission from production of 1 m³ of concrete constitutes 78 kg for concrete C30/37 with the cement amount 350 kg/m³. Increasing the amount of cement, the amount of CO₂ emissions grows proportionally reaching 82 kg/m³ for concrete C35/45 and 87 kg/m³ for concrete C40/50. If the amount of cement does not change (350 kg/m³) and 30% of cement is replaced with coal bottom ash ground for 45 minutes, the amount of CO₂ emissions is constituted from the cement production emission and coal bottom ash grinding emission. As it is seen in Table 6, for the concrete with the compressive strength class of C35/45 the amount of CO₂ emissions grows, if 20 kg of cement is replaced by 105 kg of ashes, but for concrete with the

compressive strength class C40/50 the amount of CO₂ emissions decreases. Amount of CO₂ emissions for concrete with the compressive strength class C35/45 would increase by 1 kg/m³ compared to the reference mix without coal bottom ash. The increase would be 1% compared to the reference mix without coal bottom ash, but the amount of CO₂ emissions would decrease from 87 kg/m³ to 83 kg/m³ or by 4.2% for the concrete with a higher compressive strength class. Taking into account the possible amount of CO₂ emissions, grinding of coal bottom ash would be cost effective for concrete with the compressive strength class C40/50. However, there is only a slight difference with the compressive strength class C35/45 and the concrete possibly should be adjusted according to the workability criteria and concrete plasticizers possibly should be used.

CONCLUSIONS

Conclusions

The grinding period influences particle size distribution of coal bottom ash. Extending the grinding period from 15 to 45 minutes, the amount of smaller particles grows (< 0.25 mm from 63 – 93 %). In addition, the form of particles becomes less angular. The extension of the grinding period and the increasing of the coal bottom ash amount change the particle size distribution and the amount of fine particles grows as well as the density of concrete structure increases. Coal bottom ash consists of 88% carbon indicating the presence of coal pieces which are not completely burned. Si, Al, Ca and oxides were observed in separate particles, which could further pozzolanic reactions and increase the concrete compressive strength. Adding coal bottom ash to the concrete mix changes the amount of water, which is necessary to obtain the definite consistency of fresh concrete. Coal bottom ash from a grinding period of 30 and 45 minutes replacing 10% of the amount of cement decreases the W/C ratio without decreasing the cone slump. If the amount of coal bottom ash is increased, the W/C ratio should be increased in order to preserve cone

slump class S4. Coal bottom ash in the concrete mix increases its compressive strength compared to the reference mix. The most efficient combination is 30% of coal bottom ash with the grinding period 45 minutes. The compressive strength increased from 47.0 MPa for the reference mix to 56.7 MPa for the concrete mix with coal bottom ash. Water permeability and water absorbtion of concrete specimens were tested, which are important indicators of the concrete durability. Water permeability of the specimens after 28 days was 10-42 mm. The best result was for mix with coal bottom ash with the grinding period of 30 minutes replacing 10 and 20% of cement with it - 10 and 12 mm compared to the 28 mm of the reference mix. Water absorbtion decreased significantly for mix with coal bottom ash with the grinding period of 45 minutes replacing 10-40% of cement with it, namely, 4.6-5.0% compared to the 6.1% for the reference mix. For mix with coal bottom ash with the grinding period 15 and 30 minutes changes were insignificant (5.7-6.2%). Coal bottom ash could be used as a micro additive in the concrete production.

REFERENCES

- Cheriaf M., Cavalcante Rocha J., Pera J., Pozzolanic properties of pulverized coal combustion bottom ash, *Cem. Concr. Res.* 29 (1999) 1387 - 1391.
- Council Directive, The Council of the European Union 96/61/EC "Integrated pollution prevention and control", 1996.
- Data courtesy of the American Coal Ash Association, Commercial Use of Coal Utilization By-products and Technology Trends, 2001
- ECCPA, European Coal Combustion Products Association, EESC public hearing in Cluj-Napoca, Romania on May 19,2011
- Federal Highway Administration, User Guidelines for Waste and Byproduct Materials in Pavement Construction, 06/08/2011.
- Garboczi E.J., Bentz D.P., Digital Simulation of the Aggregate-Cement Paste Interfacial zone in concrete, *J. Mater. Res.* 6 (1991) 196 - 201.
- Jankovic A., Valery W., Cement Grinding Optimisation, Minerals engineering , ISSN 0892-6875 , 2004, vol. 17, no11-12, pp. 1075-1081
- Karayigita A.I, Gayerb R.A, Querolc X, Onacakd T, Contents of major and trace elements in feed coals from Turkish coal-fired power plants, *International Journal of Coal Geology*, Volume 44, Issue 2, August 2000, Pages 169–184
- Kollebeton, <http://online.kollebeton.lv/?a=6>
- Ministry of Economics, Republic of Latvia, Report on the Economic Development of Latvia. July, 2011., Riga, 2011. P.42.
- Mohd Sani M. S. H. bin, Muftah F, Muda Z. The Properties of Special Concrete Using Washed Bottom Ash (WBA) as Partial Sand Replacement, *International Journal of Sustainable Construction Engineering & Technology* Vol 1, No 2, December 2010
- Pollocka S.M, Goodarzib F, Riediger C.L, Mineralogical and elemental variation of coal from Alberta, Canada: an example from the No. 2 seam, Genesee Mine, *International Journal of Coal Geology*, Volume 43, Issues 1–4, May 2000, Pages 259–286
- Research Profile Letter. Clinker Grinding at Breaking Point, *Concrete Sustainability Hub@MIT*, May 2011

The most effective is replacing of 20-30% of cement with coal bottom ash with a grinding period of 45 minutes.

By increasing the concrete compressive strength class from C30/37 to C40/50 the economic benefit was observed – the concrete price reduction of 3.6%. Costs of prior processing of coal bottom ash were included. The ecological benefit comes from the economizing of cement which would be necessary to ensure the compressive strength class of concrete as well as from the possible deposition costs of coal bottom ash. In order to increase the concrete compressive strength class from C30/37 to C40/50 using 105 kg of coal bottom ash, 40 kg of Portland cement are economised, namely, the amount of CO₂ emissions is decreased by 4 kg or 4.2% for each m³ of concrete.

ACKNOWLEDGEMENT

The financial support of the ERAF project Nr. 2010/0286/2DP/2.1.1.1.0/10/APIA/VIAA/033 „High efficiency nanoconcretes” is acknowledged.

Shah S.R., Rastogi S., Mathis O., Applications Of Dry Bottom Ash Removal And Transport For Utilization, Fly Ash India 2005, New Delhi

We Energies, Coal Combustion Products. Utilization Handbook. Chapter 3., 2003.

Zakharova, A., Engineering Thermodynamics and Heat, 2008, P. 272, ISBN 978-5-7695-4999-1.
Техническая термодинамика и теплотехника. Ред Антонина Захарова. Издательство: Академия, 2008.
272 стр. ISBN 978-5-7695-4999-1

ACOUSTIC AND MECHANICAL PROPERTIES OF FOAM GYPSUM DECORATIVE CEILING PANELS

Raitis Brencis*, Juris Skujans*, Uldis Iljins**

*Latvia University of Agriculture,

Department of Architecture and Building

E-mail: raitis.brencis@llu.lv; juris.skujans@llu.lv

**Latvia University of Agriculture,

Department of Physics

E-mail: uldis.iljins@llu.lv

ABSTRACT

Material structure depends on its production technology and by varying this technology it is possible to obtain similar structures. Physical and mechanical properties depend on the material structure and relating that to the material thickness, it is possible to change the maximal sound absorption coefficient position in the range of frequency. The paper examines the development of foam gypsum sound absorption material production technology, in order to obtain materials with the rules of sound absorption coefficient at the same time fulfilling the strength requirements. The sound absorption coefficient was determined with a Ø40mm impedance tube and in a reverberation chamber according LVS EN ISO 354:2003. Flexural strength for beams was determined in a three-point bending test and for ceiling panels according LVS EN 14246:2006. The study of the results was acquired from a foam gypsum production technology that simultaneously executes the strength requirements and provides a Class B sound absorption material. It has been found that foam gypsum sound absorption material and mineral wool is similar to the behavior of the sound absorption coefficient and the thickness of the product, although these materials are different structures.

Key words: Foam gypsum, acoustic panels, sound absorption, ceiling panels

INTRODUCTION

Material structure depends on its production technology. It is possible to obtain materials of similar structure using different technologies. By varying the structure it can also influence physical and mechanical properties of the material itself. In order to obtain optimal material, it is necessary to know which production technology gives certain material structure with certain properties. By the material's thickness it is possible to adjust the maximal sound absorption coefficient position in a range of frequency. Smith (Шмидт, 1969) in the last century during the '60s determined that the stone cotton sound absorption coefficient maximal value at various frequency ranges are dependent on the material's thickness.

Fine acoustic environments have to be in offices, learning classrooms, stores, and production buildings. Optimal acoustic spaces have to be reached by combining sound absorption and insulation. Latvian Building Norms LBN 016-11 "Building Acoustics" has defined requirements for reverberation time and sound insulation. Absorbents are more necessary for regulating the reverberation time, but insulators – to ensure sound insulation between the premises. Sound insulation is less changeable and the requirements during exploitation do not change so suddenly as in the case of reverberation time. Thus absorption materials have to be available with a broad absorption coefficient range. By executing acoustic indicators, absorbents have to ensure certain sound

absorption, and properties of strength may vary for different materials. Certain material structure and thicknesses are needed to ensure strength indicators. By increasing the material's thickness, the absorption coefficient does not increase indefinitely. Such cell concrete absorbents as foam concrete, aerated concrete on a cement basis and aerated concrete on a lime basis reach a maximal sound absorption coefficient already at 35 mm thickness (Laukaitis, et al., 2006). Considering the economy of raw materials, there are no grounds for choosing a thick material that does not ensure a high sound absorption coefficient. Forming composite materials, it is possible to decrease the amount of raw materials, and increase the material strength and sound absorption ability. The flexural strength of foam gypsum acoustic ceiling tiles is determined by LVS EN 14246:2006 requirements. In order to ensure the standard requirements of flexural strength, foam gypsum acoustic tiles' flexural have to be increased by 0.08 MPa. Local pressure during assembling has to be ensured for the acoustic tiles' compressive strength.

The objective of the research is to change foam gypsum sound absorption material production technology to obtain a material with properties which ensure an average weight sound absorption coefficient of $\alpha_w \geq 0.60$ at a frequency range of 250÷4000 Hz, at the same time ensuring strength requirements ($R_{flexural} > 0.08$ MPa, $R_{compressive} > 0.20$ MPa).

Table 1
Sound-absorbing board materials comparison

Material	Thickness, mm	Sound absorption coefficient α_w	Absorption class according LVS EN ISO 11645
HWL 25AB	25	0.20	E
Fibrolite F 75	75	0.65	C
Fibrolite F 100	100	0.75	C
Isover Focus A	20	-	C
Isover Master A alpha	40	-	A
Armstrong Neeva Board 15	15	1.00	A
Armstrong Perla	17	0.65	C

MATERIALS AND METHODS

Sound absorption

In order to determine the absorption coefficient in a reverberation chamber, foam gypsum panels of $300 \times 300 \times 40$ mm were produced using the method of dry mineralization (Горлов et al., 1984; Скуянс et al., 1985; Skujans et al., 2007; Iljins et al., 2009; Skujans et al., 2010). According to Standard LVS EN ISO 354:203 the minimal absorbent area of a reverberation chamber, Fig. 1., is 6.0 m^2 . In order to ensure the necessary requirements, 68 samples with a 0.09m^2 area each and with a total square of 6.12m^2 were produced. Material size was chosen in order to produce as many samples as possible to avoid mistakes. Reverberation time measurements and absorption coefficient calculations were determined after the Standard LVS EN ISO 354:2003 "Acoustics Sound Absorption Measurements in Reverberation Chamber." The sound absorption coefficient average weight value was determined after the Standard LVS EN ISO 11654:2000 "Acoustics-Sound Absorbents in Buildings-Sound Absorption Parameters."

A sound source with a 12-side (dodecahedron) all directional loudspeaker which produces a regular sound field in the chamber was placed in the reverberation chamber. A microphone was placed in 5 places by turn (Fig.1.) in an empty chamber and in a chamber with foam gypsum samples. At the beginning, the reverberation time and sound pressure level of empty and full chambers were measured. After that the average values of five microphones' measurements were determined.

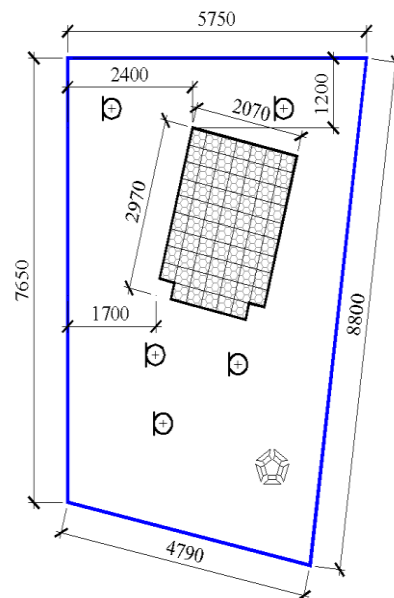


Figure 1. Foam gypsum acoustic ceiling tiles measuring scheme in reverberation chamber

After the Standard LVS EN ISO 254:2003 requirements, the sound pressure level comparison among values of side 1/3 octave band was made. If these values do not differ more than 6 dB, the sound field can be considered as diffusive. The value of sound absorption coefficient at 1/3 octave band has been determined using equation 1:

$$a_s = \frac{A_2 - A_1}{S_p} = \frac{A_T}{S_p}, \quad (1)$$

where:

A_1 - equivalent absorbent area of an empty reverberation chamber (equation 2), m^2 ;

A_2 - equivalent absorbent area with a sample (equation 3), m^2 ;

A_T - equivalent absorbent area for a sample, m^2 ;

S_p - actual geometrical area (Fig.1.) of a sample, m^2 ;

$$A_1 = V \left(\frac{55.3}{c_1 T_1} - \frac{4\alpha_1}{10 \lg(e)} \right), \quad (2)$$

$$A_2 = V \left(\frac{55.3}{c_2 T_2} - \frac{4\alpha_2}{10 \lg(e)} \right), \quad (3)$$

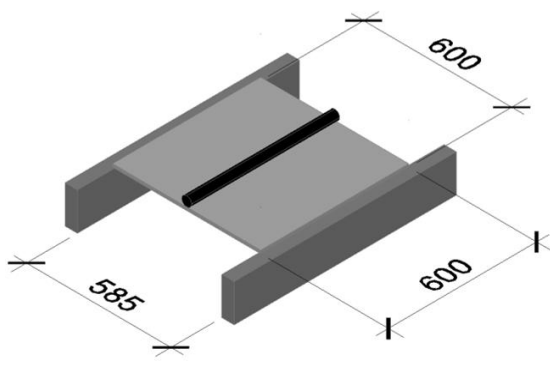
where:

V - free volume of reverberation chamber (203), m³;
 c_1, c_2 - sound velocity (LVS ISO 354:2003 6. equation), m s⁻¹;
 T_1, T_2 - reverberation time in 1/3 octave bands, s;
 α_1, α_2 - attenuation coefficient of sound in atmosphere (ISO 9613-1).

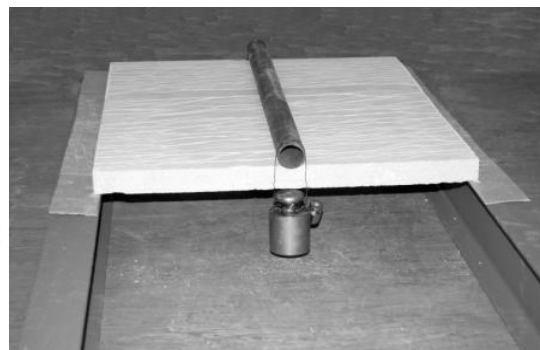
Flexural and compressive strength

Samples of 40×40×160 mm were made to determine material flexural and compressive strength. Samples were tested in a three-point bending test with a 100 mm distance between supports. The flexural strength indicator was calculated using equation 4:

$$f = \frac{3FL}{2bh^2}, \quad (4)$$



a



b

Figure 2. Foam gypsum acoustic ceiling tiles a - loading scheme; b-foam gypsum acoustic ceiling tiles loading

RESULTS AND DISCUSSION

Gypsum ceiling elements with the Standard LVS EN 14246:2006 for 600x600 tile with a length of 585 mm have to withstand a pressure of 6 kg. Knowing the pressure and possible thinner foam gypsum tile thickness (35 mm (Laukaitis et al., 2006)) by the equation (4.) the minimal allowed flexural strength was determined according to the standard – 0.08 MPa. Parameters of flexural and compressive strength are shown in Fig. 3. Foam gypsum with a production technology using 4 ml surface active stuff (SAS) corresponds to the parameter >0.08 MPa.

From these technologies foam gypsum with a production technology w/g 0.9 SAS 4 ml and w/g

where:

F - maximal load, N;
L - span between supports, mm;
b - sample width, mm;
h - sample height, mm.

Requirements of flexural and compressive strength according to LVS EN 14246:2006 "Foam Gypsum Elements of a Suspended Ceiling. Definitions, Requirements, Testing Methods" ask for 600×600 mm tiles. The tiles are produced using the same technology and thickness (40 mm) as they were tested at the reverberation chamber. Foam gypsum was dried and tested at 23±2°C and humidity 50±5 %. Testing was made for 600×600mm samples placed on supports with span 585 mm. The sample placed on supports was loaded with 6000±100 g a round loading beam on all sample length parallel to supports. Test was done for 30 min and damages (cracks) were estimated afterwards. Sample shouldn't crash and cracks are not allowed after the testing. The testing scheme is shown at Fig.2a and the test at Fig. 2b.

0.8 SAS 4 ml can't be used, because of the average weight sound absorption coefficient at 100 mm, the thickness is under 0.5. Useable technologies are w/g 0.6 SAS 4 ml and w/g 0.7 SAS 4 ml, which average a weight sound absorption coefficient at 100 mm thickness is 0.61 and 0.52 which corresponds with C class (0.61) and D class (0.52) after the Standard LVS EN ISO 11654:2000. Volume mass of foam gypsum w/g 0.6 SAS 4 ml is close to 400 kg m⁻³, which is the highest limit allowed, making the weight <15 kg m⁻². The weight of fibrolite acoustic tiles is 11.5 kg m⁻² (HWL 25... 2012).

Analyzing the data of indicators in compressive strength Fig.4. the highest indicators are for the foam gypsum with a production technology w/g 0.6 SAS 4 ml, but w/g 0.7 SAS 4 ml has been changed

by foam gypsum with a production technology w/g 0.8 SAS 4 ml, with the medium sound absorption

coefficient at 100 mm 0.43 (D class).

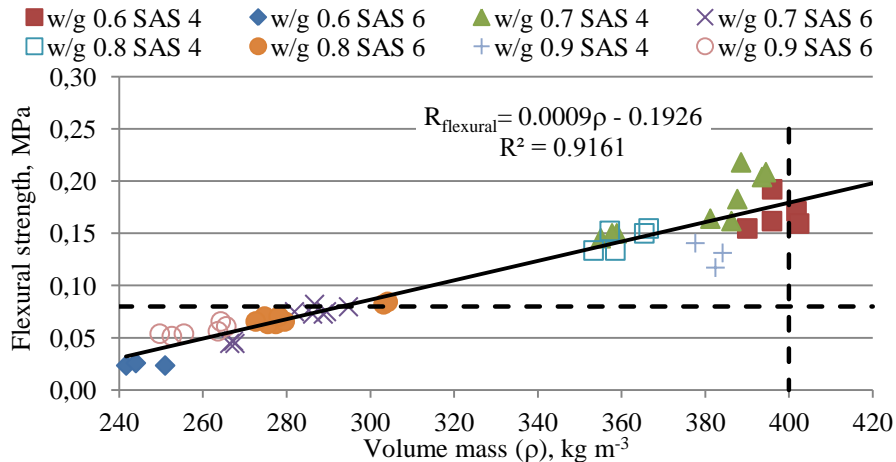


Figure 3. Foam gypsum flexural strength depending on the volume mass at different production technologies

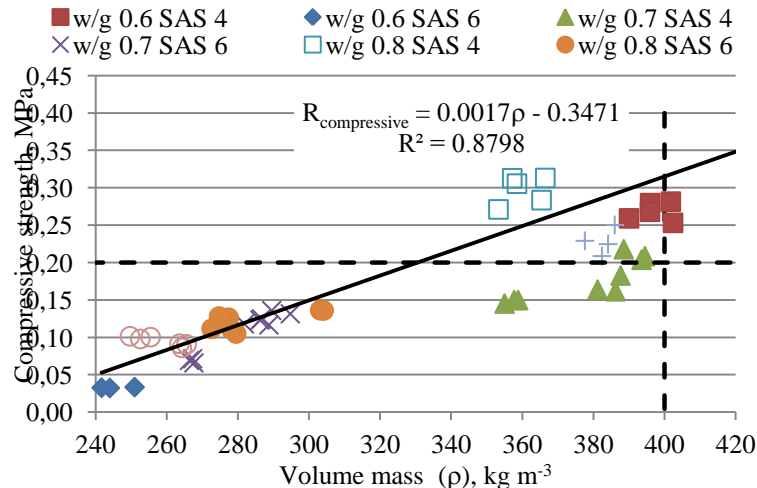


Figure 4. Foam gypsum compressive strength depending on the volume mass at different production technologies

Sound absorption tiles can be with various thicknesses depending on their usage and necessity to absorb sound. Figures 5 a,b,c,d show medium sound absorption values at different thicknesses depending on the production technology. Based on strength indicators, foam gypsum which can be used for production of sound absorption tiles, is with a production technology w/g 0.6 SAS 4ml and w/g 0.7 SAS 4 ml. From these production technologies the best sound absorption properties are w/g 0.6 SAS 4 ml at a material thickness of 30 mm; 40 mm and 50 mm, and its properties are the same as for the production technologies with 6 ml

SAS, which provide better sound absorption properties. With the material thickness of 100 mm of this production technology has lower indicators than 0.11, and this sound absorption tile isn't of practical usage.

Considering the average weight values of the sound absorption coefficients at different technologies Fig.5 a,b,c,d, as well as indicators of flexural and compressive strength, the foam gypsum with technology w/g 0.6 un SAS 4 ml was chosen for continuous material testing.

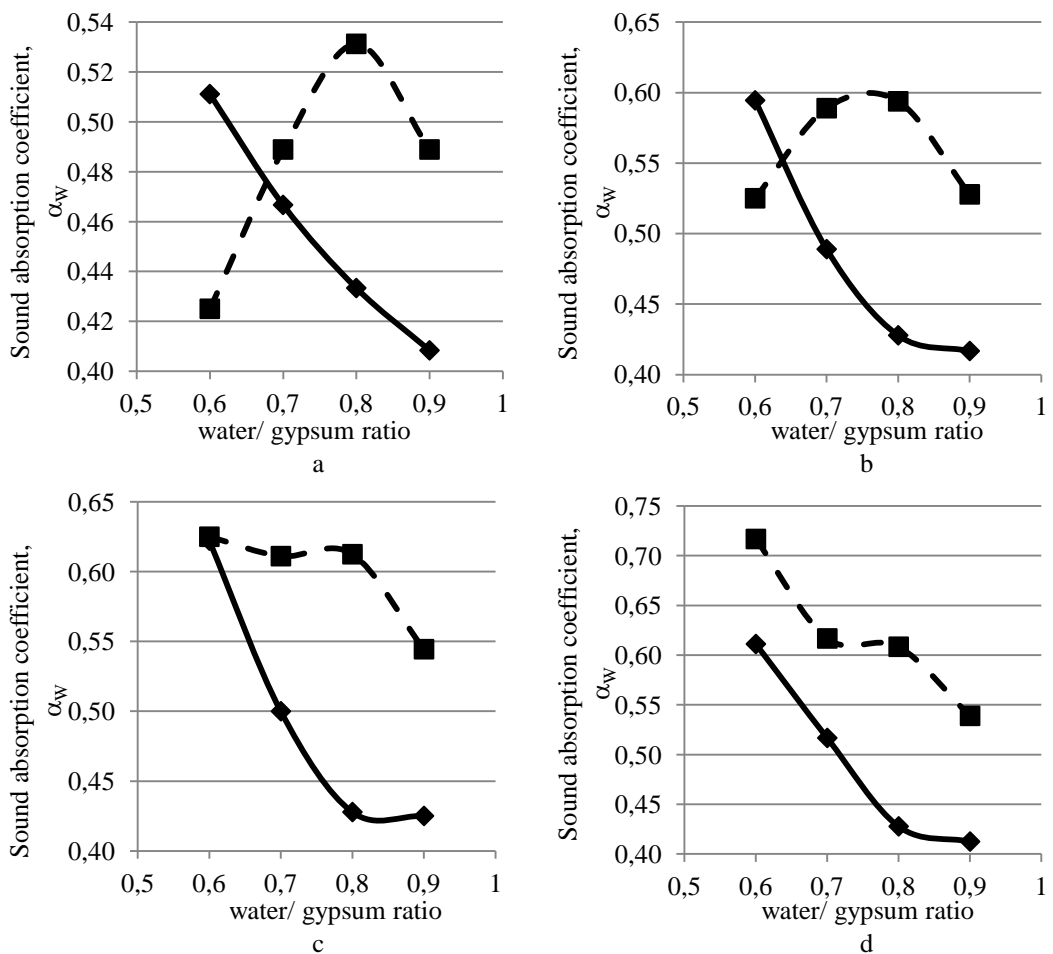


Figure 5. Foam gypsum weighed average sound absorption coefficient at different production technology. — SAS 4 ml; — — SAS 6 ml, a-30 mm thick sample; b-40 mm thick sample; c-50 mm thick sample; d-100 mm thick sample

Material thickness and frequency connection of sound absorption tiles of mineral wool basis has been researched already in the '60s of the last century. Smith (Шмидт, 1969) has determined the sound absorption coefficient for acoustic tiles and has concluded that by decreasing material thickness the maximal value of sound absorption coefficient

moves to a higher frequency range. In research with foam gypsum the same concurrence has been observed as in research with mineral wool Table 2 which is a fibrous material. We foresee that this concurrence is of a general character, and we will try to confirm it with further investigations.

Table 2
Foam gypsum of production technology w/g 0.6 SAS 4 ml average volume mass 377 kg m^{-3} , sound absorption coefficient, depending on the thickness of material

Thickness, mm	The sound absorption coefficient of the average octave bands, α					
	250 Hz	500 Hz	1000 Hz	2000 Hz	4000 Hz	Average
10	0.08	0.12	0.27	0.72	0.85	0.22
20	0.14	0.33	0.61	0.73	0.69	0.37
30	0.24	0.51	0.64	0.70	0.76	0.51
40	0.35	0.58	0.62	0.71	0.76	0.59
50	0.43	0.57	0.61	0.71	0.75	0.62
100	0.48	0.53	0.61	0.71	0.75	0.61

The results of the sound absorption coefficient of foam gypsum tested at the reverberation chamber are shown in Fig. 6. The figure shows values of the sound absorption coefficient at 1/3 octave bands and at average octave bands. The maximal value of the sound absorption coefficient is at 1 kHz (0.91) and siding 1/3 octave band frequency response is very close to 500 Hz (0.860 and 2 kHz (0.89). Decrease of absorption coefficient value of the material was observed at lower frequencies. This can be prevented by installing a material into the suspended ceiling system or placing rockwool behind the material. The sound absorption

coefficient according to the Standard LVS EN ISO 11654:2000 is 0.8 that corresponds to the B class absorbent.

The obtained result is for 0.2 higher than the sound absorption coefficient obtained in the absorption tube. That is because in the acoustic tube, sound falls on the measurement sample perpendicular to the sample surface, but in a reverberation chamber a diffused sound field has been formed, and the sound falls at various angles in such a way improving the absorption capacity.

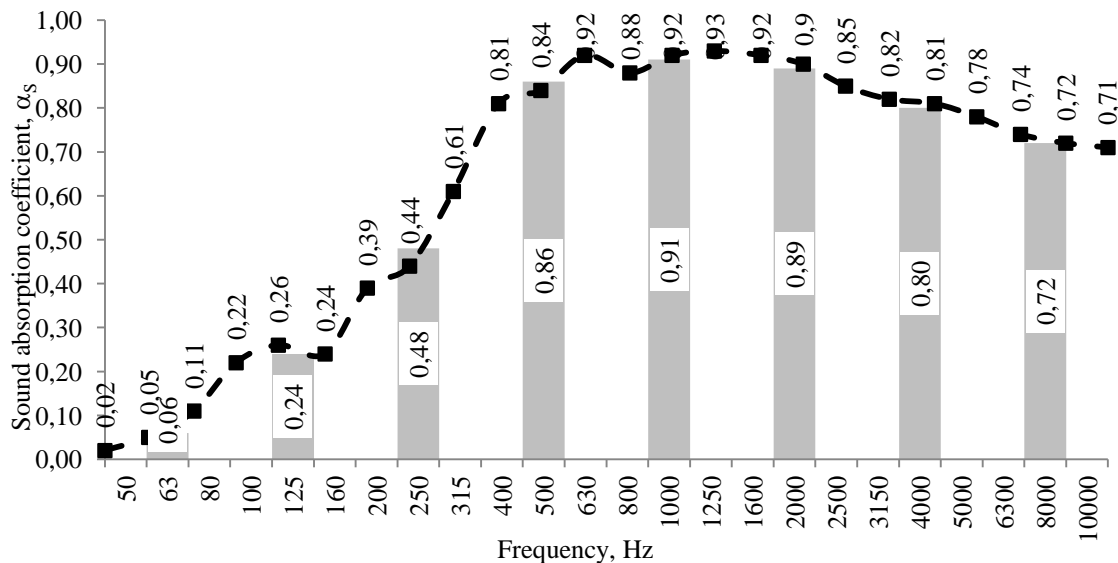


Figure 6. Measurement of sound absorption coefficient in a reverberation chamber. Frequency response curve of 1/3 octave bands foam gypsum with production technology w/g ratio 0.6, SAS 4 ml. —— α value measured frequency response (1/3 octave band); ■ - Absorption coefficient, α , average octave bands

For foam gypsum tiles tested for flexural strength in the reverberation chamber, all samples underwent a pressure test of 6 kg. The visual test didn't show any cracks, and samples were tested by Fig. 2. scheme till sample crushing, gradually increasing the pressure by 400 g till the samples were crushed. By equation 4 the determined standard material flexural strength is 0.055 MPa, but after strength tests with balks (40×40×160mm) the three-point bending test with production technology foam gypsum strength in flexural is 0.13 MPa, which is two times bigger than standard requires. For foam gypsum ceiling tiles crushing was necessary at an average weight of 15 kg, which by equation 4 in flexural strength is 0.137 MPa and 2.5 times greater flexural strength as determined by the Standard LVS EN 14246:2006 and 5% greater than the strength after material testing with balks on a three-point bending test.

CONCLUSIONS

By using production technology with composition w/g 0.6 and SAS 4 ml, the foam gypsum of volume/mass till 400 kg m⁻³ was obtained. Flexural strength 0.13 MPa, 40 mm thick tiles foam gypsum absorption increases the Standard LVS EN 14246:2003 requirements 2.5 times, reaching 0.137 MPa and compressive strength >0.20 MPa. sound absorption coefficient, measured at an impedance tube 0.62 (50 mm) C class material and reverberation chamber 0.80 (40mm) B class material.

It has been determined that foam gypsum sound absorption material and mineral wool has analogical behavior between sound absorption coefficient and the material thickness, although these materials have different structures. The sound absorption coefficient at 250 Hz is better for materials having a 100 mm thickness. By increasing the sound frequency a maximal sound absorption coefficient has been reached for samples with less thickness.

ACKNOWLEDGMENT

The research was supported by the European Social Fund, Agreement No. 2009/0180/1DP/1.1.2.1.2/09/IPIA/VIAA/017

REFERENCES

- Acoustic ceilings & walls* (2012a) [online] [accessed on 2012.11.07] Available: http://www.armstrong.lv/commclgeu/en-lv/ceilings/perla/_N-1z1416y
- Acoustic ceilings & walls* (2012b) [online] [accessed on 2012.11.07] Available: http://www.armstrong.lv/commclgeu/en-lv/ceilings/neeva-nevada/_N-1z141yeZ5n?Ntt=Neeva
- F informācija par produktu* (2012) [online] [accessed on 2012.11.07] Available: http://www.fibrolits.lv/Public/upload/09032011_F_LV.pdf
- HWL 25 AB informācija par produktu* (2012) [online] [accessed on 2012.11.07] Available: http://www.fibrolits.lv/Public/upload/09032011_HWL%2025%20AB_LV_web.pdf
- HWL informācija par produktu* (2012) [online] [accessed on 2012.11.07] Available: http://www.fibrolits.lv/Public/upload/09032011_HWL_LV.pdf
- Iljins U., Skujans J., Ziemelis I., Gross U., Veinbergs A., (2009) Theoretical and experimental research on foam gypsum drying process, In: *Chemical Engineering Transactions*. Proceeding of international scientific Conference, 17, p. 1735-1740.
- Laukaitis A., Fiks B. (2006) Acoustical properties of aerated autoclaved concrete, *Applied Acoustics*, 67, 284-296.
- LVS EN 14246:2006. *Gipsa elementi piekārtajiem griestiem. Definīcijas, prasības un testēšanas metodes*. Rīga: Latvijas Valsts Standarts, 2006.
- LVS EN ISO 11654:2000. *Akustika - Skaņas absorbētāji ēkās - Skaņas absorbcijas parametri*. Rīga: Latvijas Valsts Standarts, 2000.
- LVS EN ISO 354:2003. *Akustika. Skaņas absorbcijas mērišana reverberācijas kamerā*. Rīga: Latvijas Valsts Standarts, 2003.
- Skaņas absorbcija un izolācija* (2012) [online] [accessed on 2012.11.19] Available: <http://www.isover.lv/brochures/default.asp?aid=173&val=1&brid=19>
- Skujans J., Iljins U., Ziemelis I., Gross U., Ositis N., Brencis R., Veinbergs A. And Kukuts O., (2010), Experimental research of foam gypsum acoustic absorption and heat flow, In: *Chemical engineering transactions*, 19, p.79-84.
- Skujans J., Vulans A., Iljins U., Aboltins A., (2007) Measurements of Heat Transfer of Multi-Layered Wall Construction with Foam Gypsum, *Applied Thermal Engineering*, Volume 27, Issue 7, 1219-1224;
- Горлов Ю.П., Меркин А.П., Румянцев Б.М., Кобидзе Т.Е. (1984) Технология облегченных пеногипсовых материалов. В кн.: *Высокопрочный гипс в индустриальном строительстве: Тезисы докл.* Рига: ЛатНИИстроительства, стр. 118-121.
- Скуянс Ю.Р., Бериньш А., Беткерс Т. (1985) Применение пеногипса для декоративно – акустических плит. Тезисы докл. Рига ЛатНИИНТИ, стр. 95-96.
- Шмидт Л.М. (1969) Производство акустических материалов, Москва: Стройиздат. стр. 175

ANALYSIS OF SIMULATION MODELS OF PCM IN BUILDINGS UNDER LATVIA'S CLIMATE CONDITIONS

Janis Kazjonovs*, Diana Bajare**, Aleksandrs Korjakins***, Ansis Ozolins***, Andris Jakovics***
Riga Technical University, Chair of building materials and wares, Kalku Street 1, LV-1658, Riga, Latvia,

Phone: +371-67089132,

e-mail: [*janis.kazjonovs@rtu.lv](mailto:janis.kazjonovs@rtu.lv), [**diana.bajare@rtu.lv](mailto:diana.bajare@rtu.lv), [***aleks@latnet.lv](mailto:aleks@latnet.lv),
[***ansiso@inbox.lv](mailto:ansiso@inbox.lv), [***ajakov@latnet.lv](mailto:ajakov@latnet.lv)

ABSTRACT

This paper reviews a simulation study about Phase Change Materials (PCM) incorporated in building materials, particularly in passive applications. Due to the phase change these materials can store higher amounts of thermal energy than traditional building materials and can be used to add thermal inertia to a lightweight construction without adding physical mass. Thermal and mechanical properties of the used PCMs are presented in the paper. Thermal simulations were performed to study the optimal distribution of this material inside a building. A simulation study using WUFI®plus and EnergyPlus was carried out on PCM plaster, investigating various fusion temperatures of the PCM during day and night in hot weather conditions. The PCM effect during the heating season is also investigated. It was shown that the use of PCMs have advantages for cooling demand and building applications stabilizing room temperature variations during summer days, provided sufficient night ventilation is available. Another advantage of PCM usage is stabilized indoor temperature during the heating season.

. **Key words:** Phase change materials, cooling, thermal simulations, thermal inertia

INTRODUCTION

Demand for higher thermal comfort and climate changes have brought new challenges for designers of cooling systems, because of an increased usage of air conditioning in a building environment, resulting in higher electricity demand and CO₂ emissions. Today the thermal energy storage plays an important role in building energy conservation, which can be achieved by the incorporation of PCM into the building envelope. PCM incorporated in the building envelope, for example, in walls with plasters, absorb redundant heat, which leads to improved thermal inertia of the building, lower and shifted in time temperature peaks. References have been found for improving the thermal properties of concrete and plasters containing PCM (Cabeza, 2006; Romero et al., 2010; Schossig et al., 2005; Tyagi et al., 2011; Kuznik et al., 2011; Zamalloa et al., 2006).

PCMs can be used for cooling a building in three conventional ways (Kendrick, Walliman, 2007):

- Passive cooling: Cooling through the direct heat exchange of indoor air with PCMs incorporated into the existing building materials such as plasterboards, floorboards and furniture
- Assisted passive cooling: Passive cooling with an active component (for example, a fan) that accelerates heat exchange by increasing the air movement across the surface of the PCM
- Active cooling: Using electricity or absorption cooling to reduce the temperature and/or change the phase of the PCM

As active cooling, and supportive passive cooling, require the use of additional energy (refrigeration and fans). It is likely that the simplest, most cost-effective and environmentally friendly usage of PCM is in a purely passive way. The focus of this paper is on the use of PCMs for passive cooling, although the PCM effect during the heating period is also investigated.

The simulation models are based on five polygon test stands which have been built for the first time in Latvia. The goal of these test stands is to verify the energy efficiency and sustainability of the developed solutions for external bounding constructions, which are produced from local raw materials (ceramic blocks, foam concrete, wood, plywood, fibrolite, granules, sawdust etc.), in the conditions of the Latvian climate and, at the same time, to ensure the interior thermal comfort. Also, PCM could be incorporated in a building envelope for one stand to analyze PCM applications for Latvian climatic conditions.

Test stands are equipped with a full system for monitoring, collection and storage of data. Slightly similar polygon investigations were carried out at the Technical University of Tampere in Finland (Vinha J., 2007). However, the stands in Tampere were designed for different goals, they are smaller and without windows, which is important to ensure a sufficient level of thermal comfort. Instead of a heat pump, which will be used in the present project to reduce the consumption of fossil energy, the Tampere stands used electrical heaters. Moreover, the initial measurement data from those stands are

not available for detailed analysis, only specific results can be found in certain scientific publications. The significance of those results are also decreased for the Latvian situation due to climatic differences.

The polygon with test stands, to compare the efficiency of PCMs, are built in Lleida Technical University, Spain. The main goal of that research is to create the solution of minimal energy consumption for air conditioning systems in hot climate conditions. However, Latvian climate conditions differ significantly from Spain's climate. Moreover, the stands which are presented in Lleida do not take into account the solar energy, which comes through the window. Thereby, legacy investigations are not duplicated, and this fact substantiates the scientific and practical value of the current research in Latvian climate conditions.

MATERIALS AND METHODS

1D Integral Model

To model the heat and moisture transport in the multi-layer wall of a building, the following set of partial differential equations is used (Kunzel, 1995; Zhong, Braun, 2008):

$$\begin{aligned} \frac{\partial}{\partial x} \left(\lambda \frac{\partial T}{\partial x} \right) + h_v \frac{\partial}{\partial x} \left(\delta_p \frac{\partial(\varphi P_{sat})}{\partial x} \right) &= \\ = \rho(c + w c_w) \frac{\partial T}{\partial t} & \\ \frac{\partial}{\partial x} \left(D_\varphi \frac{\partial \varphi}{\partial x} \right) + \frac{\partial}{\partial x} \left(\delta_p \frac{\partial(\varphi P_{sat})}{\partial x} \right) &= \\ = \rho \frac{dw}{d\varphi} \frac{\partial \varphi}{\partial t} & \end{aligned} \quad (1)$$

where λ – thermal conductivity, W/(m·K);
 T – temperature, °C;
 x – wall thickness, m;
 $h_v = 2260000$ J/kg – the heat of vaporization;
 δ_p – the water vapour permeability of a material, kg/(m·s·Pa);
 φ – relative humidity;
 P_{sat} – saturation vapour pressure, Pa;
 ρ – bulk density of dry building material, kg/m³;
 c – specific heat capacity of dry building material, J/(kg·K);
 w – dry basis moisture content, kg/kg;
 $c_w = 4187$ – the specific heat capacity of water, J/(kg·K);
 D_φ – liquid conduction coefficient, kg/(m·s).

The above equations are non-linear (due to variable properties λ , δ_p and D_φ values), strongly coupled and have time-varying boundary conditions.

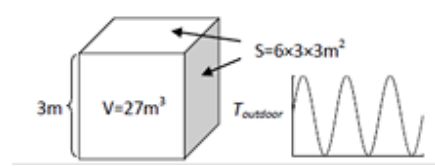


Figure 1. The integral mathematical model: graphical illustration

The simple model is created for estimating the indoor temperature variance due to varying outdoor temperatures taking into account the energy flow that crosses the wall (see Fig. 1). A similar model is inspected in (Ozolinsh, Jakovich, 2013). It is assumed that the inner load is constant q_0 . The heat amount variation indoors due to indoor temperature variation during a short time interval Δt is:

$$\Delta Q_1 = V c_{air} \rho_{air} (T_{indoor}(t + \Delta t) - T_{indoor}(t))$$

and the variation dependent on the difference with the outdoor temperature is:

$$\Delta Q_2 = \left(\sum_i S_i q_i(t + \Delta t) - q_0 \right) \Delta t$$

where S_i is the surface area of one wall, roof or floor, q_i is the heat flux corresponding to the surface with the area S_i .

From (1) and (2) it can be concluded that

$$\begin{aligned} \Delta Q_1 + \Delta Q_2 &= 0 \Rightarrow \lim_{\Delta t \rightarrow 0} \left(\frac{\Delta Q_1 + \Delta Q_2}{\Delta t} \right) = \\ &= V c_{air} \rho_{air} \frac{dT_{indoor}}{dt} + \sum_i S_i q_i - q_0 = 0. \end{aligned}$$

For calculation of the temperature and relative humidity profiles in the construction, the set of equations (1) used. From this, heat fluxes q_i on the inner surfaces are obtained.

Assuming, that indoor temperature is constant, but heating, that is necessary to ensure a constant indoor temperature, is changing, the following equation is obtained:

$$q_h = \sum_i S_i q_i$$

Simulation Methods

For calculating room climate and energy demand, two different models are used: 1D model, described on previous subsection, and 3D model which takes into account the whole building, windows etc.

For calculating room climate and energy demand, using the 3D model, the commercial software

WUFI®plus and free available software Energypluss are used.

WUFI®plus is a room climate model which connects the energetic building simulation and the hygrothermal component calculation. With the building simulation software WUFI®plus the hygric and thermal ratios in a building, in its perimeter and their interaction can be calculated and quantified as well as the energy demand and the consumption of system engineering. WUFI®plus focuses on calculating the thermal behavior of the building taking into account hourly outdoor climate values, interior thermal loads, various set-point temperatures and ventilation strategies as well as the adjusted system technology.

Energypluss is a whole building energy simulation program that engineers, architects, and researchers use to model energy and water use in buildings. EnergyPlus models heating, cooling, lighting, ventilation, other energy flows, and water use. EnergyPlus includes many innovative simulation

capabilities: time-steps less than an hour, modular systems and plant integrated with heat balance-based zone simulation, multizone air flow, thermal comfort, water use, natural ventilation, and photovoltaic systems.

Simulation Model

PCM can be impregnated into building materials such as plasters, either directly or as impregnated pellets. In the presented simulation model PCM was applied on the inner side of the building wall varying with the thickness of 2 mm, 4 mm and 6 mm. The building was a 3 x 3 m cubicle with a height of 3 m. Commercially available PCMs were used and their main properties are shown in Table 1. The most important properties of PCM are the thermodynamic properties, like transition temperature ΔT ($^{\circ}$ C) and latent heat H (kJ/kg). Heat flows of PCM are shown in (Puretemp technical data..., Rubitherm...).

Table 1

Main properties of PCM

PCM	λ , (Conductivity)	ρ , (Density)	ΔT , (Transition range)	H, (Latent heat)
	W/(m·K)	kg/m ³	°C	kJ/kg
PT 23	0.2	830	20..24	203
PT 24	0.2	860	21..24	185
SP25	0.6	1380	25..29	180

Table 2

Constructions used for modeling

Construction	Thickness mm	Conductivity W/(m·K)	Specific heat J/(kg·K)	Density kg/m ³
Wall				
Outside				
Plywood	20	0.17	1500	500
Mineral wool	200	0.036	850	40
Vapour retarder	0.25	0.15	1700	290
Plywood	20	0.17	1500	500
Fibrolite	75	0.068	2100	360
Lime plaster	15	0.49	840	1530
Roof				
Plywood	12	0.17	1500	500
Mineral wool	254	0.036	850	40
Plywood	9	0.17	1500	500
Ground floor				
Plywood	21	0.17	1500	500
Mineral wool	271	0.036	850	40
Plywood	21	0.17	1500	500

Thermal discomfort problems may arise due to outside temperature fluctuations to buildings with low inertia and large glazing areas. Using PCM as an inner layer for the building's wall may mitigate the problem. The absorbed latent heat increases the

thermal inertia of the construction while maintaining a near constant temperature.

The test stand of plywood in Fig. 2 was chosen for the simulation due to the lowest thermal inertia of the test polygon of five stands. The aim of the plywood test stand was to verify PCM usage.

The thermo physical properties and layers of the constructions were created according to the best practice guidelines. All the layers of the constructions are presented in Table 2. The heat transfer coefficient for wall was set to 0.154 W/m²K, floor 0.170 W/m²K, roof 0.158 W/m²K and triple glazed windows 1 W/m²K. The window is added on the South side.

Main parameters of the described building zone are:

- Total volume (m³) 27.0
- Floor area (m²) 9.0
- External wall area (m²) 34.2
- External transparent area (m²) 1.8
- Total PCM area (m²) 34.2
- Floor area/PCM area 0.26
- PCM relative thickness (mm) 2/4/6

To define the outside conditions, weather data for Riga, Latvia, were taken and average temperatures were used by the time step 1 hour. Summer and winter periods of the year were selected for detailed analysis.

To simplify the model, no inner heat gains from people, lightings were selected. An exception was allowed only in Fig. 5.

However, it was noted that the main factor for effective usage of PCM is night cooling for PCM solidification. Free cooling by opening the window was applied to cool and solidify the PCM.



Figure 2. Polygon of stands - in the centre: stand of plywood

PCM Application on the real test stand

The base cases were simulated with PCM usage on different places on the building wall to compare the results with standard construction without PCM usage. The base cases are given in Table 3 below.

For analyzing the influence of the window, the cases without windows were also inspected.

EnergyPlus was used for the summer period simulation, where free cooling night ventilation was applied and the window was opened at 30% by an area from the time of 20:00 to 8:00. Two temperature conditions were selected for this analysis:

1. Free floating conditions, where no temperature control is applied.
2. Controlled temperature of 25°C was selected from the time of 8:00 to 20:00. Cooling loads were measured.

For base cases it is assumed that PCM is incorporated into the lime plaster or roof. Default thickness of PCM is 6 mm, but cases with thickness of 2 and 4 mm are also inspected.

Table 1

Different cases of PCM usage on the test stand

Case	Description
A	without window, no PCM is added
A1	without window, PCM is added to the inner surface of each wall,
A2	without window, PCM is placed after lime plaster
A3	without window, PCM is placed throughout lime plaster
B	without window, PCM is added to the inner surface of one wall
C	without window, PCM is added to the inner surface of roof
WA	case A, window is added
WA1	case A1, window is added
WC	case C, window is added

RESULTS AND DISCUSSIONS

24h periodicity outdoor winter conditions

The aim of this subsection is to analyze thermal inertia for different cases of PCM PT23 usage. Simulation was done with a 1D integral model.

It is assumed that the temperature outdoors is changing periodically as a sinusoidal function within a 24-h periodicity. For analyzing thermal inertia, the inside temperature amplitude fraction was taken between case A and other cases, when PCM, with a total thickness 6 mm was added. It is assumed that the average outdoor temperature is +5°C and the temperature amplitude is 10°C, and a constant heat load is applied inside the room. Initial indoor temperature was taken to ensure maximal effect of PCM, and a simple integral model, described in subsection "1D integral model", was used. The results are summarized in Table 4.

Table 2

The ratio of the temperature amplitude for case A and given case, when PCM is used

Case	A1	A2	A3	B	C
Amplitude fraction	3.1	2.9	3.1	1.5	1.9

The results show, that the thermal inertia of the building insignificantly depended on the position of PCM (case A1, A2 and A3) in lime plaster, but PCM which was added on the floor is a better solution than case B, when PCM was added only on one wall. It could be explained by the fact that the thermal inertia of the roof is lower than that of the wall, therefore the effect of PCM usage is higher in this case. Based on these data, for a better effect and PCM placement position in the wall construction, it

was selected that for further simulation analysis PCM is placed on all inner surfaces of the walls.

PCM application on heating season

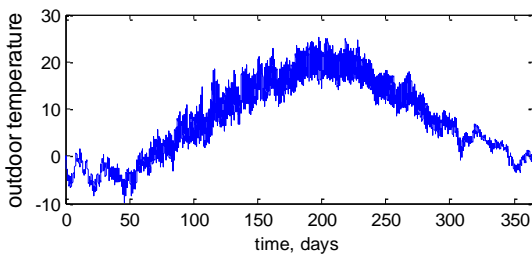


Figure 3. Annual temperature cycle in Latvia

Annual cycle (Fig. 3) was taken to analyze the yearly heat demand. Climate data for Latvia, Riga was taken by a time step of one hour as an average from the last 6 years. Data was taken from (Latvian Environment...). It is assumed, that the indoor temperature was a constant of +23,5°C during the whole year. Only the heating energy changed. For calculating the heating demand, commercial software WUFI®plus was used.

Table 3

Yearly heating demand.

Heating demand (kWh)	Without window	Window is added
No ventilation	1646	1353
Ventilation (0,7 l/h)	2508	2191

The data (see Table 5) show, that the ventilation absolutely changed the yearly heating demand. However, PCM did not effect the yearly heating demand by assumption that the inside temperature is constant. It is because PCM only helps to increase thermal inertia and there are no temperature fluctuations inside the room. A similar analyze of the yearly heating demand saving was made in (Shrestha, 2012). In this work, the yearly heating demand savings was about 1 % due to PCM usage. However, the reason for this saving was not PCM high heat of fusion, but only thermal conductivity.

However, PCM could be useful during the heating season in the following ways:

- PCM can stabilize indoor temperature by constant heat load
- In transient case from summer season to the heating season. PCM could help to increase time when the indoor temperature is decreasing below the comfort temperature.
- In specific cases, e.g., heating is switched off for brief time period. PCM application could ensure, that the inside temperature does not decrease below the optimal temperature during the brief time.

Average January temperature in Latvia is taken to analyze temperature fluctuations indoors (Fig. 4).

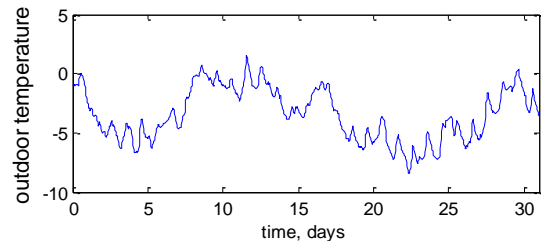


Figure 4. Outdoor temperature in January

It is assumed, that a constant heat load is applied indoors, and the indoor temperature changes are by the integral model. To see maximal effect of PCM usage, inner heat load, that ensure a maximal PCM effect, is taken.

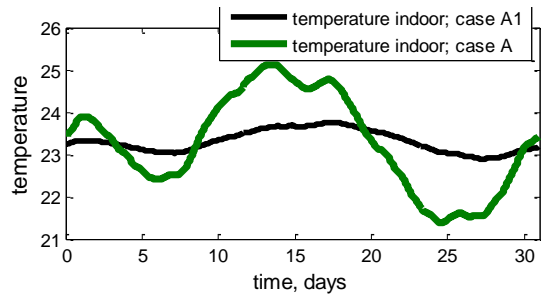


Figure 5. Indoor temperature in January

Figure 5 shows that PCM usage on walls significantly helps to stabilize indoor temperature. Without PCM the indoor temperature amplitude is about 4°C, however using PCM it is only 1°C. Due to low solar radiation during January in Latvia, the results are not significantly increased by solar radiation through the window.

PCM application on summer

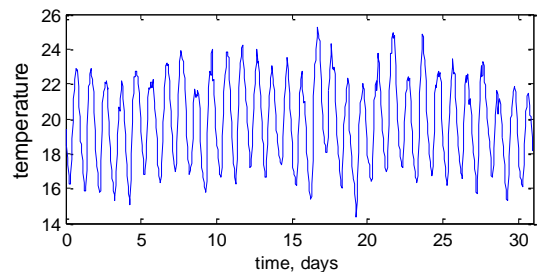


Figure 6. Outdoor temperature in July

July, which is the warmest month in Latvia, was taken for analysis (see Fig. 6).

To see the maximal effect, a constant heat load was taken indoors to ensure the maximal effect of PCM applications in this example.

1D Integral model was applied.

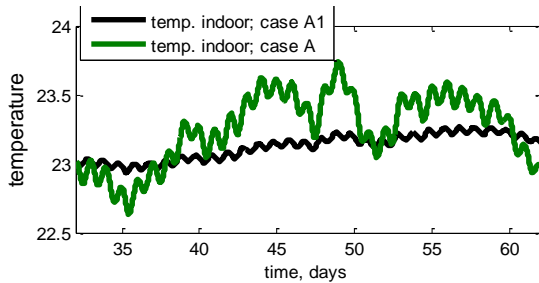


Figure 7. Indoor temperature in July

Figure 7 shows the maximal effect, when PCM's melting temperature is in the correct range. PCM usage on walls significantly helps stabilize indoor temperatures. However, the indoor temperature amplitude is relatively low without PCM usage in the building. However, the ventilation and window that were not taken into account in Figure 7 were important aspects that influenced temperature fluctuations indoors.

Also the indoor temperature fluctuations were analyzed without PCM. The air change coefficient was constant 0.7 1/h. Different cases were compared. Software WUFI®plus was used.

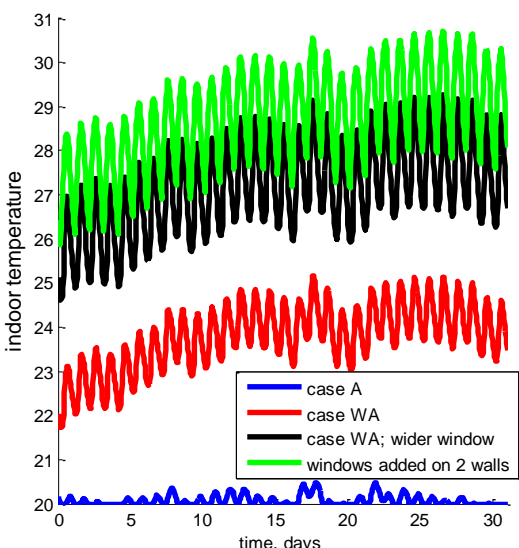


Figure 8. Indoor temperature in July. Blue curve corresponds to the real test stand of plywood. Black curve is the case, when the standard window (width 1.2m) is replaced with a wider window (2,2m). Red curve is the case, when a new window is added on the east side of the wall

Figure 8 shows that the temperature significantly differs, if window and solar radiation are taken into account. The width of a window is also an important factor that influences temperature fluctuations indoor. Also PCM could be necessary for cooling the room, especially in cases when the influence of a solar radiation is sufficiently large, and therefore the inside temperature is relatively high inside the room.

Next, the effect of PCM usage was analyzed by the assumption that the air change is constant 0,7 1/h.

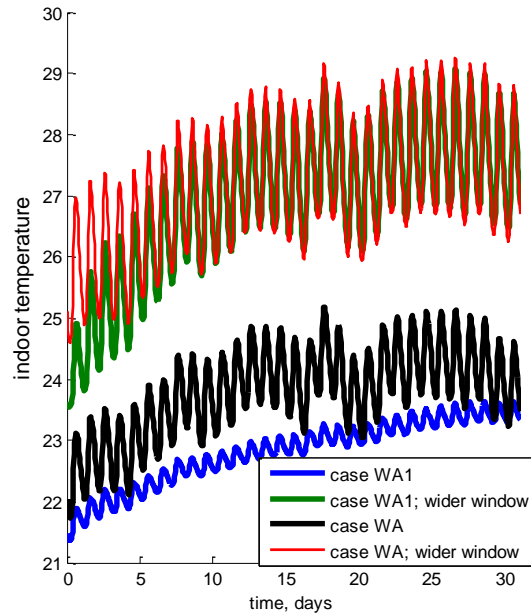


Figure 9. Indoor temperature in July

Figure 9 shows that PCM insignificantly helps to decrease the inside temperature, if the inside temperature differs too much from PCM melting temperature, because inside, the temperature does not decrease at night. This could be improved, if free cooling is applied, for example if the window is opened during the night. This situation is analyzed at the next subsection.

EnergyPlus was used for the summer period simulation, where free cooling night ventilation was applied and the window was opened at 30% by an area from the time period of 20:00 to 8:00. Two temperature conditions were selected for this analysis:

1. Free floating conditions, where no temperature control is applied.
2. Controlled temperature of 25°C was selected from the time period of 8:00 to 20:00. Cooling loads were measured.

Free floating conditions

From Figure 10 to 12 indoor temperatures with different PCMs used are shown: PT23, PT24 and SP25 with different thickness of the layer. During 5 days of July, from 05.07 to 09.07 were selected for analysis. It is seen that only PCM SP25 had some significant effect for stabilizing the temperature fluctuations and reducing the peak temperatures. Using SP25 with a thickness of 2 mm the maximum peak temperature can be reduced by 2°C, but with a 6 mm layer 3°C. Also there is a trend that proportionally increasing the thickness of the PCM layer, the maximum temperature reduction does not reduces proportionally, but reduces less. It means that it is not reasonable to increase the PCM layer to

4 or 6 mm. It is explained by less effective melting and solidification in the PCM layer.

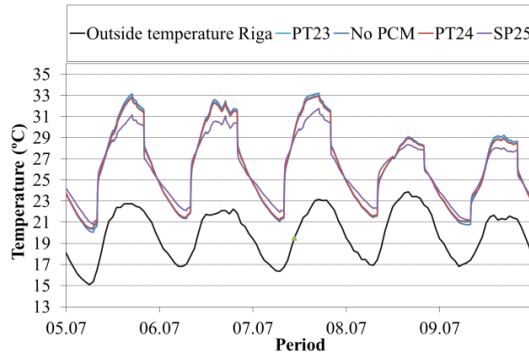


Figure 10. Indoor temperature for Free Floating conditions (PCM layer – 2 mm)

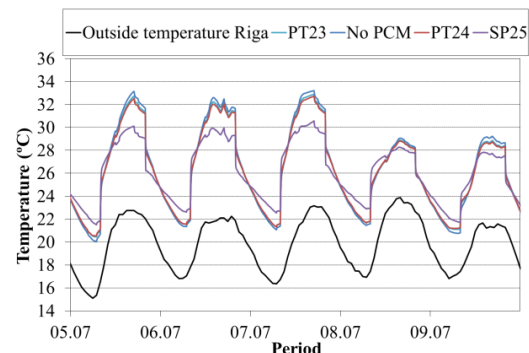


Figure 11. Indoor temperature for Free Floating conditions (PCM layer – 4 mm)

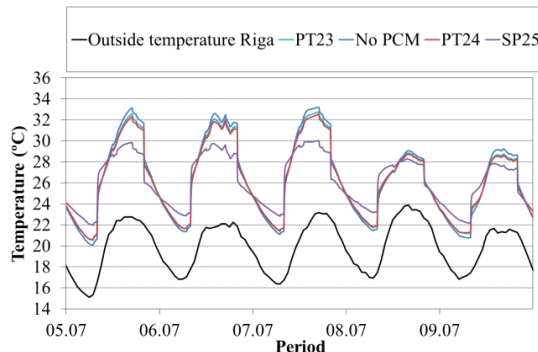


Figure 12. Indoor temperature for Free Floating conditions (PCM layer – 6 mm)

Controlled temperature conditions

To estimate the reduction in cooling loads during summer due to the usage of PCM, summer months, June, July and August were simulated. From Table 6 and Figures 13 to 16, the effects of PCMs can be seen. All three PCMs act similarly with a layer thickness of 2 mm, and reduce the cooling loads maximum to 14.4%. Maximum cooling load reduction can be observed for SP25 with a layer of 6 mm (23.1%). From Figure 16, it can be seen that

a PCM layer of up to 3 mm is the most advisable for a good and effective usage of the PCM material.

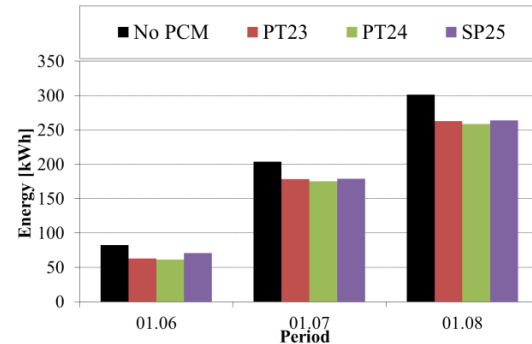


Figure 13. Cooling load for different PCMs (2 mm layer)

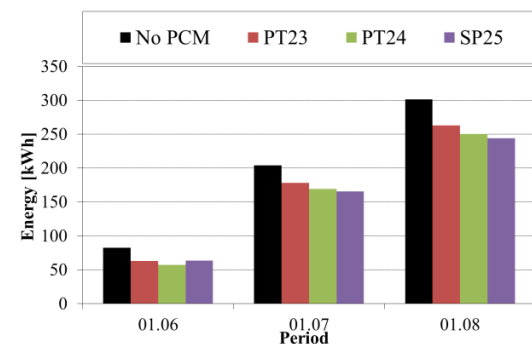


Figure 14. Cooling load for different PCMs (4 mm layer)

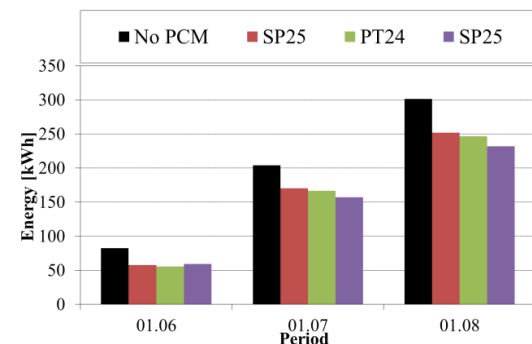


Figure 15. Cooling load for different PCMs (6 mm layer)

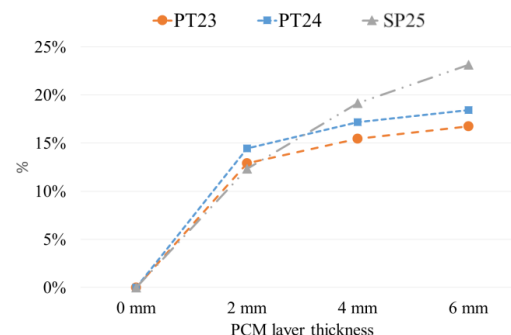


Figure 16. Cooling load decrease for different PCMs and their layer thickness

Table 6

PCM thickness	Cooling demand for different PCMs							
	No PCM		PT23		PT24		SP25	
	kWh	kWh	%	kWh	%	kWh	%	
2 mm	303.12	263.94	12.9%	259.32	14.4%	265.73	12.3%	
4 mm	303.12	263.94	15.5%	251.03	17.2%	245.05	19.2%	
6 mm	303.12	252.32	16.8%	247.20	18.4%	232.97	23.1%	

CONCLUSIONS AND FURTHER WORK

The aim of this work was to verify PCM usage on a real plywood test stand of polygon using theoretical simulation software. The results show, that PCM could be useful for Latvian climatic conditions for passive cooling. PCM usage significantly helps increase thermal inertia of building.

During the summer days in free cooling conditions, using PCM together with night ventilation, a significant indoor temperature peak decrease to 3°C can be achieved.

During the summer days in a controlled temperature of 25°C, conditions using PCM together with night

ventilation, a significant cooling load demand decrease to 23.1% can be achieved.

To make the PCM work more effective a layer of 3 mm is the most advisable.

Different PCMs with different peak temperatures can be incorporated in a building envelope to ensure thermal comfort for different indoor temperatures. Since the summer season is relatively short for Latvian climatic conditions, a detailed analysis of PCM usage during the heating season is required. The next step would be comparison of the results obtained in experiments on similar constructions with theoretical calculations. Such experiments are planned to be carried out in the future for the test of polygon stands.

REFERENCES

- Cabeza L.F., et al., Use of microencapsulated PCM in concrete walls for energy savings, Energy and Buildings, 39 (2006), pp. 113-119.
- Kuznik F. et al., A review on phase change materials integrated in building walls, Renewable & Sustainable Energy Reviews, 15 (2011), pp. 379-391.
- Kendrick C., Walliman N., Removing unwanted heat in lightweight buildings using Phase Change Materials in building components: simulation modelling for PCM plasterboard, Architectural Science Review Volume 50.3 (2007), pp 265-273.
- Kunzel, M., (1995) Simultaneous Heat and Moisture Transport in Building Components. PhD thesis. Wiley IRB Verlag, Stuttgart.
- Latvian Environment, Geology and Meteorology Centre. (2012) Relative, humidity and temperature database. <http://www.meteo.lv/meteorologija-datu-meklesana/?nid=461>
- Ozolinsh A., Jakovich A. (2013) Heat and Moisture Transport in Multi-Layer Walls: Interaction and Heat Loss at Varying Outdoor Temperatures, Latvian Journal of Physics and Technical Sciences. Vol. 49, No. 6, p. 32-43.
- Puretemp technical data. Allowed online:
http://www.puretemp.com/technology_docs/PureTemp%2023%20Technical%20Data%20Sheet.pdf
- Puretemp technical data. Allowed online:
http://www.puretemp.com/technology_docs/PureTemp%2024%20Technical%20Data%20Sheet.pdf
- Romero M.D – Sánchez et al., Phase Change Materials as thermal energy storage incorporated to natural stone. Global Stone Congress (2010).
- Rubitherm technical data. Allowed online:
http://www.rubitherm.de/english/pages/02f_latent_heat_blend.htm
- Schossig P. et al., Micro-Encapsulated Phase-Change Materials Integrated Into Construction Materials, Sol. Energy Mater. Sol. Cells, 89 (2005), pp. 297–306.
- Shrestha M. (2012) PCM Application-Effect on Energy Use and IA temperature, Norwegian University of Science and Tehnology.

Tyagi V.V et al., Development of phase change materials based microencapsulated technology for buildings: a review, *Renewable & Sustainable Energy Reviews*, 15 (2011), pp. 1373–1391.

Zamalloa A. et al., PCM containing indoor plaster for thermal comfort and energy saving in buildings, *Vitoria, Spain*, 2006.

Zhong, Z., Braun, J. E. (2008) Combined heat and moisture transport modelling for residential buildings. *Purdue University, Indiana*.

HEAT INSULATION MATERIALS OF POROUS CERAMICS, USING PLANT FILLER

Aleksandrs Korjakins*, Liga Upeniece**, Diana Bajare***

Riga Technical University, Chair of building materials and wares

E-mail: *aleks@latnet.lv, **liga.upeniece@rtu.lv, ***Diana.bajare@rtu.lv

ABSTRACT

Constantly growing energy prices and concerns about energy supplies in the future, as well as the requirements for regulating gas emissions that produce the greenhouse effect, directs us to search and realize activities allowing the reduction of energy consumption and to reach a higher energy efficiency level. Heat insulation is one such procedure for energy efficiency improvement, by reducing energy consumption in the construction field. New ecological heat insulation materials, which are made from local raw materials, can serve as an alternative for heat insulation materials already existing in the market, using clay as a binder in its production, but hemp and flax and shovels are used as burnable fillers, thus obtaining material with the necessary heat and acoustic insulation qualities, as well as fire-resistance and chemical stability in an aggressive environment and providing to the development of industries in Latvia.

In order to reduce thermal conductivity of ceramic materials, it is necessary to increase its porosity which can be realized by the usage of gas forming additives, for example, calcite and magnesite, but the second variant is to add burned out additives thus forming porous ceramics. Within this research, agricultural waste is used for the production of porous ceramics, which have not been sufficiently used for the production of construction materials with high added value in Latvia.

The aim of the research is to develop porous ceramic materials, using plant burnable filler with certain properties due to their resistance and density, based on world achievements, as well as the experimental investigations. In the present paper, the evaluation of practically obtaining material which could be used for heat insulation of buildings has been done.

The porous ceramic materials with burnable plant filler are being developed in the present investigation. The dependences, the mechanical and physical properties of porous ceramics are defined in accordance with the amount of filler, glass and the amount and size of pores, have been performed.

Key words: porous ceramics, ecological materials, insulation materials, agricultural waste, plant filler

INTRODUCTION

In the result of energy demand growth, power dependence from countries which supply primary power resources, is also increasing both in Latvia and in other European countries. Besides the growth of power dependence, worries about an unstoppable increase of energy costs in the future also extend, as well as an increase of gas emissions creating the greenhouse effect. This leads us to the realization of events that would allow us to reach an adequate level of energy efficiency, as well as promote the decrease of energy resources consumption in all sections of economic activities, including the construction branch where a greater part of energy resources are consumed for creating heat supply.

Although the speed of construction in the Baltic States has significantly slowed down during recent years, the interest in increasing the energy efficiency for building refurbishment in the public and private sector is growing.

Besides the above mentioned, society's interest about environmental and health are also issues. Understanding the importance of the quality of their surroundings, people are beginning to pay more attention towards their consumption patterns and the related potential impacts on the environment

and their health, with concerns for the wellbeing of the current as well as future generations. (Indriksone et al., 2011)

Considering both of the above mentioned modern tendencies, selection of "green" or ecological materials in the building of new houses and the building renovation process, serves as a solution for energy resource reduction not being harmful to the human health.

Municipalities and other public bodies in the Baltic States also increasingly often consider including environmental criteria or requirements for construction materials in public procurements.

Responding to this interest, producers and retailers of materials offer a wide selection of different materials to try and satisfy this demand.

Thus "ecological", "environmentally friendly", "sustainable", "green" - are popular terms used frequently nowadays by producers/retailers of materials to advertise their products. (Indriksone et al., 2011).

Using green building materials and products promotes conservation of dwindling nonrenewable resources internationally. In addition, integrating green building materials into building projects can help to reduce the environmental impacts associated

with the extraction, transport, processing, fabrication, installation, reuse, recycling, and disposal of these building industry source materials. All the materials used for construction of buildings must not harm the environment, pollute air or water, or cause damage to the earth, its inhabitants and its ecosystems during the manufacturing process, and also during use or disposal after their end of life. Materials should be non-toxic and contribute to good indoor air quality.

Using environmentally friendly building materials is the best way to build an eco-friendly building.

The following criteria can be used to identify green materials:

- a) Local availability of materials.
- b) Embodied energy of materials.
- c) Percentage of recycled/waste materials used.
- d) Rapidly renewable materials.
- e) Contribution in the Energy Efficiency of buildings.
- f) Recyclability of materials.
- g) Durability.

h) Environmental Impact (Tudora, 2011).

Porous ceramics can be used as one such ecological materials produced from local raw materials, where macro-pores are obtained using plant scorched fillers, thus the clay, hemp and flax shoves which are agricultural waste-products are mainly used for the production of material.

Flax is a versatile crop that supplies both fiber and seed for important industrial applications (Domier 1997). Flax shive is the woody, lignified inner tissues of the stem and is a by-product of fiber production. Flax fiber constitutes about 25 – 30% of the stem. Therefore, a large amount of shive is available after fiber processing. (Marshall et al., 2007). With estimates of 1 million tons of flax straw available from linseed production (Dormier, 1997) about 700.000 tons of shive could be available for a variety of uses. (Marshall et al., 2007). Traditionally flax shive is considered a waste product and as such has a limited value or is used in low-value applications such as animal bedding and burning for thermal energy (Sankari, 2000, Sharma, 1992)

Hemp is a fast growing, multi-purpose, annual herbaceous plant and almost all parts of this plant are used for processing different products. Up to now the most commonly produced and used parts are the fibers and seeds, but shoves in most cases are considered as by-product and burned or used as animal bedding, mulch, compost or a chemical absorbent.

However, in recent years, investigations of hemp shoves showed that the usage could be much wider and that they could be used in new, more high-quality products with higher added value.

Nowadays hemp shoves are used in a wide range of applications such as paper, packaging, plastics and polymers, building materials (insulation, fiber board, hemp concrete) and construction products etc., which create a more viable market with new and high-quality products from hemp shives.(Stikute et al., 2012)

Besides hemp and flax shoves, wood chips, chaff, straw, wheat bran, bark and others (Kumaoka et al., 2000) also can be used as scorched fillers, in order to produce porous ceramics. Kumaoka, 2000).

Porous ceramics are now expected to be used for a wide variety of industrial applications from filtration, absorption, catalysts and catalyst supports to lightweight structural components. (Ohji and Fukushima, 2012). Therefore their usage is natural also in the production of building materials, which has been researched in Latvia and the whole world, but has not been sufficiently and highly evaluated where the determinant role of the sphere of porous ceramics is directly related to its qualities.

The properties of porous ceramics can be tailored for specific environmental application by controlling the composition and microstructure of the porous ceramic. Changes in open and closed porosity, pore size distribution and pore morphology can have a major effect on the material's properties. All of these microstructural features are in turn highly influenced by the processing route used for the production of the porous material. For the mechanical properties, porous ceramics are determined by their structure parameters, such as porosity, pore size and pore structure (Hong et al., 2012, Gough et al., 2004). Additionally, the microstructure of the solid phase related to neck growth and solid phase continuity strongly affect the mechanical properties. (Stuart et al., 2006, Koh et al., 2006, Hong et al., 2012).

By the production of porous ceramics within the scope of this research, its qualities are regulated by varying the amount and type of the material used which has an impact on the structure of this ceramics. Planned pores are obtained in an irregular, elongated form because of the usage of hemp and flax shoves. Wood chips are historically the most popular and widely used burn-out filler.

Usage of woodchip as the burnable filler in the production of porous ceramic has been widely researched in Latvia, obtaining samples with a strength of 10 to 12 MPa in a density up to 1.5 g/cm³, by using 25% woodchip and burning the clay at a 950 – 960 °C temperature, (Sedmale et al., 2009), as well as elsewhere in the world, e.g., studies in order to assess the impact of the porous ceramic material porosity were performed at the Federal University of Kazan.

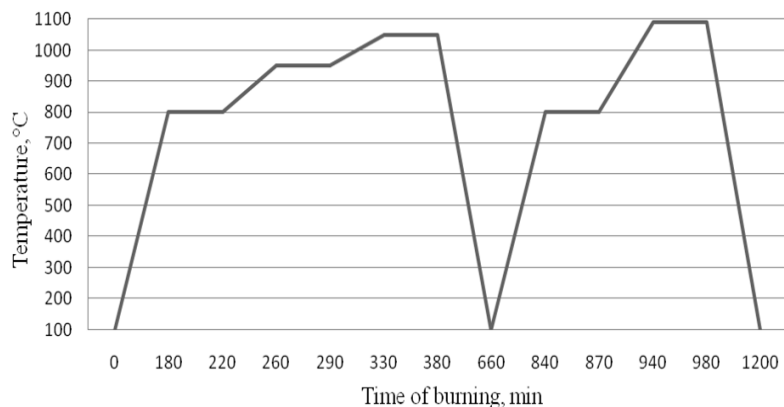


Figure 1a. The regime of sample burning 2 times

During this study, multiple samples were obtained for the purpose of pore formation, additives such as woodchips and cottonstone were used.

in series, obtaining samples that were up to 17 MPa strong upon compression (Salahov A. et al., 2011) Production of a porous ceramic material with specific features of strength and density, achieving a material that could be used to insulate buildings is the main aim of this research.

MATERIALS AND METHODS

During the stage of the sample preparation process, ceramic slurry was made, Lode clay with a humidity level of 24 % as well as ground glass and organic filler – hemp and flax shoves were used.

By preparing samples using plant fillers, such as burnable fillers, wood chips and hemp/ flaxen shoves from Kraslava region Piedruja parish, which were sieved beforehand in order to deselect admixtures of large scale, like flinders, shingles, chunk wood, as well as admixtures of organic and mineral origin, like soil and sand were used. The size of shoves used in the survey did not exceed 5 mm. Characteristics of shoves:

- Poured volume density range from 50 kg/m³ to 80 kg/m³;
- Admixture of long grain in shove mass does not exceed 8 % of the volume unit;
- Colour: Greyish green for hemp shoves, greyish yellow for flax shoves;
- With humidity level not exceeding 12 % of mass;
- There are no signs of mold on the shove surface or signs of biological degradation of shove mass.

In the beginning Lode clay was dried in a drying oven, and ground in RETSCH PM 400 mill for 30 minutes in dry condition.

When the all required components – clay, glass and hemp and flax shoves are prepared, they are dosed in the required amount and mixed in dry condition, gradually adding water until a sufficiently homogenous mixture for sample making is obtained.

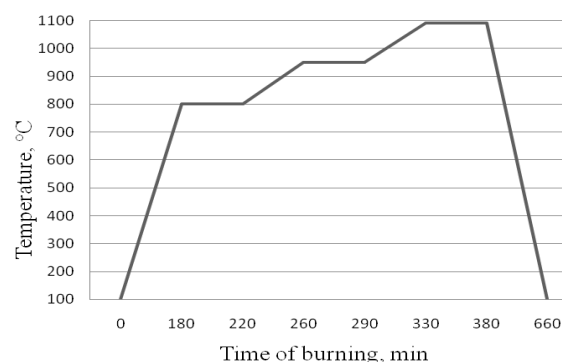


Figure 1b. The regime of sample burning 1 time

Proportion of dry clay, glass, burnable filler and water used in the investigations varied, changing the amount of glass, and amount of shoves in order to obtain larger amount of shoves in the mixture – resulting in samples with greater porosity.

Components of dry mixture are dosed according to mass, where dry, milled clay is 50 – 65 %, glass 15 – 25 %, but the burnable filler 20 – 25 %. When the dry mixture has been mixed, water is added in the amount of 35-45% from the mass of mixture.

The volume of added water shall be chosen so that it provides both the viscosity of the required mixture and strength of the obtained samples as well as probably decreasing shrinkage and energy consumption for the sample drying.

Squared samples with the side length of 100x100mm and height of 30 – 35 mm were made, which were dried without additional loading under pressure for 8 hours at a temperature of 60 °C.

By the analysis of the information available in the literature and foreign researches, it was selected that samples were burned gradually one or two times at a temperature of up to 1090 °C, for 11 – 20 hours in total.

The regime of sample burning one time is presented in Figure 1b. The regime of sample burning two times is presented in Figure 1a.

The regime of sample drying as well as burning was chosen so that time and energy resources required

for material development are minimal, but sufficient enough to provide obtaining the of material with certain properties in the end result.

Verification of samples developed using plant fillers was realized by ZWICK Z100 perpendicular to the formation direction of the samples, thus providing the establishment of a mean strength in the cross section, reducing the influence of certain weakening, which could have been formed while the samples were removed from the moulds and a non-homogenous structural density in the direction of cross section formation.

RESULTS AND DISCUSSION

The results of the research reflect on the existing and common raw material in Latvia – clay and its broad application opportunities for building material production by regulating its mechanical and physical properties with the addition of burnable plant fillers and ground glass.

Used raw materials provide acquisition of necessary properties of porous ceramics where clay serves as a cohesive substance, but glass provides higher strength and better cohesion between mixture and plant fillers within the sample formation process.

The samples with the amount of shoves 5-30% were made. The main aim of the experiment was to improve compressive strength parameters, which resulted in higher density. Maximum and minimum values of density of samples depending on the amount of used shoves are summarized in Figure 2.

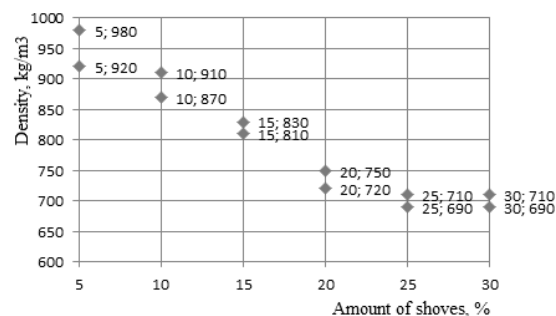


Figure 2. Volume density of samples depending on the amount of used hemp/flax shoves

Density of samples can be easily regulated, by changing the amount of fillers used. But increasing the quantity of shoves, the amount of water needed for the mixture, in order to obtain a plastic mass also increases, and in the result the time and contraction necessary for drying increases but reduces compressive strength.

Samples, in which the quantity of shoves reaches 25% - 30% and more, have low compressive strength, and a respective amount of ground glass must be chosen in further researches, in order to increase it. Compressive strength also can be increased by double burning of the samples,

choosing a higher temperature and shorter period in the second time. This topic will be studied more widely in further researches.

Weight of samples decreased per 32.1% to 38.7%, after burning. Size of samples, comparing it before and after burning, decreased per 8-12% per edge length and per 2-6% per thickness.

By comparing sample compressive strength, higher strength was observed for the samples where amount of used glass filler reached 25-30%. The highest compressive strength was 2.28 MPa for samples with content 20% of hemp/flax shoves. In comparison with previous researches, where compressive strength is 0.97 MPa, using 15% of glass, it can be seen that a greater amount of glass provides higher compressive strength. By using 40% of grinded glass in previous research for making of samples, compressive strength was 3.95 MPa was obtained, but porosity of the samples was too low.

During the control of ceramic material, water-absorption varied from 25.8% to 29.3 %.

Using hemp and flax shoves as burnable filler, macropores (Fig.3.) and micropores, shown in figure 4, can be seen within the structure of porous ceramics, where macropores have an elongated irregular form and the measure of pores in obtained the plant matrix samples is 0.033 – 1.7 mm.

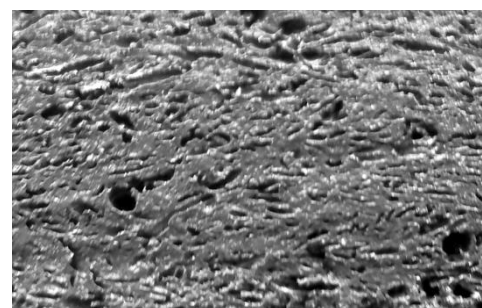


Figure 3. Macropores of porous ceramics

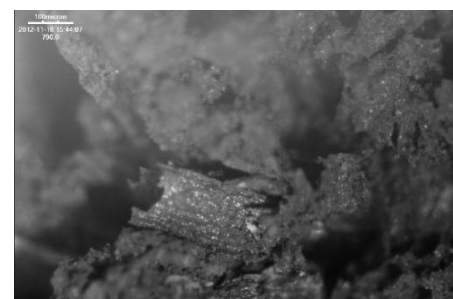


Figure 4. Micrograph of pores for samples which are made by plant fillers burning method

In comparison with the other methods for obtaining porous ceramics, this method is technologically the simplest one and has been researched more widely, allowing samples to be produced with definite porosity, but not reaching the regular form of pores.

The greater advantage is the availability and wide distribution of these raw materials.

Hemp and flax shoves used in this research which are burned during the process of burn, allow porous ceramics to be obtained with a heterogeneous porous structure, which is linked to the complex additive distribution and orientation in the volume of the sample.

By comparing this method with the other methods for obtaining porous ceramics, we can see that this method minimally limits the sizes and dimensions of obtainable samples, thus allowing production of oversized blocks, but the variation of form is not so wide as in the case when scorched filler polymer sponge is used.

In further studies of this research it is important to study and compare the impact of the sample burning regime and number of burning times and their strength, as well as to reach a higher level of sample strength without a significant increase of their volume-mass.

Usage of hemp and flax shoves in the production of porous ceramics allows us not only to produce the material itself, but also to utilize agricultural waste, which serves as the reason why hemp and/or flax fiber is used in this research, which is a valuable raw material for the production of materials with high added value in the heat insulation plate manufacturing, the textile industry and other branches.

In line with the conducted research, the addition of ground glass improves the strength of the obtained samples.

Moreover, it reduces the temperature necessary for burning as well as the amount of clay required, thus enabling to save on natural resources through an effective recycle of the glass waste.

CONCLUSIONS

Within this research samples of porous ceramics were made using clay as a matrix and scorched hemp and flax shoves in the process of pore creation.

Weight of ceramic samples decreased per 32.1% to 38.7% after burning process. Shrinkage of samples was in the range per 2-6% per thickness to 8-12% per edge length that may be explained by influence of orientation plant fillers in the samples after mixing process.

The highest compressive strength was 2.28 MPa for samples with content 20% of hemp/flax shoves and 25-30% ground glass fillers.

Water-absorption of the porous ceramic samples varies from 25.8% to 29.3 %.

Using hemp and flax shoves as burnable filler, created micropores and macropores have elongate, irregular form with sizes in the range 0.033 – 1.7 mm

Obtained samples of porous ceramics are ecologic, produced from local raw materials and waste, breathable, resistant against aggressive environment and durable.

REFERENCES

- Domier K. W. (1997) The current status of the field crop: Fibre industry in Canada, *Euroflax Newsletter*, No. 8, p. 8-10.
- Gough J.E., Clupper D.C., Hench L.L. (2004) *Journal of Biomedical Materials Research*, Vol. 69, p.621-628.
- HongC., Zhang X., Han J., Meng S., Du S. (2012) Synthesis, Microstructure and Properties of High-Strength Porous Ceramics, *Ceramic Materials – Progress in Modern Ceramics*, Pro. Feng Shi (Ed.), ISBN: 978-953-51-0476-6, InTech, p.109-110.
- Indriksone D., Bremere I., Aleksejeva I., Gratz M., Oisalu S., Svirskaitė J.,(2011) Using ecological construction materials in the Baltic States, *recommendations on using ecomaterials*, Baltic Environmental Forum, Latvia, p. 4.
- Kumaoka S.A.S. (2000) Porous ceramics provided with amorphous pore surfaces, *United States Patent No. US 6,420,292 B1*, p.16.
- Marshall W.E., Wartelle L.H., Akin D.E. (2007) Flax shive as a source of activated carbon for metals remediation, *Bioresources*, No. 2, p. 82-90.
- Koh Y.H., Lee E.J., Yoon B.H., Dong J.H and Kim H.E. (2006) Effect of Polystyrene Addition on Freeze Casting of Ceramic/Camphene Slurry for Ultra-High Porosity Ceramics with Aligned Pore Channels, *Journal of the American Ceramic society*, Vol. 89, p. 3646-3653.
- Ohji T., Fukushima M. (2012) Macro-porous ceramics: processing and properties, *International Materials Reviews*, Vol 57, No. 2., p. 115-131.

Salahov A., Tagirov L., Salahova R., Parfenov V., Ljadov N. (2011) Поры и прочностные характеристики строительных материалов, [Characterization of building material pore and strength], Строительные материалы No. 12, p. 25 -27.

Sankari H.S. (2000) Linseed (*Linum usitatissimum* L.) cultivars and breeding lines as stem biomass producers, *Journal of Agronomy and Crop Science*, No.184, p.231-235.

Sedmale G., Cimmers A., Sedmalis U. (2009) Characteristics of illite clay and compositions for porous building ceramics production, Riga Technical University, ISSN 1392 -1231, *Chemeine Technologija*, Vol. 2, p. 18-21.

Sharma H.S.S. (1992),Utilization of flax shive, *The Biology and Processing of Flax*, M Publications, Belfast, Nothern Ireland, p 537-543.

Stikute A., Kukle S., Shahmenko G. (2012) Latvian Grown Hemp Shives Processing Possibilities into Products with Added Value, In: *Sustainable business in changing economic conditions*, Proceedings of XIII International Science conference, p. 319-325.

Studart A.R., Gonzenbach U.T., Tervoort E., Gauckler L.J. (2006) Processing Routes to Macroporous Ceramics: A Review, *Journal of the American Ceramic society*, Vol. 89, No. 6, p. 1771-1789.

Tudora A.C. (2011) Assessments criteria of building materials from ecological point of view, *Bulletin of the Polytechnic Institute of Jassy*, Construction and Architecture section, p.130-131.

THERMAL CONDUCTIVITY OF WALLS INSULATED WITH NATURAL MATERIALS

Martti-Jaan Miljan*, Matis Miljan**, Jaan Miljan***

Estonian University of Life Sciences, Department of Rural Engineering

E-mail: *martti.miljan@emu.ee, **martti.miljan@emu.ee, ***jaan.miljan@emu.ee

ABSTRACT

Using of natural renewable and recyclable materials enables us to construct a comfortable space to live in. The aim of this investigation was to research thermal transmittance and relative humidity of wall fragments with different structures and insulation. Tested wall fragments were built into window openings of an actual outside wall. All the materials used were natural: wood, lightweight clay blocks, reed and straw bales, loose hemp chips and reed. Walls were rendered with clay plaster. Thermal transmittance and relative humidity were measured in four different wall structures during two years. Sensors for measuring temperature and humidity were placed at several points, for one item between the insulation and clay plaster layers. On the basis of the research it may be concluded that it is possible to fulfil minimum energy performance requirements using natural insulation materials and based on the values of the observation period it can be concluded that there was no water condensation in the wall structure. Therefore there was no threat of biodegradation.

Key words: natural construction materials, insulation with loose reed and hemp chips, lightweight clay blocks, reed and straw bales, clay plaster, thermal transmittance, relative humidity

INTRODUCTION

The use of local construction materials enables us to create a living environment many people strive for. People want to live in an environment with a healthy room climate, the creation of which would harm the surrounding nature as little as possible.

Over the centuries, people in Estonia have used local natural materials (timber, clay, reed), as well as residual materials resulting from the processing thereof (sawdust, flax shives, straw) in construction. Local materials are, in general, renewable, recyclable and, if necessary, easily disposable. These materials are predominantly used in the areas of mining or growing thereof – hence less energy is used to transport these materials. The effect of the use of such construction materials and such ways of construction is minimal to the surrounding environment.

With the use of artificial materials in the 20th century many of the local construction materials lost their importance and gradually people lost the ability to use them properly in construction. Recently more and more importance has been paid to an environmentally friendly and sustainable way of life and therefore people have started to look for alternatives to energy-intensive construction materials produced of non-renewable resources. Hence people have rediscovered local natural construction materials, including natural thermal insulation materials.

Natural construction materials have been studied at the Department of Rural Engineering of the Estonian University of Life Sciences for more than 30 years. In recent years this trend has gained priority, especially in the use of thermal insulation materials, as increasing attention is being paid to

the thermal insulation of buildings. Also, valid laws, regulations and norms set higher requirements for the thermal resistance of enclosures.

However, there is relatively little data in the literature as regards to the heat engineering characteristics of natural thermal insulation materials, hence it was extremely interesting to examine the operation and thermal resistance of enclosures insulated with natural materials and different structural solutions.

MATERIALS AND METHODS

The Department of Rural Engineering of the Estonian University of Life Sciences carried out a test in order to compare the thermal conductivity of outer walls of different structural solutions and use of material. The test was carried out in the framework of the University's baseline financing of scientific research and the Interreg IV-A project ProNatMat. The results of the tests form a basis for consulting people who use natural materials to construct buildings and give them specific recommendations as regards the use of certain materials in external enclosures.

In order to imitate the functioning of a structure truthfully in actual circumstances of the building, measurements were made on the object all year round and the test was carried out in the window openings of the laboratory of building structures. The windows were removed and four different external wall models were built in the openings using different structural solutions (figure 4a).

Test wall S1. A 130 mm thick masonry wall of flax shives and light clay blocks (figures 1 and 4b) was built in the first window opening. Wood planks of 220 x 50 mm were attached to the outer side of the

masonry wall and hemp chips were used as a thermal insulation material to fill the gap between the planks. Then 25 mm boarding was nailed on the planks and that was in turn covered with windproof film. An approximately 5 mm thick sparse reed panel was fixed to the inner surface of the wall. The wall was then covered with clay plaster inside and outside.

Test wall S2. In the next window opening vertical boards were installed on the external and internal surfaces of the existing wall, the window opening was filled with horizontally placed reed and thickened both horizontally as well as vertically (figures 2 and 4c). The wall was covered with about 50 mm thick clay plaster both inside and outside.



Figure 1. The building of a test wall of light clay blocks (wall S1)



Figure 2. The building of a test wall of horizontal reed (wall S2)

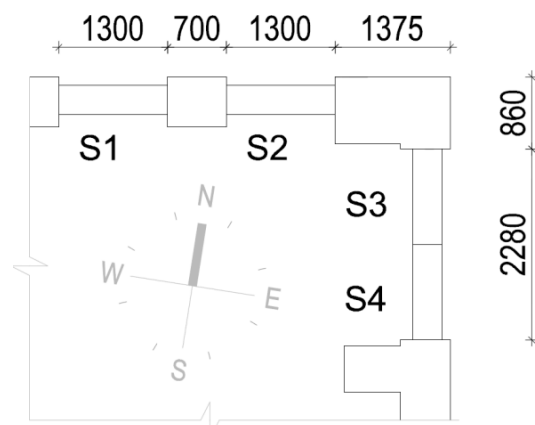
Test walls S3 and S4. The third window opening was wider and two walls of different material were built there (figures 3, 4d and 4e). The third and fourth walls were built of 450 mm thick straw and reed bales. The bales were additionally tightened with capron strips. The outer and inner surfaces of the walls were covered with 50 mm thick clay plaster.



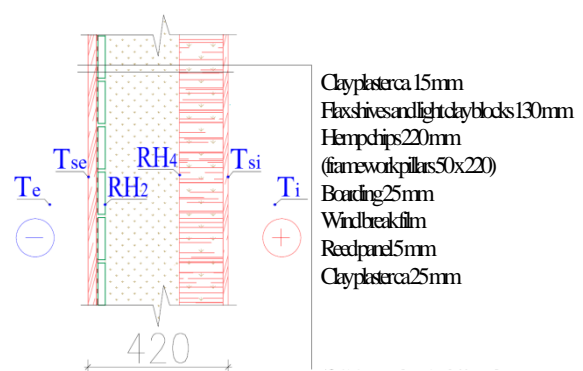
Figure 3. The building of a test wall of straw and reed bales (walls S3 and S4)

The wall structures are shown in figure 4. During construction, sensors were placed inside the walls to measure temperature and humidity.

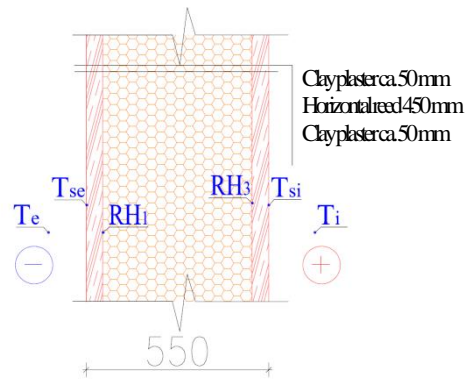
a) locations of the walls



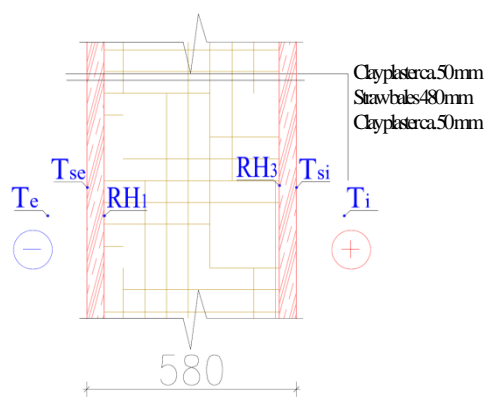
b) S1 – wall built of light clay blocks insulated with hemp chips



c) S2 – test wall built of horizontal reed



d) S3 – test wall built of straw blocks



e) S4 – test wall built of reed blocks

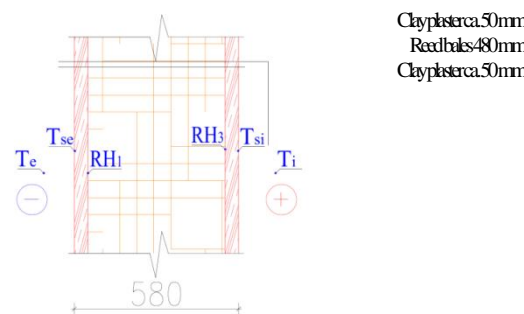


Figure 4. Test walls in the window openings of the laboratory of building structures: a) locations of walls; b)–e) cross-sections of test walls

After the completion and drying of the walls, temperature and humidity sensors were placed inside the wall to measure the characteristics of inner and outer surface and the indoor and ambient air. To measure the heat flux transmitted through the wall, heat flow measuring plates were adhered tightly to the wall (figure 5). All readings were recorded with a 15-minute interval in an Almemoo data recorder.



Figure 5. Heat flow plates to measure the heat transmittance and thermocouples to measure the temperature of surfaces of the wall

The following characteristics were measured to determine the thermal transmittance of the wall:

q – heat flow through the wall [W/m^2];
 T_e – outdoor air temperature [$^\circ\text{C}$];
 T_{se} – temperature of the outer surface of the wall [$^\circ\text{C}$];
 T_{si} – temperature of the inner surface of the wall [$^\circ\text{C}$];
 T_i – room temperature [$^\circ\text{C}$].

Based on the readings from the measuring instruments the thermal transmittance U [$\text{W/m}^2\text{K}$] of the walls was calculated:

$$U = \frac{q}{T_i - T_e}. \quad (1)$$

CONCLUSIONS

The test period lasted from December 2009 to May 2011. The measurements were made in a non-steady-state, *i.e.* the temperatures changed continuously in time and hence the heat flow through the wall varied. The data gathered as regards the measuring period can be visualised. The programme also enables thermal transmittance graphs that alter in time to be calculated and printed (Figure 6).

Figure 6 shows data received during the test period with the monthly average values calculated. The data shows clearly that thermal resistance is the best in test wall S2, *i.e.* in the wall insulated with horizontal reed bundles, and the worst in test wall S1, *i.e.* the wall built of light clay blocks insulated with hemp chips.

During the first winter the thermal transmittance decreased remarkably due to the drying of the material (clay plaster). Next year the U -value was more stable.

Based on test data the average thermal transmittance of the test walls was also calculated from October 2010 to March 2011. The results are shown in figure 7.

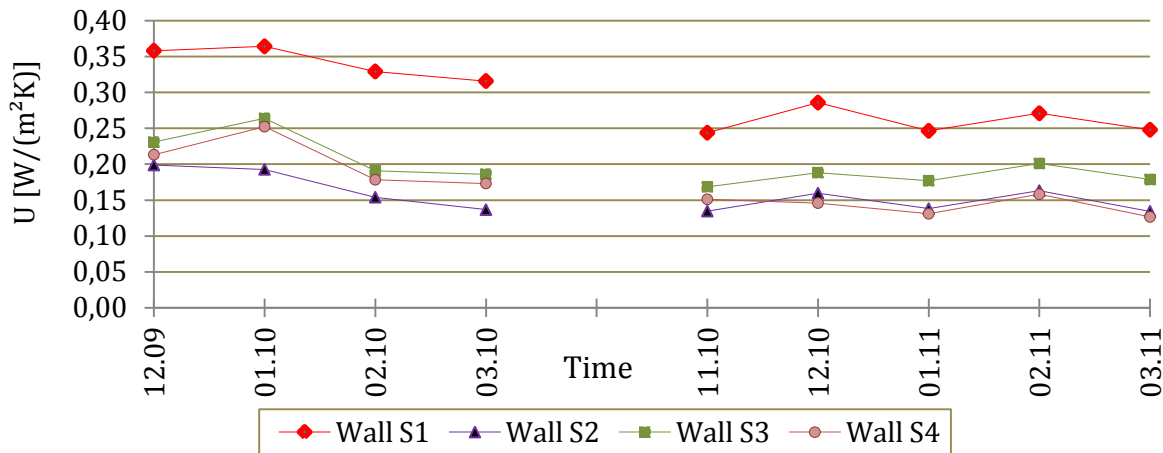


Figure 6. The thermal transmittance of different test walls, taking into account the average value in the period from December 2009 to May 2011

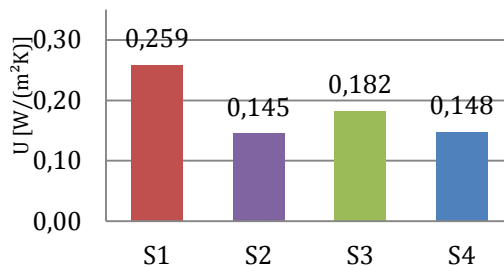


Figure 7. Thermal transmittance of test walls

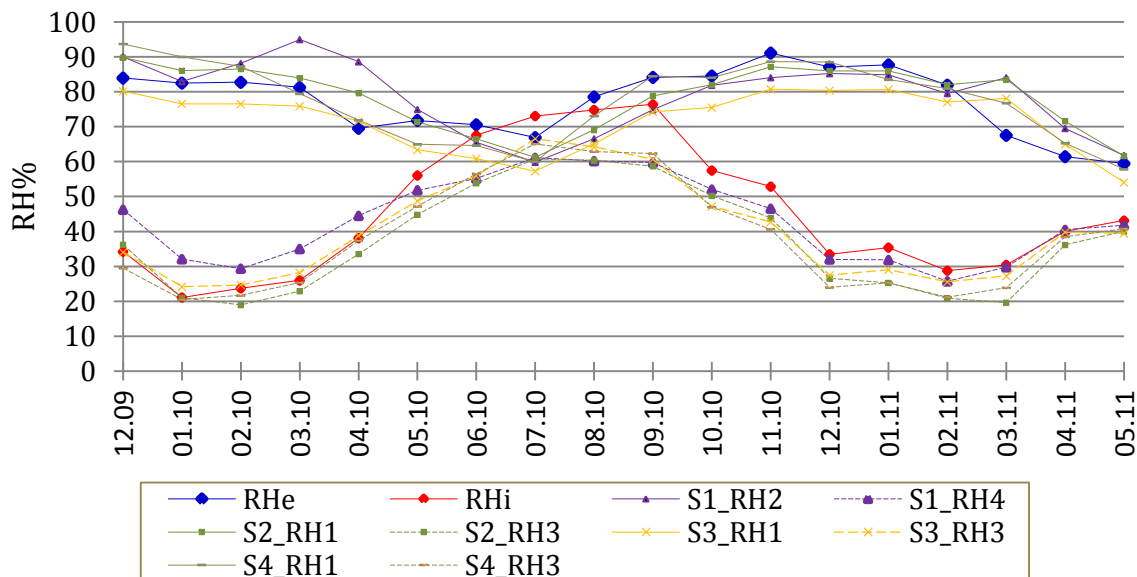


Figure 8. The relative humidity of various test walls [RH%], taking into account the average monthly value from December 2009 to May 2011 in the different layers of the walls

According to the government regulations of the Republic of Estonia Minimum energy performance

requirements the thermal transmittance value of outer walls must be at least 0,2–0,5 $\text{W}/(\text{m}^2\text{K})$ (RT

I:2007). The test results show that only one test wall (S1) does not conform to this requirement of the regulations, which, taking into account the thickness of test walls, is not at all surprising. Based on the tests carried out it can be said that natural insulation materials compete well with their insulation characteristics with artificial insulation materials and these can be successfully used in practice. When using local thermal insulation materials one needs to use thicker layers of insulation, but due to the smaller primary energy content of the material we are friendlier to nature and there are less emissions of greenhouse gases. Figure 8 shows the ratio of the percentage of relative air humidity of the walls to the level of saturation as a monthly average value in the period of December 2009 to May 2011.

The values of relative air humidity were measured at the points between the insulation and clay plaster layers in order to see whether the wall structure is saturated with humidity at that point. The line RHe shows RH changes between the outside clay plaster and the wall structure and the line RHi shows the same between the inside clay plaster and the wall structure. Based on the values of the observation period we can conclude that there was no water condensation in the wall structure.

The investigation of hygrothermal state done by the Austrians show also that there was no water condensation inside the wall and thereof no threat of biodegradation of the natural wall insulation materials due to the clay plaster layer. (Wegerer, P., Bednar, T. 2011).

REFERENCES

- The State Gazette I 2007, 73, 445, the Government of the Republic of Estonia '*Minimum energy performance requirement*'
- Wegerer P., Bednar T. 2011 Long Term Measurement and Hygrothermal Simulation of an Interior Insulation Consisting of Reed Panels and Clay Plaster. Proceedings of the 9th Nordic Symposium on Building Physics NSB 2011, Vol. 1, p. 331-338

APPLICATION OF ULTRASONIC IMAGING TECHNIQUE AS STRUCTURAL HEALTH MONITORING TOOL FOR ASSESSMENT OF DEFECTS IN GLASS FIBER COMPOSITE STRUCTURES

Marija Masonkina,

Bc. Sc.ing., assistant

Kaspars Kalnins,

Dr. Sc. ing., leading researcher

Institute of Materials and Structures, Riga Technical University

Address: Āzenes street 16, LV-1048, Riga, Latvia

Phone: +371 67089164, Fax: +371 67089254

E-mail: masonkina@gmail.com

ABSTRACT

Structural Health Monitoring (SHM) is non-destructive testing technique which implements a damage detection and characterization strategy for engineering structures. It is widely applied for rapid condition screening with the aim to provide reliable information regarding the integrity of composite structures. Key elements of the system's functionalities include detection of unanticipated structural damage events, damage location identification and characterization through images, monitoring damage growth and enabling a feedback action/alarm mechanism. Fiberglass composite materials are becoming widely utilised in the design of wind energy structures because of their performance in terms of high moduli, high corrosion and fatigue resistance, and low weight. Nevertheless the damage assessment by means of ply delamination causing stiffness and strength reduction is required by both industry and certification societies. In current research the ultrasonic imaging technique is considered as the most efficient method employed for quality control and damage growth inspection by means of ultrasound B - and C - scans for visualization and direct estimation of the nature, structure and spatial distribution of the defects in GFRP structures. More than fifty impact caused damage GFRP samples with artificial damage have been produced for the assessment study. A current research resulted in systemisation of damage and delamination identification means in glass fibre reinforced composite panels.

Key words: ultrasonic imaging technique, glass fiber reinforced composites, defects visualization, structure analysis

INTRODUCTION

Due to high cost/performance properties glass fibre reinforced plastics (GFRP) are becoming more popular in civil engineering. Areas of application include aircraft, car and marine industries. GFRP main advantages are their low cost, low weight, good thermal and acoustic insulation, low fatigue and corrosion levels (Hasiotis et al., 2011). Damage in composite structures in the form of cracks or delamination will lead to a significant loss in strength and failures in performance of the structures.

There is a large number of non-destructive testing and non-destructive inspection techniques for identifying local damage and detecting incipient failures in critical structures. Among them, ultrasonic inspection is well established and has been used in the engineering community for several decades (Giurgiutiu, Cuc, 2005). The ultrasonic method as non-destructive analysis method is very important in many industries because it allows detecting defects inside the material. SHM is extremely important and essential in various areas, including aerospace, automotive, energy, civil and mechanical engineering. Ultrasonic inspection is

frequently applied in electrical and electronic components manufacturing, in powder metallurgy, production of metallic and composite materials and in the fabrication of structures such as airframes, piping and pressure vessels, ships, bridges, motor vehicles, machinery and jet engines (Hasiotis et al., 2011; Turo et al., 2013). Ultrasonic tests even can be applicable for archaeological purposes (El-Gohary, 2013).

There have been several ultrasound technologies developed recently, which can be employed for both in the laboratory and in-service inspections. For example, Zike et.al. (Zike et al., 2011) applied ultrasonic inspections to evaluate rupture and delamination and also to compare experimental and simulation results, whereas Bartoli G. with a team applied ultrasonic tests to measure high propagation velocity in stone columns, which allowed them to judge the internal damage and evaluate the dynamic modulus of elasticity of the columns (Bartoli et al., 2012). This makes the ultrasound structural health monitoring one of most effective tool's in the market. Key elements of SHM system functionalities include detection of unanticipated structural damage events, damage location

identification and characterization through images, monitoring damage growth and enabling feedback action/alarm mechanism. SHM is extremely important and essential in various areas, including aerospace, automotive, energy, civil and mechanical engineering (Pisupati, 2009).

The pulse-echo method is the most widely used ultrasonic method. A pulse of ultrasonic energy is transmitted into the specimen, and then the energy is transmitted from the specimen into the transducer an echo. The pulse is reflected from good matrix reinforcement boundaries and also from boundaries associated with flaws. Those signals which travel back towards the probe are detected and the position and size of a flaw is determined from the total pulse travel time and detected amplitude respectively. This method is very often used for flaw location and thickness measurements. The B-scan display, a 2D slice through a specimen, is produced by scanning the probe along the surface. The C-scan display records echoes from the internal portions of test pieces as a function of the position of each reflecting interface within an area (Hasiotis et al., 2011; Shull, 2002; Kapadia..., 2013).

In the present paper, the size of the damage and damage propagation at different plies among thicknesses in glass fibre reinforced composites were inspected and visualized with the ultrasonic technique.

MATERIALS AND METHODS

Glass fibre/epoxy composite materials were used in the present investigation. Specimens were prepared with two manufacturing methods: hand lay-up (HL) method and vacuum infusion (VI) method.

Laminates were manufactured with different thickness and directions of fibre in order to assess the difference both from textile procession and specimen preparation technology. The INSTRON Dynatup 9250 HV impact tower was employed to cause artificial impact defects in composite materials. The impact nozzle used in investigation has a 20 mm diameter.

The ultrasonic inspection of specimens was made by applying the Pulse-Echo method. A 3 mm diameter pulse-receiver flat transducer of 20 MHz from PANAMETRICS was applied and the inspection was made with the specimens fully immersed in water. The ultrasonic device utilised for NDT inspection was HILLGUS USPC 3010HF. Oculus software was also used for data acquisition, control and imaging. A current Ultrasonic transducer has the ability to record 20,000 amplitudes of signal and 10,000 travel time values per second.

RESULTS AND DISCUSSION

To measure impact defect distribution in composite materials ply by ply analysis was carried using the ultrasonic imaging technique. Achieved images of selected layers of specimen 1 are shown in Figure 1. Images show a complex layer characterization of the impact defect. With the Oculus software it is possible to evaluate the size of the defect. For specimen 1, overall size of the impact is 24.4 x 24.7 mm. Defect shape and size distribution in different layers shown in Figure 2. From this image it can be seen, that the diameter of the flaw increases towards the back side of the impact for about 10 mm. This behaviour is noticeable in all specimens.

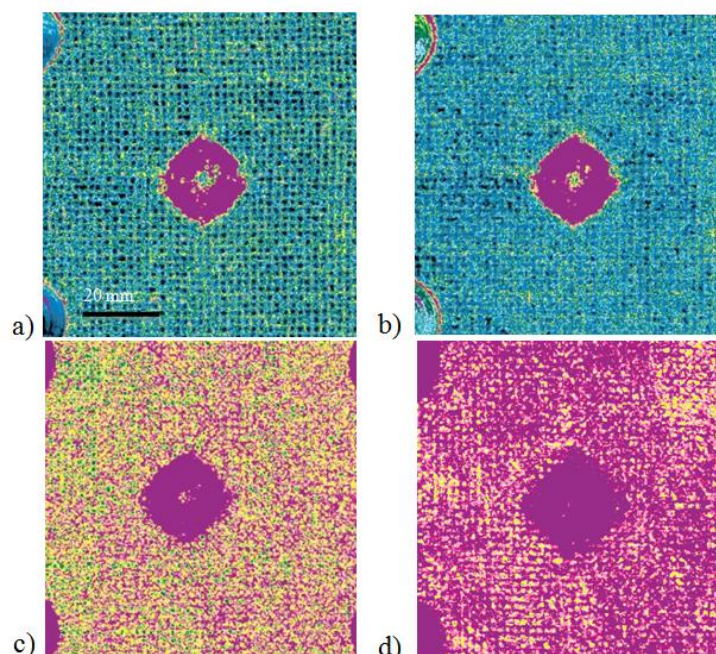


Figure 1. C-scan image of impact defects distribution on different depth of specimen 1. a) C-scan at 0.15 mm depth; b) C-scan at 0.32 mm; c) C-scan at 0.87 mm; d) C-scan at 1.31 mm depth

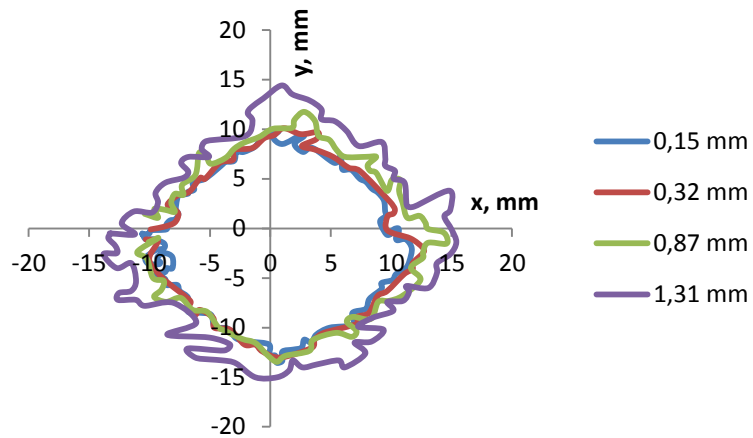


Figure 2. Distribution of defect at different depths of specimen

B-scan of the ultrasonic method can also be applied to investigate the distribution of defect in the specimen depth. Figure 3 shows distribution of the defect in specimen 1. Here it is also noticeable that the defect size increases towards the lower part of the specimen. Combining B-scan and C-scan images, the three-dimensional structure of the impact area can be reconstructed.

Figure 4 shows B- and C-scans of the specimen after impact. In this case the impact nozzle didn't penetrate through the specimen, but in B-scan (a) of this specimen only some small defects on the interface can be seen, the specimen has a vast amount of cracks and damage accumulated on the outer surface area which is demonstrated in (Figure 4.b) image.

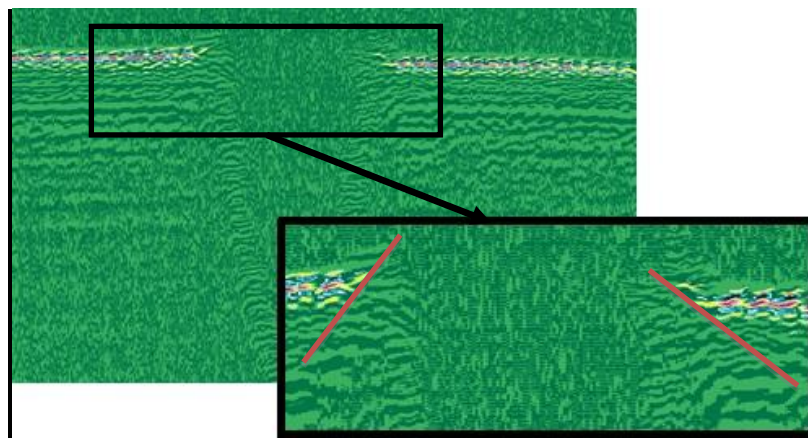


Figure 3. B-scan of specimen 1

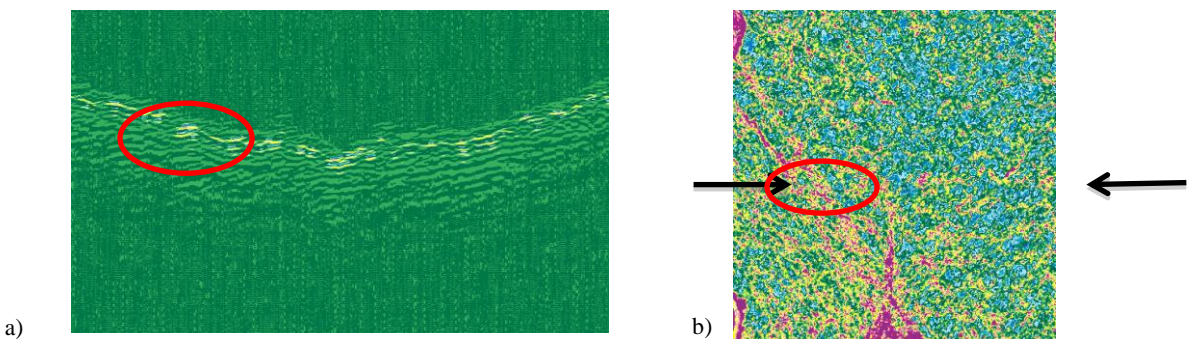


Figure 4. B-scan (a) and C-scan (b) images of the damaged area of the specimens 2. B-scan shows cross section of C-scan marked with arrows

With the ultrasonic technique it is possible to detect delamination inside the specimens. For example, in Figure 5, picture of specimen 3 and its ultrasonic C-scan images are shown. In the picture the depth cannot be identified at which delamination appears in the specimen. Whereas, with ply by ply analysis a particular ply and depth can be found where

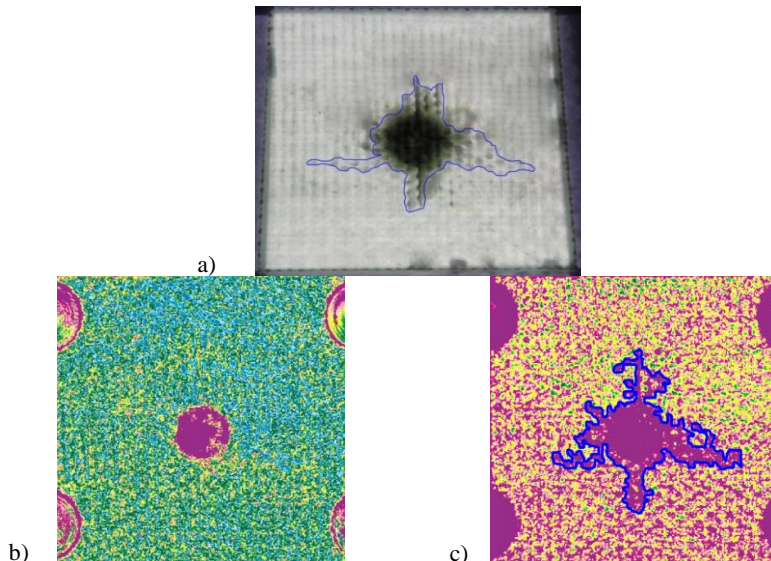


Figure 5. Picture (a) and C-scan (b, c) images of specimen 3; b) specimen at 1 mm depth and c) specimen at 1.7 mm depth

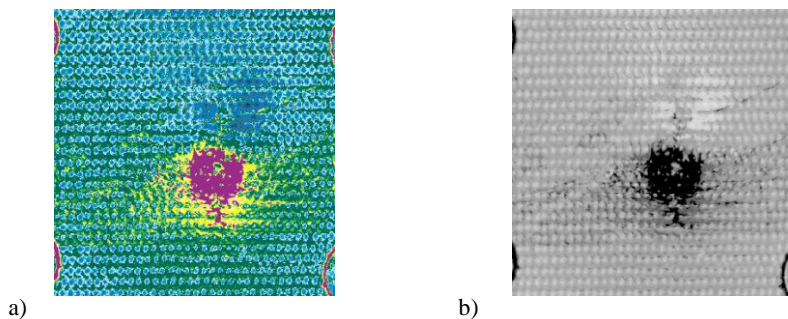


Figure 6. C-scans of specimen 4, where a) C-scan in colourful palette, b) C-scan in gray scale palette

For different applications the ultrasonic software Oculus allows the image's palette to be changed. For example, in Figure 6 specimen's 4 C-scans in different palettes are shown. Colourful palette can be used to analyze signal amplitudes distribution in the specimen. This will allow describing the specimens' composition: concentrating locations of

delamination has appeared. The delamination area seen in picture and in C-scan image is marked with blue colour. Specimen 3 has 2.77 mm thickness and delamination after impact appears at 1.7 mm depth. The size of delamination is from 40.3 to 46 mm.

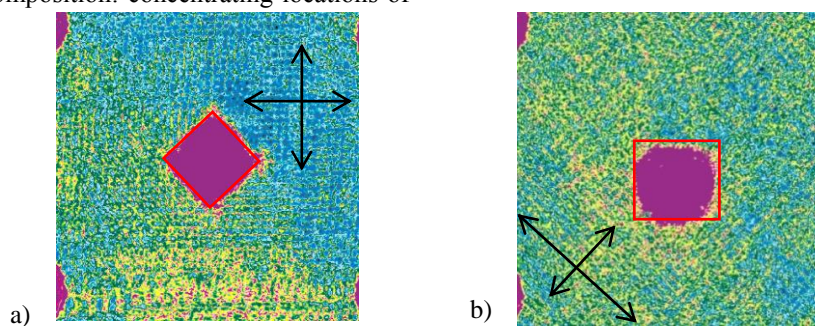


Figure 7. C-scan images of specimens with fibre direction a) 0/90 and b) 45/-45

epoxy and glass fibre. Whereas grey scale palettes allow the observer to focus and determine defect extension. In this case the amplitude of distribution doesn't overshadow the scene from defects prospect.

The shape of impact defects in specimens with different fibre direction varies. In specimen 5 fibre direction is 0/90 and the shape of impact is rhombic, but in specimen 6, the fibre direction is 45/-45 and the shape of impact is close to square. This difference is shown in Figure 7. Similar results were obtained in Zike's et.al. (Zike et al., 2011) study. With the ultrasonic imaging technique it is also possible to visualize the direction of fibre in composite materials. In Figure 7, directions of fibre are shown with arrows.

CONCLUSIONS

The ultrasonic imaging technique was successfully applied to analyse the GFRP composite materials.

REFERENCES

- Bartoli G., Betti M., Facchini L., Orlando M. (2012) Non-destructive characterization of stone columns by dynamic test: Application to the lower colonnade of the Dome of the Siena Cathedral. *Engineering Structures*, Vol. 45, p. 519-535.
- El-Gohary M.A. (2013) Evaluation of treated and un-treated Nubia Sandstone using ultrasonic as a non-destructive technique. *Journal of Archaeological Science*, Vol. 40, No. 4, 2190-2195.
- Giurgiutiu V., Cuc A. (2005), Embedded Non-destructive Evaluation for Structural Health Monitoring, Damage Detection, and Failure Prevention. *The Shock and Vibration Digest*, Vol. 37, No. 2, p. 83–105.
- Hasiotis T., Badogiannis E., Tsouvalis N. G. (2011) Application of Ultrasonic C-Scan Techniques for Tracing Defects in Laminated Composite Materials. *Journal of Mechanical Engineering*, Vol. 57, No. 3, p. 192-203.
- Kapadia. A. Non-destructive Testing of Composite Materials. [online] [accessed on 28.01.2013.]. Available: <http://www.compositesuk.co.uk/LinkClick.aspx?fileticket=14RxzdZdkjw%3D&>
- Pisupati P., Dewangan S.K., Kumar R. (2009) Structural Health Monitoring (SHM): Enabling Technology for paradigm shift in next generation Aircraft Design and Maintenance. [online] [accessed on 27.01.2013.]. Available: <http://www.infosys.com/engineering-services/white-papers/Documents/structural-health-monitoring.pdf>
- Shull, P. J. (2002) Ultrasound. In: *Nondestructive Evaluation: Theory, Techniques, and Applications*. New York, Marcel Dekker, Inc., p. 87-216.
- Turo A., Chavez J.A., Garcia-Hernandez M.J. et. al. (2013) Ultrasonic inspection system for powder metallurgy parts. *Measurment*, Vol. 46, p. 1101-1108.
- Zike S., Kalnins K., Ozolins O. (2011) Experimental Verification of Simulation Model of Impact Response Tests for Unsaturated Polyester/GF and PP/GF Composites. *Computer Methods in Materials Science*, Vol. 11, No. 1, p. 88-94.
- Zike S., Kalnins K., Ozolins O., Knite M. (2011) An Experimental and Numerical Study of Low Velocity Impact of Unsaturated Polyester/Glass Fibre Composite. *Materials Science*, Vol. 17, No. 4, p. 384-390.

Our study has shown that the ultrasonic method can work successfully for non-destructive testing of composite materials. The method demonstrates the ability to visualize internal defects in glass fibre reinforced composite and estimate the size and shape of the impact. The ultrasonic method allows the viewer to detect a particular depth of defect and its extend. Additionally by applying the B-scan method it is possible to detect the distribution of defects in the specimen's depth. This method also can be utilised to characterize specimen's structure: orientation of fibre in the specimen, epoxy and fibre concentrations location.

COMPARISON OF ASPHALT CONCRETE PERFORMANCE USING CONVENTIONAL AND UNCONVENTIONAL AGGREGATE

Viktors Haritonovs, Martins Zaumanis, Guntis Brencis, Juris Smirnovs

Riga Technical University, Department of Roads and Bridges

E-mail: viktors.haritonovs@rtu.lv

ABSTRACT

Annually up to 200 thousand tons of steel slag, a non metallic co-product of iron and steel production, are produced in Latvia. However, it has not been extensively used in asphalt pavement despite of its high performance characteristics. Dolomite sand waste, which is co-product of crushed dolomite production, is another widely available polydisperse waste material in Latvia. Its quantity has reached millions of tons and is rapidly increasing. This huge quantity of technological waste needs to be recycled with maximum efficiency.

The study investigates the use of dolomite sand waste as filler or/and sand material plus steel slag as fine and coarse aggregate for the design of high performance asphalt concrete. Both environmental and economic factors contribute to the growing need for the use of these materials in asphalt concrete pavements. This is particularly important for Latvia, where local crushed dolomite and sandstone does not fulfill the requirements for mineral aggregate in high and medium intensity asphalt pavements roads.

Various combinations of steel slag, dolomite sand waste and conventional aggregates were used to develop AC 11 asphalt concrete mixtures. The mix properties tests include resistance to permanent deformations (wheel tracking test, dynamic creep test) and fatigue resistance. Laboratory test results showed that asphalt concrete mixtures containing steel slag and local limestone in coarse portion and dolomite sand waste in sand and filler portions had high resistance to plastic deformations and good resistance to fatigue failure.

Key words: co-product, steel slag, dolomite sand waste, permanent deformations, fatigue resistance

INTRODUCTION

Asphalt concrete pavements are constructed of bituminous and polydisperse granular materials. Regardless of the thickness or type of asphalt pavement, the load is transmitted through the aggregate, the bitumen serving as a cementing agent to bind the aggregate in proper position to transmit the applied wheel loads to underlying layers where the load is finally dissipated (Huang, 1993, Mallick and El-Korchi, 2009).

Local crushed dolomite and sandstone aggregate lack the desirable qualities for asphalt concrete mix design (Skinskas et al. 2010). In the meantime, as natural supplies of high quality granular materials used in highways have become less abundant, the highway engineer is faced with the challenge of finding alternative materials to meet the requirements for these materials (Yilmaz and Sutas, 2012). Some of these alternatives are fly ash, coal dust, hydrated lime, steel slag etc. (Kandhal and Hoffman, 1997). The co-products (slag) of iron and steel production have been used commercially since 19th century (Euroslag, 2006). In the EU and North America steel slag is used in: bituminous bound materials; pipe bedding; hydraulically bound mixtures for subbase and base; unbound mixtures for subbase; capping; embankments and fill construction; clinker manufacture and fertilizer and soil improvement agent (Gintalas 2010,

Xirouchakis et al. 2011). However, in Latvia, for commercial road construction purposes, it has been used only for unbound mixtures.

The research has shown that production of asphalt mixtures with high performance characteristics is possible by using steel slag aggregate (Pasetto et al. 2011). However, the studies have also indicated that, because of the high angularity and texture of the particles, the asphalt often has poor workability (Haryanto et al. 2007). Therefore, the application of slag may have more potential in combination with conventional aggregates (Bagampadde et al. 1999). The second most widespread co-product in Latvia is the dolomite waste sand. It has been accumulating in quarries for many years and currently its quantity has reached several million tons. Previously it has been used in agriculture as the lime substitute for soil treatment and in the building industry as the quartz sand equivalent. Currently researchers in Latvia also offer to utilize the dolomite sand waste in the concrete production (Korjakins et al. 2008). However, the research on the perspective use of dolomite waste sand in the production of asphalt has received relatively little attention. For example, this material could be used to fully or partially replace the fine and filler portions.

The goal of this study is to develop asphalt mixtures with high performance properties using various combinations of BOF steel slag, dolomite sand

waste, crushed quartz sand crushed dolomite aggregates and to compare the results with the reference asphalt mixture, produced with conventional aggregates. The mix properties tests include resistance to permanent deformations (wheel tracking test, dynamic creep test) and fatigue resistance.

MATERIALS

The basic materials used in this study are fractionated steel slag, crushed dolomite aggregate; dolomite sand waste, crushed quartz sand, unmodified bitumen B70/100 and SBS modified bitumen PMB 45/80-55. Steel slag was obtained from JSC Liepajas metalurgs (Latvia), dolomite sand waste from Plavinu DM Ltd (Latvia), crushed quartz sand from Jauncerpji Ltd. (Latvia) and crushed dolomite aggregate from AB Dolomitas (Lithuania), 70-100 penetration bitumen from PC Orlen (Lithuania) and SBS modified bitumen from Grupa LOTOS S.A (Poland). Conventional aggregate and unmodified and modified bitumen are used extensively for local mixes.

Properties of dolomite sand waste

The Latvian law classifies steel slag and dolomite sand waste as non-hazardous solid materials (91/689 EEK). Chemical analysis of dolomite sand is shown in Table 1. There is no evidence of clay minerals being present in dolomite sand. The X-ray diffraction has been used to obtain mineralogical composition of the investigated dolomite waste (Korjakins et al. 2008). The main constituents of waste dolomite are $\text{CaCO}_3\text{-MgCO}_3$, which account for more than 92% of the composition.

Table 1
Chemical properties of waste materials

Steel slag		Dolomite waste sand	
Oxide	Content, %	Oxide	Content, %
CaO	30.6	CaO	31.0
MgO	18.9	MgO	17.0
SiO ₂	19.9	SiO ₂	2.5
MnO	6.3	Na ₂ O	0.82
Al ₂ O ₃	5.0	Al ₂ O ₃	0.64
TiO ₂	0.52	K ₂ O	0.76
FeO	16.3	Fe ₂ O ₃	0.34

This material contains more than 10% of fines (below 0.063mm) and therefore it has to be tested for properties of mineral filler (Fig.1). The fine particles of this material are part of the mixture mineral carcass and contribute to obtain a dense structure by filling the voids between coarse

aggregate particles. The mineral filler that is in this material, however, provides more contact points between fine and coarse aggregate thus improving the mechanical properties of the mixture. Another function of the mineral filler is to increase the bitumen viscosity and improve the properties of the binder

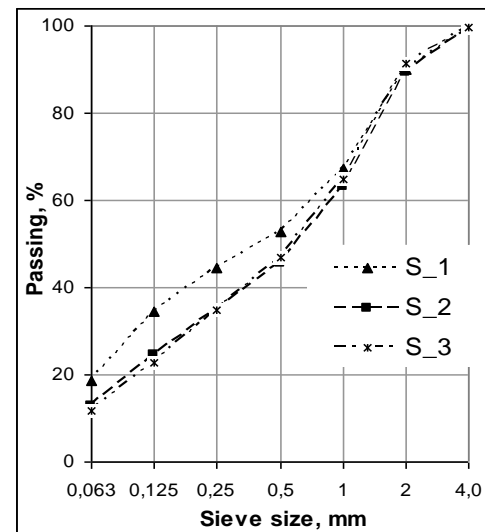


Figure 1. Particle size distribution of dolomite waste sand

Table 2
Physical and mechanical characteristics of dolomite sand

Physical and mechanical properties	Standard	Dolomite waste sand	Dolomite filler	Crushed quartz sand
Sand equivalent test, %	LVS EN 933-8	60	-	91
Flow coefficient (ECS)	LVS EN 933-6	33	-	35
Water absorption, %	LVS EN 1097-6	2.0	2.7	5.4
Grain density, Mg/m ³	LVS EN 1097-6	28.0	2.75	2.80
Fine content, %	LVS EN 933-1	12-19	78-88	0.9
Methylene blue test (MB), g/kg	LVS EN 933-9	0.5	-	0.5
Carbonate content, %	LVS EN 196-21	> 90	> 90	-
Rigden air voids, %	LVS EN 1097-4	28-30	28-30	-
Delta ring and ball test, °C	LVS EN 13179-1	8-25	8-25	-

Table 2 contains test results of conventional sand and dolomite filler for comparison of the properties of sand waste's fine portion and filler portion respectively. The properties of both of these

fractions correspond to high quality requirements. Dolomite waste sand test results present excellent angularity with an average flow coefficient of 33. Test results show that the fines quality is high – the material has low methylene blue (MB) value – 0.5 high carbonate content – more than 90%, excellent Rigid air voids and Delta ring and ball tests results

Properties of steel slag aggregate

The properties of BOF steel slag correspond to the highest category of LVE EN 13043 standard. However, because of high abrasivity of this material, the proportion of it for wearing courses according to Latvian Road Specifications 2012 has been restricted to 20 present. The test results of steel slag main properties show very low flakiness index – 2, excellent mechanical strength with average LA value of 19, high frost resistance with average MS value of 3, low fines content – 0.5% and slag expansion tests, showed that the expected swelling should be negligible (Table 3).

Table 3
Physical and mechanical characteristics of steel slag aggregate

Physical and mechanical properties	Related standard	Steel slag aggregate	Crushed dolomite aggregate	
Los Angeles (LA) coefficient, %	LVS EN 1097-2	19	22	
Resistance to wear. Nordic test (AN), %	LVS EN 1097-9	14.4	15.7	
Flakiness Index (FI), %	LVS EN 933-3	2	12	
Water absorption, %	LVS EN 1097-6	2.4	2.7	
Grain density, Mg/m ³	LVS EN 1097-6	3.25	2.80	
Fine content, %	LVS EN 933-1	0.5	0.9	
Freeze/thawing (MS), %	LVS EN 1367-2	3	9	
Expansion, %	LVS EN 1744-1	2	-	

Bitumen tests

Unmodified bitumen BND 60/90 (category defined in accordance to Russian specifications) and SBS polymer modified bitumen was used for the testing. All the test results of the bitumen BND 60/90 and PMB are shown in Table 4 and 5.

MIX DESIGN

Dense graded AC mixtures have been designed by using conventional and unconventional raw materials. The Marshall mix design procedure was used for the determination of the optimal bitumen content for the reference mixture, considering the

mixture test results for Marshall stability and flow, as well as the volumetric values: air voids (V), voids in mineral aggregate (VMA) and voids filled with bitumen (VFB) (Roberts *et al.* 2002). Test specimens for the Marshall Test were prepared in the laboratory by impact compactor according to LVS EN 12697-30 with 2×50 blows of the hammer at 140°C temperature. The optimal bitumen content was determined by optimisation of the volumetric characteristics. Variation of bitumen content even with having similar grading curves can result in high hygroscopicity of dolomite waste material, differences in aggregate bulk density and high bitumen absorption of BOF steel slag material (Sivilevičius *et al.* 2008; Sivilevičius *et al.* 2011).

Table 4
Typical characteristics of the bitumens

Parameter	BND 60/90	PMB 10/40-65	PMB 45/80-55	PMB 25/55-60	Standard
Penetration at 25°C, dmm	65.0	40.0	50.0	34.0	LVS EN 1426
Softening point, °C	50.4	65	58.4	63.5	LVS EN 1427
Fraas temperature °C	- 25	- 17	- 20	- 23	LVS EN 12593
Kinematic viscosity, mm ² /s	607	239 0	1203	171 2	LVS EN 12595
Dynamic viscosity, Pa·s	340	416 6	1074	302 1	LVS EN 12596
Elastic recovery, %	-	87	88	89	LVS EN 13398

Table 5
Ageing characteristics of bitumen under the influence of heat and air (RTFOT method)

Parameter	BND 60/90	PMB 10/40-65	PMB 45/80-55	PMB 25/55-60	Standard
Loss in mass, %	0.1	0.01	0.02	0.02	LVS EN 12607-1
Retained penetration, %	70.8	75	69.7	79.4	LVS EN 1426
Increase of a softening point, °C	6.4	7.2	5.9	6.2	LVS EN 1427
Fraas breaking point after aging, °C	-20.0	-15	-18	-19	LVS EN 12593

PERFORMANCE EVALUATION

Three different groups of mixtures were analyzed:

- Two reference mixtures without co-products (with conventional and SBS bitumen), which were used as a control;
- Mixtures containing only BOF slag and dolomite waste sand;
- Combination of conventional and unconventional materials.

Performance tests are time-consuming and the number of combinations is very large; therefore in the first phase the different mixtures were evaluated with axial and triaxial loads. The combinations that have the highest deformation resistance will be tested for rut resistance and fatigue (see Fig. 2).

Uniaxial and triaxial test

For this test the standard LVS EN 12697-25 was followed. The Uniaxial and Triaxial Cyclic Compression test is performed using specimens with 101.7 mm diameter and 63.5 ± 2.5 mm height. The laboratory specimens were compacted using the Marshall Impact compactor. The applied load had a block - pulse shape with 1sec of loading time and 1sec of rest time. The test duration was 3600 cycles and the test temperature was 40 °C for uniaxial and 50 °C for triaxial loading. The maximum axial stress for uniaxial loading was 100 kPa. The maximum axial stress for triaxial loading

was 200 kPa and 100kPa confining pressure. Figure 3 and 4 shows the uniaxial and triaxial test results. In order to reduce the number of tests, the following tests will be performed for the combinations with unmodified binder BND 60/90 and PMB 45/80-55. The combinations with PMB 45/80-55 binder showed a slightly higher resistance to deformations. In the following stages of the research the rutting resistance and fatigue performance will be evaluated for other combinations as well.

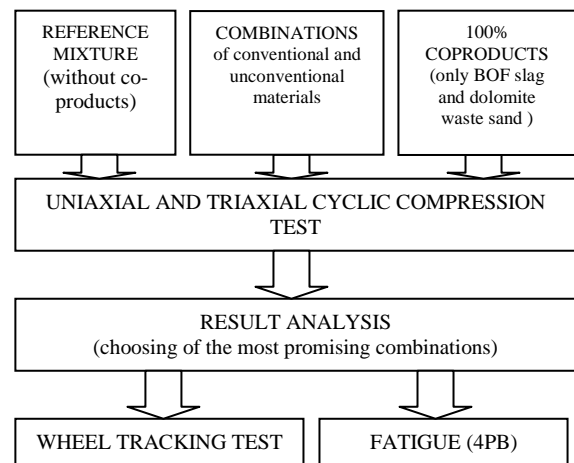


Figure 2. Performance evaluation plan

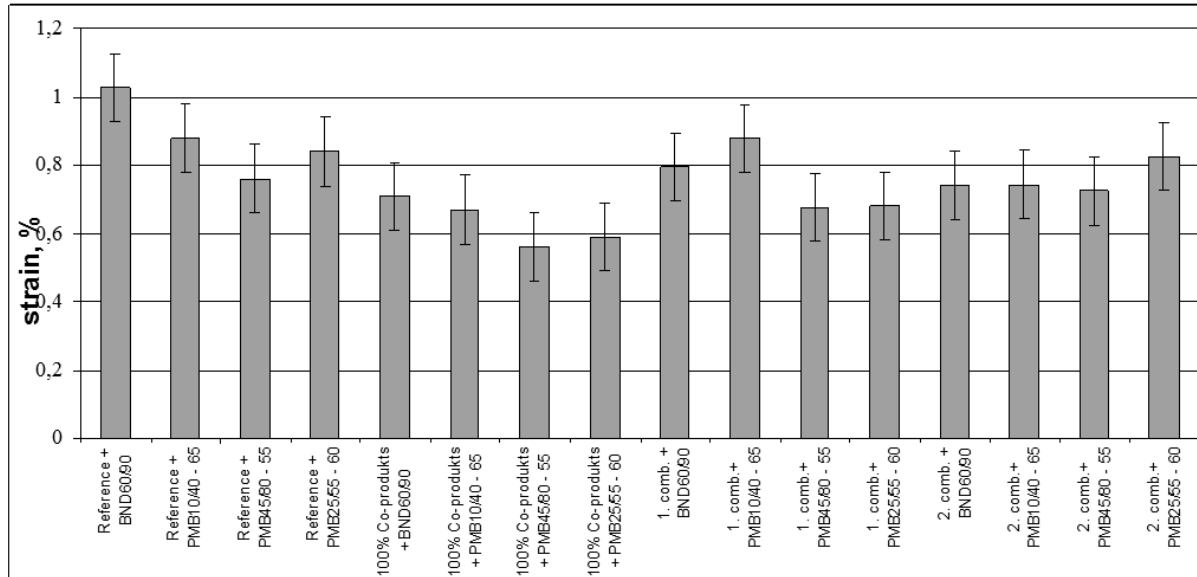


Figure 3. Uniaxial compression test results (Uniaxial compression test, 40°C, 100kPa, 3600 cycles)

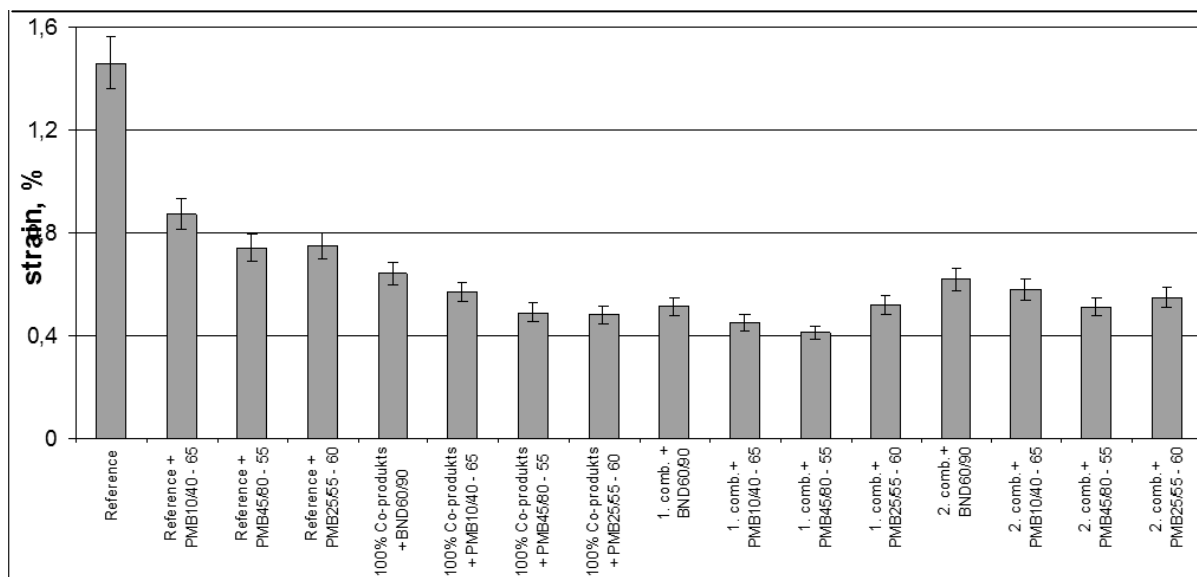


Figure 4. Triaxial test results (Triaxial test, 50°C, 200/100kPa, 1000 cycles)

Wheel tracking test

To perform a rut resistance test, a wheel tracking apparatus is used to simulate the effect of traffic and to measure the deformation susceptibility of asphalt concrete samples. Tests were performed according to standard LVS EN 12697-22 method B (wheel tracking test with small size device suspended in the air). This test method is designed to repeat the stress conditions observed in the field and therefore can be categorized as simulative. The asphalt mixture resistance to permanent deformation is assessed by the depth of the track and its increments caused by repetitive cycles (26.5 cycles per minute) under a constant temperature of 60°C. The rut depths are monitored by means of two linear variable displacement transducers (LVDTs), which measure the vertical displacements of each of the two wheel axles independently as rutting progresses. Figure 5 provides a summary of rut resistance properties of the test specimens.

The obtained results demonstrate that the largest rut depth appear for the reference mixture with unmodified bitumen. The results for the reference mixture with SBS modified bitumen are only slightly better. The asphalt concrete mixture which was produced entirely from co-products shows a high resistance to permanent deformations, having an average rut depth value of 1.54 mm and wheel tracking slope of 0.12 mm/1000 cycles. The mixture with a combination of the co-product and

conventional aggregate had somewhat worse test results.

Fatigue

To determine the fatigue life of the prepared asphalt concrete mixes, a four point bending fatigue test was conducted. The test was run at 20°C, 30Hz (according to LVS EN 12697-24) at 190 µm/m strain level. The beams were compacted in the laboratory by using roller compactor. They were sawn to the required dimensions of 50mm wide, 50mm high and 400mm long. The failure criterion used in the study is the traditional 50% reduction in initial stiffness. The stiffness reduction curves are shown in Figure 6. The obtained results indicate that the mixture with BOF steel slag and dolomite sand waste (100% co-product) showed less resistance to fatigue, compared to the results for the mixture made with conventional aggregates and combined mixture. The mix designs that include exclusively dolomite aggregates as well as the combination of dolomite and slag in a coarse portion plus waste sand in fine aggregate portion exhibit slightly higher fatigue life compared to other combinations. The fatigue life exceeded 500 thousand cycles for all the combinations with the exception of 100 percent by-product mixtures made with BND 60/90 bitumen. However, to verify the findings more extensive laboratory research is needed – this will allow to determine the relationship between tensile strain at the bottom of the beam and the number of load applications before cracking.

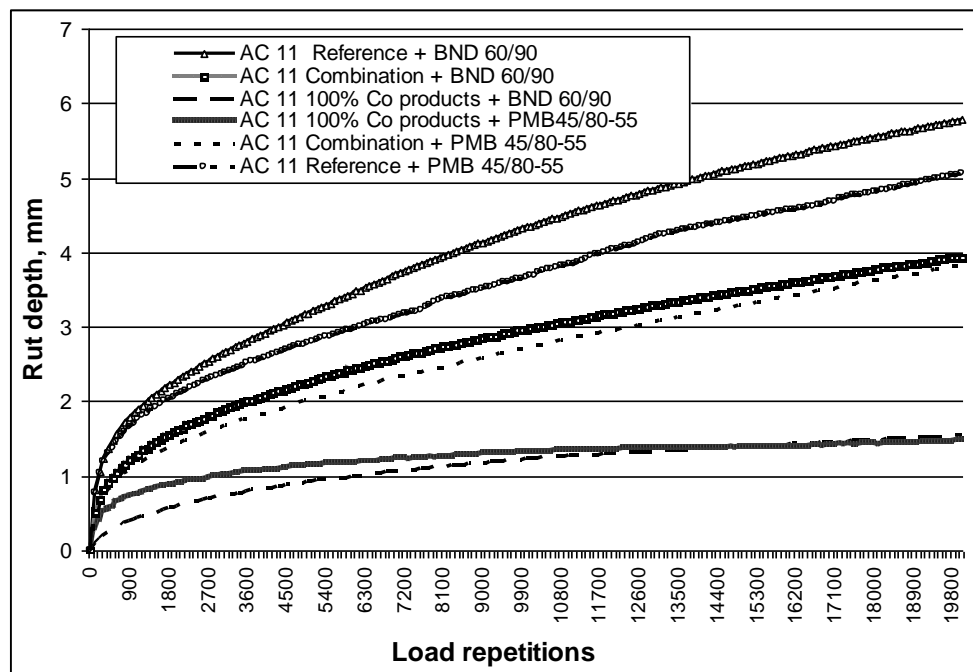


Figure 5. Wheel tracking test results

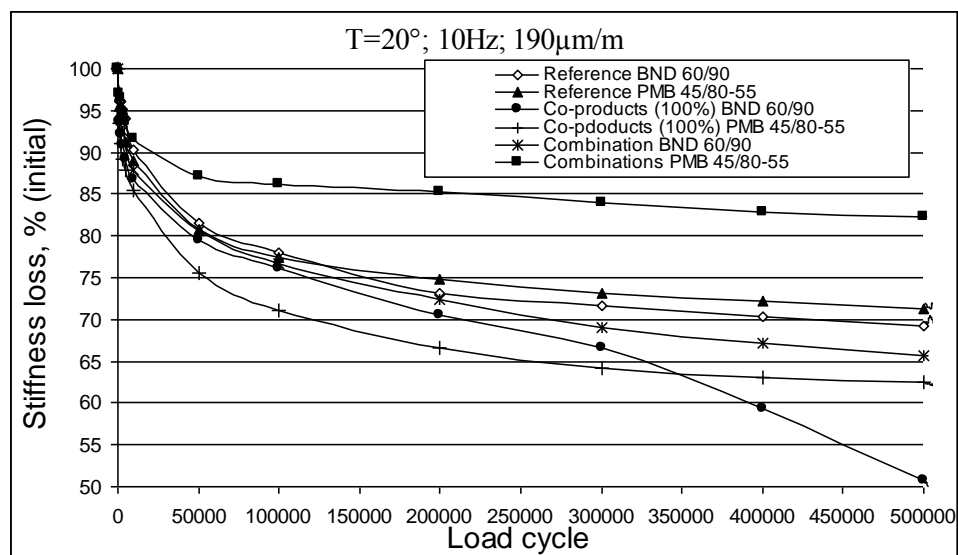


Figure 6. Fatigue test results – stiffness reduction curves

CONCLUSIONS

Physical and mechanical properties of steel slag aggregates and dolomite sand waste are comparable with the characteristics of conventional natural aggregate usually used in transportation infrastructure.

The results of wheel tracking test and cyclic compression show that mixtures with a high deformation resistance were prepared in the laboratory using two types of co-products.

The analysis of fatigue resistance results show that the mixtures made with steel slag and local

limestone in a coarse portion plus dolomite sand waste in sand and filler portions exhibit a slightly higher fatigue resistance than the conventional mixtures. However, the mixture from 100% steel slag and dolomite waste sand show less resistance to fatigue. To verify the findings more extensive laboratory research is needed – this will allow determining the relationship between tensile strain at the bottom of the beam and the number of load applications before cracking.

ACKNOWLEDGEMENT

This work has been supported by the European Regional Development Fund (ERDF) activity No.2.1.1. „Atbalsts zinātnei un pētniecībai”

(support for the science and research) within the project:No.2010/0254/2DP/2.1.1.0/10/APIA/VIA A/015.

REFERENCES

- Bagampadde U., Al-Abdul Wahhab H. I., Aiban S.A. (1999). Optimization of Steel Slag Aggregates for Bituminous Mixes in Saudi Arabia, *Journal of Materials in Civil Engineering*, Vol. 11, No. 1, p.30-35.
- The European Slag Association: „EUROSLAG” (2006). Legal status of slags. Position paper, [online] [accessed on 10.08.2011.]. Available: <http://www.euroslag.com>
- Gintalas V. (2010). Possibilities for the Improvement of the Quality of Design Solutions in the Gravel Road Reconstruction Projects, *The Baltic Jurnal of Road and Bridge Engineering* Vol. 5, No. 3, p. 177-184.
- Haryanto I., Takahashi O. (2007). Effect Of Aggregate Gradation On Workability Of Hot Mix Asphalt Mixtures, *The Baltic Jurnal of Road and Bridge Engineering* Vol. 2, No. 1, p. 21-28.
- Huang, Y. H., (1993). *Pavement Analysis and Design*. Prentice-Hall, Inc., New Jersey, USA, 805p.
- Korjaks A., Gaidukova S., Šahmenko G., Bajāre D., Pizele D. (2008). Investigation of Alternative Dolomite Properties and Their Application in Concrete Production, *Scientific Proceedings of Riga Technical university. Construction Science* Vol 2. Issue 9, p. 64-71.
- Mallick, R. B. and El-Korchi, T., (2009). *Pavement Engineering: principle and practice*. CRS Press, Taylor and Francis Group, USA, 511p.
- Pasetto M., Baldo N. (2011). Mix Design and Performance Characterization of Bituminous Mixtures with Electric Arc Furnace Steel Slags, *Proceedings of 5th Internationa Conference Bituminous Mixtures and Pavements*, p. 748 – 757, Thessaloniki, Greece.
- Roberts F., Mohammad L., Wang L. (2002). History of Hot Mix Asphalt Mixture Design in the United States, *Journal of Materials in Civil Engineering* Vol. 14, No 4, p 279 – 293.
- Sivilevičius H., Podvezko V., Vakriniene S. (2011). The use of Constrained and Unconstrained Optimization Models in Gradation Design of Hot Mix Asphalt Mixture, *Construction and Building Materials* Vol. 25, No 1, p.115 – 122.
- Sivilevičius H., Vislavičius K. (2008). Stochastic Simulation of the Influence of Variation of Mineral Material Grading and Dose Weight on Homogeneity of Hot Mix Asphalt, *Construction and Building Materials* Vol. 22, No 9, p.2007 – 2014.
- Skinskas S., Gasiūniene V.E., Laurinavičius A., Podagėlis I. (2010). Lithuanian Mineral Resources, Their Reserves and Possibilities for Their usage in Road Building, *The Baltic Jurnal of Road and Bridge Engineering* Vol. 5, No 4, p. 218-228.
- Xirouchakis D., Manolakou V. (2011). Properties of EAF Slag Produced in Greece: A Constructional Material for Sustainable Growth, in *Proceedings of .5th Internationa Conference Bituminous Mixtures and Pavements*, p. 287– 297, Thessaloniki, Greece.

INTERPRETATION OF ASPHALT MATERIAL DESIGN PARAMETERS

Atis Zarins*, Viktors Haritonovs**, Juris Smirnovs***

Riga Technical University, Department of Roads and Bridges

E-mail: *atis.zarins@rtu.lv, **viktors.haritonovs@rtu.lv, ***smirnovs@mail.bf.rtu.lv

ABSTRACT

The current situation in road design practice shows that there exists an inconsistency in using and defining some asphalt material parameters. Such inconsistency is due to the introduction of EU standards for materials while leaving the design methods unchanged. In order to find possibilities to adapt the correct modern test methods for asphalt material parameters such as deformation modulus used in road pavement design procedures, the research and theoretical grounds analysis was performed. Current research establishes that after introducing EU standards for road material requirements instead of the former GOST, road engineers were faced with the fact, that EU materials no longer conform to the former design procedure. Some of them start using other design methods different from the previously used GOST based VSN (Russian) pavement design procedure. However, both practices have not been ensured with appropriate design parameters applicable for the used procedures. The main source of inconsistency as stated above is non-compliance of the defined road pavement materials with parameters used in design procedures and, for instance, defined basing on GOST. As a result, it leads to the improperly designed pavement structures and possibly can result in significant losses for the national road industry. This paper presents the interpretation of four point bending test results and the possibility to use them in the most widely used pavement design procedure – VSN. Four point bending tests were performed on AC11 asphalt mixture with conventional (dolomite, quartz sand) and non conventional (steel slag, dolomite sand) aggregates.

Key words: dolomite aggregate, asphalt concrete, permanent deformations, fatigue resistance

INTRODUCTION

In order to find possibilities to adapt the correct modern test and assessment methods for asphalt material parameters, such as a deformation modulus used in road pavement design procedures, the research and theoretical analysis and justification were performed. Current research establishes that after introducing EU standards for road material requirements instead of former GOST, road engineers were faced with the fact, that EU standards for materials no longer conform with former design procedure. Some of them started using other design methods different from previously used GOST based VSN (Russian) pavement design procedure. However, both practices have not been ensured with appropriate design parameters applicable for used procedures. The main source of inconsistency as established is non-complying of defined road pavement materials with parameters used in design procedures and, for instance, defined basing on GOST. As a result, it leads to the improperly designed pavement structures and possibly can result in significant losses for national road industry.

This paper presents the interpretation of four point bending test results and the possibility of their acceptance for use in still mostly used pavement design procedure - Soviet Union flexible pavement design instruction (VSN 46-83, 1985). Four point bending tests were performed on AC11 asphalt

mixture with conventional (dolomite, quartz sand) and non conventional (steel slag, dolomite sand) aggregates.

Currently used pavement design philosophy in Latvia, as well as in other Baltic countries is based on former Soviet regulations VSN 46-83 established in the '70s of the last century. This design approach includes theoretical justification built on consequences following from the theory of plasticity of composite materials. The theory considers lower semi space as subsoil working in appropriate design conditions and upper semi space – as designed pavement structure, considered as a homogenous formation. No or very little modifications in the used design methodology have been made since this time, however essential changes appear in the used construction technologies and materials, as well as in actual traffic loads.

The same regulation is being used in Russia and most of the other former Soviet republics. There were, however, some essential modifications made. In this context the actual status of pavement design methodology and used parameters are analyzed in this research.

OBJECT OF DISCUSSION

The modulus of deformation is one of the main road pavement parameters used for the theoretical evaluation of a designed structure. As defined in the

current design methodology the common or equivalent modulus is the parameter, which theoretically estimates the designed pavement structure. Equivalent modulus of deformation is determined according to the used pavement layer parameters. They are - material, thickness of layer, as well as working conditions expected load: - number of standard axle passes, standard load value and character – static or dynamic, moisture and heat conditions. All of these parameters have been determined by tests or theoretically, using technologies and knowledge appropriate of the time when the methodology was developed in the '70s of the last century. The deformation modulus of road pavement can be theoretically obtained using parameters of materials used in pavement structure, or from testing particular pavement structure in situ. In both cases the possible worst working conditions for particular pavement material must be considered, while setting parameters for testing conditions.

Since parameters of elasticity and strength for bituminous bound materials dependent on loading force, speed, and duration it needs to be specified in terms of actual anticipated loading conditions.

As mentioned in the regulations on the design of non-rigid pavements VSN 46-83, the design values of the deformation modulus of asphalt concrete are determined depending on the working temperature and assigned load condition (Телтаев, 2010). This provides the ability to describe the deformation properties of pavement material by means of value – referred to as the modulus of elasticity, according to whether the load is either static or dynamic. It was required to evaluate non-rigid pavements according to the following three criteria:

- by elastic bending of the structure of the pavement;
- by the permitted shear stress in the subsoil of the roadbed and unbound material layers of the pavement;
- allowable tensile stress in bent surfaces of bound material layers.

The design values of the modules for asphalt materials of pavement in VSN 46-83 were established by results-oriented research for materials, components and technologies available at that time.

As fixed in regulations (VSN 46-83, 1985) modules of elasticity for evaluation of asphalt concrete road surfaces during dynamic loading were derived from the modulus established providing frequency of load applying an uncertain defined in interval 5 - 20Hz and was described as a dynamic modulus of elasticity. According to the above mentioned regulations the modulus was calculated applying parameters measured during a three point bending test with sample 4x4x16cm and the using equation:

$$E_{dyn} = \frac{Fl^3}{4fbh^3} \quad (1),$$

where F – effective load applied to the sample ($F=k_lk_hP$), $b=h=4\text{cm}$, $l=16\text{cm}$ – dimensions of sample. Test measurement must be done after 10 - 30 preliminary loading cycles. Design value must be set as mean from at least three samples.

REVIEW OF PROBLEM

There are many opinions in recent publications concerning the methodology of measurement and setting of design values under discussion. The paper presents overview of publications in general from researchers of countries where particular design principles are topical. Professor Teltaev points, that current standardized design parameters vaguely take into account the actual limits of grain content in composition of aggregate, type, content and physical properties of bitumen, volumetric parameters of mixture, mineral filler content and quantitative characteristics of the impact of climatic and mechanical factors (Телтаев, 2010).

Professor Rudenskiy recommend increasing standard design values for those asphalt concrete materials, with lower values of the actual modules of elasticity, but possessing greater deformative properties must be higher than the standard values from VSN 46-83 for respective grades of asphalt concrete (Руденский, 2010). This conclusion is valid, provided that the compared structures are characterized by the same energy of destruction of asphalt concrete. In case of use of asphalt concrete with greater energy of destruction (for example, using of fibrous reinforcing components), the calculated value of the modulus of elasticity also should be higher due to increased durability of asphalt concrete.

A number of researchers point to the importance of mix character and parameters if establishing design parameters of an asphalt material. Professor Teltaev makes a comparison of laboratory tests on dynamic modulus of HMA from (Flintsch et al. 2007) versus those made using standards based on VSN 46-83 and ODN method (ODN 218.046-01, 2001), and concludes that in both cases fixed modules are higher than those used as standard design parameters in VSN 46-83 and ODN 218.046 -01, and they are sensitive to the mix constituents and mix granulometry.

Professor Sibiryakova draws attention to the necessity to revise the set of standard design parameters considering new materials and technologies used in modern road industry (Сибирякова, 2007; Сибирякова, 2008).

Yeo Y. points out that the four point bending test has the added advantage that it provides a uniform stress distribution (Yeo et al., 2011). In contrast, the three point bending test has the maximum stress concentrated locally below the loading point,

exposing only a very limited area of the specimen to the maximum loads. Therefore it follows, that the four point test provides more adequate conditions for establishing of design parameters for road pavement material.

TEST METHODOLOGY

Current research includes measuring and evaluation of HMA deformation parameters during a four point bending test. Test samples were made according to the actual technical requirement (National Road Specifications 2012) and compared with results in (Flintsch et al. 2007) and VSN 46-83.

Tests were performed on AC11 asphalt mixture specimens with conventional (dolomite, quartz sand) and non conventional (steel slag, dolomite sand) aggregates. Two reference specimens were prepared containing different bitumen binders

- BND 60/90, which is most frequently applied binder in Latvian road industry, and
- PMB 45/80-55.

One specimen with hard bitumen BND 20/30 was also tested for reference.

Along with reference specimens, four specimens with experimental mix using two above mentioned binders and different combinations of non conventional aggregates were prepared and tested for stiffness loss and elasticity parameters. All tested specimen mixes were compound and prepared according to granulometry requirements set in technical requirements (National Road Specifications 2012). As seen in fig.1, specimens refer to be characterized as fine grained.

Parameters for the four point bending test were set according to the above described assumptions to simulate dynamic axis load and worst pavement working conditions for elastic bending criteria:

- Test temperature - 20 °C,
- Loading frequency - 10Hz,
- Uniform deformation - 190 µm/m.

RESULTS AND DISCUSSION

Design parameters for bituminous bound material according to methodology VSN 46-83 must be set depending on bitumen viscosity and working temperature for particular criteria, and depending on criteria to be examined. Parameters for dense asphalt mix (AC11) with bitumen used in the test for dynamic loading conditions are shown in table 1. According to ODN 218.046-01, the modulus of deformation for dynamic loading must be determined after making 1000 loading cycles.

It can be seen in fig. 2 and fig. 3 – the modulus after 1000 cycle loss of stiffness is still in progressing phase. Moreover – during design life of pavement

structure significantly more than 1000 axle load application cycles are anticipated. And one of assumptions, which the pavement design is based on, is that the pavement is still serviceable at the end of the design period. Thus, it can be concluded that the number of loading cycles are important when establishing a design value of modulus of deformation. Depending on the material, it stabilizes after 300000-400000 loading cycles and corresponds to 60-80% of initial value of deformation modulus. Nevertheless, it is seen in tab.1 that the actual values of modulus for tested specimens are up to two times greater than the standard design values.

If the deformation module values obtained in the tests are set as in the stable interval of the module exchange (after 300000 loading cycles, see. Fig.2, tab 1.), the actual value of the modulus for tested mix AC11 (dense HMA) with bitumen 60/90 are within the interval 3300-3700, for PMB 45/80-55 – 3000-3400. This means, that if using one value for all mixes, it must be considered, that dispersion in this particular case will be 12% and 13% accordingly, that could be unacceptable if considering adequately designed pavement structure.

Table 1

Comparison of deformation modulus (MPa) for different AC11 mixes and with different bitumen binders fixed as standard design value and measured in tests. (T=20 °C)

Mix and binder type	1000 cycles	300000 cycles	% loss
Dense HMA 60/90 des.value*	1800*	-	-
Dense HMA 40/60 des.value*	2600*	-	-
AC11(60/90) ref.	5000	3700	70
AC11(60/90)comb.	4700	3400	69
AC11(60/90)co-prod.	4700	3300	67
20/30 ref.	6800	3500	65
AC11 45/80-55 (PMB) ref.	4300	3300	73
AC11 45/80-55 (PMB) comb.	3900	3400	84
AC11 45/80-55 (PMB) co-prod.	4300	3000	63

* Design value VSN 46-83 (tab.13. app.3)

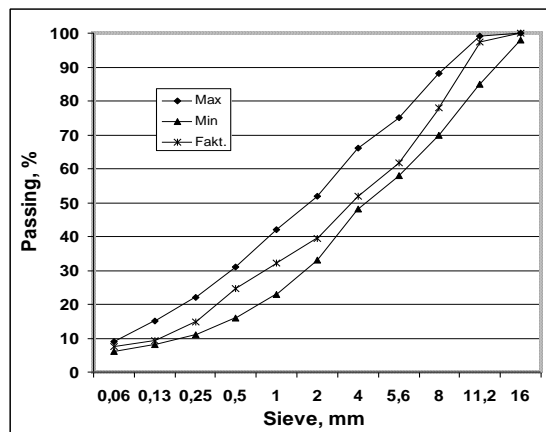


Figure 1. Granulometry of test specimens

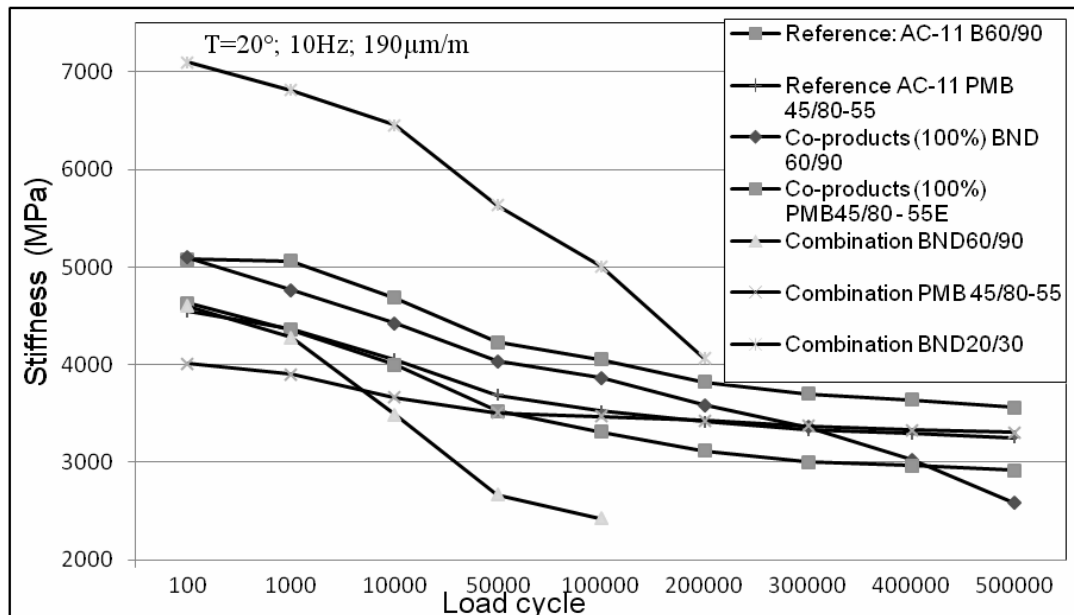


Figure 2. Diagram of stiffness exchange during loading

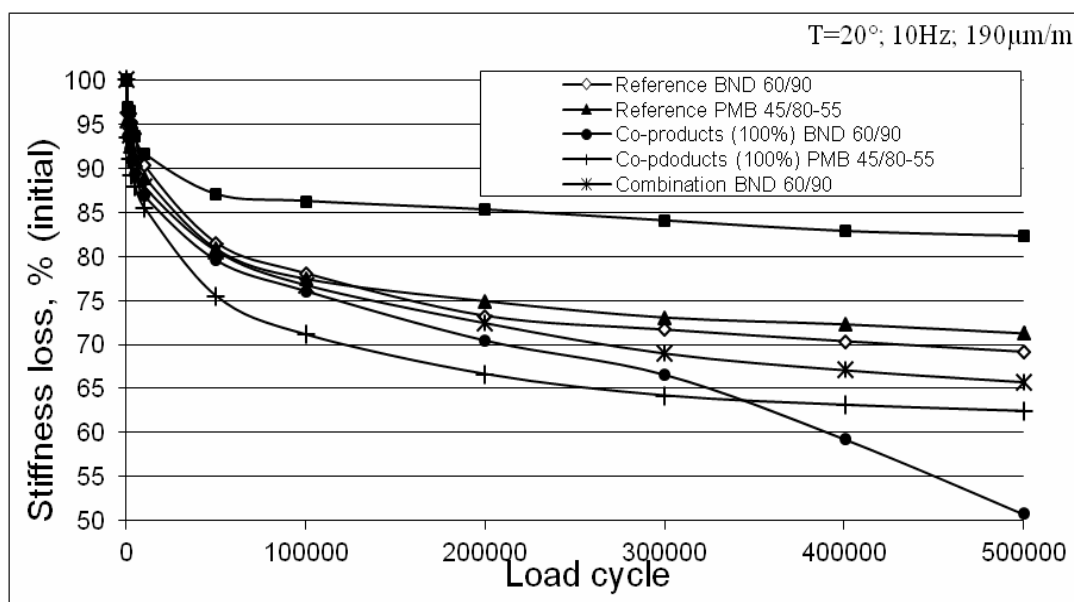


Figure 3. Diagram of stiffness loss evolution during loading

CONCLUSIONS

The four point bending test provides more adequate conditions for establishing design parameters of road pavement material if compared with the tree point bending test.

Measured value of deformation module depends on the number of loading cycles. Therefore the measured design value must depend on the design axle loadings during pavement service life and must be considered in pavement design process.

Asphalt mix made according to the particular standard granulometry and the particular regulations, does not obtain materials with uniform modulus of deformation, therefore for the design purposes it is recommend that the proposed bituminous pavement materials should be tested for establishing a proper design parameter.

Performed tests show significant discrepancy in the properties of test specimens made according to standard specifications compared with properties proposed for design purposes. Therefore, it is recommended to test proposed bituminous pavement materials for establishing proper design parameters.

ACKNOWLEDGEMENT

This work has been supported by the European Regional Development Fund (ERDF) activity No.2.1.1.1. „Atbalsts zinātnei un pētniecībai” (Support for the Science and Research) within project:No.2010/0254/2DP/2.1.1.1.0/10/APIA/VIA A/015.

REFERENCES

- Flintsch, G.W., Loulizi, A., Diefenderfer, S.D., Galal, K.A., Diefenderfer, B.K., (2007) *Asphalt Materials Characterization in Support of Implementation of the proposed Mechanistic — Empirical Pavement Design Guide*. Final report. Virginia Transportation Research Council, Charlottesville, Virginia
- National Road Specifications*, (2012), *Autoceļu specifikācijas-2012*, A/S Latvijas Valsts Čeli, Rīga. [online]. [accessed on 10.11.2012.]. Available: <http://www.lvceli.lv>
- Yeo, Y., Jitsangiam, P., Nikraz, H., (2011), *Flexural Behaviour Of Cement Treated Crushed Rock Under Static And Dynamic Loads*, in proceedings of The 7th International Conference on Road and Airfield Pavement Technology, Bangkok, Thailand.
- Инструкция по проектированию дорожных одежд нежесткого типа* ВСН 46-83 (VSN 46-83), (1985),. Минтрансстрой, Транспорт, Москва (in Russian).
- Проектирование нежестких дорожных одежд*. ОДН 218.046 -01, (2001), , Минтрансстрой, Москва (in Russian).
- Руденский, А.В, (2010), Определение расчетных значений модуля упругости асфальтобетона по результатам экспериментального определения фактических значений модуля упругости, *Дороги и Мосты*, № 23, Москва (in Russian).
- Сибирякова, Ю., (2007), Экспериментальное исследование некоторых асфальтобетонов под многократной нагрузкой //Транспортное строительство. № 4.
- Сибирякова, Ю., (2008), Расчетные параметры асфальтобетонных покрытий для проектирования нежестких дорожных одежд , doct. thesis, Moscow, .
- Телтаев, Б.Б., (2010), Анализ расчетных значений модуля упругости асфальтобетонов, Дорожная техника №10, , St. Petersburg.

DEVELOPMENT OF HIGH PERFORMANCE ASPHALT CONCRETE USING LOW QUALITY AGGREGATES

Viktors Haritonovs, Martins Zaumanis, Janis Tihonovs, Juris Smirnovs
Riga Technical University, Department of Roads and Bridges
E-mail: viktors.haritonovs@rtu.lv

ABSTRACT

Dolomite is one of the most available sedimentary rocks in the territory of Latvia. Dolomite quarries contain about 1000 million tons of the material. However, according to Latvian Road Specifications 2012, this dolomite cannot be used for average and high intensity roads because of its low quality (mainly, LA index). Therefore, mostly imported magmatic rocks (granite, diabase, gabbro, basalt) or imported dolomite are used which makes asphalt expensive. However, practical experience shows that even with these high quality materials roads exhibit rutting, fatigue and thermal cracks. The aim of the paper is to develop a high performance asphalt concrete for base and binder courses with using only locally available aggregates. In order to achieve resistance against deformations at a high ambient temperature a hard grade binder was used. Workability, fatigue and thermal cracking resistance, as well as sufficient water resistance is achieved by low porosity (3-5%) and higher binder content compared with traditional asphalt. The design of the asphalt includes a combination of empirical and performance based tests, which in laboratory circumstances allow traffic and environmental loads to be simulated. High performance ACb 16 asphalt concrete has been created using local dolomite aggregate B20/30 penetration grade bitumen. The mixtures will be specified based on fundamental properties in accordance with EN 13108-1 standard

Key words: dolomite aggregate, asphalt concrete, permanent deformations, fatigue resistance

INTRODUCTION

If the local material does not fulfill requirements, then one should seek a way for the improvement of its properties. If this is not possible, then one should seek a technological solution which will allow the application of the weaker material (Sybilski et al. 2010). One proper solution might be the use of dolomite as a component of High Modulus Asphalt Concrete (HMAC). Knowing that the binder courses, situated between 5 and 12 cm below the road surface (Fig. 1), are subject to the highest stresses, high stiffness is probably the most important requirements for HMAC (De Backer et al. 2008).

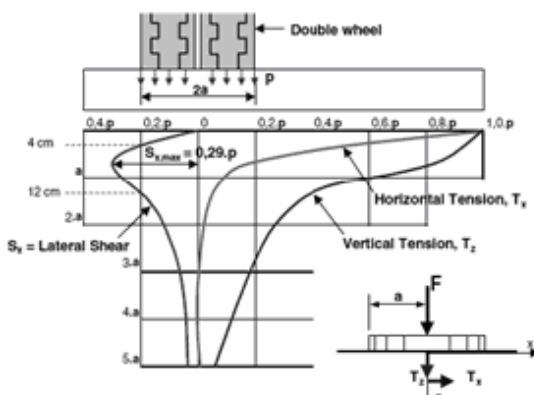


Figure 1. Lateral force diagram of heavy vehicle tire (Sivapatham et al. 2010)

HMAC is a mixture of asphalt concrete designed for use in the base and binder course of asphalt pavement. It has a closed structure with a comparatively large content of bitumen. Hard road bitumen grades are applied, mainly 10/20, 15/25, 20/30 and polymer modified bitumen. Hard bitumen assures the mixtures resistance to rutting. However a large content of bitumen assures workability, fatigue durability and water resistance (Sybilski et al. 2008).

This type of an asphalt mixture is designed not only by empirical properties but also by performance based properties (rut test, stiffness modulus test, fatigue test) (SPENS).

France was also one of the first countries in which mechanistic asphalt pavement design was introduced into general practice (AFNOR). In France, it is known under the acronym EME. In Poland, the acronym is AC WMS. The possible application of weaker mineral aggregate is one of the advantages of EMA (in English HMAC). Application of High Modulus Asphalt Concrete allows for saving on asphalt pavement's thickness thanks to a higher stiffness modulus which reduces tension strains in asphalt base layer.

The aim of the paper is to develop a high performance asphalt concrete for base and binder courses with using only locally available aggregates – crushed dolomite. In order to achieve resistance to deformations at a high ambient temperature hard grade binder was used.

MATERIALS

The basic materials used in this study are fractionated crushed dolomite aggregate and unmodified hard grade bitumen B20/30. Crushed dolomite aggregate was obtained from Plāviņu DM Ltd. (Latvia), and hard grade bitumen B20/30 from Grupa LOTOS S.A (Poland).

Bitumen characteristics

The binder properties have been tested by means of conventional binder tests: needle penetration, softening point, aging and the Fraas breaking point. The test results are listed in Table 1.

Table 1
Bitumen properties

Parameter	Result	Standard
Penetration at 25°C, dmm	25.3	LVS EN 1426
Softening point, °C	62.6	LVS EN 1427
Fraas temperature °C	- 13	LVS EN 12593
Kinematic viscosity, mm ² /s	1460	LVS EN 12595
Dynamic viscosity, Pa·s	3277	LVS EN 12596
Ageing characteristics of bitumen under the influence of heat and air (RTFOT method)		
Loss in mass, %	-0.02	LVS EN 12607-1
Retained penetration, %	75.9	LVS EN 1426
Increase of a softening point, °C	6.9	LVS EN 1427
Fraas breaking point after aging, °C	-11	LVS EN 12593

Properties of dolomite aggregate

The test results of dolomite's main properties show very low flakiness index – 5, high frost resistance with an average MS value of 7 and low fines content – 0.6%. However LA value is only 33. These aggregates are suitable for use as a component of High Modulus Asphalt Concrete, where permitted LA value up to 40 (SPENS). The properties of dolomite aggregate are shown in Table 2

Table 2
Physical and mechanical characteristics of dolomite

Physical and mechanical properties	Related standard	Result
Los Angeles (LA) coefficient, %	LVS EN 1097-2	33
Resistance to wear.	LVS EN 1097-	21
Nordic test (AN), %	9	
Flakiness Index (FI), %	LVS EN 933-3	5
Water absorption, %	LVS EN 1097-6	2
Grain density, Mg/m ³	LVS EN 1097-6	2.80
Fine content, %	LVS EN 933-1	1
Freeze/thawing (MS), %	LVS EN 1367-2	7

MIX DESIGN

HMAC-16 asphalt concrete mixtures have been designed by using conventional and unconventional (bitumen - B20/30, dolomite aggregate LA > 30) raw materials (Fig. 2). The basic idea of HMAC is to design a mix with a hard grade bitumen at a high binder content. (Rohde et al. 2008). The Marshall mix design procedure was used for the determination of the optimal bitumen content for the reference mixture, considering the mixture test results for Marshall stability and flow, as well as the volumetric values: air voids (V), voids in mineral aggregate (VMA) and voids filled with bitumen (VFB). Test specimens for the Marshall Test were prepared in the laboratory by impact compactor according to LVS EN 12697-30 with 2×50 blows of hammer at a 150°C temperature.

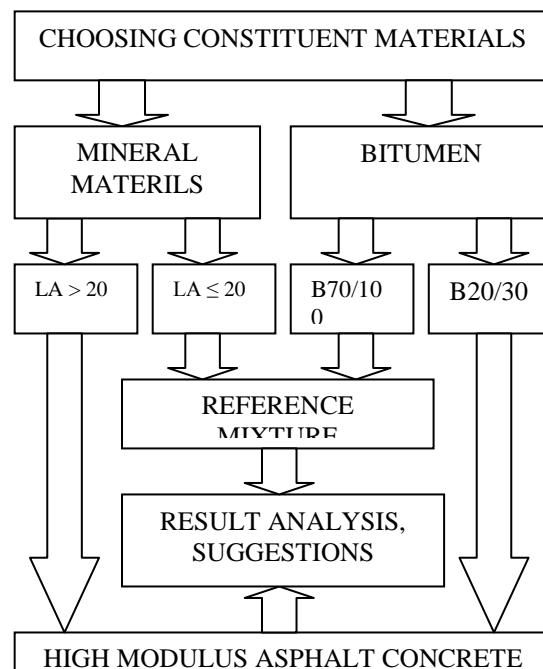


Figure 2. Experimental plan

RESULTS

Physical properties

Analysis of physical properties of the asphalt mixtures (the compaction degree), which is characterized by three volume parameter, has been made. The binder content has been optimized and conformity to HMAC requirements (SPENS) has been evaluated. Table 3 contains test results of the physical properties depending on the binder content.

Table 3
Physical characteristics of HMAC mixtures

Parameter	Mixtures					
	(HMAC-2/1)	(HMAC-2/2)	(HMAC-2/3)	(HMAC-2/4)	(HMAC-2/5)	Reference
Bulk density, kg/m ³	238 3	241 1	243 0	245 5	245 7	255 0
Maximum density, kg/m ³	260 2	258 6	258 6	255 5	255 1	268 0
Voids content, %	8.4	6.8	6	3.9	3.7	4.85
VMA	19.3	18.8	18.3	17.8	18	17.6
VFB	56.3	64	67.2	78.2	79.6	72.4
Bitumen content, %	4.56	4.99	5.06	5.67	5.83	5.0

Marshall test

Table 4 contains the Marshall test results depending on the binder content. The results show that HMAC mixtures has a higher Marshall stability compared to the reference mixture.

Table 4
Marshall test results

Parameter	Mixtures					
	(HMAC-2/1)	(HMAC-2/2)	(HMAC-2/3)	(HMAC-2/4)	(HMAC-2/5)	Reference
Stability at 60°C (kN)	Not tested (voids content > 5%)			16.6	15.4	12.0
Flow at 60°C (mm)				3.8	5.9	4.2

Wheel tracking test

To perform a rut resistance test, a wheel tracking apparatus is used to simulate the effect of traffic and to measure the deformation susceptibility of asphalt concrete samples. Tests were performed according to the standard LVS EN 12697-22 method B (wheel tracking test with small size device in air) (Fig. 3.). This test method is designed to repeat the stress conditions observed in the field and therefore can be categorized as simulative. The asphalt mixture resistance to permanent deformation is assessed by the depth of the track and its increments caused by repetitive cycles (26.5 cycles per minute) under constant temperature (60°C). The rut depths are monitored by means of two linear variable displacement transducers (LVDTs), which measure the vertical displacements of each of the two wheel axles independently as rutting progresses. The obtained results demonstrate that the largest rut depth (5.7mm) appear for the HMAC mixture with 5.83% bitumen content. The second best results are shown for reference mixture – 5.3mm. HMAC mixture with a 5.67 bitumen content, show the best result – 3.8mm. Figure 6 summarizes the wheel tracking test results.



Figure 3. Test equipment for wheel tracking test



Figure 4. Test equipment for fatigue test

Fatigue

To determine the fatigue life of the prepared asphalt concrete mixes, a four point bending fatigue test was conducted (Fig. 4.). The test was run at 10°C,

10Hz at 130 $\mu\text{m}/\text{m}$ strain level. The beams were compacted in the laboratory by using a roller compactor (Fig. 5.). They were saw cut to the required dimensions of 50mm wide, 50mm high and 400mm long. The failure criterion used in the study is the traditional 50% reduction in initial stiffness. The obtained results indicate that the HMAC mixture showed high resistance to fatigue, compared with the results for the reference mixture made with conventional aggregates and bitumen. The stiffness reduction curves are shown in Figure 7.



Figure 5. Roller compactor

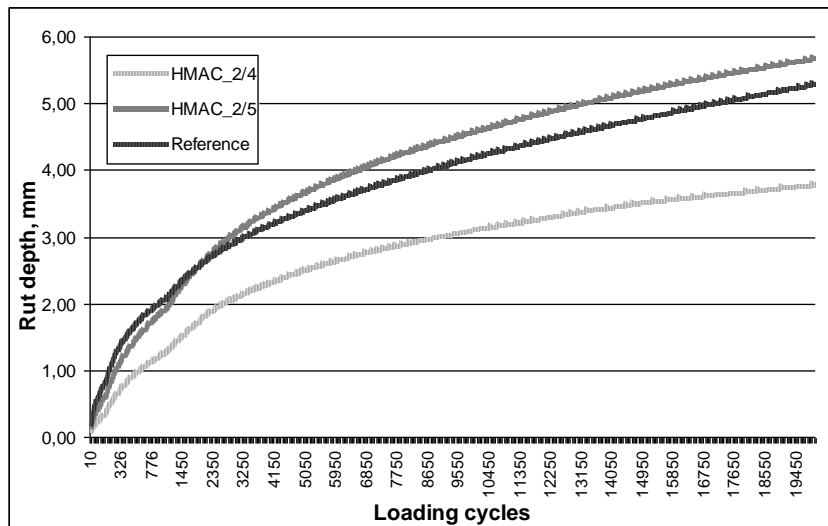


Figure 6. Wheel Tracking Test Results

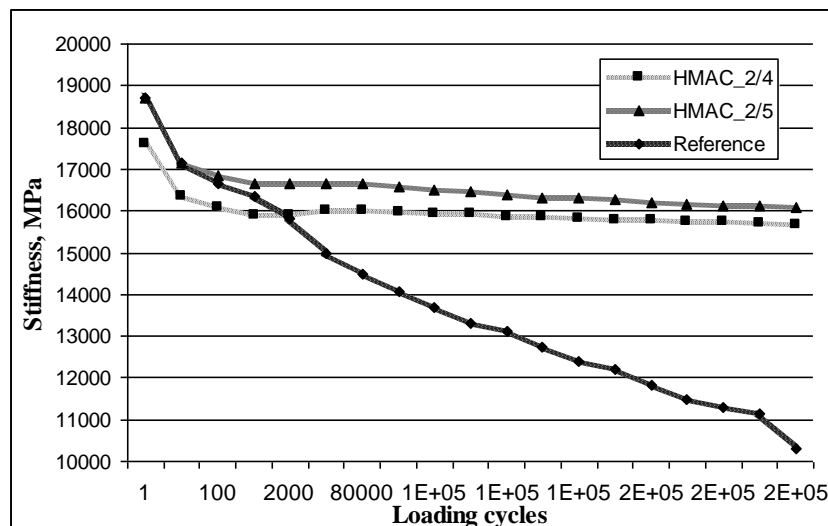


Figure 7. Wheel Tracking Test Results

CONCLUSIONS

Use of dolomite aggregate in High Modulus Asphalt Concrete was evaluated. Comparative testing was performed on the AC16_{bin} (reference) with conventional bitumen B70/100 and granite aggregate. Reference mixture proved that a low binder content resulted in lower fatigue life despite high rut resistance. However both HMAC mixtures showed high rut and fatigue resistance. Results of tests show that Latvian dolomite may be applied without any fear in High Modulus Asphalt Concrete for base and binder courses.

HMAC mixtures meet the HMAC asphalt concrete requirements in accordance with SPENS project recommendations (SPENS).

ACKNOWLEDGEMENT

This work has been supported by the European Regional Development Fund (ERDF) activity No.2.1.1.1. „Atbalsts zinātnei un pētniecībai” (support for the science and research) within the project: No.2010/0254/2DP/2.1.1.0/10/APIA/VIA A/015.

REFERENCES

- Sybilska D., Bankowski W., Krajewski M. (2010). High Modulus Asphalt Concrete with limestone aggregate, *Internationa Journal of Pavement Research and Technology* (ISSN: 1996-6814), Vol. 3, No. 2, p 96-101.
- Backer C., Visscher J., Glorie L., Vanelstraete A., Vansteenkiste S., Heleven L. (2008). A comparative high – modulus experiment in Belgium. *Proceedings of Transport Research Arena Europe 2008 (TRA 2008) Internationa Conference*. 21 – 24 April 2008, Ljubljana, Slovenia.
- Sivapatham P., Beckedahl H.J and Jannsen S. (2010) High Stable Asphalt for Heavy loaded Bus Test Lane Sections. *Proceedings of the 11th Internationa Conference on Asphalt Pavements ISAP 2010*. 1 – 6 August 2010, Nagoya, Aichi, Japan.
- Sybilska D., Maliszewska D., Maliszewski M., Mularzuk R. (2008). Experience with High Modulus Asphalt Concrete in Warsaw street overlays. *Proceedings of Transport Research Arena Europe 2008 (TRA 2008) Internationa Conference*. 21 – 24 April 2008, Ljubljana, Slovenia.
- Sustainable Pavements for European New Member States (SPENS) Document No. D8. [online]. [accessed on 10.10.2012.]. Available: <http://www.spens.fehrl.org>
- AFNOR – Association Fran aise de Normalisation. “Enrob s Hydrocarbon s: Couches d’assises: enrob s a module  lev  (EME): NF P 98-140”. Paris, 1999. (in Franch).
- Rohde L., Ceratti J. A. P., N nez P.V., Vitorello T. (2008). Using APT and Laboratory Testing to Evaluate the Performance of High Modulus Asphalt Concrete for Base Courses in Brazil. *Proceedings of the Third International Conference on Accelerated Pavement Testing (APT '08.)*. 1 – 3 October, Madrid, Spain.

UNCONFINED COMPRESSIVE STRENGTH PROPERTIES OF CEMENT STABILIZED PEAT

Peteris Skels*, Kaspars Bondars**, Aleksandrs Korjakins***

*, **Department of Civil Engineering, Technical University of Riga,

***Department of Building Materials and Products, Technical University of Riga,

Kalku street 1, Riga, Latvia, LV-1658,

Phone: 371+67089086, Fax: 371+67089086,

E-mail: *peteris.skels@gmail.com, **kaspars.bondars@j-a.lv, ***aleks@latnet.lv

ABSTRACT

Peaty soil is viewed as a weak subgrade with poor bearing capacity and high compressibility. This study presents cement stabilization of peat to improve its engineering properties. Soil samples for laboratory experiments were collected in Riga Region, Garkalne municipality, near the Riga-Pskov road, in the place where a fen is formed by the peat of up to 5 meters in thickness.

Unconfined compression tests were performed for stabilized peat specimens (cured in laboratory, soaked in water) to evaluate an increase in bearing capacity for three different Portland cement dosages- 200kg/m³, 250kg/m³ and 300kg/m³; and three different surcharge rates-0kPa, 6kPa and 18kPa; in 7, 14 and 28 days. Surcharge rates were varied in order to evaluate the effect of stabilization in different depth and under additional axial loading during the process.

Laboratory tests showed that not only the unconfined compressive strength, but also stiffness and compressibility of the peat were remarkably improved when mixed with cement. It was found that the effect of stabilization is strongly related to binder dosage, surcharge rate and curing time. The unconfined compression strength increase reached even 20 times the strength of the natural untreated and stabilized peat with 300kg/m³ cement dosage and 18kPa surcharge after 28 days curing and soaking in water.

Key words: peat, cement stabilization, hydraulically bound mixtures, unconfined compressive strength

INTRODUCTION

There are certain extents of the prospective construction areas consisting of soil layers with reduced physical and mechanical properties. In the areas with peat layers in the base, the accessibility during the construction phase and ability to construct safe, stable and serviceable structures of civil engineering projects may be greatly reduced due to the poor bearing capacity, high compressibility, and high water content.

Peat usually forms on water saturated land that is poor in oxygen and thus hinders the decomposition of dead plant matter by natural microorganisms. In these circumstances, the dying vegetation accumulates year after year in the form of a peat layer. To ensure the peat land preservation, water input must keep up with water loss.

The main aim of using stabilizers is to increase the bearing capacity and with that the compressibility and stability of the treated soil layers. The most common stabilizing agent for peats is Portland cement, although there are also other binder and additive types.

When cement reacts with water in peat, it forms calcium silicate hydrate ($3\text{CaO}\cdot2\text{SiO}_2\cdot3\text{H}_2\text{O}$) gel, which acts as glue that binds and holds the soil particles together. It is well recognized that organic soils can retard or prevent the proper hydration of binders such as cement in binder-soil mixtures

(Hebib, Farrell, 2003). Normally peat has a relatively low content of pozzolans that can enter into secondary cementation reactions. Subsequently, the interaction between hydrated lime $\text{Ca}(\text{OH})_2$ and the soil yields less effect in the secondary stabilization reactions. Therefore, no significant strength gain can be achieved from peat stabilization by cement unless cement is added to the soil in a large dosage. However, peat can be a highly variable material and the engineering properties of a peat deposit will be a result of the formation and morphology of the peat. For example, low $\text{pH}<4.8$ values usually characterize fibrous peats (raised bog), while amorphous-granular peats are rather neutral with a pH between 4.8 and 6.4 (Silami̇kele, 2010). Consequently, lower pH values will negatively affect the reaction rate of the binder, resulting in a slower strength gain in peat and vice versa.

Directly after mixing the soil with a binder, 0.5-1.0m of fill (approximately 9-18kPa) is normally laid out on top of the stabilized mass in order to create a more homogeneous stabilized mass. In addition, the fill/embankment ensures a trafficable bed for the continuous stabilization of adjacent areas. The initial preloading, applied shortly after mixing the soil with the binder, can be expected to improve the strength of the stabilized peat (Ahnberg et al., 2001).

The use of cement in peat stabilization has been studied for a long time, and in many countries codes of practice are available. In Latvia, the laboratory mechanical performance of the hydraulically bound mixtures of cement and soil is classified according to LVS EN 14227-10. Normative references to other documents applied in the study, such as LVS EN 13286-41, are also included.

The objective of this study is to evaluate the effect of the binder dosage, different surcharge rates, and also unconfined strength development in time at the laboratory. Unconfined compression tests were performed for stabilized peat specimens, cured in the laboratory and water soaked, to evaluate an increase in bearing capacity for three different Portland cement dosages - 200kg/m³, 250kg/m³ and 300kg/m³; and three different surcharge rates - 0kPa, 6kPa and 18kPa; in 7, 14 and 28 days.

MATERIALS AND METHODS

It is noted that peat can be a highly variable material depending on the formation and morphology. At one end of the scale, fibrous peats will have a visible plant structure with little humification, while amorphous peats, at the other end of the scale, will have a highly decayed structure.

The most distinctive characteristic of a peat deposit is its high water content, which generally ranges from 500% to 2000%, but can reach as high as 2500% for some coarse fibrous peats (Munro, 2004). Many of the geotechnical characteristics of peat result from this basic property.

The ash content (or non-organic content) is normally somewhere between 2% and 20% of its insitu volume and this range of ash contents can be an indicator of this type of peat (Munro, 2004).

Amorphous granular peats can have insitu undrained bulk densities of up to 1200 kg/m³ whilst for very woody fibrous peats it can be 600 kg/m³. Dry densities of peat can typically vary between 60 kg/m³ to 120 kg/m³. The specific gravity of peat typically varies from 1.5 to 1.8 with the higher ranges again reflecting a higher mineral content (Munro, 2004).

The void ratio of peat varies with the type of peat and moisture content. For example, peat with a moisture content of 1000% is likely to have a void ratio of approximately 18. Void ratios as high as 25 can be found in fibrous peats and void ratios as low as 9 are possible for the denser amorphous granular peats (Munro, 2004).

The permeability of peat in the field is highly variable and reduces dramatically when subjected to loading. The permeability of virgin peat usually ranges from 10⁻² to 10⁻⁴ cm/sec, but when loaded with a low embankment it can quickly reduce to 10⁻⁶ cm/sec and with a higher embankment construction to as low as 10⁻⁸ to 10⁻⁹ cm/sec (Munro, 2004).

The peat samples were taken in Riga Region, Garkalne municipality, near the Riga-Pskov road by the edge of the WESS Motors Auto Bergi, in the place where a fen is formed by peat of up to 5 meter in thickness (see Figure 1). The cement stabilization of this soil was studied at the laboratories of the Riga Technical University (RTU).

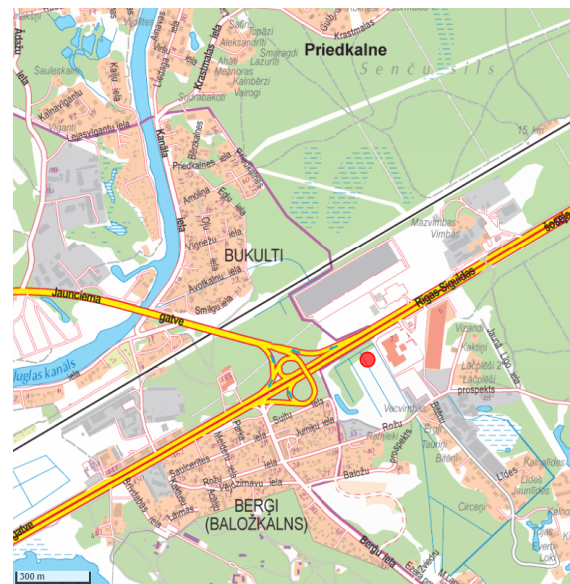


Figure 1. Map of Garkalne municipality, area by the Riga-Pskov road near the edge of WESS Motors Auto Bergi. The location is indicated with a red circle (SIA "Karšu izdevniecība Jāņa sēta" ...)

The field area is mostly flat or slightly curved in such a way that the center of the bog does not rise above the surrounding mineral ground, which is typical for fens that receive water from melting snow or from seepage flows. Fens have a tendency to contain peats that have a higher mineral content, lower water content and which are more humified than in raised bogs. According to typical fen formation as well as previous laboratory testing (Testēšanas pārskats Nr. 614-08...), sampled peat soil can be described as amorphous-granular peat with physical and chemical properties given in Table 1.

Table 1
Physical and chemical properties of natural peat

Properties	Natural peat tested
Natural water content (%)	690
Organic content (%)	91
Ash content (%)	9
Van Post classification (Hn)	H8-H10
pH	5.3

The KUNDA NORDIC CEM I 42.5N ordinary Portland cement was used for the soil stabilization

in laboratory. Binder was mixed with soil in three different dosages 200kg/m^3 , 250kg/m^3 and 300kg/m^3 using mixer KELAR EM2-1500E-2 (2000W) until the mixture was homogenous (approx. 10min). Then the soil-cement mixtures were placed by hand in plastic tubes with an inner diameter of 46mm.

Three special loading conditions for each of the different binder dosages were tested. Surcharge of 18kPa and 6kPa were put on samples filled in 200mm long plastic tubes shortly after mixing the soil, while surcharge was not put on samples filled in 100mm long plastic tubes. All the test samples were stored in a water container ensuring that water could interact with the stabilized soil at room temperature, i.e., about 20°C (see Figure 2).

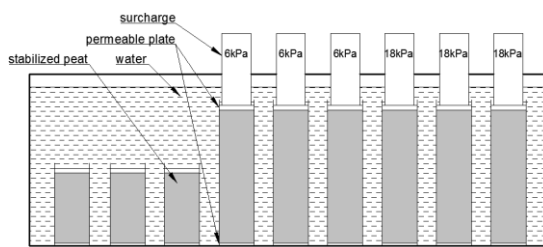


Figure 2. General design of test samples storage box

Unconfined compression tests were performed to evaluate the strength of stabilized peat samples after 7, 14 and finally 28 days stored in a water container with three different loading rates. All the test specimens were stored and then tested in triple tests, i.e., there were three equal samples for the same binder dosage and surcharge rate.

Prior to testing, the stabilized soil samples were prepared with a constant height to diameter ratio of 2. The samples were cut and smoothed to form parallel end surfaces. An unconfined compression test was performed with the electromechanical apparatus Zwick Z100 in accordance with LVS EN 13286-41.

RESULTS

It was observed during laboratory testing that the unconfined compression strength (UCS) of stabilized peat increased remarkably already after 7 days curing in water container and it enlarged continuously.

The quantitative UCS values of stabilized peat samples are plotted as a function of time in Figures 3 to Figure 8. The stabilized peat with binder dosage of 200kg/m^3 and without surcharge showed 73.2kPa, 90.5kPa, and 113.0kPa strength in average after 7, 14, and 28 days curing, respectively. While the stabilized peat with binder dosage of 300kg/m^3 and 18kPa surcharge showed 242.9kPa, 305.0kPa, and 355.8kPa strength in average after 7, 14, and 28 days curing, respectively. This is the range of

experimental data, i.e., between 73.2kPa and 355.8kPa.

It was approximately estimated that natural peat does not accomplish even UCS of about 15kPa. Therefore, the strength gain for stabilized peat was observed to be more than 20 times the strength of the natural peat and stabilized peat with 300kg/m^3 Portland cement dosage and 18kPa surcharge.

The strength gain of stabilized peat was evaluated as a function of binder dosage and also surcharge rate. It is essential to compare the effect of these different factors.

Effect of binder dosage on the strength of stabilized peat

The unconfined compression test results of stabilized peat with three different binder dosage rates and constant surcharge rate can be seen in Figure 3, Figure 4 and Figure 5 as a function of time.

It was determined that the higher the binder dosage, the higher the predictable UCS value. Strength of stabilized peat after 7 days curing under the identical preloading with binder dosage of 250kg/m^3 increased 43% and with binder dosage of 300kg/m^3 increased 124% more than with binder dosage of 200kg/m^3 in average. Furthermore, strength increase after 14 and 28 days with a binder dosage of 300kg/m^3 continued to rise 17% faster than with dosage of 200kg/m^3 and 250kg/m^3 in average. This is an indication of the optimal Portland cement content in the mixture in order to ensure a continuous stabilization process.

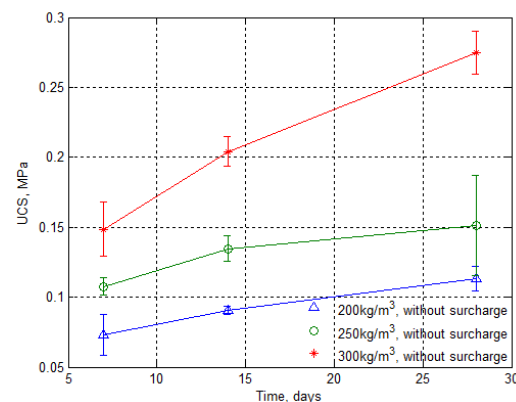


Figure 3. UCS values as a function of time for different binder dosages and without surcharge

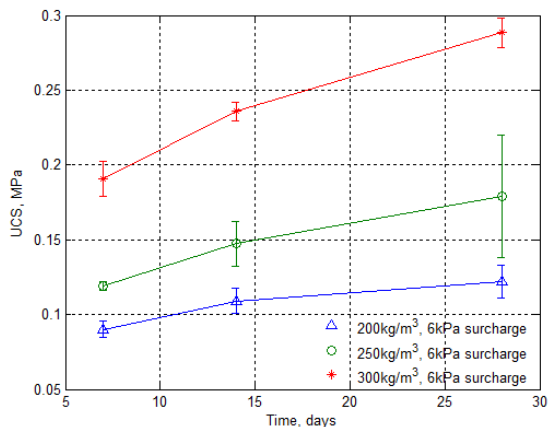


Figure 4. UCS values as a function of time for different binder dosages and with 6kPa surcharge

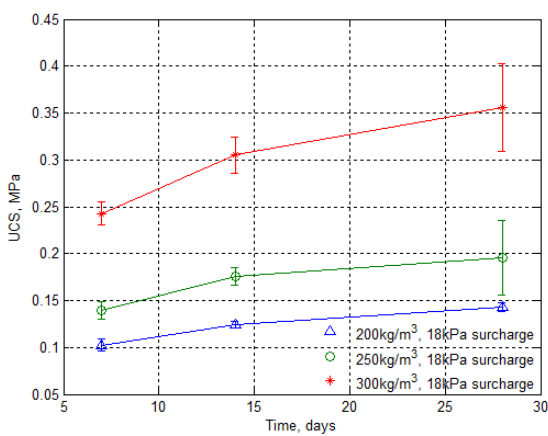


Figure 5. UCS values as a function of time for different binder dosages and with 18kPa surcharge

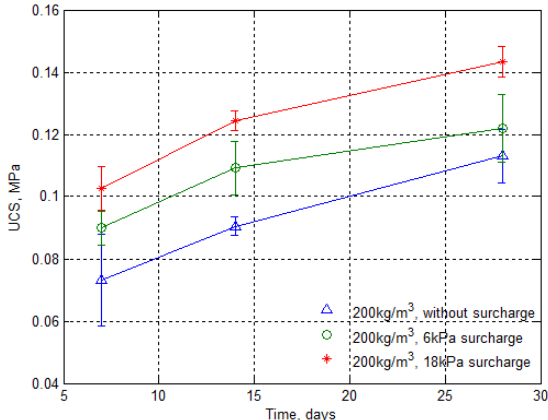


Figure 6. UCS values as a function of time for different surcharge rates and with 200kg/m³ binder dosage

Effect of preloading on the strength of stabilized peat

The unconfined compression test results of stabilized peat with three different surcharge rates and constant binder dosage can be seen in Figure 6, Figure 7 and Figure 8 as a function of time.

It was found that there is a visible UCS increase when a surcharge is applied for all three different

binder dosage rates after 7 days curing. However, both the character and the UCS increase after 14 and 28 days stayed the same in the range of the standard deviation. We can say that there is a remarkable effect of surcharge in the early stage of stabilization, while stabilization effectiveness in the later stage is determined generally by the binder dosage rate. This also might be because the surcharge rate was relatively low, i.e., only 6kPa and 18kPa.

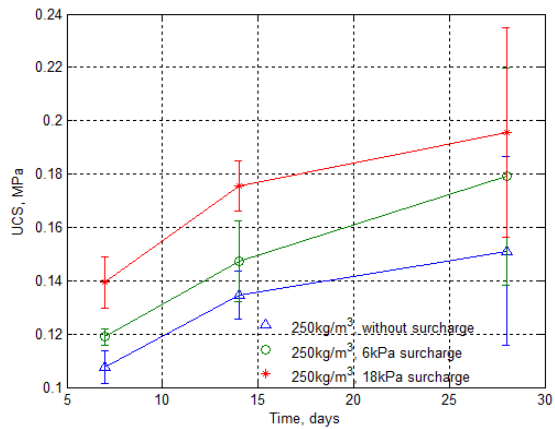


Figure 7. UCS values as a function of time for different surcharge rates and with 250kg/m³ binder dosage

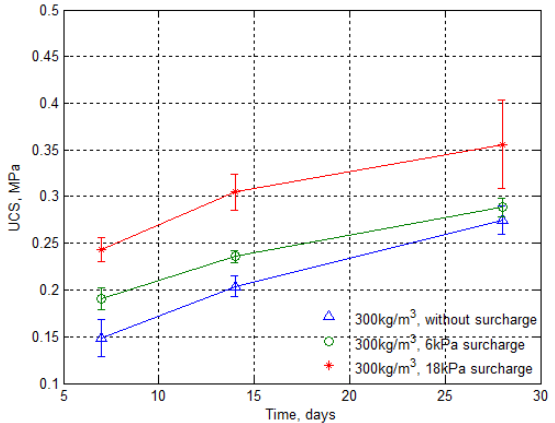


Figure 8. UCS values as a function of time for different surcharge rates and with 300kg/m³ binder dosage

CONCLUSION

Peat in its natural state consists of water and decomposing plant fragments with practically no measurable bearing strength and high compressibility. Therefore, it is of critical importance to improve its engineering properties, considering shear failure, settlements and critical plains of failure, in order to use these extents of the prospective construction area in Riga Region, Garkalne municipality, near the Riga-Pskov road by the edge of the WESS Motors Auto Bergi, in the place where a fen is formed by peat of up to 5 meter

in thickness (see Figure 1). Cement stabilization is introduced.

In this study, the stabilization of peat with ordinary Portland cement showed a considerable strength increase to more than 20 times the strength of the natural peat and stabilized peat with 300kg/m³ Portland cement dosage and 18kPa surcharge. The unconfined compressive strength of stabilized peat varied from 108.0kPa to 403.3kPa after 28 days curing depending on the binder dosage amount and the surcharge rate. Both the effect of the binder dosage and preloading on the strength of stabilized peat was evaluated.

It was found that there is a remarkable effect of surcharge in the early stage of stabilization, while stabilization effectiveness in the later stage is determined generally by the binder dosage rate. Nevertheless, this surcharge rate of 18kPa corresponds to a normal preload from approximately 1m of sand fill and it ensures the required base for construction machinery to move and continue the stabilization process. It is clearly noticed that a more homogeneous stabilized peat mixture is constructed when preload is applied.

The greatest effect on the strength of the stabilized peat was demonstrated by the Portland cement dosage. It was discovered that the larger binder dosage, the greater the predictable stabilized mass strength. But the binder amount in the mixture should be determined so to ensure that the

stabilization processes continues in time. Although the optimal Portland cement dosage for the best stabilization effect has not been determined in this study, the indication of it was found by trial and error. Comparing the effect of three different binder dosages on the strength of stabilized peat with a constant surcharge rate, it was found that the mixture with 300kg/m³ binder dosage shows a considerably larger strength increase in the later stage, i.e., after 14 days and 28 days curing, comparing with mixtures of lower binder dosages. Stabilized peat samples with 300kg/m³ binder dosage show a continuity of the stabilization processes, and therefore can be assumed to be the optimal Portland cement dose for this particular peat stabilization. However, there are more precise and advanced techniques of how to determine the optimal binder amount in hydraulically bound mixtures, e.g., pH test, Atterberg (consistency) limits analysis, used in the previous study (Skels, 2011). These tests were not in the scope of this study.

There is still plenty of room for development in the stabilization of soils with poor bearing capacity. For future work, it would be essential to evaluate the peat stabilization effectiveness in the field. This would provide results to compare with the laboratory study.

REFERENCES

- Ahnberg, H., Bengtsson, P.-E. and Holm., G. (2001), Effect of initial loading on the strength of stabilized peat. Proceedings of the ICE-Ground Improvement, Volume 5, Issue 1, pages 35-40
- Hebib, S. and Farrell, E.R. (2003), Some experiences on the stabilization of Irish peats. Can. Geotech. J. 40(1): 107-120. Digital Object Identifier (DOI): 10.1139/T02-091
- Munro, R. (2004), Dealing with bearing capacity problems on low volume roads constructed on peat. Including case histories from roads projects within the ROADEX partner districts. The Highland Council, Transport, Environmental & Community Service
- LVS EN 14227-10:2006A Hydraulically bound mixtures- Specification- Part 10: Soil treated by cement;
- LVS EN 13286-41:2003 Unbound and hydraulically bound mixtures- Part 41: Test methods for the determination of the compressive strength of hydraulically bound mixtures
- SIA “Balt-Ost-Geo” Laboratorija (10.09.2008), Testēšanas pārskats Nr. 614-08;
- SIA “Karšu izdevniecība Jāņa sēta”. Skatīts 2012.12.02:
<http://www.balticmaps.eu/?lang=lv¢erx=517575¢ery=6317714&zoom=2&layer=map&ls=o>.
- Silamiķele, I. (2010), Humifikācijas un ķīmisko elementu akumulācijas raksturs augsto purvu kūdrā atkarībā no tās sastāva un veidošanās. Promocijas darbs, Rīga: Latvijas Universitāte: Geogrāfijas un Zemes zinātņu fakultāte
- Skels, P., Ingeman-Nielsen, T., Jorgensen, A.-S., Bondars, K., Skele., E. (2011), Quicklime (CaO) stabilization of fine-grained marine sediments in low temperature areas. Proceedings of the Civil engineering 11', Jelgava, Latvia

MECHANICAL PROPERTIES OF LOW TEMPERATURE HYDRAULIC BINDERS

Bruno Kirulis*, Janis Kreilis**

Latvia University of Agriculture, Department of Structural Engineering

e-mail: *Bruno.Kirulis@llu.lv; **Janis.Kreilis@llu.lv

Linda Krage, Inta Barbane

Riga Technical University, Institute of Silicate Materials; e-mail: Linda.Krage@gmail.com

Inese Sidraba

Researcher in Latvia University; e-mail: inese@ktf.rtu.lv

ABSTRACT

The local mineral deposits – clay and dolomite are widely used for production of building materials in Latvia. Investigations of new materials and energy saving methods are today's topicality. One of the possibilities is to reduce production expenses using lower firing temperature, and, in addition, providing desired strength characteristics required for building applications (Lindina et.al., 2011). For obtaining new materials the deformation and strength properties have to be analysed and taken into account.

It is known, that a great part of architectural monuments in Latvia were built using low-temperature natural cement – dolomitic Roman cement as a binder and now it is time to start their restoration. As the production of dolomitic Roman cement stopped 60 years ago, it is urgent to develop a method on how to obtain low temperature binder from dolomite and clay similar to the historic type, from natural dolomitic marl produced Roman cement.

At first, the composition as well as physical properties of hydraulic binders were investigated (Barbane et.al, 2012). In order to study the mechanical properties, a range of uniaxial loading tests with samples were performed using the testing equipment "Instron 5985". For comparison ready-mixed calcitic Roman cement „Prompt” samples were previously tested. Analysis of the results shows stable mechanical property values. The resulting binder's mechanical parameters could be used for further improvement of the historic building restoration works.

Key words: Roman cement, clay and dolomite, mechanical properties

INTRODUCTION

Roman cements are well-known low temperature hydraulic binders. Historically Roman cements were produced and used for construction of buildings up to the middle of the 20th century, when they were replaced by Portland cement. Roman cement “rebirth” started 10 years ago (ROCEM project) due to the necessity to renovate century-old buildings of historic significance. Logically, the restoration is targeted at the use of similar materials and technologies which had been applied in restored buildings.

In Central Europe calcitic Roman cements were used as a binding agent, and extensive research work has been carried out within international projects since 2003 (Hughes et. al., 2009). It should be noted that dolomitic Roman cement has not been included in these projects because calcitic marl is dominant as a raw material in the main part of Europe. In Latvia, contrary to other parts of Europe, dolomitic Roman cement was produced as there were rich resources of dolomitic marlstone. A new method has been worked out on how to synthesize hydraulic binders for historic arhitectural renderings.

In this paper the most important mechanical properties of proposed binders are analyzed on the

experimental background. The main attention is paid to the effects of chemical composition and hardening time of the binder, as well as the influence of other factors in order to search the areas of effective application of binders.

MATERIALS AND METHODS

Materials

Mixtures from two types of clay and dolomite in powder state were synthesized. Samples were prepared by mixing the raw materials, semidry pressing and firing at 800°C temperatures. Thermochemical processes in dolomite-clay mixtures depending on the production temperature and clay type were compared by using XRD analysis and full chemical analysis (Barbane et.al, 2012).

Two compositions from Devonian clay and dolomite with a clay content of 13%, 24% (A1, A2 respectively) and one composition using Quaternary clay with a clay content of 24% (U2) were synthesized. The chosen dolomite-clay mass ratio closely conforms to the chemical composition of natural dolomitic marl – a traditional raw material of dolomitic Roman cement used in Latvia. Temperatures of 800-850°C were chosen as optimal for the synthesis of the hydraulic binder from the

mixture of clay and dolomite similar to natural dolomitic Roman cement.

For determination of mechanical properties the cylindrical samples (the ratio of the diameter-height - 1:2) of synthesized binders A1, A2 and U2 were made by adding 60% water and holding them in wet-curing conditions for 7 days (Fig.1). Tests with samples were performed after 7 and 28 days. Before the test samples were dried at 80°C for one day, they were weighed for the determination of density. Parallel, for comparison ready-mixed calcitic Roman cement "Prompt" samples were made and tested.

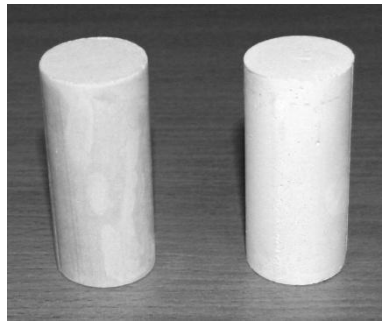


Figure 1. Cylindrical samples of synthesized binders

Methods

Testing method, sample shape and dimensions (in comparison with LVS EN 196-1) is chosen based on two considerations:

- compression of short cylinders of prismatic shapes is the most general testing method for the preliminary determination of strength of mineral materials with unknown properties;
- one of the main objectives of this investigation is to search the areas of an effective application of new material, therefore a general testing scheme was applied.

Sample size – a diameter of 28.5 mm was adopted due to a limited amount of research material.

Uniaxial compression tests were performed using the loading equipment Instron 5985, assuming the loading rate of 0.2 mm per second (Fig. 2). Conditions of uniaxial compression were provided by using of pinned joint base plates at the top and the bottom side.

As a result, data for Excel were obtained and load-extension, as well stress-deformation curves were drawn. The samples of each composition (on average five per setting group) A1, A2 and U2 were tested and the mean values assessed for sample ages of 7 and 28 days respectively.

Compression deformation modulus of the synthesized compositions is calculated using equation:

$$E = \frac{\Delta F \cdot h}{A \cdot \Delta w}, \quad (1)$$

Where:

ΔF_u and Δw – load and extension component on the linear part of the curve; A , h – cross section area and height of the sample respectively.



Figure 2. Uniaxial compression tests

Breaking compression stresses are determined and the main attention is focused on the influence of the essential factors - chemical composition, hardening time as well failure modes of the samples, water-cement ratio (W/C ratio) and the density of the binder.

Along with breaking stress and E-modulus the deformation energy is an important material characterizing factor, because of its correlation with impact resistance and fracture toughness of material (Chamis et. al., 1971). The critical deformation energy is the amount of elastic energy, accumulated in the material volume at the critical deformation or critical stress:

$$U_{cr} = \int_0^h F dh = \int_0^h E A \frac{\Delta h}{h} dh = \frac{EA\Delta h^2}{2h}$$

$$\text{or } U_{cr} = \frac{1}{2} E \varepsilon_{cr}^2 Ah \quad (2)$$

The critical deformation energy per unit volume:

$$\frac{U_{cr}}{V} = u_{cr} = \frac{E \varepsilon_{cr}^2}{2} = \frac{\sigma_{cr} \varepsilon_{cr}}{2} \quad (3)$$

$$\text{or } u_{cr} = \frac{\sigma_{cr}^2}{2E} \quad (4)$$

Mainly two failure modes were observed: 1 - crushing of the top part of the samples; 2 – crushing over the whole length or in the middle of the samples (Fig.2 and 3). The first mode lead to a reduced load capacity due to the influence of air inclusions at the top part of the samples and these results were excluded from further analysis.



Figure 3. Two failure modes of the samples

Experimental results

An overview of test results is given in the diagrams below (Fig.4–7).

Ready-mixed calcitic Roman cement „Prompt” samples were tested previously (Fig.4). The methodology was accepted and first result analysis worked out during these tests.

It can be seen, that the general level of the load bearing capacity is determined by the chemical compositions of the samples. In addition other factors affect the stress and strain properties. Hardening time has a very significant impact; only composition A1 makes an exception. In our opinion, it is caused by low clay content.

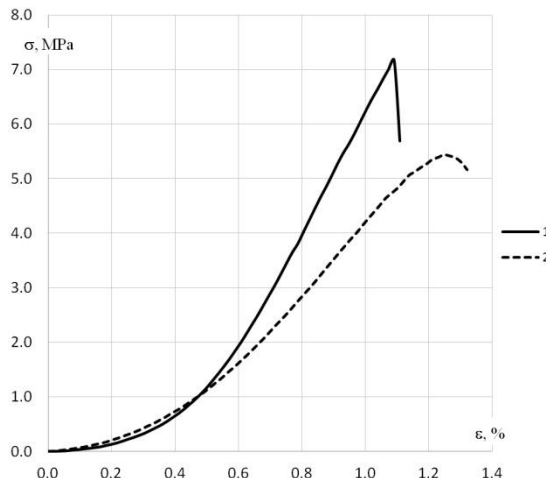


Figure 4. Test results of Roman cement “Prompt” samples: 1, 2 – hardening time of two and one week respectively

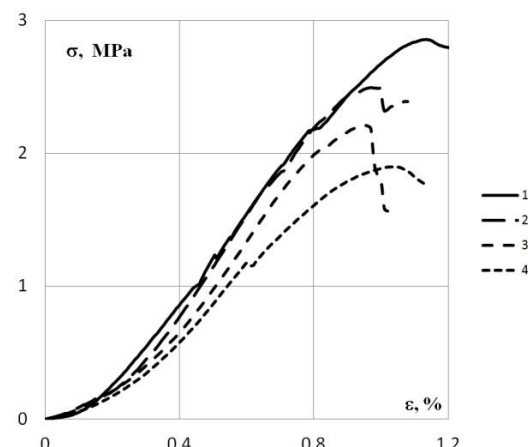


Figure 5. Test results of composition A1 samples:
1, 2 – hardening time of four weeks; 3, 4 – hardening time of one week

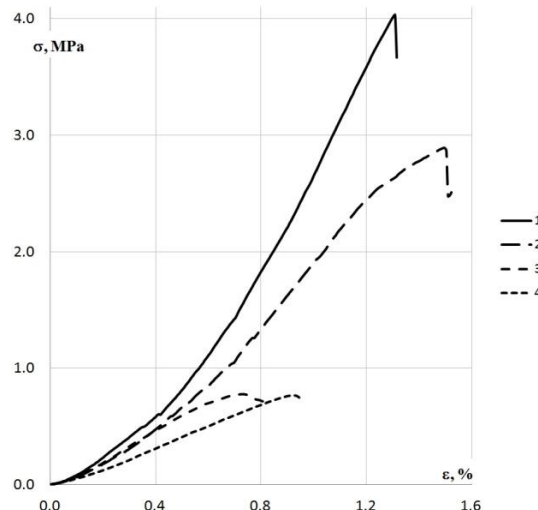


Figure 6. Test results of composition A2 samples
1, 2 - hardening time of four weeks; 3, 4 – hardening time of one week

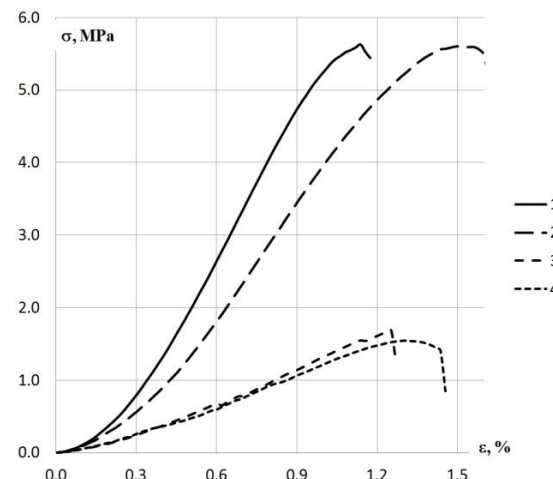


Figure 7. Test results of composition U2 samples:
1,2 – W/C ratio 60%; 3,4 – W/C ratio 70%

As mentioned before, the compositions were made by adding 60% water. It should be noted that due to rapid setting it is necessary to use a retarder – 0.6% of citric acid. The lowest possible W/C ratio is chosen to obtain a paste with sufficient workability. In order to determine the influence of W/C ratio, the additional samples of compositions U2 were made by adding 70% water. As a result a decrease in the density and strength properties can be observed (Fig. 7).

RESULTS AND DISCUSSION

The main physical and mechanical properties of the binder compositions are summarized in Table 1.

Table 1
Properties of binder compositions

Composition	No.	ρ	σ_{cr}	E	u_{cr}
		kg/m ³	N/mm ²	N/mm ²	N*m/m ³
Prompt	1``	1252	7.24	1143	22930
	2`	1190	5.44	685	21601
A1	1```	1075	4.64	354	30409
	2```	1100	4.06	387	21297
	3`	1095	3.59	349	18464
	4`	1112	3.08	259	18314
A2	1```	1200	4.03	460	17653
	2```	1160	2.89	290	14400
	3`	1190	0.76	110	2625
	4`	1200	0.78	150	2028
U2	1```	1190	5.60	600	26133
	2```	1210	5.67	720	22326
	3`	1122	1.69	180	7934
	4`	1113	1.54	160	7411

where apostrophes ` indicate hardening time (weeks)

The numerical calculation of u_{cr} was performed according to equation (4) taking into account E-modulus, obtained from the linear segment of stress-strain curves. The obtained values ($\max u_{cr} = 30409 \text{ N m/m}^3$) show that the tested specimen material critical deformation energy lays between these parameters for bulk glass ($u_{cr} = \sim 17\ 000 \text{ N m/m}^3$) and solid clay brick ($u_{cr} = \sim 46\ 000 \text{ N m/m}^3$) (Bencich et. al., 2001), (Bansal et.al., 1986).

As a result of the experimental tests the main mechanical properties of the synthesized compositions were assessed taking into account

hardening time and density (W/C ratio) of the samples. Besides, crushing modes of the samples were also considered.

In addition it should be noted that sample properties are affected by various other factors:

- influence of air inclusions due to rapid setting (beginning in 2 or 3 minutes) observed during preparation and testing. Vibration and retarder (0.6 % citric acid) partly reduced this influence;
- imperfections in loading process induced by eventual deviations from a uniaxial scheme;
- strength property was often decreased due to material brittleness.

CONCLUSIONS

Compatible binder to historic romancement has been obtained from dolomite-clay compositions containing Quaternary and Devonian period clay. In order to study the mechanical properties, a range of uniaxial loading tests with samples were performed.

Mechanical properties (σ_{cr} , E, u_{cr}) relatively reflects the chemical composition characteristics. Evaluating compositions with equal dolomite-clay ratio (A2 and U2): composition A2 shows variability of strength values due to great content of quartz; whereas composition U2 differs with stable strength properties and higher impact resistance (u_{cr}) which can be explained by higher amount of cement minerals.

Composition A1 shows less variability of compression modulus and hardening time influence. It might be caused by lower clay content.

Ready-mixed calcitic Roman cement "Prompt" (tested for comparison) has better strength properties in overall. In addition significant hardening time influence should be noted.

Given results could be used for prediction of the areas of application and further improvement of the historic building restoration works.

It is evident (Table 1) that a stable volume of compression modulus and the hardening rate should be taken into account in the choosing of the binder composition. Furthermore the rapid hardening materials (i.e. A1 compositions) have relatively lower strength and strain properties in comparison with the more clayey compositions A2, U2.

ACKNOWLEDGEMENT

The work was carried out in the framework of ERDF Project „Elaboration of Innovative Low Temperature Composite Materials From Local Mineral Raw Materials” (No 2010/0244/2DP/2.1.1.1.0/10/APIA/VIAA/152).

REFERENCES

Available: <http://www.heritagescience.pl>. Home page of the ROCEM project.

Available: http://www.romanportland.net/files/doc/cahier_technique_cr_cnp_eng.pdf

Bansal N.P., Doremus R.H. *Handbook of glass properties*. Academic Press, Inc., Orlando, FL. 1986, 704 pp.

Barbane I., Vitina I., Lindina L. *Synthesis of Roman cement from Latvia's clay and dolomite // Proceedings of International Conference on Building Materials "18. ibausil"*, Vol. 1, Weimar, Germany, September 12-15, 2012, -pp. 749-755, ISBN 978-3-00-034075-8

Brencich C., Corradi L., Gambarotta G., Mantegazza E. *Compressive strength of solid clay brick masonry under eccentric loading*. Department of Structural and Geotechnical Engineering – University of Genoa – Italy. Ruredil s.p.a. Milan, Italy, 2001, 10 pp.

Chamis C.C., Hanson M.P., Serafini T. *Designing for Impact Resistance with Unidirectional Fiber Composites*. Lewis Research Center, NASA, 1971, Cleveland, Ohio 44135, 44 pp.

Hughes D.C.; Jaglin D.; Kozlowski R. Mucha D. *Roman cements — Belite cements calcined at low temperature*. *Cement. Concr. Res.*, 2009, 39 (2), 77-89.

Klisinska-Kopacz A., Tislova R., Adamski G., Kozlowski R. *Pore structure of historic and repair Roman cement mortars to establish their compatibility*. *Journal of Cultural Heritage*, 2010, vol. 11, p. 404-410.

Lindina L., Krage L., Bidermanis L., Vitina I., Gaidukova G., Hodireva V., Kreilis J. *Formation of calcium containing minerals in the low temperature dolomite ceramics*. *Elsevier*, 2011, IOP Conf. Ser.: Mater. Sci. Eng. 25 012006 doi:10.1088/1757-899X/25/1/012006 ISSN 0921-5093

LVS EN 196-1:2005. *Methods of testing cement - Part 1: Determination of strength*

BUILDING AND RENOVATION

INDIRECT EVAPORATIVE PRE-COOLED COMPRESSOR COOLING SYSTEM PERFORMANCE UNDER VARIOUS OUTDOOR AIR HUMIDITY CONDITIONS

Arturs Brahmanis*, Arturs Lesinskis**

Riga Technical University, Heat, Gas, and Water Technology Institute

E-mail: *Arturs.Brahmanis@rtu.lv, **Arturs.Lesinskis@rtu.lv

ABSTRACT

The present study is devoted to efficiency evaluation of a combined indirect evaporative – compressor cooling system under various outdoor air humidity conditions of temperate climate. The investigated system is located in the recently restored historical building, The Art Museum Riga Bourse, which was initially built in the middle of the 19th century. The indirect adiabatic chiller supplies cooled fluid to the conventional cooling system, consisting of ventilation cooling coils and fan-coil units on separated loop. Using the data, acquired by BACnet BMS controllers and experimental data logging system, we have analyzed the cooling plant operation efficiency dependence of outdoor air humidity for a period of four month. The saved each minute data have been exported as CSV files, recalculated to each hour average values and analyzed.

Key words: indirect evaporative, cooling system, historical building

INTRODUCTION

While water side evaporative cooling arrangements are occasionally used, with air–water systems, particularly in more arid climates, the use of the technique falls far short of its potential. This is particularly the case in west European temperate climates where many opportunities to benefit from evaporative cooling techniques are often overlooked (De Saulles, 1996). This situation is attributed by (Field, 1998) to a lack of in-depth knowledge of the energy performance of water side free cooling systems, in terms of the cooling generated per unit of primary energy expended (Costelloe et al., 2002). However, the present engineering tendencies show that due to the development of HVAC system and control equipment, this method of cooling becomes even more attractive for use also in European countries with temperate climate.

The main factors for choosing one or another type of the cooling equipment are climate, cost efficiency, sizes, and availability of external recourses, such as spare heat energy, or the proximity of water sources (Borodinec et. al, 2008). The existing studies related to indirect evaporative cooling and combined systems efficiency in Northern European regions are focused mostly on high-temperature cooling systems, such as chilled beams and chilled ceilings (Duan et. al, 2012). It is obviously because of better cooling unit efficiency in higher cooling temperature conditions.

Restoration of old buildings is a complex construction process, in which engineers and architects need to solve many atypical tasks concerning not only the structural stability of the

building, but also the recovery of cultural - historical appearance of the building.

Necessity of harmonious integration of modern HVAC devices in the historical interior also enforces limits to the equipment selection. In those cases the use of high temperature cooling equipment becomes complicated because of aesthetic requirements and need for air dehumidification.



Figure 1. Riga Bourse building after restoration

Outdoor air humidity is a parameter of climate, which affects heat transfer in air heat exchangers, and needs to be taken into account in calculations (Kays et al., 1998). Recent studies have shown, that in case of water – air heat exchangers the relative air humidity level increase from 50 to 90% results in the heat transfer coefficient α growth in 1,68 times (Averkin et al., 2012). It is necessary to

clarify, that in the mentioned paper the authors did not focus on the air temperature, which implies that such distinct α changes could be explained not only by changes in the relative humidity, but also outdoor air temperature decrease (adiabatic cooling).

Latvia is located in the moderate climatic zone. Its temperature, moist climate are created by the Atlantic air masses and influenced by the Baltic Sea and the gulf of Riga. The outside air very rarely corresponds to the necessary supply air parameters. The rest of the time the air should be heated and dehumidified to achieve the necessary room air temperature and humidity (Krumins et al., 2008).

This paper focuses on the investigation of outdoor air humidity impact on the chiller COP. The investigated system is located in the recently restored historical building, the Art Museum Riga Bourse, which was initially built in the middle of the 19th century (Fig.1). To preserve artefacts, the Museum is equipped with climate – control and building management (BMS) systems.

MATERIALS AND METHODS

Cooling system description

The cooling system consists of an indirect evaporative water chiller with integrated compressor, 5 air handling units with cooling / dehumidifying coils and 98 fan-coil units on separated loop. The museum premises, which are used for storing the most valuable exhibits, are equipped also with autonomous air humidifiers to keep a constant air moisture level in winter seasons. The chiller, which we have used as an experimental unit, is equipped with an air-water heat exchanger (8), which cools secondary loop with adiabatically pre-cooled outdoor air. Outdoor air is driven by a radial fan (5), pre-cooling is provided by water nozzles located in adiabatic loop. Refrigerant – air (1), and refrigerant – water (2, right) heat exchangers utilize heat, produced by compression cycle (4). Thereby, primary loop, which supplies the building, on demand is cooled by one or two heat exchangers (3 or 2). As shown in Fig. 1, the unit has outdoor air humidity (7) and temperature sensors at air intake, temperature sensor at the exhaust. Water temperature sensors (6) are installed at primary and secondary loops, at primary loop both for the supply and return flow.

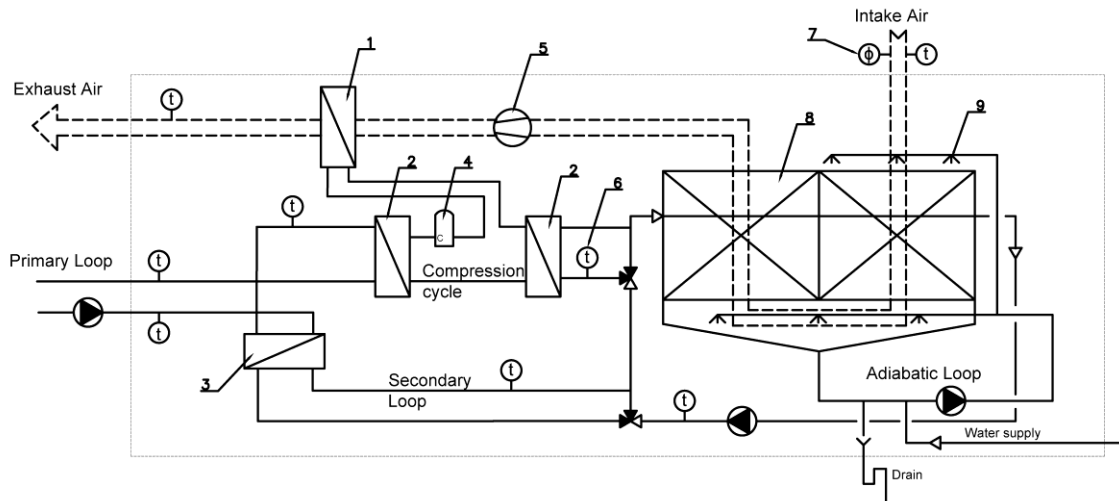


Figure 2. Scheme of the experimental unit

Water supply for “adiabatic” circuit is equipped with an impulse water meter, precision ± 1 liter. The electricity electronic meter has precision $\pm 1\text{kW}$. Both meters are not shown in Fig.2.

Data processing

Using fluid and air parameter sensors, described above, electricity consumption, water consumption, chiller operation stages, fluid temperatures, and outdoor air parameter data have been acquired for the period from August 1 till November 29, 2012. The outdoor air parameters have been acquired also by the building air handling unit automatics and incidentally in some cases slightly (o.a. temperature about $\pm 2^\circ\text{C}$) differ from the chiller sensor readings. We have ignored these deviations and taken into

account only the data collected by the sensors, installed in the chiller, due to the fact that these data are determinative for the unit automatics. As a measure of the chiller operating efficiency relation to the outdoor air moisture content, we took the unit coefficient of performance (COP) and intake air absolute humidity ratio at relatively constant temperatures. The data storing server recorded the operation data every minute, including intake air temperature, relative humidity, In / Out cooling liquid flow in primary loop, energy and water meter readings. After export to spreadsheet, the data amount had more than 163k rows (1 measurement per minute = 1 row). Hour average values were calculated for analysis. Rows, containing one or more rough errors, were ignored.

Calculations

Knowing the altitude and air temperature, saturation humidity ratio W_s can be found (ASHRAE, 2001), using equation:

$$W_s = 0.62198 \frac{P_{ws}}{P - P_{ws}}. \quad (1)$$

Where:

W_s = saturation humidity ratio, kg_w/kg_{da}

P_{ws} = saturation pressure, kPa

P = barometric pressure, kPa

The barometric pressure is assumed as the function of altitude Z , which is 6m average for Old Riga:

$$P = 101.325(1 - 2.25577 * 10^{-5}Z)^5 . 2559 \quad (2)$$

The saturated vapour pressure in kPa is calculated, using (Sensirion, 2009) Magnus formula:

$$P_{ws}(t) = \alpha \exp\left(\frac{\beta * t}{\lambda + t}\right) \quad (3)$$

Where:

t = air temperature, °C

$\alpha = 0.6112$, kPa

$\beta = 17.62$

$\lambda = 243.12$, °C

Using the intake air relative humidity data acquired, the air moisture content was obtained:

$$x = \varphi W_s. \quad (4)$$

Where:

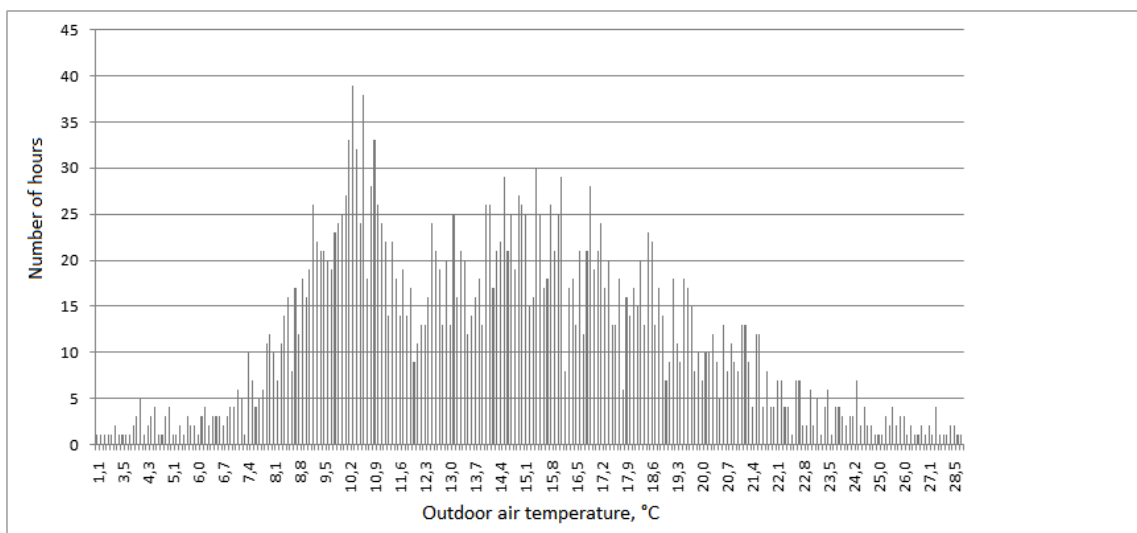


Figure 3. Average hourly temperatures – hours

Average hourly temperatures in the range $+15 \pm 1$ °C registered in 477 hours during the analyzed period. We assumed this range as constant air temperature.

φ = relative humidity, dimensionless.

The formulas above concern the intake air psychrometrics. To evaluate the efficiency of the equipment, we have calculated the cooling energy produced by the chiller per minute using equation (5), (Krieder, 2001).

$$Q = g * \rho * c_{cw} (T_{in} - T_{out}). \quad (5)$$

Where:

Q = cooling output, kW

g = cooling fluid volumetric flow, m³/s

ρ = cooling fluid density, kg/m³

c_{cw} = cooling fluid specific heat, kJ/(kg*°C)

The cooling fluid in the system is 35% ethylene-glycol and water mixture, $\rho = 1045$ kg/m³, $c_{cw} = 3.585$ kJ/(kg*°C).

The chiller COP according to the energy balance equation will be:

$$COP = \frac{\text{Cooling power}}{\text{Input power}}. \quad (6)$$

The input power was calculated for each hour of the analyzed period, using electricity meter data (every 60th minute value minus every 1st minute value of each hour).

RESULTS AND DISCUSSION

The outdoor air (OA) temperature data analysis has been performed for 2720 hours, and it showed that the most common average hourly temperatures occurred in the range from +14 to +16°C, Fig. 3.

RESULTS AND DISCUSSION

The calculated COP and OA humidity graph at all registered OA temperatures showed that the cooling unit COP dependence of the outdoor air moisture content is clearly visible, and it is inverse (Fig. 4). It

is obvious, because absolute humidity changes sharply according to the OA temperature. The higher the OA temperature, the higher the OA moisture, which results in reducing the efficiency of evaporative intake air pre-cooling. Linear approximation for COP - humidity is also shown in Fig. 4. When defining the temperature diapason $15\pm1^{\circ}\text{C}$, the COP - OA moisture dependence still persists, not so expressed, but still. In this case, humidity rise from 4,2 to 14 g/kg_{da} causes the chiller COP decrease from 2.74 to 2.56, which is

equivalent to 6.6%. The graph and approximation of this dependence are shown in Fig. 5.

The dependence shows that average chiller COP is less than 3, and it is very slightly dependent on OA moisture. According to (Kays et al., 1998) heat transfer equations, the effectiveness of the air side of the heat exchanger is dependent on the air specific heat c_p . The c_p and moisture content are in direct relation. We can conclude, that in our case refrigerant – air heat exchanger effectiveness decreasing, caused by low humidity, is compensating by adiabatic intake air pre-cooling.

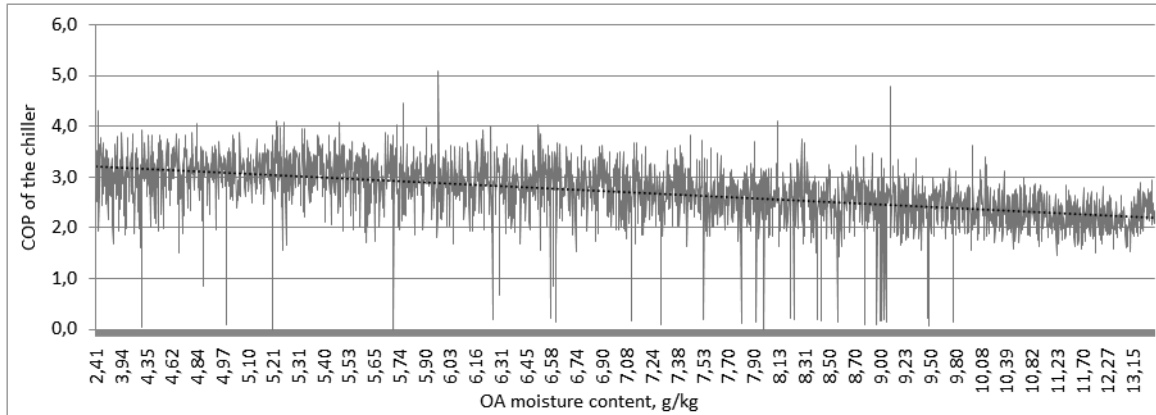


Figure 4. COP and OA moisture content at all registered temperatures,
where ---- - linear approximation of COP

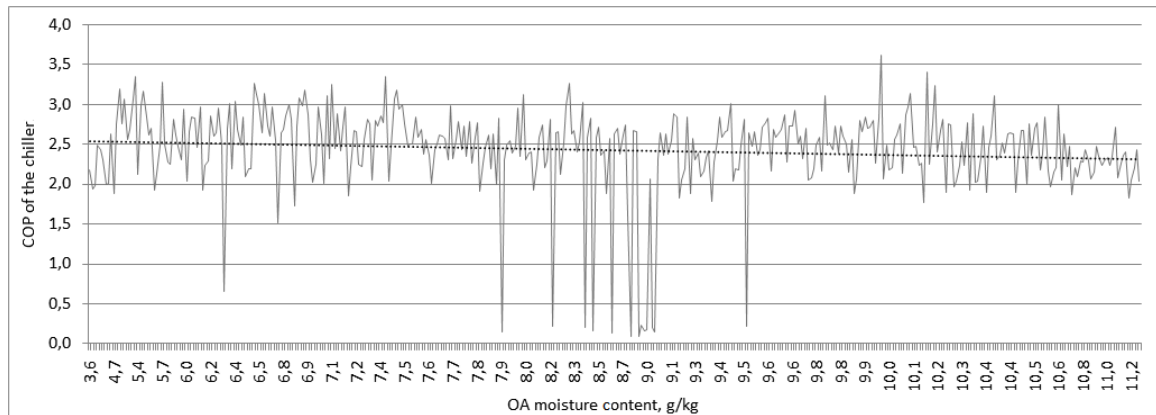


Figure 5. COP and OA moisture content at temperatures $15\pm1^{\circ}\text{C}$

CONCLUSIONS

Electricity consumption, water consumption, chiller operation stages, cooling average temperatures, and outdoor air parameter data have been acquired for the period of 4 months, during the year 2012 cooling.

The data, recorded for every minute, were processed, and recalculated for each hour average. The data analysis at constant temperature $15\pm1^{\circ}\text{C}$ showed that for the studied period of time the chiller COP very slightly depends on the outdoor air

moisture, and this dependence is inverse proportional.

The slight dependence can be explained by the adiabatic compensation effect. In our case refrigerant – air heat exchanger effectiveness decreasing, caused by low humidity, is compensated by adiabatic intake air pre-cooling.

The results of the present and related studies will clarify the efficiency of indirect adiabatic cooling systems in temperate climates.

REFERENCES

- ASHRAE. (2001) *Handbook – Fundamentals*, Atlanta: American Society of Heating, Refrigerating and Air-Conditioning Engineers, 630pp.
- Averkin, A.G., et al. (2012) *Experimental research of convective heat transfer at cooling air flow of different relative humidity in the finned coil*. Kazan: News of KSUAE, 6 pp.
- A. Borodinecs, A. Kreslins (2008). *Reduction of cooling and heating loads using building envelopes with controlled thermal resistance*. Proc. Air Conditioning and the Low Carbon Cooling Challenge Windsor 2008 Conference, 7 p.
- Costelloe, B., Finn, D. (2003) Indirect evaporative cooling potential in air–water systems in temperate climates. *Energy and Buildings*, 35, p. 573–591.
- De Saulles, T. (1996) *Free cooling system-design and application guidance*. Bracknell: BSRIA. 80 pp.
- Z. Duan et al. (2012) *Indirect evaporative cooling: Past, present and future potentials*. Renewable and Sustainable Energy Reviews 16, p. 6823–6850
- Field, J. Building analysis. 1. City Square Leeds, Building Services Journal, 12 14–18.
- Kays, W. M., London, A. L. (1998) *Compact heat exchanger, 3rd edition*. New York: McGraw-Hill. 336 p.
- Krieder, J.F. (2001) *Handbook of Heating Ventilation and Air Conditioning*. New York: CRC Press, p. 216–217.
- Krumins, A., Brahmanis, A., et.al. (2008) *Optimal control strategy of air handling unit for different microclimates in working and swimming areas of a swimming pool hall*. Proc. The 11th International Conference on Indoor Air Quality and Climate. Denmark: Indoor Air 2008, ID:173, 8 pp.
- SENSIRION. (2009) *Introduction to relative humidity*. Version 2.0. 6p. [accessed on 25.11.2012] Available: http://www.sensirion.com/fileadmin/user_upload/customers/sensirion/Dokumente/Humidity/Sensirion_Introduction_to_Relative_Humidity_V2.pdf

CONSTRUCTION WASTE MANAGEMENT PROCESS IN LATVIA: PROBLEMS AND POSSIBLE SOLUTIONS

Sandra Gusta*, Gints Skenders**

Latvia University of Agriculture, Faculty of Rural Engineers, Department of Architecture and Construction
e-mail: *Sandra.gusta@llu.lv, **gints.skenders@dome.cesis.lv

ABSTRACT

Overall in Latvia every year there are 600,000 to 700,000 tonnes of waste, about half of this amount is considered to be biodegradable municipal waste. The municipal solid waste management in their administrative areas is the responsibility of municipalities. Approximately 77% of Latvian household waste is disposed of in landfills or dumps, and every year the amount of waste disposed increases. Besides, the amount of hazardous waste is increasing and hazardous waste in the most part consists of metal production waste. Currently, hazardous waste is temporarily stored in a specially equipped commercial and waste storage sites. However, hazardous waste collection and disposal is improved, as well as the amount of recycled packaging.

Also, the construction process creates a large amount of waste. The construction waste is referred to as waste from construction, renovation and demolition, as well as debris and damaged materials resulting from the construction process, or materials used in the construction site temporarily. Usually the construction waste from residential buildings contains concrete, wood, metal, plaster panels, oil, chemicals and roof trim materials. Construction waste can contain environment and human health hazardous substances. It can cause soil contamination if improperly disposed. Precipitation may result in contaminated groundwater. These processes have defined the topicality of this article; the aim of the article is to analyze construction waste management processes, identify problems and possible solutions. This paper addresses problems related to construction waste separation, storage, transportation and disposal and the problems associated with waste management in Latvian context of sustainable construction.

Key words: construction waste, management, legislation

INTRODUCTION

Waste did not cause problems while the number of population of the Earth was small – to compare, the current population of the world exceeds six billions, but the number of population did not exceed two billions only in 1900-s; there was no deficit of raw materials, the environment was minimally polluted, there was a lot of free areas, the materials used were biologically decomposing or inert natural products (wood, clay, wool, linen, leather, etc.) which, when coming into contact with the environment, in due time vanished without a trace.

Nowadays, the situation has cardinally changed. The population of the Earth exceeds 6 billions, the stock of non-renewable natural resources (oil, gas, coal) are not everlasting. But the main thing is that synthetic materials (plastics, synthetic fiber, various chemicals, composite materials, etc.) have entered our lives extensively, but such are not common in the environment and in the majority of cases they do not decompose biologically. When such waste gets into the environment, it is being polluted because nature is not able to assimilate such waste.

CLASSIFICATION OF WASTE

Classification of waste is based on the consideration of its properties, composition and origin. It may be deemed that various types of waste are individual elements forming the total waste flow.

According to the waste properties, it may be divided into household, hazardous and inert waste. The above division is required to regulate the waste collection, burying or recycling requirements (Environment..., 2010). Classification of waste is based on consideration of its properties, composition and origin (see in Fig. 1).

Waste may be divided:

1. As to its origin:
 - a) Industrial;
 - b) Specific;
 - c) Household;
 - d) Mining.
2. As to its properties and impact:
 - a) Hazardous;
 - b) Inert.
3. As to the place of waste formation:
 - a. Industrial;
 - b. Agricultural;
 - c. Energetic;
 - d. Household;
 - e. Service.

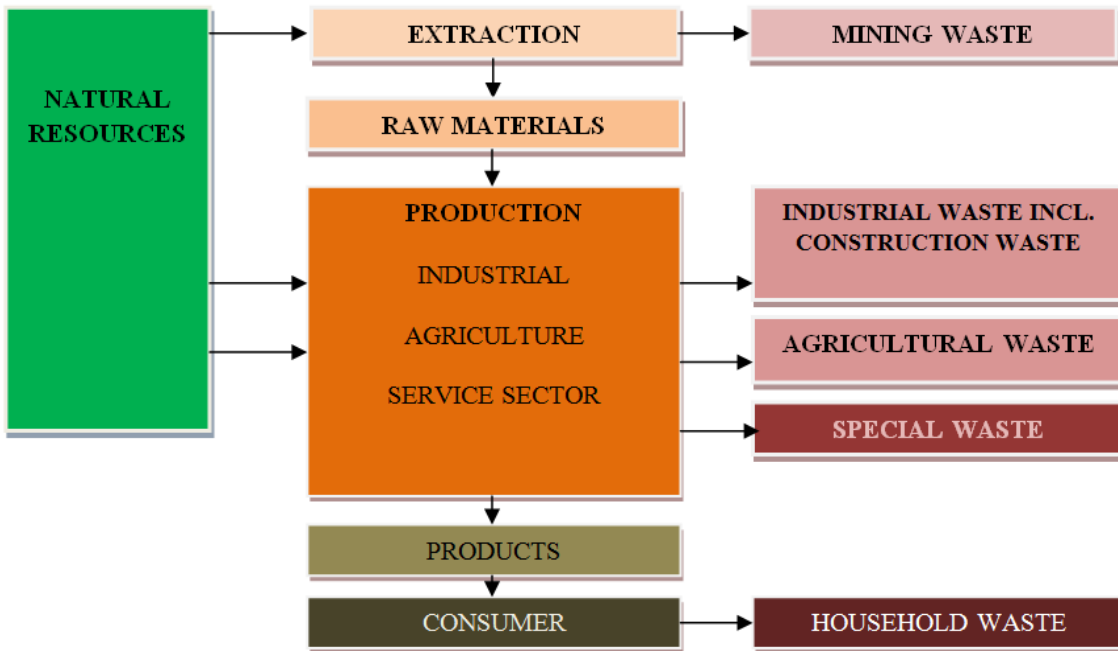


Figure 2. Waste flow

SUSTAINABLE WASTE MANAGEMENT

Sustainable waste management envisages minimizing the volume of waste produced as well as using the resources more efficiently and rationally, by recognizing that the waste of one industry serves as raw material in another industry. The main principles of sustainable waste management:

1. Self-sufficiency and proximity principle;
2. Principle "The polluter pays";
3. Principle of the producer's responsibility;
4. Good waste management practice principle.

It should be noted that during the period of operation of the previous Waste Management State Plan sufficient support from the EU Structural Funds was not available for the development of the waste recycling infrastructure. The Latvian Investment and Development Agency has granted support for investment in the development of tiny and small merchants in the especially supported territories and according to the Waste Management State Plan 2013-2020 environmental impact assessment strategic evaluation, the environmental overview for the above EU support was received by 4 projects in the waste recycling sector, one of which is the Construction Demolition Waste Recycling Service Development in LLC Jaunlaicenes kokogles.

Upon developing landfill sites meeting the requirements of legal acts in the country the preconditions were created to close and recover the waste dumping grounds not meeting the requirements of the law. By attracting the funds of the European Union in the financial planning period

for 2007 – 2013, by the end of 2011 there were 30 household landfill sites with an area of ~51 ha recovered, 7 of those landfill sites with an area of 18.185 ha in 2011.

Waste management issues have been included into the strategy "Europe 2020" (Strategy...).

The strategy "Europe 2020" nominates three priorities mutually enforcing each other:

- *Smart growth* – development of knowledge- and innovation-based economy.
- *Sustainable growth* – more effective promotion of the economy in terms of resources, less harmful for the environment and more competitive.
- *Integrating growth* - promotion of such an economy that has a high level of employment and that ensures social and territorial cohesion.

According to Section 4 of the Waste Management Law, waste management cannot adversely affect the environment, including:

- 1) creating risks for waters, air, soil as well as plants and animals;
- 2) creating disturbing noises or odors;
- 3) adversely affecting landscapes and specially protected nature territories;
- 4) polluting and littering the environment.

Especielly large volumes of waste were generated in 2008 in two fields of activity, namely in construction (NACE Section F), as a result of which 859 million tons of waste were generated (32.9 % of the total waste volume) and in the extraction industry and quarry processing (NACE Section B) which generated 727 million tons of waste (27.8 % of the total volume). A major part of waste generated in these sectors was mineral waste or soil

(excavated ground, road construction waste, demolition debris, dredging ground, useless rocks, fractions, etc.). This is an explanation for the comparatively large specific weight of mineral waste and soil (63 % of the total waste volume generated) in the total volume of waste (Regulation (EU)...).

GDP and construction amounts in Latvia from 2000 - 2012 see in Figure 2.



Figure 2. GDP and construction amounts in Latvia from 2000 – 2012 (Created by the authors according to the data of CSB)

Waste management purposes are included in the following national planning documents: Sustainable Development Strategy of Latvia to 2030 (approved by the LR Saeima on 10 June 2010), Latvian National Development Plan 2007-2013 (Regulations of the Cabinet of Ministers No. 564 "Regulations Regarding the Latvian National Development Plan 2007-2013" of 4 July 2006), Latvian Strategic Development Plan 2010-2013 (approved by the ordinance of the Cabinet of Ministers No. 203 of 9 April 2010) as well as the Basic Guidelines for Environmental Policy 2009-2015 (approved by the ordinance of the Cabinet of Ministers No. 517 of 31 July 2009).

CONSTRUCTION AND BUILDING DEMOLITION WASTE

The construction waste category included road construction and building demolition waste:

- 1) concrete and reinforced concrete constructions, concrete, bricks, tiles, roof tiles, ceramics, timber, glass, plastic and gypsum materials, insulating materials;
- 2) construction material containing asbestos;
- 3) cement, calcareous and gypsum materials as well as waste from production of items made of such;
- 4) street cracking waste – hard waste (cement together with binders, bitumen) that occurs when

cracking or renewing the street cover; extracted ground – soil excavated during construction, artificial dykes or excavated ground that cannot be used in the same place any more, rocks and bed deepening sludge,

5) old heating system elements, pipes, radiators, sanitary technical appliances, rug-type floor covers, linoleum, fabric or paper tapestry, plastic or wooden laths, dismounted doors and window blocks; all of them should be removed together with other debris. It is a mistaken attempt to burn the old floor covers, tapestry or plastic finishing elements in stoves and furnaces during refurbishment because these materials produce major heat when burned and in the event of imprudent activity it may damage the stoves or even cause fire. Many finishing materials, when burned in stoves, may distribute hazardous chemical substances thereby imposing threat to human health.

If the debris is a fine fraction clinker or crushed old plastering and it is envisaged to transport such to the container from the upper floors of the building, it is useful to perform such work by means of a debris transportation pipe; this helps avoiding littering the premises of common use (Construction...).

Pursuant to the legal acts regulating construction, when the building is renovated, reconstructed or demolished the construction materials are recycled, if possible. All debris that is qualified as hazardous waste is buried according to the requirements set forth for burying hazardous waste. Legal acts relating to the divided collection of waste, preparation for repeated use, recycling and material regeneration include the construction and building for demolition waste management purposes discussed in the plan and the methods for assessing the attainment of the goals. The rate for burying 1 ton of construction and building demolition waste has gradually increased since 2009, reaching 15 LVL per ton in 2012. Burying the construction and building demolition waste has decreased, but the volume of such waste and the volume of its recycling has increased. The total volume of construction waste collected in 2010 is 153 thousand tons. The volume of construction waste is being collected in a sorted manner or as piece-waste. Approximately 140,000 tons of the collected construction and building demolition waste have been recycled in 2010, but approximately 13,000 tons of the collected waste have been buried.

One should individually discuss the waste containing asbestos that is buried in the asbestos waste site Dūmiņi. By the end of 2010 there were approximately 4,000 tons of construction waste containing asbestos buried on the site. The possibility for burying construction waste containing asbestos is envisaged in several household waste management sites as well. It is set forth that in the future all hazardous waste will be

buried in the same site (Zebrene). When the construction waste management sector is generally evaluated with respect to attaining the regeneration goals, one may allege that the requirements have already been met and in the future the main attention should be paid to controlling the collection and transportation stages. Importing construction waste from other countries of the European Union is allowed only for regeneration purposes. No construction and building demolition waste is brought into Latvia from other countries for regeneration.

DEBRIS UTILISATION

The occurrence of debris is inevitable during any, even small, refurbishment or construction process. Each builder has to consider that the issues related to debris collection, storage, transportation and utilization will be integral and quite important parts of the construction process, the solving of which should be started in good time, at the project documentation coordination and construction permit issuance stage, so already prior to start of real works.



Figure 3. Occurrence of debris (Collection...)

The best solution is entering into an agreement with waste transporters. Even when comparatively small apartment refurbishment works are performed, one shall experience the occurrence of debris in such volumes which do not provide the opportunity to dispose of them in the usual way by dumping them into a household waste container.

It is important to know that dumping any debris into household waste containers is prohibited because the physical and chemical characteristics of the construction and refurbishment process remains and litter are essentially different from the household waste and it requires separate sorting, processing and utilization of debris.

Each repairer or builder in Latvia is bound by such construction waste management regulations as issued by the local authority in the jurisdiction of

which the refurbished or newly built object is located. It is set forth in the law that the owner of the construction waste is the legal entity or the individual in the territory of which the construction works take place, therefore the sanction for violations in the construction object may be applied to both, the builder performing the works and the customer under the assignment of which the works are performed. In this respect no discounts are allowed either to individuals or companies, but the municipal police are monitoring the situation in the territory by applying sanctions quite often for even minor violations.

In urban territories, where the works are performed in quite restricted areas, it is especially important to abide with the prohibition of placing construction waste and construction materials outside the territory where the construction works take place. The regulations impose a duty to the builder (not later than after the completion of construction works) to deliver all construction waste directly to the construction waste processing site. Quite often the persons residing next to the construction object are subject to a lengthy accumulation and storage of debris next to the place of construction because litter is dragged around the neighborhood by means of stray animals or homeless persons. The best solution for the performance of refurbishment works or the private builder is entering into an agreement with the construction waste carrier regarding the regular removal of construction waste for recycling.

THE PROCEDURE IN WHICH CONSTRUCTION WASTE IS MANAGED

In construction works of a larger volume (if the occurrence of construction waste is envisaged in the construction project), upon the receipt of the construction permit the customer must, within five days after the commencement of works, enter into an agreement with the construction waste carrier regarding the removal of construction waste for recycling. Quite often the customer delegates this task to the builder performing the works. Excerpts from the "Construction waste management regulations" of Riga: the "Owner of construction waste – any individual or legal entity generating construction waste by its activity or who is the owner of the construction waste." "Upon accepting the construction for operation and taking into account the envisaged volume of construction waste, starting from 10 m³, Riga City Construction Inspectorate shall require the act regarding the total volume of construction waste removed for recycling that has been signed by the construction waste carrier or the construction merchant (if the construction merchant has removed the construction waste) as well as by a representative of the construction waste recycling company." "Tanks, containers and vehicles fitted for the purpose shall

be used for the collection and transportation of construction waste."

Transportation and recycling of debris is often performed by the same companies who offer to place a specialized debris container in the object. The rent for the idle period of the container is symbolic and is calculated for the presence of the container in the object for a day or more. The main costs are formed by the container transportation and debris utilization charges that are calculated according to the cubic capacity. Containers of 5, 8, 9, 10, 15 and 25 m³ are offered for rent. Already, at the stage of drafting the construction work cost estimate, the customer should require the builder to include the transportation and utilization of debris in the costs as well as follow up that the volume of debris is calculated in the cost estimate as accurately as possible. Saving funds on account of the debris removing works, including carrying it out from the object and loading into the container, quite often leads to conflict situations with municipal police or neighbors.

LIABILITY AND DUTIES OF THE CONSTRUCTION WASTE OWNER

The owner of the construction waste in the territory of which the construction works take place is forbidden to place construction waste and construction materials outside the territory in which the construction works take place. It is his duty, not later than after the completion of construction works, to deliver the construction waste directly to the construction waste recycling companies or to enter into an agreement with the construction waste carrier regarding the removal of construction waste for recycling. When issuing the architectural and planning assignment, the City Council Development Department shall specify therein that the delivery of the construction waste for recycling is mandatory and that the envisaged volume of construction waste (m³) must be specified in the construction project.

Upon accepting the construction for operation and taking into account the envisaged volume of construction waste, starting from 10 m³, the City Construction Inspectorate shall require the act regarding the total volume of construction waste removed for recycling (Form "Act regarding the volume of construction waste delivered for recycling", sample 1) that has been signed by the construction waste carrier or the construction merchant (if the construction merchant has removed the construction waste) as well as by a representative of the construction waste recycling company. After the receipt of such acts, the Riga City Construction Inspectorate shall file those with the Environmental Department within five days.

If the occurrence of construction waste is envisaged in the construction project, upon the receipt of the

construction permit the customer must, within five days after commencement of the works, enter into an agreement with the construction waste carrier regarding the removal of construction waste for recycling or receive a permit from the Regional Environmental Authority for the independent removal of the construction waste to the recycler. When construction and refurbishment works financed from the city budget funds are performed, upon commencing the works the customer must require the contractor to present the agreement regarding the delivery of construction waste for recycling entered into the construction waste recycling company.

CONSTRUCTION WASTE COLLECTION

Tanks, containers and vehicles fitted for purpose shall be used for the collection and transportation of construction waste.

It is the duty of the construction waste tank and container owner to maintain these in technical order. The owner or the lessee of the construction waste tanks and containers is responsible for their cleanliness (Collection...).



Figure 4. Available containers - 4 m³, 5.5 m³, 8.5 m³, 15 m³, 22 m³, 35 m³, 40 m³ (Collection...)



Figure 5. Transportation of construction waste (Collection...)

CONSTRUCTION WASTE SORTING AND ACCEPTING FOR RECYCLING

To ensure a quality construction waste recycling process, the owner of the construction waste must sort such as follows:

- separate other household waste and hazardous waste, including asbestos;
- concrete and reinforced concrete constructions (larger than 100x70 cm, thickness of up to 30 cm);
- concrete and reinforced concrete constructions (larger than 100x70 cm, thickness from 30 cm to 70 cm);
- concrete and reinforced concrete constructions (larger than 100x70 cm, thickness exceeding 70 cm) as well as all T-shape and double T-shape beams;
- all types of construction waste (smaller than 100x70x30 cm) by sorting them as follows:

Owners and carriers of the construction waste are strictly prohibited to remove and store away construction waste in household landfill sites and the managers of the household landfill sites are prohibited from accepting such. In the construction waste recycling company the delivered construction waste is weighted and the type of construction waste is registered by filling in the form "Construction waste acceptance waybill" delivered by the cargo carrier; two copies of which shall be retained by the carrier. The construction waste recycling company is entitled to handle the construction waste after weighing the waste and accepting it for recycling. The construction waste carrier must deliver the "Construction waste acceptance waybill register" to the Environmental Department monthly, by the 15th date of the following month. If the construction waste recycling company refuses to accept the construction waste due to its low quality or any other reason, such shall be confirmed by an entry in

the construction waste acceptance waybill by specifying that it is permitted to take the construction waste to the household landfill site for storing away.

When construction waste is accepted for storing away in the household landfill site, the construction waste acceptance waybill containing the entry by the construction waste recycling company regarding its refusal to accept the construction waste for recycling shall be required. One copy of the construction waste acceptance waybill shall be left with the person accepting such cargo at the landfill site.

If the construction waste delivered to the construction waste recycling company or the household landfill site contains substances hazardous to the environment and human health, the construction waste shall be returned to the supplier to handle, according to the provisions of Part One of Section 14 of the Law of the Republic of Latvia "Waste Management Law".

The excavated ground should be used or removed so that it is not mixed with the construction or other household waste. If possible, it should be used for landscaping the construction site or removed to another object or piece of land by agreeing such a place with the Riga City Council Environmental Department as well as not permitting the destruction of the productive upper soil layer or lowering its quality.

The construction waste recycling company must quarterly, by the 25th date of the following month, deliver to the City Council Environmental Department the overview of the volumes of construction waste brought in and recycled, of its suppliers and the types of construction waste.

If during sorting the construction waste prior recycling it is discovered that the construction waste contains other household waste then the construction waste recycling company must deliver such to the household landfill site (Riga City Council...) .

CHARGE FOR ACCEPTING THE CONSTRUCTION WASTE FOR RECYCLING AND SALE OF THE PRODUCTS

The supplier of the construction waste pays the construction waste recycling company for accepting the construction waste for recycling. The upper limit of the construction waste acceptance and recycling rates is set forth by the City Council. The construction waste recycling company may determine its own construction waste acceptance and recycling rates, but such cannot be higher than the ones set forth by the resolution of the City Council. The City Council is not responsible for the sale of products of the construction waste recycling companies (Riga City Council...) .

LIABILITY FOR FAILURE TO COMPLY WITH THE REGULATIONS

Complaints about the quality of services provided by the construction waste recycling company as well as about the failure to comply with these regulations should be filed with the City Council Environmental Department. If a violation of these regulations is discovered in the activities of the construction waste recycling company or the construction waste carrier, the City Council Environmental Department is entitled to unilaterally terminate the agreement on the recycling or transportation of the construction waste. For the failure to comply with these regulations, individuals and legal entities may be penalized with the fine set forth in the Latvian Administrative Violations Code. The administrative violation protocol may be drafted by:

- police officers, because the right of the police to control the performance of these regulations is regulated by the Law of the Republic of Latvia "On Police";
- head of the construction inspectorate and the construction inspectors;
- inspectors of the State Environmental Inspectorate (Riga City Council...) .

NATURAL RESOURCES AND WASTE

While the energy efficiency of the building during its use is still the most important aspect in terms of sustainability, the choice of materials used for construction have significant importance for the environmental impact – the primary energy content in the materials themselves (during the process of extraction, processing, transportation and waste management), use of toxic and hazardous substances and use of non-renewable resources. A large portion (40-50%) of the raw materials used in the world is converted annually into materials and products useful for construction.

Moreover, 40% of the total amount of waste generated annually comes from construction and demolition of buildings, followed by waste from renovation works. A major part of such waste may be recycled or used repeatedly, for example, for making roads or railway dams. The choice of materials used for construction has essential importance with respect to the environmental impact as well, especially the use of natural resources and the generation of waste flows (during the construction process as well as at the phase of demolition).

CONCLUSIONS

Due to its considerable volume, construction waste occupies huge territories of landfill sites. They may also contain substances hazardous for the environment and human health. If improperly

buried, they may cause serious soil pollution. As a result of precipitation, underground waters may be polluted as well. It is necessary to order special containers for collecting construction waste. Construction waste management is governed by the legal acts of each region and the construction waste management regulations. Construction waste, as well as other waste, endangers the environment and the ecosystem. Quite a lot of construction waste is generated as a result of the construction process. It is possible to recycle a large part of the construction waste and to use it repeatedly. According to the Waste Management State Plan 2013-2020 environmental impact assessment strategic evaluation environmental overview:

1. In the field of waste management – in 2013-2014 it is envisaged to introduce a strict accounting system for the transportation of construction waste;
2. In the field of divided waste collection – to set forth in legal acts administrative penalties for the failure to sort waste;
3. In the field of waste preparation for regeneration, waste regeneration and recycling - to set forth quality criteria for the compost/digestate so that it may be used elsewhere in the economy (agriculture, construction, forestry, road construction, etc.);
4. In the field of waste burying – to assess the possibility of setting forth prohibitions/limitations for burying such waste that has the potential for recycling.

According to the Directive 2002/98/EC (Non-hazardous...), to increase to at least 70 % by 31 December 2019, the preparation of non-hazardous debris and building demolition remains for repeated use, recycling and other material regeneration, including filling by using waste as a substitute for other materials.

PROPOSALS:

1. To set forth in the General Construction Regulations that it is the duty of the customer to ensure that debris is collected.
2. Regulation (EU) No 305/2011 of the European Parliament and of the Council of 9 March 2011 laying down harmonized conditions for the marketing of construction products and repealing Council Directive 89/106/EEC. The Regulation enters into force on 1 July 2013 and the transitional period is ongoing at the moment (Regulation (EU)...).

Principal requirements for the buildings are set forth in Annex I to the Regulation, and there is a new requirement for sustainable use of natural resources (Requirement 7): Sustainable use of natural resources.

The construction works must be designed, built and demolished in such a way that the use of natural

resources is sustainable and in particular ensure the following:

- a) reuse or recyclability of the construction works, their materials and parts after demolition;
- b) durability of the construction works;
- c) use of environmentally compatible raw and secondary materials in the construction works.

The first six requirements are already set forth in Part Three of Section 3 of the Construction Law and in the Latvian Construction Regulation LBN 006-01 "Essential requirements for buildings" (LBN 006-01...); all 7 principal requirements for the constructions will be specified in the new draft Construction Law.

3. It is required to envisage such a system as BAPUS. Otherwise unfair competition occurs – cargos that do not reach recycling, illegal debris management is also present;

4. Promotion of recycling. Stimulating the attraction of EU funds for the purchase of recycling equipment (in proximity to large cities). Support of the EU Structural Funds to slum demolition.

5. The NRT rate for the volume of buried debris should be increased.

6. Sales of recycled materials should be stimulated.

7. Stricter control is required, but it should be evaluated whether setting forth such strict requirements is needed in B category permits – as of 2014 there must be concrete laid everywhere? Is it a requirement to lay concrete on the debris acceptance areas or on the whole area?

90% may be recycled in Latvia. Debris may be recycled to full amount.

8. It may be forecasted that the content of waste will change because construction technologies change and there will be other kinds of construction waste (for example, filled panels will not be made of reinforced concrete any more), thus also other recycling technologies.

Waste containing asbestos is brought into the Brocēni site Dūmiņi minimally because the costs are high (50 LVL/ton) and the distances are large, and storing in other sites is possible.

REFERENCES

Environment and sustainable development / Vide un ilgtspējīga attīstība. Riga: LU Akadēmiskais apgāds. 2010.II., p. 231

Strategy "Europe 2020" (European Commission statement) EUROPE 2020,
Available at: <http://eurlex.europa.eu/LexUriServ/LexUriServ.do?uri=COM:2010:2020:FIN:LV:PDF>
February 15, 2013.

Construction and building demolition waste.

Available at: www.videsprodukti.lv February 15, 2013. (in Latvian).

Collection and transportation of construction waste.

Available at: www.zaaoo.lv February 15, 2013. (in Latvian).lv

LBN 006-01 "Essential requirements for buildings",

Available at: <http://www.likumi.lv/doc.php?id=6234likumi.lv>. February 15, 2013. (in Latvian).

Regulation (EU) No 305/2011 of the European Parliament and of the Council of 9 March 2011 laying down harmonised conditions for the marketing of construction products and repealing Council Directive 89/106/EEC.

Available at: <http://eur-lex.europa.eu/LexUriServ/LexUriServ.do?uri=OJ:L:2011:088:0005:0043:LV:PDF>, February 10, 2013.

Principal requirements for the buildings are set forth in Annex I to the Regulation, and there is a new requirement for the sustainable use of natural resources (Requirement 7): Sustainable use of natural resources.

Available to:<http://eur-lex.europa.eu/LexUriServ/LexUriServ.do?uri=OJ:L:2011:088:0005:0043:LV:PDF>

Non-hazardous debris and building demolition remains (Directive 2002/98/EC)

Riga City Council Binding Regulations No.36 "Construction Waste Management Regulations" ("LV", 159 (2734), 01.11.2002.) [Valid from 02.11.2002.; Lapsed 18.11.2010.]

Available at: <http://www.likumi.lv/doc.php?id=67863>, February 10, 2013. (in Latvian).

DESIGN OF FLOW AND HOLDING CAPACITY OF ESCAPE ROUTES IN BUILDINGS

Prof. Peter H.E. van de Leur MSc.

DGMR Consulting Engineers and University of Ghent

Dr. Nico P.M. Scholten PhD.

Foundation Expert centre Regulations in Building (ERB)

E-mail: n.scholten@bouwregelwerk.org

ABSTRACT

A method was developed to dimension escape routes in a multi-storey building, controlling both the flow capacity of egress elements and the holding capacity of floor sections. The method is an extension of a current more traditional approach that requires the staircases in a building to provide sufficient holding capacity on each storey to accommodate all occupants of the storey. The width of stairs and doors is governed by the requirement that the building can be evacuated in 15 minutes. The existing method, mandatory in the Netherlands for office buildings, is unsuitable for high density occupancies such as assembly and education.

The new method recognizes the protection offered by smoke and fire compartments on the same floor as where the fire originated. It allows using these other compartments to hold occupants for a limited time before they can move into the staircases, thus making the method practicable for high occupant density buildings.

A side benefit of the new method is that it forces the designer to consider the likely exit routes taken by escaping groups depending on the location of a fire, not only in the originating fire compartment but in all other parts of the building as well. This is valid not only for the average distribution of occupants over the various parts of the building, but also for any other foreseeable distribution of occupants. The new method was published in 2011 as a Dutch Standard NEN 6089, and was introduced in a modified form in the Dutch Building Decree in April 2012.

The paper describes the method, and compares it to popular methods in current use worldwide.

The authors argue that the new method overcomes some relevant limitations of the conventional methods, while remaining simple enough to be acceptable as a mandatory analysis for a building permit.

Key words: NEN 6089, escape routes, holding capacity

CONCEPTS AND PRACTICE RELATED TO EVACUATION ROUTE SIZING

In case of a fire in a multi-storey building, the evacuation routes should have sufficient capacity to allow occupants to evacuate the area close to the fire or the building as a whole before they are threatened by smoke and fire or collapse. Unfortunately, widely different ideas have developed worldwide over what constitutes 'sufficient capacity'. These ideas have been translated into corresponding requirements in building codes to the size of egress elements such as doors, corridors, lobbies and stairways. The ideas reflect different answers to questions such as: which portion of the evacuation must be controlled? Which occupants need to be provided with egress capacity? How long? How much capacity do they need? How much safety margin is needed in the capacity? How fast are people assumed to move? How fast are fire and smoke assumed to grow? How do we account for delays between alarm and start of movement? Which routes are occupants assumed to take?

Also unfortunately, the concepts are in most cases not explicitly stated but have to be re-engineered from the codes themselves. (Bukowski, 2009) does that in a representative overview of international approaches, from which major elements are used in this paper. The discussion focuses on staircase dimensions, omitting doors, corridors and other floors outside staircases.

From a 1935 NBS report, Bukowski distinguishes several different concepts, including:

- Capacity method, where all occupants are stored within a protected staircase, and subsequently evacuate the building.
- Flow method, which regulates stair width by requiring that all occupants are able to leave the building within the time that it is safe to be in the building.
- Combined method, which means the flow method for lower buildings, shifting to the capacity method for taller buildings.
- Probability method, considering only the population of the six most densely populated floors, implying a phased evacuation.

Bukowski found that regulations worldwide are mostly based on the capacity method, with slight differences in the details.

US CODE REQUIREMENTS

In the US model building codes IBC and NFPA 5000, the required capacity of stairs and doors on any floor is related to the number of occupants served on that floor, with 7.6 mm (0.3 in) of stair width required per person for an unsprinklered building. IBC reduces the required capacity to 5.1 mm (0.2 in) per person where sprinklered. The minimum 1100 mm (44 in) wide stair thus accommodates 147 persons unsprinklered or 220 persons sprinklered.

Bukowski considers this a capacity approach. We note however that a staircase containing a 1100 mm wide stair and associated landings can store around 40 persons on every floor at 0.25 m² per person, far less than the 147 or 220 persons allowed. In a general and simultaneous evacuation of the whole building, assuming an occupant load close to maximum on most of the floors, most people will have to wait outside the staircase for a considerable time.

It can be argued that this is not necessarily unsafe since some phasing will occur even if the alarm is activated on all floors at the same time. The fire floor would effectively respond to the alarm before the other floors, allowing its occupants to find shelter on the lower levels of the staircase. Occupants of the non-fire floors will take longer to enter the staircase, but since there is much less urgency for them, that is not a problem. This argument is clearly not very robust. If the non-fire floors start to evacuate at the same time as the fire floor, occupants of the fire floor will again find themselves blocked outside the staircase.

A phased evacuation, with sufficient delay to allow all occupants of the fire floor to enter the protected staircases before the other floors are alarmed, eliminates the above problem to a large degree. Measures should be taken to prevent occupants on other floors from noticing the alarm on the fire floor.

If unrestricted access to the stairs is guaranteed, objections can still be raised as to the safety of the dimensioning rules in the US code.

- Even with unrestricted access to the staircase, the occupants on the fire floor may take considerable time to enter the staircase since they must proceed down over the stairs in order to make place for others. Using Bukowski's recommended numbers, the flow rate over the 1100 mm stair is 52 or even only 32 persons per minute. Assuming the latter value, it takes almost 7 minutes before the last of 220 persons on a sprinklered fire floor can enter the staircase. If the fire floor is laid out as undivided office space and the staircases have

no protected corridor or lobby, 7 minutes cannot be considered safe to stay in the room of fire origin.

The danger of accidents is obviously greater if access to the staircase is restricted on the fire floor as discussed above.

- On the floors directly above and below the fire floor, the time delay before the last person can enter a protected staircase can be many minutes. The delay may be large enough to see smoke and heat propagating to these floors, causing persons to have to wait in rapidly deteriorating conditions;

A robust way to deal with the above discrepancy between the basic concept of the capacity method and the actual US implementation would be to provide storage area for all occupants of each floor on the flights and landings of the staircase or in a protected lobby or corridor, a provision apparently not required in the US building codes. Bukowski recommends this approach in his suggestions for performance objectives, with a specific escape for floors with assembly spaces: a refuge area next to the staircase, large enough to store all occupants of that floor, would exempt the staircase from the extremely large size requirement on the staircase on the floors below the floor in question.

The corresponding code requirements in the other countries Bukowski studied are actually very similar to those in the USA, so the same comments hold.

- Australia, deemed to satisfy solutions: a 1000 mm (between handrails) stair serves 100 persons; a storey accommodating between 100 and 200 persons requires an aggregate stair width of 1000 mm plus 250 mm for each 25 persons; over 200 persons, the required stair width increases less, 500 mm for each 60 persons.

The approach is similar to the US. A stair serves on any storey more persons than it can store, but substantially less than the US rules allow: 100 instead of 147/220 persons on a 1100 mm clear width stair.

- The UK approved document B (ADB) follows the capacity approach more fully. For a simultaneous evacuation, a staircase must have sufficient capacity to store all persons it serves, with an allowance for the number of persons that can have left the staircase after 2.5 minutes given a flow capacity of 80 persons per minute per meter clear width. Each storey in a staircase is assumed to store 50 persons per meter of effective stair width (Bukowski and Kuligowski, 2004).

The worked examples in ADB show that the rule can lead to rather strange and unsafe results in case of an uneven distribution over storeys: A staircase serving 50 persons on each storey but 100 persons on the upper two

storeys, would need less stair width than serving 50 on all floors!

For phased evacuation, the required stair width is only determined by the number of persons on any storey, implying that only the persons on the fire floor need to find space in the staircase directly. A 1100 mm stair accommodates 120 people per floor, each additional person requiring 10 mm more. The 120 persons having unrestricted access, and the 1100 mm allowing a flow rate of 88 persons/minute, the fire floor is emptied in 1.4 minutes.

Bukowski's less optimistic assumption of 32 persons/minute leads to 3.8 minutes, lower than the US value.

In addition, the UK assumes one person for every 6 m² of office area. Whether this represents a substantial safety margin taken in the UK egress capacity requirements, or simply a more Spartan use of space in Britain is not known.

DISCUSSION

The various approaches discussed appear to deal quite differently with buildings with high occupant densities above the ground floor. The UK effectively requires that the stairways accommodate everyone in the building (Communities and Local Government, 2006). That is a quite safe requirement, far more constricting than other countries that allow smaller staircases; countries such as Australia and the USA apparently rely on unspecified safety factors that make it acceptable if people on the fire floor take several minutes before they can enter a protected staircase. These countries have adopted that margin since their industries consider strict application of the capacity concept too burdensome.

This does raise the question of whether the UK does construct the very substantial staircase dimensions that the rule prescribes for high occupant densities; or have they adopted other, more practical ways to ensure safety, without changing the rule accordingly?

The methods described do not appear to explicitly value some of the factors that have been used in developing the Dutch standard, notably:

- A distinction between the need for rapid evacuation by persons in the compartment of fire origin, and those in an adjacent fire compartment. By controlling the flow capacity and the storage capacity of a storey as a whole, the rules make no such distinction. Thus, an open plan office storey requires identical staircase capacity as the same storey divided in fire compartments. From a point of view of hazard, significant differences exist. As discussed above, occupants of the open plan fire floor may have to wait 7 minutes before the last person is in a staircase. The same storey divided in two equal fire compartments

connected by wide doors offers a different view: occupants of the compartment where the fire starts now have a high capacity additional exit to the safety of the second fire compartment.

- The capacity of a staircase is mostly coupled to the width of the stair. Actually, a standard staircase stores more persons on the landings than on the stair, and the size of the landing on floor levels is often relatively easy to enlarge without resorting to adding lobbies.
- No direct control of the overall evacuation time of the staircase.

DUTCH CODE REQUIREMENTS

The Dutch Building Decree up to April 2012 specified a rule similar to the UK, but more restrictive (van de Lier et. al, 2009). It is a combination of:

- full capacity method, requiring that protected staircases provide room on every floor for all occupants of that floor;
- flow method, which states that the flow capacity of the stairs must allow all staircases to be evacuated within 15 minutes (20 minutes in staircases with additional protection by a smoke proof lobby, 30 minutes in 'safety staircases' that can only be accessed from the outside).

A less strict interpretation of the rule allows for storage in a protected staircase lobby.

The requirements to the capacity of stairs come on top of a basic rule that governs the total door width of rooms and smoke compartments. Sufficient door width must be available to allow occupants to leave the room or compartment in not more than 1.5 minutes.

Basic parameters of calculations are prescribed as follows. Flow capacity: 90 persons per min per m clear width for doors and passageways, 45 persons per min per m clear width for stairs. Storage capacity is set at 4 persons per m² on floors, 0.9 persons per m stair width on each tread on stairs.

The Dutch code requirements are set in addition to a set of basic rules:

- Fire compartments are limited to 1000 m², separated by 60 minutes fire resistant constructions (EI60 according to the European standard EN 13501-2);
- Each fire compartment must be divided in smoke compartments such that the maximum walking distance to the nearest compartment exit does not exceed a limiting value varying between 30 m high occupant densities down to 1 person per 8 m² usable floor area, and 60 m for occupant densities lower than 1 person per 20 m² usable floor area. Smoke compartments are separated by 20 minutes fire resistant constructions (E20 or Sa by NEN-EN 1634-3).

NEED FOR ADVANCED EVACUATION MODELLING

A discussion of the hazards mentioned above in this chapter does not need advanced calculation models such as Building EXODUS, Steps and similar to quantify them. As long as cases simplified to their essential core are discussed, the simple calculation rules in the prescriptive and deemed-to-satisfy methods are sufficient to discuss the value and safety issues of the different approaches. The modern evacuation models can make their analysis simpler, and they become essential when the added effects of varying occupant number and density, mobility issues and the like need to be addressed. Most literature on application of these models seems to consider these ‘building regulations’ cases less interesting than, e.g., complex structures and crowd management issues. The authors disagree.

THE NEED FOR AN ALTERNATIVE MODEL

The formal implementation of the Dutch code method for dimensioning of stairs is applicable only up to 15 floors, offering no guidance for higher buildings.

The strict application of the capacity concept makes it very restrictive, and completely impractical even for relatively low buildings with high occupant loads such as assembly or education. Building owners strongly object against the excessive loss of rentable space that must be reserved for staircases and protected lobbies, and in practice the method is rarely applied in full except for less densely occupied buildings such as offices and hotels.

Practitioners realized that where a floor is subdivided in fire or smoke compartments, the protected staircase is not the only safe place on the floor. In case of fire in one compartment, the other compartments on the same floor provide a safe place, at least for a short time. That eliminates or at least reduces the need for the provision of storage area in protected staircases or lobbies.

DEVELOPMENT OF NEN 6089

This idea has lead to the development of a model that allowed for temporary storage in smoke compartments or fire compartments adjacent to a protected staircase. Phased evacuation was to be introduced at the same time. For all other parts of the model the objective was to stay as close as possible to the existing Dutch building code. That included keeping the model as simple as possible, a prerequisite for getting a mandatory role in building permit procedures.

In the discussions over the development, new problems were identified that required additional features in the method.

- Limits needed to be set to the time that people are forced to wait in the ‘holding space’ adjacent to the protected staircase. Consensus

was reached over maximum waiting times of 3.5 minutes in a smoke compartment (E20 protection), and 6 minutes in a fire compartment (EI30 protection).

- A scenario with no fire is checked for compliance of the overall evacuation time of the building with the standard 15/20/30 minutes, depending on staircase protection.
- A fire can start in the compartment adjacent to a protected staircase. In that case, it is not reasonable to allow an extended waiting time, the directly threatened compartment must allow evacuation in 1.5 minutes as per the building code (or: the building construction must allow evacuation in 1.5 minutes).
- It was found necessary to introduce fire scenarios, at least by making a distinction between the compartment where the fire starts and all others. The latter are protected from the fire by E20 or EI30 constructions and can serve as waiting space. Since a fire can start in any compartment, this means that the analysis of a building involves many calculations, one for each scenario.
- No further specification of the fire location within the compartment is required. Effects of exits being blocked by the fire are not treated.
- Further scenarios are introduced if different major occupant distributions can be distinguished, each offering a different challenge to the egress system. An example is an educational building; at ordinary school hours virtually everyone is in the classrooms, but at specific times the whole school may be assembled in a main hall. By treating each as a different scenario, a common problem is avoided that arises when the maximum occupant load is assumed in all areas.
- The previous allows for a rather straightforward prediction of the distribution of persons over the exit doors of the compartments on the fire floor and on other floors.
 - In the ‘directly threatened compartment’ where the fire starts, occupants may be assumed to use all exits available to the compartment, since in the very first phase of fire development blockage of exits by fire or smoke is improbable. The assumption is moreover in line with the code requirement governing only the total exit door width.
 - In a compartment on another floor, occupants are likely to evacuate all taking the same ‘normal’ route, since there is no immediate threat that would cause them to look for the closest possible exit of their compartment. They are also unlikely

- to have information as to the exact location of the fire, so they have no reason to deviate from their designed evacuation route. They will obviously take longer to evacuate their compartment than 1.5 minutes, but that does not threaten their safety.
- In other compartments on the fire floor, the situation for occupants is more complex. Their normal evacuation route may lead through the compartment of fire origin; occupants trying that route are likely to track back as soon as they see smoke or fire, or people fleeing towards them. A reasonable assumption is that they avoid all escape routes running through the directly threatened compartment, and choose another available route. This other route is then taken by a) occupants for whom this is the normal escape route, b) occupants of other compartments avoiding the directly threatened compartment, and c) a fraction of the occupants of the directly threatened compartment, who used a 'non-standard' exit. These numbers can normally be estimated in a simple way, easily defended when reviewed.
 - It is to be expected that on the fire floor, the distribution of persons over staircases is different from the standard, whereas the distribution remains unchanged on other floors. In an extreme case, with a fire in the compartment adjacent to a staircase, almost all occupants of the fire floor must be expected to use the only other staircase. The waiting time to enter that staircase on the fire floor could be critical.
 - It is the responsibility of the applicant to propose reasonable distributions of occupants over compartment exits and staircases in the various scenarios. The above principles may serve as starting points, but the specific situation of the building may lead to modified distributions.
 - Apart from fire scenarios, the model allows for treatment of varying occupation of the building. The same population could be distributed over classrooms during working hours, but concentrated in an assembly hall at another time. Treating every relevant distribution as a separate scenario avoids the problems of designing for simultaneous maximum occupancy for all spaces.
 - An important simplification is the assumption that walking distances and walking times are negligible, and that the evacuation process is governed by flow and storage capacity. This assumption loses its validity with extremely low occupant densities, a situation rarely found in buildings where stairway dimensioning is a relevant issue.
 - In order to deal with waiting times and uneven distributions of persons, the model was cast in the form of a time development, tracing numbers of persons along their egress paths. To keep the model reasonably simple, a fixed time step of 30 s is imposed;
 - A consequence of the assumption of negligible walking times is that walking speeds do not pose a limit on the vertical distance over which persons can move within a time step. A specific rule limits that distance;
 - Waiting times outside the staircases are strongly influenced by the assumptions regarding the process of mixing the stream from a storey with the stream from the storeys above in the staircase. A local 50% - 50% mixing on each storey is assumed. This does have rather important consequences in that high occupant loads are far easier to handle on the lowest storeys than high in a building.
- The standard NEN 6089 was published in 2011, accompanied by a practical instrument NPR 6080 in the form of a computer program that practitioners can use to carry out the necessary calculations (NEN 6069, 2011). The software was developed by DGMR for the Dutch Standards organisation NEN. The example calculations below were made using the software.
- Within the Building Decree 2012 rules for different flow capacities are giving depending on the maximum openings angle of a door. These figures are not well validated and suggest an accuracy that cannot be proved. Within NEN 6089 in case of a fire people are directly projected in front of the exit doors of a compartment. The distance to be walked or differences in floor levels within a compartment are ignored. The Building Decree 2013 takes these effects in account which suggest accuracy that is not important at all but influence the outcome highly in some premises.
- Also the time to evacuate the smoke compartment were the fire started is returned to 1 minute instead of 1,5 minute. In international perspective there is no reason for such a severe requirement.
- The outcomes of the Building Decree 2012 calculations are much more severe than that of calculations by NEN 6089. In practise this lead to a lot of discussions and to unnecessary building costs and pressure on the income of a company because of diminishing the amount of people that is permitted in the premises.
- ## EXAMPLES
- Example calculations are presented that correspond to a worked example in ADB par. 4.25, an office building designed for simultaneous evacuation. The

building has 11 office storeys above the ground floor, each of two stairs serving 600 persons, distributed evenly over the storeys. The required stair width according to ADB is 1100 mm.

For the purpose of this paper, two scenarios are selected to illustrate the method. In an actual building project permit application, the applicant must make plausible that all relevant scenarios have been tackled, and that all show compliance.

The main parameters used to make the calculations according to NEN 6089 are reproduced in Table 1.

Table 1

Calculation parameters, simultaneous evacuation

Parameter	Value
Scenario	No fire
Stair width	1100 mm
Landing dimensions	2500 mm x 1100 mm
Number of treads per storey	18
Number of persons on each storey	110
Total number of persons	990
Distribution of persons over staircases	55/55 on all floors
Protection level	EI30
Evacuation type	simultaneous

Scenario 1	Scenario 2	Trappenhuis 1	Trappenhuis 2	Resultaten:	Trappenhuis	Max. toegestane ontruimingstijd [mm:ss]	Berekende ontruimingstijd [mm:ss]	Voldoet?
Gebouw								
Ontruimingstijd [min.]		13:00	13:00					
Voldoet?		Ja	Ja					
Verdieping 11								
Aantal personen [-]		55	55					
Wachttijd [min.]		4:00	4:00					
Voldoet?		n.v.t.	n.v.t.					
Verdieping 10								
Aantal personen [-]		55	55					
Wachttijd [min.]		4:30	4:30					
Voldoet?		n.v.t.	n.v.t.					
Verdieping 9								
Aantal personen [-]		55	55					
Wachttijd [min.]		4:30	4:30					
Voldoet?		n.v.t.	n.v.t.					
Verdieping 8								
Aantal personen [-]		55	55					
Wachttijd [min.]		4:00	4:00					
Voldoet?		n.v.t.	n.v.t.					
Verdieping 7								
Aantal personen [-]		55	55					
Wachttijd [min.]		3:30	3:30					
Voldoet?		n.v.t.	n.v.t.					
Verdieping 6								
Aantal personen [-]		55	55					
Wachttijd [min.]		3:30	3:30					
Voldoet?		n.v.t.	n.v.t.					
Verdieping 5								
Aantal personen [-]		55	55					
Wachttijd [min.]		3:00	3:00					
Voldoet?		n.v.t.	n.v.t.					
Verdieping 4								
Aantal personen [-]		55	55					
Wachttijd [min.]		2:30	2:30					
Voldoet?		n.v.t.	n.v.t.					
Verdieping 3								
Aantal personen [-]		55	55					
Wachttijd [min.]		2:00	2:00					
Voldoet?		n.v.t.	n.v.t.					
Verdieping 2								
Aantal personen [-]		55	55					
Wachttijd [min.]		2:00	2:00					
Voldoet?		n.v.t.	n.v.t.					
Verdieping 1								
Aantal personen [-]		55	55					
Wachttijd [min.]		1:30	1:30					
Voldoet?		n.v.t.	n.v.t.					
Begane grond								
Aantal personen [-]		0	0					
Wachttijd [min.]		0:00	0:00					
Voldoet?		n.v.t.	n.v.t.					

Explanation: gebouw: building; Verdieping: floor; wachttijd: waiting time; trappenhuis: staircase; aantal personen: amount of people; begane grond: ground floor; voldoet: satisfied; max. toegestane ontruimingstijd: maximum permitted egress time of the building; berekende ontruimingstijd: calculates egress time; ja: yes.

Figure 3. Results for scenario 1, simultaneous evacuation

The results for the ‘no fire’ scenario 1 are presented below. The screen dump shows the results for both staircases. Waiting times before the last of the 55 persons assigned to each

staircase has entered the staircase increase from 1.5 min on the first floor, to 4 minutes on the highest floor. The overall evacuation time is 13 minutes. In the no fire scenario, waiting times are

considered irrelevant. The report section reproduced to the right of the screen dump checks only the staircase evacuation times against the 15 minutes limit.

Scenario 2 introduces a fire in an area served by staircase 1 on storey 6. The storey is assumed to be separated in two smoke or fire compartments. Half of the occupants of the directly threatened compartment served by staircase 1 now evacuate to staircase 2, bringing the distribution on that storey to 27/83. allowed 1.5 minutes. The waiting time at staircase 2 is 4.5 minutes. Because this is higher than the allowed 1.5 minutes for the directly threatened compartment, an open plan configuration is not acceptable. The waiting time

is also higher than 3.5 minutes, and as a consequence a smoke resistant (E20) separation is not sufficient. With a EI30 fire resistant separation the maximum waiting time increases to 6 minutes, which is not exceeded. The overall evacuation time is slightly reduced for staircase 1 and slightly increased for staircase 2, but since no limit is set to evacuation time in a fire scenario these are irrelevant for the overall judgment. The report section reproduced to the right of the screen dump checks only the waiting times on the fire storey times against the 1.5 minute limit for the directly threatened compartment, and against 6 minutes for an EI30 protected ‘influenced’ compartment.

Scenario 1	Scenario 2	Trappenhuis 1	Trappenhuis 2			
Gebouw						
Ontruimingstijd [min.]		12:30	13:30			
Voldoet?		n.v.t.	n.v.t.			
Verdieping 11						
Aantal personen [-]		55	55			
Wachttijd [min.]		3:30	4:30			
Voldoet?		n.v.t.	n.v.t.			
Verdieping 10						
Aantal personen [-]		55	55			
Wachttijd [min.]		4:00	5:30			
Voldoet?		n.v.t.	n.v.t.			
Verdieping 9						
Aantal personen [-]		55	55			
Wachttijd [min.]		3:30	5:00			
Voldoet?		n.v.t.	n.v.t.			
Verdieping 8						
Aantal personen [-]		55	55			
Wachttijd [min.]		3:30	4:30			
Voldoet?		n.v.t.	n.v.t.			
Verdieping 7						
Aantal personen [-]		55	55			
Wachttijd [min.]		3:00	4:00			
Voldoet?		n.v.t.	n.v.t.			
Verdieping 6						
Aantal personen [-]		27	83			
Wachttijd [min.]		0:30	4:30			
Voldoet?		Ja	Ja			
Verdieping 5						
Aantal personen [-]		55	55			
Wachttijd [min.]		3:00	3:00			
Voldoet?		n.v.t.	n.v.t.			
Verdieping 4						
Aantal personen [-]		55	55			
Wachttijd [min.]		2:30	2:30			
Voldoet?		n.v.t.	n.v.t.			
Verdieping 3						
Aantal personen [-]		55	55			
Wachttijd [min.]		2:00	2:00			
Voldoet?		n.v.t.	n.v.t.			
Verdieping 2						
Aantal personen [-]		55	55			
Wachttijd [min.]		2:00	2:00			
Voldoet?		n.v.t.	n.v.t.			
Verdieping 1						
Aantal personen [-]		55	55			
Wachttijd [min.]		1:30	1:30			
Voldoet?		n.v.t.	n.v.t.			
Begane grond						
Aantal personen [-]		0	0			
Wachttijd [min.]		0:00	0:00			
Voldoet?		n.v.t.	n.v.t.			

Resultaten:					
Trappenhuis	Verdieping	Status opvangruimte	Max. toegestane wachttijd [mm:ss]	Berekende wachttijd [mm:ss]	Voldoet?
Trappenhuis 1	Verdieping 6	Direct bedreigd	01:30	0:30	Ja
Trappenhuis 2	Verdieping 6	Beïnvloed - B30	06:00	4:30	Ja

Explanation: gebouw: building; Verdieping: floor; wachttijd: waiting time; trappenhuis: staircase; aantal personen: amount of people; begane grond: ground floor; voldoet: satisfied; max. toegestane ontruimingstijd: maximum permitted egress time of the building; berekende ontruimingstijd: calculates egress time; ja: yes.

Figure 4 Results for scenario 2, fire on storey 6

ANALYSIS

These examples illustrate how the model values alternative egress paths in specific scenarios if they are protected from the location of the fire source. This makes it possible to go beyond the strict capacity method without losing sense of the safety of the design. The examples illustrate that the method does not sanction occupant loads far above the strict capacity of the staircases. Even if

the directly threatened compartment can then evacuate within the limit of 1.5 minutes, the other compartments on the fire storey will easily slip beyond the maximum of 6 minutes.

Some relief of this is offered in situations with very uneven occupant load (a heavily loaded storey with almost empty storeys directly below and above can evacuate very fast). Phased evacuation is also very efficient in guaranteeing free staircases.

The recently published standard has gone through only a limited testing period. As practical results become available from building projects with its introduction in the building regulations, the model and its parameters will face a first large scale reality check. It should be expected that modifications are needed to satisfy both safety targets and economy.

CONCLUSIONS

The newly published Dutch standard NEN 6089 was developed to fill the need for a more practical design rule for staircase sizing than the strict

capacity method that has been mandatory in the Netherlands until April 2012.

This paper discusses its design, and analyses how it compares to approaches in other countries. The new method offers a distinct advantage over the existing methods in dealing explicitly with the time that people have to wait before they can enter a protected staircase, applying limits dependent on the level of protection offered by smoke resistant or fire resistant separating structures.

Practical experience with the method is growing because the standard can be used from the end of 2011.

REFERENCES

- Bukowski R. (2009) Emergency Egress from Buildings. NIST Technical Note 1623.
- Bukowski R., Kuligowski E. (2004) The Basis for Egress provisions in US Building codes. InterFlam 2004. Edinburgh. UK, July 2004
- Communities and Local Government (2006) Approved Document B, volume 2 – buildings other than dwellings.
- NEN 6089 (2011) Determination of the collection capacity and the throughput capacity of circulation spaces. Netherlands Standardization Institute (in Dutch).
- Van de Leur P., Peters B., Haas M. (2009) A Method For Dimensioning Stairs And Door Widths For Dutch Building Regulations. *Human Behaviour In Fires Symposium*. Cambridge. UK.

NON-DESTRUCTIVE EVALUATION OF FIBER ORIENTATION IN FIBERCONCRETE PRISM

Arturs Macanovskis ^{*}, Vitalijs Zaharevskis ^{**}, Andrejs Krasnikovs ^{***}

^{*}Riga Technical University

Institute of Mechanics

E-mail: artursmacanovskis@inbox.lv

^{**}Riga Technical University

Institute of Mechanics

E-mail: vitalijs.zaharevskis@rtu.lv

^{*,**}Riga Technical University

Institute of Mechanics and Concrete Mechanics Laboratory

E-mail: Krasnikovs.Andrejs@gmail.com

ABSTRACT

Macro crack propagation in mechanically loaded steel fiber reinforced concrete is characterized by fibers bridging the crack, providing resistance to its opening. Suppose about homogeneous distribution of spatially arbitrary oriented fibers in a volume is leading to homogeneous spatially arbitrary distributed fiber orientation on the surface of the crack. At the same time, high experimental results scatter in fiberconcrete bending tests is experimentally observed, proving non-homogeneous fiber distribution in a volume and according to spatial orientations. One possibility to solve this problem is to use fiberconcrete with internal oriented fiber structure. In this work fiberconcrete prisms with oriented (in each prism longitudinal direction) short steel fiber structure were elaborated (Lapsa et al., 2010). Two metallic combs were prepared, a mould with fiberconcrete was placed on the shaking table and fibers in the mould were combed. The fiber orientation results were controlled by X-ray analysis and by ultrasonic device. All prisms were loaded by 4 point bending and Load bearing – crack opening curves were obtained.

Key words: steel fibers, concrete prisms, non-destructive testing, four point bending

INTRODUCTION

Usually fibers are homogeneously distributed in concrete body having arbitrary spatial orientations (Laranjeira et al., 2010; Gettu et al., 2005; Krenchel, 1982; Krasnikovs; Kononova, 2009).

Macro crack propagation in mechanically loaded steel fiber reinforced concrete is characterized by fibers bridging the crack, providing resistance to its opening. Supposition about homogeneous distribution of spatially arbitrary oriented fibers in a volume is leading to homogeneous spatially arbitrary distributed fiber orientation on the surface of the crack. At the same time, high experimental results scatter in fiberconcrete bending tests is experimentally observed, proving non-homogeneous fiber distribution in a volume and according to spatial orientations. The question of how to reduce experimental results scatter is important. A number of test methods have been proposed, but all have significant problems associated with either the variability of the results or their application in structural design calculations. One possibility to solve this problem is to use fiberconcrete with internal oriented fiber structure. In the present work fiberconcrete prisms with oriented (in each prism longitudinal direction) short steel fiber structure were elaborated (Lapsa et al., 2010). Precise amount of fibers was mixed with

concrete and fresh fiberconcrete was placed into a mould. Two specially elaborated metallic combs (see Fig.1.) were prepared, a mould with fiberconcrete was placed on the shaking table and simultaneously fibers in the mould were combed. This operation was executed few times. Displacement between each comb two adjacent teeth was smaller than the length of a fiber, and was bigger than the cross-section size of a bigger concrete aggregate largest linear size. Vibration was applied during the process. The fiber orientation results were controlled by X-ray picture analysis. The prisms with oriented and chaotically (non-oriented) distributed fibers were tested by an ultrasonic device, measuring the ultra-sound wave velocity dependence on the fiber orientation in the samples and fiber concentration. The ultra-sound wave velocity dependence on fiber orientation was experimentally obtained. After that all prisms were tested by 4 point bending till failure.

EXPERIMENTAL SAMPLES FABRICATION

Experimentally fiberconcrete samples with the following recipe were made:

- First type of cement 42,5
- Sand (fraction 0 - 2.5 mm)
- Sand (fraction 0 - 1 mm)
- Dolomite filler

- Micro silica
- Dramix fibers
- Water

27 prismatic samples were elaborated having dimensions 10x10x40 cm.

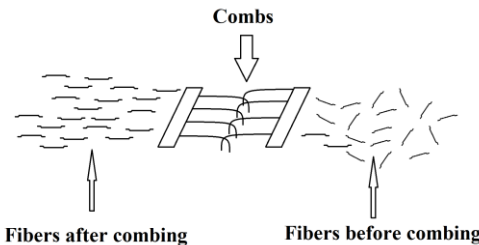


Figure 1. Fiber orientation process

The samples were divided into 4 groups:

- 1) Benchmarks- specimens having chaotic fiber distribution in the sample volume (fiber content was 40, 60 and 80 kg/m³).
- 2) Laminated beams (non-oriented) - fibers were located in two layers, the first non-oriented (fiber content was 20 kg/m³), and the second layer was non-oriented (fiber content was 60, 100 and 140 kg/m³).
- 3) Beams with oriented fibers - fiber reinforced concrete samples were processed by the method of combing (see Fig.1and Fig.2).
- 4) Laminated beams (oriented) - fibers were located in two layers, the first non-oriented (fiber content 20 kg/m³), the second layer oriented (fiber content 60, 100 and 140 kg/m³).



Figure 2. Combing fibers on the vibrating table

FIBER ORIENTATION

To get oriented fibers two combs were used by which fibers were oriented and a steel form placed on a vibrating table. In Fig. 1 the combing scheme can be seen, while in Fig. 2 you can see the real process. Combing occurred when two combs were dragged in opposite directions and that way fibers were oriented in a concrete mix.

USE OF ULTRASOUND IN CHARACTERIZATION OF FIBERCONCRETE

Determining the time of distribution of ultrasound waves in different materials

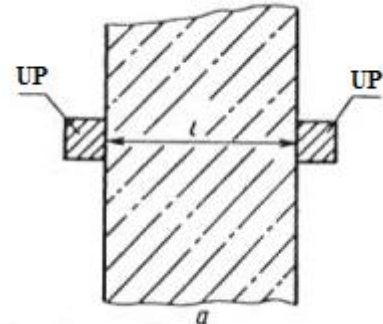


Figure 3. Scheme of concrete sample testing by sound transmission method,
where UP – ultrasonic transducers

their mechanical properties and internal structure can be indirectly characterized. In the present work attempts were made using ultrasound testing to determine the degree of fiber orientation in fiberconcrete samples.

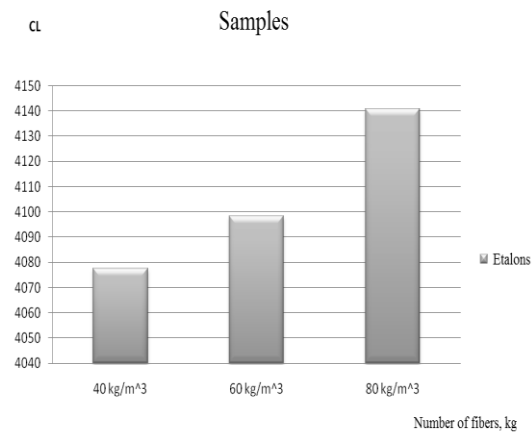


Figure 4. Correlation between ultrasound wave speed and fiber concentration in fiberconcrete with chaotic fiber distribution in fiberconcrete volume

Ultrasound converters were placed on opposite sides of the sample determining the ultrasound wave velocity (v), m/s, is given by the formula 1

$$v = \frac{l}{t} * 10^3 \quad (1)$$

where: t is time of ultrasound wave distribution in microseconds;
l – distance between the centers of the transducer in mm.

During the test on samples with chaotic fiber distribution (the first group of materials - the

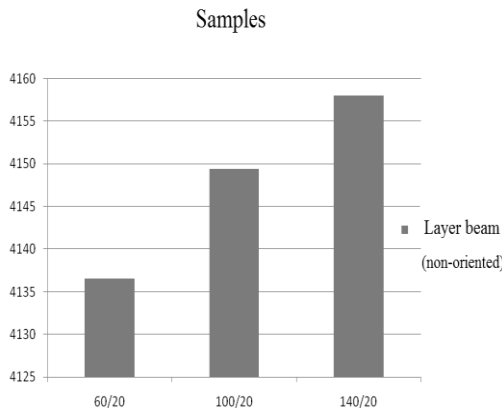


Figure 5. Correlation between ultrasound wave speed and fiber concentration in layered fiberconcrete with chaotic fiber distribution in each layer volume

benchmarks) the results were obtained for the ultrasound wave propagation velocity dependence on the steel fiber content in samples, which are shown in Figure 4.

The graph compares three samples with different amount of fibers per m^3 , as follows:

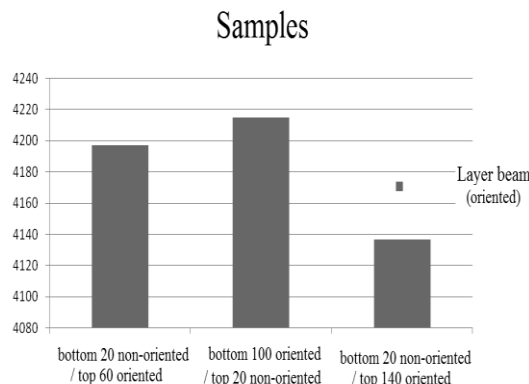


Figure 6. Correlation between ultrasound wave speed and fiber concentration in layered fiberconcrete with oriented fiber distribution in each layer volume

From the graph it is easy to conclude that with increasing of the fiber concentration the velocity of waves increases. Explanation of such phenomenon is as follows: ultrasound velocity in steel is greater than in concrete and if the steel fiber part in the mix is higher, then also the speed increases.

In Fig. 5 the testing results for samples consisting of layers with non-oriented fibers (samples from the second group) are shown. The trend to increase the wave propagation speed increasing the fiber concentration was maintained. In Fig. 6 the results of layered samples testing comprising oriented fibers (samples from the fourth group) are shown. In the following figure it is possible to see that with increasing of the fiber concentration, the rate of increase remains at the beginning and is decreasing

later. The reason here is the fact, that in the samples located on the vibrating table, uncontrolled standing waves were created in the sample body forming fiber density non-homogeneous distribution along the longitudinal axis of the sample what highly affected the experimental results, reducing the speed of wave propagation. This picture is easy to recognize in x-ray photos that were done and possible to see in Figures 7 and 8.

FIBROCONCRETE SAMPLE X-RAY INVESTIGATION

With the goal to perform fiberconcrete sample internal structure control, the samples were subjected to X-ray study. X-ray sample pictures from the fourth group (viewed from the side shown in Figure 7, and viewed from the top in Figure 8) are presented. The pictures show a pronounced effect of vibration on the fiberconcrete internal structure, vibration creates non-predictable fiber density non-homogeneous distribution along the longitudinal axis of the sample. The sample vibration time does not exceed 1 minute.

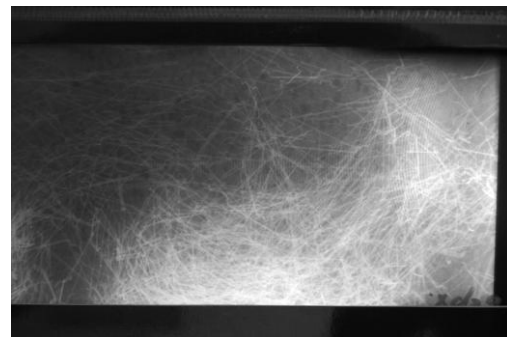


Figure 7. X-ray image of fiber distribution in oriented layered fiberconcrete (sample from the fourth group, view from a side)

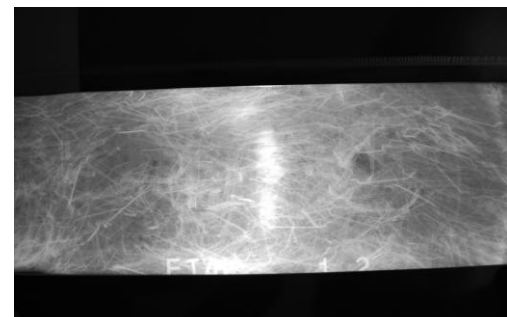


Figure 8. X-ray image distribution of fibers in oriented layered fiberconcrete (sample from the fourth group, view from above)

TESTS ON FOUR POINT BENDING FIBERCONCRETE PRISMS

All 18 samples that were made were tested by four-point bending (Fig. 9.) using "CONTROLS" Autamax 5. The tests were continued till the macro crack opening reached 6 mm.

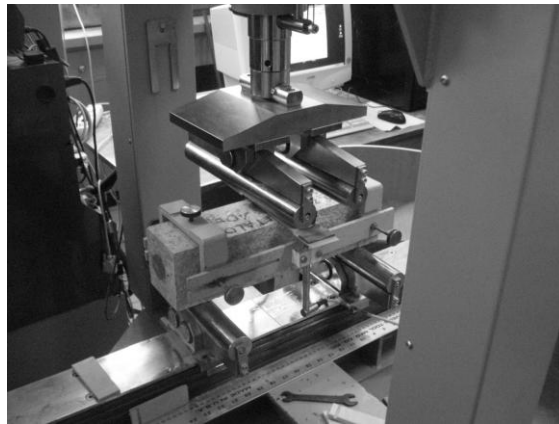


Figure 9. Sample test by four point bending

The first group (benchmarks with chaotically orientated fibers) sample curves applied force - the mid-point prism vertical deflection are shown in Fig.10a. In figure the testing results for samples with different amounts of fibers 40 kg/m³- samples P10, P13, with 60 kg/m³- samples P16, P19, with 80 kg/m³- samples P22, P25 are shown. As it can be seen from the graphs, if the fiber amount increases the load carrying capacity is increasing too, the sample P25 with the highest content of fibers (80 kg/m³) withstood the highest load. Least amount of load withstood the sample P10 with fiber concentration of 40 kg/m³. At the same time, the result has large dispersion.

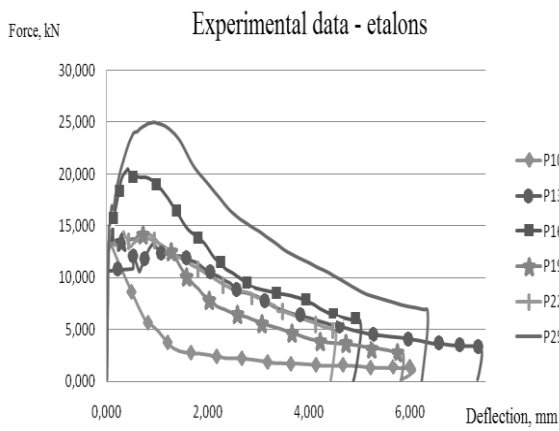


Figure 10. (a) Load - deflection curves for samples (P10, P13, P16, P19, P22, P25), where force was measured in kN and deflection in mm

Layered beam (with non-oriented fibers in layers) with the fiber concentration 40 kg/m³ - samples P11, P12, with 60 kg/m³- samples P14, P15, with 80 kg/m³- samples P17, P18. The four-point bending curves: applied force - the mid-point of prism vertical deflection are shown in Fig.10b.

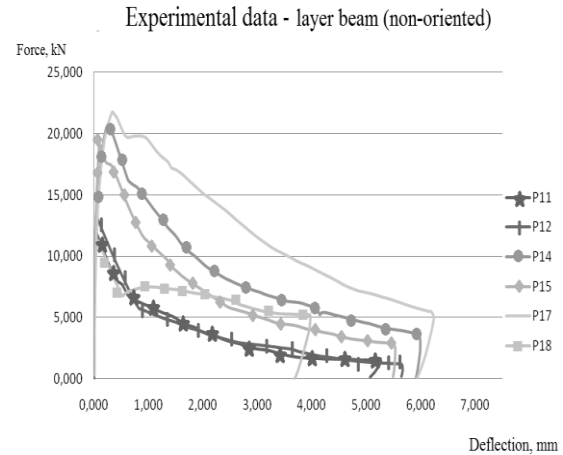


Figure 10. (b) Load - deflection curves for samples (P11, P12, P14, P15, P17, P18) - layered samples with not oriented fibers in layers, where force was measured in kN and deflection in mm

According to Fig. 10b it can be concluded, that the highest load bearing capacity in bending was shown by the sample P17, the sample with a higher concentration of fibers, and the sample P11 which withstood the lowest load had the lowest amount of fibers. The peak load for the sample P17 was 22 kN and for the specimen P11 the peak load was 12 kN. The experimental data that were obtained for laminates with oriented fibers in layers are shown in Fig. 10c. The graphs belong to the beams with various quantities of fibers: 40 kg/m³- samples P20, P21, 60 kg/m³- samples P23, P24, 80 kg/m³-samples P26, P27.

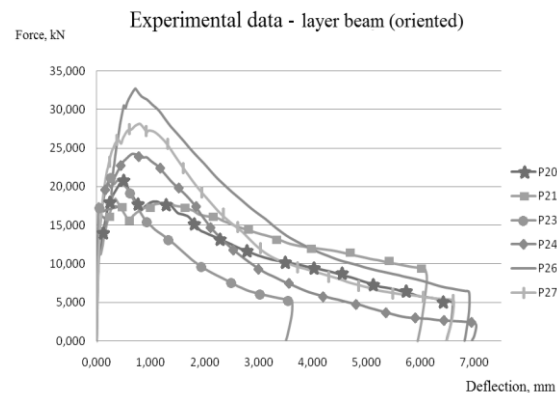


Figure 10. (c) Load - deflection curves for samples (P20, P21, P23, P24, P26, P27) - layered samples with oriented fibers in layers, where force was measured in kN and deflection in mm

The sample P26 with the fiber amount of 80 kg/m³ withstood the highest load and the sample P21 with fiber concentration of 40 kg/m³ withstood the least load. The sample P26 withstood the maximal load equal to 26 kN and the sample P21 equal to 18.

Comparison of the three groups of the results shows that despite the relatively large scatter of the results laminated samples with orientated fibers in layers showed the highest load carrying capacity. The sample P27 - sample with 80 kg/m³ fiber quantity with oriented fibers in plies showed higher maximal peak load. It can be concluded that not only the amount of fibers is affecting the load bearing capacity, but also the fiber orientation.

NUMERICAL MODELING

In parallel to the experimental study, the non-homogeneous fiberconcrete prisms subjected to four-point bending were modeled numerically (using the finite element method (FEM) program ANSYS (Release...)) with the goal to show internal stress fields in the beam before the macro crack opening and after that. 2D beam FEM model was created with dimensions 40x10 cm. The model was realized for:

- ✓ beam with non-oriented fibers;
- ✓ beam with oriented fibers;
- ✓ laminated beam (top layer fiber concentration - 20 kg/m³, bottom layer fiber concentration - 60 kg/m³);
- ✓ laminated beam (top layer fiber concentration - 20 kg/m³, bottom layer fiber concentration - 100 kg/m³);
- ✓ laminated beam (top layer fiber concentration - 20 kg/m³, bottom layer fiber concentration - 140 kg/m³);
- ✓ beam with cracks and non-oriented fiber beam with cracks and oriented fibers;
- ✓ laminated (oriented fibers) beam with crack.

For benchmark specimens having chaotic fiber distribution in the sample volume fiberconcrete Young's modulus was determined in the experiments with ultrasound wave velocity determination. In layered samples fiberconcrete Young's modulus was calculated according to "rule of mixture" formulas (Young's modulus for concrete without fibers was taken equal to 30GPa). Poisson's ratio $\nu = 0.2$. Laminated beam loading case is shown in Fig. 11a. The stress distribution is shown in Fig. 11b-e. Three fiberconcrete beams were considered: laminated beam (top layer had fiber concentration - 20 kg/m³, bottom layer had fiber concentration - 60 kg/m³); laminated beam (top layer had fiber concentration - 20 kg/m³, bottom layer had fiber concentration - 100 kg/m³); laminated beam (top layer had fiber concentration -

20 kg/m³, bottom layer had fiber concentration - 140 kg/m³).

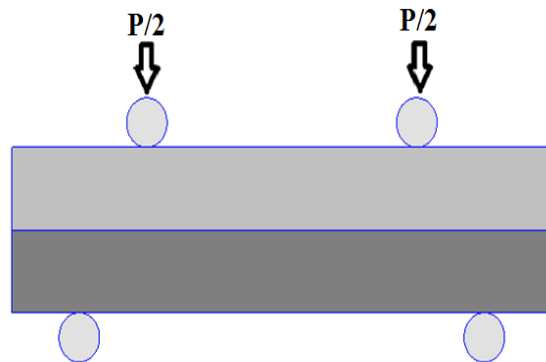


Figure 11. (a) Layered samples on four point bending

The numerical results for laminated beam (if the top layer had fiber concentration 20 kg/m³ and the bottom layer had fiber concentration 60 kg/m³) are shown in Figures 11b-e.

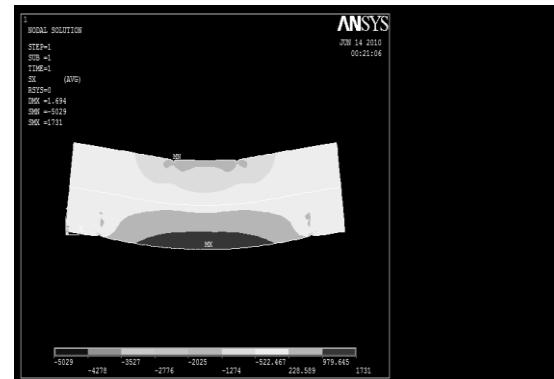


Figure 11. (b) Normal stress σ_{xx} distribution in the layered sample during bending

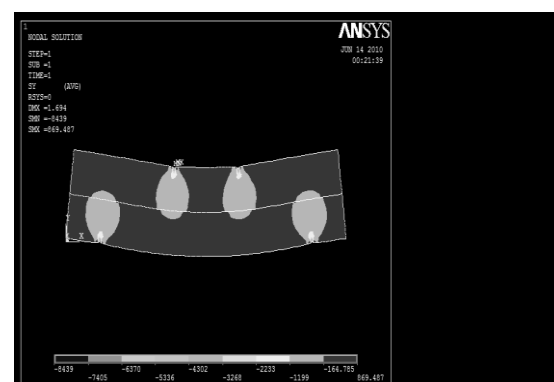


Figure 11. (c) Normal stress σ_{yy} distribution in the layered sample during bending

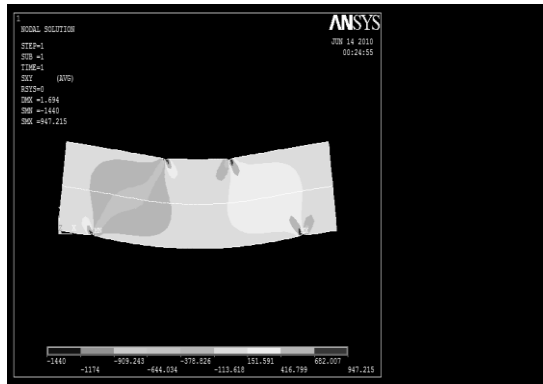


Figure 11. (d). Tangential stress τ_{xy} distribution in the layered sample during bending

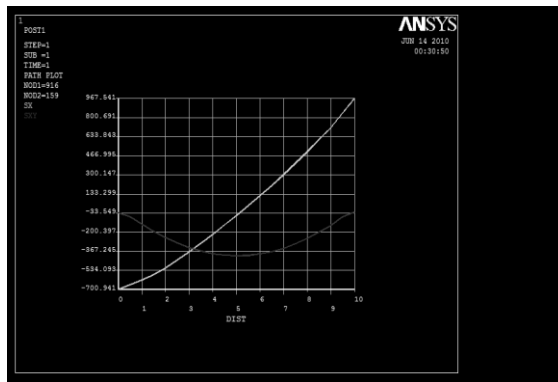


Figure 11. (e). Normal and tangential stress distribution through thickness of the beam (in the middle between the left and the top support of the applied load)

With the goal to numerically simulate stress fields in the beam with open macro crack, the crack was modeled by an isotropic layer having relatively low Young's modulus (3Gpa). Laminated beam with a crack is shown in Fig. 12a.

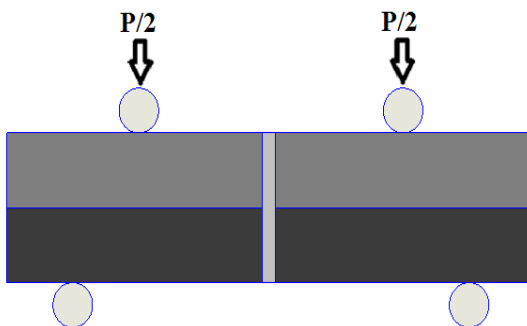


Figure 12. (a). Layer beam with crack (crack is modeling as a soft layer) under four point bending

Stress distribution in laminated beam (with one non-oriented layer and one oriented layer) with crack is shown in Fig. 12b-e.

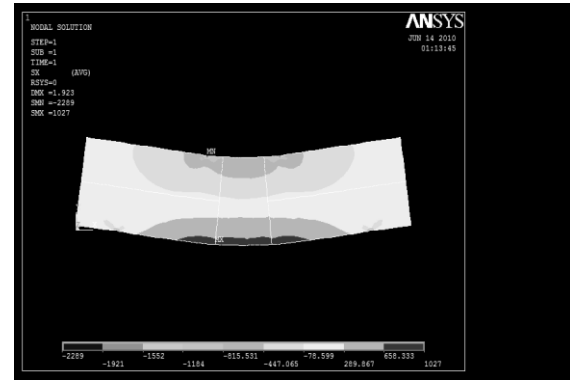


Figure 12. (b) Normal stress σ_{xx} distribution in the layered (fibers are oriented) sample under bending

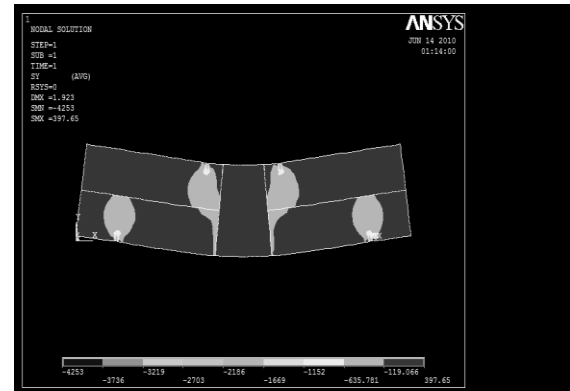


Figure 12. (c) Normal stress σ_{yy} distribution in the layered (fibers are oriented) sample under bending

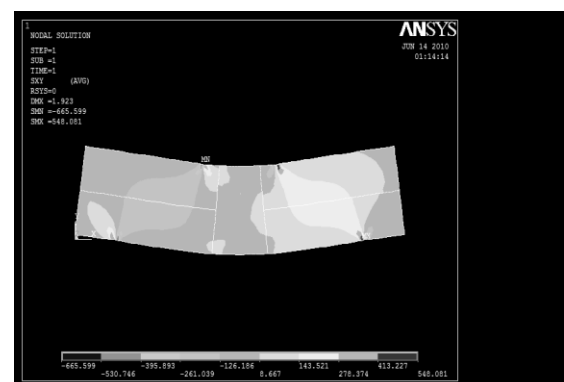


Figure 12. (d). Tangential stress τ_{xy} distribution in the layered (fibers are oriented) sample under bending

CONCLUSIONS

The non-destructive methods:

- a) Ultrasound wave velocity method;
- b) X-rays analysis;

were experimentally used in investigation of the possibility to obtain anisotropy in fiberconcrete. Fiberconcrete samples were elaborated and investigated:

- 1) Samples with chaotic fiber distribution in the sample volume.
- 2) Laminated samples (non-oriented) - fibers were located in two layers, the first non-oriented, and the second layer was non-oriented.
- 3) Samples with oriented fibers - fibers were processed by orientation procedure.
- 4) Laminated samples (oriented) - fibers were located in two layers, the first non-oriented, the second layer - oriented.

Because fiber concretes, that were under investigation, contained relatively small amounts of fibers (up to 3.5 % of volume) the ultrasound method showed low sensitivity (high dispersion of results) to the fiber content change and their orientation. It was found that by the X-ray method it is possible to give most thorough information about the internal structure of the sample. In order to explain the results of the measurements fiberconcrete beams (chaotic oriented, oriented, layered, layered-oriented) FEM model was created. The simulation data showed the most loaded areas

in the prisms during loading and cracking of the fiberconcrete beams.

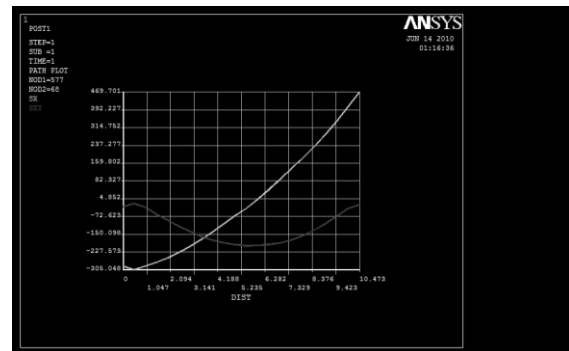


Figure 12. (e). Normal and tangential stress distribution (fibers are oriented) throw the thickness of the beam (in the middle between the left and the top support of applied load)

References

- Gettu R., Gardner D.R., Saldivar H. and Barragan B. „Study of the distribution and orientation of fibers in SFRC specimens”, Materials and Structures, 38, 2005, P.31-37.
- Krasnikovs A. & Kononova O., „Strength Prediction for Concrete Reinforced by Different Length and Shape Short Steel Fibers”, Sc. Proceedings of Riga Technical University. Transport and Engineering, 6, vol.31, 2009, pp.89-93.
- Krenchel H., Jensen H. W. Organic Reinforcement Fibers for Cement and Concrete. – 1982. - Serie R, No 151. – Denmark: Department of structural Engineering, Technical University of Denmark;
- Lapsa V., Krasnikovs A., Strauts K., (2010) „Fiberconcrete non- homogeneous structure element building technology, process and equipment”, Latvian patent Nr. P-10-151, November 10.
- Laranjeira F., Grunewald S., Walraven J., Blom C., Molins C. and Aguado A. (2010) „Characterization of the orientation profile of steel fiber reinforced concrete” Materials and Structures, Published online 06 November 2010. RILEM. www.rilem.net.
- Release 10.0 Documentation for ANSYS “ANSYS Inc. Theory Reference”.

CASE STUDY OF ENERGY EFFICIENCY IN AIR HANDLING UNITS WITH HEAT EXCHANGERS FOR RESIDENTIAL APPLICATION IN LATVIA

Gatis Plavenieks*, Arturs Lesinskis**

Riga Technical University, Institute of Heat, Gas and Water technology

E-mail: *gatis.plavenieks@rtu.lv, **arturs.lesinskis@rtu.lv

ABSTRACT

This paper presents a case study of the heat recovery of air handling units with heat exchangers for residential application in Latvia. The paper will be summarizing the measurements of configuration for air handling units with air-to-air heat exchangers. The research carried out analytical studies analyzing an optimum variant of the energy savings with regard to different type of the air-to-air heat exchangers and their technical performances. The results show that basic methods of air handling unit's optimization should be encouraged due to the potential of energy savings in Latvia's residential area. Reduction of consumption of energy, improvement of energy efficiency and optimization of air handling units for the residential area are important issues to address the improvement of indoor air quality.

Key words: heat exchanger, energy efficiency.

INTRODUCTION

The European Union's (EU) as well as Latvia's energy consumption is increasing each year, thus increasing the dependency on external oil and gas suppliers. EU buildings consume 40% of the total energy consumption in Europe. It has been predicted that by the year 2020 energy consumption of air-handling systems will increase two times, and it should be limited to a higher standard for air handling units (AHU). In private houses mechanical ventilation with heat recovery has become common. Natural ventilation is not suitable for use in cold climates due to the cold supply of air that creates drafts and heat losses of ventilation. According to researchers in Scandinavian countries, mechanical ventilation with heat recovery is compared to natural ventilation and extract fans. It is found to be the most effective system for maintaining a low humidity level. But the biggest challenge is to find solutions to avoid ice forming in the heat exchangers reduce electricity consumption for the fans and deal with pressure drop reduction in ventilation systems (J. Lavergé, A. Janssens, 2012; Kragh J., Rose J., Svendsen S. 2013; Borodiņecs, A., Kreslīņš, A., Dzelzitis, E., Krumiņš, A. 2007). This paper presents a case study of available types of air-to-air heat recovery in air handling units for residential houses in Latvia. In the article test data from measurements of pressure, air flow tests for three different types of heat exchangers and measurements of power consumption have been presented. Comparison was made of heat exchangers to search for an optimum variant of the energy savings and optimization. Reduction of energy consumption, improvement of energy efficiency and optimization of air handling units in

residential area is important to address the improvement of indoor air quality.

MATERIALS AND METHODS

According to statistics, new standard private houses in Latvia have an average area of 200 square meters - 2 floors, a living room and a kitchen and toilet on the first floor, on the second floor - 3 bedrooms, one toilet and bathroom, usually combined. The air handling units with 400 cubic meters of air per hour and heat exchanger of air-to-air type were usually selected. Using equipment sales data collected from 2000, it can be concluded that since 2000 originally only air handling units equipped with plate heat exchangers were used, that can be explained by a limited offer from manufacturers and building technologies. Since 2005, setting up air handling units with rotary heat regenerator has become popular in Latvia. But in recent years, statistics showed a significant increase in the units with rotary heat regenerator- 75%, in 24% of cases with a counter flow heat exchangers that are associated with the European Union's goals to reduce energy by 20% by 2020, and support programmes, and only in some cases the equipment with plate heat exchangers will be used.

According to one of Latvian internet surveys-during the winter time most of the population, 70% of people spend less than one hour a day in the open air. It shows the importance of indoor air quality of houses.

The measurements were performed in Systemair AB Research& development laboratory. The test setup was in accordance with BS 848, AMCA standard 210-99 and DIN 24 163.

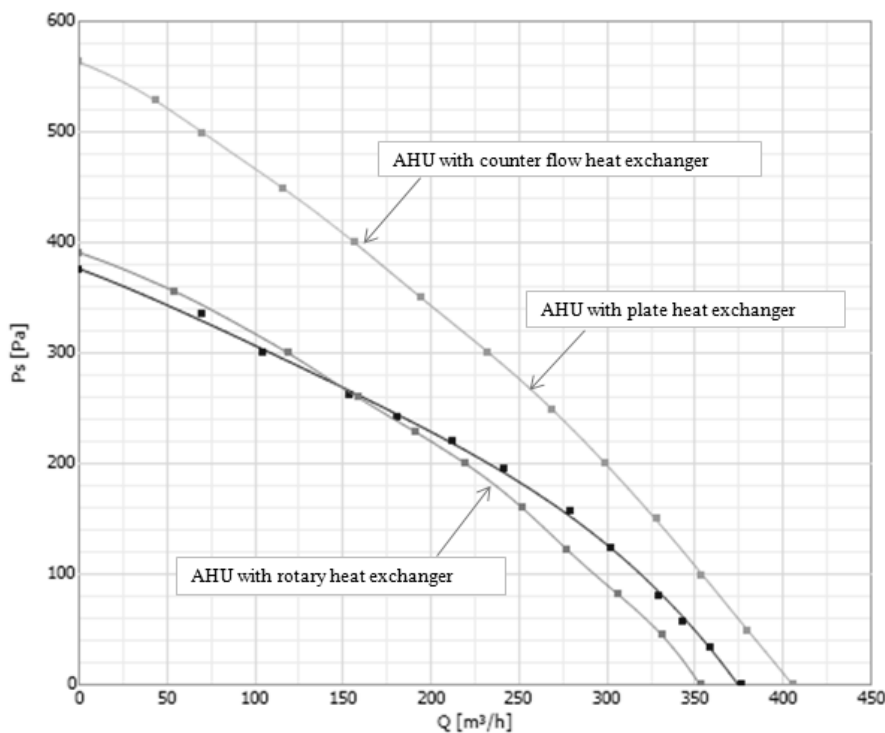


Figure 1. Supply side air flow and pressure diagram for air handling units with different type air-to-air heat exchangers, where Y – pressure, P_s (Pa); X – air flow, Q (m^3/h)

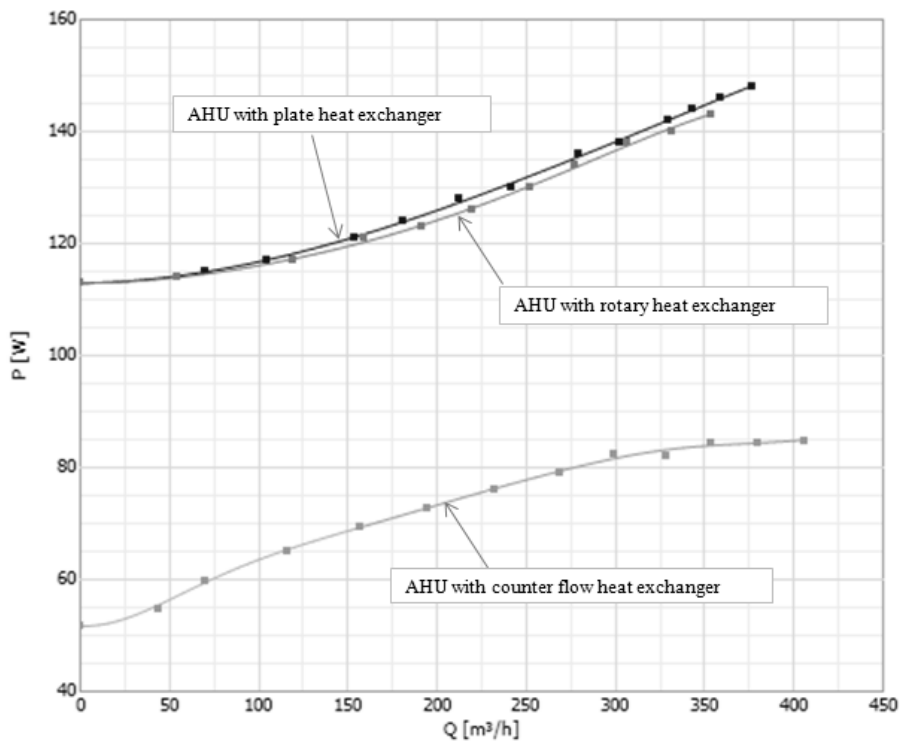


Figure 2. Power consumption and air flow of supply side air flow for air handling units with different type air-to-air heat exchangers, where Y – pressure, P (W); X – air flow, Q (m^3/h)

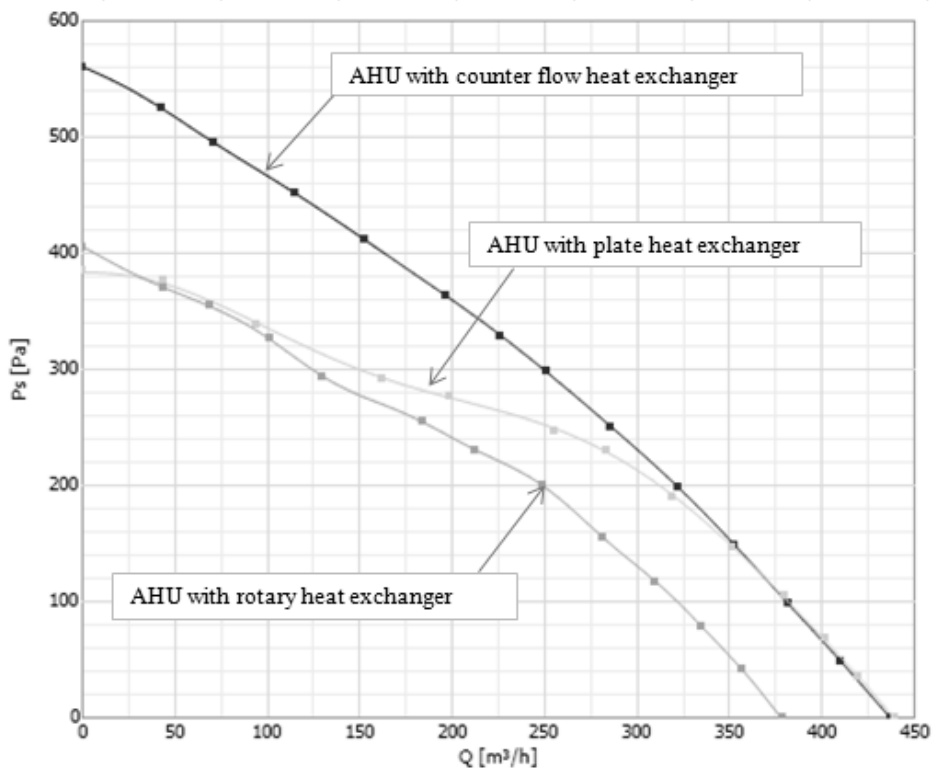


Figure 3. Exhaust side air flow and pressure diagram for air handling units with different type air-to-air heat exchangers, where Y – pressure, P_s (Pa); X – air flow, Q (m^3/h)

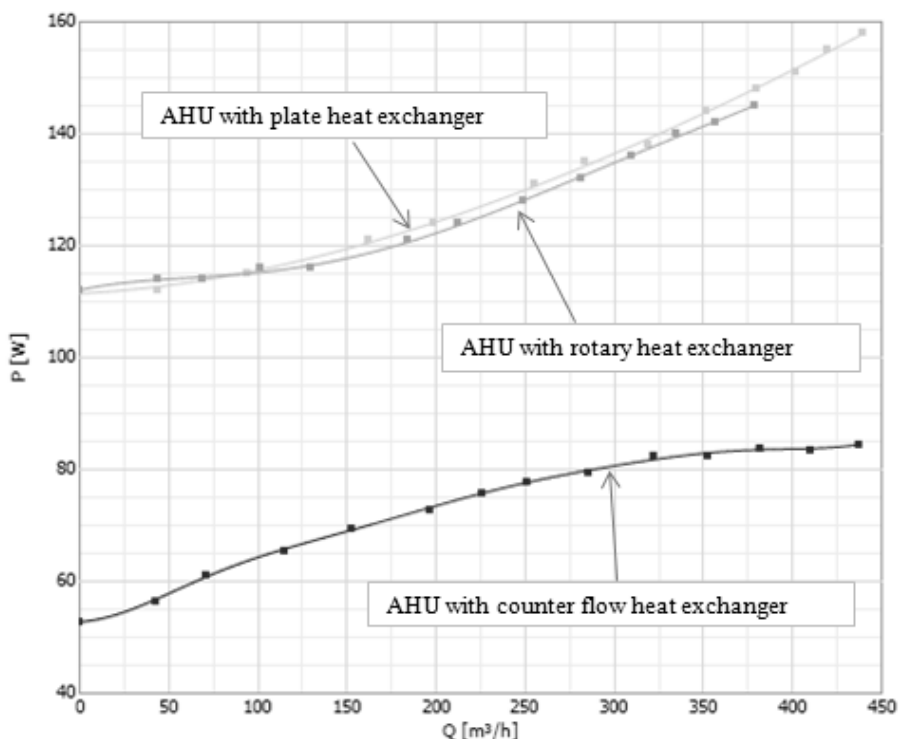


Figure 4. Power consumption P (W) and air flow Q (m^3/h) of exhaust side air flow for air handling units with different type air-to-air heat exchangers, where Y – pressure, P (W); X – air flow, Q (m^3/h)

Air handling units with different type heat exchangers were measured, separately for supply and exhaust units as well as power consumption at the air flows.

In the current research the calculations of heat transfer were made for three air-to-air types of heat exchangers - plate and counter flow heat exchangers and rotary regenerator as well. Calculations were made for Riga area 5 coldest days air temperature - 20°C. Heat transfers were calculated base on distance between plates for all three type heat exchangers. The calculations were made in accordance with the European norm EN308 and its sub documents. The selection programs of Heatex AB and Klingenborg Gbmh were used.

Table 1
Heat transfer of heat exchangers

Heat transferred, kW	Nominal plate distance, mm	Type of exchanger
4.3	3.3	Plate heat exchanger
3.8	4.2	
3.2	5.0	
2.7	6.5	
5.2	1.5	Rotary heat regenerator
5.2	1.7	
5.0	2.0	
4.7	2.0	Counter flow heat exchanger

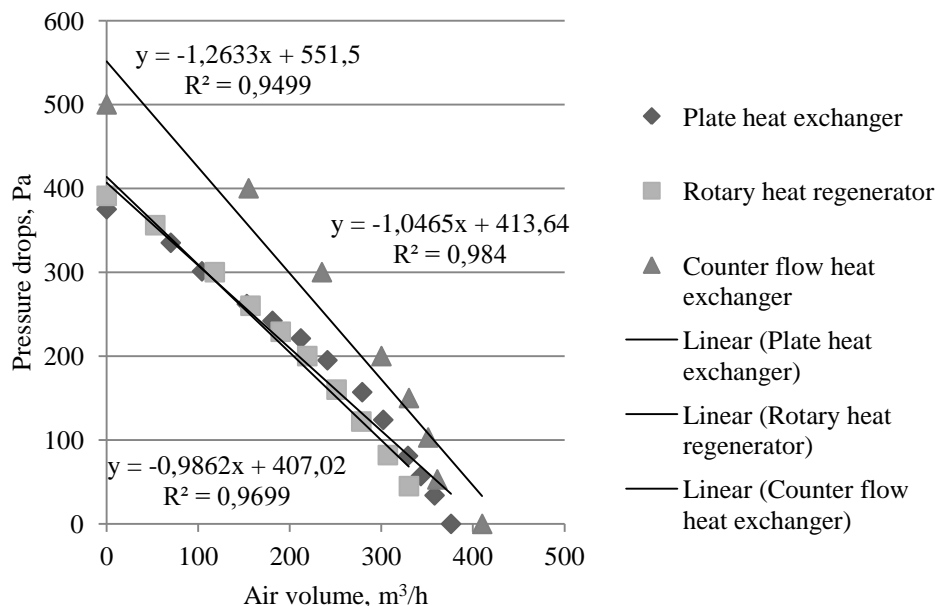


Figure 5. Air flow rate for three different types of heat exchangers

Summarizing the literature sources, calculations and technical options, we can create the optimal air processing for air handling unit configuration, which would be suitable for use under the climatic conditions of Latvia:

1. Air handling units have to be on supply and exhaust fans equipped with electronically communicated motors. It is connected with low energy consumption of this type and it is important if the scenario of electricity price increasing will take force in the future.

RESULTS AND DISCUSSION

Within this research analytical studies on three types of air-to-air heat exchangers were carried out. The main focus was to compare air flows at the pressure drops of heat exchangers equipped air

2. Rotary regenerator and counter flow heat exchanger provide higher efficiency from heat recovery viewpoint compared to plate heat exchanger.

3. Lower class filters which allow outdoor air pollution. Latvia is environmentally green country with low outdoor air pollution. Usually residential areas are located away from high pollution sources. Low level of outdoor air pollution allowed reduced SFP value for air handling units due to low pressure drops in supply filters.

handling units. Analyses of diagrams showed significant power reduction due to using new type of fans with EC motors comparing to asynchrony motors used in residential area. Air handling units with counter flow heat exchangers have a good air flow performance. The best air flow performance

was provided by air handling unit with counter flow heat exchanger as can be seen in Figures 1 to 4. Table 1 shows the data calculated heat transfer in kW for three different types of air-to-air heat exchangers depending of plate distance.

CONCLUSIONS

According to data from table1, we can see that heat recovery of plate heat exchanger is from 57% to 91% comparing to counter flow heat exchanger. Heat recovery of plate heat exchanger is from 53% to 84% comparing to rotary regenerator. Heat recovery of counter heat exchanger is practically the same comparing to rotary regenerator. All

calculations were made for Riga area 5 coldest days by air temperature -20°C at the air flow 400 m³/h. As a result of the test and analysis on the most effective combination of air handling units suitable for Latvia's climate, it can be concluded that the unit with heat recovery rotary regenerator and counter flow heat exchanger combination with fans having electronically communicated motors, proved to be the best.

ACKNOWLEDGEMENT

With great appreciation to the technical staff of Research and development centre of Systemair AB (Sweden) which supported the research.

REFERENCES

- AMCA standard 210-99. Laboratory methods of testing fans for certified aerodynamic performance rating / The American National Standards Institute. -2007. – 77 p.
- ASHRAE Standard. Method of Testing Air-to-Air Heat Exchangers/ The American National Standards Institute. -1992. – 10 p.
- Astrom J. (2008) Investigation of Issues related to electrical efficiency improvements of pump and fan drives in buildings, Chalmers university of technology, Goteborg, Sweden.
- Borodiņecs, A., Kresliņš, A., Dzelzitis, E., Krumiņš, A. (2007). Introduction of hybrid ventilation systems of dwelling buildings in Latvia. Paper presented at the IAQVEC 2007 Proceedings - 6th International Conference on Indoor Air Quality, Ventilation and Energy Conservation in Buildings: Sustainable Built Environment, , 1 361-368.
- Jaboyedoff P., Roulet C.-A., Dorer V., Weber A., Pfeiffer A., (2004) Energy in air-handling units—results of the AIRLESS European Project, Energy and Buildings, Volume 36, Issue 4, p. 391-399, ISSN 0378-7788.
- Kragh J., Rose J., Svendsen S. Mechanical ventilation with heat recovery in cold climates. http://web.bvv.kth.se/bphys/reykjavik/pdf/art_157.pdf accessed 02.01.2013.
- Krēsliņš A. (1969) Gaisa kondicionēšana:- Rīga: Liesma, – 96.lpp.
- Krēsliņš A. (1975) Gaisa kondicionēšana rūpnieciskajās un sabiedriskajās ēkās Rīga: Liesma, 256.lpp.
- Креслинь А.Я. (1972) Автоматическое регулирование систем кондиционирования воздуха Москва : Стройиздат, 96.р.
- Laverge, J., Janssens, A. (2012) Heat recovery ventilation operation traded off against natural and simple exhaust ventilation in Europe by primary energy factor, carbon dioxide emission, household consumer price and energy. Energy and Buildings.
- Nyman M., Carey J. Simonson A. (2005) Life cycle assessment of residential ventilation units in a cold climate, Building and Environment, Volume 40, Issue 1, p. 15-27, ISSN 0360-1323.
- Рымкевич А.А. (1990) Системный анализ оптимизации общеобменной вентиляции. М.: Стройиздат, 409с.
- Sterling V.A.(2009). A handbook of sustainable building design and engineering: an integrated approach to energy, health and operational performance. London: Earthscan 435 p.
- Yilmaz T. (2002) Influence of rotational speed on effectiveness of rotary type heat exchanger. Heat and mass transfer No 38.
- Хаузен Х. (1981) Теплопередача при противотоке, прямотоке и перекрестном токе. М.: Энергоиздат, 365с.

ENVIRONMENTAL PERFORMANCE REGULATIONS IN THE NETHERLANDS

Dr. Nico P.M. Scholten, PhD

ERB Foundation Expertcentre Regulations in Building

E-mail: N.Scholten@bouwregelwerk.org

Harry A.L. van Ewijk, MSc

IVAM UvA BV Amsterdam, research and consultancy on sustainability

ABSTRACT

The Dutch Building Decree, as in force since April 2012, stipulated that by January 1st, 2013 a calculation of material environmental performance for a dwelling or office building should be delivered at submission of the environmental (building) permit.

The aim of this requirement is to encourage more conscientious decisions by a regulated uniform determination method. Environmental and life cycle properties of the materials chosen and design variants should so be enabled to be subject to consciousness. Furthermore, the development of sustainable initiatives and innovation should be stimulated.

During the preparation of the Building Decree 2012 the so called "Determination Method Environmental Performance of Buildings and Infrastructural Works in Combination with the National Environmental Database" and the "Green Deal Environmental Performance Calculation" became available for application. Precurring the publication of limit values for sustainability in the Building Decree, exercises are executed based on these methods and promoted by the Ministry and market parties.

The paper will elaborate on this development, the methods used and the results obtained.

Keywords: sustainability, regulations, environment, performance

INTRODUCTION

Sustainability of buildings is an important subject of policy for the government and the supply industry. The environmental issue (sustainability) is from October 1st, 1998, based on the clause 2 of the Housing Act, the foundation for regulation by the Dutch Building Decree. In the period 2001-2003 various R&D organizations namely TNO, W/E, Intron, IVAM environmental Research University of Amsterdam and CML, University of Leiden run an extensive R&D project (Scholten et al., 2004) to develop a determination method for the environmental performance of buildings to use in the building regulations. Standardization of the determination method and code of practice was at the end of this period almost finished by the Dutch Standardization Body. In the end the determination method was blocked by building industry because of the expected complexity of the regulations and the influence on the freedom of the choice of materials.

Earlier the production industry started a project to introduce material based environmental relevant product information (MRPI), a so-called environmental material product declarations (EPD) according to ISO 14025 (ISO 14025:2006, 2006). Later, the standardization body transformed the 'MRPI manual' to the Dutch standard NEN 8006:2004, the determination method for the MRPI of building products, amended in 2007 (NEN 8006:2004, 2004). This NEN 8006 is at the moment the base for the determination method in use in the building regulations (Method of calculation, 2011) (See www.milieudatabase.nl).

Meanwhile, also in Europe on voluntary base there was the standardization process. The Dutch NEN 8006 was brought to the table in that process. EN 15804:2012 'Sustainability of construction works - Environmental product declarations - Core rules for the product category of construction products' was published. This caused NEN 8006 to be withdrawn on July 1st, 2012, but it is still the base of the determination used in the Building Decree 2012. To determine the environmental performance of a building EN 15978:2011 'Sustainability of construction works - Assessment of environmental performance of buildings - Calculation Methods' was published. No A-deviations are questioned by the Dutch Standardization Body.

DUTCH BUILDING DECREE 2012

On January 1st, 2013, a calculation report of environmental performance shall be handed over as a part of the environmental (building) permit procedure. This is regulated in the paragraph 5.2 of the 2012 Building Decree (Building Decree, 2012). This paragraph applies to new buildings (residential and offices with a floor area larger than 100 m²). The environmental building performance shall be calculated following the determination method "Environmental performance Building and Infrastructure works" (Method of calculation, 2011). The determination method is in good consultation with the delivery industry and building industry developed, but remarkably it is not a standardized determination method by the Dutch Standardization Body.

Emission and resources related indicators have to be demonstrated. There are no performance levels or classes yet to be met. For the calculation some calculation tools are available now.

Every calculation shall meet certain requirements. For demonstrating that the used calculation tool meets these requirements the tool owner can request the Foundation for Building Quality (SBK) proof of acceptance. For this procedure SBK has developed a special website: National Environmental Database (NMD).

TOOLS

Both the Dutch assessment tool developer "GPR Bouwbesluit", 'GreenCalc' and the Dutch EPD (Environmental Product Declaration) software operator MRPI developed already tools for the required building calculations. Free downloads of the tools are available. Both tools use environmental product data taken from the National Environmental Database. Other tools will follow.

DETERMINATION METHOD ENVIRONMENTAL PERFORMANCE OF BUILDINGS AND INFRASTRUCTURE WORKS

This method can be used by construction professionals together with the pertaining database. This method and database allow assessing the environmental impact of the used materials at construction and maintenance of a dwelling or office building based on the design documentation of those works. The results of these calculations are expressed in one or more figures. So designers can see which building components cause the most important (negative) environmental effects. Subsequently optimization of the design becomes possible. Thus, professionals can choose for sustainable solutions based on sound information, as to realize a building with less negative environmental effects and thus a better performance.

The determination method is used by private measuring-and calculation instruments to evaluate the environmental impact of buildings and infrastructure. The method is developed using the Life Cycle Analysis approach. This LCA is available for the calculation of environmental effects of construction materials, products, systems and complete building works. LCA takes the complete product life cycle into account, resource extraction, manufacturing, transport, use and demolition of works.

The determination method was developed to calculate the environmental performance of buildings and infrastructure transparent and verifiable over their full lifecycle. The basis for the method is NEN 8006:2004, including the May 2007 amendment. Because these methods were developed on the product level, it was necessary to develop

supplementing rules for determination on the building/works level.

These are additional rules to NEN 8006, published by SBK in their determination method, so that it can be applied on the project level. To understand the method to the full extent, knowledge about NEN 8006 and the LCA methodology is required. If and when the calculation of the environmental performance of buildings and infrastructure steps outside the border of the NEN 8006 standard, it is explicitly shown in the SBK determination method.

There are arguments to supplement the standard:

- NEN 8006 concerns construction materials, building products and building elements, while the method needs to determine the environmental performance on building or works level;
- NEN 8006 bases itself on manufacturers data provided to establish an Environmental Product Declaration (EPD). While inescapable generic, producer independent data are required to determine the environmental performance on the building or works level when specific product data are not available.

A more fundamental aim of the determination method is to harmonize and unify calculations of, for instance, the existing software like the Dutch GPR Building, GreenCalc, DuboCalc and Eco-Instal such that the calculation regardless of the used tool delivers the same environmental effect scores and environmental ratios.

Only for this purpose at SBK (Foundation Building Quality) deposited data may be used as registered in the National Environmental Database. This consists of:

1. Product cards;
2. Background processes that result in 'basic environmental profiles'.

The database is partly public accessible and partly only after signing a license agreement with SBK.

In the determination method the ten 'baseline' impact categories' of the CML2 impact categories are used. Because CML2 does not discern within abiotic depletion (in fossil energy carriers and other), and the determination method does, this results in eleven effect categories instead of ten.

DATABASE (NMD)

The national database consists of product cards, basic profiles, and the base- or background processes, in a LCA database in SimaPro format.

The product-cards contain information on functional unit, product composition, life span, auxiliary materials, maintenance frequency and general product information. (i.e., no environmental data) on building components.

The product 'External glazing' is divided in the card in various components: profile, glazing putty, double glazing and distancer. The unit is m². Per m² components are represented in kg. Additional information, like service life, is given. So, there are no

environmental data in the card-base. Basic profiles are the environmental impacts (environmental profiles) following the calculation of the basic processes in SimaPro. These are modular in principle so per unit of material for instance kg cradle-to-gate and per unit of energy for instance kWh electricity etc. To be used for implementation in LCA's, applied in calculation of buildings.

The base- or background processes, in a LCA – database in SimaPro format, are used to calculate the environmental impacts (environmental profiles) of base processes like manufacturing and demolition. The maintenance thereof in the database ensures the base profile database to be in line with the SimaPro database.

The various private calculation software use the product cards and the base profiles – together the product profile card. The information of a material or process on the product-cards is so coupled in the calculation software with the information thereof in the base profiles. More specific: the calculation of top processes in the basic process database gives these base profiles. For instance, a certain type of cement in concrete is coupled with a specific quantity per unit of concrete with the base profile of cement.

The base profile database is mainly filled according to the analyses that have been performed with SimaPro (calculation software) and the Swiss database Ecoinvent2.2, corrected for the Dutch situation where necessary and possible. To generate figures choices have been made. The choice consisted of the decision which available processes would be used. If no process is available, it has to be developed; in some cases the existing processes have been adapted to be in line with the Dutch circumstances.

Furthermore, a characterization method is required to be able to generate data. With this method the environmental impacts are determined like abiotic depletion, global warming, etc. At this moment one works with CML2 baseline 2000.

The SBK web application contains the data in MySQL converted to SQLite. The format of the SQLite file is described in the Calculation rules project.

The National Environmental Database contains the following data categories:

Category 1: brand data, third party verified; for manufacturers and suppliers. Comparable with a declaration bases on EN 15804.

Category 2: generic (brand less) data, third party verified and notice of representativity (i.e., for the Dutch market or a specific group of products); for product groups, groups of manufacturers, groups of suppliers.

Category 3: brand less generic data, not third party verified, validated in general by the SBK Technical Committee; for product groups, groups of manufacturers, groups of suppliers, clients.

In the product-cards it is differentiated into the lifespan of a product in its application and the lifespan

of the material applied. For instance, a building has a lifespan of 50 years, double glazing 25 years, which means that the environmental effect of double glazing counts twice in the calculation software.

Within the determination method one has chosen for a fixed lifespan of a building to make mutual comparison on environmental performance feasible. All calculation software uses this fixed lifespan. As soon as regulations will stipulate the limit values this is not acceptable and a determination method that allows the determination of the adaptive property of a building must be made available. At the end of the functional lifespan the building represents a rest value in terms of usability of the Casco.

Flexible construction in the form of replaceable/removable/reusable interior separation walls is not yet valued in the NMD.

The following environmental effect categories are recognized:

1. Abiotic depletion, non fuel;
2. Abiotic depletion, fuel;
3. Global warming;
4. Ozone layer depletion;
5. Photochemical oxidation;
6. Acidification;
7. Eutrophication;
8. Human toxicity;
9. Ecotoxicity, fresh water;
10. Ecotoxicity, marine water;
11. Ecotoxicity, terrestic.

The following environmental ratios are recognized:

1. Energy, primary, renewable;
2. Energy, primary, non-renewable;
3. Energy, primary;
4. Water, fresh water use;
5. Waste, hazardous;
6. Waste, non hazardous.

The determination method pays in depth attention to the transport-distance. In the base profile with the environmental effect categories the LCA must be founded on raw material extraction to the factory gate plus the transport distance from the factory exit abroad to the city of Utrecht. Concerning the transport distance in Holland one calculates them from Utrecht to the construction site, if no specific data are available. This distance is recorded in the product-card.

What is the difference between the product data category 1 & 2 and category 3?

Let us, for instance, overlook a flexible interior separation wall.

A category 1 or 2 LCA interior wall is executed over the life cycle of the complete interior wall. This analysis produces a product-card with base profiles with environmental information pertaining to this wall. These base profiles refer to the product interior wall (composed of, for instance, gypsum board, insulation and steel profiles) including the in company processes of the supplier of the interior wall, its transport profile and its waste scenario. The file

describing the end result is the third party validated according to a fixed protocol (registered under menu item base documents in the website) and that results in the status of category 1 (brand determined) or category 2 (brand less).

An interior wall category 3 (brand less, not validated) will be composed from different base profiles (gypsum board, insulation, and steel profile) also standard transport profiles and waste scenarios will be used from the database.

Important difference between category 3 and the other two categories data is that in case of a movable wall in category 3 the manufacturing process to produce the wall (energy, factory waste etc.) and to pose the wall is not included in the calculation. Therefore, it is desirable to use as much as possible validated data and that is the aim in the future.

Category 3 data will be replaced by category 1 and 2 data. To stimulate this process the environmental effects of category 3 are ameliorated by 30% on January 1st, 2013.

DATABASE ACCESSABILITY

It was decided for the time being not to make the National Environmental Database accessible via the internet. Only data suppliers and parties that contract a license like developers of calculation software have access. It is not reluctance of SBK but outside the expert-circuit and without calculation software the database has no information value. This is not in accordance with the legal provisions. Laws and elements thereof may not consist of non-accessible parts and have to be fully accessible and understandable for professional users.

Accessibility is arranged as follows:

- a. Manufacturers and associations thereof; they can read the data uploaded by them;
- b. Software/tool developers; tool developers like GPR Building, GreenCalc+ and Dubo Calc, SBK have license agreements; they can use the National Database; also new developers can buy a license;
- c. LCA agencies; third parties can obtain a part-licenses that is limited to the database of base profiles including the complete database in SimaPro format.

To be included in the NMD an Environmental Product Declaration (EPD) is required according to the Determination Method/SBK validation protocol. A MRPI certificate is not per se required, since the SBK validation protocol is in practice identical to the MRPI validation protocol.

MANAGEMENT AND ADMINISTRATION OF THE METHODS AND DATABASES

The Foundation Building Quality (SBK) manages the Determination Method, the National Environmental Database and the pertaining documents and protocols. SBK is the only organization that may expand the

database. This is at the least a strange situation, especially because the method is not fully transparent and verifiable for everyone. This is in conflict with the national Rules for Regulations and Regulatory bodies (Instructions for regulations, 2011).

RELATION TO EUROPEAN DETERMINATION METHODS

NEN and SBK do research to the differences and similarities between the European and Dutch National developments to be able to chart and monitor them as well as possible.

To a large extend (>95%) the European standards and the SBK method together with NEN 8006 are in line. Since the development of the European standards and the Dutch system were parallel processes in time there are differences on details. At the moment it is clear that one of the main differences between NEN 8006 respective the SBK method and EN 15804 respective EN 15978 are the environmental indicators (EN 15978:2011, 2011). In NEN 8006 10 indicators are mentioned and in NEN-EN 15804 there are 22 + 2 indicators (in EN 15978 it is 22) (EN 15804:2012, 2012; EN 15978:2011, 2011). Besides this EN 15804 does not recognize weights allotted to the indicators, the relative importance of different indicators. The last important difference consists of the modular approach with obligatory differentiation, and a voluntary 'Module D' for the loads and benefits of recycling of materials

Is it possible to include manufacturers EPD data established according to EN 15804 in the NMD? It is quite possible that such an EPD is established without using the background data from the NMD like energy generation and transport. In such a case the EPD is not comparable with the requirements of the SBK validation protocol. Aimed at mutual recognition of EPD's international talks are ongoing. No results have come out yet and the following operational action can be taken.

If and when a product of "foreign" origin is applied in a building one can use category 3 in the NMD with a correction for the transport distance. An EPD according to EN 15804 can be the basis for category 3 data (EN 15804:2012, 2012). In such a way there are no trade impediments for the use of "foreign" data on the Dutch market. Question marks can be placed to this related to trade barriers within the EU because what has happened to this category by January 1st 2013, is mentioned before.

As such the chosen modus operandi is surprising because the European standards are leading and case history shows that the European Commission calls Member States to the European Court when products under the European standards experience unfair trade obstruction under National Regulations. Differences in impact scores because of the transport distance corrections lead not to a trade barrier.

HOW ARE INNOVATIVE PRODUCTS TREATED IN CASE OF LACKING DATA?

Innovative products mostly lack base profiles and specific product data like service life. This also may be applicable for products from abroad on which not yet LCA has been performed. Companies with such products could together with their LCA –agency propose how to provide the necessary data required for inclusion in the NMD.

Proposed could be: we take base profile X with an assumption about the differences of Y % because it is not possible to generate a base profile of material Z and base profile X is nearest to material Z.

These proposals are discussed with the SBK-product data committee and/or the Technical Committee and if agreed the product will be included as category 3.

LIMIT VALUES TO BE REQUIRED

In the Building Decree 2012 – part new Construction-provisions are given to calculate the environmental performance of dwellings and office buildings.

Upon explicit request from the construction sector limit values are not yet implemented. One wants to obtain experience to see what will be the impact on the environment and the application of materials and products.

At the moment in the running Green Deal environmental performance project the Dutch Architectural Organization and the Royal Metal Union use the determination method to gain experience and stimulate the building industry in the light of realization a level playing field and innovation.

To be able to establish appropriate limit values fitting within the system of the national technical building

REFERENCES

Building Decree 2012

EN 15804:2012 (2012) Sustainability of construction works - Environmental product declarations - Core rules for the product category of construction products.

EN 15978:2011 (2011) Sustainability of construction works - Assessment of environmental performance of buildings - Calculation Methods.

Instructions for regulation, Circular of the Prime-Minister of November 18th 1992, last amendment of May 11th 2011, OJ 2011, 6602.

ISO 14025:2006 (2006) Environmental labels and declarations. Type III *Environmental declarations – Principles and procedures*

Method of calculation for the determination of the Environmental performance of buildings and infrastructure during their whole lifetime, based on the life cycle analysis method (LCA-CML2) of July 1st 2011, published by Foundation Building Quality, Rijswijk.

NEN 8006:2004 (2004) Environmental Data Of Building Materials, Building Products And Building Elements For Application In Environmental Product Declarations - Assessment According To The Life Cycle Assessment (lca) Methodology (in Dutch).

Scholten N.P.M., de Wit S., Kortman J., Huppens G., Schuurmans A., Anink D. (2004) The development of an environmental performance standard for materials in buildings for the Dutch building decree CIB-congress 2004, Toronto, Canada.

regulations (Building Decree 2012 juncto article 2, first member, a, of the Housing Act) a series of questions requires further and deeper analysis. Ongoing research by a consortium of ERB Expertcentre Regulations in Building Delft, RIGO Research Amsterdam, IVAM Environmental Research Amsterdam and CML University of Leiden has to solve these questions.

In all situations attention has to be given to the sensitivity of the results in relation to the definition of the materialization of the functional use, determining the environmental performance and as such the determination and choice of the limit values.

There are eight specific fields of attention:

1. Allocation of function;
2. Location dependency;
3. Infill, finishing;
4. Provision/regulation free building components;
5. Extent of dwelling (sub)- and other functions;
6. Quality level;
7. Multi-functionality;
8. Governance and differentiation in standardization.

CONCLUSIONS

The regulations in the 2012 Building Decree are the first step forward with no other aim than to stimulate the building industry to invest seriously in sustainable thinking.

There is still a long way to go before reaching a situation comparable to the energy conservation requirements. Both, regarding acceptability by the consumer as well as solutions in practice.

LANDSCAPE ARCHITECTURE

INTERACTION AREAS OF THE CULTURAL AND HISTORICAL TERRITORIES AND THE SOVIET PERIOD RESIDENTIAL AREAS

Una Ile*, Silvija Rubene**

Latvia University of Agriculture, Department of Architecture and Building
E-mail: *una.ile@llu.lv, **silvija.rubene@llu.lv

ABSTRACT

Based on the carefully studied historical material, a research was carried out on the interaction zone between the cultural and historical territories and the Soviet period residential territories in the urban environment. The visual structure analysis of the landscape in the urban environment was analyzed, choosing the Old Town area of the city of Jelgava, Jelgava St Anne's Evangelical Lutheran Church, and the soviet period residential territories located between these objects. In this defined area the elements of the visual structure of landscape were analyzed, including both the compositional and aesthetical aspects, and the evaluation of sights in the urban environment context. Consequently, the aim of this research is to obtain new findings from the analyses preformed in the research and the groups of respondents.

Key words: visual landscape structure, cultural and historical territories, residential areas

INTRODUCTION

Jelgava is the only Latvian city, which had been destroyed during the world wars, losing a great part of its cultural and historical housing. Jelgava used to be the pearl of Latvian urban construction of the early 20th century. But from July 27 to 31 of 1944 the beautiful city of the baroque, classicism and renaissance era masterpieces, and all of its architectonic, cultural and national values were destroyed – bombarded and burnt down. 93 % of the city territory was turned into ruins. During the Soviet occupation from the 1944–1945 the General Plan of the Jelgava city housing was developed by a group of professionals with V. Laka in the lead. It was decided that a brand new city will be constructed instead of reconstructing the old one. The new city was supposed to have wide streets and squares, new residential housing quarters which would vaguely remind of the earlier Jelgava. The old housing was supposed to be subordinate to the new constructions; also the unaffected buildings were pulled down. The area which is presently known as the Old Town is only a small part of the city outskirts with a historical wooden architecture which has surprisingly survived, see Figure 1 (Jelgava city hall project, 2011; Soldatovs, 1949; Suhecka, 1990; Riekstiņš, 1991).

Presently the city of Jelgava is not one of the most attractive places with its half-collapsed houses and neglected courtyards, but at the same time this area is the only witness of the former luxury of Mītava – some of the buildings have remained from the 18th and 19th century. The present cultural and historical

heritage comprises urban construction, architecture, art and historical monuments, thus composing the historical environment of Jelgava. In the process of city development it is crucial to maintain the cultural and historical heritage because it composes an essential and diverse spatial image. These fragments of historically spatial architectonic environment are unique elements of the whole city planning system. One of the base units of the urban structure is its residential areas; therefore, a great attention is paid to the development and housing improvement in these territories in the urban development strategic and operative planning documents. The residential area is a populated environment of an appropriate size which has its own maintenance, identity, character that follows its type of housing, physical borders and the sense of community between the landscape and the residents (Treija et al., 2003). Along with rapidly developing processes of industrialization in the period of the '60 – '80s in Riga and in other cities of Latvia, a chain of new industrially-made type residential and industrial building complexes were built, which attracted to Latvia a large number of workers from other republics of the USSR. This impressive constructing process in the post-war Soviet period disrupted the historical planning principles and the urban scale. Rapidly deteriorating, this apartment market caused social, economic and technical problems, as well as issues that concern their maintenance (Asaris et al., 1996; Briņķis et al., 2001)

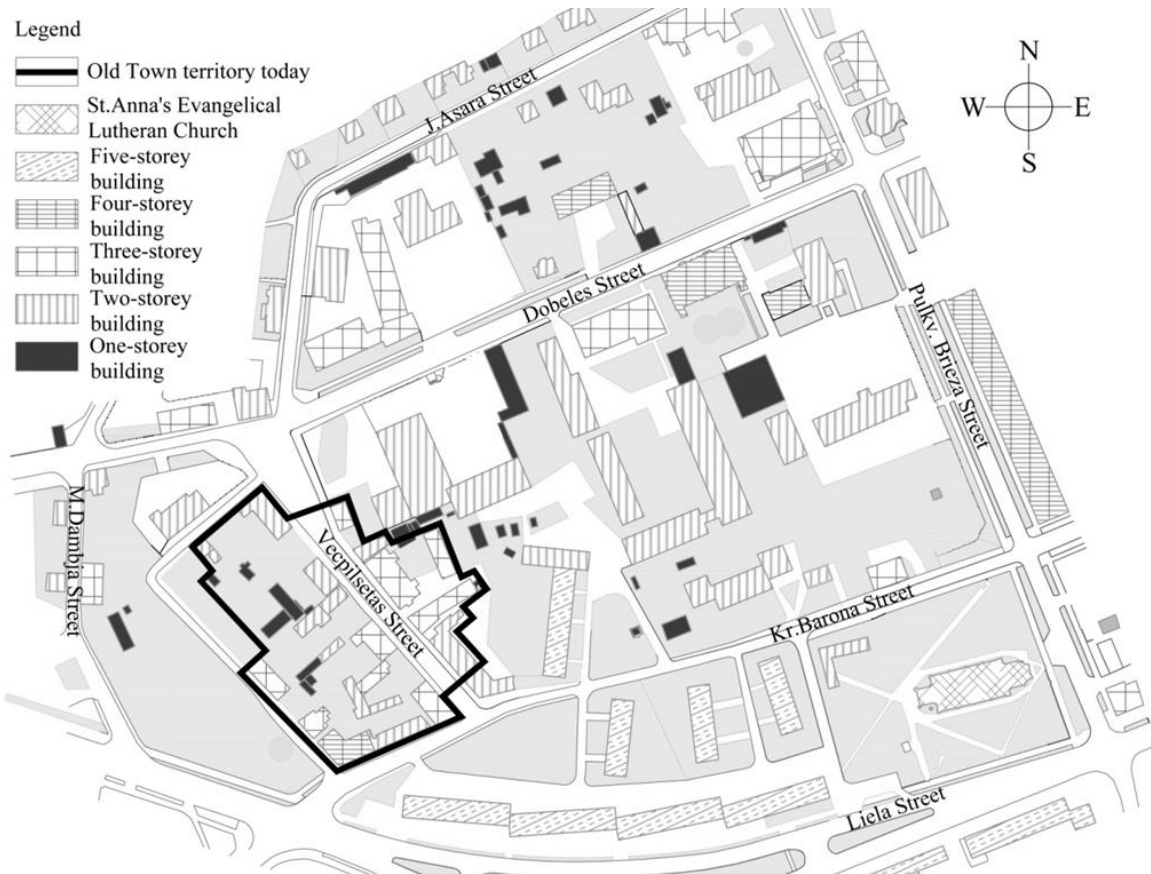


Figure 1. In the crossing of Dobeles, Vecpilsētas and Jāņa Asara Streets remains the oldest part of the Jelgava housing that has not been destroyed during the World War II
(Source: construction made by the author, 2013)

MATERIALS AND METHODS

The research of the interaction area between the cultural and historic territory and the territory built during the Soviet period in the city of Jelgava was carried out from October 2012 till December 2012. In order to reach the set goal, the following scientific research literature was studied – publications, documents and electronic resource analyses. By involving a group of students (K. Aizups, K. Cirse, D. Lapsa, A. Mengots, S. Pastare, S. Sarkanbārde, A. Katlapa, J. Gertmane, T. Patrina from the Latvian University of Agriculture, Faculty of Rural Engineering, Landscape architecture and planning specialists), a study of the present situation was carried out, and a visual structure analysis was performed. In order to qualitatively study the present situation, the group of students interviewed 52 respondents. 32 of whom lived in the analyzed territory, whereas, 20 respondents worked (pastor, civil servant, businessmen, store employees, printing workers, secretaries, teachers, shop assistant-consultant), spent their whole day in the Old Town territory of Jelgava. The group of respondents comprised 54 % male, and 46 % female respondents aged 20–70 years.

In order to raise the quality of the research, several experts were chosen and interviewed according to the specifics of the research. The group of experts consists of 12 professionals respondents: historian A. Tomašūns, engineer A. Dambergs, land surveyor M. Mengots, landscape architect of the Jelgava City Council Administration Building Authority A. Lomakins, professors-architects A. Ziemeļniece, I. Lāčauniece, V. Liepa, assistant architect L. Daga, designer J. Borgs, chief geodesist of the Jelgava City Council Administration Building Authority V. Veinbergs, Jelgava Local Government Investment Division Project Manager S. Zīverte and head of the History and Education Division I. Deksne.

In order to establish and define the results, a monographic (descriptive) method was applied, which was based on the scientific data and established facts obtained from the analyzed territory. All the developed schemes of analysis were obtained in the process of research (authors: group of students: K. Aizups, K. Cirse, D. Lapsa, A. Mengots, S. Pastare, S. Sarkanbārde), applying digital topography. The photographs used in the research were created by authors during a period from 2006 until January 2013. The historical maps

and historical photographs were taken from the archive of the Scientific Library of Jelgava and the State Inspection for Heritage Protection of Latvia.

RESULTS AND DISCUSSION

Transformation of the analysed territory over the centuries

In the second half of the 19th century the activities of economic life began to increase, which caused an economic growth that created an impulse for the housing development. New modern plants were constructed. Kramer's Grebner's, Westerman's – Dering's and Gauderer's plants could be successfully running even nowadays, because a part of these buildings are still existing. In several places of the city streets, instead of wooden houses, first multi-storey residential houses were built according to the individual projects, which established that the top storeys of these buildings would rise above the traditional panorama of the Jelgava city church



Figure 2. Residential building on Dobele Street, the '30s of the 20th century (Source: <http://www.zudusilatvija.lv/objects/object/10275/>, National Library of Latvia, Latvian Studies, from project collection "Gone Latvia")



Figure 3. Jelgava. Courtyard of the residential house with a balcony and a woodpile (Source: <http://www.zudusilatvija.lv/objects/object/10652/>, National Library of Latvia, Latvian Studies, from project collection "Gone Latvia")

towers. At the end of the century the construction spread outside the borders of the historical city

(Dābols, 2003). Another three new facade image collections were published before 1824. These examples of copper carving techniques offered a great variety, and their authors were the great architects Luigi Rusca, Vasily Stasov and William Geste; however, the new system lead to a housing creativity stagnation and the loss of individuality. The permit for every new building or rebuilding could only be obtained if the facade was adapted to one of the examples in the book (Lancmanis, 2010). Until the end of July of 1944, Jelgava could undoubtedly be characterized as a monument of the wooden architecture complexes. Only few drawn city overviews, drawings of housing fragments, illustrated publications, pictures of maps, and several photographs of old city housing, which were taken shortly before the fire demolition in Jelgava, are left today; see Figures 2 and 3. Whereas, the multi-storey residential housing of the analyzed territory, which is located along the Liela Street, was created during the Soviet period, see Figure 4. This housing is visually unattractive and heavy in comparison to the nearby Old Town buildings. They are located in between cultural and historical heritage housing territories and St Anne's Evangelic Lutheran Church. Part of these multi-storey residential houses was built very close to St Anne's Evangelical Lutheran Church and it completely transforms the characteristics of the housing. The transformations of the visual space of the landscape are reflected in Figures 5 and 6. The church history explorer Ernst Herman Bush considered the approximate construction time of St Anne's Church to be around the period of Duchess Anne's spiritual patronage around the end of the 16th century, respectively, after the death of Duke Gotthard Kettler. Although the Latvian Lutheran congregation in Jelgava was established and had existed a lot earlier, the name of the Patron saint given to the church is an obvious glorification of the Benefactress- Duchess Anne, which allows dating the approximate time of its construction. It can be assumed that until her death in 1602, St Anne's Church was almost constructed, but only from timber. It lacked the throne, which was finally built in between 1619 and 1621, but since 1638 the newly built stone church was ordained on July 26 in 1640 (Spārītis, 2011). The construction of the 5 km long Duke Jacob's canal along the St Anne's Church was begun from the 17th to 18th century, and it connected the rivers Svēte and Driksa. The canal was flowing through the centre of the city. It served as the drainage for gutter water and as a water supply for the whole city, but unfortunately was not successful. The canal ramified into three arches, thus, being the most characteristic construction of the city of Jelgava, which crossed the whole city in a straight line from the river Driksa until Dambja street (Jelgava, Duke Jacob's Canal ... ; Lancmanis, 2010), see Figures 7 and 8.

The Plan illustrates the city street network quarters surrounded by the Jelgava fortification bands, Jacob's Canal, newly built baroccal planning of the

Jelgava city (Lancmanis, 2010.) The historical view and the present condition of the Duke Jacob's Canal are illustrated in the Figures 9 and 10.



Figure 4. Multi-storey residential housing along Liela Street (Source: photo by the author, 2006)



Figure 5. St Anne's Church surrounding area in the end of the 1920 (Source: Dāboliņš, 2006)



Figure 6. View at the analysed territory from Kr. Barona Street (Source: photo from N. Reča's private archives)

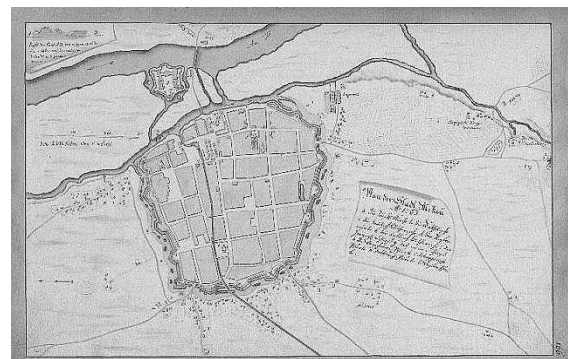


Figure 7. Plan of the Jelgava city with the Duke Jacob's Canal, 1763 (Source: LU AB: <http://www.3.acadlib.lv/broce/> 4. vol. part 2, figure 255)



Figure 8. Duke Jacob's Canal that joined the rivers Svēte and Driksa (Source: <http://www.zudusilatvija.lv/objects/object/10303/>, National Library of Latvia, Latvian Studies, from project collection "Gone Latvia")



Figure 9. Duke Jacob's Canal (Source: <http://www.zudusilatvija.lv/objects/object/13637/>, National Library of Latvia, Latvian Studies, from project collection "Gone Latvia", Original keeper: R. Zalcemanis)



Figure 10. Kr. Barona Street nowadays
(Source: photo by the authors, 2012)



Figure 11. Multi-storey residential housing and St Anne's Church in the middle of 20th century
(Source: photo from A. Tomašūn's private archives)



Figure 12. Multi-storey residential housing and St Anne's Church today
(Source: photo by the authors, 2013)

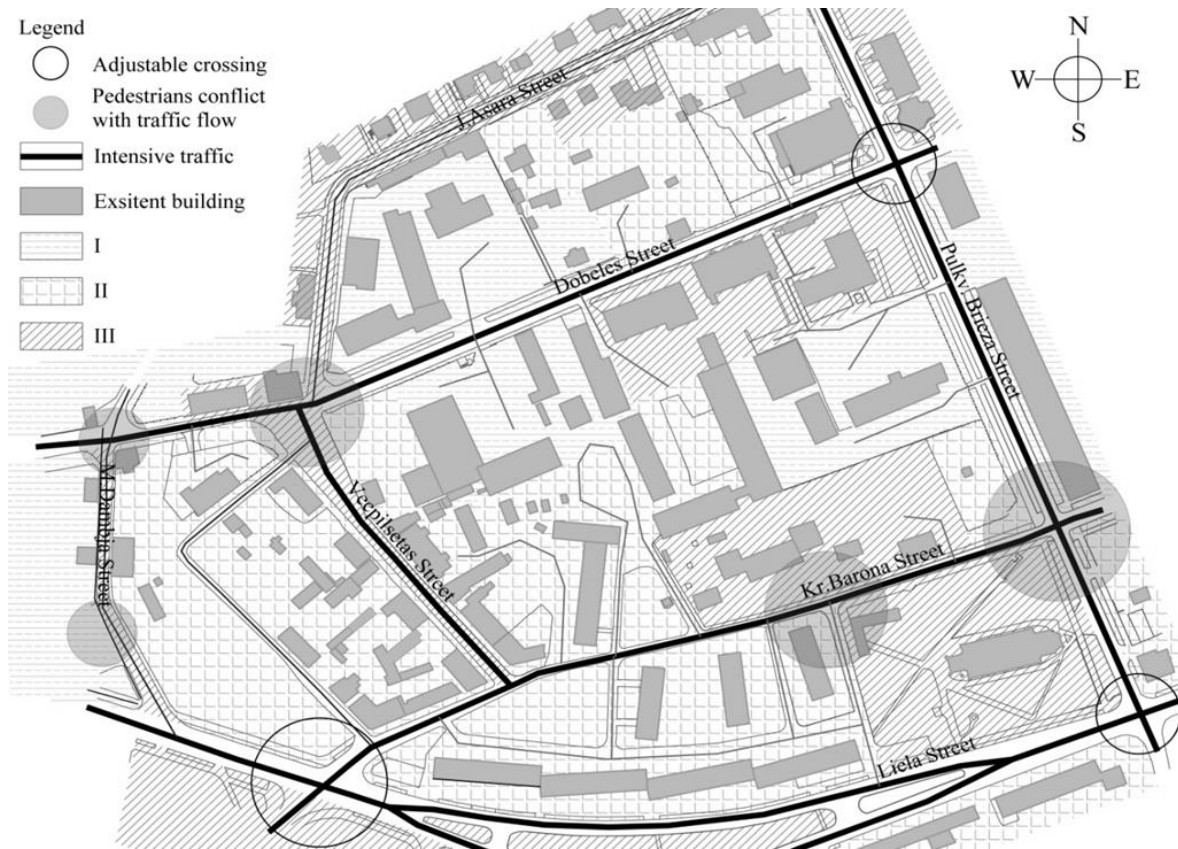


Figure 13. Transport and pedestrian traffic conflict zones. Functional territory zoning
(Source: construction photo by the students group, 2012), I – degraded urban environments landscape space, industrial or abandoned territories; II – unexploited territories without landscape; III – landscaped territories with positive landscape values

Visual structure analysis of the territory analyzed in the research

Performing the visual structure analysis in the process of research, it was established that in Jelgava only a small part of the unique historical housing been left, which should be allocated the most attention and resources in order to perform conservation of these historical buildings. The dominant structures of the territory are the two-storey building, which offer pleasant sights and comfortable atmosphere in the modern urbanised urban environment. The Soviet period five-storey residential areas overshadow the most significant dominance – St Anne's Church. Moving along the Liela Street in the direction to the point R, the five-storey buildings obstruct the view onto the Jelgava Old Town territory. The main part of this multi-storey residential housing is located along the sides of Liela street. The visually unattractive landscape is reflected in the historical information of the middle of the 20th century in Figure 11, and the present situation in the analysed territories is reflected in Figure 12. The overemphasized scale of the multi-storey residential housing is too hulking for the analysed territory because it obstructs important views.

The research established that the present functional zoning of the area is chaotic, and the examples can be observed in Figure 13. The main part of the analyzed territory is occupied by the residential, functionally unexploited, and commercial zones. Today the present cultural and historic heritage takes up around $\frac{1}{4}$ of the analyzed territory. In the process of research it was established that there are multiple conflicting cases involving pedestrian and traffic flow in the Old Town territory of the Jelgava city, which is also reflected in the survey data, see Figure 14, and 20 % of residents wish to diminish transport flow and 60 % want to construct recreational areas suitable also for people with special needs. 11 % of residents wish that in the process of development, new children playgrounds would be constructed, 26 % want new walking areas, 19 % want new restaurants, bars and 15 % expressed a desire to have new cinema in the area. Whereas, 8 % of residents want new multi-storey car parks constructed in the new the Old Town in order to easily access all the entertainment facilities in the Old Town's territory, whereas none of the

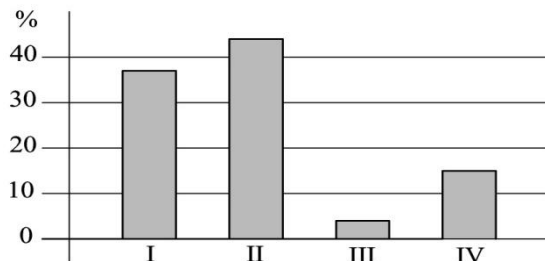


Figure 14. Survey data from 32 respondents.
I – 37 % of the respondents use private cars; II – 44 % travel on foot; III – 4 % use public transportation; IV – 15 % use other vehicles
(Source: authors construction, 2013)

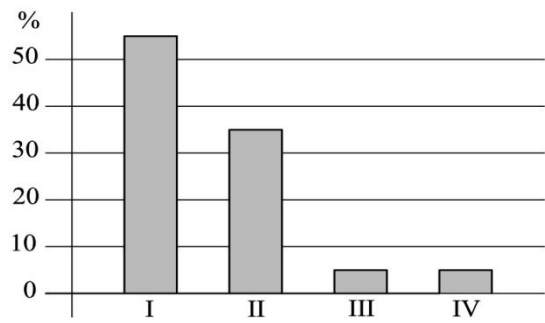


Figure 15. Survey data from 20 respondents.
I – 55 % functions should be renovated only partially; II – 35 % of the working group would prefer the total renovation; III – 5 % do not find the renovation necessary; IV – 5 % do not express any concern on this topic
(Source: authors construction, 2013)

residents who work in this area consider this construction necessary. The data collected from the survey on the respondents who work in this area differ from those of the other respondents: 10 % of respondents want new greenery, 5 % want better open views at the St Anne's Church. 5 % want more car parks, 8 % for new children playground, 10 % want new recreational areas, 9 % want water elements, 9 % – new tourism objects, 8 % – more litter bins, 11 % want qualitative pavements for pedestrian pathways and road surface, 6 % want cobbled streets and 10 % want improved lighting. The research established that no one would prefer to leave the territory in its present condition.

Opinions from the other group are shown in Figure 15. According to the findings 88 % of respondents are not satisfied with the quality of the pedestrian pathways and roads, and the other 12 % of respondents find that the quality of road surface is decent. 55 % of people want the territory to have several changes – the historical buildings should be renovated. 96 % of the respondents affirmed that they would exploit these territories after their renovation, reorganization and landscaping but 4 % would not change their opinion of these territories and would not use them even after their

reconstruction. 60 % of residents who work in this area would gladly spend their spare time in the Old Town territory, whereas 40 % would prefer other places. 27 % of respondents would prefer to transform the location of industrial areas, moving them to other parts of the city territory.

To summarize, the surveyed group of residents have distinguished the following urban environment issues in the Old Town territory of the Jelgava city: 13 % mention the car parking problems, 13 % – disorganized pedestrian flow (especially early in the morning, near public institutions such as kindergartens, see Figure 16), 25 % consider the analysed territory to be neglected and unattractive, 19 % emphasize that there are no resting areas and 13 % find the lighting in the territory to be very poor. The research established that 15 % of residents find this territory to be unsafe and 60 % of the respondents who work in the area find it unsafe to be in this territory in the night hours. The amount of data proves that 90 % of respondents who work in this area feel safe in this area during the daytime. 57 % would rely on the proper work of municipality and professionals. In addition, 43 % of the residents wish that the territories were qualitatively developed and reorganized. 88 % of inhabitants would prefer the Old Town territory to be transformed into a pedestrian area, which would attract more tourists in the future and would provide more recreational possibilities for every visitor and resident. The research established that also the experts unanimously consider that it is necessary to move all the industrial areas outside the city borders or at least outside the Old Town territory, and to transform Vecpilsetas street with the square near Dobeles street into walking area, prohibiting the traffic along the narrow streets, except the servicing transport. To achieve the set goal, an accounting of the most valuable, aesthetically qualitative elements in the analyzed territory was carried out, and the opening views of the vertical dominances were analyzed, which is reflected in Figure 17.



Figure 16. On the right side of kindergarten
(Source: photo by the authors, 2013)



Figure 17. Analysis of vertical dominances in the analysed territory (Source: construction photo by the students group, 2012), I – negative views of the vertical dominances; II – positive views of the vertical dominances; III – view of the chimney; IV – view of St Anne's Church from the Dobeles street; V – view of St Anne's Church in the direction to point A; VI – view of the St. Anne's Church in the direction from point R to point A

The results obtained in the research are also confirmed by the group of experts and their opinions as regards the present condition of the territories. 33 % of experts find that the main problem lies in the poor condition of the historical objects. They explain it with the location of this territory as opposed to other cultural and historical objects of the city. They consider it necessary that these objects are united into a one „historical path”, and 45 % of them suggest improving the facades of the five-storey residential buildings along the Liela Street. Whereas, 22 % of experts shared their opinion that it is necessary to transform this housing with different construction solutions that agree with the style of the analysed territories.

The process of research analysis established wide, unattractive sights of the multi-storey residential housing and their courtyards. The conflicting aspect

was established in the direction heading from the point R to St Anne's Church, where the view is fully obstructed by soviet period housing. The research established that 32 % of respondents, who work in this area, consider the most valuable landscape element to be St Anne's Church, 12 % – the massive tree that grows in the territory – Canadian aspen, 23 % – the Old Town territory itself, 20 % – the paved streets, 5 % – house chimneys, and 8 % of respondents have no opinion as regards this issue. Whereas, 50 % of experts consider St Anne's Church tower to have the main vertical dominance. Experts suggested that in the future perspective, the main point of attention might be another building, which would be constructed in a historical style with the facades similar to the style of Old Town. 29 % of experts agree with the statement that the green territories should be

constructed mostly in the courtyards and squares, in order to reveal the fronts of the historical building as much as possible. 50 % of experts consider that it is necessary to construct new buildings with historical elements, and 17 % of them wish to

integrate both the historical, and modern elements in the Old Town territory, while 16 % of them emphasize that it is necessary to completely renovate the historical identity for the analyzed territory.

CONCLUSIONS

The findings obtained during the research process are essential for the further development of the cultural and historic objects and Soviet period residential courtyards. By performing the historical research and photo fixation in the Old Town territory of the city of Jelgava, multiple unresolved and neglected issues were established. Consequently, the amount of the material obtained, considerably reflects the present condition of these territories. Qualitative and objective information was obtained from the data collected from respondents, as regards the issues that the residents would prefer to change, and their desire to participate in any activities that would help improve

the poor conditions of the analysed territories. The residents of the territory are unanimously ready to collaborate with the members of municipality and other specialists in order to find gradual improving solutions for the neglected territories. A great contribution for the research was given by the expert opinions that have accentuated even more the existing variety of problems of the urban construction that affects the improvement and maintenance of the cultural and historic objects, as well as the improvement of the planning structure, supplementing the existing housing with new historical buildings, organizing and improving the landscape of the courtyards and resting areas.

REFERENCES

- Āboļiņš, A., Tapiņa, I. (2001) Latvijas pilsētu vēsturiskie centri. Rīga: Valsts Kultūras pieminekļu aizsardzības inspekcija, 87 lpp.
- Asaris, G., Marana, A. (1996) Riga, Latvia: Demography and Housing. Royal Swedish Academy of Sciences, 2(25), pp. 97–102.
- Briņķis, J., Buka, O. (2001) Teritoriālā plānošana un pilsētbūvniecība. Rīga, Rīgas Tehniskās universitāte, 219 lpp.
- Būmane, L., Butāne, O. (2008) Jelgavas Vecpilsētas iela atdzimst [online] [accessed on 12.04.2008.]. Available: <http://webcache.googleusercontent.com/search?q=cache:4bg3zQdZp6oJ:www.jelgavniekiem.lv/%3Fact%3D4%26art%3D9943+Jelgava+atdzimst&cd=11&hl=lv&ct=clnk&gl=lv>
- Dābols, A. (2003) Jelgavas būvvēstures eksplikācijas. G.Eliasa Jelgavas vēstures un mākslas muzejs. Raksti I, 8-14. lpp.
- Dābols, A. (2006) Lielā iela, “Pie baltās zostiņas”, “Pie zelta zirga” – ceļojums pagātnē, retrospekcija nāktonei. G.Eliasa Jelgavas vēstures un mākslas muzejs. Raksti II, 20–27. lpp.
- Jelgava. Hercoga Jēkaba kanāls Kanāla ielā [online] [accessed on 10.01.2013.]. Available: <http://www.zudusi.latvija.lv/objects/object/10303>
- Jelgavas pilsētas domes projekts (2011). Jelgavas vecpilsētas bruģakmeņa stāsts [audiovizuāls materiāls]: The Tale of a Paving Stone from the Old Town of Jelgava / scenārijs un režija Aiga Dzendoletto; tehniskā montāža un režija Guntis Šūpuļnieks; tulkojums Kārlis Streips; balss Zigurds Ķeizars; operatori Ojārs Zariņš, Uģis Jakubāns, Mikus Andersons; producents AGD grupa; vāka dizains - Santa Teimonen.
- Lancmanis, I. (2010) Klasicisms Jelgavas arhitektūrā. Senā Jelgava. Rīga: Neputns, 216–234. lpp.
- Leiburga, A., Laukšteina, D. (2003) Koka namu ceļš no skaistuma līdz postam. Zemgales Ziņas, Nr. 2989, 3. novembris
- Riekstiņš, K. (1991) Atjaunotu vecpilsētu – rīt uz brokastu laiku? Jelgavas Ziņotājs, 5. aprīlis
- Soldatovs, N. (1949) Atjaunosim mīlo Jelgavu. Zemgales Komunists, Nr. 77, 14. maijs
- Spārītis, O. (2012) Versija par Jelgavas Sv. Trīsvienības baznīcu. Jelgava: Jelgavas pilsētas pašvaldība, 139–143. lpp.
- Suhecka, M. (1990) Vecpilsētai – vienotu koncepciju. Jelgavas Ziņotājs, 22. decembris
- Treija, S., Bratuškins, U. (2003) Development Problems of Large Scale Housing Estates in Riga. Scientific Journal of Riga Technical University, 2(4), pp 77–83.

THE IMPACT OF LEGISLATIVE RULES AND ECONOMIC DEVELOPMENT ON THE COASTAL LANDSCAPE IN LATVIA

Natalija Nitavskā*, Daiga Zigmunde**

Latvia University of Agriculture, Department of Architecture and Building

E-mail: *natalija.nitavskā@llu.lv, **daiga.zigmunde@llu.lv

ABSTRACT

The development of the coastal landscape in Latvia was affected by various factors during different periods of time; the economic development and legislative rules are among them. The aim of this paper is to study and analyse how these factors have influenced the coastal landscape, identify spatial, functional and visual changes as well as inter-relationships between the factors and changes in the landscape. The study presents the analysis of the impact of legislative rules and economic development on the coastal landscape in Latvia during three historical periods: the Soviet period, the period of regaining independence in Latvia as a period of transition, and the present period. The selected objects of the study - Ainaži, Saulkrasti, Kolka, Liepāja - are of different scales and with individual historical development. The main conclusion of the study is that both heavy restrictions in the Soviet period and rapid yet unclearly defined development in the period of transition and present period are in contradiction to the landscape, thus irreversibly changing the identity of the coastal landscape as well as the spatial, visual and functional aspects. Taking all this into consideration, when planning the coastal landscape and improving the legislative rules in future, it is important to establish a vision of sustainable development, take actions at the regional as well as national levels, and identify the priorities at the local level emphasizing the identity of the landscape, cultural, archaeological and natural values.

Key words: landscape changes, coastal landscape, Baltic Sea, impact of legislative rules

INTRODUCTION

For years the coastal area of the Baltic Sea and the Gulf of Riga has seemed appealing for people as a permanent living place, recreational space, and a biologically and archaeologically diverse landscape. Meanwhile, this part of Latvia is politically and strategically important, as it is the state border and the door to the international zone. The coastal landscape is multifarious. Currently the total stretch of specially protected territories along the sea is approximately 232 km, which composes 47 % of the total coastline length which is 490 km (Eberhards, 2003; Laime, 2005). There are 7 towns and more than 20 populated areas located on the coast having direct access to the sea (Piekrastes telpiskās...).

When looking to the Baltic Sea region as a whole, one should note the special role of coastal territories in development of this area. A considerable number of the population has already been there historically and economic activities have been performed for a long time. At the same time natural and aesthetically attractive landscapes have formed on the coast under the influence of nature's factors. The value of the coastal landscape is also formed by the unique cultural environment with the identity immanent to each place. Therefore preservation and protection of the coastal landscapes is important. Nowadays the topicality of the coastal landscape research is mainly related to the increase of human activities in this territory. By the towns and villages

expanding, new architecture that is often not typical of the rural landscape sets in; tourism industry is developing by attracting an increasing numbers of visitors. Development of infrastructure is related to it as well: construction of roads, bridges and various service objects. During the last recent years the trend of port operation rebirth is evident and new oil terminals have also been built. Coastal territories are increasingly used for obtaining alternative energy by developing wind generator parks. Thereby these territories are becoming increasingly attractive for economic and recreational activities of people (Melluma, 2003). In the Latvian Sustainable Development Strategy the Baltic Sea coast has been recognised as one of the greatest values of Latvia where cultural and historical heritage and natural wealth must be balanced with economic development (Latvijas ilgtspējīgas..., Hohlovska, Trusinš, 2010).

As already noted earlier, development of the coastal landscape is affected by various nature and human factors (Nitavskā et al, 2011). By human influence increasing, the role of planning for sustainable development of these coastal territories is becoming more topical. It also includes the analysis of existing and projected economic development and perfection of legislative rules.

The influence of legislative rules on landscape changes is related to two aspects. On the one hand it is the use of the term 'landscape' itself in legal documents. On the other hand there are legislative rules affecting the economic activity of people that

facilitate or minimise one or another activity on the coast thus directly or indirectly affecting the overall visual image and function of the landscape.

Latvian scientists have also characterised the influence of legislative rules and economic development on landscape changes in their studies by emphasizing coastline protective belt problems (Pižulis, 2010), coastline recreation development trends and problems (Hohlovska, Trusinš, 2010), relation of landscape management and planning to legislation and legislative rules (Melluma, 2002).

According to the suggestion of the Latvian scientist Aija Melluma (Melluma, 2003) sustainable development of the Latvian coastline directly depends on planning where it is important to adhere to the requirements of the Latvian legislative rules in nature protection and territory planning context. It is also important to consider the sustainable development principles and coastline protection guidelines that have been recognised in European countries and have been included in several international documents. Those are: HELCOM (The Baltic Marine Environment Protection Commission, also known as Helsinki Commission) recommendation 15/1: Coastline protection , adopted in 1994; joint recommendations for the coastal territory planning in the Baltic Sea region adopted by the 1996 Stockholm conference of the Baltic Sea region ministries responsible for spatial planning and development; the European spatial development perspective in which the sea coast territories have been distinguished as special spatial structural units (1999); the Spatial Development Action Programme VASAB (Baltic Sea Region Spatial Planning Initiative) 2010+ developed within the Vision and Strategies around the Baltic Sea 2010 that has been adopted by the 2001 Wismar conference of the Baltic Sea region ministers responsible for spatial planning and development; Recommendation 2002/413/EC of the European Parliament and of the Council concerning the implementation of Integrated Coastal Zone Management in Europe (Melluma, 2003). Principal emphasis in these documents is laid on coastal spatial planning, development, protection and management.

A regulatory approach was adapted in Latvia for coastal protection that was started in the 19th century. Nature protection is currently regulated by means of the Protective Belt Law and of major importance is the law On Specially Protected Nature Territories which provides for development of protection plans for protected nature territories. The laws On Environmental Protection and On Protection of Cultural Monuments provide for protection and preservation of environment and monuments. The documents governing planning in Latvia are: Regional Development Law, Territorial Planning Law, regulations of the Cabinet of Ministers regarding individual types of planning

(local and district local authorities, planning region, national planning) (Melluma, 2003). It should be admitted that quite often coastal protection is perceived very narrowly, only for the purposes of regulation. For the purpose of generalisation, the Protective Belt Law, unfortunately, does not respect the coastal diversity. Nowadays the principles of planning are justified by territory diversity, identity and development definitions that are based on balance of the economy and the social sphere (Brīnķis et al, 2009).

Within the long-term development strategy of Latvia in 2008 the Regional Development and Local Authority Ministry was entrusted with drafting the coastal spatial development strategy and setting forth for the coast the status of the territory of national importance. "Proposals for ensuring sustainable management of the Baltic Sea and the Gulf of Riga coastline" have been prepared within this task and the work "Reviews regarding problems and conflict situations on the coast" for Kurzeme and Riga planning regions has been drafted as well. Notwithstanding such a large deposition in the direction of coastal development the many authors still note that planning regions are not being involved. Scrupulous work on the detailed plans with modelling approach should be regarded as one of the solutions (Brīnķis et al, 2009).

Coastal development is important at the European Union level and is governed by the following international documents and documents of the Baltic Sea region and national level. Environmental protection and biodiversity issues are discussed by the Convention on the Protection of the Marine Environment of the Baltic Sea Area (Helsinki, 1974, 1992); Convention on Wetlands of International Importance especially as Waterfowl Habitat (Ramsar, 1971); Conventions on Biodiversity (Rio de Janeiro, 1992); Convention on the Conservation of European Wildlife and Natural Habitats (Berne, 1979); Convention on the Conservation of Migratory Species of Wild Animals (Bonn, 1979); General Convention on Climate Change (1992) and the Kyoto Protocol (1997); the EU directives on the conservation of wild birds (79/409 EEC) and on the conservation of natural habitats and of wild fauna and flora (92/43 EEC); the Helsinki Commission (HELCOM).

The landscape exploration, planning, management and development issues have been included in the European Landscape Convention (Florence, 2000); Recommendation (2002/413/EC) concerning the implementation of Integrated Coastal Zone Management (IPZP) in Europe (adopted on 30 May 2002); the EU Strategy for the Baltic Sea Region; the Baltic Sea region spatial planning documents (VASAB); Sustainable Development Strategy of Latvia till 2030; National Development Plan of Latvia for 2014 - 2020 (approved by the Republic of Latvia Saeima resolution of 20 December 2012);

the River basin section management plans; Land Policy Principal Guidelines for 2008 – 2014 (Ordinance of the Cabinet of Ministers No. 613 of 13 October 2008); Environmental Policy Principal Guidelines for 2009 – 2015 (approved by the Ordinance of the Cabinet of Ministers No. 517 of 31 July 2009); Riga Planning Region Spatial (Territory) Plan for 2005 – 2025 (approved on 2 February 2007); Kurzeme Planning Region Spatial (Territory) Plan for 2006 – 2026 (approved on 9 January 2008).

The national cooperation and security issues are discussed by the Convention on Access to Information, Public Participation in Decision-making (Aarhus, 1998); Convention for the Prevention of Pollution from Ships (1973); International Convention on Oil Pollution Preparedness, Response and Co-operation (1990); Convention on the Transboundary Effects of Industrial Accidents (1992); European Council Directive 91/271/EEC of 21 May 1991 concerning urban waste-water treatment; the EU Water Framework Directive 2000/60/EC; Directive 2003/105/EC of the European Parliament and of the Council of 16 December 2003; Council Regulation (EC) No. 2371/2002 on the conservation and sustainable exploitation of fisheries resources under the Common Fisheries Policy; Energetic Development Principal Guidelines for 2007 – 2016 (approved by the Ordinance of the Cabinet of Ministers No. 571 of 1 August 2006); Strategic Plan of the Fishery Sector for 2007 - 2013 (approved by the Ordinance of the Cabinet of Ministers No. 201 of 11 April 2007 “On the Strategic Plan of the Fishery Sector for 2007 - 2013”).

Coastline sustainable development planning should be looked through at all planning levels: national, regional as well as local level. Each of these levels has different aims and approaches to their implementation; however they are closely interlinked and supplement each other. Researchers and planners see several important tasks that would be desirable to include and solve in each level of planning. On the national level the principal goals of sustainable development and coastline protection should be declared; the natural and cultural and historical values of national importance should be defined and revealed on maps; the coastline should be reasonably divided into sections based on natural, cultural and historical and development peculiarities; individual aims and priorities should be distinguished for each of these sections; coastline development and management strategies should be developed; spatial limits and management of the urbanisation process development should be foreseen (Melluma, 2003; Brīnkis et al, 2009; Pižulis, 2010). The developed Latvian Coastline Spatial Development Principle Guidelines for 2011-2017 foresee developing the coast as a multi-functional and economically balanced space by

facilitating business specific to the coast, recreation and tourism (Piekrastes telpiskās...; Hohlovska, Trusinš, 2010).

On the regional level it is important to ensure an integrated approach to coastline management and planning which is based on detailed knowledge of landscape starting from the sea shore types, town and village positioning and current condition, types of landscape characteristic for the coast, nature processes, their dynamics and frequency, economic activities of people and their intensity, and ending with defining and recognition of places having great development potential.

Plans at the local level play the most important role since they are based on the existing real situation and conditions, not forecasts. At the local level it is important to involve the public in both the planning process and its implementation and management. It is exactly at the local level where it is possible to maintain the identity of particular landscape and to develop an individual approach to sustainable development of such a landscape. Plans and legislative rules at the local level can influence maintenance of local natural and cultural values and traditions which, in turn, create original landscapes. It is advisable to base local level plans on the following materials: existing values (both legally protected and formally unprotected) – excellent landscape places, nature creations, habitats, cultural and historical heritage; gathered information about the natural coastline process development places and risk assessment of such places – coast erosions, new creations and active sand travelling; consequences of economic activities of humans – damage, pollution, erosion, abandoned objects; opinions and conclusions regarding the individual place environmental capacity, admissible load of use, required activities for preserving cultural heritage (Melluma, 2003; Brīnkis et al, 2009; Pižulis, 2010).

The purpose of this particular study is to determine how economic development and legislative rules affect the Latvian coastal landscape, what spatial, functional and visual changes happen under their influence and what mutual interrelations may be evidenced between these factors and landscape changes. Therefore the main tasks of the article are to research such influences in different periods of time and to obtain principal guidelines that should be included into coastal territory sustainable development planning.

MATERIALS AND METHODS

Selecting Representatives

The objects for research have been selected possibly different to obtain more diverse results regarding landscape changes in the Baltic Sea coastal territories in Latvia. The selected objects of the study are Ainaži, Saulkrasti, Kolkja, and Liepāja

(Fig. 1). They are of different scales and with individual historical development.

Liepāja is situated on the Baltic Sea on the SW side

of Latvia. On the inland side the town is limited by the Tosmare and Liepājas lakes.



Figure 1. Location of study objects - Ainaži, Saulkrasti, Kolka, and Liepāja

The rights of a town were acquired in 1625. Town area is 60.37 km², population - 89 448, arranged green territories of 0.93 km² or 1.5% of the total territory of the town, forest territories occupy 10.12 km² or 17% of the total territory of the town, water territories 10.12 km² or 17% of the total territory of the town (*Liepājas pilsētas...*).

Kolka village is located near Kolkasrags - Cape Kolka that stretches into the sea and is a meeting place of the Baltic Sea and the Gulf of Riga. Kolka is one of the Liv villages. Kolka village dates back to the year 1387. Kolka civil parish current area is 116.9 km² and the population in Kolka village is 873 (*Dundagas pagasta...*). Kolka civil parish is now part of Słītere National Park.

Ainaži is located on the coast of the Gulf of Riga and borders on Estonia. Ainaži acquired the rights of township in 1926, but since long ago it has been a place populated by the Liv fishermen. The town area is 5 km², rural territory 149 km². At the end of 2003 there were ~ 1800 people residing in the territory, including 1200 in Ainaži town and ~ 600 in rural territories. The green areas are composed of forests, marshes, waters and bushes occupy 73 % of the territory (*Ainažu pilsētas...*).

Saulkrasti is located on the Gulf of Riga, 45 km north of Riga. The rights of township were acquired in 1991. Total area of the territory is 48 km², including the territory of Saulkrasti town of 6.8 km², rural territory 41.2 km². At the beginning of 2003 the number of permanent residents in Saulkrasti town with its rural territory was 5398 (*Saulkrastu pilsētas...*).

Analysed historical periods

The analysed period is from 1939 to 2012. It has been divided into three sections: Soviet period, the period of regaining independence of Latvia and the present period. Characteristics of those are given above.

The Soviet period. For the Baltic Sea coastal territories the Soviet period was characterised by sharp changes because these territories became the external border of the USSR. The largest towns on the Baltic Sea western coast became the Soviet military navy bases (Ciganovs, 2010). A special borderland regime was developed on the Baltic Sea coast and border guard units, posts, tank practice areas, aviation firing grounds, military airports, weapon and ammunition storages, military intelligence objects, etc. were concentrated there (*Militārais mantojums...*). Resources and territories were required for placing these objects as well as for army living quarters. This facilitated pressing local residents out of their native places of residence, adjustment of several cultural heritage objects for military needs as well as announcing the coastline as a restricted movement zone. The border status imposed on the landscape cardinally changed the cultural and historical development of this area, both the historically formed lifestyle and the type of economic activities.

Parallel to these processes on the coast, the Latvian rural landscape was also affected by the land reform that had already started in 1940 and collectivisation. Its task was nationalisation of land by decreasing

the existing peasant households to 20-30 ha; land was declared property of the state (Boruks, 2003). Collective farms united the land formerly owned by peasants the inventory and cattle, which they were deprived of during the nationalisation of land. Economic development of collective farms differed and this facilitated the migration of people from less developed rural areas to the towns. During the period of 1940 to 1985 the rural population in the territory of Latvia decreased from 65 % to 30 %. After collectivisation the number of homesteads in the territory of Latvia decreased from 89.8 % (in 1948) to 3.5 % (in 1950) (Boruks, 2003).

This period which is characterised by forced industrialisation and collectivisation of agriculture also caused a migration of people from other Soviet republics thus changing the ethnical composition of Latvia (Zvidriņš, Vanovska, 1992). Development goals of the new government affected the existing construction system; changes appeared in the field of city planning, standardised architectural solutions were adopted (Brīnķis, Buka, 2001). Later, in 1959, the building of new industrial plants began. The number of military industrial complexes increased in Latvia, but sufficient attention was not paid to environmental protection (Butulis, 2010).

As of 1956 the CPSU CC 1st Secretary N. Khrushchev condemned the Stalin's totalitarian regime and started a partial liberalisation that was reflected in many areas of life. This period was characterised by improvement of cultural and social life. People who had come during the migration lived in many places, also in barracks and in the 1960s mass construction of residential houses began based on the model projects. The apartment fund increased twice from 1960 to 1985, but all the needs of the population were not satisfied (Butulis, 2010). When developing the social sphere, there were several legislative rules and national standards issued in the Soviet Union that regulated the nature protection field and use of water objects for recreation. This legislation had started to operate by the '80s by controlling both location of recreation places with respect to the national economy objects and arrangement of such territories, water quality, sanitary protective zone size and type of control. For example, 20-40% of green areas were foreseen for recreation zones which in certain places did not correspond to natural conditions of the beach (Библиотека нормативно...). Recognising the consequences of industrialisation, the resolution of the Council of Ministers was issued in 1988 regarding reviewing and transforming the cardinal nature protection issues. In the introduction part of this document all imperfections of the system and the already existing problems were discussed (Библиотека нормативно...).

Regaining independence of Latvia. After Latvia regained independence in 1990 the Soviet army left its bases. Several thousand hectares of vast

territories were abandoned in coastal territories unpopulated, but with rocket bunkers, underwater ports, neglected cultural heritage monuments that served earlier for the needs of the army, soldiers' barracks and other constructions. Quite often these areas were polluted (Luksa, 2007). When the Soviet army left, the military territories were quite often handed over to the management of local authorities. There were not enough funds to manage and guard those, therefore they were robbed most often (Belta, 2008). A part of these territories was denationalised or privatised.

At the beginning of the '90s the collective farms were transferred into joint stock companies or liquidated (Boruks, 2003). Territories of collective farms and the army were left without legal owners which facilitated the degrading of these territories, vandalism, destruction of nature and cultural heritage objects and violation of laws, since the new legislation had not yet been prepared to protect such territories. During this period the most common violations on the coast were - dunes destroyed by cars and illegal construction in the protective zone. Notwithstanding the fact that the Soviet laws also prohibited construction in the dune areas, local authorities deemed these laws as having lost their effect (Matulis, 2000). These times of change, in general, changed the town construction policy because a new form of private property and market relations entered into force in both town and rural construction (Brīnķis, Buka, 2001).

The former border of Eastern Europe and Western Europe gained attention also for the great biological diversity of these territories that was facilitated by limited access to this zone. After the collapse of the Berlin Wall an idea for developing the Green Belt project arose that is valid nowadays as well. The Baltic Green Belt project operated within it, which is implemented by 15 governmental and non-governmental organisations from five countries in the eastern and southern shores of the Baltic Sea. There are the German, Lithuanian, Latvian, Estonian as well as international nature and nature protection resource union (IUCN) in Belgium and the Coalition for Clean Baltics (CCB) in Sweden. The task of this project is preserving, using and developing natural and cultural heritage on the Baltic Sea coastline; developing an international cooperation platform for nature protection and sustainable coastal development organisations; demonstrating good examples in tourism, ecological farming and involvement of the public into regional planning. (Project "Baltic...; Sliteres nacionālais..."). Another such project that took place in the '90s was the European Union INTERREG IIIB a co-funded project Sustainable Reintegration of the Post-Soviet Military residential territories as a Challenge and Opportunity for Regional Development – ReMiDo. Within the project territories - they were evaluated, their development trends were defined, experience

of other countries was assessed, action plans on governmental and local authority level were developed and some pilot projects were implemented (Luksa, 2007).

Present period. After the Soviet army left many territories remained with an unclear status and an unarranged environment. Former military territories on the coast were polluted and dangerous. It was not only the pollution of ground waters and soil, but also unexploded ammunition that was in the ground. The Ministry of Defence, the Ministry of Environment, local authorities and National Armed Forces (NAF) are currently responsible for putting these territories in order. There are more than 100000 ha of such territories currently in Latvia, which is one seventh of the territory of Latvia. Approximately 80000 sea ammunition units are in the Baltic Sea, including the territorial waters of Latvia. The Defence Property State Agency has been operating since 2003. It performs and organises environmental protection activities in military defence objects as well. Planned research of such territories has been performed together with NAF, but implementation of protection and cleaning activities is delayed by the need for large financial investments (Polītis, 2007).

An increasing number of tourists are interested in military heritage and a lot of specialists consider this field as a unique and competitive direction of tourism having its target audience. Several objects have been inspected already and recommendations have been provided for sustainable management of military heritage and its use for tourism in the Natura 2000 and other protected nature territories. Quite often the USSR military bases used military constructions dating back to the Tsar's period and World War I. A data base of these military heritage objects and the military heritage tourism map have been developed. Recommendations have been summarised and the Military Object Use Guidelines have been drafted that include information about the data base, examples from other countries and Latvia (Militārais mantojums...; Militāro objektu...).

Assessment materials and approaches

In order to study the impact of legislative rules and economical development on spatial, functional and visual changes in the coastal landscape cartographical materials from different periods of time, historical photographs and images, development plans, legislative rules and statistical data are used.

Legislative rules at the local level have been used in research, because they most directly affect the decision-making in relation to development of particular territories. For the purpose of historic research the electronic archives of legislative rules of the USSR for the period from 1939 to 1990 has been used (Библиотека нормативно...), for the purpose of research on the situation of the present

period – the nature protection and management, construction legislative rules and the local municipality development plans for the period from 1990 to 2012. According to those the main causes for landscape changes were defined, which were influenced by decisions adopted during the particular period based on these legislative rules. The findings of previous studies (Nitavskā et al, 2011; Nitavskā, Draudiņa, 2012) regarding the town of Ainaži and the Liv coast territory historic development have been used to characterise economic and historic development. They mark the principle development stages and events that had a significant impact on the coastal landscape changes. The USSR General Headquarters military topographic maps of scale 1:10000 for the territory of Latvia of 1942 as well as the Latvian Geospatial Agency topographic map based on surveys of 1994 – 1999 were used for cartographical analysis. For the analysis of historical changes also the Latvian National Library map coverage possibilities were used by using historical maps of different periods and modern maps (Latvijas Nacionālā...). Based on the cartographical material the spatial and functional changes of landscape were defined: increase or decrease of construction, forest, road and water territories.

Black-and-white and coloured photographs from archives, books, internet resources and photo materials from the personal archives that had been obtained by inspecting the territories in 2010, 2011 and 2012 were used for additional analysis as well. Visual changes in landscape were defined based on the photographs: changes in the objects important for the place in the course of time as well as occurrence or disappearance of new man made or nature elements (Nitavskā et al, 2011).

The obtained data have been summarised in tables which distinguish three periods of research, and the main development stages and changes in landscape relevant to those have been defined for each of them (Fig. 2, 3, 4, 5).

RESULTS AND DISCUSSION

Changes in each populated area landscape caused by legislative rules and economic development are depicted in the schemes (Fig. 2, 3, 4, 5) and the detailed descriptions following further.

Liepāja

After research of the cartographical material it was determined that the main spatial changes have taken place in the town of Liepāja expanding when the urban territory increased and natural territories shrank. By the town expanding, the anthropogenic load increased as well, because the number of inhabitants in Liepāja till today has increased almost tenfold. It did not increase during the Soviet period as fast as in other places in Latvia because a

closed military port zone was established there. Thereby the principle growth in population during this period was due to the fact that several parts of the town were allocated for military persons that were operating in the coastal military objects. Legislative rules of that time set forth that these territories were not accessible or had limited access. Thus, closed territories with specific infrastructure appeared in the landscape of Liepāja. After regaining independence, when the Soviet army left, entire parts of the town were left unpopulated and abandoned. Thereby territories started to gradually appear in the town landscape that were, and in some places still are non-functional and degraded.

To overcome a hard economic crisis, in '90s Liepāja was established as the SEZ (special economic zone).

Its establishment and the laws and legislative rules related thereto, in their turn, facilitated flourishing of the town (Latvijas pilsētas...). Some parts of the territories obtained new functionality. The improvement of the visual quality of landscape was promoted which, in its turn, facilitated the development of tourism. The most popular tourist objects at the moment are Liepāja Karosta and Karosta prison, but one must admit that the infrastructure has not yet developed to a sufficient extent.

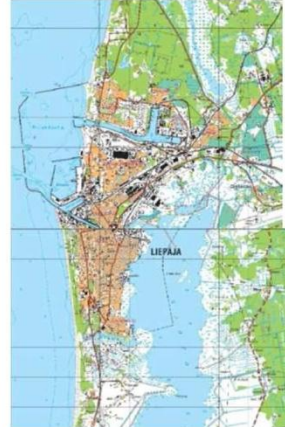
	Soviet period – 1939–1990	Latvian independence period -1990s	Present period – from 2000
Events	Closing of port area because of World War II Closing parts of the city and its infrastructure for military purpose Movement of inhabitants from country to the city; growth of population affected by migration and industrialization	Abandonment of several parts of the city become Decrease in economic development affected by economic crisis Establishment of Special Economic Zone; city development	Tourism development The coastal nature protection Comtinuation of degradation of former military areas
changes in the landscape	Increase of built-up areas Increase of urbanization in the area	Degraded landscape of former military areas Uncontrolled use of natural areas Apiering of new architectural objects	Still degraded landscape of the military areas New architectural and tourism objects
maps, photos	    	  	

Figure 2. Development of Liepāja city.

(Source: PSRS Ģenerālštaba...; Latvijas Ģeotelpiskas...; Liepāja vēstures...; Izstāde "Karosta..."; Latvijas pilsētas...)

Kolka

After research of the legislative rules and historic materials, it was determined that the first significant landscape changes in the territory of Kolka were

related to the strict protection regime established during the Soviet period. This facilitated inaccessibility of landscape. The territory could be visited only by a limited range of persons; local fishermen could not go into the sea freely. Such

closed territory status facilitated increase of biodiversity, because anthropogenic load in the territory decreased rapidly. However, it was defined as a negative feature that along with the re-naturalisation processes in this territory several cultural and historical objects were lost or degraded, traditions and traditional territory management types were lost. Many residents were forced to move out of the nearby Liv villages because military army bases were placed there.

Basing on the cartographic material it could be evidenced that the territory of Kolka village expanded during the Soviet period. After studying historical materials and legislative rules, it could be concluded that this was facilitated by the development of Kolka as the civil parish centre.

Thereby new elements came into the landscape. Collective farms and new infrastructure were developed, the number of inhabitants increased because of migration (Šuvčāne, 2010; Lībiešu krasts). The architectonic structure of landscape changed rapidly. Model-type multi-storey construction appeared that did not match with the cultural and historical traditions of the coastal village. The scale and visual image of landscape were changed. After regaining independence the collective farm collapsed and vast unmanaged territories remained that were reflected in the landscape as degraded territories. As long as Kolka civil parish is currently a part of Slītere National Park, specific conditions are imposed on

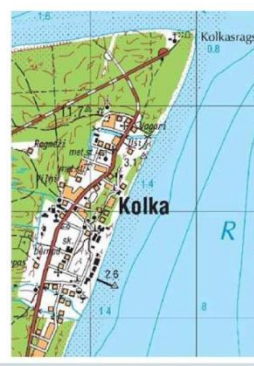
	Soviet period – 1939–1990	Latvian independence period -1990s	Present period – from 2000
Events	Strict protection regime of the Soviet Army; development of military zones Denationalization of private properties Building of collective farms; collectivization Development of new infrastructure Population growth in urban centres	Establishment of Slītere National Park Collapse of collective farms Regaining of private properties Abandonment and degradation of the military areas	Tourism development The coastal nature protection Insufficient financing for maintenance of territories of former collective farms
changes in the landscape	Increase of built-up areas Increase of urbanization in the village A loss of traditional way of economic activities Increase of biological diversity and loss of heritage values in restricted areas	Nature degradation as the result of illegal construction Degraded landscape of collective farms of the Soviet period Uncontrolled use of natural areas	Improvement of the infrastructure in protected areas Continuation of landscape degradation in the areas of former collective farms Aforestation of unmanaged areas
maps, photos	 	 	 

Figure 3. Development of Kolka village.
(Source: Generālštaba...; Latvijas Ģeotelpiskas...; Fotostasts "Senais..."; Šuvčāne, 2010; author's photo)

management and development planning of this territory. The village itself is located in a neutral protective zone which allows developing this territory comparatively freely. But the territories

adjacent to the village are within the landscape protection zone that sets forth much stricter restrictions by minimising the anthropogenic load (Slīteres nacionālais...). The territory of the former

collective farm that is on the sea shore is abandoned and still degraded. As long as sufficient funding for territory management or transformation is not available, the territories will continue to be gradually overgrown. Nowadays tourists are attracted more by the Cape Kolka itself and less by Kolka village, because its most important cultural and historical values had practically been lost or degraded during the Soviet period.

Ainaži

Ainaži flourishing period is related to shipbuilding and port flourishing at the end of the 19th and the

beginning of the 20th centuries. During this period Ainaži port developed rapidly, there was also a railway. After World War II the town infrastructure developed in Ainaži and the number of inhabitants increased. By natural territories decreasing, the town environment increased in the landscape. One can see the evidence by researching historic photographs that during the Soviet period, like in other towns of Latvia, the model-type architecture appeared. The multi-storey block-house construction in conjunction with the collective farming infrastructure elements (hothouses, cattle-sheds,

	Soviet period – 1939–1990	Latvian independence period -1990s	Present period – from 2000
Events	Building of collective farms Development of new infrastructure Population growth in urban centres Closing a rail line	Establishment of the border control point in the town Regaining of private properties Dissolution of the collective farms and many other companies Establishment of North Vidzeme Biosphere Reserve status	Tourism development The coastal nature protection Still existing degraded areas of former collective farms Population decline
changes in the landscape	A loss of traditional way of economic activities The increase of built-up areas Enclosed areas of natural recovery The increase of urbanization in the village	Degraded landscape of collective farms of the Soviet period	Improvement of the infrastructure in protected areas Continuation of landscape degradation in the areas of former collective farms Aforestation of unmanaged areas
maps, photos	 	  	 

Figure 4. Development of Ainaži town.

(Source: Latvijas Ģeotelpiskas...; Ainažu baka; Renemanis, 2006; Ainažu jurnieku...; Latvijas pilsētas...; author's photo)

warehouses, etc.) explicitly changed the scale of the landscape. Collective farms and many other enterprises ceased to exist after regaining independence in the '90s. People had to look for work elsewhere, but the number of unmanaged and

degraded territories increased in the landscape. Nowadays the flourishing shipping days are bygone, only by the lighthouse is a reminder of those times, the museum and the breakwater also dominate the landscape (Latvijas pilsētas; Ainažu

pilsētas...). Currently, the territory of the town, together with the Randu meadows and forest areas, has been included into the Northern Vidzeme Biosphere Reserve. This facilitates landscape protection and controls use of natural resources.

Saulkrasti

Saulkrasti formed by gradually uniting several populated areas that had existed since 1641. When the town environment expanded and new territories gradually joined in, the number of inhabitants

increased also from 1935. Based on the historic and modern photographs it was possible to establish that after World War II, when Skulte fishing port and several productions were built, the scale and visual image of landscape changed explicitly. Specifics of Ainaži town landscape are mainly related to the increasing use of this territory and the anthropogenic load. Already Saulkrasti has been a favourite summer holidaymaker place since the Soviet times, also there are many campgrounds, guesthouses and summerhouse districts there.

	Soviet period – 1939 – 1990	Latvian independence period -1990s	Present period – from 2000
Events	Development of new port area Denationalization of private properties Development of collective farms Establishment of new infrastructure Population growth in urban centres	Collapse of collective farms Gaining a town status; covering larger area Regaining of private properties Many factories and enterprises have been privatized	Tourism development, The coastal nature protection Development of new road around the town Increase of guest houses, holiday home areas
changes in the landscape	The increase of built-up areas The increase of urbanization in the rural landscape	Nature degradation as the result of illegal construction Degraded landscape of the farms of the Soviet period Uncontrolled use of natural areas	The increase of built-up areas The increase of urbanization in the rural landscape
maps, photos	 	 	 

Figure 5. Development of Saulkrasto town.

(Source: Generālštaba...; Latvijas Ģeotelpiskas...; Regional policy...; Uzņēmējdarbība – ieskats...; Neubad, Pension...; Latvijas pilsētas...)

After regaining independence in the '90s many productions and enterprises were privatised (Latvijas pilsētas...). The number of degraded territories is not so large comparatively, because the territory of Ainaži town is attractive for various types of use. However, expressed uncontrolled use of natural resources is evident that was facilitated by lack of relevant legislative rules during the transformation period from the ones developed during the Soviet period to the ones drafted in Latvian period, as well as a prolonged unclear granting of the nature object protection status and property right conflicts. The town is currently developing the coastal infrastructure by arranging the beach area, coastal walking trails and visiting objects; such processes are partially hindered by lack of financial support. In its development strategy the town is planning the transformation of summerhouse districts into residential quarters as well as the development of Zvejniekciems port (Saulkrastu pilsētas...).

CONCLUSIONS

The main conclusion of the study is that both heavy restrictions and rapid yet unclearly defined development are in contradiction with the landscape, thus irreversibly changing the identity of the coastal landscape as well as the spatial, visual and functional aspects.

After researching different size and character populated areas on the coast it should be concluded that the effect of economic development and

legislative rules on coastal landscape may be both direct and indirect. As the result of their influence the main trends in landscape changes may be proposed.

Economic growth and increase of population is reflected in the landscape by an increase of construction and a decrease of natural territories. Introduction of closed zones and strict protection regime facilitates an increase of natural diversity, though at the same time it facilitates also the disappearance of traditional landscape and individual cultural and historical objects.

The slow development of laws and new legislative rules n conditions of changes, facilitates illegal use of natural resources and quite often also degrading of natural territories.

Unarranged property right issues and lack of financial investment is reflected in landscape as chaotic and in some places also uncontrolled territory development or landscape degrading and inaccessibility of landscape.

National and local level planning issues should be closely related to research of historic events by clearly recognising mistakes and benefits provided by the earlier planning and management processes. Taking all this into consideration, when planning the coastal landscape and improving the legislative rules in future, it is important to establish a vision of sustainable development, take actions at the regional as well as national level, and identify the priorities at the local level emphasizing the identity of the landscape, cultural, archaeological and natural values.

ACKNOWLEDGEMENTS

The work had developed within the framework of European Social Fund support for doctoral (No. 2009/0180/1DP/1.1.2.1.2/09/IPIA/VIAA/017) program of Latvia University of Agriculture.

REFERENCES

- Ainažu bāka. Foto autors: Arturs Dimenšteins [online] [accessed on 8.12.2012]. Available: <http://www.bakas.lv/lv/bakas/25/>
- Ainažu jūrnieku un uzņēmēju ģimenes Veides māja. Foto [online] [accessed on 15.12.2012]. Available: <http://www.zudusilatvija.lv/objects/object/5651/>
- Ainažu pilsētas ar lauku teritoriju teritorijas plānojums.* I. Daļa. Paskaidrojuma raksts (2003) [online] [accessed on 2.09.2012.]. Available:http://www.rpr.gov.lv/uploads/filedir/Ter_plaanojumi/Pilsetas/Ainazi/I.dala-Ainazi- Paskaidrojuma-raksts.pdf
- Belta D. (2008) *Daba un cilvēki cenšas tikt galā ar militāro mantojumu* [online] [accessed on 8.09.2012]. Available: <http://www.liepajniekiem.lv/lat/zinas/aktuali/2008/07/24/daba-un-cilveki-censas-tikt-gala-ar-militaro-mantojumu/>
- Boruks A. (2003) *Zemnieks, zeme un zemkopība Latvijā. No senākiem laikiem līdz mūsdienām.* Jelgava: Latvijas Lauksaimniecības Universitāte. 317 lpp.
- Briņķis J., Buka O. (2001) *Teritoriālā plānošana un pilsētbūvniecība.* Rīga: Rīgas Tehniskā universitāte. 219 lpp.
- Briņķis J., Strautmanis I., Bērziņš E. (2009) Baltijas jūras piekrastes zonas attīstība kā viens no būtiskiem faktoriem vietējās ainaviskās savdabības saglabāšanā. *Scientific Journal of Riga Technical University*,13 (1), p. 161-170.

- Butulis I. (2010) *Latvijas vēsture*. Rīga: Jumava. 206.lpp.
- Ciganovs J. (2010) 1939: *Latvijas teritorijā iekārto padomju bāzes* [online] [accessed on 20.10.2012]. Available: http://www.sargs.lv/Vesture/Vesture/2010/12/Padomju_bazes.aspx#lastcomment
- Dundagas pagasta teritorijas plānojums* (apstiprināts 19.12.2005.), un Kolkas pagasta teritorijas plānojums (apstiprināts 13.06.2003.) [online] [accessed on 14.10.2012]. Available: http://www.dundaga.lv/dokumenti/planojums#dundagas_pagasta_teritorijas_planojums
- Eberhards G. (2003) *Latvijas jūras krasti : morfoloģija. Uzbūve. Mūsdienu procesi. Monitorings. Prognozes. Aizsardzība*. O.Āboltiņš (red.). Rīga: Latvijas Universitāte. 296 lpp.
- Fotostāsts "Senais lībiešu ciems Kolka" [online] [accessed on 20.12.2012]. Available: <http://www.kolka.lv/?cat=17PSRS>
- Hohlovska I., Trusins J. (2010) Ilgtspējības principi piekrastes rekreācijas plānošanā. *Scientific Journal of Riga Technical University*, 14 (1), p 21-24.
- Izstāde "Karosta – foto osta 2012" [online] [accessed on 6.12.2012]. Available: <http://www.karosta.lv/fotoosta/>
- Laime B. (2005) *Augi jūras krastā*. Rīga. 64 lpp.
- Latvijas Geotelpiskas aģentūras topogrāfiskā karte pēc 1994. – 1999. gada uzmērījumiem*
- Latvijas ilgtspējīgas attīstības stratēģijas pamatzinojums*. Latvijas ilgtspējīgas attīstības stratēģija [online] [accessed on 25.10.2012]. Available: http://latvija2030.prakse.lv/files/liai_pamatzinojums.pdf
- Latvijas Nacionālā digitāla karšu bibliotēka* [online] [accessed on 20.09.2012]. Available: <http://kartes.lndb.lv/>
- Latvijas pilsētas*. Enciklopēdija (1999). A.Iltnere, U.Placēns (red.). Rīga: Preses nams. 592 lpp.
- Lībiešu krasts* (2008). B.Šuvcāne (sast.). Talsi: Talsu tipogrāfija. 37 lpp.
- Liepāja vēstures līkločos [online] [accessed on 7.12.2012]. Available: <http://liepajasvesture.blogspot.com/search/label/karosta>
- Liepājas pilsētas attīstības stratēģija 2008. – 2014. gadam* (2007). Liepājas pilsētas Dome [online] [accessed on 20.10.2012]. Available: http://www.liepaja.lv/upload/Bizness/Attistiba/pilsetas/Strategija_GALA_VERSIJA.pdf
- Luksa M. (2007) Lētāk ir kaut ko darīt nekā nedarīt neko. *Komersanta vēstnesis*, Nr.48 (104)
- Matulis J. (2000) Latvijas piekraste pārdota kopā ar Latvijas valsti. *Vides Vēstis* 2000, Nr. 11/12 (36)
- Melluma A. (2002). Landscape as a development resource: case of Kurzeme region. *Geogrāfiski raksti*, 10, p. 5–15.
- Melluma A. (2003) *Latvijas piekrastes ilgtspējīga attīstība*. Rīga: McĀbols. 16 lpp.
- Militārais mantojums* [online] [accessed on 5.10.2012]. Available: <http://www.latvia.travel/lv/militaraismantojums>
- Militāro objektu izmantošanas vadlīnijas*. LLTA "Lauku ceļotājs" (2010). Baltic Green Belt Project [online] [accessed on 21.10.2012]. Available: http://www.celotajs.lv/cont/prof/proj/GreenBelt/results/Militario_objektu_apsaimniekosanas_vadlinijas_2010.pdf
- Neubad, Pension Frau H. Winek [online] [accessed on 22.12.2012]. Available: <http://www.zudusilatvija.lv/objects/object/7309/>
- Nitavskas N., Draudiņa I. (2012) Development tendencies of the Livonian coastal landscape identity in Latvia. *Power of landscape: International Scientific Conference ECLAS 2012 proceedings*, p.352-357.
- Nitavskas N., Zigmunde D., Lineja, R. (2011) The Forming Elements of the Baltic sea Coastal Landscape Identity from the Town Ainaži to the Estuary of the River Salaca. *Civil Engineering 11: International Scientific Conference proceedings*, Vol. 3, p.182 – 193.
- Piekraistes telpiskās attīstības pamatnostādnes 2011.-2017.gadam. stratēģiskais ietekmes uz vidi novērtējums* (2010) [online] [accessed on 2.05.2011.]. Available:http://www.mk.gov.lv/doc/2005/RAPLMpamn_230410_piekri.502.doc

- Polītis P. (2007) Nacionālie bruņotie spēki gan aizsargā, gan atveseļo. *Vides Vēstis* 2007, Nr.11 (104).
- Project "Baltic Green Belt" [online] [accessed on 20.12.2012]. Available: <http://www.erlebnisgruenesband.de/en/gruenes-band/europa/baltic-green-belt.html>
- PSRS *Generālštāba militārās topogrāfiskās kartes* mērogā 1:10000 Latvijas teritorijai 1942.g.
- Pužulis A. (2010) The Baltic coastal area management issues in Latvia. *Tiltai*, no1, p. 89-100.
- Regional policy – inforegio*. Seaside resort benefits from big bypass. Saulkrasti, Latvia [online] [accessed on 22.12.2012]. Available: http://ec.europa.eu/regional_policy/projects/stories/details_new.cfm?pay=LV&the=60&sto=1716&lan=7®ion=ALL&obj=ALL&per=2&defL=EN
- Renemanis V. (2006) *Ainažu pilsētai 80*. Rīga: Pērse. 171 lpp.
- Saulkrastu pilsētas ar lauku teritoriju teritorija plānojums*. Paskaidrojuma raksts. Saulkrastu pilsētas ar lauku teritoriju dome 2003. gads ar grozījumiem 2007.gadā [online] [accessed on 20.10.2012]. Available: http://www.rpr.gov.lv/uploads/filedir/Ter_plaanojumi/Pilsetas/Saulkrasti/saulkrastu_terplana_2._redakcija_010903_.pdf
- Slīteres nacionālais parks* [online] [accessed on 7.08.2012]. Available: http://www.daba.gov.lv/public/lat/iadt/nacionalie_parki/sliteres_nacionalais_parks/ (in Latvian).
- Šuvcāne B. (2010) *Senais lībiešu ciems Kolka*. Rīga: Jumava. 622 lpp.
- Uzņēmējdarbība - Ieskats Saulkrastu "Padomju tūrisma"* [online] [accessed on 20.12.2012]. Available: [v/old/lv/uznemejdarbiba/11/ieskats_saulkrastu_padomju_turisma_perioda/520](http://old/lv/uznemejdarbiba/11/ieskats_saulkrastu_padomju_turisma_perioda/520)
- Zvidriņš P., Vanovska I. (1992) Latvieši: statistiski demogrāfiskais portretējums. Rīga: Zinātne. 163 lpp.
- Библиотека нормативно – правовых актов Союза Советских Социалистических республик* [online] [accessed on 27.12.2012]. Available: <http://www.libussr.ru/>

REGIONAL STRUCTURE OF CULTURALLY-HISTORICAL LANDSCAPE OBJECTS AVAILABILITY IN LATGALE UPLAND AREA

Lilita Lazdane*, Madara Markova**, Aija Ziemelniece***

Latvia University of Agriculture, Department of Architecture and Building

E-mail: *l.lilita@inbox.lv, **madara.markova@inbox.lv, ***aija@k-projekts.lv

ABSTRACT

Culturally-historical landscape formation is based on certain functional meanings of elements in landscape space, and subdual of the surrounding space to specific functional needs. Over the last 50 years, the landscape space of Latgale Upland has changed along with territorial policy changes. The aim of the research is to analyse two object groups of culturally-historical importance in the context of regional and local structures such as church landscapes, watermill and small-scale hydroelectric power plant spaces, to define landscape transformation tendencies. The research territory was chosen to be Latgale Upland and its locality (surrounding territory) – Latgale Upland area. The research illustrates that, changes in the processes of regional planning have become an important reason for the transformation of culturally-historical landscapes' available structure, however, the characteristic of culturally-historical attributes and scale proportions in local landscape still exist.

Key words: Regional landscape, Church, Watermill, Hydropower

INTRODUCTION

This research is introducing a part of culturally-historical landscapes in Latgale Upland area. The term, ‘culturally-historical landscape’, is used throughout this research to include the following types of landscapes in Latgale Upland area: Churches and hydropower objects (watermills and a small-scale HPP (hydroelectric power plant)).

Transformations in culturally-historical landscapes are increasing along with the processes of globalisation. The aspect of accessibility could have an impact on culturally-historical landscape development possibilities for more active public use.

Historic landscapes are important national assets, and they provide some of the most special and valued places for public recreation and education (English ..., 2005). Church and hydropower object landscapes are an important culturally historic part of the history of Latgale region. Churches and places of hydropower objects can be found often in the contemporary landscape of Latgale. The importance, functionality and number of these objects have changed dynamically in the past, thereby influencing the landscape transformation processes. These changes are rooted in different historical periods, mainly involving a complete change of ethnicity and socio-cultural field (Fjodorovs, 2009).

For the local population, the countryside in Latvia is perceived as an important contributor to a sense of identity (Bell et al., 2007). Those landscapes, which are perceived daily, are mainly ‘every day’ landscapes, but usually these landscapes are in danger because of their unprotected status.

According to literature review, church gardens previously had too little attention from researchers.

Gardens were usually established and built without taking into account the church buildings’ composition, but they are one entity. Garden and church landscape includes different culturally-historical elements – fences, crucifixes, free standing bell towers and separate compositional plantings (Markova, 2012). The division in denominations (Orthodox, Catholic, Lutheran, Old Believer) also has an impact on landscape design and functions in each territory. The denominational membership of the church territory is very important, because in the main contours, it already defines the landscape character (Markova, 2012). Each type of the churchyards has differences in architecturally compositional form, and also in element groups, that supplement the church architecture. Some experienced researchers have carried out their research in connection with churches and sacred art in Latgale, but the landscape issue has been left behind so far. Extensive research regarding wooden churches in Latgale, especially the Roman Catholic Church construction in the 18th century, has been done by Krūmiņš (2003), who was a multi-faceted architect, writer and scientist. An art scientist, R. Kaminska, whose works are mainly dedicated to the artistic heritage of eastern Latvia, particularly concerning the 17th to 19th century heritage, has published several books and articles related to church architecture and art researches (Kaminska, 2008). Kaminska together with Bistere have started work on sacral architecture, art heritage and existing inventory study ,compiling and and documenting the findings, and have already published their results in several books (Kaminska et al., 2006, Kaminska et al., 2011). These researchers reveal the wide meaning and value of churches, churchyards

and church landscapes that are important for the place development, one of which is tourism.

Hydropower objects have been researched in different fields of studies (Lazdāne, 2011; Lazdāne, 2012; Raitis et al., 1944; Silke, 2008; Tveins, 1985). These landscapes are the result of interaction between the human-made and natural landscape elements. Water reservoirs, historical watermill buildings, industrial character (watermill, power plant) united with public (watermill) and private (dwelling house) character in one landscape. Landscapes in these historically actively used territories are changing nowadays.

Several researchers focusing on the research of landscape structures and historical regional development in Latvia, including Latgale region, could be mentioned as Zariņa (2008), Penēze (2009), Melluma (2012).

The importance of globalisation processes is increasing (Reenberg et al., 2009). A lot of research has been carried out on urbanisation and globalisation processes and landscape transformation that is influenced by these processes. Among the processes that have an impact, local landscapes nowadays can be influenced from external driving forces, and the economical profitability of time consumed affects the urbanisation density and movement of people migrating (Reenberg et al., 2009; Harvey, 1996). At the European Union level, theoretically, free movement of labour and finances mean transformation from more remote territories to main economically powerful cities and towns, and thus demographic situation in border territories is changing, and population density particularly in the countryside is decreasing (Antrop, 2003).

To understand what qualities are important to people's quality of life, we need to acknowledge the diversity that exists in people's capabilities, experience, desires and needs (Thompson et al., 2007). For example, a person's decision to visit the historic landscape will be influenced by how easy it is to get there and back again (English ..., 2005). One of the key factors for good cultural landscape development is availability (Jongman, 2002). In this context, roads are one of the compositional elements, influencing not only object availability and accessibility, but also form object visibility. It is necessary to think about the functionality of these landscapes. If functional landscape transformation means space reorganisation and modelling of needed architectural elements, changes can be in shifting perception not in the form of object (Landecker et al., 1998). Landscapes are transformed around us with the aim to adjust them for our everyday needs; they define arrangement, style, and materials of the features, as they represent many eras of natural evolution and generations of human efforts (Yatsko, 1997). After passing time, needs and functions change and so do the

landscapes. But in all this process, we cannot leave the quality of life space behind.

In this research, in addition to the culturally-historical object availability and placement studies, specific connection to the tourism has been made, as it is an important sector for regional development. In researches about tourism territories and the importance of their location, tourism regions are emphasised. It is an idea about complex regional development. In one single regional development, idea is placed together with architectural monuments, landscapes and other elements (Banica et al., 2011). The territory of Latgale is a region with such dimensions. Those objects that are more difficult to reach have to be individual and varied in their cultural, historical and architectural meanings (Banica et al., 2011). On the other hand, the accessibility of a destination clearly influences the attractiveness and potential for tourism and development (Banica et al., 2011).

Latgale Upland is located in the southern part of Latvia. This territory is rich in lakes and has a very picturesque landscape that is complemented with different culturally-historical elements. Today the situation and placement of these objects are part of regional structural research for church and watermill landscape and their involvement in sustainable territorial planning.

Solutions for different landscapes have to be different, and at the same time, one has to consider all kinds of sustainable development of cultural landscape. There are landscapes, where people's presence needs to be limited and total rearrangement of territory functions is needed. One such example is Aglona church landscape. The basilica annually unites a lot of people, and that is the reason why this territory has changed considerably through the years. The vast frontal space substantiates functionality only once a year on the occasion of the Assumption on August 15.

We have to think also about the territories that are left behind and have lost their functional meaning. Environmental qualities often have a direct impact on human well-being, so we have to maintain them as much as we can.

The aim of this research is to analyse two object groups of culturally-historical importance in the context of regional structure, to define landscape transformation tendencies in the aspect of availability.

Both objects of this research – hydropower objects and churches – are evaluated in respect to the surroundings. They are architectural point objects that have wider visual, economic and ecological influence. In hydropower objects, the impact is on the presence of water, working places, economic and social activities and place maintenance. Water reservoirs in these objects can be up to several thousand square meters. Churches are not only architectural monuments, but also these are places

where people gather, and there is social interaction, participation, and spiritual growth. Life space in both of these landscape types has to be qualitative.

MATERIALS AND METHODS

Latgale Upland is a territory located in the south-east of Latvia. Latgale Upland occupies the territory of approximately 6300 km² (Markots, 2011), and only a small part of it (in the south) is located outside Latvia (Мейронс, 1975), which will not be taken into account because the aim of the study is to research the territories only in Latvia. The area of this research is wider than the area of Latgale Upland, because of the densely built-up territories which are researched, and because of the fact that the visibility and availability can't be strictly demarcated in nature, as it might be possible to mark on maps.

The small-scale hydropower territories for this research were selected from maps of the 1920s

(Геодѣзіјас ...), where the places of watermills were marked, and the scheme of 2008 (Latvijas ..., 2008) where the places of small-scale HPP were located. The church territories were selected from the map of Jāņa sēta (2006) 'Dienvidlatgale. Latvijas tūrsma kartes - Tourism maps of Latvia' 1:200000, where the places of churches were located. In the map of Latgale Upland area, the number of territories for this research was marked on the map. In the research, 14 territories of hydropower objects (watermills and small-scale HPP) (Table 1.), and 15 territories of churches (Table 2.), (Figure 1) were included. They were chosen randomly from the region, by the criterion of even dispersion and location in different landscape types of urbanisation (rural, peri-urban, and urban).

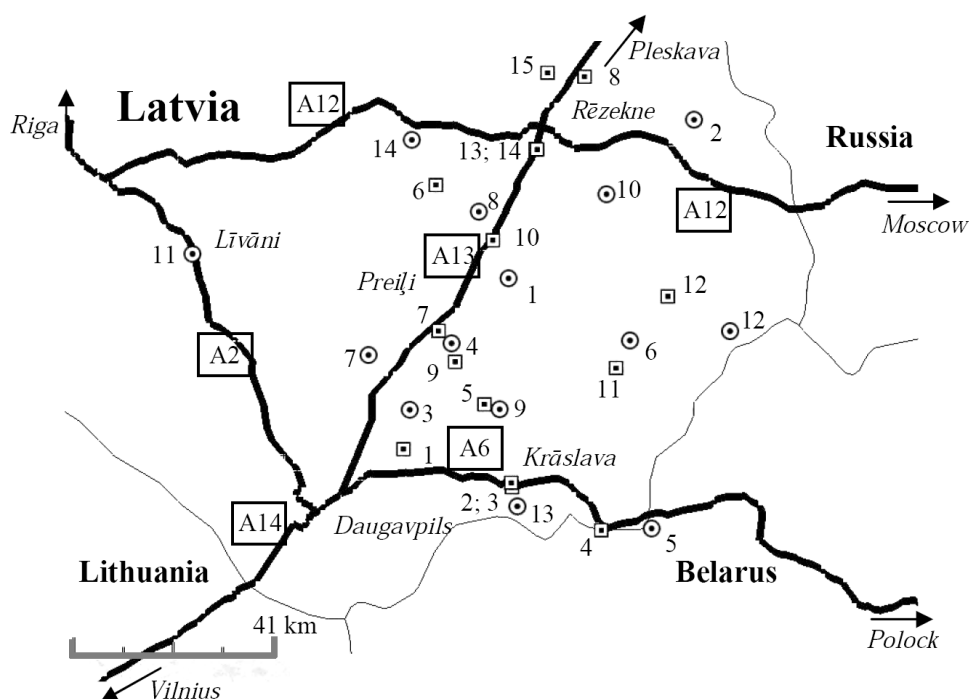


Figure 1. Location of objects in Latgale Upland area, where — Main country roads; ○ - Hydropower objects: 1- Balda w., 2 - Felicianova w/ HPP, 3 - Galvāni HPP, 4 - Jaunaglona HPP, 5 - Koškoviči w., 6 - Obiteļi w., 7 - Pelēči w/ HPP, 8 - Prezma w., 9 - Sakova w., 10 - Sprukti HPP, 11 - Straumes w/ HPP, 12 - Tīmaņi w., 13 - Upmaļu w/ HPP, 14 - Viļānu w/ HPP; ■ Churches: 1 - Bikernieki old believer 2 - Krāslava Catholic 3 - Krāslava Old Believer 4 - Piedruja Orthodox and Catholic 5 - Kovalova Old Believer 6 - Paramonovka Old Believer 7 - Rušona Catholic 8 - Bērzgale Catholic 9 - Aglona Catholic 10 - Malta Old Believer 11 - Dagda Catholic 12 - Vertulova Orthodox 13 - Rēzekne Orthodox 14 - Rēzekne Lutheran 15 - Ilzeskalne/Kuļneva Orthodox

This research was carried out during the period between 2010 and 2012. In this research, a cartographical method has been used to show location of researched territories in region (Figure 1), and to measure the distances for analysing the accessibility (Table 1., Table 2.); a literature survey

method was employed. The territories were visited and various photo materials collected. Measurements were made in base map, which was drawn using Internet tools by Google Earth. In assessment, the tables were designed, and the data were marked according to the researched

measurements. The distance measurements precision is up to 1.0 kilometre. Division by type of roads was used are: street; main country road (A); main regional road (P); main local road (P); and local road. Types of roads were taken from roads division by Latvian law on roads (Likums..., 1992). For availability survey, both the distance from the main roads and the distance from the main cities was taken into account. Administrative centres are places where all services are available.

In Table 1, in addition, the function of hydropower objects' buildings is marked. In Figure 1, the denomination of church is marked with the functions which are included in this research.

RESULTS AND DISCUSSION

Regional Accessibility

By the results of research made by European data project (ESPON), it was mentioned that 'regions with a high accessibility are most often also economically and competitively successful'

(ESPON, 2009). The accessibility in Latgale region and Latvia, in general, by 'potential accessibility by rail' (ESPON, 2006a) and 'by potential accessibility by road' (ESPON, 2006b) is in one of the lowest positions in Europe.

If the most accessible sites are usually those that offer different travel options (bus, car, public transport, etc.) (English ..., 2005), then the territories, which are located out of the cities, have fewer possibilities for diverse public transport and easy accessibility (two territories of hydropower objects are located in towns, but 12 in rural or village areas; nine objects of churches are located in towns, but six are in rural or village areas). The second important aspect is the time spent on the way to the destination. In Latvia, generally, the maximum allowed speed is 90 kilometres per hour. Then, using the road distance numbers form Table 1 and Table 2, we could get to the objects of this

Table 1.
Watermills and small-scale HPP landscapes, and their connections to different road types and biggest cities
(created by L. Lazdāne)

Nº	Name of object and – watermill, HPP - hydropower plant station.	Near which road the object is placed (Attributes: street; A- main country road; P- main regional road; V- main local road; local road)	Closest main country road (attribute) / distance (km)	Distance (km) to the closest city of republic's significance	Distance (km) to the closest city of republic's significance	Distance (km) to the capital city - Rēzekne	Functions of buildings
1.	Balda w	P	A13/9	30	79	247	dwelling house
2.	Felicianova w/ HPP	V	A12/11	44	133	281	HPP, old w. building abandoned
3.	Galvāni HPP	V	A13/10	72	39	232	new HPP
4.	Jaunaglona HPP	street	A13/9	59	56	234	Abandoned
5.	Koškovici w	local road	A6/4	115	82	302	Ruins
6.	Obiteļi w	V	A6/44	53	91	277	guest house
7.	Pelēči w/ HPP	V	A13/11	59	39	220	HPP
8.	Prezma w	V	A13/10	22	80	247	Ruins
9.	Sakova w	P	A6/17	70	61	246	dwelling house
10.	Sprukti HPP	local road	A13/26	22	112	266	HPP
11.	Straumes w/ HPP	A	A6/0	91	63	167	HPP
12.	Timaņi w	V	A12/37	69	116	303	Ruins
13.	Upmali w/ HPP	local road	A6/7	94	51	270	HPP
14.	Viljāni w/ HPP	street	A12/3	32	89	215	HPP

research from Riga in two to three hours. However, by the way of Google Earth Internet calculations (Google...), we could obtain more or less precisely calculated time that we could travel on road, which shows that it would take from 2.5 to 4.5 hours to get to these objects.

It has been researched for different types and needs for accessibility for several functions. Mainly, the longest distance to go to work by car, if the driver is driving alone, is 70 km, but to travel for recreation it is less than 50 km, but if there is a shared ride trip, the distances are shorter (In that case, it is

possible to travel to work 50 km, but for recreation 55km) (Iacono et al., 2008). In the case of the Latgale Upland area, if researched territories could be the place for work, for a driver alone (for the 70 km distance) ten of the 14 hydropower objects, and 11 of the 15 churches are accessible from Rēzekne town; 6 of the 14 hydropower objects, and 7 of the 15 churches are accessible from Daugavpils; none of the objects is accessible for daily work from Riga (Capital city). The possibilities to use territories for daily recreation (50 km distance) are: five of the 14 hydropower objects and seven of the 15 churches are accessible from Rēzekne town; two of the 14 hydropower objects and four of the 15 churches are accessible from Daugavpils city and none from Riga . Accessibility to Riga for daily work is impossible for both object groups, but the accessibility to both local towns have two of the 14 hydropower objects and three of the 15 churches.

According to Peneze (2009), in regional developments, the roads and infrastructure objects development at the local scale could be one of several factors, which will have an impact to landscape structure and quality. This development

could provide possibilities for access to work places or recreational territories (Peneze, 2009). But as a potential danger, she mentioned the depopulation and marginalisation of rural territories because of the negative attitude toward living in rural areas among the younger generations (Peneze, 2009).

The results regarding the territory's accessibility at the local scale show that locations of territories regarding the road intensity also vary. Hydropower objects locations are: by street - two; by main country road - one; by main regional road – two; by main local road – six; and by local road – three. Churches locations are: by street – eight; by main regional road – two; by local road - five. It can be concluded that most churches are near the main roads and in urban landscapes. A question as to why some of the churches in rural landscapes are with less households around them is a question that needs to be answered in further research studies.

The results of the criterion used here are different because it determines functional differences in landscapes. The accessibility in local scale differs by types of selected objects of research.

Table 2.
Church landscapes and their connection to different road types and biggest cities (created by M. Markova)

Nº	Name of church object	Near which road the object is located (street, A-main country road, P-main regional road, V-main local road, local road)	Closest main country road/ distance	Distance (km) to the closest city of republic's significant city - Rēzekne	Distance (km) to the closest city of republic's significant city - Daugavpils	Distance (km) to the capital city of Latvia – Rīga
1.	Bikernieki	local road	A6/7; A13/14	76	24	236
2.	Krāslava Catholic	street	A6/0	88	44	264
3.	Krāslava Old Believer	street	A6/0	88	44	264
4.	Piedruja Orthodox	street	A6/3	104	71	291
5.	Kovalčova	local road	A6/23; A13/23	70	66	246
6.	Paramonovka	local road	A12/19; A13/29	48	96	231
7.	Rušona	local road	A13/1	45	49	228
8.	Bērzgale Catholic	local road	A13/3	22	118	258
9.	Aglona	P	A 13/8	56	53	232
10.	Malta Old Believer	street	A13/1	20	70	238
11.	Dagda Catholic	street	A6/27	59	80	266
12.	Vertulova	P	A13/50; A12/37	51	99	286
13.	Rēzekne Orthodox	street	A12/4; A13/4; A15/4	0	90	240
14.	Rēzekne Lutheran	street	A12/4; A13/4; A15/4	0	90	240
15.	Ilzeskalne/Kuļneva	street	A13/6	16	111	251

From researched hydropower objects by functions are as follows: Two territories are used as dwelling-houses; seven as small-scale HPP; one as guest house; main watermill or small-scale HPP building is in ruins or abandoned in five territories; newly constructed small-scale HPP in place, where never watermill was constructed is in one territory. The distance, of course, is not the only one reason why the territory is not used. From previously detected distances (70 km), hydropower objects areas with good access to both towns one territory out of two is abandoned; and with good access only to Rēzekne town, two territories are in ruins; a ruin can be found in one territory, which the location has a distance from both local towns of more than 80 km.

The territories of churches are located at different distances, but all of the researched territories are functionally used today. The active function and placement is a valuable characteristic for church landscape involvement in regional tourism establishment and development. Involvement of churches and churchyards in regional development plans and territorial planning promotes church landscape vitality. In church landscapes, functions are kept the same nowadays, but only not so intensively (Figure 1).

Landscape availability for tourism market

In tourism object evaluation, the possibility for people to get out of the city and then be able to return to it in the most comfortable way in quite a short time is an important evaluation. At the same time, if destination is one of a kind, or somehow differs from another, then accessibility has no influence on its attractiveness (Celata, 2007). One of the examples of being different from other objects could be Aglona church, where, at least once a year, the distance does not have any impact on the accessibility.

There are three scales of tourism potential planning. First is site scale. It deals with the single tourism unit (Inskeep, 1994; Formica 2000; Gunn et al., 2002; Pearce, 2012). In our case, there are several possible responsible stakeholders: private owners, companies, country or municipality, and religious organisations. In hydropower objects landscapes, most of the responsibility comes from private persons and companies. In church landscapes, responsibility for development is divided between the state and religious organisations. From the researched objects in the territories of churches, almost all are used as a tourism object occasionally by enthusiastic tourists, mostly devoting a large amount of time to travelling.

Second is the destination scale. This potential planning involves such objectives as socio-cultural, environmental, political and economic factors. In this scale, single sites are put together (Inskeep, 1994; Formica 2000; Gunn et al., 2002; Pearce,

2012). In this scale, an object provides variable components – natural and/or man-made attractions. Here the key role is for regional geographical qualities together with a wide range of culturally-historic objects. In the destination scale, the data according to accommodation places with offers in Latvia could show the prospect of existing possibilities to use the region for the tourism market, and according to the data in 2011, in the Latgale region, 8.4% places for accommodation were located, providing 5% of places to sleep from the total in Latvia (Latvijas..., 2012b). The Latgale region has the second lowest places to sleep for tourists in Latvia. The potential tourism market could be prognosticated according to the existing data of tourists' visits in Latvia. The visits to different regions in 2011 are: in Riga - 88%; in the suburbs of Riga - 8%; in the Vidzeme region - 0% (1591 people); in the Kurzeme region - 2%; in the Zemgale region - 1% (3603 people); in the Latgale region 1% (5412 people) (Latvijas..., 2012c). The main tourism market is located in the biggest city of Latvia – in Riga, the administrative centre which is densely populated. In group of regions with the lowest number of tourist visits, Latgale region is the second most visited rural region in Latvia, so there is a need for different objects in rural landscape, in order to make a variety of offers for different tourism interests.

The third scale is the regional scale. Planning the regional level of tourism potential includes a comprehensive structured activity geared towards the integration of attractions located in a region (Inskeep, 1994; Formica 2000; Gunn et al., 2002; Pearce, 2012). As the research objects are part of regional landscape identity, factors have to be taken into account, such as in transportation, ecology and forestry plans. For the tourism market, on the regional scale, it is important to take into account the population size, and its tendencies. The population of local residents in Latvia is decreasing, and from 1995 to 2012 the population has decreased by 18.4%, but if separately compared, then the population decrease in the last two years only in the Latgale region is much higher – 26.4% (Latvijas..., 2012a). The data according to population density also are important, and according to data of Eurostat, the population density in Latvia, in 2006 was 37 inhabitants per 1 km² (European..., 2008). If we compare this number in the region located along the Baltic Sea with the population density in 2006, the count in Lithuania was - 54, Estonia – 31, Finland – 17, Sweden – 22, Poland – 122, Germany – 231, Denmark – 126 (European..., 2008). The population density is higher in countries, which are closer to the central part of Europe. These data lead one to think that the tourism market that was researched in the Latgale Upland region can't be developed based only on local population, or on regionally the closest countries along the Baltic Sea.

Centrally tended economic development in Latvia promotes the biggest growth in cities; similarly as it is in other countries under the influence of globalisation, and the territories in the country side are less actively used. Each landscape needs individual development according to its accessibility and intensity for everyday use. The existence of tourism resources in Latgale Upland is a necessary element of tourism attractiveness, but it cannot predict the significance of the attraction of the region. The pulling force of a region depends not only on the number of tourist objects located in a given area, but also on how these resources are valued and perceived by tourists (Formica, 2000). By simply increasing the number of tourism trails and objects, we would not always be able to increase the overall attractiveness of a region.

Local Landscape Character

The centralisation processes according to financial possibilities and the development of dense areas of private house villages in last 20 years are concentrated in Riga, and this has saved the territory of Latgale region from an over-development of territories in rural areas, close to cities, to suburban territories, and to main roads. Such situations last until today and preserve the unique landscape character for the Latgale Upland area, but the economic recession has impacted the landscape with new issues, and the culturally-historical landscape of Latgale Upland has to cope with pressure from the economic reality. The rural lands, private and public houses are becoming abandoned more and more by each passing year,



Figure 2. Wood-carving elements on an abandoned private house (Author: Lazdāne, 2012)



Figure 3. Wood-carving elements on a private house part of a watermill building (Author: Lazdāne , 2012)

and the loss of old, decorative, structurally diverse and historically-cultural rich buildings is increasing. The high-quality architectural values are still visible in these landscapes (wood-carving elements in architecture as seen in decorative elements of windows shutters, openings and frames, in doors, fences, facade cornice laths, rafters, etc.) (Figure 2, Figure 3). The culturally-historic objects and natural elements such as rivers and lakes, hill-relieves are connected in one system of interpretive values. This system of connections has to be researched in future. As the example of the existing situation for this interpretive system, the landscape of Līksna church could be mentioned. In the rural landscape of this territory, the height of church towers are approximately 45 meters, which is not common for these rural areas. Also the location of this church is in a hilly area, on the one of the highest tops of the hills, quite high in comparison to the surrounding landscape. The visibility of this churches' silhouette can reach up to 10 km in distance. In the formation of new private housing in the 20th century in the '1920s and 1930s, in the first period of Latvia's independence, the views of this landmark, was taken into account in surrounding landscapes (Figure 4).



Figure 4. View from a private house area to the church (Author: Lazdāne, 2012)



Figure 5. Old building has lost its function as a cattle-shed, and in the front, the decorative

plantings are not cared for. (Author: Lazdāne, 2012) In the character of Latgale Upland area, the views of churches still exist. The connection with traditions to religion historically was strengthening the development of Latgale region inhabitants' families. This is one of aspects, which characterises the identity of the Latgale Upland region.

Today the transformation of old private houses is developing, and the new inhabitants in rural landscapes are now using these houses as places for recreation during the weekends and holidays. The existence of traditional hard work on farms is disappearing, but the environment of a psychological culture is still developing (the maintenance of historical architecture, apple-garden, vegetable patches, site views to the surrounding landscape features). With the disappearance of historical meaning to each building (Figure 5.) today we are obtaining a new functional belonging (public centre for crafts; a place for summer camping; a place for artists' workshops, etc.). These functional transformations are acceptable because they are not reducing the quality of architecture and culture.

Of course, the processes of centralisation and the global economic recession also have an influence on the agricultural structure, which is changing the agricultural lands to unmanaged territories and worsen soil territories nowadays, and more bushes and tree seedlings are seen growing. The new, uncontrolled forest territories are destroying the system of irrigation and structure of the cultural landscape, changing it to a post-natural landscape.

CONCLUSIONS

The tendencies of landscape transformations in culturally-historical importance objects were researched. There is obvious tendency of globalisation, and local population is decreasing. The access to the common territory of Latgale Upland area from capital city of Riga is low. Landscapes are also different in access to territories

from republic's significant towns. Possibility to attract tourists or potential inhabitants form capital city to Latgale region is low, especially for longer period of time, which is required for visiting each territory included in this research. If the landscape development (for public or private use) is important, it has to be accessible in the shortest time period, especially from big cities and towns, but the territory of Latgale is located too far away. The connection between Riga and Latgale Upland area has to be developed for faster traveling time and for a better quality of accessibility. The need for high speed roads and a good rail transport system is extraordinarily urgent.

Church landscapes mostly are placed near main streets and main roads and this is a good starting point for the development of these objects as tourism objects as dominance of the landscape is not only as ceremonial buildings, but also as qualitative architectural objects which are an important part of cultural history.

In the development of culturally-historical traditions in building constructions in the Latgale area, locally dimensional parameters in scale, proportions, colour scheme, disassociation between buildings and areas for living and the branch of wood trade are seen developing. These parameters are special determinants only to the Latgale Upland area which has a characteristic that is uniquely national aesthetic quality with a sense of scale, which has been formed in several generations and are definitely socio-political, economic, and it has to be protected and developed.

The development of technologies, the financial and economic situation, and cultural activity in both local and on a global scale will have an impact on the future development scenario, and has to be taken into account for future planning strategies.

Historical meaning of churches, as local cultural centres, may have lost their importance, but they are still places with not only religious, but also cultural and social importance. This existing possibility has to be used for future regional development strategies.

Of the researched territories of hydropower objects, most of them are developing as industrial territories or degraded, abandoned territories; a tourism possibility as a guest-house is used only in one territory, but the number of visitors in other territories (as to objects of tourism attraction) is not known. Of the researched church territories, almost all are used as tourism objects, but the number of visitors with the aim to use these territories as tourism objects is minimal and uncounted because of the small capacities. Culturally-historical landscape of Latgale is a resource for further tourism development and for providing landscape diversity.

ACKNOWLEDGMENTS

This research work was supported by European Social Fund project „Realization assistance of LLU doctoral studies”, Agreement No. 2009/0180/1DP/1.1.2.1.2/09/IPIA/VIAA/017.

REFERENCES

- Antrop M. (2003) Landscape change and the urbanization process in Europe. *Landscape and Urban Planning* 67, p. 9-26.
- Banica A., Camara G. (2011) Accessibility and Tourist Function Development of the Romanian Small Towns. *GeoJournal of Tourism and Geosites*. Vol.7, p. 122-133.
- Bell S., Penēze Z., Nikodemus O., Montarzino A., Grīne I. (2007) The value of Latvian rural landscape. In: *European Landscapes and Lifestyles: The Mediterranean and Beyond*. Z. Roca, T. Spek, T. Terkenli, T. Plieninger, F. Höchtl (ed.). Lisbon, Portugal: Edições Universitárias Lusófonas, p. 347–362.
- Celata F. (2007) Geographic marginality, transport accessibility and tourism development. In: *Global Tourism and Regional Competitiveness*, Celant, A. (ed.). Bologna: Patron, 37-46.
- English Heritage (2005) Easy Access to Historic Landscapes [online] [accessed on 10.12.2012.]. Available: <http://www.sensorytrust.org.uk/resources/eahl.pdf>
- ESPON (2006a) Map 3. Potential accessibility by rail [online] [accessed on 09.01.2013.]. Available: http://www.espon.eu/export/sites/default/Documents/Publications/TerritorialObservations/TrendsInAccessibility/map3_accessibility_rail_2006.pdf
- ESPON (2006b) Map 5. Potential accessibility by road [online] [accessed on 09.01.2013.]. Available: http://www.espon.eu/export/sites/default/Documents/Publications/TerritorialObservations/TrendsInAccessibility/map5_accessibility_road_2006.pdf
- ESPON (2009) Territorial Dynamics in Europe: Trends in Accessibility, Territorial Observation No. 2 [online] [accessed on 14.12.2012.]. Available: <http://www.espon.eu/export/sites/default/Documents/Publications/TerritorialObservations/TrendsInAccessibility/to-no2.pdf>
- European Communities (2008) Eurostat Pocketbooks. Tourism statistics [online] [accessed on 20.12.2012.]. Available: http://epp.eurostat.ec.europa.eu/cache/ITY_OFFPUB/KS-DS-08-001/EN/KS-DS-08-001-EN.PDF
- Fjodorovs F. (2009) The spiritual space of Latgale. In: *Latgale as a culture borderzone: comparative studies Vol II (1)*. Daugavpils: Saule, University of Daugavpils, p. 9-19.
- Formica S. (2000) Destination Attractiveness as a Function of Supply and Demand Interaction. Ph.D.dissertation, Blacksburg, Virginia [online] [accessed on 23.11.2012.]. Available: <http://scholar.lib.vt.edu/theses/available/etd-11142000-15560052/unrestricted/FrontMatterDissertationDefense.pdf>
- Ģeodēzijas topogrāfijas daļa. *Latvijas topogrāfiskā karte*. (Latvijas topogrāfisko karšu mērogā 1 : 75 000 komplekts, izgatavotas pēc 1911.–1927. gadu uzņēmumiem un rekognoscijas) [Topographical Set of Maps of Latvia 1920-1937]. Rīga: Armijas štāba Ģeodēzijas-Topogrāfijas daļa
- Google Earth Plug-in Driving Simulator [online] [accessed on 07.10.2012.]. Available: <http://earth-api-samples.googlecode.com/svn/trunk/demos/drive-simulator/index.html>
- Gunn C.A., Var T. (2002) *Tourism Planning: Basics, Concepts, Cases*. London: Taylor & Francis Books, 442 p.
- Harvey D. (1996) *Justice, Nature and the Geography of Difference*. Oxford: Blackwell Publishers. 480 p.
- Iacono M., Krizek K., El-Geneidy A. (2008) Access to Destinations: How Close is Close Enough? Estimating Accurate Distance Decay Functions for Multiple Modes and Different Purposes, Report No. 4 [online] [accessed on 07.10.2012.]. Available: <http://www.lrrb.org/PDF/200811.pdf>
- Inskeep E. (1994) *National and Regional Tourism Planning: Methodologies and Case Studies*. London: Routledge, 249 p.
- Jāņa sēta (2006) Dienvidlatgale. Latvijas tūrisma kartes - Tourism maps of Latvia. Scale 1:20000. Rīga: SIA Karšu izdevniecība Jāņa seta, 1 p.

- Jongman R.H.G. (2002) Homogenisation and fragmentation of the European landscape: ecological consequences and solutions. *Journal Landscape and Urban Planning*, Vol. 58, Issues 2–4, p. 211–221.
- Kaminska R. (2008) Austrumlatvijas rekatolizācija un tās ietekmētais baznīcu arhitektūras un mākslas mantojums. In: *Sakrālā arhitektūra un māksla: mantojums un interpretācija*. K. Ogle (ed.). Rīga: Neputns, p. 31-47.
- Kaminska R., Bistere A. (2006) *Sakrālās arhitektūras un mākslas mantojums Daugavpils rajonā*. Rīga: Neputns. 296 p.
- Kaminska R., Bistere A. (2011) *Sakrālās arhitektūras un mākslas mantojums Rēzeknes pilsētā un rajonā*. Rīga: Neputns. 335 p.
- Krūmiņš A. (2003) *Latgales koka baznīcas Romas katoļu draudzēs 18. Gadsimtā*. Rīga: Jumava. 192 p.
- Landecker H., Mayer E.K., Vance S. (1998) *Marta Schwartz: Transfiguration of the Commonplace*. Washington, D.C.: Spacemaker Press. 175 p.
- Latvijas Mazās hidroenerģētikas asociācija (2008) *Mazā hidroenerģētika Latvijā*. Rīga: SIA Adverts, 96 p.
- Latvijas Republikas Centrālā statistikas pārvalde (2012a) Centrālās statistikas pārvaldes datu bāze. ISG12. Pastāvīgo iedzīvotāju skaits statistiskajos reģionos, republikas pilsētās un novados gada sākumā [online] [accessed on 20.12.2012.]. Available: <http://data.csb.gov.lv/DATABASE/ledz/databasetree.asp?lang=16>
- Latvijas Republikas Centrālā statistikas pārvalde (2012b) Centrālās statistikas pārvaldes datu bāze. TUG091. Viesnīcas un citas tūristu mītnes Latvijas statistiskajos reģionos, republikas pilsētās un novados [online] [accessed on 18.12.2012.]. Available: <http://data.csb.gov.lv/DATABASE/transp/Ikgad%C4%93jie%20statistikas%20dati/T%C5%ABrisms/T%C5%ABrisms.asp>
- Latvijas Republikas Centrālā statistikas pārvalde (2012c) Centrālās statistikas pārvaldes datu bāze. TUG16. Tūrisma komersantu apkalpoto personu skaits Latvijas statistiskajos reģionos [online] [accessed on 18.12.2012.]. Available: <http://data.csb.gov.lv/DATABASE/transp/Ikgad%C4%93jie%20statistikas%20dati/T%C5%ABrisms/T%C5%ABrisms.asp>
- Lazdāne L. (2011) The Historical Development of Watermills and small-scale Hydroelectric Power Plants Landscape in Latvia. In: *Research for Rural Development 2011. Annual 17th International Scientific Conference Proceedings*. Latvia, Jelgava: Latvia University of Agriculture, Vol. 2, p. 200-206.
- Lazdāne L. (2012) Public Perception about Landscapes of Watermills and Small-Scale Hydroelectric Power Plants in Latvia. In: *Research for Rural Development 2012. Annual 18th International Scientific Conference Proceedings*. Vol. 2. Latvia, Jelgava: Latvia University of Agriculture. p. 141-147.
- Likums ‘Par autoceļiem’ (1992) pieņemts 11. 03. 1992. (Ziņotājs, 13, 02.04.1992.) [stājas spēkā 02.04.1992.] ar grozījumiem: [stājas spēkā ar 01.01.2012.] Latvijas Republika [online] [accessed on 10.11.2012.]. Available: <http://www.likumi.lv/doc.php?id=65363>
- Markots A. (2011) Plakanvirgas pauguru morfoloģija, uzbūve un veidošanās apstākļi salveida akumulatīvi glaciostukturālajās augstienēs Latvijā. Promocijas darba kopsavilkums [online] [accessed on 18.12.2012.]. Available: http://www.lu.lv/fileadmin/user_upload/lu_portal/zinas/Kopsavilkums-Aivars-Markots.pdf
- Markova M. (2012) Characterization guidelines for churchyard in Latgale Upland. In: *Peer reviewed proceedings of ECLAS 2012 Conference - The Power of Landscape at Warsaw University of Life Sciences – SGW*. Warsaw: Warsaw University of Life Sciences, p. 59-64.
- Melluma A. (2012) Historical Contexts and Development Paths of Latvian Landscapes [online] [accessed on 18.12.2012.]. Available: http://www.lza.lv/LZA_VestisA/66_3/5_Aija%20Melluma.pdf
- Pearce D.G. (2012) *Frameworks for Tourism Research*. New Zealand: Victoria University of Wellington, 224 p.
- Peneze Z. (2009) *Transformations of the Latvian Rural Landscape in the 20th and 21st Centuries: Causes, Processes, Tendencies*. PhD Thesis. Rīga: Latvijas Universitāte.
- Raitis J., Virsnieks R. (1944) *Lauku dzirnavas*. Otrais iespiedums. Rīga. 10 p.
- Reenberg A., Primadahl J. (2009) Editorial: Globalisation and the local landscape [online] [accessed on 21.12.2012.]. Available: http://rdgs.dk/djg/pdfs/109/2/Pp_iv-vi_109_2.pdf

- Silķe K. (2008) Ūdens enerģijas izmantošanas vēsture Latvijā. In: *Mazā hidroenerģētika Latvijā*. Rīga: SIA Adverts, Latvijas mazās hidroenerģētikas asociācija, p. 6-11.
- Teivens A. (1985) *Latvijas dzirnavas*. Stockholm: Daugava. 298 p.
- Thompson C.W., Takemi S., Bell S., Millington C., Southwell K., Roe J., Aspinall P. (2007) Landscape quality and quality of life [online] [accessed on 18.12.2012.]. Available: http://www.openspace.eca.ac.uk/conference2007/PDF/Summary_Paper_CWT_31_Aug_07.AB_edit.pdf
- Yatsko M.S. (1997) Ethnicity in Festival Landscapes: An Analysis of the Landscape of Jaialdi '95 as a Spatial Expression of Basque Ethnicity, Master's Thesis [online] [accessed on 18.12.2012.]. Available: http://scholar.lib.vt.edu/theses/available/etd-2230102449761431/unrestricted/etd5_chap2.pdf
- Zariņa A. (2008) *Vietas ainavas raksturs un tā izmaiņas attīstības pēctecīguma teorijas perspektīvā. Landscape path dependency: landscape development's historical and biographical aspects in Latgale [Latvia]*. Promocijas darbs. PhD Thesis. Rīga: Latvijas Universitāte. 91 p.
- Мейронс З. (1975) Рельеф Латгальской возвышенности и сопредельных районов Восточно-Латвийской низменности. – В кн.: *Вопросы четвертичной геологии*, 8. Рига: Зинатне, с. 48-81. (In Russian).

FLOODING AS A MEANS OF MILITARY DEFENCE: LANDSCAPE OF THE 20TH CENTURY FORTRESS WROCŁAW

Lukasz Pardela

Ph. D., Eng., Wrocław University of Environmental and Life Sciences,
Department of Environmental Engineering and Geodesy, Institute of Landscape Architecture
E-mail: lukasz.pardela@up.wroc.pl

ABSTRACT

The article presents the historical importance of the military flooding system around the city of Wrocław (Breslau) at the beginning of the 20th century. The research was carried out in the years 2010-2012 to investigate the elements of the former “barrages d'eau” (Archives de la Societe des Nations, 1920b) of Fortress Wrocław (Festung Breslau), situated on the River Odra. The author of this paper focuses on the structures built along the following two Odra tributaries: the Widawa and the Ślęza. On 9 May 1889 a decision on the modernisation of the fortress was made (Bayerische Hauptstaatsarchiv, 1911). From that moment on, the city was repeatedly renovated network in order to maintain its military effectiveness. To allow defensive flooding operations in the foreground areas in both sectors of the fortress, a number of hydrotechnical structures were erected. At the same time after the great flood of 1903, large earthworks were launched. The construction of weirs on the River Widawa coincided with the necessary expansion of the city's flood control system. Both, the fortress weirs and the canals with sluices, became an important part of the modernized system of the Wrocław Water Junction. This improvement was of major importance to the fortification of the fortress's right sector. However, Fortress Wrocław was never completed and during the Great War fortress weir's were never used for military purposes. Today the fortress weirs constitute a historical value as part of the hydrotechnical heritage.

Key words: military flooding, fortress landscape, festung breslau

INTRODUCTION

Wrocław's geographical location, with its high density of the river network, was favourable for defence. As far as the history of military conflicts is concerned, intentional floodings were crucial for defence (Pardela et al., 2012). Engineering work could be used to combine artificial and natural obstacles in roads and weirs *designed or employed to disrupt, fix, turn, or block the movement of an opposing force, and to impose additional losses in personnel, time, and equipment on the opposing force.* (Department of Defense, 2010). Guard-protected hydrotechnical structures were necessary to control the water level of defence flooding on rivers, streams and polders.

On 14 June 1910, Wrocław (Breslau) was officially named a 2nd-class fortress (*Festung Breslau*) (Bayerische Hauptstaatsarchiv, 1911). The principal line of resistance that included *Festung Breslau* as well as other fortresses, e.g. *Festung Custrin* and *Festung Stettin*, ran along the Odra River, from north to south, along the eastern border of the German Empire.

The author of this paper focuses on landscape transformations resulting from historical flooding structures deployed for military purposes, i.e. with a view to defending the 20th century *Festung Breslau* and two Odra tributaries: the Widawa (*Weide*) River and the Ślęza (*Lohe*) River (*op. cit.*). The overall aim of the research was to investigate the historical background of the river landscape around the

fortress to define the defence flooding range by using ongoing simulations with HEC-RAS flood flow models.

RESEARCH METHODS

The Archives

The analysis of the local historical military structures and the Widawa and Ślęza river landscapes, which failed to attract scientists' interest for almost seven decades, was started by collecting historical data available at various archives located in the cities of Wrocław, Berlin and Geneva. The principal, pioneering archival research was conducted between March 2010 and June 2012 and was aimed at acquiring copies of the original drawings and cartographic materials related to the defence weirs and the hydrotechnical aspects of Wrocław's river network. The archival study was carried out at the State Archives in Wrocław, the Departmental Archives of the Lower Silesian Land Drainage and Water Structures Management Board, the Departmental Archives of the Regional Water Management Board in Wrocław, the Herder Institute collections, the Berlin State Library – the Prussian Cultural Heritage, and the Secret State Archives of the Prussian Cultural Heritage in Berlin. The most valuable source materials, including detailed drawings of the weirs, among other things, were obtained by the author from the Military Inter-Allied Commission of Control in the

League of Nation Archives in Geneva in September 2012 (Archives de la Societe des Nations, 1920a).

Terrain works

The secondary, exploratory research consisted in fieldwork aimed at locating and identifying weirs on the Ślęza and the Widawa. This was undertaken between November 2010 and June 2012. All the locations of the defence weirs and other fortifications were classified as secret and so were not marked in the relevant sources. The author was searching for the locations on the basis of old military plans and descriptions of the fortress, i.e. 20th-century schematic maps, and aerial photographs taken in 1944 and 1947. However, the river landscape changed over time, depending on the season. The sites were overgrown in the summer and the metal frames and concrete or stone walls were hardly visible. All recognized historical hydrotechnical structures were measured, described and photographed during various times of the year. The collected data were catalogued and compared with old drawings and manuscripts gathered during secondary research (*op. cit.*).

MILITARY AND FLOOD PROTECTION ASPECTS

The fortress, being a complex system, needs more attention to prevent simplifications when discussing its operation. As a sub-discipline, 'military history' is often neglected by researchers, who concentrate instead on architecture, heritage protection, hydrotechnical or landscape aspects. In order to analyze 20th century landscape related to flooding operations, some elementary guidelines were adopted. The study covered some military aspects, e.g. those contained in handbooks for German pioneer units D.V.E. 230 some general military solutions, and technical manuals presenting typical fortification erection methods (*Technische forschrift*). The following information can be found in one of the field fortification manuals: '*It is possible to raise the effectiveness of water obstacles through piling them up if they exist or if it is possible to direct the inflow out and to close the drain hole. However, flooding the neighboring terrain improves the obstacle. Any structures for damming the water should withstand the associated pressure and be protected against softening or being washed away*', and '*The top of the weir should reach 0.5 m above the planned water level; in the case of earth dams it is sufficient if the embankment is 1-2 meters higher than its width. If possible, embankment slopes should be flat. Depending on the terrain, more than one flooding polders may be necessary to create a defence flooding line. In order to prevent the dam from being flooded or washed away, supporting installation made of channels or pipes should be*

provided to drain excess water and to ensure the stability of river banks' (Wichrowski, 2005).

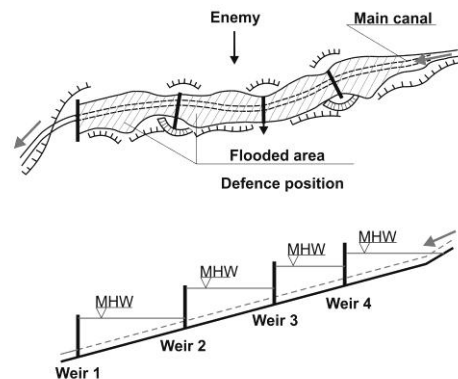


Figure 1. The flooding scheme (Source: Ministry of Defence, 1991)

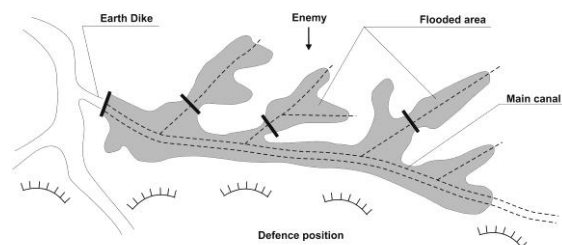


Figure 2. Turning the land along the river into a swamp (Source: Ministry of Defence, 1991)

Most attention was paid to a comparison of the guidelines discussed in the Fortress Combat Guide (1911) with the floodings of the Fortress Wrocław, which enabled the defence characteristics of the city and its surrounding landscape, hidden from non-military people, to be noticed. A highest cabinet order (*Allerhöchste Kabinetts-Ordre*) of 9 May 1889 (*Bayerische Hauptstaatsarchiv, 1911*) initiated the process of planning new fortifications around the city, and dividing the fortress into a left sector and a right sector along the Odra. On 10 October 1889, the Engineering Committee of the Main Inspection of Fortresses and German General Staff (*Generalstab*), decided, among other things, to erect dams on *Schwarzwasser* (Czarna Woda), the *Weide* and *Lohe* rivers. Between 1890 and 1901 main infantry shelters (*Infanterie Raum*) in Wrocław were constructed, and between 1906 and 1912, they were upgraded and converted into infantry forts (*Infanterie Stützpunkt*). Plans were drawn up to build other field fortifications during fortress mobilization. Following a disastrous flood in the summer of 1903, the right sector of the fortress was redeveloped in 1914, and received an extra line of ten group shelters (*Unterkunft*), expanding the defence eastward. But at the same time, the floodwater essentially proved its strength, so the military authorities had a clearer view of the

importance of flooding used for defence purposes. After that, the city began to build new protective structures along the Widawa River valley, and to replace the meandering stream of the Czarna Woda with new canals added to the Wrocław Water Junction. The construction work was started in 1912 and completed one year before the Great War ended. (Born, 1948). After 1912, the lower course of the Widawa river became part of the Wrocław Floodway System, which had a hydraulic capacity of 2,300 m³/s, and a portion of the discharge amounting to 150 m³/s was dropped from the Odra to the Widawa by the Odra-Widawa discharge channel. (Parzonka, 2012) What was the significance of the weirs and the other defence flooding structures to the fortress itself? The natural barrier in the north-western section of the fortress was strengthened with a new important artificial obstacle. Simultaneously, in the left sector the natural valley of the Ślęza River was turned into a defence line as well. However, the fortress weirs were not used during the Great War.

THE FORTRESS WEIRS

The first fortress weir in Cavallen (Kowale) was ready to be built just after the regulation work was officially approved. Between 1913 and 1915, a total of 14 fortress weirs were erected on both rivers – nine on the Widawa, and five on the Ślęza (Politisches Archiv, 1920).

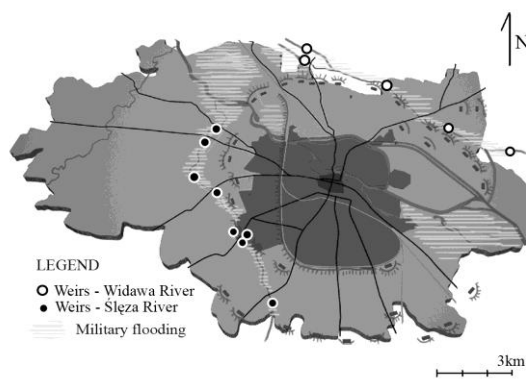


Figure 3. The scheme of the Fortress Wrocław defensive flooding in 1914. (Source: the author)

The following three types of constructions were mainly used: a needle weir (*Nadelwehr*), a stop log weir (*Dammbalkenehr*) and a sheet pile weir dam (*Schützenwehr*). The structure names (*St. W*, *St. W I-XII*, *St. W XI a*) did not reflect their types or locations, which most probably were regarded as military secret. All fortress weirs dammed the river flow and caused the backwater effect, increasing the base flood elevation and the distance for which the effects extended upstream. The fortress weirs had to be low to avoid detection by enemy artillery

observers located on hills surrounding the fortress or in balloons. The structures fulfilled the same function as typical civil weirs, i.e. they dammed the river flow, serving to regulate the water level or to measure the river flow (Licker, 2003). The description of each civil weir contains the following information: the state of repair, the operating status



Figure 4. The fortress weir no IV (*Schützenwehr - St. W. IV*) with armour steel plates, 2012 (Source: photo by the author, 2012)



Figure 5. The fortress weir XI (*Nadelwehr - St. W. XI*) in a state of major disrepair, 2012 (Source: photo by the author, 2012)

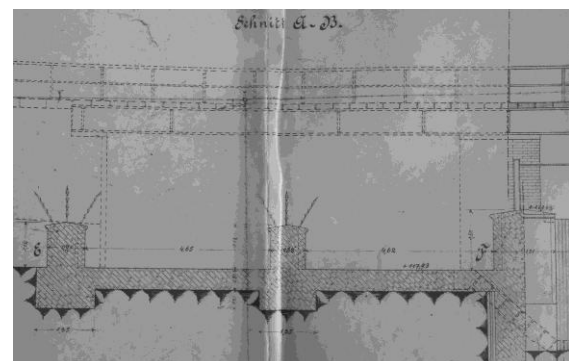


Figure 6. The steel picks of the underwater barbed wire obstacle (*St. W. XI a*) (Archives de la Société des Nations, 1920b)

and the water lifting level. Based on the typical weir structure, the following technical data were recorded during the cataloguing of the fortress weirs: the foundation, the still and stilling basin, upstream and downstream slope protections, pillars, weir heads and bulkheads, dykes, and earthen embankments. Some differences in construction were noted (Pardela et al., 2012). Furthermore, in the case of the military weirs the following were also taken into account: armour steel plates, steel fencings and land or underwater barbed wire netting protecting the structure against sabotage or demolition (Deutches Reich, 1911), guardhouses with telephone communication, alarm installations, and field fortifications with infantry positions around the weirs.

THE LANDSCAPE AND THE LAND USE

The military landscape of the 20th century Fortress Wrocław was carefully designed to prevent the enemy from discovering the exact positions of the forts and shelters. All military zones were overgrown with tactical clusters of local tree and shrub species that ensured extra protection by natural camouflage (mimetism and mimicry features). The weakest, southern front of the fortress was protected by a high rail embankment equipped with five positions prepared for artillery. The cultural landscape, nowadays defined as cultural properties representing the combined effect of nature and human labour. (World Heritage Convention, 1992), in the case of the fortress was shaped by a piece of restrictive legislation known as *The Act on Limiting the Ownership of Land in the Vicinity of Fortresses*, promulgated on 21 December 1871. Under the Act, on 4 April 1910, zones (so-called *rayons*) were established in the Fortress Wrocław. According to the Act, all infantry forts and shelters along the Widawa and Ślęza rivers were subject to building restrictions; the ring of forts in the case of the Fortress Wrocław had a protected zone 2,250 meters deep (rayon I – 600 m, rayon III – 1,650 m) (Deutches Reich, 1871). The weirs constructed within the reach of rayon I had a massive impact during construction and operation, *inter alia*, on landscape, land use and the environment.

Changes in soil moisture levels lowered agricultural productivity, and loss of vegetation growing in or alongside the rivers resulted in losses to the associated animal communities. The rural valleys along the rivers could be intentionally flooded or turned into marshes by receding floodwater.

Shallow ponds were supposed to repel the invader's cavalry (e.g. the Russian cavalry establishment, which was the largest of all among the nations fighting in 1914), infantry and light artillery carts (horse-drawn artillery guns) by preventing or delaying military manoeuvres (Pardela et al., 2012).



Figure 7. The ruined fortress weir (St. W. I), 2010
(Source: photo by the author, 2010)



Figure 8. The fortress weir (St. W. X), 2010.
(Source: photo by the author, 2010)

After the Second World War, the Ślęza river valley was radically redeveloped in line with the flood-protection regulations, so the natural rural landscape vanished. The historical landscape of the Widawa also changed after the city's northern beltway was constructed.

CONCLUSIONS

Nowadays, the Wrocław Floodway System is being modernized to enable trouble-free passage of 3,100 m³ of water per second through Wrocław and via the Odra-Widawa discharge channel (Parzonka, 2012). The digging and expansion of the channels influenced landscape, heritage, nature conservation fisheries, water quality, and recreation. Concrete structures are frequently an eyesore, but some, which are partly made of stone, blend well with the landscape. The fortress weirs constitute an outstanding historical value and comprise a number of untypical design solutions. The rehabilitation of the existing weirs, especially those located on sites of historic importance along the Widawa River, offers an opportunity for further research thanks to archaeological exploration. None of the weirs were officially regarded as part of the listed historic

landscape. So the first step taken by the author aimed at protecting two of the best preserved fortress weirs (*St. W. IV* and *St. W. XI*) after the pioneer research was completed was to put them on the list of protected structures in accordance with Articles 5 and 21 of the Polish Monument

Protection and Care Act of 23 Jul 2003. The landscape of the Widawa river valley was not changed for almost a century until the last decade. Is the rehabilitation of the exiting, hydrotechnical heritage of the fortress weirs possible? Only time will tell.

ACKNOWLEDGMENTS

This study was part of a bigger project funded by the Ministry of Science and Higher Education under the research project entitled 'The impact of Wrocław's river network on the city's fortifications created at the turn of the 20th century, with a special focus on defence weirs' (N N305 363738). The study was conducted in cooperation with the Institute of Environmental Engineering and was led by Prof. Włodzimierz Czamara, Jacek Śląski helped with the English translation.

REFERENCES

- Archives de la Societe des Nations (1920a). COL 64. *Dossier de recensement place de Breslau*, Fascicule I. *Ogranisation generale de la place. Annexe No I*
- Archives de la Societe des Nations, Geneve (1920b). COL 64. *Dossier de recensement place de Breslau*, Fascicule VII. *Dispossites des barrages d eau. Annexe No VII/1*, p.1
- Bayerische Hauptstaatsarchiv (1911), Munchen, Mkr 4605/2. *Die Entwicklung des Deutschen Festungssystem seit.1870*, Denkschrift, p. 236
- Cornish, N. (2001). *The Russian Army 1914-18. Men-at-Arms*. Osprey Publishing, 13 p.
- Department of Defense (2010), *Dictionary of Military and Associated Terms*, Joint Publication 1-02, 213 p. [accessed: 2.02.2013]. Available: http://www.dtic.mil/doctrine/new_pubs/jp1_02.pdf
- Deutches Reich (1871). *Gesetz, betreffend die Beschränkungen des Grundeigentums in der Umgebung von Festungen* vom 21. Dez. 1871. Reichsgesetzblatt, Berlin. [accessed on 2.01.2013] Available: http://commons.wikimedia.org/wiki/Category:Deutsches_Reichsgesetzblatt_1871
- Deutches Reich (1911). D.V.E. 275. *Feld-Pioneerdienst aller Waffen*, 12.12.1911. pp. 161-164
- Licker, M.,D. (ed.). (2003). *Dictionary of Engineering* McGraw-Hill. New Jersey. 614 p.
- Ministry of Defence. The Command of Military Engineering (1991) *The Manual for Military Engineering and all sorts of the army and departments*, Warsaw, 284 p.
- Pardela, Ł., Stodolak, R., Olearczyk, D., Czamara, W. (2012). *The hydrotechnical structures of Wrocław fortifications . Structural Analysis of Historical Constructions*. Vol. 2, 1226 p.
- Parzonka, W. (2012). *Rola kanalu zrzutowego Odra - Widawa dla ochrony przeciwpowodziowej miasta Wrocławia*. 6 p. [accessed on 1.03.2013.]. Available: http://www.donnees.centre.developpement-durable.gouv.fr/symposium/expose/SP3-13_pol.pdf
- Politisches Archiv des Auswärtigen Amts Berlin (1920), Bonn, II-FM 152/10, F 6/1, *Erlauterung über die Festung Breslau*.
- The Library of the University of British Columbia, LPA B08A, (1910). *Deutsches Reich, Kriegsministerium Anleitung für den Kampf und Festungen* 13.07.1910, Ernst Siegfried Mittler und Sohn, Berlin
- Wichrowski, M. (trans.), D.V.E. 230. (1906). *Felbefestigungs Vorschrift*, 28.06.1905 Berlin,. Poznań, 2005, 10 p.
- World Heritage Convention (1992). *Cultural landscape* [accessed on 10.05.2009]. Available: <http://whc.unesco.org/en/culturallandscape/online>

THE ROOF LANDSCAPES, THE HISTORIC CITY CENTRES AND CONTEXTUAL SEARCHES OF THE GREEN STRUCTURE

Aija Ziemelniece

Latvia University of Agriculture, Department of Architecture and Building

E-mail: aija@k-projekts.lv

ABSTRACT

The expressiveness of the historic urban space alongside with the shape of the outer facades of the building is largely determined by the roof landscape and its separate compositional elements – color, the form of the cover, the pitch game of the roof plane, the roof pitch or the building's turn to the rest of the building construction, roof constructions, chimneys, etc.. The lower is the construction, the easier it is to read the roof character. Both groups of the big trees have often broken in the old building construction where the foliage masks the perception of expressiveness of the historic space, narrowing the view angle and obscuring the silhouette of the wooden building construction of the street. This is particularly true in areas where wooden buildings have disappeared from the continuous building construction, being replaced by tree seedlings which, not removed in a timely manner, form huge sizes covering facades of buildings but the root system and the amount of leaves destroy the constructive structure of buildings. Getting used to it every day, the location of the tree is assumed to be correct. Without going into detail of the structure of the historical composition of the urban constructed space, series of faulty assumptions are formed that undermine the expressiveness and harmony of the urban space.

Key words: urban structure, urban landscape, roof landscape, wedges of green plantations, green structure, visual aesthetics and quality, contextualism, harmony

INTRODUCTION

The urban planning organizes the space in which a human being will live. Architecture is also a compromise between the man-created space and natural environment. Thus, as the attitude and requirements of the society towards architecture are changing, architecture changes on the whole. The dominant instrument in the architect's work, instead of the empirical proof or theories, is creativity as the main driving force (Rukmane-Poča, 2011).

Any inhabited locality has its own physical structure and symbolical identity which may be weak but the urban landscape often forms the city's uniqueness, therefore great importance is given to the creation of aesthetical quality of the urban environment. The city has to be flexible in relation to perception habits of users and change of the function and meaning. The city is a continuous and complex form, which, at the same time, is chaotically changing (Liepa-Zemeša, 2010).

With the increase of pace of life and the amount of daily sociability of space and time, people are increasingly looking for support and comfort in the harmony of their internal environment. The supporting point in the urban space is commonly found in the historical building zone, the scale, color, form, rhythm, the semantics of which is psychologically very readable. The old pavement makes to slow down the pace and enhances the emotions instigated visually by the overall urban construction ensemble (Strautmanis, 1977).

A link is created where the external spatial environment stabilizes the human inner world. The

scale and proportions are features that by themselves are able to give to the informational structure of the spatial environment an unprecedented and unique individuality. A sense of scale or the ability to compare the dimensions of the external space and its elements with human dimensions essentially belongs to the information in the formation and development of which a great importance is given to personal experience (Strautmanis, 1977). The sense of scale is inextricably linked to the sense of proportion and it will always stimulate harmony of the spatial environment (Strautmanis, 1982).

The elements belonging to the urban space - engineering constructions, advertising displays, small forms of architecture, cars, greenery, trees - with their vast diversity of forms and composition, existing within a definite architectural spatial framework, generally form a spatial substantiative environment in which our life is going on (Strautmanis, 1982).

MATERIALS AND METHODS

People assess the space around them intuitively, looking for an element that could stabilize the mental and physical comfort of their internal environment. It is important that the users could perceive it clearly and mentally abstract and structure it in space and time. It must be linked to the values of residents. If the town loses its notion and accuracy, it becomes more difficult to be understood (Strautmanis, 1977).

The expressiveness of the urban construction space of the 80s and 90s of the 19th century of Bauska, Jelgava and Kuldīga is characterized by a similar architectural compositional image of the building construction that highlights the stylistic trends and the scale of the building construction period that is vividly marked by the roof plane pitches and their covering material. For the method of research, there are used the research results of individual building blocks of the historical parts of the above towns derived by comparing the existing situation of building construction with the character of the gone or partially transformed historical building construction. The material under examination includes the results of the architectural survey of the old building construction where the dominant view lines are evaluated and compared with the perception of the roof landscape, amount of the green plantations and their locations in the historical center.

By the evaluation of existing tree planting areas and architectural shape of the historical building construction, there is explored the context of the urban construction environment which consists of several spatial elements – a tree plantation line along the street, a backyard with a garden, the tree height, their spacing, foliage density, color in seasons and its accent in the silhouette of the building construction, etc.. For the historical centers of Bauska, Jelgava, the harmony of the compositional elements is different but in the research a number of similarities are used between these towns which affect the construction time, architectural and stylistic trends, intensive conservation and tree planting time during the post-war years.

Describing these dimensions, there is an opportunity to analyze the shape of the historical space where the results of the research are important in the aspect of further urban planning and restoration works.

RESULTS AND DISCUSSION

Nowadays, not only the general knowledge of comfort and its determining factors is widening, but changes are taking place in the human requirements and attitudes to the closest surroundings (Strautmanis, 1977).

The architecture acts as information that creates a spatial environment and it is able to influence a positive formation of the public emotions (Strautmanis, 1977). Any spatial form has its own information. The ambient urban construction environment is an endless source of signals that people perceive as

something in its own right to understand. This set of signals which reflects quality of the environment is the most important part of the information exchange process of our psyche and spatial environment (Strautmanis, 1977).

The expression of the building construction of the 80s and 90s of the 19th century is most vividly marked by the ridged planes of roofs of houses that have survived in the towns of Courland which have not undergone serious war damage. The historic centers of Aizpute, Kuldīga, Alsunga, Grobiņa, etc., are characterized by a building construction, the height of which does not exceed two storeys. The basis of the architecturally - constructive shape of the facades of buildings is wooden stand, wooden corner-jointed and brick buildings with board sidings or mortar plastering on splints. In order to obtain research materials, for the needs of comparison there were used separate old building blocks in the historical centers of Kuldīga, Bauska and Jelgava. The research was based on the main view lines of courtyards and some of the street segments with tree plantations and without them.

Examining individual fragments of the old town street building, a number of arguments were selected, concerning the harmony and balance issues of the urban space:

- The trees and the green planting context in the scale of the building construction;
- The nature of intimacy for the building zone of the historical construction;
- The opportunities of perception of the roof landscape.

In the example of Bauska, the historical Riga street has been surveyed. This street is characterized by a continuous 1 - 2 storey buildings without street plantations and it has been developed in parallel to the Mēmele river, creating a visual association with the water landscape. Such street location of the urban construction character gives it the opportunity to develop a promenade, the uniqueness of which is possible to supplement with the base of the natural elements or the green - blue wedge expression. Between the street and the river a continuous building construction is located, which distances the promenade from the water's edge in about 50 m in width. For the landscape space of Riga street, in the postwar years a number of the historic building interruptions have appeared, allowing the development of the green zone. Evaluating the tree scale and proportion, it is evident that some of them cause a visual disharmony and quench in the view line to perceive expressiveness of the architectural form creation.



Figure 1. The tree cover that hides the historic building construction of Riga street (Author's photo, 2012)

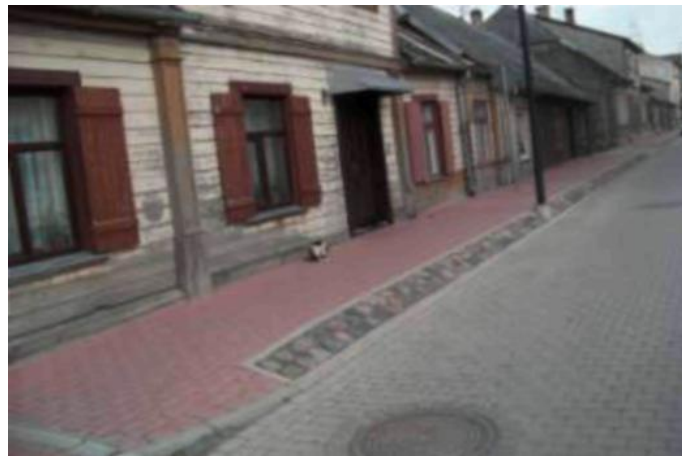


Figure 2. The roof landscape and the colouring scheme of the street structure. Bauska, Riga street (Author's photo, 2012)



Figure 3. Bauska, Kaleju street. The wooden building construction losing its building, in its place there is a self-growing tree. (Author's photo, 2012)

In the building construction of Riga street at the Town Hall Square (33 Riga street), by the river side a green zone approximately 30 m in width has been created, enabling to spatially interconnect the square and the water landscape. At present, the view lines to the river are broken by the tree and

shrub cover, hiding the expressiveness of the brick architecture of the building at 37 Riga street. While at this point, it is not visually seen that about 30 m away, there is a picturesque view to the the river bluff with rapids that should be exposed, spatially searching the context with the building construction

of the Town Hall Square. Historically this point was important since it served as a place where the goods were unloaded from the boats and taken to the marketplace. Creating a wide lawn zone in this place, visually there would be obtained continuation of the Town Hall Square. For the new Town Hall Square cover in this place, a wedge pattern has been built that emphasizes the historical walk from the river to the square. Moving through Riga street eastwards or along the upstream of the Mēmele river, on the side of even number by 60 m there is a green square with recreational zones. It is created with tree plantations distanced from the red line of the street and covers about 50 m long zone along a pedestrian sidewalk. The square has appeared after disappearance of the wooden building construction in this place. Its scale and green plantations are balanced with the adjacent historic building construction and it is not overpowering it.

From the square, up Riga street there dominates a dense one-storey wooden building construction with roof constructions, giving the street a romantic feeling of a small town. Thanks to the small height of buildings, the roof plane landscape is readable. During the postwar years, the roofs had lost their historical colour and structure which was given by the red clay tiles or tin and they are replaced by gray slate sheets. Opposite the building of 16 Riga street, approximately in a band about 80 m long, the compositional expressiveness of the building construction of the street is absorbed by the existing

brick fence along areas of production area, creating monotony of forms. Here architecturally new composition solutions are possible, that could save the flow of the building construction scale and harmony. The buildings of 20 Riga street and 22 Riga street continue the character of the historic building structure with expressive roof constructions. In the distant view lines, the roof plane game of both buildings is not visible as it is covered by a group of maple trees planted in the red line zone of the street. The same is true for the viewpoints in the opposite direction of the street where maple trees are hiding the roof landscape of 16 Riga street and 18 Riga street.

By the architectural expression of the buildings being hidden behind the tree foliage, the balance and rhythm of the scale of the building construction are lost. This is true not only in the summer time but also during the rest of the season as the branches of trees without leaves are visually heavy and overpower fragility of the building facades. The nature of the branches of the trees competes with the facade elements - window shutters, door panels, wall board sidings, pitches of roof constructions providing additional shading.

The character and harmony of the roof constructions on both sides of the street in the short view lines are readable in the houses at 20, 43, 41, 39 Riga street. Between the buildings No. 43 and 45, the partially hidden household yard with wooden sheds opens the view to the river landscape.



Figure 4. The roof landscape of the old town of Bauska missing the convincing red roof tile dominance (Author's photo - 2012)

By disappearing of the building construction between the buildings at 22 Riga street and 24 Riga street, in the post-war years, at the street side 8 linden trees have been planted, the huge crowns of which have toppled to the side of the road and cover the street in the eastern part of the building construction. The scale of the trees destroys both the composition of the street building and diminishes expressiveness of the adjacent buildings

(the wooden corner-jointed one-story residential building at 47 Riga street).

The interruption of the northern side of the building construction along the river every 60-80 m allows to maintain pulsation in the urban construction space between a natural base and character of the building construction. Under the influence of various spatial transformation processes, the street has a small green recreation pocket that can be

supplemented by the rest functionality - cafes, hotels, crafts and art exhibition centers.

Examining the landscape space of Riga street from the Town Hall Square to the west, as a vertical dominant here must be visible the spire of Ev. Lutheran Ann's church which is marked in the town's silhouette from the right bank of the Mēmele river. The church opposite the building at 21 Riga street is not visible as it is densely covered by massive birch trees and trees of the garden of the Church. Hiding in the dense tree cover zone to the church, a strong visual expression is obtained by the historic building on the street. In this segment the cover reconstruction of Riga street has been completed, bringing in a new colorite, form and structure. In the renewal of the cover, no enclosed concrete kerbs are used, but the rubble line with a slight slope, forming a rainwater collection for the edge of the carriageway. In the segment of Riga street from Kalna street, there is no interruption of the old building construction, therefore the visual interconnection with the Mēmele river is more scarce. The gardens are huddled behind the one-storey building construction and they are not visible from the street. The access to the river is opposite the junction with Baznīcas street where a pedestrian path leads to the river floodplains, past the

courtyards with flower beds. At the junction of Riga street and Baznīcas street, alongside with disappearing of the old building construction in the 70s of the 20th century, a public building is built, which looks heavy against the fragile wooden building construction of Riga street with a romantic facade expression. At the junction of both streets, a recreation zone is located with a successful architecture small form search, stressing the philosophical "turning point" in the city's historic building construction. It is a place where different centuries, thinking and stylistic trends meet. Down Riga street along the Mēmele river, the historic building construction closes with a river meadow and the ruins of the former windmill, in the distance of which the Bauska Castle is visible. The dense tree cover on the left bank of the Mēmele river is interfering with the construction volume of the castle, opening only fragments of it for the view. Consequently, the most powerful culminating point in the view lines of the end of Riga street – the old castle with the slope of the embankment edge – visually is demarcated. Cleaning river floodplain meadows and the steep castle mound from self-sown trees, the town would regain a compositionally strong architectural landscaped space.



Figure 5. Ev. Lutheran Church in Bauska. One of the most expressive dominants in the town, the volume of which is hidden by a dense overgrowth of trees (Author's photo, 2012)

Jelgava City - the old building construction and its roof landscape expression today is associated with only a small part of the historical territory of the town (80s and 90s of the 19th century) which has escaped from the war and the post-war years of devastation. They are individual fragments in the town's northwestern part along Vespilsētas, Kr. Barona and Dobeles streets. The thin old building construction has contributed to the penetration of new buildings in the historic part of the town which is particularly visible in the view lines from 68 Dobeles street. The background of the silhouette is

formed by the nine - storey residential building construction of the 70s of the 20th century but the foreground of the view point – the one-storey volumes of the historical buildings with gabled roof planes and trussed gables in the end pediments. The contrast of the scale and proportions of building construction of the end of the 19th century and the post-war years, and the contrast of proportions as well as the different stylistic trends in the building construction - in the above mentioned view line form a silhouette that marks the transformation process of the urban space. The background shape

of the existing high - rise residential buildings is simple and linear, and their building volumes are distanced approximately 200 m away, without competing with the foreground visible architectural character and scale of the historic buildings, the facades of which are enriched by detailed elements - tiny window panes, shutters, board siding for exterior walls, color tones, lining around of the window opening, roof constructions, etc.. Unfortunately, the old buildings have lost the red clay tiled roofs, thus reducing the expressiveness of the roof landscape. The historical building construction zone and the high - rise residential building area are separated by Lielā street of a transitional character with a regular linden plantation lines and a wide lawn. The current height of trees on Lielā street is small and their crown does not exceed the height of the historic building construction.

Gradually, by disappearing of the old buildings of the second half of the 19th century, green wedges or gardens, lawns or tree plantations have been appearing in their place in the small historical block of houses. These wedges conquer the places where due to the emergency situation the wooden building construction is dismantled (3 J. Asara street). In a few years the green areas are transformed into a new building construction zone, so breaking into the spacing of the building construction of the historical blocks of houses.

The scale expressiveness of the old urban space is most vividly readable in the junction of M. Dambja street and Dobeles street with a building structure line of approximately 60 m long for each of the four bottoms of the street. The street junction of the southeastern part is marked by a two-storey plastered wooden pillar building with a corner bay (1 M. Dambja street, 90s of the 19th century). Beside it, there is an orchard that fills in the missing continuous wooden building construction interruption near M. Dambja street. The distance to the next building along the street is 30 m and visually it creates a street space fragmentation, especially in summers when the green garden expression dominates, wrapping the old buildings in the green foliage (3M. Dambja street).

Similarly, the northeastern part of the junction has been evaluated where the piece of land (68 Dobeles street) has lost the perimetral building construction and the free area is occupied by a large quantity of trees, the foliage of which covers both the backyard and the building construction of the street. Only the one - story red brick building with a luxurious facade has survived which is decorated by a risalite of the central entrance, eight window opening axes with arc-type lintels, roof constructions and a brick cornice ledge. The adjacent street bottom is covered by a wrought granite cobbles (the end of the 19th century). For the mentioned area, a number of projects have been

developed to restore the old building construction on the corner of the block of buildings (Jelgavas ...,2008).

The northwestern part of the junction (2 Dobeles road) continues the historic brick building character. Here one can find 2- and 3 - storey volumes of the former manufacturing buildings that are retracted from the building line of the street, so finding an opportunity to create a small front square in the junction zone of the streets.



Figure 6. The character of the building construction of Old Jelgava (the end of the 19th century)

The factory buildings have lost their historical significance and in the perspective it is possible to create an industrial park there. In the southwestern portion of the junction, the one - story wooden buildings are decorated with an expressive fachwerk pattern in the pediment. Between the buildings at 2 M. Dambja street and 3 Dobeles road in approximately 50 m line there has disappeared the wooden building construction which has been replaced by a kitchen garden along the street. Since there are no large plantations of trees, the view lines are not covered to the building construction's silhouette of Lielā street. Behind the one - story wooden pillar building at 3 Dobeles street, a hangar-type commercial building was built (2005), the proportion of which is too huge and it suppresses the expressiveness of the old building construction. In order to reduce the scale disproportion in the view lines, it is necessary to create a regular line of street tree plantations which will not only hide the construction volume of the supermarket but also compositionally extend the southern part of Dobeles road. In the eastern part of M. Dambja street, the parallelism is created by J. Asara street in which the greatest part of the historic building construction has disappeared, in some places creating 30-60 m long interruptions. Along the pedestrian zone of the western part of J. Asara street – in an approximately 70 m long belt there are gardens, stretching from the courtyard side of the building construction of M. Dambja street. In summers, in the view lines from J. Asara street, the garden merges with the adjacent square and

together with the old block of houses forms a compositionally large green landscape space. The tree canopy height inhibits the scale of the building construction. This is also attributable to the area at 5 J. Asara street where the mentioned green zone merges with the garden on Vecpilsētas street. The existing trees are giant and in summers cover the roofs of Vecpilsētas street in the view lines from J. Asara street. The old building construction's spacing is so overwhelming that the tree and bush groups form diagonal green wedges that cross the street bottoms and compositionally split the area of the old building construction, altering the scale of the historic urban space. The transverse green areas spatially are much wider than the streets, thus disrupting the proportion of the historic structure of the building construction. The 2 - storey wooden pillar building with board sidings at 3 M. Dambja street is the last pile building which is preserved in this street. The constructive position of the building is severely damaged by the huge oaks in its both ends, the canopy of which covers the roof of the building, covering also the historical building construction at J. Asara street and the view lines to the spire of the bell tower of St. Ann's Church. The building construction has disappeared in the piece of land at 5 M. Dambja street as well and it is

covered by self - sowing trees, obscuring the building construction of the southern part of J. Asara street. The scale of the historical building construction of Old Town and its street width is best read between the buildings of 1 M. Dambja street and 3 M. Dambja street. Opposite the old building of 1 J. Asara street, a building at 2 J. Asara street has been restored, describing the width of this street so well. The romanticism of the small street is enriched by the restored carriageway and cobble cover of the sidewalk which are separated by a sloping edge of round cobbles rather than typical concrete borders. The line of trees in front of the buildings at 5, 7, 9 J. Asara street in the distant view lines from Lielā street hide expressiveness of the old building facades, so the trees should be sawn out, leaving only the huge willow which marks the line where once there was the city's rampart with the canal. The building at 9 J. Asara street is situated at the street junction with Kr. Barons street. After reconstruction of the street cover on Kr. Barona street, trees have been planted anew but the overgrown trees are cut down revealing expressiveness of the building construction's facade of the western part of Vecpilsētas street and romanticism of the roof landscape.



Figure 7. The context of different construction periods and architectural stylistics in the view points in Dobeles street, Jelgava (Author's photo, 2012)



Figure 8. The northeastern part of the junction of M. Dambja street and Dobeles street. The lost perimetral building construction line is occupied by a dense tree cover (Author's photo, 2012)



Figure 9. The interruption of the historical continuous building construction line disrupts the compositional character of the urban space. The scale of tree branches suppresses expressiveness of the old building construction
(Author's photo, 2012)



Figure 10. In the junction of M. Dambja street and Kr. Barona street, the tree canopy exceeds the building's crest (Author's photo, 2012)



Figure 11. The brick architecture of the old manufacturing buildings adjacent to the wooden building construction on Dobeles street, Jelgava
(Author's photo, 2012)



Figure 12. The color scheme of Jelgava Old Town in paintings.
Watercolor by Uldis Roga (2002)

During the war, **Kuldiga** was guarded by the Courland front line and the post-socialism time has affected the wooden building structure very little. Consequently, the city's historic center is not characterized by long street building construction interruptions and a vanished old building construction. Panorama of Kuldiga Old Town reflects peculiarities of the natural base and illustrates semantics of the building construction, highlighting the most important in the different periods of time. Determining the protective zones of panorama or silhouette peculiar to Kuldiga is an important object of planning – an individual approach must be followed in areas that succumb to Kuldiga Old Town or due to the relief affecting the view both from it and to it. There are identified several sites that disrupt the harmony of the old town's silhouette (Jākobsone, 2012). Like in Bauska and Jelgava, one of the tasks of the historical part of Kuldiga is to report on the removal of the trees that are to be included in the

conservation and protection program of the old town (Jākobsone, 2012; Dambis, 2012).

In the silhouette of Kuldiga, the church spires play an important role. Now, they are just noticeable in fragments in some of the points of the historical part of the town as a large part of the shrine is hidden by chaotic groups of tree plantations. In the middle part of the historic center at the junction of Baznīcas - Tīrgus-Strautu streets there is situated St. Trinity Roman Catholic Church. Its volume, as a dominant, forms the end of Strautu street but the elegance of the church facade and the spire of the bell tower from Strautu street is not readable as its southern side is hidden behind a dense pine group and linden trees. The shrine's altar part or the eastern side at the junction of Baznīcas-Tīrgus streets is blocked by a huge canopy of deciduous trees. The northern part of the church includes the courtyard space. Thus, the shrine's architectural expression in its perimeter in the viewpoints from the pedestrian zones is not visible.



Figure 13. Kuldiga. The huge tree crowns in year 1905 street (Author's photo)

In the view lines from Pasta street, the tree canopies hide not only the eastern end of the church but also

the buildings of 1 and 3 Strautu street, losing the silhouette of the flow of the building construction

from 2/4 Baznīcas street. The spire of St. Ann's Ev. Lutheran Church is visible in the distance for a moment. In the mentioned view line, by removing trees near the catholic church, the silhouette of the street building construction would reveal its expressiveness between the buildings of 2/4 Baznīcas street and 1 Baznīcas street (city council). This would give a picturesque view point with two church spires. In turn, in the view lines from the church to Strautu street, one-storey wooden buildings with mansard constructions occupy its western side. On the other side of the street there is a square where the tree height is three times higher and suppresses playfulness and expressiveness of the facades of the one-storey buildings. The small width of Strautu street and height of the trees of the square form shading of the street building construction. The large quantity of autumn leaves laying on the roofs of the old buildings damages their cover and board sidings. Density, distancing and height of tree plantations adjacent to the historical building construction are exaggerated. Walking down Baznīcas street in the northern direction, on the odd number side between the old buildings where there are formed interruptions (4-6 m), there are created the so-called green gates that



Figure 14. Kuldiga. Continuation of the street building construction is hidden in the branches of the tree (Author's photo, 2012)

CONCLUSION

In the recovery of the historical centers, not only the restoration work of architectural monuments is important. The visual informative perception in the distant view lines is just as important.. Restoration work includes authenticity recovery not only of the street cover material, coloring and window openings but also considering the density and proportion of location of the green structure. Restoration allows to recover not only the construction volume but also the outer space around it – the recreation zone, the height of the green plantations, their dendrological peculiarities, etc..

link the pedestrian area of Baznīcas street with the square adjacent to Year 1905 street. The green gate or entrance spaces to the square between the buildings at 12 Baznīcas street and 14 Baznīcas street is highlighted by the vine cover in the ends of the building but between the buildings at 14 Baznīcas street and 18 Baznīcas street there are formed circle - shape steps that form the second green entrance gate to the square. As an accent to the entrance there serves the symmetrical position of linden trees, symbolizing the entrance gate. The third enormous - size tree at the end wall of 18 Baznīcas street is removable. It is not only competitive in terms of the scale but the tree branches damage the external wall of the building. At the junction of Baznīcas street and Kalķu street, there St. Catherine's Ev. Lutheran Church is located. As a dominant, it belongs to the longitudinal axis of Kalķu street but it is not visible because of the tree cover in the junction. From the side of Baznīcas street, the church volume is notable only in the street turning place just shortly before the front square of the church which is partially hidden by trees. The gracefulness of the church in the distant view lines is not readable.



Figure 15. The proportion game of the historical building construction and the tree crown in Kuldiga (Author's photo, 2012)

For the planning of the historic urban space, the cultural heritage is an economic value – the resources, which are wisely managed bring ensure an economic benefit. In the current economic situation and in the future, for ensuring preservation of the cultural heritage, the public - private partnership is particularly important.. For the development, which is focused on people's quality of life, a balanced and a long-term approach there is required.

A discussion on the transformation of sites of cultural heritage in order to ensure a wider public access is particularly topical in the last few years

when there has been recognized the particular importance of the cultural heritage in the creation of the quality of life of people. Professionals in the field of cultural heritage are still discussing the admissibility of the transformation of cultural monuments and preservation of authenticity, so a dialogue and consultations are necessary on the

solutions of the accessibility of cultural monuments, respecting all the interest groups involved. Local authorities in particular need more information about positive solutions and the role of the cultural and historical heritage in the recovery of economics.

REFERENCES

- Dambis J. (2012) Jaunā arhitektūra vēsturiskās pilsētās. Ieguvumi un draudi. Zinātniski praktiskās konferences materiāli. Kuldīga.
- Jākobsone J. (2012) *Kultūrvēsturiskais mantojums Kuldīgas pilsētvilē: promocijas darbs*. Rīga: RTU. 17;19 lpp.
- Jelgavas pilsētas teritorijas plānojums 2009.-2021.* (2008). Jelgavas pilsētas pašvaldība [online] [accessed on 20.10.2012]. Available: <http://www.jelgava.lv/pasvaldiba/dokumenti/dokumenti0/attistibas-planosana/jelgavas-pilsetas-attistibas-planosanas-8/index.php?cmd=get&cid=75891>
- Liepa-Zemeša M. (2010) *The Creation Conditions of City Visual Integrity*. Rīga: Scientific Journal of RTU. 10. series., Arhitektūra un pilsētplānošana, Vol 4. p. 57-61.
- Rukmane-Poča I. (2011) *Contemporary urban space in the context of formal currents of architecture*. Rīga : Scientific Journal of RTU, Vol 5. p. 58-65.
- Strautmanis I. (1977) Dialogs ar telpu. Rīga : Liesma. 16, 23, 48, 227 p.
- Strautmanis I. (1982) Māksla arhitektūrā. Rīga : Liesma. 100 p.

LAND MANAGEMENT AND GEODESY

EVALUATION OF INDICATORS OF CADASTRAL ASSESSMENT

Vivita Baumane*, Armands Celms**

Latvia University of Agriculture, Department of Land Management and Geodesy

E-mail: *vivita.baumane@llu.lv, **armands.celms@llu.lv

ABSTRACT

To justify the importance of the indicators affecting the cadastral value, surveys were carried out, by help of which opinions of different respondent groups were summarized. The interviewed respondent groups were real property specialists of municipalities and experts. The thematic blocks of the questions included in the questionnaires are designed with the aim to clarify the quality of the indicators of cadastral assessment models, as well as their significance. The paper summarizes the survey findings about the correspondence and significance of the indicators of cadastral assessment models of land as evaluated by municipality specialists, as well as the assessment and solutions to actual problems are offered. Based on the findings of the municipality specialists' survey and the research results, the indicators for the improvement of cadastral assessment models of building land and rural land offered to the experts' assessment are summarized and evaluated.

Key words: cadastral assessment, cadastral assessment models, indicators of cadastral assessment models, building land, rural land.

INTRODUCTION

Cadastral assessment is a systematic assessment of property groups on a particular date, performing the assessment according to a standardized procedure (Nekustamā..., 2005). Cadastral assessment in Latvia is mainly used for calculating the real property tax.

The value determination models, using the real property data for calculations, explain the value of the property. These models were designed based on the costs, revenue and deals comparison methods. For the cadastral assessment to be implemented, the country should have accumulated stored computerized information about objects and their indicators, the information about real property market deals should be summarized, the assessment procedure and calculation models should be provided by the legislation (Baumane, Parsova 2010).

Due to the limitations of the scientific research the authors have studied improvement opportunities for the assessment models of building land and rural land in their paper from the aspect of the indicators affecting them.

Recognising research (Baumane, 2010; Baumane, 2012) developed a basis for the following hypothesis - the most important indicators provide objective cadastral assessment.

According to the hypothesis, the goal of the paper is to analyze and evaluate indicators for cadastral assessment models. To attain the goal, the following objectives were set:

- evaluate the indicators of cadastral assessment models as assessed by municipality specialists;

- evaluate the indicators of cadastral assessment models as assessed by experts.

MATERIALS AND METHODS

In the study regulatory acts were used, where indicators for cadastral assessment are determined (Kadastrālās..., 2006).

A questionnaire was designed and real property specialists of municipalities were interviewed. The survey was designed to implement a questionnaire about the influencing indicators of the cadastral assessment. The questionnaire included unstructured answer questions and structured answer questions. The questionnaire was implemented with the most widely used electronic questionnaire method. The questionnaire respondents were chosen and inquiry forms were sent to real property specialists of 110 municipalities.

It was necessary to obtain the questionnaire data to be attributable to the respondent groups for determining the sample size. A simple selection case without repetitions can be used, the calculation formula (Krastiņš, Ciemīņa, 2003):

$$n = \frac{t^2 N \nu (1-\nu)}{t^2 \nu (1-\nu) + \Delta_\nu^2 N}$$

where:

- n - selection volume;
 Δ_ν - relative frequency of random error,
or permissible level of materiality;
 t - probability coefficient;

N - number of respondents;
v - relative frequency in selections.

Therefore, the necessary number of respondents was calculated in the selection that the questionnaire obtained would be applicable to the general group. In total 87 respondents were interviewed, that draw up 80% from the total number of municipalities.

The study used expert experience, and in the result processing the American scientist's T.Saaty hierarchical analysis method was applied (Saaty, 1981). Experts included high-level practitioners, experienced specialists and scientists.

Expert assessment of the rural land and building land cadastral valuation model improvement possibilities with the authors' developed algorithm of the hierarchical analysis method, where used for assessment of the influencing indicators of rural land and building land cadastral assessment. The expert working process was based on the authors' matrices. Each pair evaluation for matrices was calculated in special vectors groups, and then the results normalized to 1, so the priority vectors were obtained for the indicators of cadastral evaluation.

RESULTS AND DISCUSSION

The main indicators that characterize the qualitative situation of land are the area of land useful for agriculture (arable land, meadows, pastureland, and orchards) and its amelioration situation. The survey results indicated that actual information on agricultural use of the land is not available in municipality villages or municipalities.

Assessing the correspondence of the qualitative assessment of the useful land (Fig.1), it can be concluded that there is a significant number of municipalities where the qualitative assessment of agriculture use of the land has decreased, but not more than by 5 points, and there are municipalities where the qualitative assessment of agricultural use of the land has decreased by 5 – 10 points.

To improve the data quality of agricultural use of the land qualitative assessment, when summarizing the specialists' opinions, it can be concluded that a large complex of measures should be taken on the state scale, as a result of which the qualitative assessment of the land useful for agriculture would be actualized, as well as the meliorated areas and their functional situation would be recognized.

Whereas, before starting building a complex assessment of the territory should be performed, including the assessment of the geological situation. Geological research is also necessary due to the existence of such geological formations as caving falls and the increase of new territories they occupy. The survey findings indicated that 9% of the municipalities face this problem, but 37% indicated

that the municipality does not have information about the existence of caving falls.

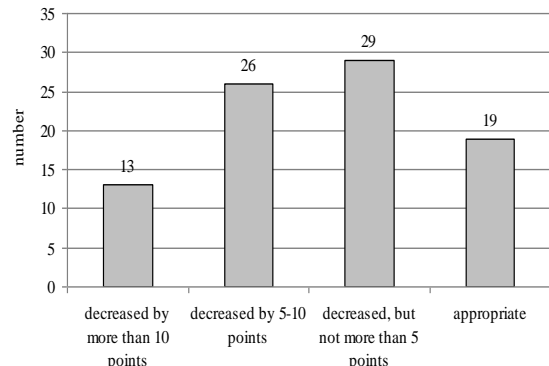


Figure 1. Respondents' assessment of the correspondence of the qualitative assessment of the agricultural use of the land (Source: authors' research assessing every case n=87)

Most of the respondents admit that geological research should be performed with a complex of state level activities (Fig.2), whereas, a similar distribution of answers is observed for the other types of the suggested answer choices. 25 respondents consider that geological research is not necessary and 23 respondents consider that geological research is necessary but only upon the initiative of the owner of the real property.

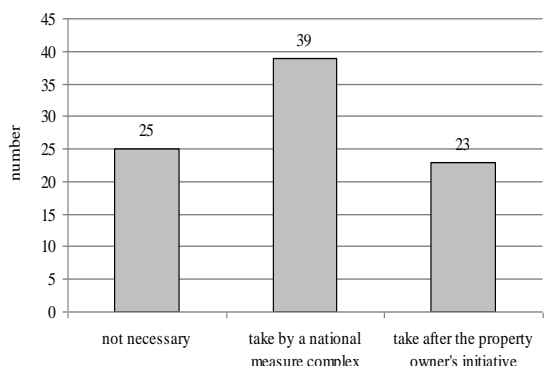


Figure 2. Respondents' assessment about the need of geological research (Source: authors' research assessing every case n=87)

According to laws and regulations, the purposes of use of real property are determined for the purposes of cadastral assessment, therefore, the determined purpose of use of real property should correspond to its actual purpose of use. When assessing the respondents' opinion about the determined purpose of use of real property and their correspondence to the actual use (Fig.3), 44 respondents indicate that the purposes of use determined in their municipalities fully correspond to their actual or perspective use and 35 respondents admit that the determined purposes of use of real property

correspond to the actual use, only with few exceptions, which increases the cadastral assessment.

As the base value has been determined for every group of the purposes of use of real property, to calculate an objective cadastral value, it is very important to determine a correct purpose of use for the real property and its objects, therefore, in some situations it is necessary to propose a change of the purpose of use of real property to a purpose that corresponds to the actual use of the real property.

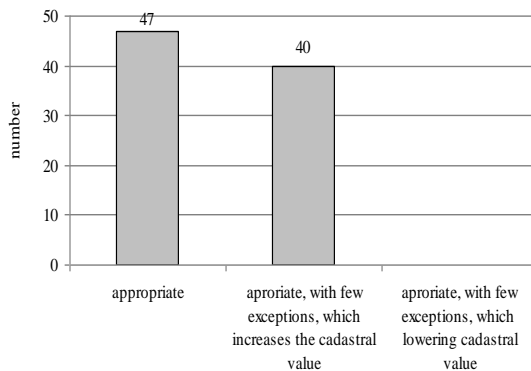


Figure 3. Respondents' assessment of the determined purposes of use of real property (Source: authors' research assessing every case n=87)

The indicators characterizing the cadastral assessment models of building land (Fig.4) and rural land (Fig.5) were offered to the real property specialists of municipalities to assess the significance of these indicators.

Assessing the indicator "purposes of use of building land", 99% of the respondents admitted that this indicator has a very significant impact on the calculation of the cadastral value and only 1% of the respondents admitted that this indicator only partly affects the cadastral value. 69 respondents, or 79%, admitted that the indicator "encumbrances" has a significant impact on the calculation of the cadastral value and 18 respondents (21%) admitted that this indicator partly affects the cadastral value. 17% of the respondents assessed that the indicator "pollution" has a significant impact on the calculation of the cadastral value, but 71% of the respondents indicated that this indicator partly affects the cadastral value. 86% of the respondents evaluated the indicator "supply with engineering communications" as significant and 14% of the respondents admitted that this indicator only partly affects the cadastral value. 60% of the respondents admitted that the indicator "geological situation" has a significant impact in the calculation of the cadastral value, but 40% of the respondents admitted that this indicator only partly affects the cadastral value but it has to be taken into consideration. Only 3% of the respondents admitted

that the indicator "social infrastructure" has a significant impact on the calculation of the cadastral value and 37% of the respondents admitted that this indicator partly affects the cadastral value but it has to be taken into consideration, but 60% of the respondents admitted that this indicator partly affects the cadastral value and it does not have to be taken into consideration. 59% of the respondents indicated that the indicator "real property market situation" has a significant impact on the calculation of the cadastral value and 40% of the respondents admitted that this indicator partly affects the cadastral value but it has to be taken into consideration, but only 1% of the respondents admitted that this indicator partly affects the cadastral value and does not have to be taken into consideration.

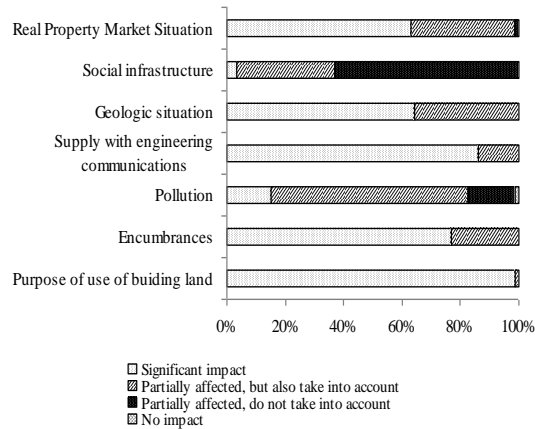


Figure 4. Respondents' assessment of the indicators of cadastral assessment of building land (Source: authors' research assessing every case n=87)

According to the assessment of the real property specialists of municipalities of the significance of the cadastral assessment model of building land, it can be concluded that the least significant indicator that does not affect the cadastral assessment of land is "social infrastructure", but the most significant indicators are "purpose of use of building land", "encumbrances", "provision with engineering communications" and "geological situation". These are significant indicators and they have to be taken into consideration when improving the cadastral assessment model of building land.

When assessing the significance of cadastral assessment models of rural land, the respondents evaluated equally the indicators "agriculture use of the land qualitative assessment" and "qualitative assessment of forest land", 97% and 98% respectively admitted that these indicators have a significant impact on the calculation of the cadastral value.

63% of the respondents assessed that the indicator "encumbrances" has a significant impact on the calculation of the cadastral value but only 2% of the respondents admitted that this indicator partly

affects the cadastral value but it has to be taken into consideration.

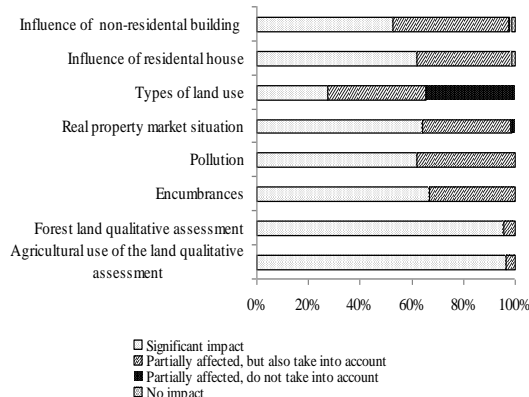


Figure 5. Respondents' assessment of the indicators of cadastral assessment of rural land (Source: authors' research assessing every case n=87)

Whereas, 58% of the respondents admitted that the indicator "pollution" has a very significant impact on the calculation of the cadastral value, but 42% of the respondents admitted that this indicator partly affects the cadastral value but it has to be taken into consideration. 61% of the respondents admitted that the indicator "real property market situation" has a significant impact on the calculation of the cadastral value, but 38% of the respondents admitted that this indicator partly affects the cadastral value but it has to be taken into consideration and 1 respondent, which corresponds to 1%, admitted that this indicator partly affects the cadastral value and it does not have to be taken into consideration. 20% of the respondents admitted that the indicator "types of land use" has a significant impact on the calculation of the cadastral value, 42% of the respondents admitted that the indicator partly affects the calculation of the cadastral value but it has to be taken into consideration, 38% of the respondents admitted that the indicator partly affects the cadastral value and it does not have to be taken into consideration. 58% of the respondents admitted that the indicator "influence of the residential house" has a significant impact, 41% of the respondents admitted that this indicator partly affects the cadastral value but it has to be taken into consideration, but 1 respondent admitted that this indicator does not at all affect the cadastral value. 48% of the respondents admitted that the indicator "influence of the non-residential building" has a significant impact on the calculation of the cadastral value, 50% of the respondents admitted that this indicator partly affects the cadastral value but it has to be taken into consideration, 1 respondent, which constitutes 1%, admitted that this indicator partly affects the cadastral value and does not have to be taken into consideration and 1 admitted that this

indicator does not at all affect the cadastral assessment.

The analysis of the survey findings allows concluding that the least significant indicator that partly affects the cadastral assessment of rural land, according to the respondents' assessment, is "types of land use", but the most significant indicators are "agriculture use of the land qualitative assessment", "qualitative assessment of forest land" and "encumbrances". In this case all selected indicators have received a significant recognition; therefore, these indicators should be taken into consideration when elaborating the cadastral assessment model of rural land.

In the research the experts' experience was also used, and to process the results, the American scientist T. Saaty's hierarchy analysis method was applied. The experts performed the assessment of the elaboration opportunities of the cadastral assessment models of rural land and building land with the algorithm of the hierarchy analysis method developed by the authors, using the information about the main indicators affecting the cadastral value of rural land and building land. To improve the cadastral assessment model of rural land the following criteria were selected for the experts' assessment: agricultural use of the land quality assessment; assessment of the quality of forest land; influence of the non-residential building; influence of the residential house; encumbrances; pollution; real property market.

The experts' assessment of the cadastral value model of rural land for the above characterized groups reflects sharper differences of the experts' opinions (Fig.6), but yet most of the experts admit that agricultural use of the land qualitative assessment has more significance. The experts have also emphasized land pollution as a very significant indicator, which largely affects the agricultural use of the land. The experts have prioritized the offered indicators in the following order: agricultural use of the land quality assessment; pollution; assessment of the quality of forest land; real property market situation; influence of the non-residential building; influence of the residential house.

To improve the cadastral assessment model of building land the experts were asked to assess the following criteria: purpose of use of the building land; encumbrances; pollution; supply with engineering communications; geological situation; level of social infrastructure; real property market.

The experts' assessment of the above characterized groups of the cadastral assessment model of building land reflects differences in the experts' opinions; however, most of the experts admit, that the purpose of use of real property with a code from 06 till 12 has a more significant role in the calculation of the cadastral value of building land. 4 experts have also emphasized the geological situation as a very significant indicator. The

experts' opinion about the significance of the real property market indicator approves that too much attention is paid to real property market during the cadastral assessment process, not to the data characterizing each property.

The experts have prioritized the offered indicators in the following order (Fig. 7): purpose of use of the building land; supply with engineering communications; encumbrances; geological situation; pollution; level of social infrastructure; real property market situation

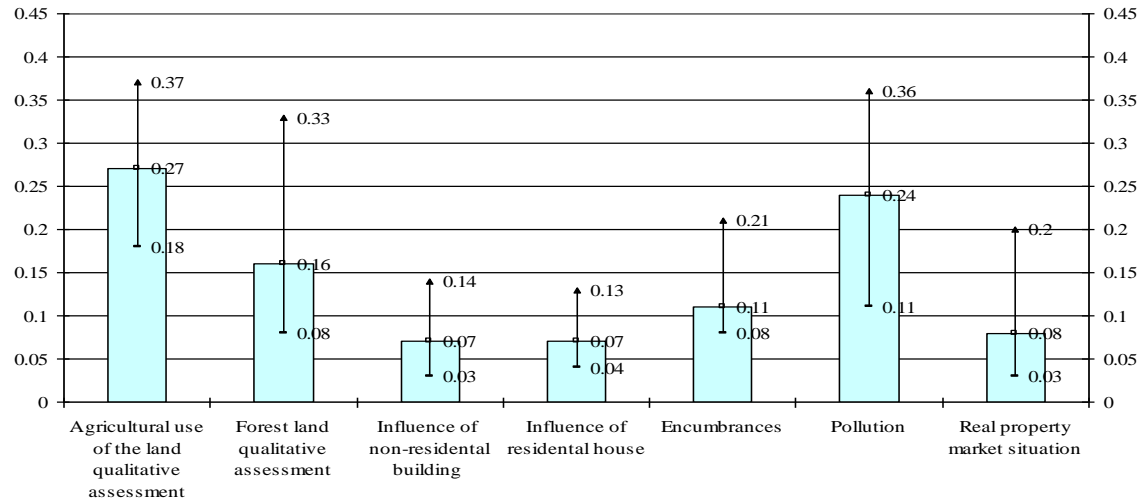


Figure 6. Priorities for elaboration of the cadastral assessment model of rural land (Source: authors' calculations)

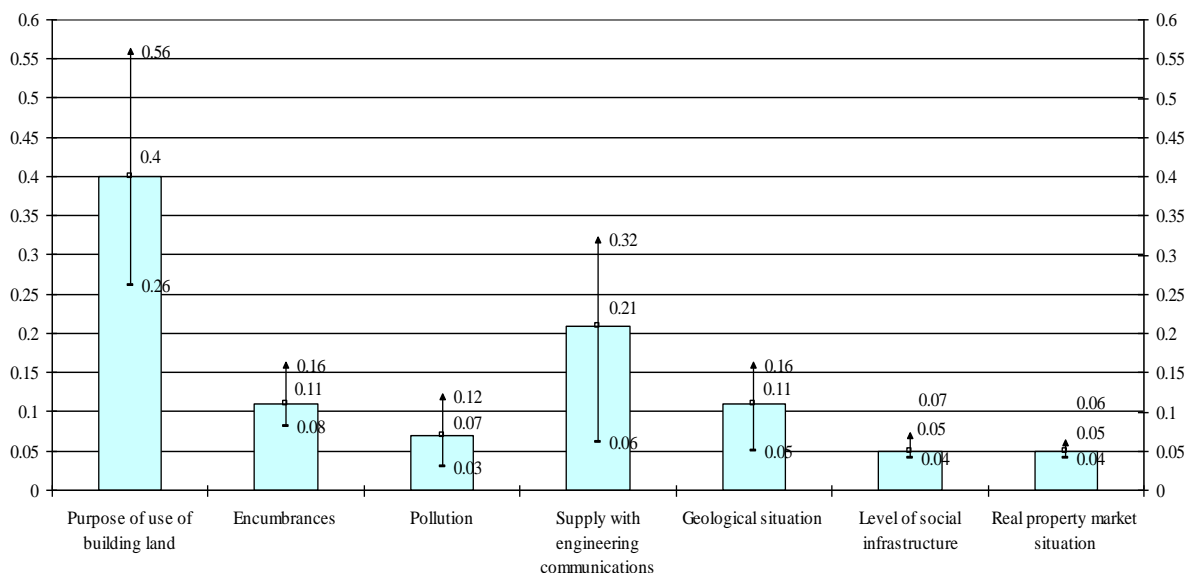


Figure 7. Priority of elaboration of the cadastral assessment model of building land (Source: authors' calculations)

Summarizing the research results and experts' opinion about the opportunities for the improvement of cadastral assessment models of building land, it can be concluded that the assessment model should comprise correction coefficients that will characterize the existence of engineering communications, as well as geological conditions, alongside with the elaboration of the data storage system.

CONCLUSIONS

1. The findings of the municipality specialists' survey allow concluding that a large complex of activities should be implemented on the state scale, in the result of which the qualitative assessment of the agricultural use of the land would be actualized, the meliorated areas and their functional situation

would be acknowledged; geological research information is very necessary and its acquisition is possible implementing the complex of state-scale measures.

2. Based on the experts' assessment of the improvement opportunities for the cadastral assessment model of building land, it can be concluded that the assessment model should include correction coefficients that will characterize the existence of engineering communications, as well as the geological situation, alongside with improving the data storage system, but after the assessment of the improvement opportunities for the cadastral assessment model of rural land, it can be concluded that qualitative data about the quality of soils and pollution are necessary.

ACKNOWLEDGEMENTS

The work was supported by European Social Fund project "Realization assistance of LLU doctoral studies". Contract No. 2009/0180/1DP/1.1.2.1.2/09/IPA/VIAA/017.

REFERENCES

- Baumane V. (2010) Cadastral Valuation Models. *Economic Science for Rural Development*: proceedings of international scientific conference No.22. Jelgava: LUA, p. 68.-75.
- Baumane V. (2012) The Applications of Factor Analysis in Assessment of Cadastral Valuation Models. *University, society, innovative development: experience, perspectives: proceedings of the international scientific practical conference*. Koksetay: State Koksetay University of A.Ualihanov (Kazakhstan), p.315.-318.
- Baumane V., Paršova V. (2010) *Kadastra datu izmantošana kadastrālās vērtēšanas modeļos*. *Geomātika: RTU zinātniskie raksti*, 70.-75. lpp.
- Kadastrālās vērtēšanas noteikumi (2006): Ministru kabineta 2006. gada 18. aprīļa noteikumi Nr. 305. *Latvijas Vēstnesis*, Nr. 72, 2006. gada 10. maijā.
- Krastiņš. O., Ciemiņa I. (2003) Statistika. Rīga. 267 lpp.
- Nekustamā īpašuma valsts kadastra likums: LR likums (2005). *Latvijas Vēstnesis*, Nr.205 (3363), 2005.gada 22.decembrī.
- Saaty T. (1981) The Analytic Hierarchy Process. p. 387.

DISPLACEMENTS AT THE GNSS STATIONS

Diana Haritonova*, Janis Balodis**, Inese Janpaule***, Madara Normand****

*****, **Institute of Geodesy and Geoinformation of the University of Latvia, Riga Technical University

**Institute of Geodesy and Geoinformation of the University of Latvia

E-mail: *Diana.Haritonova@inbox.lv, **Janis.Balodis@lu.lv, ***inesej@inbox.lv,

****_madaracaunite@yahoo.lv

ABSTRACT

The daily movements of EUPOS®-Riga and LatPos permanent GNSS network stations have been studied. Time series of GNSS station results of both the EUPOS®-Riga and LatPos networks have been developed at the Institute of Geodesy and Geoinformation of the University of Latvia (LU GGI). Reference stations from EUREF Permanent Network (EPN) have been used and Bernese GPS Software, Version 5.0, in both kinematic and static modes was applied. The standard data sets were taken from IGS database. The impact of solid Earth tides on the site coordinate changes has been studied. The Moon and the Sun tide effect is a significant factor causing the GNSS station displacements together with the Earth crust local part. Earth tidal displacements have been obtained by modifying the routine of Bernese GPS Software computing tidal station displacements in accordance with the latest IERS Conventions.

Key words: GNSS, permanent networks, displacements, solid Earth tides

INTRODUCTION

In the framework of EUPOS® regional development project, there have been two GNSS station networks developed in Latvia – LatPos and EUPOS®-Riga, which have been operating since 2006.

The EUPOS® initiative is an international expert group of public organisations coming from the field of geodesy, geodetic survey and cadastre. Partners from 19 Central and East European countries work on the provision of compatible spatial reference infrastructures by using the Global Navigation Satellite Systems (GNSS) GPS, GLONASS and as soon as available - GALILEO by operating Differential GNSS EUPOS® reference station services. The EUPOS® services allow a high accuracy and reliability for positioning and navigation and provide a wide range of geoinformation applications on this basis (EUPOS, 2013).

Time series of GNSS station results of both the EUPOS®-Riga and LatPos networks have been developed at the Institute of Geodesy and Geoinformation of the University of Latvia (LU GGI). The impact of solid Earth tides on these results has been studied.

Earth tide is a phenomenon which has been recognized for more than a thousand years, and its careful analysis started in the 19th century and flourished afterwards. However, the high precision calculations on Earth tides became available just after a reliable model of the Earth's physical properties and digital computers had been acquired (Sung-Ho Na et al., 2010).

Earth tides and tide deformations are the Earth's crust vertical movements with a maximum amplitude of up to 30 cm and theoretically precisely

determined oscillations. The Earth's periodic oscillations occur, mainly, as a result of gravitational forces between the Earth, the Moon and the Sun and centrifugal forces of the rotation system (Мельхиор, 1968).



Figure 1. EUPOS® reference station subnetwork in the Baltic countries including LatPos and EUPOS®-Riga

The Moon and the Sun tide effect is a significant factor causing the GNSS station displacements together with the Earth crust local part (Poutanen et al., 1996).

DATA PROCESSING

Static processing

The daily solutions yielding the time series of site X, Y and Z geocentric coordinate variations for EUPOS®-Riga and LatPos permanent GNSS network stations were obtained applying Bernese GPS Software, Version 5.0.

The reference stations were selected among the EUREF Permanent Network (EPN) stations in the surroundings of Latvia. Most frequently 5–8 reference stations were selected from a set of stations: BOR1, JOEN, JOZE, MDVJ, METS, POLV, PULK, RIGA, TORA, VAAS, VISO, VLNS.

The standard data sets were taken from the IGS database – ionosphere and troposphere parameters, satellite orbits, satellite clock corrections, as well as the Earth rotation parameters.

The results of GNSS data processing are station coordinates in the IGS05 coordinate system of the daily solution. These coordinates first were transformed to the European reference frame ETRS89, and then to the Latvian Geodetic Coordinate System LKS-92 with the view of obtaining station horizontal and vertical displacements.

Kinematic processing

The Bernese GPS Software allows the estimation of kinematic, i.e., epoch-wise receiver coordinates (Beutler et al., 2007). This feature has been applied for computing solid Earth tides caused by horizontal and vertical displacements at one of the EUPOS®-Riga network stations – LUNI.

Such displacements can be obtained by modifying the Bernese GPS Software routine TIDE2000.f computing tidal station displacements in accordance with the latest IERS Conventions. Modification is necessary to define that the tidal impact corrections will not be introduced for kinematic stations during data processing.

Processing of mixed, kinematic and static stations has been performed in the same solution allowing to process data from several stations in the baseline mode, one of them kinematic – LUNI, the others static. Eight EPN stations: JOZE, MDVJ, METS, PULK, RIGA, TORA, VISO, VLNS, were fixed, i.e., static for datum definition in each kinematic double-difference network solution.

The result file of GNSS data kinematic processing includes a priori station coordinates in the IGS05 coordinate system and estimated displacements and RMS in North, East and Up components of rover station in meters with 5-minute sampling interval.

Use of theoretical data

For data control the program ‘solid’ has been applied. It writes solid Earth tide components – North, East, Up, in the local Transverse Mercator system with a central meridian 24°; an Earth-centered GRS80 ellipsoid is applied. The solid Earth tide components are computed for 24 hours at 1 minute intervals in GPS time.

The program implements the conventions described in Section 7.1.2 of the IERS Conventions (2003) (McCarthy et al., 2004). ‘Solid’ does not implement ocean loading, atmospheric loading, or deformation due to polar motion (Milbert, 2012).

RESULTS AND DISCUSSION

Time series analysis

Fig. 2 shows a small part of a 4-year continuous GNSS time series developed at the LU GGI – 18-day vertical displacements at the LatPos and EUPOS®-Riga stations. The figure represents data for 20 LatPos network stations and for 5 EUPOS®-Riga permanent network stations. The dispersion of station vertical displacements is located at a 1,5 cm interval.

An observation time period – from 14th to 32nd day of the year 2010, was selected considering phases of the Moon and other phenomena which increase the impact of tidal forces.

Fig. 3 shows solid Earth tide theoretical vertical displacements at the EUPOS®-Riga station LUNI with coordinates Lat 56.950613022° and Lon 24.116529489° in the GRS80 system for a selected observation time period. The maximum height of the tidal wave was on 28th–29th day of the year 2010 and was equal to 34 cm in the territory of Riga according to the theoretical estimates.

Comparing these charts shown in Fig. 3 and Fig. 4, some coherence can be observed between extreme values of the vertical displacements at the GNSS stations and tidal wave distribution. As well as dissimilar height values at the LODE (orange curve), JEKA (red) and SIGU (violet) stations can be distinguished.

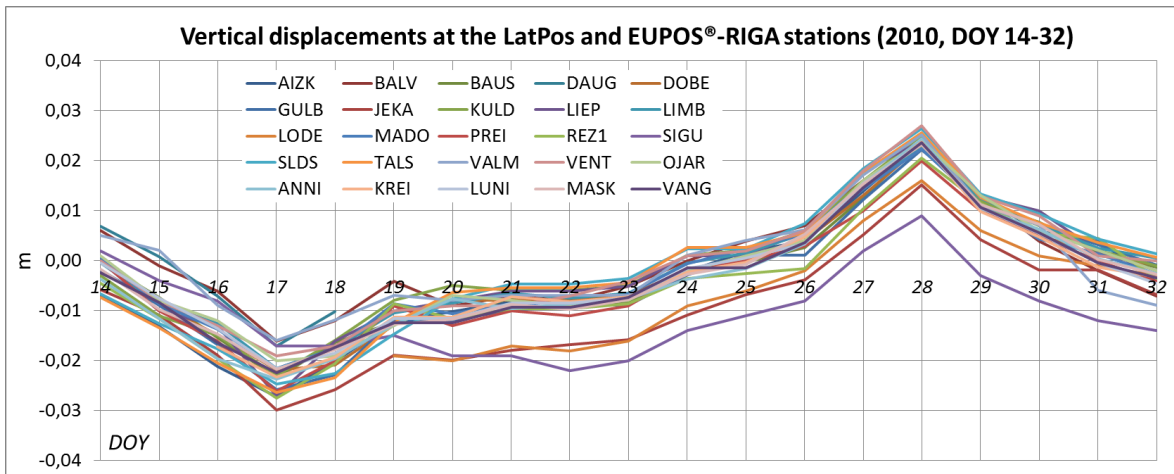


Figure 2. Time series of GNSS station height coordinate, where DOY – day of year

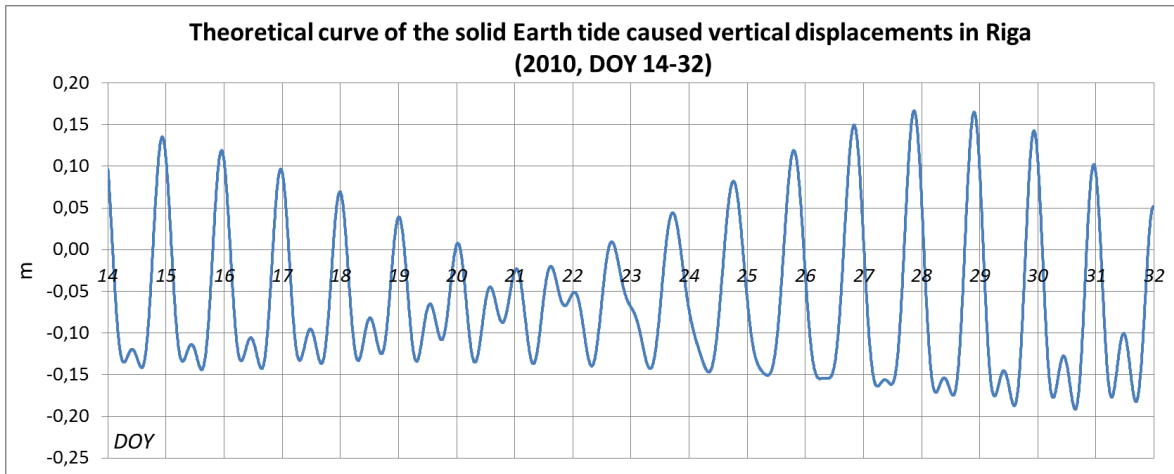


Figure 3. Theoretical vertical displacements due to the solid Earth tide effect obtained by the program ‘solid’, where DOY – day of year

Subdaily displacement analysis

The impact of solid Earth tides on the GNSS station coordinate changes during the day has been studied. Earth tidal displacements were obtained by modifying the routine of Bernese GPS Software TIDE2000.f. Consequently, the solid Earth tide corrections of LUNI station displacements were not taken into account in the computing process.

Fig. 4 shows 5-day horizontal and vertical displacements caused by the solid Earth tides at the central station of the EUPOS®-Riga network – LUNI.

Observation time interval – from 27th to 31st day of the year 2010, was also selected considering the strong impact of tidal forces of that time.

For data control, the theoretical curves were obtained by the program ‘solid’. LUNI station

coordinates Lat 56.950613022° and Lon 24.116529489° were used for this purpose.

Fig. 5 represents comparisons obtained by GNSS data kinematic processing and theoretical results of tidal displacements at the LUNI station in Up (a), North (b) and East (c) components.

The maximum height of the tidal wave in the Up component is about 35 cm. In the case of the North component, this value is about 10 cm.

As can be seen from the Fig. 5, data from the Up and North components correspond to the theoretical curves of tidal waves, but the East component data coincide with the theoretical tidal oscillation curve just partly. Such East component results can be explained by the delayed site reaction to the Earth tidal forces. Of course, human error cannot be ruled out as well.

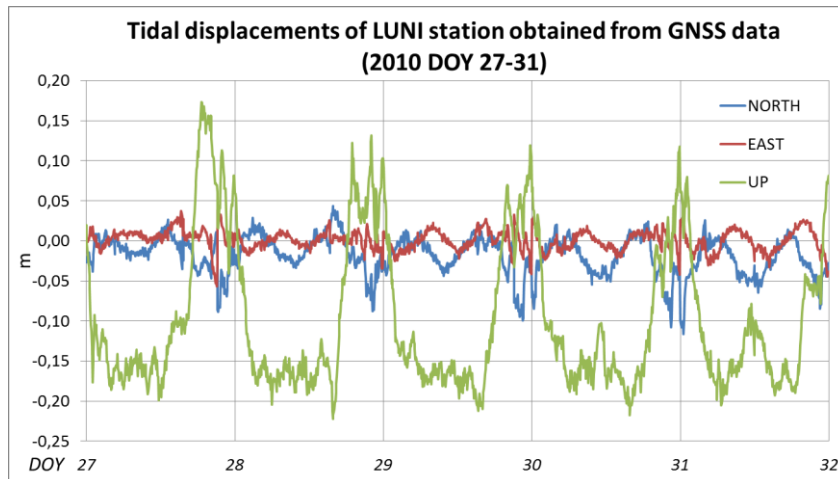


Figure 4. Estimated tidal displacement trajectory in North, East, and Up components for LUNI station

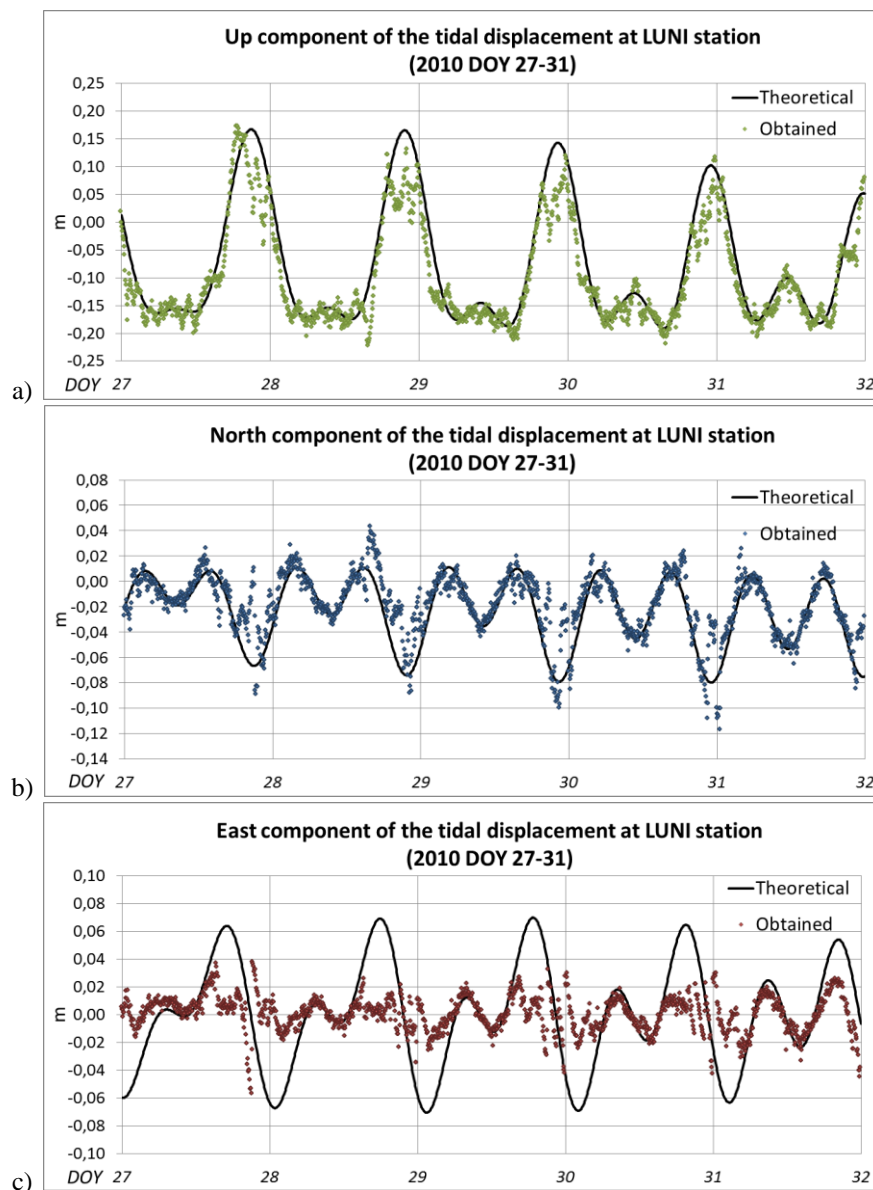


Figure 5. Estimated and theoretical tidal displacement data in Up (a), North (b) and East (c) components for LUNI station

CONCLUSIONS

Some coherence can be observed between extreme values of the vertical displacements at the LatPos and EUPOS®-Riga permanent GNSS network stations and the solid Earth tide caused vertical displacements.

Outlying height values of LODE, JEKA and SIGU stations were identified for a selected period of time. The possible reason could be the seismic activity at some areas of Latvia, or periodic influence of solid Earth tide impact, or GNSS station antenna problems.

An assessment of the influence of the above mentioned factors on the obtained data is in

progress and will be prepared, when complete information and all results of the 4-year continuous GNSS time series are summarized.

The effect of solid Earth tides on the GNSS antenna's position may be obtained by applying kinematic processing.

The maximum height of the tidal wave in the Up component at the EUPOS®-Riga station LUNI is about 35 cm, and in the North component this value reaches 10 cm for selected observation time interval. However, the East component estimates of the solid Earth tide caused displacements show delayed reaction to the tidal forces.

ACKNOWLEDGEMENT

We would like to express our thanks to Izolde Jumare for the necessary data processing support.
The research was funded by ERAF, project Nr 2010/0207/2DP/2.1.1.1.0/10/APIA/VIAA/077.

REFERENCES

- Beutler G., Bock H., Dach R., Fridez P., Gäde A., Hugentobler U., Jäggi A., Meindl M., Mervart L., Prange L., Schaer S., Springer T., Urschl C. and Walser P. (2007) *User manual of the Bernese GPS Software Version 5.0*. Astronomical Institute, University of Bern. 612 p.
- EUPOS Web Pages [online] [accessed on 14.01.2013.].
Available: <http://www.eupos.org>
- McCarthy D. D. and Petit G. (2004) *IERS Conventions (2003)*, *IERS Technical Note No. 32*. Frankfurt am Main: Verlag des Bundesamts für Kartographie und Geodäsie. 127 p.
- Milbert D. (2012) GPS Software Index Page. Solid Earth Tide [online] [accessed on 14.01.2013.].
Available: <http://home.comcast.net/~dmilbert/softs/solid.htm>
- Poutanen M., Vermeer M., Mäkinen J. (1996) The permanent tide in GPS positioning. *Journal of Geodesy* 70: p. 499–504.
- Sung-Ho Na, Moon W. (2010) Analysis of Earth Tide as a Whole-Earth Forced Oscillation and Its Computation. *Journal of the Korean Physical Society*, Vol. 56, No. 6, p. 1866–1872.
- Мельхиор П. (1968) *Земные приливы*. «МИР», Москва. 482 p.

PRECISION OF LATVIA LEVELING NETWORK NODAL POINT HEIGHT

Armands Celms*, Maigonis Kronbergs, Vita Cintina***, Vivita Baumane* ****

Latvia University of Agriculture, Department of Land Management and Geodesy

E-mail: *Armands.Celms@llu.lv, **Vita.Cintina@llu.lv, ***Vivita.Baumane@llu.lv

ABSTRACT

This study provides an assessment of the accuracy of performed first order leveling at the period from 2000 to 2010. For the newly created leveling network, the standard deviation of each leveling network nodal point, in relation to the starting points, chosen in different parts of the country, is defined. Furthest from the century benchmark fr002 the fundamental benchmark 1174 is located in Zilupe, which heights standard deviation is 9,7 mm and the fundamental benchmark 1463 in Jurkalne, which height standard deviation is 8,2 mm. The obtained accuracy value influencing factors are discussed and recommendations for further research are provided. In general, the performed leveling provides the opportunity to use the estimated height values for the existing height system actualization and successful inclusion in the European Vertical Reference System.

Key words: nodal points, leveling network, standard deviation

INTRODUCTION

First order leveling network is a decisive factor for development of the national height system. Therefore, leveling must be carried out with the highest possible accuracy.

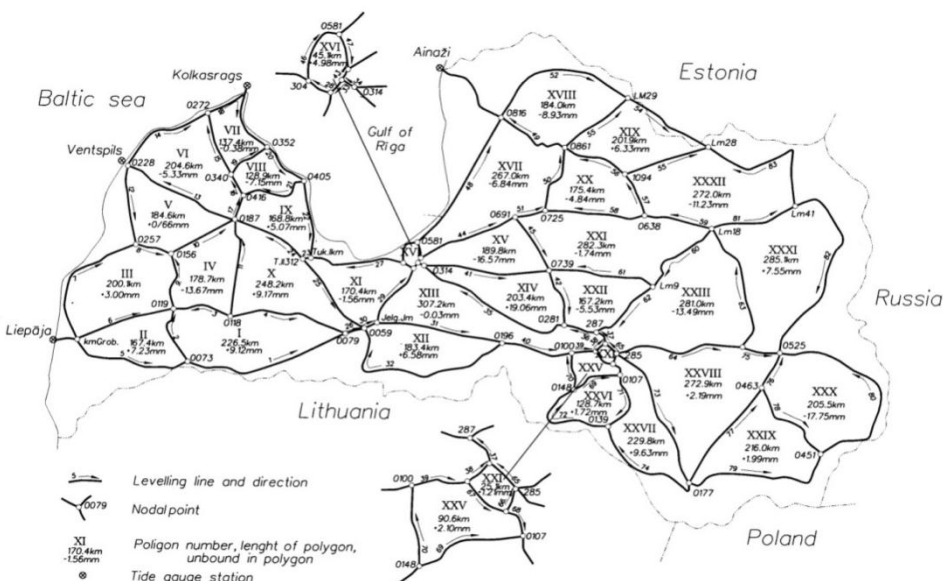
This research deals with Latvia I class leveling network nodal points accuracy. For this research The Latvian Geospatial Information Agency data about performed leveling from 2000 to 2010 were used.

The aim of the research is to provide accuracy assessment of the most topical leveling data. The standard deviation of each leveling network nodal point, in relation to the starting points, chosen in different parts of the country, is defined.

This type estimation of the leveling network accuracy so far has not been done.

MATERIALS AND METHODS

National leveling core network is the height system developer and maintainer of a given territory. The established leveling core network accuracy gives guarantees for other studies that the data from this network are of high quality. As an example, studies on the Earth crust vertical movements, their speed and amplitude of values. To accurately determine the exact changes that occurred, the leveling must be executed with the best possible accuracy (Ellmann et al., 1999). In case, if precise leveling final results for some reason are not with the highest certainty, then it is very difficult for further data application in the national economy (Celms et al., 2012).



In the territory of Latvia during the last seventy years three precise leveling campaigns were performed. In the territory of Latvia the core leveling network was created from 1929 to 1939 (Fig.1). During this period in the territory of Latvia the overall first order leveling network was set and surveyed. The leveling network reached the total length of 4422 km and included 1262 leveling signs (Latvijas PSR ..., 1941). The leveling network was unsystematic, re-leveled in the last century two more campaigns – at the time from 1947 to 1948 (Fig.2). During this period leveling was performed by separate existing core network leveling lines. It was done in order to include the leveling core network in the Soviet Union geodetic space. During the period from 1967 to 1974 precise leveling was carried out again (Fig.3). Almost all lines were leveled again. In the leveling lines, where measurements were not fulfilled, the elevation values between the unit points were taken from the previous (1929 – 1939) epoch measurement data.

Fragmentarily precise leveling was organized and carried out until 1990.

The most recent first order leveling in Latvia was performed during the period from 2000 to 2010 (Fig.4). At the time period from 2000 to 2005 precise leveling works were organized and performed by the State Land Service. In the following period – from 2006 to 2010 these works were continued and successfully completed by the Latvian Geospatial Information Agency experts. Leveling was performed by the existing lines, including in previous campaigns leveled leveling signs, which were preserved till the present day. In this epoch, separate lines in some sections were leveled by new sites (Instruction of ..., 2001). As an example, in the line Zilupe – Demene leveling in the section Indra – Demene was prepared and fulfilled not by the previous epoch measured lines. It was related to the Latvian border geodetic surveying grounds preparation.

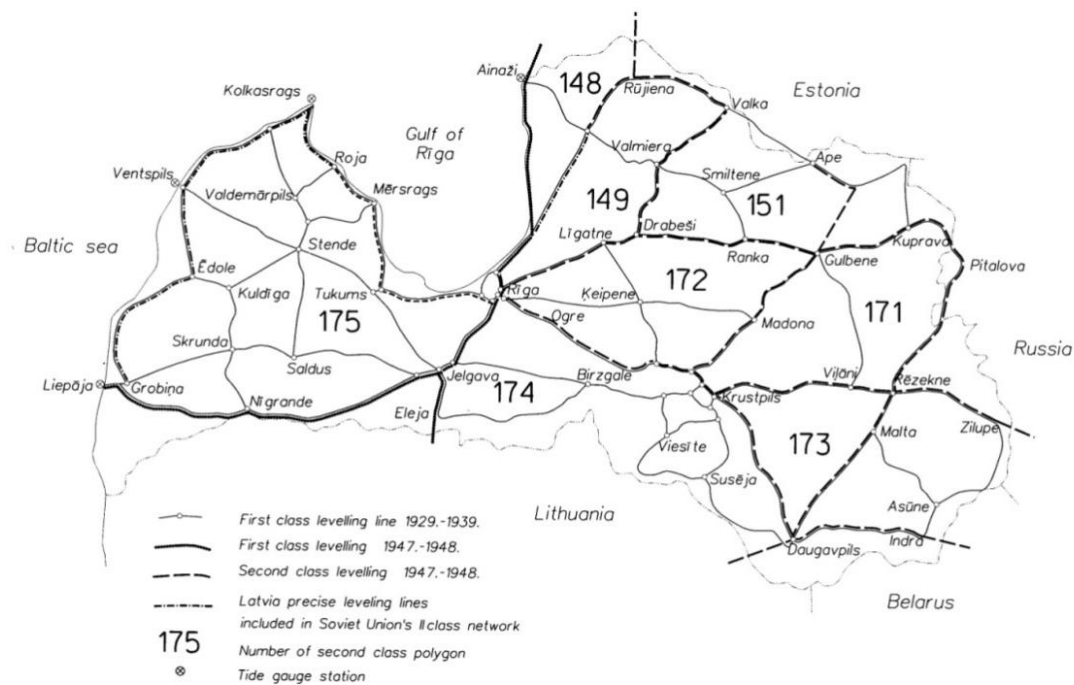


Figure 2. Scheme of precise leveling network from 1947 to 1948

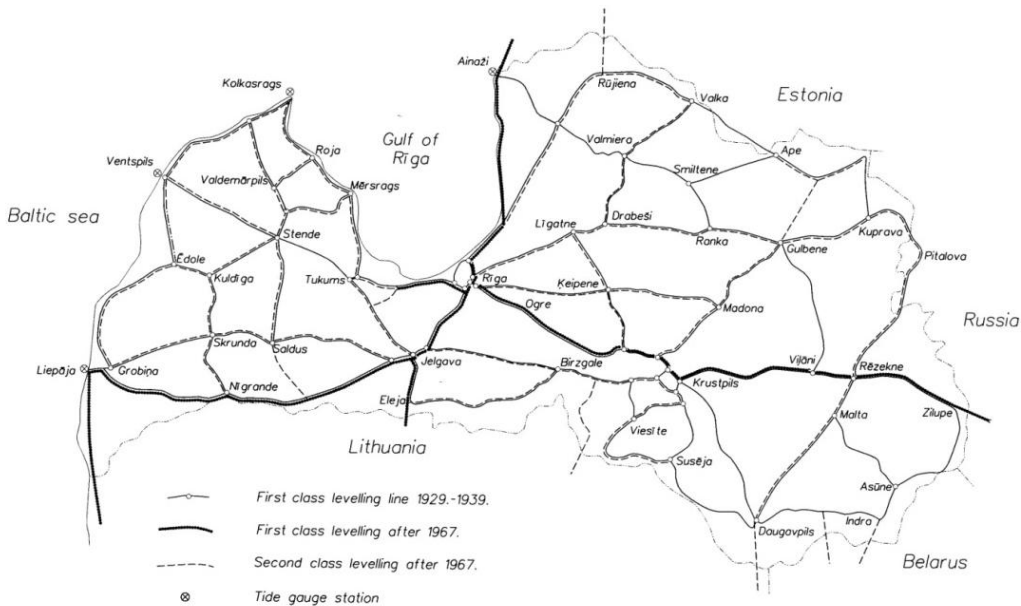


Figure 3. Scheme of precise leveling network from 1967 to 1974

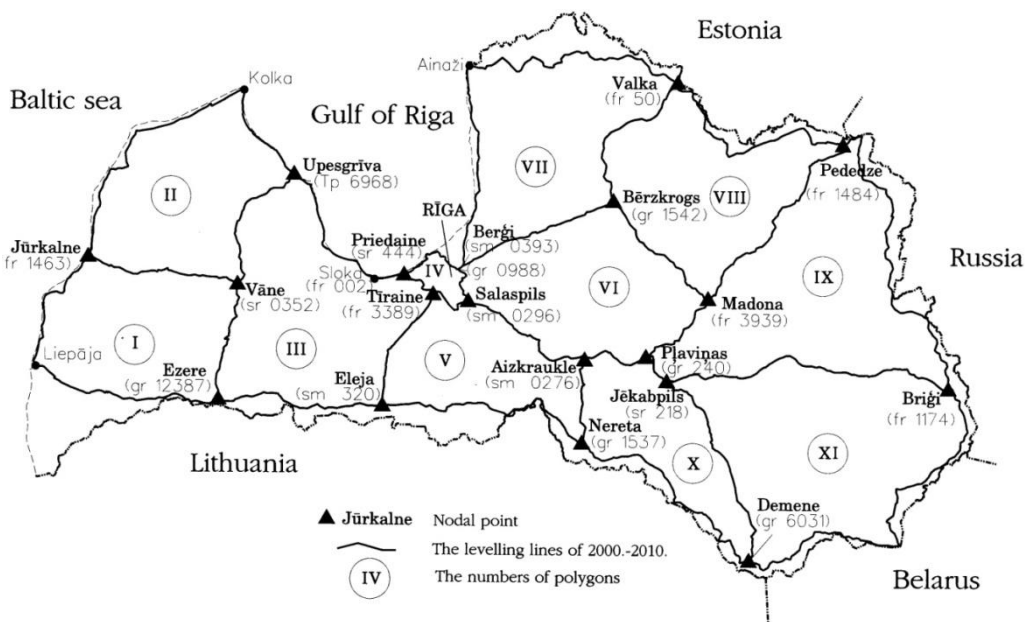


Figure 4. Scheme of first order leveling network

Only for the 1929–1939 leveling, the farthest placed nodal point standard deviation, in relation to the central part of the leveling network, has been calculated (wall mark Sm304 in Zasulaiks) (Jakubovskis et al., 1994). These calculations were performed only in 1992, because in the 30's it took massive additional calculations, which were not performed. In total, there were 51 nodal point height standard deviations determined to the wall

mark Sm304 in Zasulaiks (Table 1). Standard deviation in the west direction (280 km) is less than 5 mm and east direction (350 km) – less than 6 mm. The estimated standard deviations of the nodal points are shown in Table 1. The obtained results show that, despite the technical possibilities of that time and experience, leveling works were performed with the highest accuracy.

Table 1

Nodal points height standard deviations in relation to wall mark Sm304 in Zasulauks

Nodal point	Height mean square error, mm	Line Nr.
0079	±3,9	1,4,26
0073	±5,3	1,2,5
0119	±5,0	2,3,4,9
00118	±4,8	3,4,11
Grobiņa	±5,7	5,6,7
0257	±5,3	7,8,12
0156	±5,1	8,9,10
0187	±4,5	10,11,13,17,24
0228	±5,4	12,13,14
0272	±5,5	14,15,18
0340	±5,1	15,16,19
0416	±4,8	16,17,21
0352	±5,3	18,19,20
0405	±4,9	20,21,22
Tukums I	±3,8	22,23,27
312	±3,8	23,24,25
0059	±3,4	25,26,30,32
303	±1,1	28,29,33
Jelgava	±3,3	29,30,31
0196	±4,3	31,32,40
0254	±1,6	33,34,43
0314	±1,9	34,35,41
0281	±3,8	35,36,42
287	±4,0	36,37,62
0168	±4,1	37,38,65
0102	±4,2	39,39,47
0100	±1,3	39,40,70
0739	±3,7	41,42,45,61
0346	±1,8	43,44,47
0691	±3,7	44,45,51
0581	±2,1	46,47,48
0816	±4,6	48,19,52
0861	±4,4	49,50,53,56
0725	±4,0	50,51,58
29	±5,1	52,53,54
28	±5,2	54,55,93
1094	±4,7	55,56,57
0638	±1,3	57,58,59
18	±4,6	59,60,63,81
9	±4,4	60,61,62
22	±5,1	63,64,75
285	±4,2	64,65,66,73
0106	±4,2	66,67,68
0107	±4,7	68,69,71
0148	±4,7	69,70,72
0139	±5,3	71,72,74
0177	±5,4	73,74,77,79
0525	±5,2	75,76,80,82
0463	±5,5	76,77,78
0451	±6,0	78,79,80
41	±5,2	81,82,83

In this study, the most recent leveling network data were used. The raw data were obtained from the Latvian Geospatial Information Agency. These data were arranged by lines; in the result from these lines polygons were created. For each line the leveling data were arranged in a specific sequence showing the leveling signs, elevation between them and the distance between the leveling signs. The elevation values between the leveling signs are given as average, taking into account the "forward" and "back" measurements. The elevation values are given with the calibration corrections and including coefficients for the transition to the normal height system (Instruction of, 2001).

To achieve the objectives stated in this study the Latvian class I leveling network equation by the parametric method was carried out (Gaidaev et al., 1969). In calculations by this method, for measurement results elevations, measured between the nodes are taken, but for the parameters (unknown) – node adjusted heights. Then the numbers of the parametric equations are equal to the numbers of the leveling network lines n, but the numbers of the parameters are equal to the leveling network nodes t.

Defining the node M_j adjusted height $H_j = (H_j) + \xi_j$, where (H_j) is the node height approximate value, but ξ_j is correction to $j = 1, 2, \dots, t$ (Table 2), parametric equations in following form are obtained:

$$a_i \xi_1 + b_i \xi_2 + \dots + t_i \xi_t - \lambda_i = v_i$$

$$i = 1, 2, \dots, n \quad (1)$$

where:

n – number of lines

v – elevation correction

λ – mathematical difference between the measured elevation value and leveling network node height approximate values

$$\lambda_i = l_i - (h_i) \text{ with weight } p_i \quad (2)$$

where:

l_i – measured elevation of leveling line

(h_i) – height approximate value (Table 3)

Using the Gauss lemmas equations $[av]=0$; $[bv]=0$; ... $[tv]=0$, following the correction parametric equations, a normal equation system is drawn up (Fig. 5).

Table 2
Leveling network point heights

H ₄₄₄	=	2,9700		
H _j	(H _j)	ξ_j		
H ₁	= 12,6510	+ ξ_1	Tp6968	
H ₂	= 13,4018	+ ξ_2	Fr1463	
H ₃	= 87,5046	+ ξ_3	Sr0352	
H ₄	= 72,7757	+ ξ_4	Gr12387	
H ₅	= 33,5612	+ ξ_5	Sm320	
H ₆	= 12,3026	+ ξ_6	Fr3389	
H ₇	= 13,3314	+ ξ_7	Gr0988	
H ₈	= 10,4439	+ ξ_8	Sm0393	
H ₉	= 17,8528	+ ξ_9	Sm0296	
H ₁₀	= 80,2234	+ ξ_{10}	Gr1537	
H ₁₁	= 95,2382	+ ξ_{11}	Sm0276	
H ₁₂	= 179,1619	+ ξ_{12}	Gr1542	
H ₁₃	= 49,6972	+ ξ_{13}	Fr50	
H ₁₄	= 84,5788	+ ξ_{14}	Gr240	

H ₁₅	=	141,1518	+	ξ_{15}	Fr3939
H ₁₆	=	156,6380	+	ξ_{16}	Fr1484
H ₁₇	=	132,1347	+	ξ_{17}	Gr6031
H ₁₈	=	91,3675	+	ξ_{18}	Sr218
H ₁₉	=	130,3630	+	ξ_{19}	Fr1174

The normal equation system is derived using the Gauss algorithm (Freij, 1957). As a result ξ adjusted values are obtained, by which the leveling network node adjusted heights are calculated.

For the performed calculations as a starting point of the height system the leveling sign sr444 was taken. It was set because that the wall benchmark sr444 is located 10 km away from the wall mark sm304. Therefore, the obtained results can be comparable to the 1929 - 1939 leveling standard deviation of the leveling network node points.

The height standard derivation is calculated for XIX nodal point, which naturally is embedded as a fundamental ground mark fr1174.

Table 3
Correction parametric equations

																				weight (p)	
H _{II}	-	H _I	-	h ₁	=	v ₁	13,4018	-	12,6510	-	0,7561	=	-5,3		-	ξ_1	+	ξ_2	+	-5,3 = v ₁	0,0049
H _{II}	-	H _{III}	-	h ₂	=	v ₂	13,4018	-	87,5046	-	-74,0977	=	-5,1			ξ_2	-	ξ_3	+	-5,1 = v ₂	0,0117
H _{III}	-	H _I	-	h ₃	=	v ₃	87,5046	-	12,6510	-	74,8532	=	0,4		-	ξ_1	+	ξ_3	+	0,4 = v ₃	0,0122
H _{IV}	-	H _{II}	-	h ₄	=	v ₄	72,7757	-	13,4018	-	59,3844	=	-10,5		-	ξ_2	+	ξ_4	+	-10,5 = v ₄	0,0054
H _{IV}	-	H _{III}	-	h ₅	=	v ₅	72,7757	-	87,5046	-	-14,7289	=	0,0		-	ξ_3	+	ξ_4	+	0,0 = v ₅	0,0138
H _V	-	H _{IV}	-	h ₆	=	v ₆	33,5612	-	72,7757	-	-39,2228	=	8,3		-	ξ_4	+	ξ_5	+	8,3 = v ₆	0,0110
H _V	-	H _{VI}	-	h ₇	=	v ₇	33,5612	-	12,3026	-	21,2669	=	-8,3		-	ξ_5	-	ξ_6	+	-8,3 = v ₇	0,0144
H ₄₄₄	-	H _{VI}	-	h ₈	=	v ₈	2,9700	-	12,3026	-	-9,3326	=	0,0		-	ξ_6	+	0,0	=	v ₈	0,0409
H _I	-	H ₄₄₄	-	h ₉	=	v ₉	12,6510	-	2,9700	-	9,6814	=	-0,4			ξ_1	+	-0,4	=	v ₉	0,0108
H _{VII}	-	H ₄₄₄	-	h ₁₀	=	v ₁₀	13,3314	-	2,9700	-	10,3614	=	0,0			ξ_7	+	0,0	=	v ₁₀	0,0233
H _{VII}	-	H _{VIII}	-	h ₁₁	=	v ₁₁	13,3314	-	10,4439	-	2,8875	=	0,0		-	ξ_7	-	ξ_8	+	0,0 = v ₁₁	0,3472
H _{VI}	-	H _{IX}	-	h ₁₂	=	v ₁₂	12,3026	-	17,8528	-	-5,5447	=	-5,5		-	ξ_6	-	ξ_9	+	-5,5 = v ₁₂	0,0374
H _{IX}	-	H _{VII}	-	h ₁₃	=	v ₁₃	17,8528	-	13,3314	-	4,5268	=	-5,4		-	ξ_7	+	ξ_9	+	-5,4 = v ₁₃	0,0400
H _X	-	H _V	-	h ₁₄	=	v ₁₄	80,2234	-	33,5612	-	46,6622	=	0,0		-	ξ_5	+	ξ_{10}	+	0,0 = v ₁₄	0,0079
H _X	-	H _{XI}	-	h ₁₅	=	v ₁₅	80,2234	-	95,2382	-	-15,0159	=	1,1		-	ξ_{10}	-	ξ_{11}	+	1,1 = v ₁₅	0,0199
H _{IX}	-	H _{XI}	-	h ₁₆	=	v ₁₆	17,8528	-	95,2382	-	-77,3842	=	-1,2		-	ξ_9	-	ξ_{11}	+	-1,2 = v ₁₆	0,0125
H _{VIII}	-	H _{XII}	-	h ₁₇	=	v ₁₇	10,4439	-	179,1619	-	-168,7180	=	0,0		-	ξ_8	-	ξ_{12}	+	0,0 = v ₁₇	0,0113
H _{XIII}	-	H _{VIII}	-	h ₁₈	=	v ₁₈	49,6972	-	10,4439	-	39,2487	=	4,6		-	ξ_8	+	ξ_{13}	+	4,6 = v ₁₈	0,0041
H _{XII}	-	H _{XIII}	-	h ₁₉	=	v ₁₉	179,1619	-	49,6972	-	129,4601	=	4,6		-	ξ_{12}	-	ξ_{13}	+	4,6 = v ₁₉	0,0115
H _{XI}	-	H _{XIV}	-	h ₂₀	=	v ₂₀	95,2382	-	84,5788	-	10,6594	=	0,0		-	ξ_{11}	-	ξ_{14}	+	0,0 = v ₂₀	0,0261
H _{XIV}	-	H _{XV}	-	h ₂₁	=	v ₂₁	84,5788	-	141,1518	-	-56,5768	=	3,8		-	ξ_{14}	-	ξ_{15}	+	3,8 = v ₂₁	0,0203
H _{XII}	-	H _{XV}	-	h ₂₂	=	v ₂₂	179,1619	-	141,1518	-	38,0138	=	-3,7		-	ξ_{12}	-	ξ_{15}	+	-3,7 = v ₂₂	0,0125
H _{XV}	-	H _{XVI}	-	h ₂₃	=	v ₂₃	141,1518	-	156,6380	-	-15,4846	=	-1,6		-	ξ_{15}	-	ξ_{16}	+	-1,6 = v ₂₃	0,0078
H _{XVI}	-	H _{XIII}	-	h ₂₄	=	v ₂₄	156,6380	-	49,6972	-	106,9424	=	-1,6		-	ξ_{13}	+	ξ_{16}	+	-1,6 = v ₂₄	0,0078
H _{XVII}	-	H _X	-	h ₂₅	=	v ₂₅	132,1347	-	80,2234	-	51,9249	=	-13,6		-	ξ_{10}	+	ξ_{17}	+	-13,6 = v ₂₅	0,0075
H _{XVIII}	-	H _{XVII}	-	h ₂₆	=	v ₂₆	91,3675	-	132,1347	-	-40,7748	=	7,6		-	ξ_{17}	+	ξ_{18}	+	7,6 = v ₂₆	0,0081
H _{XVIII}	-	H _{XIV}	-	h ₂₇	=	v ₂₇	91,3675	-	84,5788	-	6,7887	=	0,0		-	ξ_{14}	+	ξ_{18}	+	0,0 = v ₂₇	0,0563
H _{XIX}	-	H _{XVIII}	-	h ₂₈	=	v ₂₈	130,3630	-	91,3675	-	38,9902	=	5,3		-	ξ_{18}	+	ξ_{19}	+	5,3 = v ₂₈	0,0060
H _{XVI}	-	H _{XIX}	-	h ₂₉	=	v ₂₉	156,6380	-	130,3630	-	26,2698	=	5,2		-	ξ_{16}	-	ξ_{19}	+	5,2 = v ₂₉	0,0054
H _{XVII}	-	H _{XIX}	-	h ₃₀	=	v ₃₀	132,1347	-	130,3630	-	1,7505	=	21,2		-	ξ_{17}	-	ξ_{19}	+	21,1 = v ₃₀	0,0047

RESULTS AND DISCUSSION

After correction the parametric equations were calculated, elevation corrections v measured and each line weight p value, as well as $p v^2$ sum were determined (Table 4).

Table 4

Data for leveling accuracy assessment

weight (p)	correction v	$p v^2$
0,00495	-1,10	0,0060
0,01168	-3,07	0,1101
0,01224	2,57	0,0808
0,00545	-7,66	0,3196
0,01376	4,87	0,3263
0,01096	2,36	0,0610
0,01440	-5,58	0,4483
0,04090	-1,17	0,0560
0,01084	2,40	0,0624
0,02330	-3,17	0,2342
0,34722	-0,15	0,0078
0,03738	-3,43	0,4398
0,03998	-3,13	0,3917
0,00786	-6,88	0,3721
0,01986	-0,04	0,0000
0,01254	-0,26	0,0008
0,01133	-1,80	0,0367
0,00407	7,51	0,2298
0,01153	3,48	0,1396
0,02614	-0,15	0,0006
0,02029	2,20	0,0982
0,01254	-4,83	0,2925
0,00777	-2,01	0,0314
0,00778	-1,18	0,0108
0,00751	-7,34	0,4047
0,00814	3,50	0,0997
0,05634	0,86	0,0417
0,00598	12,84	0,9860
0,00539	-1,20	0,0078
0,00474	17,67	1,4800
Sum:		6,7763

The calculated value is used to describe the accuracy of the leveling network; it is for calculation of the leveling kilometric standard deviation S_{km}

$$S_{km} = \sqrt{\frac{[pv^2]}{n-t}} = \sqrt{\frac{6,7763}{30-19}} = 0,785 \text{ mm} \quad (3)$$

where:

S_{km} – leveling kilometric standard deviation
n – number of lines

Since node 19 (fr1174) is located farthest from the selected leveling network starting point sr444, than its adjusted height weight, in the process of reduction of the equation system by Gauss

algorithm is a coefficient at ξ_{19} . ξ_{19} is the last unknown, and at the same time this node adjusted the height weight and also the height standard deviation S_{H19} .

$$S_{H19} = \frac{S_{km}}{\sqrt{p_{19}}} = \frac{0,785}{\sqrt{0,0072}} = 9,2 \text{ mm} \quad (4)$$

In the process of carrying out the entire leveling network adjustment with software NivNet, there was obtained the same standard deviation value for this node height. This indicates that the applied software for calculations provides authentic equalization results and their accuracy evaluation. Therefore, to reduce large amount of calculations, the rest of the node adjusted height standard deviations are determined by the computer program NivNet.

Table 5
Height standard deviations calculated from the starting point sr444

Leveling sign	Point height, m	Standard deviation, mm
Tp6968	12.65378	6.52
fr1463	13.40877	8.42
sr0352	87.50955	7.56
gr12387	72.78554	7.44
sm320	33.56510	5.90
fr3389	12.30377	3.35
gr0988	13.32823	4.03
sm0393	10.44087	4.22
sm0296	17.85190	4.12
gr1537	80.22040	6.94
sm0276	95.23634	6.31
gr1542	179.16068	6.80
fr50	49.69712	7.84
gr240	84.57710	6.88
fr3939	141.15170	7.26
fr1484	156.63834	8.55
gr6031	132.13794	8.54
sr218	91.36666	7.36
fr1174	130.36976	9.24

For practical use of the leveling network, it is important to know the height of the points and their accuracy. According to the Cabinet of Ministers rules Nr.879, as the starting point the century benchmark fr002 in Sloka was chosen; and then the leveling network nodal points adjusted height standard deviations were determined. Considering the above mentioned the leveling network node point height standard deviation values were calculated both, for the starting point sr444 and the century benchmark fr002. The obtained values are summarized in Table 6.

	a	b	c	d	e	f	g	h	i	j	k	l	m	n	o	p	q	r	s	t	u	
a	0.0279	ξ_1	-0.0049	ξ_1	-0.0122	ξ_1															0.0168 a	
b	-0.0049	ξ_1	0.0220	ξ_1	-0.0117	ξ_1	-0.0054	ξ_1												-0.0290 b		
c	-0.0132	ξ_1	-0.0117	ξ_1	0.0377	ξ_1	-0.0138	ξ_1												0.0646 c		
d	-0.0024	ξ_1	-0.0138	ξ_1	0.0302	ξ_1	-0.0110	ξ_1												-0.1480 d		
e		-0.0110	ξ_1	-0.0144	ξ_6				-0.0079	ξ_{10}										-0.0232 e		
f		-0.0144	ξ_5	0.0927	ξ_6	-0.0374	ξ_6	-0.0400	ξ_6											-0.0822 f		
g				0.4105	ξ_7	-0.3472	ξ_7	0.3626	ξ_7											0.2160 g		
h					-0.3472	ξ_7	0.3626	ξ_7												-0.0159 h		
i					-0.0374	ξ_6	-0.0400	ξ_7	0.0899	ξ_9	-0.0125	ξ_{11}								-0.0233 i		
j						-0.0079	ξ_5	0.0353	ξ_6	-0.0199	ξ_{11}									0.1239 j		
k						-0.0125	ξ_6	-0.0199	ξ_{10}	0.0585	ξ_{11}	-0.0261	ξ_{14}							-0.0075 k		
l							-0.0113	ξ_8	0.0353	ξ_{12}	-0.0115	ξ_{13}	-0.0125	ξ_{15}						-0.0059 l		
m							-0.0041	ξ_8		0.0234	ξ_{13}	-0.0115	ξ_{12}	0.0261	ξ_{14}	-0.0203	ξ_{15}	-0.0078	ξ_{16}		-0.0215 m	
n								-0.0041	ξ_8		-0.0125	ξ_{11}	-0.0125	ξ_{12}	0.0127	ξ_{14}	-0.0203	ξ_{15}	-0.0053	ξ_{16}		0.0717 n
o									-0.0075	ξ_{10}		-0.0078	ξ_{13}	-0.0203	ξ_{14}	0.0405	ξ_{15}	-0.0078	ξ_{16}		-0.0434 o	
p										-0.0075	ξ_{10}		-0.0078	ξ_{13}	-0.0210	ξ_{16}	0.0203	ξ_{17}	-0.0081	ξ_{18}		0.0231 p
q											-0.0075	ξ_{10}		-0.0563	ξ_{14}	-0.0704	ξ_{17}	0.0704	ξ_{18}		-0.0640 q	
r												-0.0075	ξ_{10}		-0.0054	ξ_{16}	-0.0060	ξ_{17}	0.0161	ξ_{19}		0.0298 r
s													-0.0075	ξ_{10}		-0.0047	ξ_{17}	-0.0060	ξ_{18}		-0.0959 s	
t														-0.0075	ξ_{10}		-0.0047	ξ_{17}	-0.0060	ξ_{18}		-0.0959 t
	2.7085	6.9882	4.9662	3.8978	9.8411	1.1731	-3.1718	-3.0245	-1.8425	-2.9806	-0.8980	-1.2279	-0.1112	-1.6914	-0.0952	0.3102	3.2744	-0.8275	6.7080			
	ξ_1	ξ_2	ξ_3	ξ_4	ξ_5	ξ_6	ξ_7	ξ_8	ξ_9	ξ_{10}	ξ_{11}	ξ_{12}	ξ_{13}	ξ_{14}	ξ_{15}	ξ_{16}	ξ_{17}	ξ_{18}	ξ_{19}			

Figure 5. Normal equations unknown coefficients

Table 6
Height standard deviations calculated from the starting point fr002

Leveling sign	Point height, m	Standard deviation, mm
Tp6968	12.65252	6.04
fr1463	13.40750	8.27
sr0352	87.50828	7.39
gr12387	72.78428	7.49
sm320	33.56384	6.41
fr3389	12.30250	4.55
sr444	2.96874	3.25
gr0988	13.32696	5.10
sm0393	10.43961	5.25
sm0296	17.85063	5.15
gr1537	80.21913	7.51
sm0276	95.23508	6.98
gr1542	179.15942	7.46
fr50	49.69585	8.42
gr240	84.57583	7.50
fr3939	141.15043	7.86
fr1484	156.63707	9.07
gr6031	132.13668	9.03
sr218	91.36539	7.94
fr1174	130.36850	9.71

In general, the performed leveling will give the opportunity to use the calculated elevation values

for the existing height system update and successful inclusion in the European Vertical Reference System (Sacher et al., 1999).

As well as the given leveling product – elevation values are useable as support for various public sector research and development. For example by the Earth crust vertical movement studies, updating the cartographic material components of height and other (Lazdāns et al., 2009).

CONCLUSIONS

1. Furthest from the century benchmark fr002 the fundamental benchmark 1174 is located in Zilupe, which height standard deviation is 9,7 mm and the fundamental benchmark 1463 in Jurkalne, which height standard deviation is 8,2 mm.
2. Considering the current leveling network standard deviation $S = 0,785$ mm/km, that affects the accuracy of nodal points, to recognize the causes, there is a further need to determine the leveling systematic error and study its influencing factors.
3. The leveling network point height accuracy may directly affect the lower classes leveling accuracy.
4. The nodal point height standard deviation is required for calculations of the geoid model latest versions.

ACKNOWLEDGEMENTS

The work was supported by European Social Fund project “Realization assistance of LLU doctoral studies”. Contract No. 2009/0180/1DP/1.1.2.1.2/09/IPA/VIAA/017.

The authors want to thank the Latvian Geospatial Information Agency for the provided data.

REFERENCES

- Celms A., Kronbergs M., Cintīņa V. (2012) Accuracy Estimation of the Latvia First Order leveling Network. In: *International scientific and technical conference GEOFORUM 2012*. Lvivska Politehnika ISSN 1819-1339, Pp.44 – 47.
- Ellmann A., Torim A., Abols N., Kaminskis J., Sleiteris E. (1999) Different solutions adopted to modernize the height networks in the Baltic countries. In: The importance of Heights Proc. “Geodesy and Surveying in the future”, March 15–17, 1999, Gavle, Sweden, p. 349–360.
- Freijs V. (1957) Novērojumu izlīdzināšana pēc vismazāko kvadrātu metodes. Rīga, 110 lpp.
- Instruction of 1-st, 2-nd and 3-rd order leveling (2001) State Land Sevice, Riga 98 p.
- Jakubovskis O., Kronbergs M., Helfriča B. (1994) Pastāvošā precīzā augstuma atbalsta tīkla analīze un novērtējums. Latvijas ģeodēziskā augstuma atbalsta tīkla rekonstrukcijas projekts, Jelgava
- Latvijas PSR precīzā nivellēšana (1941) (*Precise Leveling in the Latvian SSR*) ZTK Zemes ierīcības un meliorācijas pārvaldes Zemes ierīcības daļas izdevums, Rīga, 117 lpp. (In Latvian and Russian)
- Lazdāns J., Aleksejenko I., Kaminskis J., Celms A., Kaļinka M., Klīve J., Reiniks M. (2009) Aktualitāte Latvijas sasaistē ar Eiropas augstumu sistēmu. //LU 67. Zinātniskā conference Astronomijas un ģeodēzijas sekcija 2009. g. 12. februārī Rīgā.
- Sacher M., Ihde J., Celms A., Elmann A. (1999) The first UELN stage is achieved, further stepa are planned // Report on the Symposium of the IAG Subcommission for the European Reference Frame (EUREF) held in Prague, June 2–5, 1999, p. 87–94
- Гайдаев П., Болышаков В. Д. (1969) Теория математической обработки геодезических измерений [Theory of mathematical processing of geodetic measurements]. Москва: Недра. с 399

ENVIRONMENT AND ENVIRONMENTAL EFFECTS

COMPARISON OF MUNICIPAL SOLID WASTE CHARACTERISTICS AFTER SEPARATION BY STAR AND DRUM SCREEN SYSTEMS

Dace Arina

Latvia University of Agriculture, Faculty of Rural Engineering
E-mail: dace.arina@gmail.com

Ausma Orupe

Institute of Physical Energetics in Latvia
E-mail: jkalnacs@edi.lv

ABSTRACT

The research provides the results of experimental work in the waste mechanical pre-treatment in Latvia. The goal is to detect and to compare the composition and main parameters of sorted waste components after separation by the star screen and drum screen systems. Samples were taken in three fractions - coarse, medium, fine from the star screen system and coarse and fine from the drum screen system. The parameters – upper, lower heating values, moisture, ash content, S and Cl were determined. Results - the waste content of the fine fraction after the star screen system pre-treatment has less additional material, than after the drum screen system pre-treatment. The coarse fraction after the star screen system pre-treatment contains high calorific energy raw materials for the production of alternative energy materials. However this fraction needs an additional separation if the drum screen system pre-treatment is used for it. The same is necessary for the medium fraction after the star screen system pre-treatment.

Key words: star screen technology, drum screen technology, mechanical pre-treatment, composition of waste, parameters of waste

INTRODUCTION

Most of the waste in the Baltic States is not sorted and is landfilled (Eurostat, 2010). According to national statistics the total amount of disposed municipal waste in 2011 was around 572195 tons and the largest part of it - 89%, consisted of unsorted household refuse and similar waste material. The production of alternative fuels is one of the ways to reduce the amount of waste for landfilling. The method used to reduce organic waste disposal is pre-treatment of the unsorted mass before its disposal. The waste separation lines are one of the technological solutions that is planned to be used in all landfills to separate biological waste in Latvia. Automatic sorting by the linear star screen and rotating drum screen sorting lines was investigated as the pre-treatment method. Sorted waste quality as a solid recovered fuel depends on the content, moisture and other factors. The best solutions were found for pre-sorted waste containing small quantities of biodegradable waste and moisture. The mechanical pre-treatment of solid municipal waste was found as a perspective method for improving the sorting properties of waste.

MATERIALS AND METHODS

The effectiveness of two mechanical separation lines has been evaluated – the linear star screen and the rotating drum screen sorting line.

Waste samples were taken from the *Ziemeļvidzeme* solid municipal waste landfill *Daibe*, with the first waste mechanical Pre-treatment Centre in Latvia and facilities for mechanical shredding, screening (the star screen system – model of *Komptech Multistar L3-Flowerdisc* – throughput performance of up to 40 t h⁻¹; screen sections: 0/10-25 mm; 10-25 /60-80 mm; >60-80 mm) and the separation of metal of the municipal solid waste (Arina, Orupe, 2012; Arina, Bendere *et.al*, 2012). The operation of the Pre-treatment Centre included separation of a high calorific value fraction prior to landfilling and composting of biodegradable waste. The system of the collection of sorted waste is widely developed in the region unlike in the rest of the territory of Latvia. There is approximately 10 % in source sorted waste.

Waste samples were taken from the separation and reloading waste station of *Vibsteri* in *Broceni* (*Viduskurzeme* waste management organization) with the first facilities for alternative fuel (refuse derived fuel and solid recovered fuel) production in Latvia. *Vibsteri* is equipped with a mechanical shredder, screener, magnetic separator of metal, manual sorting line (places for 8 people), a metal detector and cutting mill (30x30 mm). The screener (drum screen) – model of *Technobalt DS-6000* – with screen: 60x60 mm. The typical scheme of screening technologies (Tchobanoglous *et.al*, 1993) and pictures are shown in Fig.1.

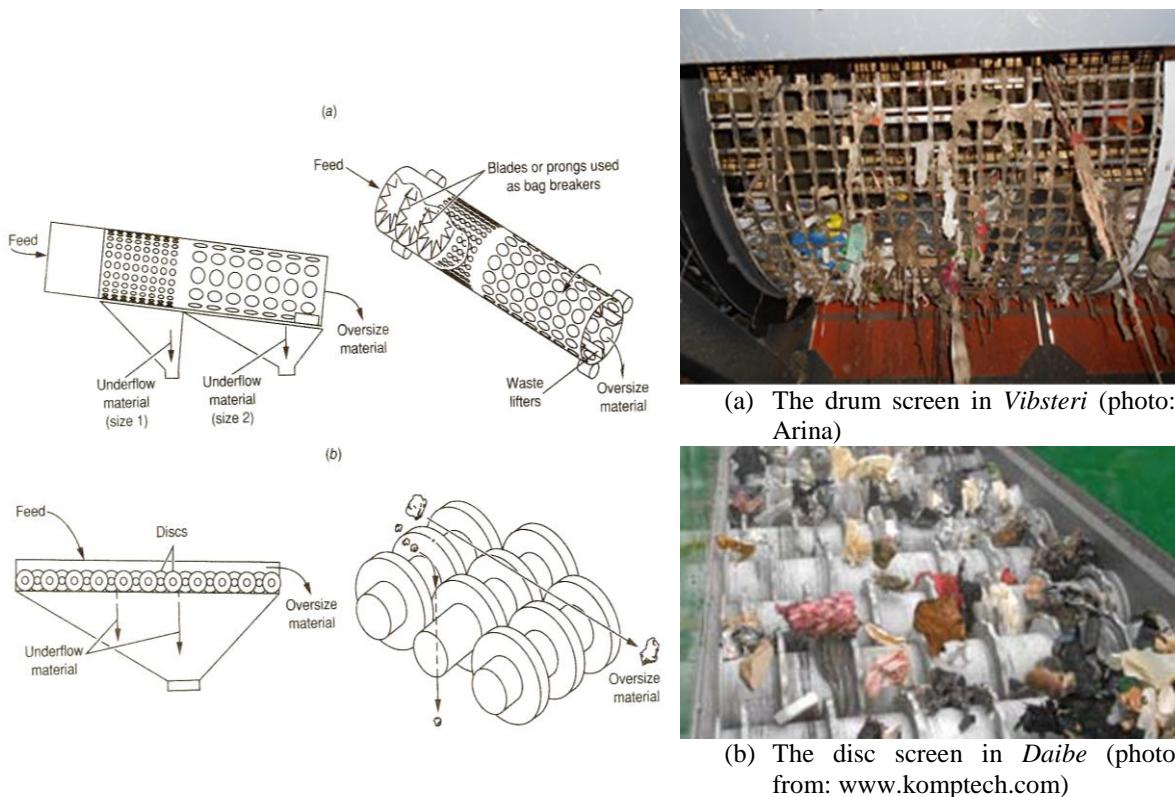


Figure 1. Typical screens used for the separation of solid wastes: (a) rotary drum screen, (b) disc screen

The mass of household refuse waste was screened to the following components in average firstly using pre-shredding:

- After the star screen technology: coarse fraction ~22% (18-25%), medium fraction ~40% (38-43%), fine fraction (putrescible) ~35% (30-36%), metal ~3 % (2-3%);
- After the drum screen technology: coarse (combustible) fraction (size >120mm) ~53% (50-55.5%), fine fraction or putrescible (size <60mm) ~45% (43-47%), metal ~2 % (1.5-3%). Afterwards the coarse fraction is forwarded to the manual sorting line where about 5-8% of it is separated: biodegradable (food) waste ~1%, inert (glass, rocks) ~3%, aluminum cans ~1%. About 45-50% of refuse derived fuel is generated after shredding.

The sampling was carried out according to the Standards *LVS CEN/TR 15310-(1-5):2007* and *LVS EN 14899:2011*. Samples were taken from each fraction: coarse, medium and fine (excluding metal) from the landfill *Daibe* and coarse (refuse derived fuel) after cutting mill and two fine fractions (excluding metal) from *Vibsteri*. The samples of the fine fraction were taken separately from both the start and the end of the drum screen, because of the visual difference between them after their fall out from the drum from its start and end respectively. The experimental

truckloads of the collected refuse waste were chosen from the city in the four seasons in *Daibe* and only in the summer season in *Vibsteri* (one truck load per season) – waste from apartments, private houses and small companies; containers were removed 1-2 times a week.

About 150 samples were taken. The sample size was 1-2 kg. The samples were weighed in the laboratory, dried and weighed again. The composition was determined manually (sorted components were weighed and the respective weight percentage was calculated) in 11 parts – paper and cardboard (soft paper, journals, packing, wallpaper); plastic (soft and hard plastic); putrescible (kitchen waste, garden waste); small particles (miscellaneous small particles); hygiene (diapers and pads); textile (fabric); rubber and leather; wood; metal (ferrous, non-ferrous); glass; mineral (stones, ceramics). In order to prepare the representative samples for laboratory analyses after drying, the samples were grained and formed. The following parameters: moisture, heating value, chlorine and sulphur content, ash, amount of metals in ash were determined according to the series of Standards (from Latvian National Organization for Standardisation) – *Characterization of waste* and *Solid recovered fuels*. Data were evaluated statistically using the SPSS 17.0 computer program. A One-Way ANOVA was used to analyze the effects of the variables.

RESULTS AND DISCUSSIONS

The average percentage distribution of the waste composition of dry mass after the star screen

technology is shown in Table 1 and after the drum screen technology in Table 2.

Table 1

The average composition of waste fractions after waste pre-treatment by the star screener (%, for dry waste)

Composition of waste	Coarse fraction (%) Mean; Std.error	Min; Max	Medium fraction (%) Mean; Std.Error	Min; Max	Fine fraction (%) Mean; Std.Error	Min; Max
Paper and cardboard	39.5±2.90	2.0; 92.1	23.9±1.73	7.6; 48.3	2.4±0.16	0; 4.8
Plastic	38.7±2.84	4.8; 77.9	24.5±1.55	5.4; 44.3	2.1±0.19	0; 5.6
Putrescible, green	0.7±0.17	0; 3.9	6.6±0.85	0; 23.6	12.3±1.38	2.6; 30.0
Small particles (<10mm)	3.2±0.63	0; 16.0	6.3±0.69	0; 18.5	43.7±2.01	21.5; 71.8
Hygiene (diapers, pads)	5.1±0.99	0; 30.6	7.1±1.06	0; 24.6	0.7±0.12	0; 2.9
Textile	5.5±1.27	0; 37.5	4.0±0.81	0; 19.4	0.1±0.03	0; 0.8
Rubber/ leather	4.1±1.32	0; 41.9	3.4±1.34	0; 43.9	0.1±0.02	0; 0.4
Wood	1.1±0.47	0; 19.1	3.6±0.86	0; 20.9	0.5±0.10	0; 2.3
Metal	1.5±0.35	0; 10.3	3.5±0.66	0; 23.4	0.5±0.15	0; 3.3
Glass	0.2±0.08	0; 2.6	9.1±1.17	0; 25.3	32.1±1.86	1.9; 52.0
Inert, mineral	0.4±0.33	0; 13.4	8.1±1.66	0; 36.7	5.5±0.52	0; 14.2

Table 2

The average composition of waste fractions after waste pre-treatment by the drum screener in summer (%, for dry waste)

Composition of waste	Coarse (refuse derived fuel) fraction (%) Mean; Std.error	Min; Max	Fine fraction (from the start of the drum) (%) Mean; Std.Error	Min; Max	Fine-2 fraction (from the end of the drum) (%) Mean; Std.Error	Min; Max
Paper and cardboard	25.8±1.69	17.0; 36.5	6.2±0.53	4.4; 9.8	18.5±2.41	6.0; 31.4
Plastic	24.8±2.23	16.4; 44.9	4.3±0.56	2.4; 9.2	9.9±1.38	3.6; 18.2
Putrescible, green	0.6±0.32	0.0; 3.3	13.6±1.55	2.9; 19.5	17.2±2.60	8.6; 35.3
Small particles (<10mm)	26.0±2.16	10.0; 33.9	40.1±3.59	27.1; 58.2	15.6±2.34	5.4; 29.7
Hygiene (diapers, pads)	2.4±0.56	1.0; 7.7	1.8±0.42	0.0; 4.5	10.3±1.55	2.6; 18.7
Textile	8.9±1.72	0.0; 17.0	1.4±0.30	0.0; 3.1	5.4±1.35	0.0; 13.5
Rubber/ leather	3.9±0.93	0.0; 10.1	0.9±0.38	0.0; 4.0	2.2±0.84	0.0; 9.5
Wood	5.3±0.99	0.9; 11.5	1.1±0.27	0.0; 2.5	3.1±0.68	0.4; 8.6
Metal	0.7±0.26	0.0; 2.9	2.1±1.26	0.0; 14.5	2.2±0.65	0.0; 6.5
Glass	0.4±0.12	0.0; 0.9	21.5±3.24	2.3; 37.9	11.1±1.90	1.9; 22.7
Inert, mineral	1.3±0.66	0.0; 7.4	7.1±1.09	1.4; 13.4	4.4±1.84	0.0; 21.9

The fine fraction from the start of the drum screen was used to compare fine fractions from both screening technologies, because the fine fraction from the start of the drum differs significantly from the fine fraction from the end of the drum.

The drum screener produces more heterogenic mass than the star system screener within fine fraction – there is about three times more paper after drum screening as shown by the data. There is more glass in the separated fraction after the star

screening, because glass is reduced to a smaller size during this process and therefore reaches a fine fraction as smaller and heavier parts. Whereas there are larger pieces of glass (even whole bottles) after

drum screening, therefore arriving at a combustible fraction (afterwards separated manually). The mean values of the parameters for all waste fractions are represented in Table 3.

Table 3
The mean values of the parameters for all waste fractions

Fraction	Moisture (%)	Lower Heating Value (as received) MJ kg ⁻¹	Ash content (dry basis)	S (%)	Cl (%)
After star screen system					
Coarse f.					
Summer	43±3.0	13	17	0.2	1.1
Autumn	36±2.7	13	19	0.2	2.2
Winter	36±4.2	20	8	0.1	0.2
Spring	24±1.6	14	9	0.3	0.3
Medium f.					
Summer	49±1.6	11	15	0.3	4.1
Autumn	48±1.7	8	32	0.2	0.7
Winter	43±1.3	11	33	0.3	1.7
Spring	30±1.7	15	12	0.9	0.5
Fine f.					
Summer	49±2.5	7	46	0.2	2.0
Autumn	44±2.8	3	63	0.2	0.2
Winter	49±1.0	5	65	0.2	0.3
Spring	28±1.2	7	79	0.2	0.1
After drum screen system					
Coarse f., Summer	33±1.1	14	13	0.4	0.7
Fine f., Summer	43±1.7	4	63	0.3	0.5
Fine-2 f., Summer	50±1.6	6	29	0.3	0.4

The moisture of spring significantly differs from the moisture amount for summer coarse fraction, for summer, autumn and winter medium fraction and for summer, autumn and winter fine fraction after the star screen technology (at the $\alpha=0.05$ level; at analyze of ANOVA).

There is a significant difference ($P<0.01$) of moisture between all three summer fractions obtained from the drum screen technology.

There is no statistically significant difference ($P\geq 0.01$) between moisture of the fine fractions from the star and the drum screening technologies in summer.

The lowest calorific value for the coarse fraction was not significantly different between both screening technologies.

The large amount of moisture in the waste influences the calorific value. The amount of moisture depends on the weather conditions, on the proportion of biologically degradable food waste, on the storage of waste and on the waste capacity to absorb moisture. It is characteristic of Latvia that rainfall exceeds evaporation. As paper, cardboard and some hygienic waste and textiles absorb moisture, plastic being relatively dry, forms the largest part of the coarse fraction. In that way moisture is greater if the largest part of the sample is formed from moisture absorbing waste.

The amount of ashes for summer coarse fraction differs significantly between both screening technologies ($P<0.05$). There are more ashes after star screening. The large amount of paper and cardboard within the coarse and medium fraction explains its high proportion of ash. But fine fraction contains more sand and other incombustible materials.

The large amount of cardboard and paper explains the content of chlorine for samples of the coarse fraction. There was relatively less chlorine within the medium fraction, nevertheless this fraction contained an significant part of plastic with chlorine as well as paper and cardboard.

The amount of sulphur was significantly different only for the spring medium fraction, being relatively small for all other fractions.

CONCLUSIONS

- 1) The drum screening technology (screens of 60x60mm) separates more mass of waste than the technology of the star screen. This is useful if the aim of the screening is to separate biologically degradable waste from the waste to be landfilled.
- 2) To obtain more material (fine-2 fraction) for the production of refuse derived fuel, it would be

- advisable for this case to have smaller screens for the distal part of the drum.
- 3) The qualitative material for the production of fuel cannot be obtained from wet unsorted household waste (typical of Latvia's circumstances) by only pre-shredding and screening either with the drum or star screen.
 - 4) Depending on financial resources both technologies (star or drum) of the screening can be used if the aim is not to produce fuel.
 - 5) The waste fractions separated by the star screen technology can be used more widely in landfills. As the fine fraction can be composted and used as a cover material for landfills or can be used for the production of biogas. The medium fraction can be landfilled or used for direct combustion and the coarse fraction can be used to produce fuel.
 - 6) Mechanical sorting lines do not give the possibility to fully separate biological waste.
 - 7) To decrease the amount of moisture in the waste and to increase the amount of waste for RDF or SRF production it is advisable to introduce the source separation system for biowaste (including kitchen waste) – thus it is possible to obtain a qualitative mass of biowaste that can be used for the production of compost or biogas (Bendere, 2012).

ACKNOWLEDGEMENT

Acknowledgement to the European Social Fund (ESF) agreement No: 2009/0180/1DP/1.1.2.1.2/09/IPIA/VIAA/017 for the doctoral research grant award to the first author.

REFERENCES

- Arina D., Bendere R., Teibe I. (2012) Pre-treatment Processes of Waste Reducing the Disposed Amount of Organic Waste and Greenhouse Gas Emission. In: The ISWA World Solid Waste Congress 2012. Proceedings. Florence, Italy, 517 pdf
- Arina, D., Orupe, A. (2012) Characteristics of Mechanically Sorted Municipal Wastes and Their Suitability for Production of Refuse Derived Fuel. *Environmental and Climate Technologies*, Issue 1, Jun 2012, p. 18
- Bendere R., Smigins R., Arina D., Teibe I. (2012) Bioreactor cells as waste pre-treatment method – starting statements, maintenance, final recovery and landfilling. In: 18th International Conference Linnaeus ECO-TECH 2012. Kalmar, Sweden. Proceedings, p. 260-267.
- Eurostat (2010) The Statistical office of the European Union, Waste generation and treatment, 2010, [online] [accessed on 30.01.2013].
- Available:http://appsso.eurostat.ec.europa.eu/nui/show.do?dataset=env_wastrt&lang=en
- Tchobanoglou G., Theisen H., Vigil S.A. (1993) Separation and processing and transformation of solid waste. In: *Integrated Solid Waste Management: Engineering principles and management issues*. USA: McGraw-Hill, Inc. 260 p.

FORECAST FOR DRAINAGE RUNOFF AT DIFFERENT THICKNESS OF HUMUS SOIL LAYER

Otilija Miseckaite, Liudas Kincius,
Aleksandras Stulginskis University, Institute of Water Resources Engineering
E-mail: Otilija.Miseckaite@asu.lt

ABSTRACT

Soil properties and water regime can be improved in various ways, depending on the soil texture and climatic conditions. Drainage hydrological performance often depends on the quality of the installation, anthropogenic and climatic factors. It is important to assess the functioning of drainage under different weather conditions. The article summarizes findings and presents the forecast of drainage flow dynamics bold (up to 40-50 cm) thick and natural (20-30 cm) layer of soils and the impact of meteorological conditions on drainage runoff.

Key words: drainage runoff, thick layer, forecast

INDRODUCTION

Climate change impact on flora is receiving increasing attention around the world (Fuhrer, 2003). Precipitation distribution in a territory and their change within a year has a great impact on the hydrological phenomena, soil formation and plant-growing seasons (Bukantis et al., 2009). Climate changes (temperature increase, precipitation decrease) may be related to environmental pollution. The most important is the size of drainage runoff (Bučienė, 2008). Climatic conditions and physical geographical factors determine the fact that in the territory of Lithuania there are 3.4 million hectares of overly wet land or about 86% of the total agricultural area, which may be used extensively and productively only after draining (Lukianas et al., 2009). The efficiency of land use also depends on the speed of removal of excess water. The changes of climate (temperature increase, precipitation decrease) can be linked to environmental pollution. The role of production agricultural systems as a non-point source of these nutrients in surface waters has come under increasing scrutiny in recent years (Grigg, 2003). Subsequent transport of nitrate N to surface waters occurs through subsurface drainage (tile lines) or base flow (Randal et al., 2001). Compared to surface drainage alone (surface runoff), subsurface drainage increased loss of nitrate from these agricultural fields under both climate regimes, but particularly during drought (Grigg, 2004). At low temperatures and low moisture, the plants intake nutrients worse, therefore, they are eluted from the soil with drainage runoff more intensively (Soussana et al., 2006). Spatial variability of humus layer thicknesses can have important impacts upon soil water dynamics, nutrient storage and availability, as well as plant growth (Bens et al., 2006). The impact of humus on heavy-textured soil is multiple, since not only the moisture regime is

related with its quantity (Maikštėnienė ir kt., 2007). The fertility and erosion of soil is determined by the content of organic materials in it. Humus accumulation depends on the soil texture and fertilization level, climatic conditions (Janušienė, 2002), grown plants (Jankauskas ir kt., 2005). The thickness of humus layer influences not only elution of biogens, but also the speed of surface water drainage to deeper layers of soil. Land drainage is one of the most active areas of the anthropogenic activities which influence the runoff of the rivers (Ruminaite et al, 2011). River flow forecasting has always been one of the most important issues in hydrology (Nayak et al., 2005). Drainage network architecture in a basin is an expression of the surface water hydrological characteristics, and it is a function of the climate, geology and relief of the basin (Pakhmode et al., 2003).

Geomorphological characteristics can be treated as signatures of hydrological responses (Bhagwa et al., 2011). The size of water resources and the unevenness of distribution in time depend on the climatic and meteorological conditions of a specified territory and change every year – very watery and very dry periods occur (Meilutyte-Barauskienė et al. 2008). In most cases, the water table remains within the organic soil throughout the thaw period (Quinton et al., 1999). Soil moisture is an important variable as it affects the soil thermal properties, and therefore the amount of energy available to lower the frost table, which controls the hydraulic conductivity of the saturated layer, and ultimately the rate of subsurface drainage (Quinton et al., 2003).

The aim of research: to determine the influence of thickness of humus layer by using the data of research of 20 years and to make a runoff forecast under conditions of changing climate.

MATERIALS AND METHODS

The investigation was carried out in Lithuania. In the territory of investigations the soil was calcareous deeper gleyic leached soil, (the experiment according to FAO: calcar - HypogleyicLuvisol), according to mechanical composition – loam of medium-heaviness and light loam. Soil volume mass in the layer of 1 m varies from 1.3 to 1.7 g/cm³, porosity - from 50.9 to 32.0 %, hygroscopic moisture – from 0.95 to 2.36 %, the filtration coefficient in arable layer – 0.31–0.94 m/day.

The scheme of the experiment: field I – 1.71 ha with thickened layer of 45–50 cm; field II – control, 1.72 ha with natural humus layer of 20–30 cm.

The results obtained were subjected to the statistical analysis program Statistica. The treatment effects were compared using the least significant difference test at the level of 95% ($p=0.05$) probability. Correlation relation is assessed, according to the value of correlation coefficient R.

RESULTS AND DISCUSSION

Drainage runoff size and duration affect the humus layer thickness: in the field with an artificially thickened humus content (up to 50 cm) frequency curve is steeper, and shorter than outside with natural humus content (up to 30 cm) (Fig. 1).

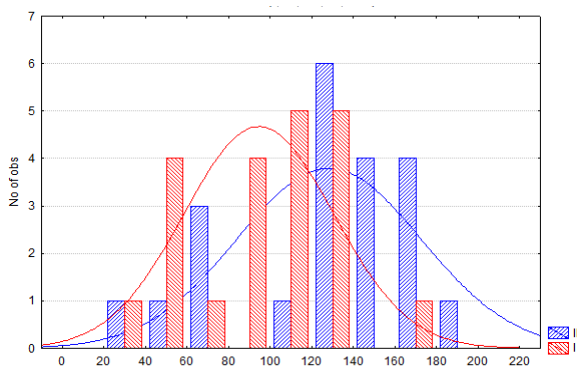


Figure 1. Runoff frequency curve

Analysing the drainage runoff during a twenty-year period between the annual values outside with the artificially thickened humus content (up to 50 cm) and in the control field, with natural humus content (up to 30 cm), a statistically significant difference ($p < 0.05$) was defined (table 1).

Table 1
Analysis of Variance

SS Effect	df Effe ct	MS Effect	SS Error	df Err or	MS Error	F	P
12001.25	1 25	12001.01	86715.40	2167.88	5.54	0.02	

Fig. 2 presents annual runoff and its linear trend. As it can be seen, drainage runoff increases in both versions, however, the curve is sharper in the control field with natural humus layer.

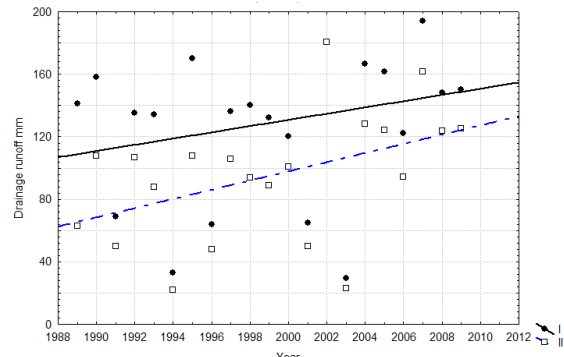


Figure 2. Annual runoff and the linear trend

While analysing the dependence of the size of annual drainage runoff on the annual amount of precipitation, annual temperature and evaporation individually, it was determined that the greatest impact on drainage runoff outside with thickened humus layer is by precipitation, as in the control field. Correlation relation is moderate ($r=0.40$ (I field), $r=0.46$ (II field)). By correlation analysis and the curve estimation of Statistica, the result showed that there were significant relationships ($p<0.05$) between the runoff and precipitation in I field. There was no significant relationship between the runoff and rainfall in I field, but the rainfall had an impact on the runoff. The results of statistical analysis are presented in Table 2.

Table 2

Results of statistical analysis

	Beta	Std. Err. of B	B	Std. Err. of B	t	p-level
I field						
Temperature	0.17	0.21	9.1	11.76	0.78	0.45
Precipitation	0.46	0.21	0.35	0.16	2.20	0.04
Evaporation	-0.06	0.21	-0.04	0.16	-0.28	0.79
II field						
Temperature	0.21	0.22	9.1	9.63	0.94	0.36
Precipitation	0.41	0.22	0.25	0.13	1.90	0.07
Evaporation	0.03	0.22	0.02	0.13	0.13	0.89

Following the method of group linear regression, the dependence of height of drainage runoff on precipitation, evaporation and temperature was analysed. While analysing field II (with thickened humus layer), the correlation coefficient $r=0.49$ was obtained. A similar correlation coefficient was obtained, when analysing the dependence of drainage runoff under natural humus ($r=0.46$).

The results of simple exponential smoothing method (initial data and smoothed data as well as forecast) are presented in Fig. 3. While forecasting

by simple exponential smoothing (FSES) method, the best results are obtained as $a=0.1$.

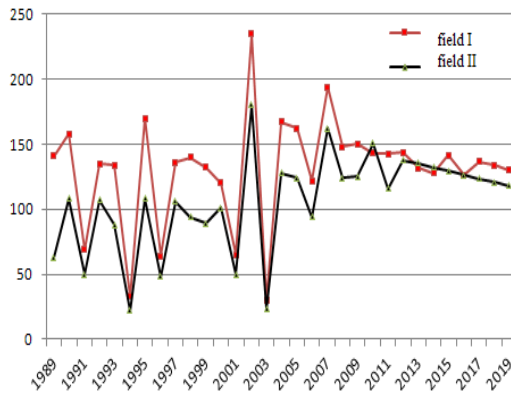


Figure 3. Forecast by applying the forecasting model of simple exponential smoothing

By applying the forecasting model ARIMA (2.0), it was revealed that the size of drainage runoff with a natural or thickened humus layer will become equal or close to the drainage runoff outside with the natural layer (Fig.4). It is explained by the decay of the thickened humus layer through 30 years.

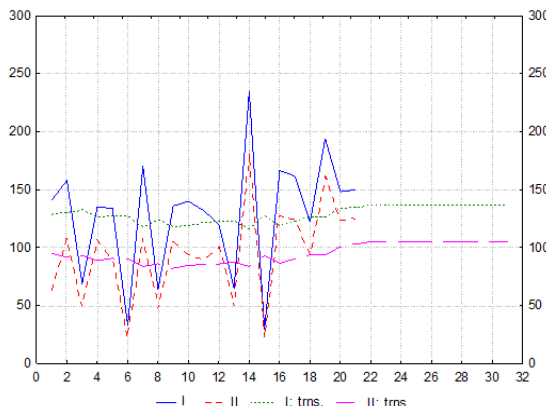


Figure 4. Forecast by applying the ARIMA (2.0) model

Thus, although the forecasts in both cases differ insignificantly, using the model ARIMA (2.0), lower error was obtained. The estimates of forecast accuracy are presented in Table 3.

Table 3
Forecast accuracy

Mean square	I	II
FSES	2714,10	1684,68
ARIMA	1808,7	1029,9

During the twentieth century the global air temperature increased by 0.6°C , while in Europe – 0.95°C . Moreover, due to a more intensive hydrological cycle and an increased atmospheric circulation in the middle and high latitudes, the

warming is accompanied by an increased average amount of precipitation (Bukantis, 2005). In the 21st century air temperature is expected to rise by $2\text{--}5^{\circ}\text{C}$ in Lithuania (Rimkus, 2007).

In case the annual air temperature increases by 2°C and the annual amount of precipitation is the same, the forecasted increase of drainage runoff will be equal to 15% (I field) or 20% (II field), while in case the annual air temperature increases by 5°C – 37% (I field), 52% (II field) (Fig.5).

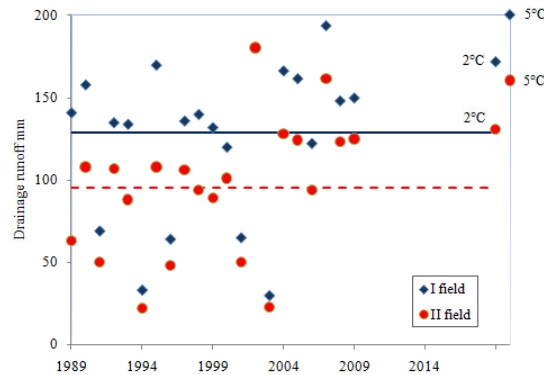


Figure 5. Predicted annual drainage runoff the temperature will increase to 2°C or to 5°C

In Fig. 6 the predicted runoff is presented, in case the temperature will increase to 2°C or 5°C , and the average annual rainfall increases 100mm: the forecasted increase of drainage runoff will be equal to 34% (I field), 37% (II field), while in case the annual air temperature increases by 5°C – 56% (I field), 69% (II field).

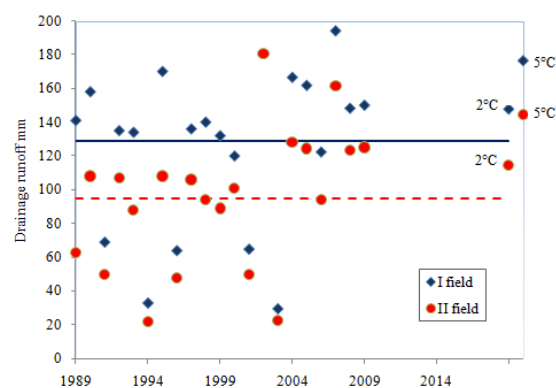


Figure 6. Predicted annual drainage runoff

CONCLUSIONS

Analysing the drainage runoff during a twenty-year period between the annual values outside with the artificially thickened humus content (up to 50 cm) and in the control field, with natural humus content (up to 30 cm), a statistically significant difference ($p < 0.05$) was defined. The size of drainage runoff is mostly influenced by the amount of precipitation ($r=0.46$). In case of thickened humus layer, a statistically reliable result was obtained.

By expecting that the annual air temperature increases by 2°C , the forecasted increase by drainage runoff will be 17.5%, while in case the annual air temperature increases by 5°C , under the current average annual amount of precipitation, an increase of 44.5% is forecasted. In case the annual air temperature increases by 2°C and the annual amount of precipitation grows by 100 mm, the forecasted increase of drainage runoff will be equal to 35.5%, while in case the annual air temperature increases by 5°C - 62.5%.

REFERENCES

- Bens O., Buczko U., Sonja Sieber S., Hutt R. F. (2006) Spatial variability of O layer thickness and humus forms under different pine beech–forest transformation stages in NE Germany. *J. Plant Nutr. Soil Sci*, Vol. 169, p. 5-15.
- Bhagwat N. T., Shetty A., Hegde V. S. (2011) Spatial variation in drainage characteristics and geomorphic instantaneous unit hydrograph (GIUH); implications for watershed management—A case study of the Varada River basin, Northern Karnataka [online] [accessed on 09.08.2012.].
Available: <http://www.sciencedirect.com/science/article/pii/S0341816211000919>
- Būcienė A. (2008) Azoto ir fosforo išplovos drenažu problematika plėtojant ekologinius mišrios gamybos ūkius. *Gyvulininkystė*, Vol. 52, p. 13-29.
- Bukantis A., Kažys J., Rimkus E. (2009) Gausus krituliai Lietuvoje 1961-2008 metais. *Geografija*, Vol. 45, No.1, p. 44-53.
- Fuhrer J. (2003) Agro-ecosystem responses to combinations of elevated CO₂, ozone and global climate change. *Agriculture, Ecosystems and Environment*, Vol. 97, p.1-20.
- Grigg B. C., Southwick L. M., Fouss J. L., Kornecki T. S. (2004) Climate impacts on nitrate loss in drainage waters from a southern alluvial soil. [online] [accessed on 12.10.2012.].
Available: <http://naldc.nal.usda.gov/catalog/9688>
- Grigg, B. C., Southwick, L. M. , Fouss J. L., Kornecki T. S. (2003) Drainage system impacts on surface runoff, nitrate loss, and crop yield on a southern alluvial soil. *American Society of Agricultural Engineers*, p. 1531-1537.
- Jankauskas B., Jankauskienė G., Šlepeliene A. (2005) International campa-rison of analytical protocols for determining soil organic matter content on Lithuanian Albeluvisols. *Earth and Environmental Sciences*. Latvijas Universitatis Raksti, Vol. 692, p. 66-75.
- Janušienė V. (2002) Augalų liekanų ir mėšlo skaidymo intensyvumas bei humifikacija priesmėlio dirvožemyje. *Žemdirbystė: mokslo darbai*, Vol. 77, p. 102-111.
- Lukianas A., Ruminaite R. (2009) Periodiškai šlapiai žemių sausinimo drenažu įtaka upių nuotekui. *Journal of Environmental Engineering and Landscape Management*, Vol. 17, No. 4, p 226-235.
- Maikštienė S., Šlepeliene A., Masilionytė L. (2007) Verstuvinio ir neverstuvinio pagrindinio žemės dirbimo poveikis glėjiškų rudžemių savybėms ir agrosistemų energetiniam efektyvumui. *Žemdirbystė*, Vol. 1, p. 3-23.
- Meilutytė-Barauskienė D., Kovalenkovičienė M., Irbinskas V. (2008) Lietuvos upių vandens ištekliai klimato kaitos fone. *Geografija*, Vol. 44, No. 2, p.1-8.
- Nayak P. C., Sudheer K. P., Ramasastri K. S. (2005) Fuzzy computing based rainfall–runoff model for real time flood forecasting. [online] [accessed on 05.09.2012.].
Available: <http://onlinelibrary.wiley.com/doi/10.1002/hyp.5553/abstract>
- Pakhmode, V., Kulakarni, H., Deolankar, S. B. (2003) Hydrological drainage analysis in watershed programme planning: a case from the Deccan basalt, India. *Journal of Hydrogeology*. Vol. 11, p. 595–604.

- Quinton W. L., Gray D. M. (2003) Subsurface drainage from organic soils in permafrost terrain: the major factors to be represented in a runoff model. *Swets & Zeitlinger*, p. 917-922.
- Quinton, W. L., Marsh, P. (1999) Image Analysis and Water Tracing methods for examining Runoff Pathways, Soil Properties and Residence Times in the Continuous Permafrost Zone. Integrated Methods in Catchment Hydrology. *IUGG 1999 Symposium HS4, Birmingham, UK, July 1999. IAHS Publ.* 258, p. 257–264.
- Randall W. G., Mulla J. D. (2001) Nitrate Nitrogen in Surface Waters as Influenced by Climatic Conditions and Agricultural Practices. *J. Environ. Qual.* 30, p. 337-344;
- Rimkus E., Kažys J., Junevičiūtė J., Stonevičius E. (2007) Climate change predictions for 21st century in Lithuania. *Geographia*, Vol. 43, No. 2, p. 37-47.
- Ruminaite R., Barvidiene O. (2011) Impact of land drainage and natural factors on the changes of the hydrological regime of the Tatula river. Environmental Engineering. The 8th International Conference May 19–20, 2011, Vilnius, Lithuania Selected papers, Vol. 2, p. 654-658.
- Soussana J. F., Lüscher A. (2006) Temperate grasslands and global atmospheric change. *Grassland Science in Europe*, Vol. 11, p. 739-748.

CALCULATION OF RAINWATER SEWAGE SYSTEMS

Eriks Tilgalis, Reinis Ziemelnieks

Latvia University of Agriculture, Department of Architecture and Building

E-mail: eriks.tilgalis@llu.lv; reinis.ziemelnieks@llu.lv

Marcis Sipols

Latvia University of Agriculture, Department of Architecture and Building, Master student

ABSTRACT

Rain intensity is highly variable, making it difficult to accurate calculation of runoff and the flow rate that results in periodic flooding of streets and squares disturbing the traffic and making material damages. The developed rainwater system calculation method is capable of determining the rainfall maximum flow rates of different surfaces with different surface probability (1-200%) in the whole territory of Latvia. The maximum stormwater flow rates are determined according to the expression based on A.Ziverts' formula that is refreshed by R.Ziemelnieks in the promotion work. The gully between the placing distance ridged edge of the road is determined by the expression which was calculated at the end in this publication. LBN 223- 99 was used for rainwater calculation time for gully flow and the formula for calculating the minimum slope of the rainwater collector. The paper gives the k-values of Latvian towns, depending on the desirable flow of rainwater. The method developed enables the calculation of the maximum rate flow of rainwater in urban areas with different probability and the distance between two adjacent intermediate gullies.

Key words: rainwater, rain flow, surface runoff, gullies.

INTRODUCTION

Media news show that heavy downpours in Riga and other Latvian cities become more intensive year after year. Rain or co-system sewerage systems are not able to carry away all surface waters quickly from the squares and streets having the heavy impermeable cover (Ziemelnieks, Tilgalis, Juhna, 2008). At present, parking places, pavements and roads having the impermeable hard cover increase fast in towns (Ziemelnieks, Tilgalis, 2009). The problems caused by rain waters in the city territories have become actual recently beginning more and more to feel the presence of rain waters in the sewerage systems. The situation becomes worse by connection of the rainwater sewerage collectors to the sewerage networks, which creates an additional load to the sewerage networks of the co-systems and pumping stations during the rain. Pumping and purification of rain waters create additional costs of electro energy for the service establishments. A topical dissolved problem is not yet developed method of rainwater gully trap placement calculation.

MATERIALS AND METHODS

Processing of rain data

This study makes use of the rain observation data from different inhabited locations and towns using the publicly accessible information of the agency of Latvia environment, geology and meteorology (LVGMA) (Tables of Meteorological Observations..., Meteorological and hydrological...). The rain observation data rows were summed up and supplemented in order to improve the existing

calculation method of maximum rainwater discharge in the town of Latvia by means of the new k-coefficient. The data of the rain intensity during the warm period from April till September were chosen and used when the downpours with the maximum intensity are observed in Latvia causing the flooding of territories and streets. The precipitation model groups were drawn up selecting the maximum empirical data quantities, in addition by taking into consideration the air temperature regime, the period of warm weather, thus the hard kind of precipitation – snow, ice was not estimated and was excluded from the investigation.

Rainwater discharge calculation methods

The developed rainwater system calculation method is capable of determining the rainfall maximum flow rates of different surfaces with different surface probability (1-200%) in the whole territory of Latvia. The maximum stormwater flow rates are determined according to the expression of the basic formula (1) that is refreshed by E.Tilgalis and R.Ziemelnieks:

$$Q_{\max} = q \cdot k \cdot F \cdot \Psi, [m^3 s^{-1}] \quad (1)$$

where:

Q_{\max} – maximal rainfall flow rate, $m^3 s^{-1}$;
 q – runoff module 1 ($s \cdot ha^{-1}$) calculated using the formula E.Tilgalis;
 k – coefficient depending on the probability of calculation;
 F – surface run-off area to be calculated, ha;
 Ψ – surface runoff coefficient (0,1-0,95% depending on the surface, Table (1)).

The calculation simplified expression of the existing discharge module by E.Tilgalis (Tilgalis, 2004) was used as the calculation basis (2) presuming the length of the specific downpour up to 20 min and its average rain intensity 1 mm min⁻¹.

$$q = 0.13 \cdot \alpha, [(s \cdot ha)^{-1}] \quad (2)$$

where:

α - rainfall amount in millimeters (mm), during the period without frost according to the summed up date by A. Zīverts in Table 2.

The kind of material use of the surface cover may be different in the location of use of a conformable area, therefore, the rainwater discharges change. In Latvia the coefficients of surface discharge have not been summed up in literature. The coefficients of rainwater discharge surface for the present surface cover areas are shown in Table 1.

RESULTS AND DISCUSSION

By determining the values of the precipitation intensity of maximum minutes and by specifying the coefficients of surface runoff for different kinds of covering materials, the calculation method of the existing discharge has been improved. The popular method used in Latvia for the calculation of the discharge amount is a simplified method worked out by A.Zīverts and Ē.Tilgalis (Tilgalis, 2004). Using this method it is possible to calculate the discharges with the possibility up to 200%.

In addition, the determined k-coefficient dependent on the calculation possibility was determined based on the previously carried out investigations in the promotion work (R.Ziemelnieks). The method elaborated provides for the possibility to calculate the maximum rainwater discharges in inhabited locations with a different possibility. In the result of the investigation it is possible to conclude that in Latvia it is advisable to use the calculations with the repetition possibility or 25% (frequency of According to the table drawn up by A.Zīverts (Zīverts, 1997) several values of k-coefficients for the inhabited locations of Latvia are determined. improvements was carried out, repetition once in 2 or 4 years).

The gully between the placing distance ridged edge of the road is determined by the following expression:

$$L = \frac{Q_{kan} \cdot E \cdot t_r^{1,2n-0,1} \cdot 10^7}{Z_{mid} \cdot A^{1,2} \cdot (a+x)} [m] \quad (3)$$

where:

L- inlet spacing between two intermediate gullies (m);

t_r - time for water to travel from the furthest point on the road surface to the gully grating (by LBN 223-99, 3-5 min);

F- area included between two adjacent inlets (ha);

Q_{kan} - peak flow approaching the inlet (sub-catchment outlet) (l/s);

Z_{mid} - runoff coefficient (by LBN 223-99,0.29)

A- parameter related by LBN 223-99

n- parameter related by LBN 223-99

a- width of the sidewalk (m)

x- half width of the roadway (m)

E - grate effectiveness of the collect rain water is determined by *UPC* methodology.

Table 1
Coefficients Ψ

Use of areas or type of covering material of surface area	Coefficient, Ψ
Use of areas	
Town office	0.70 - 0.95
Commercial premises	0.50 - 0.70
Populated areas	
Detached house	0.30 - 0.50
Flat in a dwelling house	0.40 - 0.60
Flat(apartments)	0.60 - 0.80
Inhabited suburb district	0.25 - 0.40
Industrial district	
Light industry	0.50- 0.80
Heavy industry	0.60 - 0.90
Parks, green areas, cemeteries	0.10 - 0.30
Railway carriage park, playground	0.20 - 0.40
Meadows for pastures	0.10 - 0.30
Surface area covering material	
Street, pavement covered by asphalt or concrete	0.70-0.95
Concrete area	0.80-0.95
Concrete cobble stone covering	0.70-0.80
Pedestrian pavements and part for transport	0.75-0.85
House roof covering material (depending on material)	0.75-0.95
Grassland having sandy soil composition	
Sandy soil with 2% decline or less	0.05-0.10
Sandy soil with 2%-8% decline	0.10-0.16
Sandy soil with 8% decline or more(precipice, slope)	0.16-0.20
Grassland having clayey soil composition	
Decline 2% or less	0.10 - 0.16
Decline 2%-8%	0.17 - 0.25
Decline 8% and more (precipice, slope)	0.26 - 0.36

Source: Computer applications in hydraulic engineering (basic hydrology-rainfall)(translation report by R.Ziemelnieks)

Recently, the Hydraulic and Hydrological Engineering Section of the Technical University of Catalonia (UPC) promoted a new research line in the field of the road grate efficiency, (DEHMA-UPC, 2004):

$$E = A \cdot \left(\frac{Q}{y} \right)^{-B} \quad (4)$$

where:

Q- total flow approaching the inlet (l/s)

y- hydraulic depth upstream to the grate (mm)

A and B are two characteristic parameters related to the grate geometry.

Eq. 4 is the result produced by a series of tests on a platform of 3 m width corresponding to a common lane in Latvia.

Table 2
Values of k-coefficients

No	City, populated place	Duration of observation, years	a, rainfall April-September, mm	k-coefficient with the possibility						
				200%	100%	50%	25%	10%	5%	1%
1	Cīrava	33	272	0,75	1,25	1,54	1,92	2,37	2,67	3,35
2	Dagda	27	268	0,75	1,23	1,50	1,84	2,33	2,60	3,30
3	Daugavpils	42	276	0,77	1,27	1,58	1,95	2,40	2,70	3,40
4	Dzērbene	33	428	1,17	2,00	2,47	3,00	3,70	4,12	6,10
5	Gulbene	39	391	1,0	1,77	2,23	2,74	3,40	3,80	4,75
6	Gureļi	37	447	1,23	2,07	2,54	3,15	3,85	4,35	6,65
7	Ieriķi	35	391	1,0	1,77	2,23	2,74	3,40	3,80	4,75
8	Jelgava	50	335	1,0	1,54	1,86	2,37	2,90	3,25	4,00
9	Kabile	41	291	0,80	1,33	1,63	2,05	2,50	2,80	3,57
10	Kolka	57	250	0,71	1,15	1,37	1,73	2,15	2,45	3,10
11	Kosa	25	428	1,17	2,00	2,47	3,00	3,70	4,12	6,10
12	Kuldīga	42	291	0,80	1,33	1,63	2,05	2,50	2,80	3,57
13	Lejasciems	29	484	1,33	2,27	2,74	3,45	4,24	4,63	7,90
14	Liepāja	63	235	0,68	1,05	1,30	1,63	2,03	2,30	2,85
15	Mālpils	38	409	1,12	1,86	2,35	2,85	3,55	3,95	5,60
16	Ogre	31	335	1,0	1,54	1,86	2,37	2,90	3,25	4,00
17	Pilskalne	35	277	0,77	1,27	1,58	1,95	2,43	2,70	3,40
18	Priekuļi	47	409	1,12	1,86	2,35	2,85	3,55	3,95	5,60
19	Ranka	34	391	1,0	1,77	2,23	2,74	3,40	3,80	4,75
20	Rēzekne	37	264	0,73	1,20	2,10	1,82	3,13	2,54	3,22
21	Rīga	71	368	1,00	1,68	2,10	2,60	3,12	3,60	4,50
22	Saldus	27	263	0,73	1,20	1,45	1,82	2,30	2,54	3,18
23	Stāmeriene	38	447	1,23	2,07	2,54	3,15	3,85	4,35	6,65
24	Stende	46	304	0,85	1,37	1,70	2,12	2,64	2,95	3,75
25	Subate	37	228	0,65	1,03	1,27	1,60	1,97	2,19	2,77
26	Užava	25	272	0,75	1,25	1,54	1,92	2,37	2,67	3,35
27	Ventspils	59	298	0,83	1,35	1,65	2,10	2,57	2,85	3,65

Source: Calculated and created by R.Ziemelnieks

$$A = \frac{0,39}{A_g^{-0,35} \cdot p^{-0,13}} (n_t + 1)^{0,01} \cdot (n_l + 1)^{0,11} \times (n_d + 1)^{0,03} \quad (5)$$

$$B = 0,36 \cdot \frac{L}{W} \quad (6)$$

where:

Ag- area that includes the void area of the grate inlet (AH)

p- ratio of the Ag to the AH

nt, nl, nd- are, respectively, the numbers of transversal, longitudinal and diagonal bars
L- length of the grate inlet
W- width of the grate inlet

The rainwater diversion gravity self-flow collector internal diameters were calculated assuming the full pipe filling and a minimum allowable internal pipe diameter of 250 mm (200 mm are usually used for inside section nets) to calculate the minimum pipe slope (LBN 223-99), which will challenge the self-cleaning process of the pipe systems using expression:

$$Q = \omega \cdot v, \text{ m}^3\text{s}^{-1} \quad (7)$$

$$I_{\min} = \tau (\rho g R)^{-1} \quad (8)$$

where:

τ – flow stress, N/m²;

ρ – gravity of waste water, kg/m³;

g – acceleration due to gravity, m/s²;
R – pipeline filled hydraulic radius, m.

CONCLUSIONS

1. The newly formed formulas (1; 3) and the real values (Tables 1; 2) given offer an accurate calculation of the rainwater discharge.
2. According to the values of k-coefficient numbers obtained, it can be concluded, that one may take into consideration larger possibilities of the consequences of the flood, while choosing the surface covering material with a less repetition possibility.
3. It is recommended to make calculations with 50% probability. The calculation method of the distances between gullies gives designers a new footing based on the hydraulic calculation.
4. The proposed stormwater drainage system calculation method will prevent grave errors of stormwater discharge and gully mutual distance calculations.

REFERENCES

- Metodiskie norādījumi lietus kanalizācijas projektēšanā (1983) Komunālās saimniecības pārvaldes ministrija LPSRS projektēšanas institūts „Latkomunālprojekts”, izlaidums HBK -3-83. Rīga: institūts „Latkomunālprojekts”, 66 p.
- Meteoroloģisko novērojumu tabulas TMS, Rīga, I-XII, stacijas Nr. 5692410. Laika josla Griničas.\Regions Zemgale, Stacija: Rīga. Kods: RIAS99PA. Latvijas Republikas hidrometeoroloģijas pārvaldes dabas vides stāvokļa valsts datu fonds jeb LVGMA.
- Hydraulic Department (DEHMA-UPC) (2004). Course of Urban Hydrology. Technical University of Catalonia, Barcelona, Spain.
- Ziemeļnieks R., Tilgalis E. (2009) „Calculation method of rainfall flow rate”, LUA Annual 15th International Scientific Conference Proceedings, Research for Rural Development 2009. Jelgava, Latvia University of Agriculture, pp. 315-319.
- Ziemeļnieks R., Tilgalis E., Juhna V. (2008) „Rainfall effect on sewage co-system activity in Riga”, LUA Annual 14th International Scientific Conference Proceedings, Research for Rural Development 2008. Jelgava, Latvia University of Agriculture, pp.194-199.
- Ziemeļnieks R., Tilgalis E. (2009) „Calculation method of rainwater discharge”, LUA 3rd International Scientific Conference Civil Engineering'11. Jelgava, Latvia University of Agriculture, pp. 267-271.
- Tilgalis Ē. (2004) *Notekūdeņu savākšana un attīrīšana*: mācību grāmata. Jelgava: LLU, LVAF. 239 lpp.
- Zīverts A. (1997) *Ievads hidroloģijā*: mācību palīglīdzeklis, Jelgava: LLU. 111 lpp.
- Meteoroloģisko un hidroloģisko novērojumu dati* [online] [accessed on 04.01.2010]. Available: http://www.meteo.lv/public/hidrometeo_dati.html
- Noteikumi par LBN 223-99 Kanalizācijas ārējie tīkli un būves: MK noteikumi Nr.214* [online] [accessed on 07.05.2010]. Available: <http://www.likumi.lv/doc.php?id=19996>

GROUND TEMPERATURE REGIME IN THE COWSHED ENVIRONMENT

Dainius Ramukevicius*, Petras Milius**

Aleksandras Stulginskis University

Institute of Hydraulic Construction Engineering

E-mail: *dainius.ramukevicius@asu.lt, **petras.milius@asu.lt

ABSTRACT

The investigations of ground temperature fixings in a cowshed building environment and under the building are presented in the article. Ground temperatures have been fixed on the surface and in various depths up to 3 metres. Ground surface and premise's air temperatures have been fixed inside the building. Three temperature fixing borings have been arranged inside the building and as many outside. The temperature has been fixed at 5 points and in various depths of every boring.

With the help of the ground temperature fixings on the premises of the cowshed building's animal resting area, it has been determined that in winter time the temperature from the floor's surface distributes from 14 °C up to 20 °C. It is influenced by outside and inside air temperature as well as by the animal's heat transfer to the ground surface. A more active ground temperature variation of the building environment is noticeable at the depth of up to 3 metres. The fixed ground temperatures in the boring (which is moved away from the building at 5 metres) showed that the climate influences the temperature distribution most of all.

Keywords: cowshed, ground, temperature

INTRODUCTION

One of the ways to reduce the uses of heat and electricity energy in agricultural buildings and to improve microclimate is the improvement of heat isolation of the building while using effective building materials of barrier constructions.

It has been known that between outdoors and the ground (that is in structure's zone) and between the lodgment's air, intense heat interchanges go through the floors on the ground as well as through the foundations. These interchanges have a huge influence on the microclimate of the whole building (Montsvilienė, 2003; Phillips et al. 1992). When the microclimate is optimal, the animal efficiency may increase to 30 %. When the microclimate is incorrect, 15-20 % of animals (especially the young ones) could die because of diseases, their weight decreases to 25 % and 15-20 % of the feed is overdraft (Sallvik, 1998).

The microclimate of the cowshed very much depends on the building's construction, the state of the building's temperature, the temperature of inside surfaces of barriers. 50 % and more of their time the animals usually rest, that is why the temperature of the floor's surface influences the heating control process of the animal's organism as well as its metabolism, heat generation and feed usage (Sallvik, 1998; Bleizgys et al., 2008).

Despite the fact that many articles concerning the questions of heat waste reduction have been published in Lithuania and are dedicated to analytical and experimental investigations of the state of temperature of the superstructure, different measures have been started to be applied, different variants of building heating have been suggested,

nevertheless the influence of soils in the structure's zone is underrated (Hilti et al., 2002).

Heat interchanges through the ground are very complex. One must know the theoretical basis of physics of building heating as well as heating-moisturizing ground and material conditions, building climatology.

In foreign countries (USA, UK, Norway, Sweden, Russia etc.) different calculation methods of heat interchanges of the buildings are used while designing buildings. At present in foreign countries computer programs are used for the calculations of heat interchanges of the buildings (Ehrlemark et al., 1996). More detailed investigations in Lithuania concerning this problem started this decade. However in scientific research works published in Lithuania as well as abroad, the detailed investigation data about the influence of ground on the state of temperature of the whole structure is lacking. Besides, the influence of outdoor factors is underrated. That is why when trying to evaluate the influence of the ground on the state of temperature of a cowshed (on which the microclimate parameters depend only partially), first of all experimental investigations must be carried out in order to determine the temperature of the ground of the animal-breeding structure. While having the factual ground temperature, it is easy to determine the heat losses of the structure through the floor on the ground.

MATERIALS AND METHODS

While selecting the place in the object for the measuring of ground temperature, the building configuration, lodgement layout, windows and

doors arrangement, animal resting and standing areas have been taken into account as well as the potential influence of outdoor factors. Temperature measurements of the ground were carried out in the cowshed in 80 places. The length of the cowshed – 66.6 m, the width – 12.5 m, the height of the lodgement – 2.4 m. Constructions of the cowshed: foundations – concrete strip, width – 40 cm, deepening – 1.1 m. Floor construction: concrete – 5 cm; gravel – 15 cm; ground – clay. There are 80 cows in two roped rows in the cowshed. The cowshed plan is shown in Figure 1.

It is very important that the borings must be arranged very close to the foundation from the inside as well as from the outdoor areas. While trying to evaluate the ground influence of the building zone on the state of temperature of the whole building, the temperature of the ground of the nearby building should be taken into account as well. Inside the cowshed 3 borings I, II, III with a diameter of 4 cm were made for the ground temperature investigations from the outside of the foundation up to the middle of the cowshed.

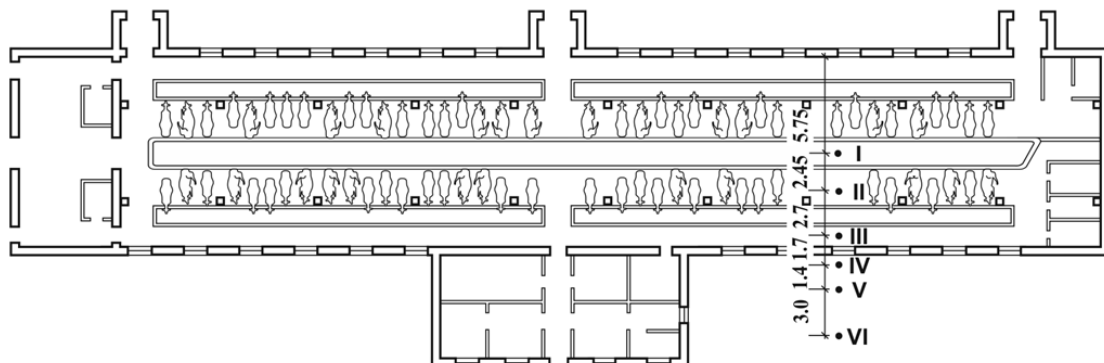


Figure 1. Plan of the cowshed: I-VI – borehole numbers

Semiconductor transistor sensors were placed to measure the temperature in every boring in a vertical direction at a distance of 0.25 m, 0.5 m, 1.0 m, 2.0 m and 3.0 m from the land's surface. Also outside of the building at a distance of 0.6 m, 2.0 and 5.0 m from the outdoor wall and in IV, V, VI borings, the above mentioned sensors were placed into duplicate depths in the land surface. All borings up to the land surface were filled up with a mix of sand and gravel.

The computer program "Surfer" was used for graphical presentation of temperature spreading in cowshed base and in its surroundings. The heat transmission from higher to lower temperature zones are displayed by pointers.

The measuring of the grounds of the cowshed was carried out from 11/2004 till 05/2005. The temperature measuring wasn't equal. They were fixed with 3-5 day intervals.

RESULTS AND DISCUSSION

The ground temperature measurements of the cowshed base and its external environment showed that the ground temperature field (under the building) is in a constant dynamic state. The heat exchange between the outside ground and the one

under the building as well as on the floor is influenced by the external temperature regime. A very intense heat exchange takes place during the stable period, i.e. during the winter months. For example, in November, when the outdoor temperature drops below 0 C°, the base ground temperature under the floor near the foundation (0,25 m) drops to 6-8 °C. At that time, the surface temperature of the foundation is 5.0 °C lower than the surface of the area in the middle of the floor (Fig. 3., 4 curve). At lower outdoor temperatures the cowshed's interior ground and floor chilling occurs partly due to the cold wall of the premises, because the wall thermal resistance is $\approx 1 \text{ m}^2\text{K/W}$. When the outdoor temperature dropped more than -10 °C, the temperature of the floor near the foundation (III ground temperature measurement point) was 5 °C lower than in the middle floor area (I ground temperature measurement point) (Fig. 3., 1 and 2 curves). In May and June, when base ground thaws, the temperature fluctuations in floor surface are relatively small – from 1 to 3 °C (Fig. 3., 6 and 7 curves). A computer program was used for the graphical presentation of the temperature distribution of the ground in the cowshed inside base and its external environment. Using the data of

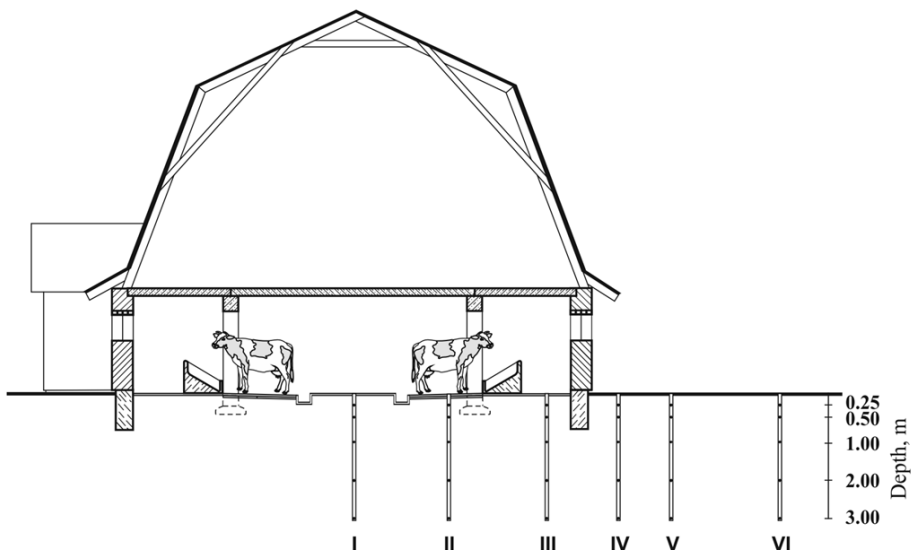


Figure 2. Arrangement of the measuring boreholes of the ground temperature of the cowshed internal base and external environment as well as temperature sensing depths in them

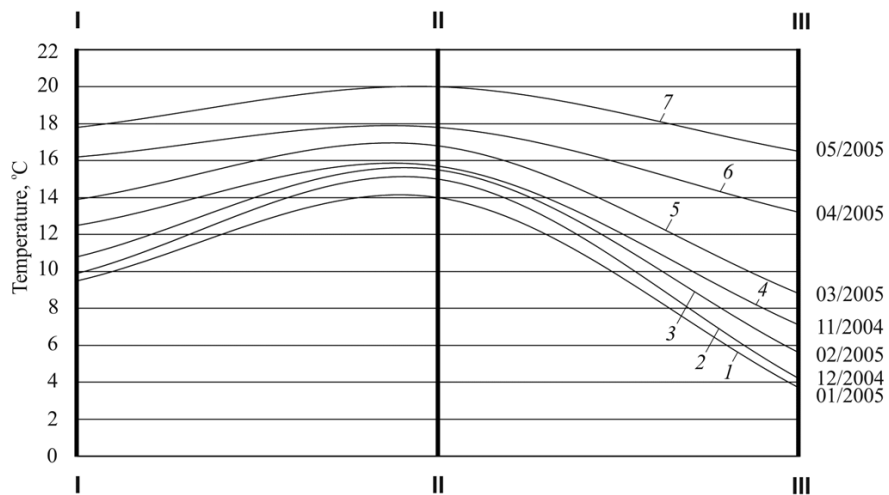


Figure 3. The temperature of the floor surface of the cowshed building in various periods of the year:
I-I – in the middle of the cow housing room; II-II – in the cow standing area;
III-III – inside the building near the outside walls

the cowshed internal base ground temperature measurements, the cowshed building base ground uniform temperature distribution lines - isotherms were obtained (Fig. 4). A set of isothermal surface consists of these lines. The temperature difference and the distance between the two isotherms ratio gives the temperature gradient, which describes the propagation of heat. Heat propagation directions from a higher temperature area to a lower temperature range, as well as directions of the grounds in the cowshed inside base and its external environment are presented by arrows (Fig. 4).

Following the building's external environment, the ground temperature measurement analysis of the results showed that the ground frost depth of the building (farthest from the remote wells) (Figure 4., VI ground temperature measurement point) was

only 0.6 m in winter time. Such shallow ground frost could affect the cowshed building internal base ground temperatures. Therefore, it can be said that to some extent, the cowshed building internal base temperature depends on the outdoor air temperature. However, the cowshed internal base temperature experimental measurements show that the radiated heat from the animals in their living quarters has a significant influence on the internal base temperature field. This is apparent in Figure 3., where the highest temperature is on the floor surface of the living quarters (II ground temperature measuring point). The radiated heat from the animal at the site of its living quarters is transmitted not only to the surrounding surface of the living quarters and the floor, but to the ground floor in the deeper layers as well. Particularly intense

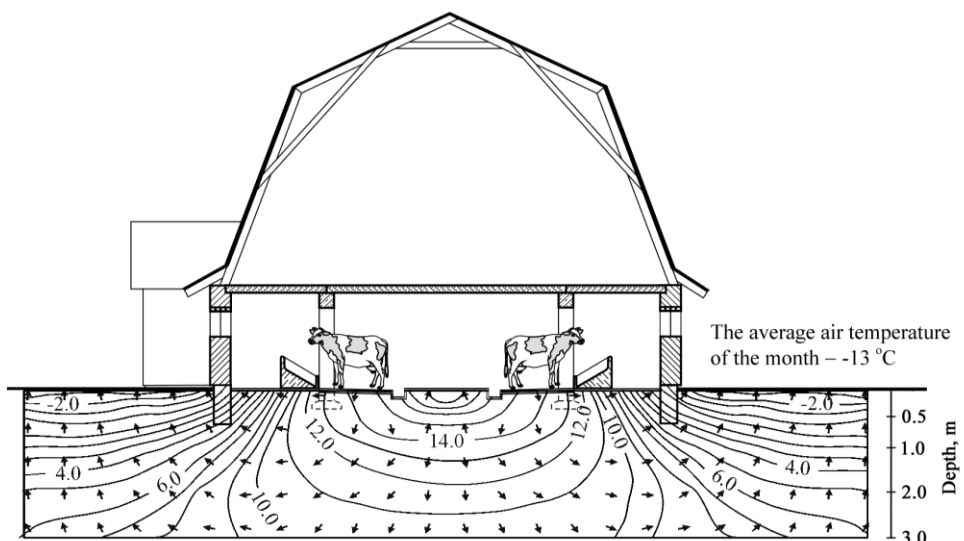


Figure 4. The average ground temperature of the cowshed base and its environment, when the coldest month outside air temperature was during the research period (01/2005)

heat exchange between animal living quarters and the building external environment air manifests in cold season through the base ground and building foundations. However, not all the heat is transferred to this direction. Some heat radiated from the animals through the floor comes back into the room next to the floor area into the ground living quarters due to the air temperature difference in the ground floor and ground surface. Such thermal movement of the subfloor ground is possible when the outside air temperature is much lower than -10°C. When the weather gets warmer, the temperature distribution of the building internal base ground and its external environment becomes more equal (according to depth) (Fig. 4).

CONCLUSIONS

Intense heat exchange between the outside air and ground-based cowshed through the

foundation manifests itself during the coldest time of the year. When the outdoor temperature drops below 0 °C, the base ground temperature under the floor near the foundation drops to 6-8 °C. When the outdoor temperature has dropped more than -10 °C, the temperature of the floor near the foundation is 5 °C lower than in the middle floor area (9-10 °C).

The experimental temperature measurement data show that heat radiated by animals, that is absorbed not only in the air, but also in the base ground through living quarters floor has a significant influence on the internal base ground temperature field. Some heat radiated from the animals through the floor comes back into the room next floor area into the ground living quarters due to the air temperature difference on the ground floor and ground surface.

REFERENCES

- Bleizgys R., Česna J., Kavolėlis B. (2008) *Perspektyvios galvijų laikymo technologijos*. Kaunas: Akademija, 56 p.
- Ehrlemark A., Sallvik K. (1996) Model of Heat and Moisture Dissipation for Cattle Based on Thermal Properties. *Transaction of the ASAE*, Vol. 39, No. 1, p. 187–194.
- Hilty R., Kaufmann R., Van Canegem L. (2002) Building for Cattle Husbandry. *Yearbook Agricultural Engineering*, VDMA Landtechnik, No.14, p. 163-170.
- Montsvilienė E. (2003) *Fizinių, cheminių ir biologinių aplinkos veiksnių tyrimai ir jų įtaka šaltose karvidėse laikomoms kareivėms*. Dr. disertacijos santrauka. LVA, Kaunas, 28 p.
- Phillips C., Piggins D. (1992) *Farm Animals and the Environment*. Wallingford C. A. B. International cop., 54 p.
- Sallvik K. (1998) Environment for Animals. *CIGR Hanbook of Agricultural Engineering, Animal Production*, Vol 2. p. 32-54.
- Sirvydas A., Kerpauskas P., Nadzeikienė J., Stepanas A., Teresciuk V. (2006) Temperature Measurements in Research of Thermal Weed Extermination. *Proceedings of the International Conference, Development of Agricultural Technologies and Technical Means in Ecological and Energetic Aspects*, No. 11, p. 321-331.

LIMIT DEFORMATIONS OF RETAINING WALLS IN LITHUANIAN HYDROSCHMES

Raimondas Sadzevicius*, Tatjana Sankauskiene**, Feliksas Mikuckis***

Aleksandras Stulginskis University, Institute of Hydraulic Construction Engineering

E-mail: *raimondas.sadzevicius@asu.lt, **tatjana.sankauskiene@asu.lt, ***feliksas.mikuckis@asu.lt

ABSTRACT

In accordance with Standard STR 2.05.04:2003 all deformations of hydraulic structures are divided in two groups: 1) main – deformations of whole structure and 2) local – deformations of joints, supports, etc. Retaining walls of the used hydraulic structures are under the influence of climatic conditions, water, soil pressure and other types of loads. Deformations appear because of the aggressive environment and the load influence. The aim of the work is to evaluate the limit deformation of retaining walls on hydroschemes.

The state of 14 reinforced concrete retaining walls of hydroschemes was evaluated during the scientific expedition in the period 2007–2012. Retaining walls of hydraulic structures in Kaunas, Marijampolė, Kėdainiai, Panevėžys, Šilutė districts were examined and main deformations were determined.

Key words: retaining walls, limit deformation, hydroschemes.

INTRODUCTION

After the analysis of the state of 155 dams' hydraulic structures constructed in Lithuania was made (Patašius, 2009), it was found out that the most common deformations are these: cracked, leant, displaced, crumbled retaining walls (RW) of reinforced concrete. RW are considered as the main constructions of hydraulic structures (main constructions are those, which hold the pressure of soil and water). The questions of the evaluation of the state and reliability of these constructions are important because, if the evaluation of deformations of RW is carried out and the repair or reconstruction works are made in time, not only the collapse of RW but also the breakdown of the whole hydroscheme is prevented. Field observations and analytical methods were used for the evaluation of limit deformations of hydraulic structures' (HS) retaining walls. In accordance with Standard STR 2.05.04:2003 all deformations of hydraulic structures are divided in two groups: 1) main – deformations and displacements of the whole structure and 2) local – deformations of joints, supports, etc. This Standard does not specify which limit values define the deformations of RW. Limit cases of RW construction deterioration are given in Standard STR 2.05.14:2005, nevertheless it is not specified in this document, what limit values of vertical and horizontal deformations (fig. 1) are applied in the evaluation of the state of RW.

Vertical and horizontal deformations of building constructions and their limit values are defined in Standard STR 1.12.01:2004 app. 1, however the

document does not say anything about RW deformations' limit values. In science literature, they were described by Lithuanian (Gurskis, 2006; Patašius, 2009; Jokūbaitis, 2007) and foreign (Witzany, 2007; US Army Corps of Engineers, 2002) scientists. In accordance with the analysis of reviewed literature, it was found out that the characteristics of materials' physical and mechanical properties are correctly evaluated not in all cases, there is a lack of data about the values of RW deformations, calculation methods are complicated and do not give accurate results, consequently additional research of the evaluation of RW deformations' limit values have to be carried out.

Object of research – Retaining walls of hydroschemes, which are located in Kaunas, Marijampolė, Kėdainiai, Panevėžys, Šilutė districts.

Aim of research – to evaluate limit values of deformations of retaining walls in hydraulic constructions.

Tasks to reach the aim:

- To evaluate retaining walls' geometrical characteristics and to measure deformations in Kaunas, Marijampolė, Kėdainiai, Panevėžys, Šilutė districts;
- To evaluate the compressive strength of concrete of retaining walls;
- To determine the inclination of retaining walls dependence on wall's height.

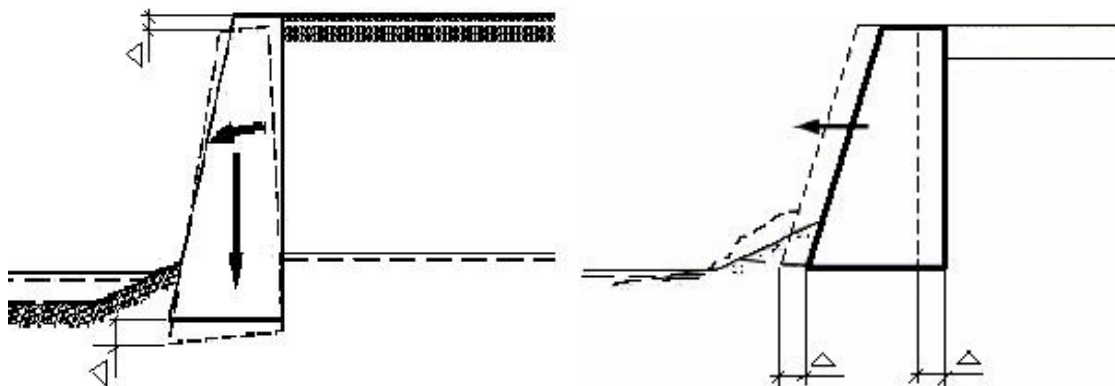


Figure. 1 The illustration of retaining wall horizontal and vertical deformations

METHODS OF RESEARCH

According to the researches carried out earlier (in 1998 – 2007) by the researchers of the Department of Building Constructions in Aleksandras Stulginskis university, hydroschemes with noticed considerable deformations of retaining walls were chosen. In Kaunas, Marijampolė, Kėdainiai, Panevėžys, Šilutė districts, RW inclinations were noticed in retaining walls of 14 hydroschemes. Analyzing in detail, how limit deformations depend on RW geometry, RW deformations' dependencies on wall's geometrical properties were determined. Analyzing the state of retaining walls, the following diagnostics methods were used: visual examination,

deformations photofixation, nondestructive methods for the estimation of RW strength, field observations.

Visual examination is the examination of an object at the same time making the simplest necessary measurements and using simple tools such as a tape-measure, a ruler, a sliding caliper, a camera and a plumb line.

RW lengths, widths, heights, inclinations and deflections were measured during field observations (fig. 2).

Photofixation method – everything was sequentially photographed.



Figure. 2 Illustration of retaining walls deformations' measurements

Using the nondestructive method with a rebound hammer of concrete Cat.58-CO181/N (Schmidt's system), an actual compressive strength of concrete was measured.

Testing concrete with the rebound hammer in specially prepared construction's places, 10-12 hits were made in accordance with the usage instructions of the instrument. Research results were statistically evaluated – an average compressive strength of concrete f_c , variation coefficient v and

root-mean-square deviation σ were calculated using „Microsoft Excel“ macros.

RESULTS AND THEIR REVIEW

Table 1 represents construction sites' names, minimal values of RW compressive strength of concrete f_c , variation coefficient v , root-mean-square deviation σ , RW inclination and RW height which were investigated in 14 hydroschemes.

Table 1

Results of the research of retaining walls' compressive strength
of concrete and deformations in hydroschemes

No.	Name of hydroscheme	Minimal values of compressive strength of concrete, f_c , MPa	Variation coefficient v , %	Root-mean-square deviation σ	RW inclination, cm	RW height, cm
Kaunas district						
1.	Gailiušai	7.6	40.74	3.08	12	320
2.	Panevežiukas	5.6	21.74	1.22	7	237
Marijampolė district						
3.	Pilviškiai	16.8	32.12	5.9	R 7.2 L 5.3	R 165 L 170
4.	Totorvietės	14.1	20.22	3.0	—	—
5.	Marijampolės marios	22.1	24.73	5.8	R 15 L 6.5	—
Panevėžys district						
6.	Jotainiai	19.0	24.77	5.0	R 4.5 L 12	880 – 440
7.	Pažibai	11.2	32.97	3.9	R 8.5 L 13	280
8.	Žibartony II	25.4	39.82	10.7	R 6 L 5	235
9.	Paviešiečiai	4.4	42.54	2.0	—	—
10.	Žibartony I	14.5	35.77	5.5	R 6	300
Kėdainiai district						
11.	Kėdainiai town	11.9	24.46	3.1	11.5 and 5	780 – 260
12.	Dotnuva	4.7	46.76	2.3	4	250
13.	Kruostas	31.2	30.42	10.8	R 2	910
Šilutė district						
14.	Žemaičių Naumiestis	25.3	15.77	4.9	L 3 R 17	480

Notice: R – right RW, L – left RW, “–“ Measurements not carried out.

According to the research results presented in table 1, it was established that, out of 14 hydroschemes, the smallest compressive strength of concrete was in Paviešiečiai dam's RW (4.4 MPa), the biggest one – in Žibartony II dam's RW. In accordance with earlier (during the course of design) valid requirements of regulations, the class of compressive strength of concrete in these constructions should have been no lower than B15, these days it would correspond to the C12/15 class. The concrete of retaining walls of Marijampolės marios, Jotainiai, Žibartony II, Žemaičių Naumiestis hydroschemes meets the requirements of these standards. In accordance with currently valid Standard STR 2.05.05:2005 constructions, used in the conditions of XC4 and XF3 exposure classes, must designed from the concrete whose the least strength class is C30/37. The RW concrete of

none researched hydroscheme meets this requirement.

The smallest RW inclination was found in Dotnuva hydroscheme (4.0 cm), the largest – in Žemaičių Naumiestis dam (17.0 cm). According to the indices of emergency state described in Standard STR 1.12.01:2004 app. 1, it is considered that vertical or horizontal deformations, which are larger than 1/50 of wall's height, are one of the indices of the emergency state of RW. Taking into consideration that Žemaičių Naumiestis RW height is 4.8 m, its limit deformation is 9.6 cm. Since the measured wall deformation is 17 cm, it can be stated that such deformation exceeds the limit value almost twice (deformations are larger than 1/50 of wall's height). Retaining wall is in emergency state.

Analyzing the reasons of RW deformations appearance in hydraulic structures, it was established that various deformations can appear

due to an increased load (i.e. due to the weight of motor vehicle on the slope), an increased pressure of soil or groundwater (Panėvėžiukas and Dotnuva hydroschemes), an undermining of the base under the foundation (Pilviškiai hydropower station's RW inclinations could appear due to this reason), seepage effects etc.

During the researches in 2007 – 2012, RW inclination was the most frequently recorded deformation. The main possible reason of inclination is the increased soil pressure. RW "blowouts" are also frequently noticed when the wall is canted as a result of not functioning drainage, especially when water gathers after a heavy rain beside the RW construction. Pressure notably increases in winter, when the gathered water freezes, its volume expands (up to 9 %) and it pushes the wall (Kėdainiai and Pažibai hydroschemes).

On the basis of the research results presented in table 1, RW inclination was plotted as a function of wall's height (fig. 3).

As the results of RW deformations' research shows (fig. 3), the inclinations of almost every examined construction exceed the limit value of 1/50 of wall's

height (this value is marked with the above straight line).

The deformed retaining walls of reinforced concrete in hydroschemes can be strengthened using the following principles described in literature (Venckevičius, 2000; Hidrotechninė statyba, 2000):

- Cross-section enlargement (using concrete encasement in the compression zone; using reinforced concrete encasement in the compression zone; using reinforced concrete encasement in a tension zone (at the same time the baseplate of a wall is strengthened); using reinforced concrete core in a tension zone; using double-sided reinforced concrete encasement).
- Reinforcement extension (using internal, external or external prestressed reinforcement).
- Changing the design model (with additional supports, cantilever beams, reinforcing steel strings with prestressed muff).
- Changing the tension state (by reducing the load, with a prestressed reinforcement or relieving plates).

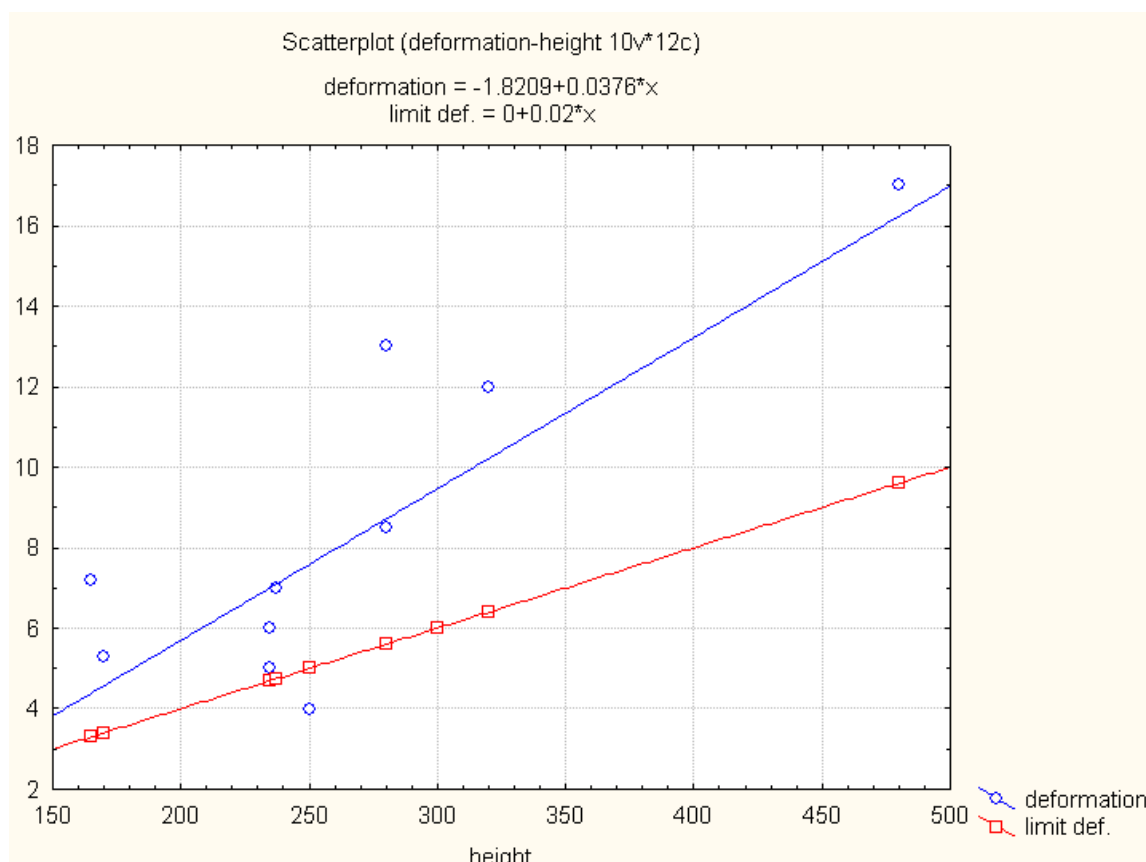


Figure. 3 Retaining walls' deformations-height dependence

CONCLUSIONS

1. According to the results of the field observation of 14 hydroschemes, it was established that the smallest retaining walls inclination was in Dotnuva hydroscheme (4.0 cm), the largest – in Gailiušiai (12.0 cm), Pažibos (13.0 cm) and Žemaičių Naumiestis (17.0 cm) dams.

2. Taking into consideration that the limit deformation is equal to 1/50 of wall's height value, it was established that the inclination in Pažibai

hydroscheme (13.0 cm) exceeds the limit value (4 cm) more than three times and the inclination in Žemaičių Naumiestis hydroscheme (17.0 cm) exceeds the limit value (9.6 cm) almost twice.

3. After the retaining walls inclination analysis was made, it was established that the retaining walls of 150 – 300 cm height are most commonly prohibitively inclined, their inclination reaches from 4 to 13 cm.

REFERENCES

- Gurskis V., (2006) *Pilviškių hidroelektrinės ant Šešupės upės gelžbetoninių konstrukcijų tyrimai ir rekomendacijos defektams šalinti*. Kaunas, Akademija, 25 p.
- Jokūbaitis V. (2007) *Statinių gelžbetoninių ir mūrinių konstrukcijų techninės būklės tyrimai ir vertinimas*. Vilnius, 85 p.
- Patašius A. (2009) *Natūrinių ir anketinių duomenų apie Lietuvos hidromazgų techninę būklę analizė ir rekomendacijų parengimas*. Kaunas, 102 p.
- Ramonas Č. (2000) *Hidrotechninė statyba*. Metodiniai patarimai. Kaunas, Akademija, 324 p.
- STR 1.12.01:2004. Valstybei ir savivaldybėms nuosavybės teise priklausančių statinių pripažinimo avariniai tvarka, Vilnius, LSD, [online] [accessed on 24.09.2012].
- Available: http://www3.lrs.lt/pls/inter3/dokpaieska.showdoc_1?p_id=390038&p_query=&p_tr2=
- STR 2.05.04:2003. Poveikiai ir apkrovos, Vilnius, LSD, [online] [accessed on 24.09.2012].
- Available: http://www3.lrs.lt/pls/inter2/dokpaieska.showdoc_1?p_id=213447
- STR 2.05.14:2005. Hidrotechnikos statinių pagrindų ir pamatų projektavimas. Vilnius, LSD, [online] [accessed on 24.09.2012].
- Available: http://www3.lrs.lt/pls/inter3/dokpaieska.showdoc_1?p_id=252567
- STR 2.05.05:2005. Betoninių, gelžbetoninių konstrukcijų projektavimas. Vilnius, LSD, [online] [accessed on 24.09.2012].
- Available: http://www3.lrs.lt/pls/inter3/dokpaieska.showdoc_1?p_id=249853
- US Army Corps of Engineers (2002) *Structural Deformation Surveying*. Washington, 292 p.
- Venckevičius V., Žilinskas R. (2000) *Statinių rekonstrukcija ir remontas*. Kaunas, 315 p.
- Witzany J., Cejka T. (2007) Reliability and failure resistance of the stone bridge structure of Charles Bridge during floods, *Journal of civil engineering and management*, No 3, Vol XIII, pp. 227–236.

INDUSTRIAL ENERGY EFFICIENCY

DEVELOPMENT OF INDUSTRIAL ENERGY EFFICIENCY IN LATVIA, LEGISLATION AND STATISTICS

Anda Kursisa*, Laura Gleizde**

NGO Passive House Latvija, Latvian Cluster of Industrial Energy Efficiency
E-mail: anda@virtu.lv; ** laura.gleizde@gmail.com

ABSTRACT

This article analyzes the legislation of the Republic of Latvia and available statistical data about industrial energy efficiency. The European legislation in the sector of industrial energy efficiency is reviewed and compared to the Latvian legislation. LR and EU statistics is summarized, data of OECD countries in respect of energy consumption by industries and savings estimates are informatively reviewed. Latvian industrial energy efficiency scenarios are estimated based on EU and OECD studies. Recommendations include the need for a more detailed analysis of data on industrial energy consumption by sectors, strategic choice of a best available technology (BAT) development scenario; and the need for support measures in the SME sector.

Key words: industrial energy efficiency, industrial statistics, legislation in energy efficiency

INTRODUCTION

This article is devoted to the manufacturing industries, not including construction industry. The data collection methodology includes collection of data from the Central Statistical Bureau (hereinafter – CSB) with required indicators, however, in cases when CSB statistical data are collected under a joint sector “Industry and Construction”, they are shown together. Market influence, energy efficiency incentives; availability of funding, energy consumption benchmarks, energy price increase dynamics, CO₂ saving and balances and other factors available in studies of the Ministry of Economy and other sources, as well as in state reports are beyond the scope of this article. Measures performed within the CCFI state support programme and their impact on energy efficiency in industries are analyzed in the article “Energy Consumption and its Decrease Potential in Industry Sectors”, authors A. Kursiša, L. Gleizde.

EUROPEAN LEGISLATION ON ENERGY EFFICIENCY IN INDUSTRIES

The most topical document describing and determining energy efficiency measures binding for industrial companies currently is Directive 2012/27/EU of the European Parliament and of the Council of 25 October 2012 on energy efficiency, amending Directives 2009/125/EC and 2010/30/EU and repealing Directives 2004/8/EC and 2006/32/EC, hereinafter – the Directive. The Directive supports 20% primary energy saving (p.(2)) by 2020, and to perform further measures (p.(7)) to achieve these targets. Furthermore, Paragraph 56 provides that “Directive 2006/32/EC

requires Member States to adopt, and aim to achieve, an overall national indicative energy savings target of 9% by 2016, to be reached by deploying energy services and other energy efficiency improvement measures.” Paragraphs referring to the industrial sector determining measures for enterprises in general “2. Member States shall develop programmes to encourage SMEs to undergo energy audits and the subsequent implementation of the recommendations from these audits. 4. Member States shall ensure that enterprises that are not SMEs are subject to an energy audit carried out in an independent and cost-effective manner by qualified and/or accredited experts or implemented and supervised by independent authorities under national legislation by 5 December 2015 and at least every four years from the date of the previous energy audit.” (Directive 2012/27/EU of the European Parliament and of the Council, Article 8 Energy audits and energy management systems, p.(2), p.(4))

Article 1(2) provides that “The requirements laid down in this Directive are minimum requirements and shall not prevent any Member State from maintaining or introducing more stringent measures. Such measures shall be compatible with Union law. Where national legislation provides for more stringent measures, the Member State shall notify such legislation to the Commission.” (Directive 2012/27/EU of the European Parliament and of the Council, Article 1 Energy audits and energy management systems, p.(2))

Directive implementation deadlines by sections are defined, in some cases allowing Member States to define them individually, however in compliance with the provisions of the Directive.

LATVIAN LEGISLATION IN ENERGY EFFICIENCY SECTOR

In Latvia, energy efficiency directions in general and by sector are defined by documents of the European Commission, and subsequently adopted laws of the Republic of Latvia and Regulations of the Cabinet of Ministers.

In this article we note only those documents that directly refer to energy efficiency in industrial sectors, focusing more on manufacturing industry.

Law on Energy Efficiency of Buildings

The Law on Energy Efficiency of Buildings, in force since 06.12.2012, reviews issues related to buildings, the building envelope, and high efficiency engineering systems in buildings.

Section 3 provides that "*Minimum requirements of energy efficiency are applicable to buildings to be reconstructed or to be renovated, if: 1) the design documentation for reconstruction applies to more than 25 percent of the surface of the building envelope; 2) a reconstruction or renovation of utilities of the building is performed.*"

Section 5 defines high efficiency systems, the description of which is largely applicable also to industrial buildings and objects, and they are also a component of energy efficiency specification:

(1) *When designing buildings, the possibility to use the below mentioned high efficiency systems must be evaluated: 1) decentralized energy supply systems using renewable energy resources;*

2) cogeneration systems for simultaneous generation of heat energy and electric energy or mechanical energy; 3) systems using heat pumps that transfer heat from its natural environment to buildings or utilities of buildings by changing natural heat flow; 4) centralized heat supply or centralized cooling systems, especially those using renewable energy resources, and which are used for several buildings or territories by transferring energy from the central energy generation source.

(2) *If it is planned to reconstruct or renovate the utilities of buildings, the possibilities of use of the high efficiency systems must be evaluated.*

In an ideal situation, such reconstruction must be applicable in any case, when plant management plans any renovation works, even more in the case, if energy efficiency is the only and primary objective of the works.

Regulations on industrial energy audit

Regulations on industrial energy audit (Draft, version of 08.11.2012.) are made as a support document for the successful implementation of the

Directive in respect of industrial energy audit, and defines: "*1.2. requirements for the performance of industrial energy audits set in respect of legal entities;*

1.3. significant requirements to the evaluation of compliance of an industrial energy auditor and a mechanism of surveillance of observance of these requirements;

1.4. responsibility of an industrial energy auditor."

This draft legislation, in the context of the Directive, refers to large enterprises, and energy auditors who will perform audits in large enterprises. Audits and industrial audits of SMEs may be performed voluntarily, this draft legislation does not envisage any state support mechanism or quality control for them. With regard to the fact that "*the category of micro, small and medium-sized enterprises is made up of enterprises which employ less than 250 people and which have an annual turnover not exceeding EUR 50 million, and/or an annual balance sheet total not exceeding EUR 43 million*" (Directive 2012/27/EU of the European Parliament and of the Council, Article 2, Definitions, p. (26)), there is a risk that such companies with high energy consumption, that is significant by Latvian standards, may stay outside the framework of enterprises to be audited, will not receive information about energy saving possibilities, thus not including energy efficiency measures in the plans of the enterprise, until forced to do so by the economic situation – tariffs or decrease of competitiveness.

STATISTICAL INDICATORS IN ENERGY EFFICIENCY IN COUNTRIES OF THE EUROPEAN UNION, OECD AND THE REPUBLIC OF LATVIA

One of the comparative indicators used in the European Union is **energy consumption of kg or ton of fuel equivalent (kg/T of oil equivalent) per 1000 EUR of gross domestic product (GDP)**. This indicator is closely related to the economic development, because it includes energy consumption not in manufacturing only, but also in the households, service and transport sector, as well as GDP growth.

LR document "On Guidelines for Energy Sector Development for 2007-2016", CM Order No.571 of 01.08.2006, Sec.4, provides that: "Energy intensity (The ratio between the total consumed amount of primary energy resources and the GDP unit, "On Guidelines for Energy Sector Development for 2007-2016", CM Order No. 571, 01.08.2006) in 2010, 2015 and 2020 shall reduce to 0.35, 0.28 and

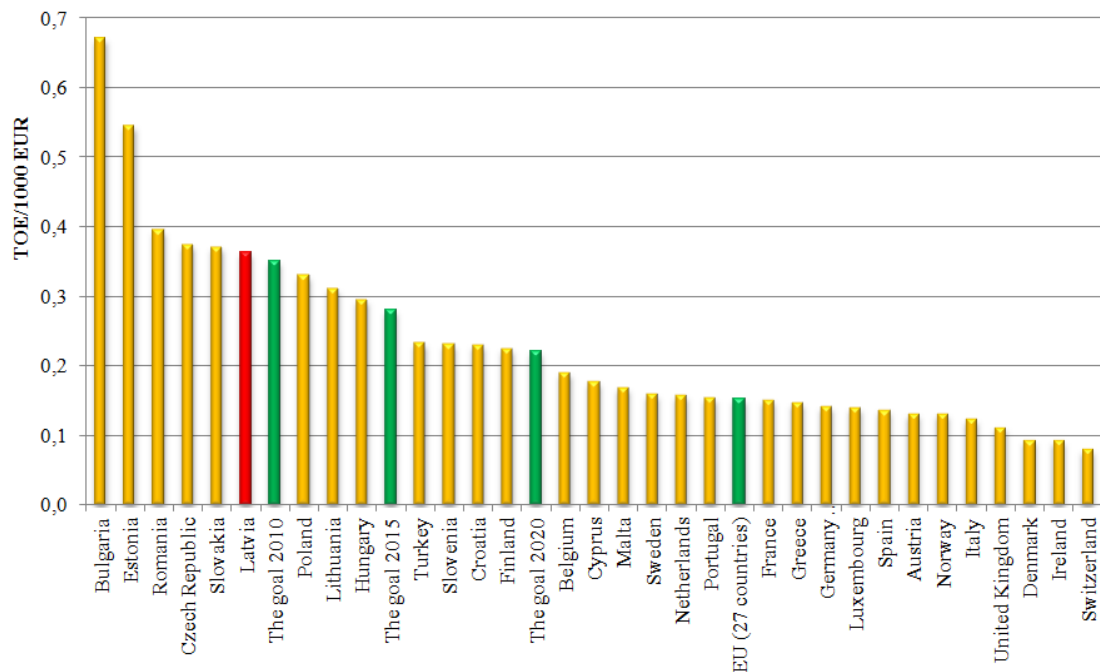


Figure 1. Energy use intensity in Europe and Latvia in 2010: country indicators, Latvian target indicators for 2010, 2015, 2020. Source: Eurostat

0.22 TOE/1000 EUR, respectively". In accordance with Eurostat data, Latvia showed 0.363 TOE/1000 EUR GDP in 2010 compared to the target index 0.350 TOE/1000 EUR GDP.

It shall be taken into account that Latvian statistics shows a negative GDP increase for the period from 2008 to 2010. In 2011 the GDP increase was 5.5%, in 2012 - 5%. The Ministry of Economy (Informative Report "On the Performance of Objectives Set in the Guidelines for Energy Sector Development for 2007-2016") forecasts a GDP increase of 4-5% per year till 2020. As far as energy consumption in the industrial sector is about 20% from the total energy consumption (2011), while industry in total makes 27% from GDP, the decrease in the energy intensity index depends on several factors:

- increase of GDP in general, incl. the industry sector;

- decrease in the energy consumption in the country in general, incl. the industry sector. Furthermore, households are significant energy consumers (32% in 2011, CSB), while they do not cause a GDP increase.

"Energy Efficiency Monitoring Report for 2011" prepared by the Ministry of Economics in 2012 provides: "*In the time period from 2000 to 2007 GDP increased faster than energy consumption affected by the energy efficiency improvement both in energy generation and management, and in energy end consumption sectors. Positive example of other countries (Denmark) shows that countries with high energy efficiency may ensure a GDP increase while energy consumption remains unchanged.*" In Latvia, the negative line of development of energy intensity is also confirmed by statistics of the last years.

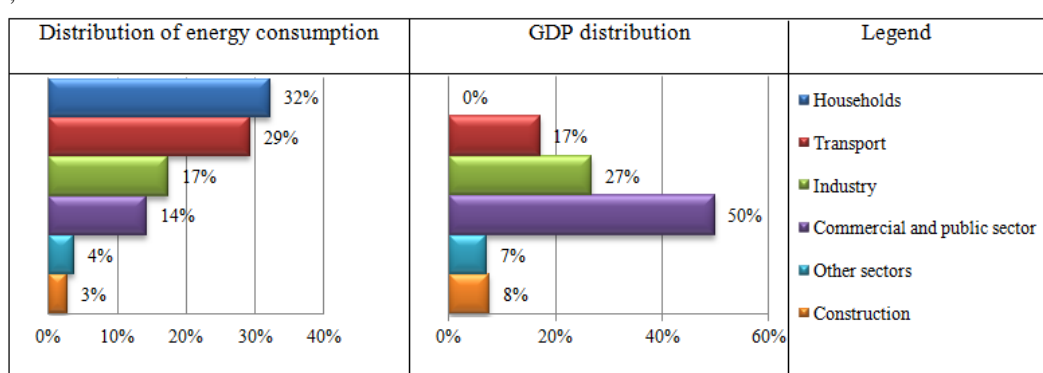


Figure 2. Distribution of energy resources consumption and GDP consumption in Latvia. (Source: CSB (2011))

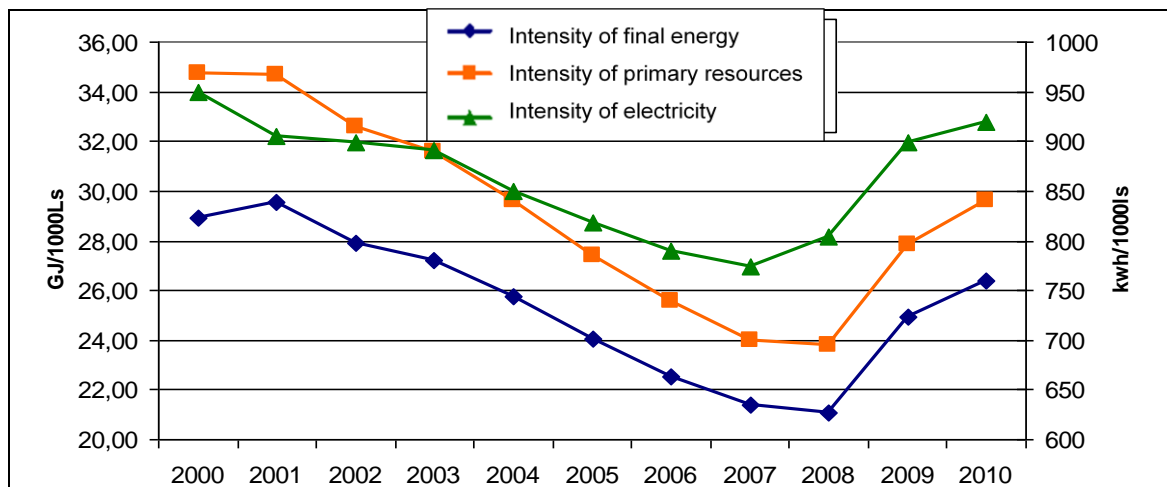


Figure 3. Changes in energy intensity indicators in Latvia in 2000-2010 (in prices of 2000). ("Energy Efficiency Monitoring Report for 2011", ME)

At the same time the total energy consumption of industry sectors increases. The Figure 4 shows that percentage of industrial energy consumption in the total energy consumption in 10 years has increased by 11%. The last 2 years showed an especially fast increase, showing that the percentage of the industry sector in the total energy consumption has a growing trend. Figure 5 shows the largest energy consumers in the industry sector. If we further review the development of these four sectors in the 5-year run (Figure 6), it is seen that the consumption in the "Manufacture of food and beverages" reduces with a minimum trend. The fastest increase in energy resources consumption is in the "Wood industry" having consumed 46% of all consumers of energy resources in the industry sector in 2011.

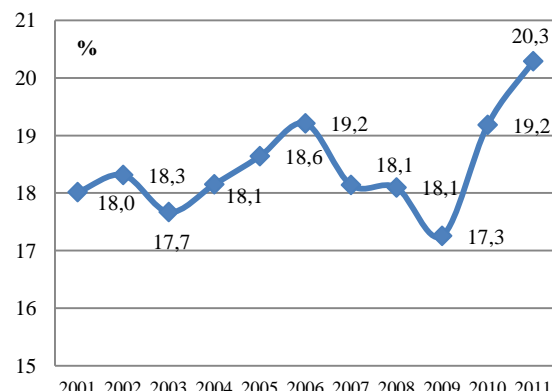


Figure 4. Energy consumption of industry sectors, % of the total consumption. (Source: CSB)

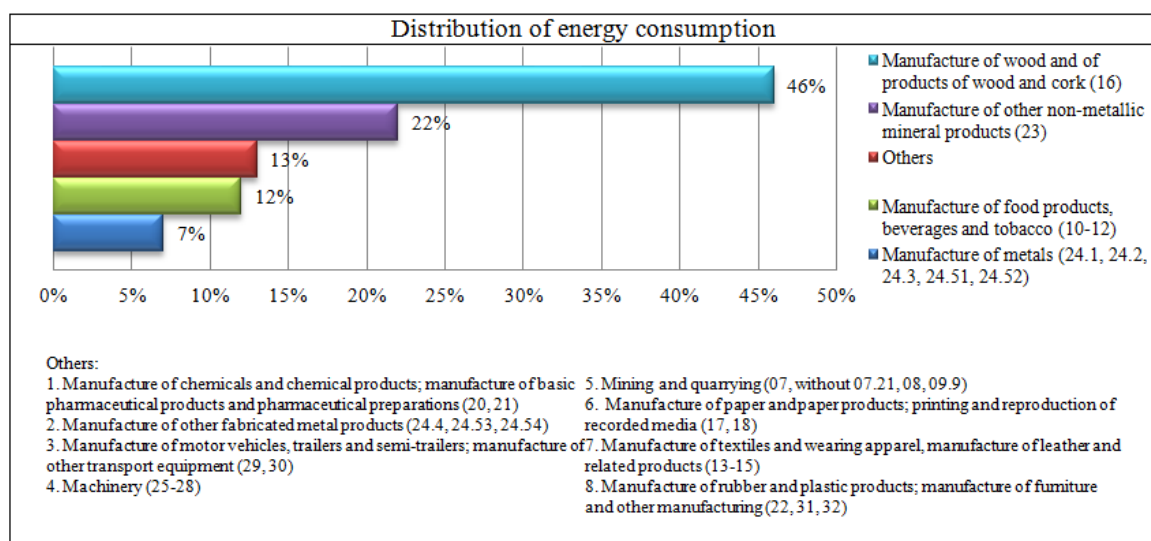


Figure 5. Most energy-intensive industry sectors according to NACE 2 code classification.
(Source: CSB (2011))

Summarizing sector data (EM, Energy Efficiency Monitoring Report for 2011) on energy efficiency, ME concludes: "...in the woodworking sector, the manufacturing of products, including for export, is done with comparatively low energy efficiency.

Taking into account the high percentage of woodworking in the total energy consumption of industries, the total energy saving in industries has a minus sign, or there were no energy savings in the industry sector. It should be noted that at the same time many sectors show a positive trend, such as food industry, light industry and machinery manufacturing. Energy efficiency measures implemented with a state support up to now were mostly directed to the improvement of energy efficiency of industrial buildings."

To perform a more detailed study of the relation between energy consumption and the development of industry sectors, we analyze the added value factor. The added value is "A value an enterprise has added to purchased raw materials, materials, semi-finished products during the manufacturing of goods (or rendering of services). A is calculated by

subtracting the value of purchased material resources used for manufacturing a product (or rendering a service) from the sales price of the product (or the service)." Unfortunately, due to confidentiality issues, these data were not available about the metal industry sector. The data on 2011 shown in Figure 7 are estimates, they were not confirmed at the time of conducting this study. These data let conclude that in three sectors about which comparable data are available:

- in the sector of non-metal mineral products the energy consumption curve follows the added value curve;
- in the manufacture of food it was possible to reduce energy consumption at the same time maintaining a stably changing added value; a negative trend is found in woodworking sector – on the background of 50% added value drop, the energy consumption from 2007 to 2011 had a double increase, i.e. – energy intensity per added value worsened four times in a short period of 5 years.

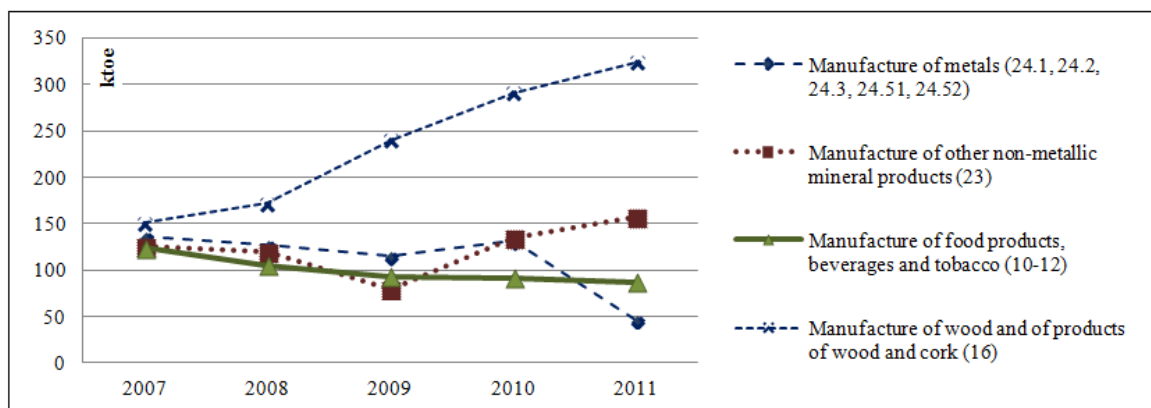


Figure 6. Changes in energy consumption in main industry sectors. (Source: CSB)

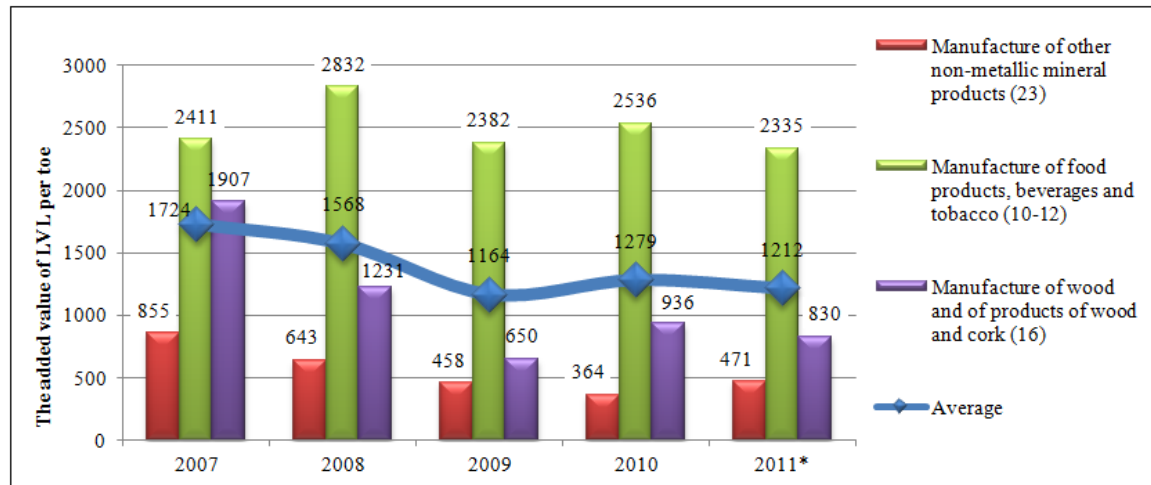


Figure 7. Added value created by main industry sectors per energy consumption unit. (Source: CSB)

The data summarized in Figure 8 show that the industries that have not achieved any energy saving are Manufacture of chemical products, Manufacture of non-metallic mineral products, and Manufacture of wood and products of wood, the latter being especially characterized by wastefulness of energy resources. The authors consider that part of this negative trend is formed by manufacture in non-heated, adjusted buildings, as well as energy Individual national industry structure, past development and expected industrial growth play major roles. A high achievement in the past relates to a low future potential, and vice versa. Good examples are Greece, Hungary and Latvia with a low potential". (Altmann M, Michalski J, Brenninkmeijer A, Tisserand P. 2010)

4 scenarios are modeled within the framework of this article: based on OECD study (Saygin D., Patel M.K., Gielen D. (2010)), and based on the summarized energy consumption in industries for 2011, and a conservatively accepted GDP increase of 4% ("Ministry of Economy forecasts a GDP increase of 4-5% per year by 2020, and 3-4% per year – by 2030" p.19, ME Report).

Energy efficiency is modelled based on OECD's estimated scenarios, EU research data (potential by 2020 >4%) are considered as a reference only.

resources required for driers that mainly consist of biomass – woodworking production residues with low market value. This sector needs special attention, because even if energy consumption is

increased due to biomass, it has no economic character in respect of the abovementioned Added value factor.

REVIEW OF DEVELOPMENT SCENARIOS

In the Latvian state energy strategy, the energy consumption forecasts in industries are usually analyzed as a single factor – GDP increase curve, without any evaluation of energy efficiency. In reports of European and OECD countries, Latvian data are analyzed in a broader context. In general, the energy efficiency potential in industries by 2020 is evaluated below 4%, while in Europe it is above 6% (Altmann M, Michalski J, Brenninkmeijer A, Tisserand P. 2010, Sec.2.). If we calculate it arithmetically, it would be ~0.5 % per year in Latvia starting from 2013. Section 2 of this document also provides that after 2000, the rate of energy efficiency improvements reached the average of 1.7%. This EU document gives a positive evaluation to the previous Latvian performance, Section 29 provides that "This analysis shows that there is no simple rule for energy savings potentials in the 27 Member States. In the CCFI state support programme, that is in the stage of implementation, the energy balance of enterprises embraced only 1.6% of the total energy consumption of industries, however, the total heat and electric energy saving is 0.4% of industries' total saving.

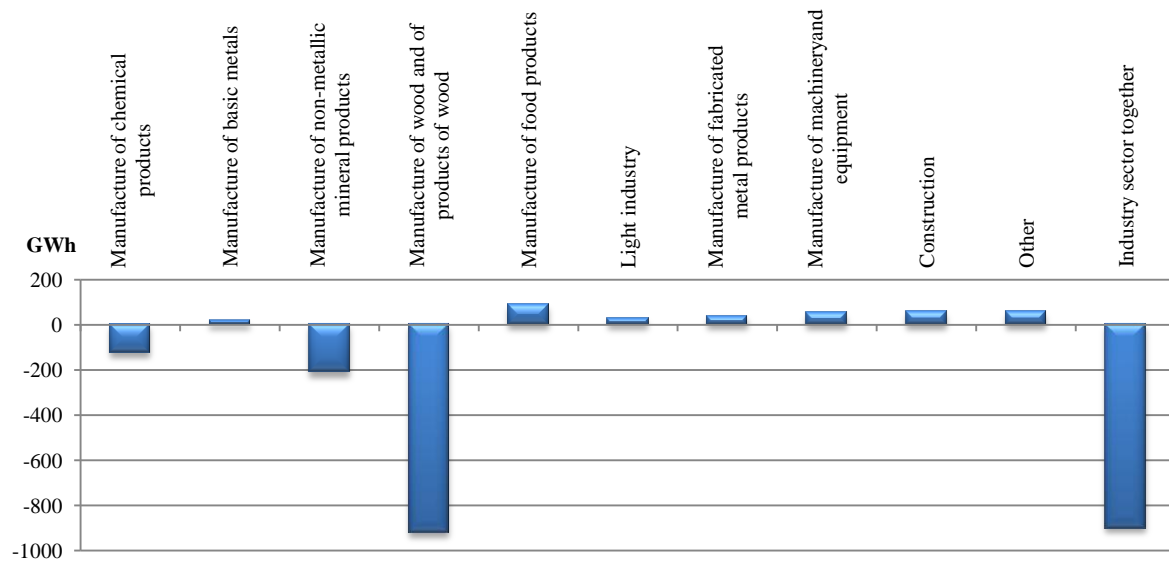


Figure 8. Energy consumption in industries in 2010, GWh. (Source: ME, Energy Efficiency Monitoring Report for 2011)

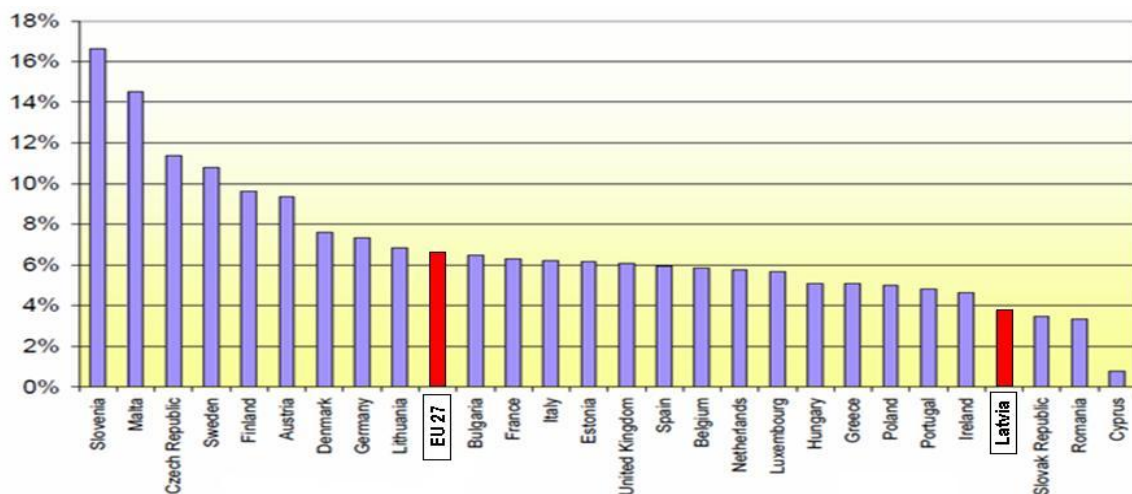
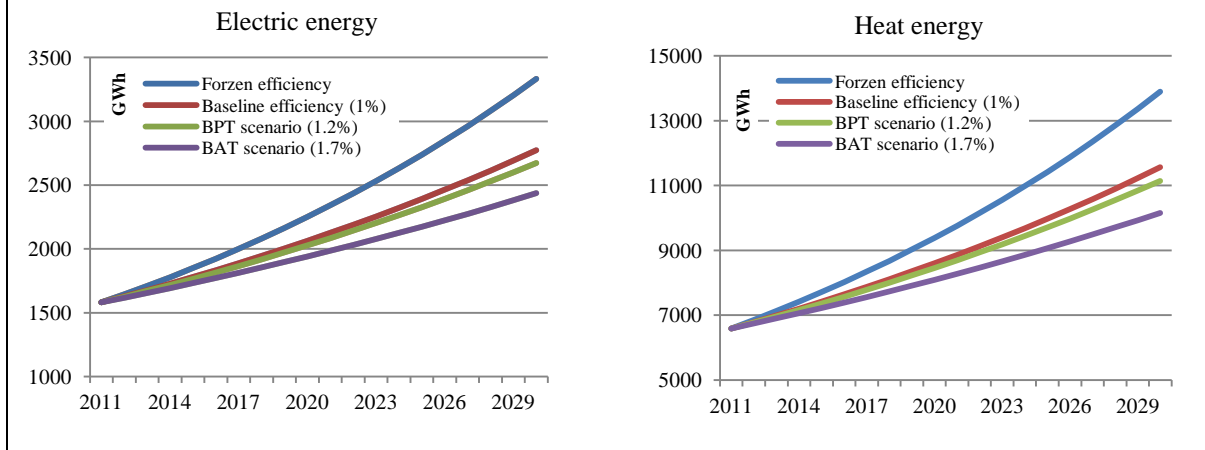


Figure 9. Energy savings potential in the HPI (High Policy Intensity) scenario by 2020

Table 1

Development scenarios	
4 scenarios, according to OECD	Possibility in Latvia
Frozen efficiency: no additional energy efficiency savings are made, i.e. the current levels of energy efficiency are not improved upon	Such development forecast is hardly probable, because the increase in energy prices is a determining factor for energy efficiency as far as investment payback periods are relevant.
Baseline efficiency: energy efficiency improves at a rate of 1% a year	The scenario is close to the one evaluated in the EU study, when measures take place “by themselves”, at the initiative of the market and entrepreneurs.
BPT scenario: all plants are operating at the current levels of best practice technology by 2030. This is equivalent to an energy efficiency improvement of 1.2% a year in the period 2007 to 2030	The best practice technology is a scenario, according to which Latvia continues (or would continue) state support programmes, such as CCFI, and implements measures of the Directive for large enterprises.
BAT scenario: all plants are operating at current levels of BAT by 2030. This is equivalent to an energy efficiency improvement of 1.7% a year in the period 2007 to 2030	The best available technology is a set of targeted measures combining support of state, ESCO and commercial banks with all the measures specified in the Directive – mandatory energy audits in large enterprises, technical support for SMEs, and introduction of a monitoring and benchmarking system.



CONCLUSIONS AND RECOMMENDATIONS

The regulatory framework of EU and Latvia on the improvement of industrial energy efficiency is reasonable and its content is appropriate, however, it does not specify particular targets and measures to achieve a real improvement in energy efficiency in Latvia.

The European and OECD scenarios, reviewed in this article envisage an improvement in energy efficiency for Latvia from ~ 0.5% per year to 1.7%, or slightly less than 4% in total by 2020. At the same time, industry sectors in Latvia in total, as evaluated by the EP, have a low energy saving potential. Conversely, Latvia is one of the worst of EU Member in terms of energy intensity. OECD research (Saygin D., Patel M.K., Gielen D., 2010) provides that: "A high growth rate implies many new production facilities to be installed and put into operation, which in general have close to best available efficiency. Thus, by 2020, a large portion of the industrial installations will be efficient and have low potential for further efficiency improvements. Especially for energy intensive industries, new installations are often the only possibility for major energy savings. These energy savings will in general be realised without a need for targeted policies. (...) Romania and Latvia for example show a strong correlation of a low energy savings potential with a high projected growth rate of energy consumption in industry".

Along with a positive evaluation, energy efficiency of Latvian industries has not met focused planning yet. Therefore, despite the fact that an independent evaluation (OECD, EP) defines low energy efficiency potential, Latvia must make its own detailed and a substantive analysis.

To perform it, newly installed energy consumers (for instance, opening of new enterprises, or significant extension of existing ones) in the sector need to be separated in the future, that would allow to structure energy efficiency statistics both by actual saving and by restructuring. Currently available data can be analyzed only in respect of the added value increase.

In this context, the need to increase the competence of local professionals also in the industrial sector is explained in the Directive, Art.6 "*A sufficient number of reliable professionals competent in the field of energy efficiency should be available to ensure the effective and timely implementation of this Directive, for instance with regard to the compliance with the requirements on energy audits and implementation of energy efficiency obligation schemes. Member States should therefore put in place certification schemes for the providers of energy services, energy audits and other energy efficiency improvement measures.*"

Therefore, a detailed evaluation of energy efficiency targets and scenarios by sectors must be

performed, especially in the industries of Chemical products, Non-metallic mineral products, and paying special attention to Woodworking.

Reviewing several energy efficiency scenarios in industries, and taking into account both the problems reviewed in this article – lack of data and analysis by sectors; and opportunities of Latvia as a growing economy, the authors of this article recommend the **Best available technology** scenario as a target strategy. The BAT is a set of measures which combine support of state, ESCO and banks with all the measures specified in the Directive – energy audits in large enterprises, technical support for SMEs, and introduction of a monitoring and benchmarking system. The target audience should be split into groups by size, as the measures to be performed and the savings to be achieved by SMEs and large enterprises are radically different.

When planning energy efficiency measures, it should be taken into account that enterprises with high energy consumption are also addressees of Directive 2003/87/EC with regard to the emission allowance trading (ETS) system, therefore (p.(55)) "...the Commission will have to monitor the impact of new measures on Directive 2003/87/EC establishing the Union's emissions trading scheme (ETS) in order to maintain the incentives in the emissions trading system rewarding low carbon investments and preparing the ETS sectors for the innovations needed in the future". As industrial energy audits will be mandatory for large enterprises from 2014, these companies in general will be provided audit and monitoring procedures.

In its turn, SME's in the Latvian economics have a great impact both on employment and export, they form a significant portion of energy consumption, and however, they are frequently not provided with a technical information or financial support. P.41 of the Directive provides: "...To help them adopt energy efficiency measures, Member States should establish a favorable framework aimed at providing SMEs with technical assistance and targeted information."

Research limits. CSB statistics does not include the period during which measures of the CCFI were implemented, therefore the research must be continued, analyzing the monitoring data, and studying the impact on the sector in total. Other factors limiting the research must also be taken into account: the enterprises implementing energy efficiency without state support are not included. Also ETS is not included, and it "...represents roughly 50% of the energy consumption in terms of total industrial final energy consumption. So far knowledge of the impacts of the ETS on energy efficiency is very limited." (Altmann M, Michalski J, Brenninkmeijer A, Tisserand P., 2010).

ABBREVIATIONS

ECM – European Commission
ME – Ministry of Economy of the Republic of Latvia
EU – European Union
ECN – European Council
EP - European Parliament
GDP – Gross domestic product
CCFI – Climate Change Financial Instrument
LR – Republic of Latvia
NACE Rev.2 – Statistical classification of economic activities in the European Community
CM – Cabinet of Ministers of the Republic of Latvia
SME – Small and medium enterprises
OECD – Organisation for Economic Co-operation and Development
TOE – ton of oil equivalent

REFERENCES

- Akadēmisko terminu datu bāze. [online] [accessed on 28.01.2013.]
Available:
<http://termini.lza.lv/term.php?term=pievienot%C4%81%20v%C4%93rt%C4%ABba&list=pievienot%C4%81%20v%C4%93rt%C4%ABba&lang=LV>
- Altmann M, Michalski J, Brenninkmeijer A, Tisserand P.(2010), European Parliament: Overview of Energy Efficiency measures of European industry. [online] [accessed on 24.01.2013.]
Available:
<http://www.europarl.europa.eu/committees/en/itre/studiesdownload.html?languageDocument=EN&file=33970>
- Website of the Central Statistical Bureau. [online] [accessed on 20.01.2013.]
Available:
<http://www.csb.gov.lv/>
- Directive 2012/27/EU of the European Parliament and of the Council of 25 October 2012 on energy efficiency, amending Directives 2009/125/EC and 2010/30/EU and repealing Directives 2004/8/EC and 2006/32/EC.
- Website of Eurostat. [online] [accessed on 25.01.2013.]
Available:
<http://epp.eurostat.ec.europa.eu/portal/page/portal/eurostat/home/>
- Latvijas Republikas „Ēku energoefektivitātes likums” (“Law on Energy Efficiency of Buildings” of the Republic of Latvia), in force since 06.12.2012
- Ministry of Economy of the Republic of Latvia. „Energoefektivitātes monitoringa pārskats par 2011.gadu” (“Energy Efficiency Monitoring Report for 2011”)
- Cabinet of Ministers of the Republic of Latvia. Noteikumi par rūpniecisko energoauditu (Regulations on industrial energy audit) (Draft, version of 08.11.2012.)
- Latvijas Republikas dokuments „Par Enerģētikas attīstības pamatnostādnēm 2007.–2016.gadam”, MK Rīkojums Nr.571, 01.08.2006 (Document of the Republic of Latvia “On Guidelines for Energy Sector Development for 2007-2016”)
- Saygin D., Patel M.K., Gielen D. (2010). United Nations Industrial Development Organization. Global Industrial Energy Efficiency Benchmarking. An Energy Policy Tool. Working paper. [online] [accessed on 24.01.2013.]
Available:
http://www.unido.org/fileadmin/user_media/Services/Energy_and_Climate_Change/Energy_Efficiency/Benchmarking_%20Energy_%20Policy_Tool.pdf

ENERGY AUDIT METHOD FOR INDUSTRIAL PLANTS

Karlis Grinbergs, Bc. Sc Ing.

Energy Case

E-mail: grinbergs.karlis@gmail.com

Sandra Gusta, assist. prof., Dr. oec.

Latvia University of Agriculture, Faculty of Rural Engineers, Department of
Architecture and Building
E-mail: sandra.gusta@llu.lv

ABSTRACT

Different studies have shown that there are opportunities for major energy efficiency improvements in the industrial sector and many of them are cost effective. These energy conservation measures are general and also niche specific.

Owners or managers of industrial parks and factories are not always aware of the possibilities for energy efficiency improvements. Energy audit is the first step in order to discover the possibilities of energy savings, prioritizing projects, tracking progress and making system adjustments after investments.

Industrial energy audit is a process that makes saving of energy and raw materials possible. Quality of the end product often is also increased. By improving a local electricity grid and overall building and manufacturing process characteristics there is also often observed a decrease in factory down time.

Industrial energy audit is quite new in Latvia, but by using the world experience and following standards, projects have been elaborated where the energy savings exceed 70% of total energy demand (Latvijas..., 2011). These processes have defined the topicality of this article; the aim of the article is to analyze energy audit method for industrial plants.

Keywords: industrial energy audit, energy efficiency, energy savings, industrial energy audit guidelines

INTRODUCTION

Global competition, carbon emission regulations and integration in the European electricity market will most probability increase the demand for energy efficiency on the part of companies all over Europe.

Conducting an energy audit is one of the first steps that must be done in order to identify the possible energy efficiency positions. Even by knowing the exact procedure of the industrial energy audit many plants do not have the capacity to conduct an effective energy audit without any external help. The existing regulations for industrial energy audits are only descriptive and do not provide any specific action plan or process description; the audits conducted by professional certified energy auditors are unique and hardly comparable. But usually manufacturing companies lack the knowledge about the possibilities of energy savings and increased productivity. And because of the lack of quality information only limited technical and financial resources for improving energy efficiency are available, especially for small and medium-sized companies. Information in industrial energy auditing and energy efficiency practices should be prepared and distributed to industrial plants and other related companies (National..., 2005).

STEPS OF INDUSTRIAL ENERGY AUDIT

An industrial energy audit is a process that facilities energy usage patterns, equipment efficiency, and overall building efficiency is determined in order to propose energy efficiency measures. The result of a successful energy audit is decreased energy consumption, reduced raw material usage and increased quality of the end product. The data collected by an energy auditor is the basis on which the energy efficiency suggestions will be created. The implementation of these measures will reduce manufacturing costs and also the negative effects on the environment. "Industrial energy audit is a new term in Latvian. It is a process aimed at finding loopholes in the production process, a design task in order to save raw materials and energy. Performing industrial energy audits makes it possible to save raw materials, energy, optimizing the manufacturing process or raising the company's profits and increase competitiveness. After an industrial energy audit, the client data will have an accurate list of energy efficiency measures which will reduce costs and the environmental impact. The industrial energy audit consists of the following steps (International..., 2007)" (see Figure 1):

Step 1. Data collection:

- The presentation of the process or stage. The first task of the energy audit is getting acquainted with the entire production process or stage. What is produced, which inputs are used?

How much water is supplied, the amount of energy used, characteristics and quantity of raw materials used and other specific information that can be useful in the audit process, for example waste treatment.

- The principal scheme. When gathering data for the energy audit the principal scheme can be very useful because it includes all of the energy flows and process relationships.
- Data collection. Collection of data on the entire production process and a specific period is one of the main steps of the energy audit. When collecting data about the manufacturing process and systems, it is very important to collaborate with the employees as they know the systems very well.
- The benchmark. The collected data are compared with the data from similar companies across Europe or Latvia.
- Defining the problem. After comparison of the consumption problematic systems, systems with relatively high energy usage can be defined.

Step 2 Data processing:

- Creating a team of specialists. After defining the problem, the specialists from the appropriate fields are incorporated into the audit process.
- Necessary calculations. Calculations are carried out for all of the manufacturing steps, and the possible energy efficiency improvements are identified.
- Accurate scheme for the production of energy and raw material flows. A pre-established production scheme is improved, supplemented with information acquired in the energy audit process

Step 3 Analysis of results:

- The most appropriate solutions are identified and justified.
- Exact energy efficiency suggestions are presented. The goal of the suggestions is improving the manufacturing process and decreasing energy and raw material consumption.
- All of the suggested improvements are integrated in an overall process diagram or scheme in order to obtain a better understanding on how these changes will affect the overall manufacturing process.
- Selection of an appropriate solution based on the potential savings, the impact on production processes and technologies, as well as potential investments are selected for energy efficiency measures to be economically justified.

Step 4 Recommendations for improvement:

- Proposed technology integration in the scheme. Improvements are included in the scheme in a way to better understand how it will affect the entire process.

- The choice of the right solution . Based upon the potential savings, the impact on production processes and technologies, as well as potential investments and ROI, energy efficiency measures are selected.

Step 5 Economic foundations:

- All of the energy efficiency suggestions are justified for their economic benefit. Measures considered most often: pay-back time and ability to attract EU structural funds.
- Choosing economically reasonable energy efficiency measures. After an economical analysis, the most advantageous measures are chosen. Pay off times and capital costs are considered.(International..., 2007)

ANALYSIS

The main purpose of an energy audit is to find out the energy usage patterns, the amount of energy used, and most important - the amount of energy needed. Next, based on these findings the auditor must develop possible scenarios of energy efficiency with precise recommendations and return on the investment analysis. In Figure 1, the general energy flow is shown, two main parts are considered – total facility energy use and facility energy production (National..., 2010). Often the only measured branch from the facility energy production chart is thermal energy production, but even more often this energy is used in a non-efficient way. A different situation is in the “Total Facility Energy

Use” branch, because the energy consumed by the facility is precisely metered due to the fact that this is the metric by which the facility is billed by the energy supply company. But if the energy is used in different processes and facilities, the need for local energy monitoring devices arises. Detailed energy consumption monitoring provides the information necessary for adjusting the manufacturing process in order to obtain higher energy efficiency and lower energy costs even without changing any equipment. This information can also be used to determine the main energy consumers and create an action plan to lower the overall facility energy usage (Canadian..., 2010). Tier 1 layer in Figure 2 accounts for facility energy production and facility energy usage. The total facility energy usage can be either positive or negative depending on the facility type and equipment used. Most of the time the net facility energy use will be negative, because the majority of the companies are only energy consumers and not producers. This is especially true in Latvia; most of the companies lack the capabilities of energy production either for themselves or for selling to the grid. Often this is due to the fact that there are no additional resources to spend on new, energy producing systems and most commonly due to the difficulties of selling energy back to the grid (International..., 2007).

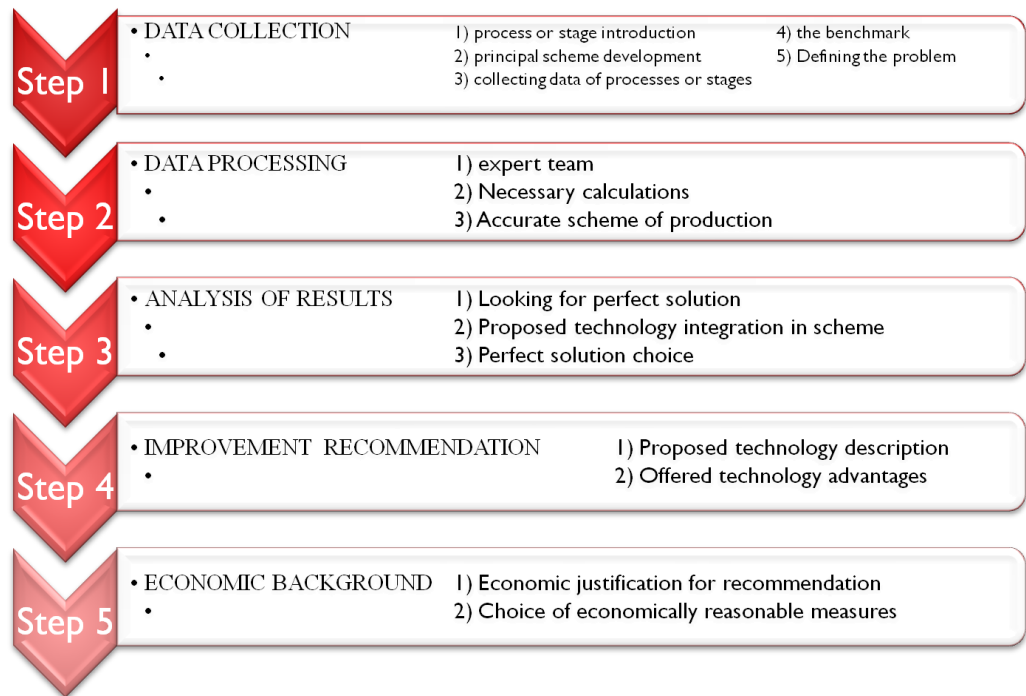


Figure 1. Steps of industrial energy audit (Gusta, 2012)

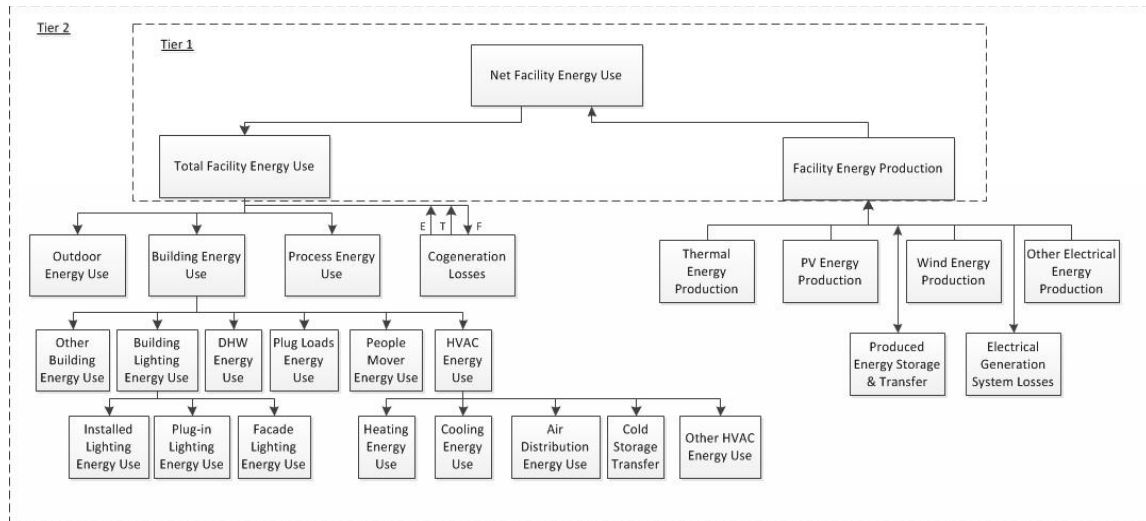


Figure 2. Net facility energy use

Tier 2 in Figure 1 provides a closer look at energy consumption and production systems. This allows the energy auditor to analyze the energy consumption patterns and suggest possible energy efficiency measures. The most energy efficiency measures are taken for overall building energy use, including energy for heating, ventilating, air conditioning, indoor lighting, facade lighting, domestic hot water, plug loads, people and production movers, other building energy use and also process energy use (National..., 2005). When a building is multifunctional, the energy use

may be determined to each functional area for the comparison with other building areas of the same type.

In the industrial sector often the most energy consuming position is the “Process Energy Use”. Process energy use is the energy consumed in a building or elsewhere at a facility to support a manufacturing, industrial or commercial process other than conditioning and maintaining comfort for the occupants. Examples include an electrical welder, machine tools, steel melting furnace, wood drying chamber and other high power appliances. In

an office environment, typical personal computers are not categorized as process loads; nor are servers that support building operations. However, server computers at an Internet service provider company are process loads. Process energy use does not include the effect of this energy use on heating, ventilation and air conditioning loads. Any heat recovered and used at the facility in a way that offsets the consumption of purchased energy or

other energy generated at the facility is subtracted from process energy use and included in the metric that corresponds to the energy use (European..., 2012). The flow diagram in Figure 3 illustrates the relationship between the energy usage and energy production in a facility, the diagram accounts for the majority of possible energy usage or production capabilities.

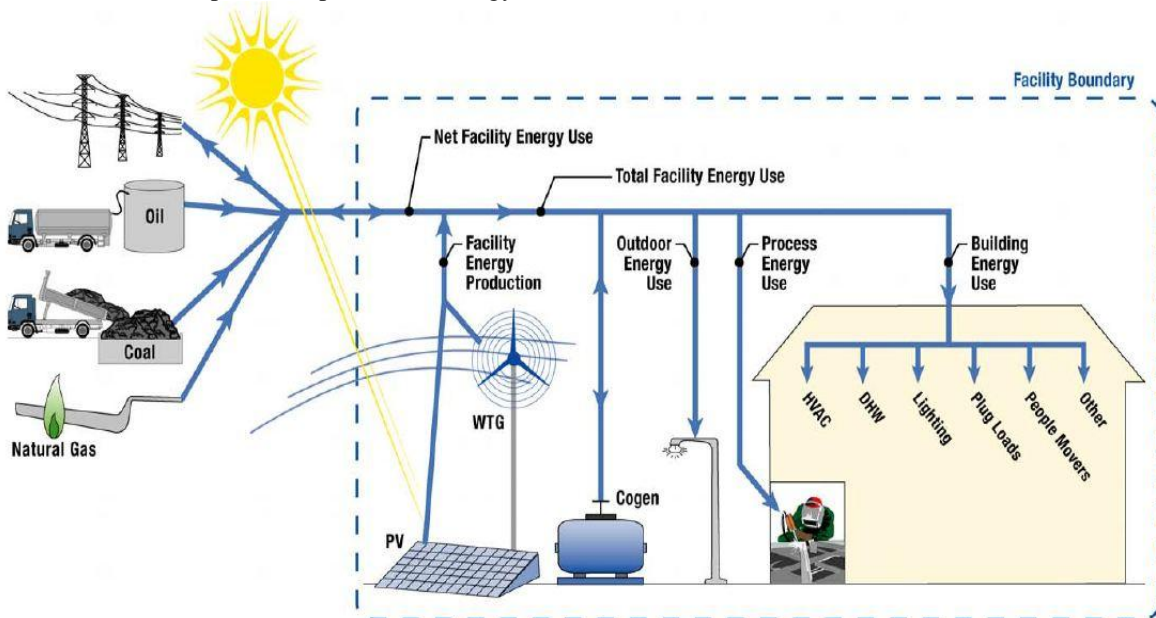


Figure 3. Energy flow diagram providing an illustrative view of energy consumption and production (National..., 2005)

Gathering data through an array of different methods such as measurements, bill analysis and other available sources, is one of the main activities of energy auditing. Without accurate data the energy audit cannot be successfully accomplished. A lot of data are readily available and can be collected from different divisions of the plant that is being audited. But some data require precise and detailed measurements, often over a period of time. The energy audit team is usually well-equipped with all of the necessary measuring instruments (European..., 2012). The most common energy types measured during the auditing process are:

- Liquid and gas fuel flows.
- Electrical measurements (voltage, current, load diagrams, power and power factor).
- Temperatures of solid and liquid surfaces, including surface thermography.
- Building infiltration and exfiltration parameters.
- Pressure of fluids in pipes, furnaces or vessels.
- Fume gas parameters (CO_2 , CO , O_2 and PM).
- Relative humidity.
- Luminance levels.

All of the acquired data must be carefully processed and interpreted in order to obtain the most accurate result possible (United..., 2009).

Benchmarking is a very important step in order to acquire plausible energy efficiency expectations. Although in Latvia there is no database where to compare the findings. The most common benchmarking unit for industrial plants is energy usage per one unit of production. Also it is common to compare types of energy used in common industries or energy used per activity as seen in Figure 3.

The main advantage of an energy balance diagram is that all energy inputs can be quantified and balanced against all energy outputs. The most convenient graphical representation of this is the Sankey diagram. In the Sankey diagram, the energy losses/outflows, the energy gains/inflows, as well as the usable energy in a given energy system are represented quantitatively and in proportion to the total energy inflow, according to the existing data from energy bills and invoices, calculations and on-site measurements in the plant. Presenting the energy flows in a visually appealing way with the aid of the Sankey diagram helps to locate the most critical energy-consuming areas of the energy system and, at the same time, to identify the sources that lead to energy losses. Figure 3 provides an example of the Sankey diagram with energy flow patterns (Ernest..., 2010).

Improvement of energy efficiency is the most important step towards the three goals of the energy policy: security of supply, environmental protection and economic growth. Nearly all of the global energy demand and CO₂ emissions are attributable to manufacturing, especially in the large primary material industries such as chemicals and petrochemicals, iron and steel, cement, paper and aluminum. Understanding how this energy is used and distributed is a national and international responsibility; and the potential for efficiency gains is crucial for decreasing CO₂ emissions. In Latvia

the industrial audit idea is new and there have been only a few audits conducted, but the trend is clear, there is a great saving potential in the Latvian industrial sector (Kursiša, Gleizde, 2013). The main investments in industrial energy efficiency in Latvia cover renovation of the building envelope, improvement of inner heat supply, ventilation systems, hot water systems, lighting system and mainly improvements in the technological process itself.

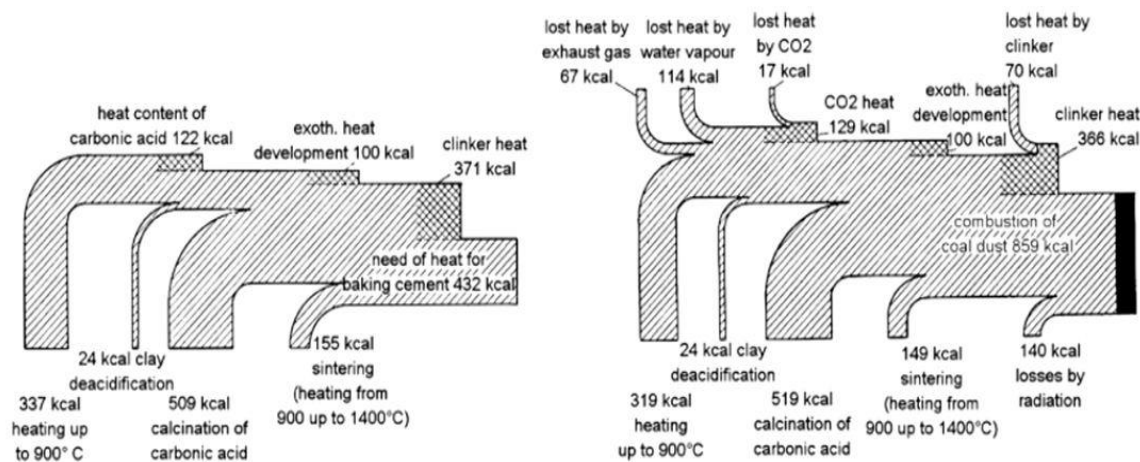


Figure 4. Sankey diagram shows the theoretical heat outlay (left) and practical heat consumption (right) in cement production (Ernest..., 2010)

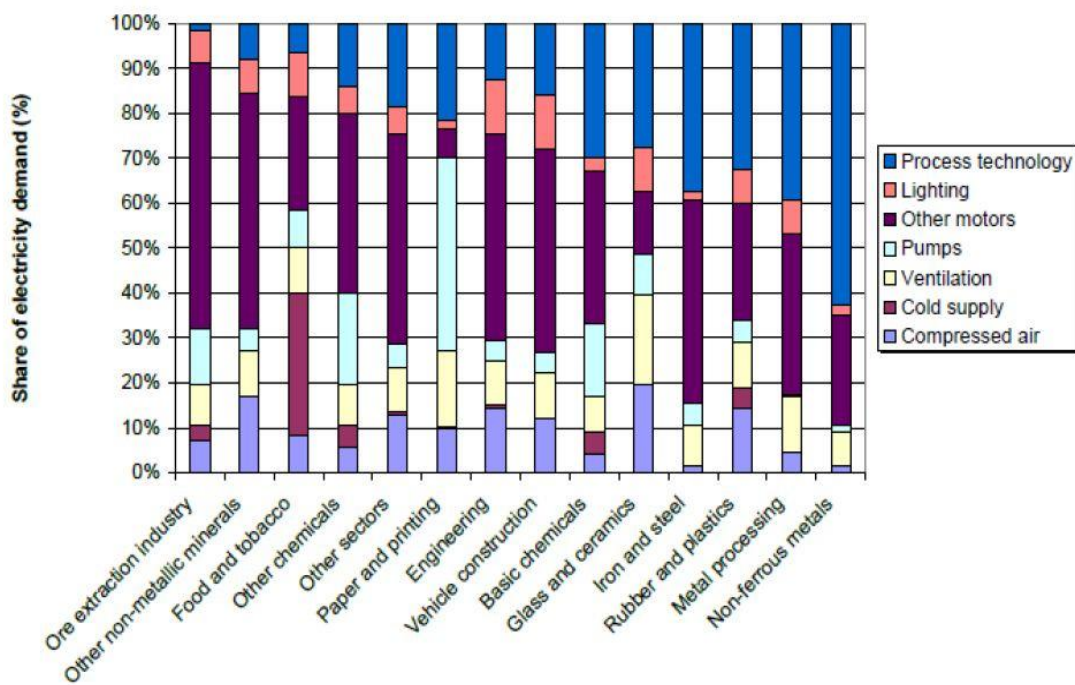


Figure 5. Share of electricity demand by application (European..., 2012)

CONCLUSIONS

1. Energy efficiency is one of the most important and most cost effective tools that can be applied for any facility. The goal of energy efficiency is to reduce the amount of energy required to provide products and services, or a healthy indoor climate.
2. Although world wide the industrial energy audit is a common practice, in Latvia it is something new and yet to be applied for most companies and facilities.
3. Improving facility energy efficiency gives the possibility to decrease CO₂ emissions and overall fuel consumption. The decrease of fuel consumption often is the main goal of an energy efficiency program.
4. There is a lack of knowledge about energy efficiency and what it has to offer. The concept of energy audits usually is understood only as a process of assessing energy flow for residential buildings, not factories, office buildings or similar industrial facilities.
5. In order to increase energy efficiency the need for additional energy monitoring devices are recommended. Monitoring devices should be installed for every big energy consumer or at least for every facility in order to be able to monitor energy usage and the usage patterns.

REFERENCES

- Gusta S. Industrial energy efficiency and sustainable development // Proceedings of the Green Economics Institute 7th Annual Green Economics Conference: *Green Economy: Reform and Renaissance of economics and its methodology – Green Economics – the solutions for the 21st century Green Economy: Rethinking Growth: RIO+20*, 19-21 July 2012, Oxford University, pp.144-148., ISBN:978-1-907543-30-2
- Kursiša A., Gleizde L. (2013) The development of energy efficiency for industries in Latvia: Legislation and statistics. *Civil Engineering 13*
- Latvijas Vides Investīciju Fonds (LVIF) (2011) Kompleksi risinājumi siltumnīcgāzu emisijas samazināšanai rūpniecības objektos, *account*
- Canadian Environmental Agency (CEA) (2010) Realizing Potential of Energy Efficiency
Available: http://www.globalproblems-globalsolutions-files.org/unf_website/PDF/realizing_potential_energy_efficiency.pdf
- Ernest Orlando Lawrence Berkeley National Laboratory (EOLBEL) (2010) Industrial Energy Audit Guidebook: Guidelines for Conducting an Energy Audit in Industrial Facilities [online] [accessed on 27.01.2013.].
Available: <http://china.lbl.gov/publications/industrial-energy-audit-guidebook>
- European Parliament (EP) (2012) Overview of Energy Efficiency measures of European Industry [online] [accessed on 27.01.2013.].
Available: <http://www.europarl.europa.eu/committees/en/itre/studiesdownload.html?languageDocument=EN&file=33970>
- International Energy Agency (IEA) (2007) Tracking Industrial Energy Efficiency and CO₂ Emissions [online] [accessed on 27.01.2013.].
Available: http://www.iea.org/publications/freepublications/publication/tracking_emissions.pdf
- National Renewable Energy Laboratory (NREL) (2005) Procedure to Measure Indoor Lighting Energy Performance [online] [accessed on 27.01.2013.].
Available: <http://www.nrel.gov/docs/fy06osti/38602.pdf>
- Natural Resources Canada (NRC) (2010) Energy Savings Toolbox – an Energy audit Manual and Tool [online] [accessed on 27.01.2013.].
Available: <http://oee.nrcan.gc.ca/sites/oee.nrcan.gc.ca/files/files/pdf/energy-audit-manual-and-tool.pdf>
- United Nations (UN) (2009) Global Industrial Energy Efficiency Benchmarking [online] [accessed on 27.01.2013.].
Available: http://www.unido.org/fileadmin/user_media/Services/Energy_and_Climate_Change/Energy_Efficiency/Benchmarking_%20Energy_%20Policy_Tool.pdf

ENERGY EFFICIENT ELECTRICITY USAGE AND LIGHTING SOLUTIONS FOR INDUSTRIAL PLANTS

Karlis Grinbergs
Energy Case, Bs. Sc. Ing.
E-mail: grinbergs.karlis@gmail.com

ABSTRACT

In recent years, there has been a growing interest about energy efficiency and conserving the environment in general. The study aims to evaluate industrial plant energy usage patterns and the potential for their improvement. Current electrical systems at factories often are inefficient according to present day technical standards. Technologies that are used in industrial plants are old and there is room for improvements. Transition towards a low-carbon emission economy for industrial plants will change the method of power production and also the way of how it is consumed. Converting conventional electrical grids to smart grids is an important step in energy economy. The focus on improvement of existing lighting systems has the potential of being one of the most significant short term actions to cut the expenses and decrease CO₂ emissions.

Keywords: industrial energy efficiency, efficient electricity usage, energy efficient lighting

INTRODUCTION

Industrial energy auditing method attempts to resolve differences among various auditing approaches. There are three main issues that have caused problems with performance monitoring of energy audit results and measures taken in the past.

- Standardization: Standard performance metrics provide a consistent basis for comparing energy performance among buildings;
- Versatility: The analysis is customized to the facility boundaries, energy configuration, goals and budget of analysis that apply to a given project;
- Economy of Effort: The data collection is carefully matched to the goals of the analysis and the study questions to avoid the common mistakes of too few or too many data.

Each procedure in this series should be done according to a standardized protocol that helps to quantify performance metrics (NREL, 2005).

Technical potential for improving industrial energy efficiency is substantial. The economic potential appears favorable even without putting any price on excess CO₂ emissions. Most of the improvements include various adaptations of existing technology (EOLBNL, 2010). However it is well known that there are numerous issues regarding the adaptation of such technologies. Yet, the main problem is lack of information, shortage of recognized professionals and no or limited access to capital needed for investments (CEA, 2010). In this paper two possible energy efficiency measures are considered - smart grids and efficient lighting systems.

Smarts grids provide a way to reduce transmission and distribution losses, optimize usage of operating

infrastructure by providing regulation for power flows, shifting peak demands, channeling decentralized and renewable energy into the grid and managing consumption patterns of all users connected to the grid (EC, 2006).

Electrical lighting is one of the major energy consumers in industries where lighting is used constantly or inefficiently. Large energy savings are possible by using energy efficient lighting, effective illumination sensor usage, optimal system design and rising awareness about energy economy for workers. Correct and energy efficient usage of electric lighting provides a wide array of benefits. First, carefully designed lighting system, improves work conditions, visual performance and visual comfort. (NYCDoDC, 2005/2006). Next, it reduces heat gains, thus saving energy in air conditioning systems, and increasing thermal comfort.

ANALYSIS

Manufacturing and construction industries are the third largest energy consumers in Latvia after household and transport branches. Energy consumption in manufacturing and construction industries in 2007, 2008, 2009, and 2010 years were as follows: 16.6%, 16.4%, 16.2% and 18.3% of total energy consumption in Latvia. Energy efficiency measures are usually applied in order to maintain or increase competitiveness in given industry (EM, 2011).

As it is stated in Figure 1, energy consumption for manufacturing and construction industries had been very steady over the years. There are potentials for energy efficiency in every industry.

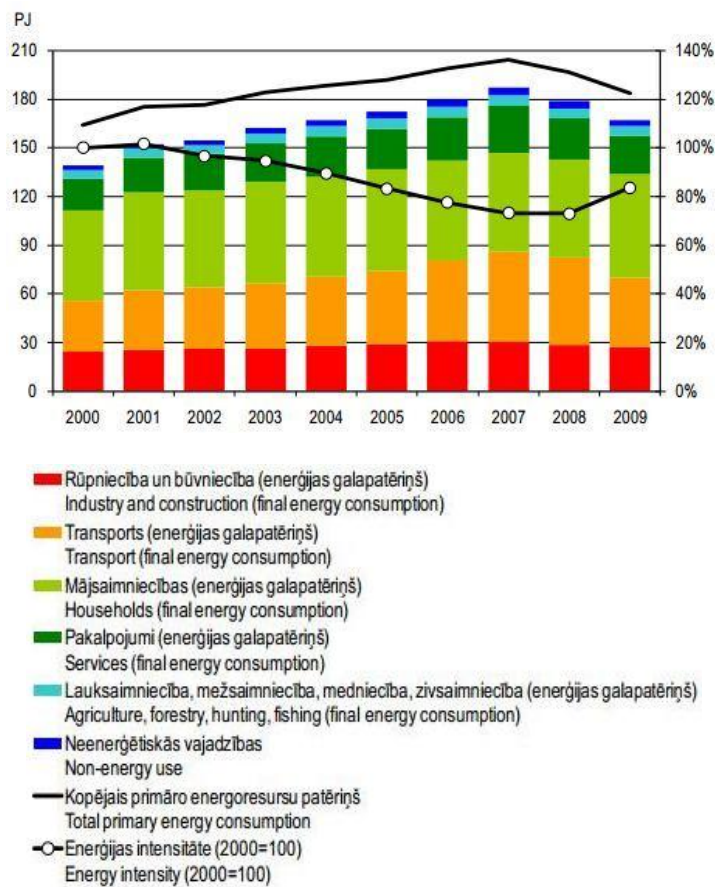


Figure 1. Final energy consumption by sectors (EM, 2011)

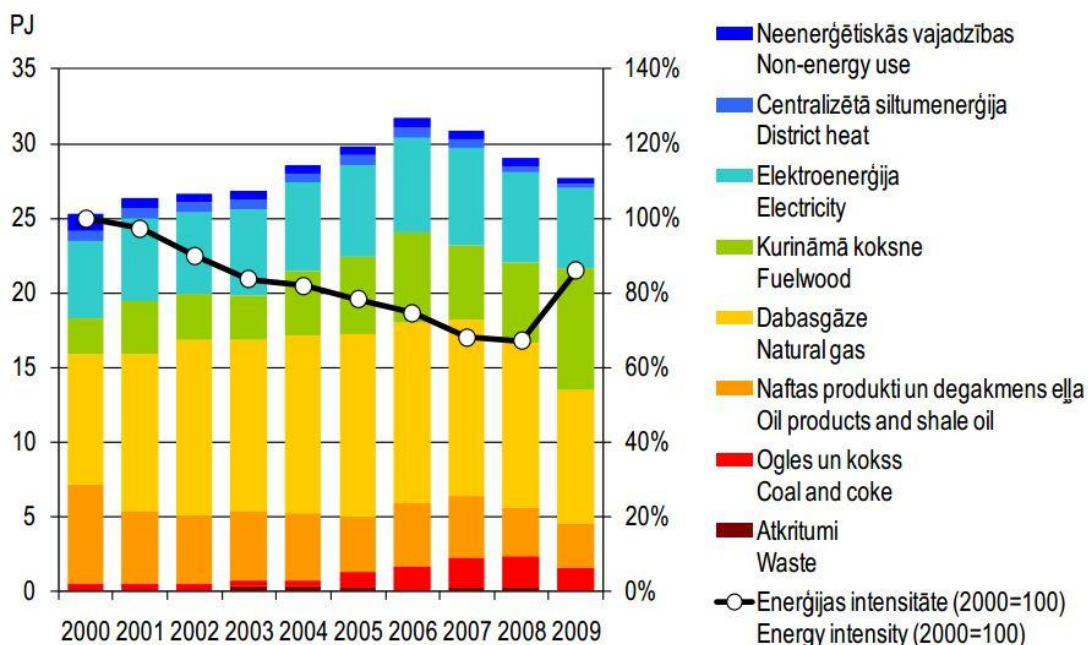


Figure 2. Final consumption in industry and construction (EM, 2011)

The share of electricity in total energy demand had been steady over the years and was as follows: 19.8% in 2009, 21.3% in 2008, and 21.6% in 2007

and similar for the previous years as well. But the total energy demand has been increasing over the years. World experience and overall world practice

show that energy efficiency has a great potential in the industrial sector and the potential savings are ranged from industry, individual companies and buildings, but the savings are often in the range from 10 to 40% of total energy usage (EM, 2011).

SMART GRIDS

Conventional electricity distribution systems are very complicated and extensive, but almost entirely passive, with little inter-communication and very limited control ability. Only the biggest consumers have commercial electricity monitoring systems either by voltage or by drawn current. The interaction between consumer loads and the power system itself is very poor (EC, 2006).

Smart communication systems offer the possibility of much greater control and monitoring of the grid than it is utilized in most cases now. Monitoring and controlling the grid offers the possibility of energy management and economy. Smart grid is an opportunity to use information and communication technologies in order to revolutionize the electrical power system. But due to the large size of the system and scale of the required investments switching to smart grid requires careful justification.

Smart grids are beneficial not only to power producers, but also consumers; the technologies used in smart grids provide information about energy usage and the possibility to manage the energy flow. This is achieved through advanced sensors and computerized remote controls that are designed to limit outages and network losses. These devices are interlinked to communication networks to enable consumer participation and to manage the integration of distributed energy sources (renewables, energy storage, combined heat and power). This allows the interconnected components to be optimized and monitored, and to help ensure efficient and reliable system operation. Figure 3 represents general smart grid vision and the different participants involved, converting a traditional one-directional power grid into a fully interconnected network. For the smart grid to become fully functional and usable, the energy sector will have to overcome two main challenges (CEA, 2010):

1. Level of implementation: issues of standardization and certification, operation, system testing, and consumer participation;
2. Financial issues: large amounts of funding are needed throughout the lifecycle of the smart grid development.

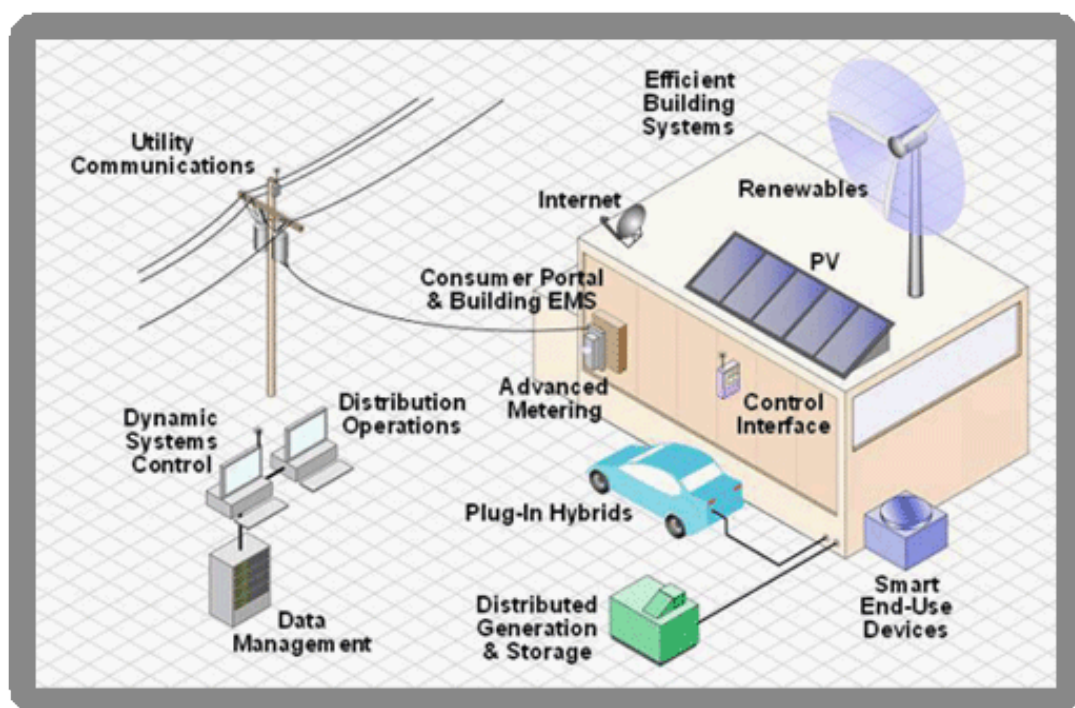


Figure 3. Schematic representation of smart grid idea (Bassein, 2010)

ENERGY EFFICIENT LIGHTING

The focus on improving the efficiency of electric lighting has the potential to be one of the most significant short-term initiatives to decrease power

consumption and CO₂ emissions. There are multiple possibilities of energy economy regarding lighting usage and the physical lighting fixture itself. But there are numerous barriers that industries must

overcome in order to introduce energy efficient lighting systems:

- Financial barriers are due to the higher initial cost of energy efficient lighting products, relative to conventional lighting and control systems;
- Market barriers may include: high quality lighting systems are not widely available due to low demand; the lack of promotion of energy efficient lighting products;
- Information barriers result from the lack of awareness and information about energy efficient lighting among professionals and the general public;
- Regulatory institutional barriers involve: lack of government interest; insufficient enforcement of policies; the need for more qualified personnel; priority on increasing supply rather than on reduction of consumption;
- Technical barriers include a lack of resources and infrastructure such as recycling and testing facilities, also pilot projects; and problems with electrical power supply, including outages, power surges and voltage variations;
- Environmental and health risk perception barriers include concerns about quality of light; possible exposure to electromagnetic fields; and possible exposure to hazardous materials that may be contained in the electronics or other lamp components.

The most efficient lamps for general illumination in the consumer sector use one-fifth to one-sixth of the electrical power to produce the same amount of light as the least efficient lamps and last up to 35 times longer (UNEP, 2012)

The first step in deciding whether a company would benefit from phasing out inefficient lighting is to understand how much electricity is currently being consumed for lighting, and what potential savings are available by moving towards more efficient lighting. Moving towards energy efficient lighting can be beneficial to other building systems as well, for example efficient lighting systems generate less heat and therefore the load for cooling or the air conditioning system is reduced. Another important thing is using those lighting patterns that can be modified and adopted as energy efficiency measures.

RESEARCH

Research was conducted in order to obtain lighting usage patterns and determine possible measures for energy saving by optimizing the lighting system and adding sensor controls for lighting appliances.

Research was conducted using the Steinel PROLog (Figure 4.) lighting audit sensor. Usually this sensor is placed in the areas where the potential energy losses could be found due to unnecessary artificial lighting. The sensor must be placed where people would cross the sensors reception area (Figure 5.) and it registers the movement patterns and frequency in a 21-28 day period. The sensor is designed for rooms without any automatic lighting control systems. The sensor data processing enables the system to determine the important data set for the lighting system design:

1. Amount of daylight. Daylight is often available through windows or skylights. But natural light is present only at certain times of the day and the amount of light from windows changes throughout the seasons. Availability of daylight is also affected by window properties such as g-value and percentage of glazing; also dirt on windows can sometimes play a huge role in reducing the amount of daylight.
2. Usage patterns of the room measured. Due to a built in occupancy sensor it is possible to register how often and for how long the light is actually needed in the room. By coupling usage patterns and time of available daylight it is possible to determine when artificial lighting is needed (or when auditing existing systems – whether artificial lighting is needed at all). In order to decide when artificial lighting is needed a normative illuminance at a specific workplace must be determined and set in the audit sensor.

Economical calculations have been conducted. Two scenarios are calculated and the economic data compared. The first scenario is the existing real life situation (existing lighting fixtures, for window condition and room usage patterns). The second scenario is calculated with new lighting fixtures and using an occupancy sensor, window condition is treated as unchanged (although often only by cleaning the window glass significant savings can be achieved). The scenarios are calculated for one, three, five and ten years. In the economical calculations three main parts of savings are considered, cost of used energy (and therefore CO₂ emissions), cost of changing lighting fixtures and the maintenance cost itself. Measurements were conducted in a room with low worker movement intensity, but the lighting was controllable only manually. Existing room parameters and results are shown in Table 1 and Figures 6 to 8.



Figure 4. Steinel PROLog audit sensor (Steinel, 2012)

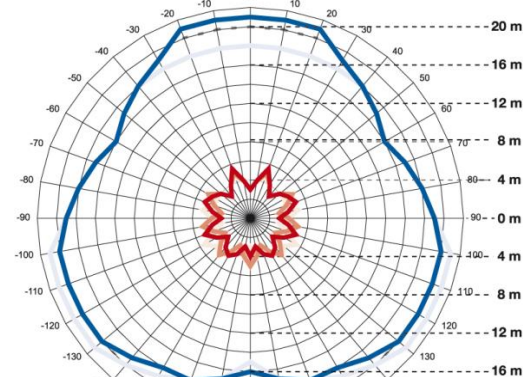


Figure 5. Sensor active range (Steinel, 2012)

Table 1

Room data		Results	
Windows type	Old wooden windows	Sunlight under the needed 300 lx	7515h
Amount of sunlight	50 lx	Currently used artificial lighting	8590h
Power of one lighting appliance	58W	Workers present	3103h
Existing lights	13 rows, 3 columns 2x58W	Artificial lighting actually needed	2575h
Total power of one lighting fixture including ballast	130 W	Annual energy for lighting	130657 kWh
Total lighting power	15.2 kW	Truly needed energy for lighting	39172 kWh
Normative (needed) lighting	300 lx	Lighting fixture life expectancy, existing	1.16y
Existing lighting usage pattern	24 h	Lighting fixture life expectancy, with sensors	3.11y
Data of measurement		Service cost, existing system	Ls 552.78
Month	September of 2012	Service cost, with sensors	Ls 207.16
Results obtained	299650	Energy economy for 1 year	82038.88 kWh
Duration of measurement	21 day	CO ₂ economy for 1 year	41019.44 kg

(Source: Created by the author)

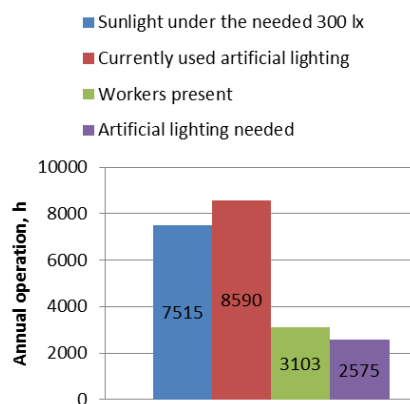


Figure 6. Annual operation, h
(Source: Created by the author)

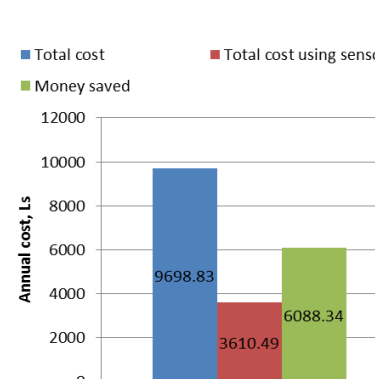


Figure 7. Annual cost, Ls
(Source: Created by the author)

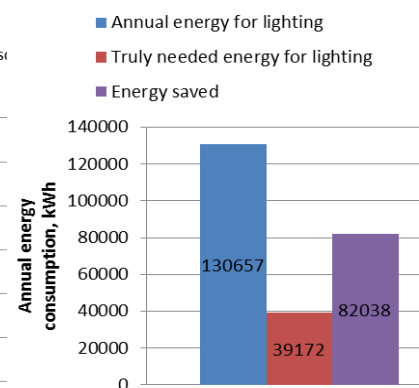


Figure 8. Annual energy consumption
(Source: Created by the author)

In figures 6-8 possible energy savings and costs are illustrated. The following issues were identified:

- The daylight is not sufficient for most of the time for quality work conditions, Figure 6.
- Artificial lighting is used all of the time, despite some of the time daylight is available and most of the time there are no workers present, Figure 6.

- Artificial lighting is needed only 29.9% of the time, Figure 6.
- The possible achievable savings per year are up to Ls 6083.34 - reduction of 62.8 %, Figure 7.
- The total energy needed for lighting is only 29% or 39172 kWh of the energy currently used, total energy saved by using sensor lighting systems – 91485 kWh, Figure 8.

CONCLUSIONS

1. In order to obtain the best possible result of the industrial energy audit the need for standardization is identified. Standardization gives the best possible opportunity to compare similar facilities in the same industry and analyze the results.
2. There is a large technical potential for improving industrial energy efficiency. Economic potential of energy efficiency in industrial appliances is substantial not only because of the CO₂ emission quotas, but also because most of the improvements include various adaptations of existing technology.
3. There are numerous issues regarding adaptation of technologies such as lack of information, shortage of recognized professionals and no or limited access to capital needed for investments.
4. Energy consumption in Latvian manufacturing and construction industries in 2007, 2008, 2009, and 2010 were as follows; 16.6%, 16.4%, 16.2% and 18.3% of total energy consumption.
5. Conventional electricity distribution systems are very complicated and extensive, but are almost entirely passive with little communication and very limited control ability and therefore only the biggest consumers have electricity monitoring system. The interaction between consumer loads and the power system itself is very poor.
6. Electricity grid monitoring and controlling offer the possibility of energy management and economy. Smart grid is an opportunity to use information and communication technologies in order to monitor and control the grid.
7. Smart grids are beneficial not only to power producers, but also consumers; the technologies used in smart grids provide information about energy usage and the possibility to manage the energy flow. The main advantages of smart grid limited outages and decreased network losses.
8. The focus on improving the efficiency of electric lighting has the potential to be one of the most significant short-term initiatives to decrease power consumption and decrease CO₂ emissions.
9. There are multiple possibilities of energy economy regarding lighting usage and the physical lighting fixtures itself.
10. Barriers of implementing energy efficiency measures for lighting systems: financial, informational, technical, environmental and governmental.
11. Results of the research shows that there is significant savings potential by using sensor controlled lighting systems. In this particular case, the total money saved per year is as much as Ls 6088.34.

REFERENCES

- Canadian Environmental Agency (CEA) (2010) Realizing Potential of Energy Efficiency Available: http://www.globalproblems-globalsolutions-files.org/unf_website/PDF/realizing_potential_energy_efficiency.pdf
- Ekonomikas Ministrija (EM) (2011) Latvijas enerģētika skaitļos, Latvian Energy in Figures [online] [accessed on 27.01.2013.]. Available: [http://www.em.gov.lv/images/modules/items/Latvijas_energetika_skaitlos_2011\(1\).pdf](http://www.em.gov.lv/images/modules/items/Latvijas_energetika_skaitlos_2011(1).pdf)
- Emma Bassein (2010) What is the Smart Grid [online] [accessed on 27.01.2013.]. Available: <http://www.carbonlighthouse.com/2010/08/smart-grid/>
- Ernest Orlando Lawrence Berkeley National Laboratory (EOLBEL) (2010) Industrial Energy Audit Guidebook: Guidelines for Conducting an Energy Audit in Industrial Facilities [online] [accessed on 27.01.2013.]. Available: <http://china.lbl.gov/publications/industrial-energy-audit-guidebook>

European Commission (EC) (2006) European SmartGrids Technology Platform [online] [accessed on 27.01.2013.].

Available: ftp://ftp.cordis.europa.eu/pub/fp7/energy/docs/smartgrids_en.pdf

National Renewable Energy Laboratory (NREL) (2005) Procedure to Measure Indoor Lighting Energy Performance [online] [accessed on 27.01.2013.].

Available: <http://www.nrel.gov/docs/fy06osti/38602.pdf>

New York City Department of Design + Construction (NYCDoDC) (2005/2006) Manual for Quality, Energy Efficient Lighting [online] [accessed on 27.01.2013.].

Available: <http://www.nyc.gov/html/ddc/downloads/pdf/lightman.pdf>

Steinel (2012) Steinel PROLog [online] [accessed on 27.01.2013.].

Available: http://www.eauc.org.uk/steinel_uk

United Nations Environment Programme (UNEP) (2012) Achieving the Global Transition to Energy Efficient Lighting Toolkit [online] [accessed on 27.01.2013.].

Available: http://www.thegef.org/gef/sites/thegef.org/files/publication/Complete%20EnlightenToolkit_1.pdf

ENERGY CONSUMPTION AND ITS REDUCTION POTENTIAL IN LATVIAN INDUSTRY SECTORS

Anda Kursisa*, Laura Gleizde**

NGO Passive House Latvija, Latvian Cluster of Industrial Energy Efficiency
E-mail: * anda@virtu.lv; ** laura.gleizde@gmail.com

ABSTRACT

This article, firstly, compares the distribution of energy consumers by industry sectors in Latvia. Next, the manufacturers which have received state support within the Climate Change Finance Instrument (CCFI) programme are examined by their industry sectors (food products, chemical products and metalworking). The energy saving calculated by companies (by NACE sectors) and its distribution by energy efficiency measures are analyzed. The planned savings structure is compared to statistical indicators of OECD countries, European Union and Latvia both by data available in sectors and during operation of industrial buildings. Further, the distribution of planned measures by types of energy efficiency is examined, and savings in megawatt-hours (MWh) and as total company consumption are compared. When comparing the percentage of energy efficiency measures with the EU study, the statistics of the CCFI tender does not depict the indicators specified by the EU: first, crosscutting electric energy and manufacturing processes, then heat savings. The heat energy saving for heating of buildings dominates in CCFI tender measures; the next significant indicator is energy savings in the manufacturing process. This article provides an example of planned and achieved results of two companies based on the monitoring data at the disposal of the authors. Energy efficiency in industries needs more studies, especially in terms of utility solutions and measure payback periods. A more detailed statistics by sectors is required, surveys of companies that have not received state support and ETS companies would provide more information about energy efficiency possibilities.

Keywords: industrial energy audit, energy efficiency, energy savings, industrial energy audit guidelines

INTRODUCTION

The purpose of this article is to analyze energy efficiency measures in industry sectors (excl. constructions) in Latvia, reviewing them in the context of statistics of the European Union and OECD (Organisation for Economic Co-operation and Development). Conclusions and recommendations are given to increase the competitiveness of Latvian industrial companies by reducing energy consumption.

This article is based on Latvian statistical data (Central Statistical Bureau – hereinafter CSB), openly available foreign studies, and the Climate Change Financial Instrument ((hereinafter – CCFI), CM Regulation No.521, 2010) data collected with the support of the Latvian Environmental Investment Fund (hereinafter – LEIF). The choice of the authors to analyze data of the state support programme, CCFI Open Tender “Complex Solutions for Greenhouse Gas Emission Reduction in Manufacturing Buildings” (hereinafter CCFI tender) is explained as follows: although the measures planned in 2010 were performed mainly in 2011, though monitoring data have been summarized in 2013, energy audits and saving calculations of ~40 of companies provide a broad overview of the sector. Therefore, this study will be continued analyzing monitoring data both for the programme implemented in 2010 and the one planned in 2012 – 2013, tracing it until 2015.

The method of the authors includes collection of CSB data and quantitative data of CCFI companies from LEIF documents (Project applications and energy audits), their comparison with statistics of other countries, and an analysis by types of energy efficiency measures and energy saving types. Shortcomings in the CCFI data analysis are caused by different formulations of energy efficiency measures in energy audits; also investments are not split according to activities thus restricting to analyze the payback periods, in some cases contracts were changed. However, these shortcomings do not affect the total result more than by 5%, because the responsibility of funding receivers for quantitative and qualitative indicators in the 5 year monitoring period is legally binding, not allowing less CO₂ savings as calculated, and not more than 5% changes in investment indicators. Limits for the application of foreign statistics is the structure of their data, for example, LR statistics shows a significant woodworking sector, while EU and OECD – manufacture of pulp and paper that have a smaller percentage in LR. Latvian legislation and statistics are analyzed in the article “Development of Industrial Energy Efficiency in Latvia, Legislation and Statistics”, authors A. Kursiša, L. Gleizde.

STRUCTURE OF ENERGY CONSUMPTION IN LATVIA AND SECTORAL BREAKDOWN OF COMPANIES RECEIVING CCFI SUPPORT

In the state support programme (CCFI) analyzed in this study, 49 projects were approved, agreements were concluded about the implementation of 41 project. Energy efficiency projects submitted by 39 companies, 57 buildings in total (companies could submit plans of measures for several buildings) were analyzed in this study. All industry sectors are represented at least by few companies, however, manufacturers of food and beverages (4 companies) show higher energy consumption. By the quantity, there are more companies from metalworking (6) and woodworking (5) sectors. 4 industry sectors (descending order) are leading in the energy consumption structure in Latvia:

- manufacture of wood and related products ;
- manufacture of non-metallic mineral products;
- manufacture of food and beverages;
- manufacture of metals.

Participants of CCFI, according to the energy consumption ratio of companies, shows a slightly different trend:

- manufacture of food and beverages – with high prevalence;
- manufacture of chemicals and chemical products;
- manufacture of other fabricated metal products;
- repair of equipment and storage functions.

It should be noted that the companies that have received state support form an incomplete picture, because the total energy consumption per pre-performance of measures makes 1.6 % from the total consumption of the industry sector. 33 companies in the ETS (Emissions trading scheme) system, larger energy consumers and respective creators of emissions making about 40% of energy consumption were excluded from support. Latvian ETS members are operators, who, according to the requirements of the Law "On Pollution" received greenhouse gas emissions permits. The structure of these companies is led by:

- manufacture of non-metallic mineral products;
- manufacture of food products;
- manufacture of wood and of wood and cork products ;
- manufacture of chemicals and pharmaceutical products.

In the European Union (Altmann M, Michalski J, Brenninkmeijer A, Tisserand P. (2010)), companies operating in the ETS system make ~50% from industry's energy consumption, however the impact of ETS trading on energy efficiency is poorly studied.

Therefore, the limits of this study are defined by the analysis of the companies that have received state support and measures (project of 2010, implementation in 2011 – 2012).

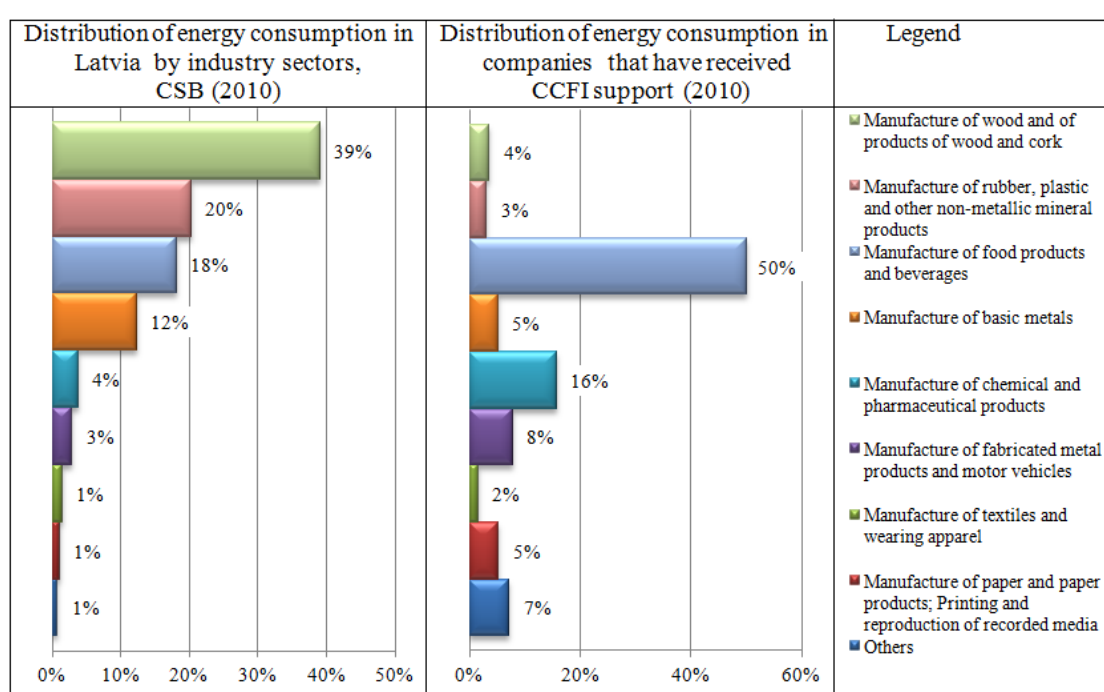


Figure 1. Energy consumption structure in Latvia by industry sectors, CSB and CCFI, 2010. Calculated based on total electric energy and heat energy consumption, MWh

ENERGY SAVING BY TYPES OF ENERGY AND INDUSTRY SECTORS

When reviewing energy supply of companies supported by CCFI, the total distribution of fuel supply for industries includes all type of energy resources available in Latvia: centralized heat supply and electricity; and local boiler houses using natural gas and liquefied gas, biomass (wood), diesel oil, mazut and coal. The saving of energy resources by their type matches the power supply structure of companies.

If the most used power fuel resources are: **central heating, natural gas, wood (biomass) and**

electricity; then the most highly ranked savings are provided by: **central heating, natural gas, electricity, wood (biomass).** In total, 27% of the forecasted savings is formed by electricity reduction, the other part consists of heat energy. We view energy saving by sectors in the context of the total consumption of companies, where the most significant consumption is in the “Manufacture of food products and beverages”, that is followed by “Manufacture of chemical and pharmaceutical products”.

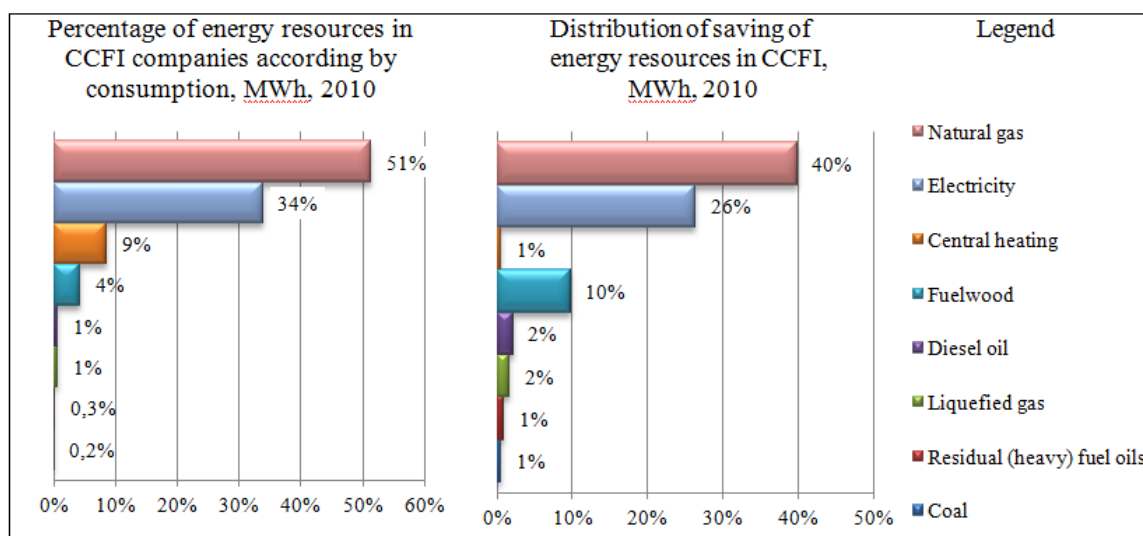


Figure 2. Distribution of percentage saving of energy resources in CCFI projects

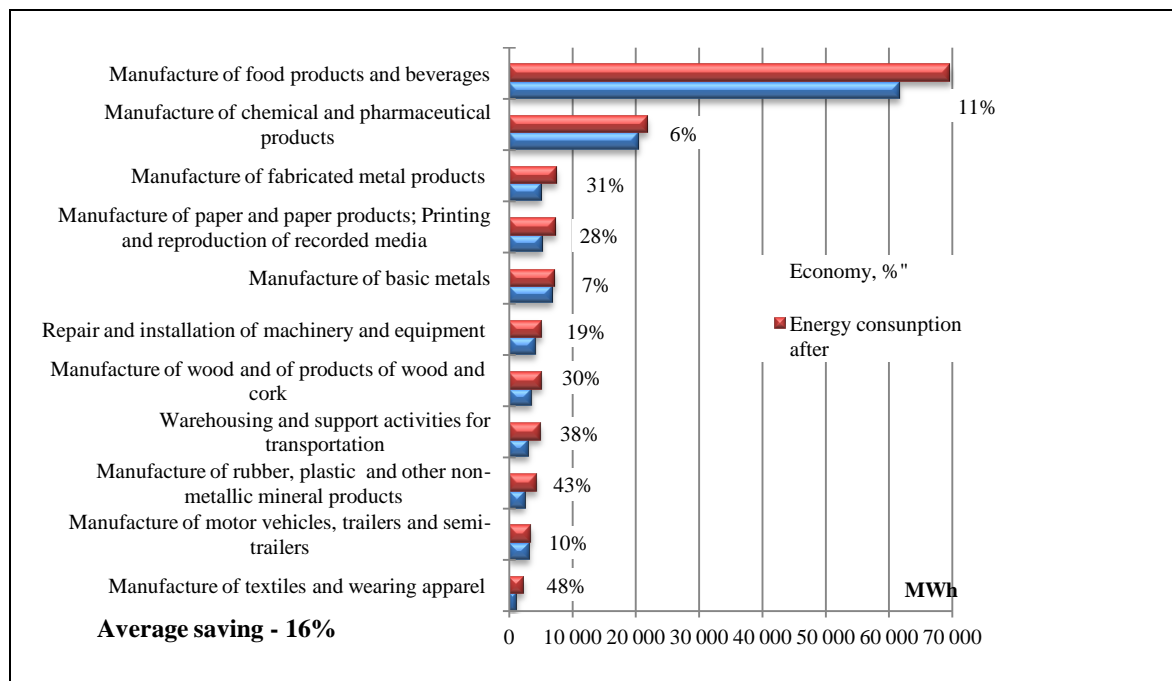


Figure 3. Distribution of saving in CCFI projects by sectors of operation

COMPARISON WITH EU AND OECD STATISTICS; INDUSTRIAL BUILDING AGE FACTOR

Comparison with EU and OECD statistics

When reviewing savings in the most significant sectors, EU benchmarks cannot be applied due to the lack of sector data, however, we may compare estimates of EU and OECD countries for energy cost ratio in companies and the savings forecast for the sector in general or on average in the company. Considering that the European and OECD study had no data collected on the woodworking sector, which is specific to Latvia due to its high energy consumption, this sector is not included in the table.

Table 1
Comparison of industry sectors' data

Sector	Data source	Energy cost ratio (%) in company	Potential energy saving (%)
Manufacture of basic metals	OECD ¹	10-30	10
	EU ²	n/d	6-7
	CCFI ³	1-4	3-45
Manufacture of food products and beverages	OECD	1-10	25
	EU	10	11-13
	CCFI	2-7	3-37
Manufacture of chemical and pharmaceutical products	OECD	50-85	9-25
	EU	n/d	17
	CCFI	1-5	1-13
Manufacture of non-metallic mineral products	OECD	25-50	20-35
	EU	n/d	n/d
	CCFI	1-4	6-79
Manufacture of textiles and wearing apparel	OECD	5-25	10
	EU	n/d	n/d
	CCFI	1-7	33-63

1- Saygin D., Patel M.K., Gielen D. (2010);

2 - Altmann M, Michalski J, Brenninkmeijer A, Tisserand P.(2010).; 3- LEIF, CCFI

In total, the companies analysed have a smaller energy cost ratio (it is still explained by comparatively low prices of energy resources in Latvia); however, the potential energy saving in companies significantly exceeds the average of EU and OECD sectors. As a result, the impact of energy efficiency measures on financial indicators of companies is a significant factor.

Industrial building age factor and impact of industry restructuring

In Latvia, according to the most successful energy saving estimates of CCFI projects, saving may reach up to 79%, showing an average saving of 43% in the manufacture of non-metallic mineral products and 48% saving in the manufacture of textiles and clothing.

Along with the general knowledge that insulation of building may provide about 50% saving of heat energy, we also study the OECD explanation about

the impact of the life cycle of industrial buildings to the energy saving forecast. In the study (Saygin D., Patel M.K., Gielen D. (2010)), it was concluded that older factories are smaller by size, have lower energy efficiency, and lower efficiency of production technologies. In its turn, the turnover of the companies is frequently not sufficient to transfer manufacturing to a technologically modern building; that is especially characteristic for Russia and former USSR. This aspect forces to continue manufacturing in non-effective buildings. However, it is also specified there that the growth of energy consumption in developing countries is expected from new, effective plants.

In accordance with the data collected by the European Union (Altmann M, Michalski J, Brenninkmeijer A, Tisserand P. (2010)), about 30% of the total energy efficiency reduction is caused by structural changes in industry sectors, innovation of technologies or transfer of energy-intensive manufacturing plants.

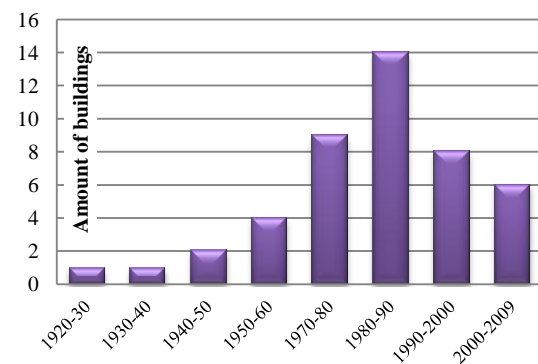


Figure 4. Distribution by the year of construction of buildings, supported by CCFI. Source: LEIF, CCFI

In the CCFI program, 47% of investments go into the building and building envelope, both by saving structure (mainly heat energy) and by investments. The companies that wished to transfer their manufacturing to modern buildings before the economic crisis (for example, AS "Staburadze", AS "VG Kvadra Pak") decided to improve energy efficiency of the existing buildings and the manufacturing process.

Moreover, the buildings that were built before 2000 do not meet Latvian heat insulation standards, the buildings have large losses of energy in heating and also ventilation, that is especially significant in manufacturing plants with high air exchange intensity.

According to the structure of CCFI projects, the trend to renovate the existing buildings and to improve technologies will be maintained, however, in the future, in case of positive economic growth, the development of new manufacturing plants is expected to improve Latvian energy efficiency balance (Kursiša A., Gleizde L. 2013)

CCFI ENERGY SAVING ANALYSIS: PERCENTAGE AND MEASURES

First of all, we must consider that for analysis of savings statistics, a larger number of companies is required, because several sectors are represented by just a few companies (1-3) that do not show a trend, but rather provide only an example of the sector. Measures for building envelope – insulation, replacement of windows, doors and gates – dominate in energy efficiency by MWh savings; they are followed by measures for energy efficiency in production technologies, and the reconstruction of the heating system. It should be noted that even using energy audit methods, heating efficiency measures in calculations are rarely precisely separable from savings caused by the improvement of the building envelope. Only some companies did not use the opportunity to insulate their building and to replace windows and doors, yet - exactly these few companies achieved the biggest saving with their measures for energy efficiency of equipment and heat recovery. The most frequently used activities, by quantity, are: insulation, replacement of windows, and doors in combination with reconstruction of heating and/or lighting. Activities in manufacturing are less frequent; however, they take an equivalent position in the investments section along with reconstruction of buildings or renovation measures, including both building envelope and utilities. The popularity of insulation may be explained by the long life cycle of buildings and non-compliance with Latvian heat engineering standards that cause large heat losses.

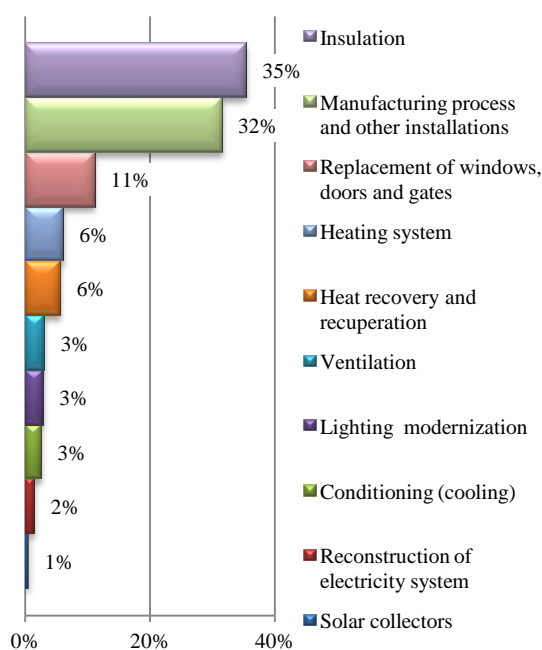


Figure 5. Distribution of saving by types of measures, MWh

The authors of the article analyzed whether the number of energy efficiency measures in the company correlates with the saving ratio (%) in the total consumption, and in megawatt-hours. If we split energy efficiency activities by types according to the saving chart, no mutual relationship is stated, i.e. – large energy saving ratio may be forecast only when insulating buildings, while the largest economy in megawatt-hours could be achieved with individual measures in manufacturing equipment and heat recovery. It is characteristic that insulation may provide a significant saving in up to 79% of buildings that have no significant manufacturing energy consumption. In its turn, if industrial consumption is several times higher than the energy consumption caused by building heating losses, it is possible to achieve a much higher quantitative saving in megawatt-hours (MWh). See the structure of energy efficiency measures to forecast results in Figure 7. The EC document (Altmann M, Michalski J, Brenninkmeijer A, Tisserand P., 2010) tells about the ratios of saving: “Roughly speaking, the energy savings potential in the industry is equally distributed between the three categories of electricity consumption by process specific energy consumption, space heating and crosscutting technologies including lighting, electric motors, pumps, ventilation, cold supply and compressed air.” In the same document, p. 15, it is noted that electricity consumption by crosscutting technologies provides for the largest economic savings potential, process specific consumption has medium potentials, and space heating has the lowest potential.

Paying attention to the section with the largest potential, EC, p.16, indicates that “On average over all sectors and over all EU Member States, crosscutting electricity consumption in industry represents some 70% of total industry electricity consumption [IISI, 2009]. This demonstrates the importance of improving these seven crosscutting groups of technologies.”

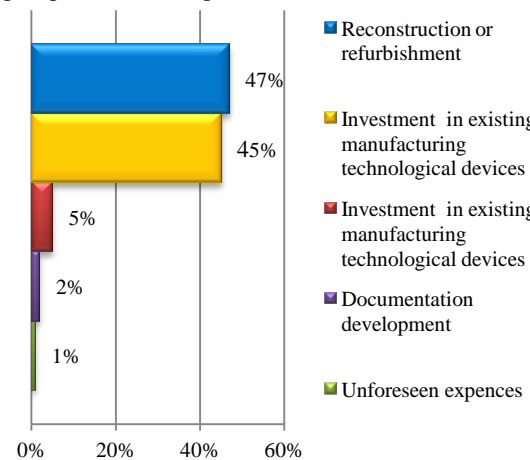


Figure 6. Distribution of investments, Ls

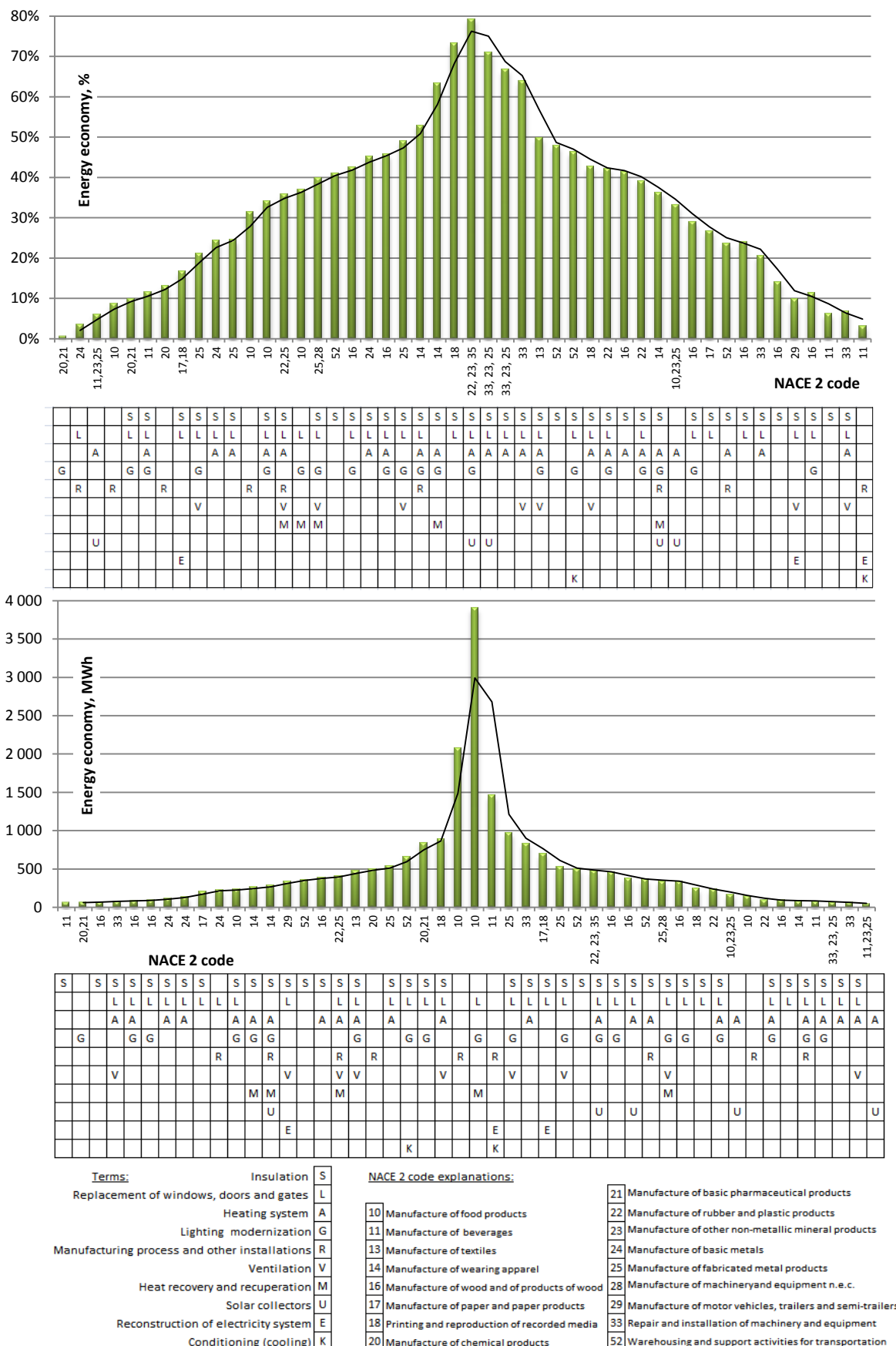


Figure 7. Saving in % and MWh by industrial buildings of sector's companies, with NACE 2 codes

When studying the resulting ratio of savings per activities; and comparing it to the EU study, it must be concluded that the statistics of the CCFI tender does not reflect the indicators that are specified in the EU. The heat energy saving for heating of buildings dominates in the measures, the next significant indicator is energy savings in manufacturing processes. The authors may explain it by auditors' insufficient knowledge of crosscutting technologies, especially in ventilation, cooling and electric systems. The method of calculations for building envelope is known to auditors due to their experience in the sector of buildings, manufacturing processes and saving opportunities are frequently recommended by technologists of companies, however, the remaining savings from processes asks for the interrelation of specific knowledge in several engineering sectors beyond the competence of one professional.

EXAMPLES

SIA “Valmiera-Andren”

SIA “Valmiera-Andren” manufactures large-sized glass fibre containers, including custom design containers. Within the framework of the CCFI project, dismantling of the unused story, insulation of external walls and the roof, replacement of windows, doors and gates, reduction of the area of windows, installing of recuperation-based ventilation, and transfer of the fuel of hot water system from electricity to gas were performed in 2011. The heat energy saving calculated during the CCFI audit was ~40%. Actual heat energy savings according to first heating period monitoring data reach almost 60% saving, see Figure 8.

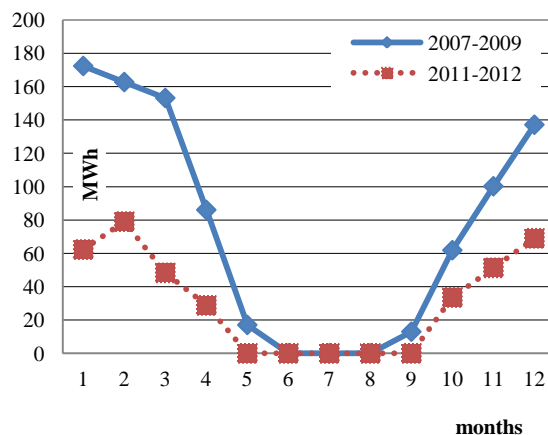


Figure 8. Changes in heat energy consumption in SIA “Valmiera-Andren”

AS “Dinex Latvia”

Metalworking company AS “Dinex Latvia” manufactures exhaust systems and filters for trucks. Within the framework of the CCFI project, insulation of external walls and the roof, replacement of windows, doors and gates, reduction of the area of windows, reconstruction of the ventilation system with air recirculation and improvements of the electrical network were performed in 2011. The heat energy saving calculated during the CCFI audit was ~40%. Actual heat energy savings according to first heating period monitoring data are doubled and reach almost 90% saving, see Figure 9.

CALCULATION OF THE IMPACT OF SAVING AND INVESTMENTS ON HEAT AND ELECTRICITY CONSUMPTION OF INDUSTRY SECTORS AND LATVIA

The companies studied in the CCFI program make 1.6% from the total industry consumption before the implementation of measures, and the planned calculated saving is 0.24%. A higher saving percentage (0.37%) is planned for electricity, it also provides other positive forecasts: larger reduction of CO2 emissions and shorter payback periods due to electricity tariffs.

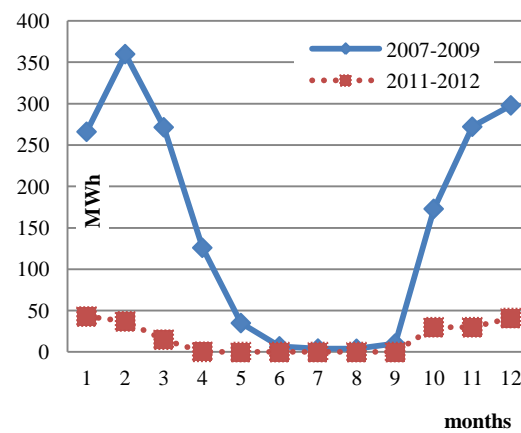


Figure 9. Changes in heat energy consumption in AS “Dinex Latvia”

Table 2

Calculation of saving			
Total saving	Saving in MWh	Average tariff (excl. VAT) in 2011, Ls/kWh	Cost saving, Ls
Electricity, 27% from CCFI's total	6 184	0.073	451 420
Heat energy, 73% from CCFI's total	16 585	0.035	580 490
Total CCFI saving, 100%	22 769		1 031 910
Total investments, Ls			10 675 025
Total payback period without state support, years			10.3
Payback period with state support (on average >50%), years			4.3

Table 3

Calculation of investments			
	Consumption in industries LR 2011	Saving in CCFI	% from LR
Electricity, MWh	1 674 720	6 184	0.37%
Heat energy, MWH	7 943 290	16 585	0.21%
Total	9 618 010	22 769	0.24%

CONCLUSIONS AND RECOMMENDATIONS

The companies that have received CCFI support do not fully reflect all sectors, because their total energy consumption before the measures makes 1.6% of the total consumption of the industry, while, for example, companies of the ETS system together make 40% of the total consumption. However, the structure of CCFI sectors sufficiently illustrates the companies representing the leading industry sectors of LR in food, chemical products and metalworking sectors.

The saving of energy resources by types corresponds to the power supply structure of companies; the most highly ranked savings are provided by: **central heating, natural gas, electricity, wood (biomass)**. 27% of the forecast saving are formed by electricity reduction, the other part consists of heat energy.

If we compare the ratio of energy costs of companies and the saving potential with available EU and OECD data, a lower percentage of energy costs is stated in companies, however, the potential energy saving significantly exceeds the average value of EU and OECD sectors. As a result, the impact of energy efficiency measures on financial indicators of companies is evaluated as a significant factor. When comparing the resulting ratios of energy efficiency measures with the EU study, the statistics of the CCFI tender does not depict the indicators specified by the EU: first, crosscutting electric energy and manufacturing processes, then heat savings. The heat energy saving for heating of buildings dominates in CCFI measures, the next significant indicator are energy savings in manufacturing processes. The authors may explain it by auditors' insufficient knowledge of crosscutting technologies, especially in ventilation, cooling and electric systems. The method of

calculations for building envelope is known to auditors due to their experience in the sector of buildings; manufacturing processes and saving opportunities are frequently recommended by technologists of companies, however, the remaining savings from processes asks for the interrelation of specific knowledge in several engineering sectors beyond the competence of one professional.

Therefore, recommendations for crosscutting technologies and payback periods in manufacturing sectors require more analysis. It is not simple to analyze due to data confidentiality issues, as well as because accurate information is required on energy efficiency technologies, energy saving and tariffs; up to now, Latvia has paid much greater attention to heat energy audits and economy, but methods of electricity savings, that are very important for manufacturers, require a more detailed study in the future.

When analyzing whether the number of energy efficiency measures in the company correlates with the saving ratio (%) in total consumption and in megawatt-hours, no mutual relation is stated, i.e. – large energy savings in the percentage may be forecast only when only insulating buildings, while the largest economy in megawatt-hours may be achieved with individual measures in manufacturing equipment and heat recovery.

Although the analysis performed in this article is based on calculations and forecasts, examples with monitoring data of two companies provide evidence that the forecasts may be achieved and significantly exceeded.

The companies studied in the CCFI program make 1.6% from the total industry consumption before the implementation of measures, and the planned calculated saving is 0.24%. A higher saving ratio is planned for electricity, it also provides other

positive forecasts: larger reduction of CO₂ emissions and shorter payback periods due to electricity tariffs. Energy efficiency in industries needs more studies, especially in terms of utility solutions and investment payback periods. A more detailed statistics by sectors is required; surveys of companies that have not received state support and ETS companies would provide more information about energy efficiency possibilities.

Due to the fact that the companies that have received CCFI support submit monitoring data on the first year of operation till 31 January 2013, the

analysis of actual savings must be performed within the framework of another study.

Research limits. The companies implementing energy efficiency measures without state support and the companies operating in the ETS (European Union Emissions trading scheme) system are not included; market influence, energy price increase dynamics, energy efficiency incentives and disincentives, availability of funding, benchmarks, CO₂ saving and other factors included in other studies and report are not analyzed.

REFERENCES

- Altmann M, Michalski J, Brenninkmeijer A, Tisserand P.(2010), European Parliament: Overview of Energy Efficiency measures of European industry. [online] [accessed on 24.01.2013.] Available:<http://www.europarl.europa.eu/committees/en/itre/studiesdownload.html?languageDocument=EN&file=33970>
- Kursiša A., Gleizde L. (2013) „Rūpnieciskās energoefektivitātes attīstība Latvijā; likumdošana un statistika” (Development of Industrial Energy Efficiency in Latvia, Legislation and Statistics)
- Ministru kabineta 2010.gada 8.jūnija noteikumi Nr.521 "Klimata pārmaiņu finanšu instrumenta finansēto projektu atklāta konkursa "Kompleksi risinājumi siltumnīcefekta gāzu emisiju samazināšanai ražošanas ēkās" nolikums" (Cabinet of Ministers Regulation No.521 Regulations of the Open Tender of projects funded by the Climate Change Financial Instrument “Complex Solutions for Greenhouse Gas Emission Reduction in Manufacturing Buildings” of 8 June 2010)
- Saygin D., Patel M.K., Gielen D. (2010). United Nations Industrial Development Organization. Global Industrial Energy Efficiency Benchmarking. An Energy Policy Tool. Working paper. [online] [accessed on 24.01.2013.] Available:
http://www.unido.org/fileadmin/user_media/Services/Energy_and_Climate_Change/Energy_Efficiency/Benchmarking_%20Energy_%20Policy_Tool.pdf
- Statistical classification of economic activities in the European Community (*NACE rev.2*) codes.